Memoirs of Museum Victoria 74: 5–15 (2016) Published 2016

ISSN 1447-2546 (Print) 1447-2554 (On-line)
http://museumvictoria.com.au/about/books-and-journals/journals/memoirs-of-museum-victoria/

Quantifying scientific significance of a fossil site: the Gogo Fossil sites (Late Devonian, Western Australia) as a case study

John A. Long

School of Biological Sciences, Flinders University, GPO Box 2100 Adelaide, South Australia 50901 and Geosciences, Museum Victoria, GPO Box 666, Melbourne, Victoria 3001, Australia (john.long@flinders.edu.au)

Abstract

Long, J.A. 2016. Quantifying scientific significance of a fossil site: the Gogo Fossil sites (Late Devonian, Western Australia) as a case study. *Memoirs of Museum Victoria* 74: 5–15.

Assessing the scientific significance of fossil sites has up to now been largely a matter of subjective opinion with few or no metrics being employed. By applying similar metrics used for assessing academic performance, both qualitative and quantitative, to fossil sites we gain a real indication of their significance that enables direct comparison with other sites both nationally and globally. Indices suggested are those using total pages published for both peer-reviewed and combined peer-reviewed and popular publications, total citations from the papers, total impact points for site (citing palaeontology-related papers only), total number of very high impact papers (VHIP; journal impact factor>30) and social media metrics. These provide a measure of how much the published fossil data from a site has been utilised. The Late Devonian fossils of the Gogo Formation of Western Australia are here used as an example of how these metrics can be applied. The Gogo sites for example, have produced c.4384 pages of peer-reviewed papers (c.5458 total combined with popular works); generated papers with a total impact point score of 611, including 10 VHI papers, and generated 4009 citations. The sites have an overall h-index of 33. Combing these into a Scientific Site Significance Index (SSSI) will permit direct comparisons of site significance to be made for initiating discussions about site protection, tourism, geopark status, local heritage listings or potential future world heritage nominations.

Keywords natural heritage, palaeontology, Paleozoic.

Introduction

Tom Rich once said in an interview with Natalie O'Brien of The Australian, that Gogo was "the most important fossil vertebrate site in Australia" (The Australian, 2nd August, 2001, p.4). Whether or not one agrees with such a statement is completely arbitrary, but such statements raise a number of questions concerning how we routinely assess the scientific significance of a fossil site. Fossil sites are non-renewable resources that may hold values ranging from the tangible, in terms of scientific significance and economic values to local tourism, but they may hold other values in terms of cultural significance when fossil sites coincide with places valued by indigenous peoples, or be historically significant in their own right (e.g., Wellington Caves, New South Wales; Lake Eyre Basin, South Australia; Rich & Archbold, 1991). Fossils can also hold intangible natural heritage values making them far more significant than their net scientific worth as can geological sites (Pena do reis & Henriques, 2009; Long, 2012a). An example of this is the Gogo fish *Mcnamaraspis* (fig. 2A) which in December 1995 became historically significant as the first state fossil emblem to be formally decreed in Australia (Long, 2004; https://www.dpc.wa.gov.au/GuidelinesAndPolicies/SymbolsOfWA/Pages/FossilEmblemGogoFish.aspx).

Although there are several papers evaluating geoheritage sites (e.g. Pena do reis & Henriques, 2009) there are none the author knows of that specifically attempt to evaluate the scientific significance of a fossil site using an applied approach. To initiate discussion on potential methods to evaluate the significance of any fossil site, this paper will analyse the Gogo fossil sites in north Western Australia, of late Devonian age (Frasnian), in terms of various metrics which allow a comparative measure of scientific significance as is generally applied to measuring academic performance. This approach is based on the premise that a site rich in fossils of high diversity and significance will have been targeted for primary research. If the papers are indeed significant they will have been used in other studies and thus be cited frequently. If the work has high international significance then the work will most likely have been published in high impact multidisciplinary science journals, if the discoveries were made in relatively recent times. Many highly significant sites lack extensive publications in these journals as I acknowledge that the need to publish in high impact journals is a relatively recent phenomenon tied to increased grant success and even academic promotion. If the fauna from a site is highly diverse it should also result in large number of publications being developed, and possibly have

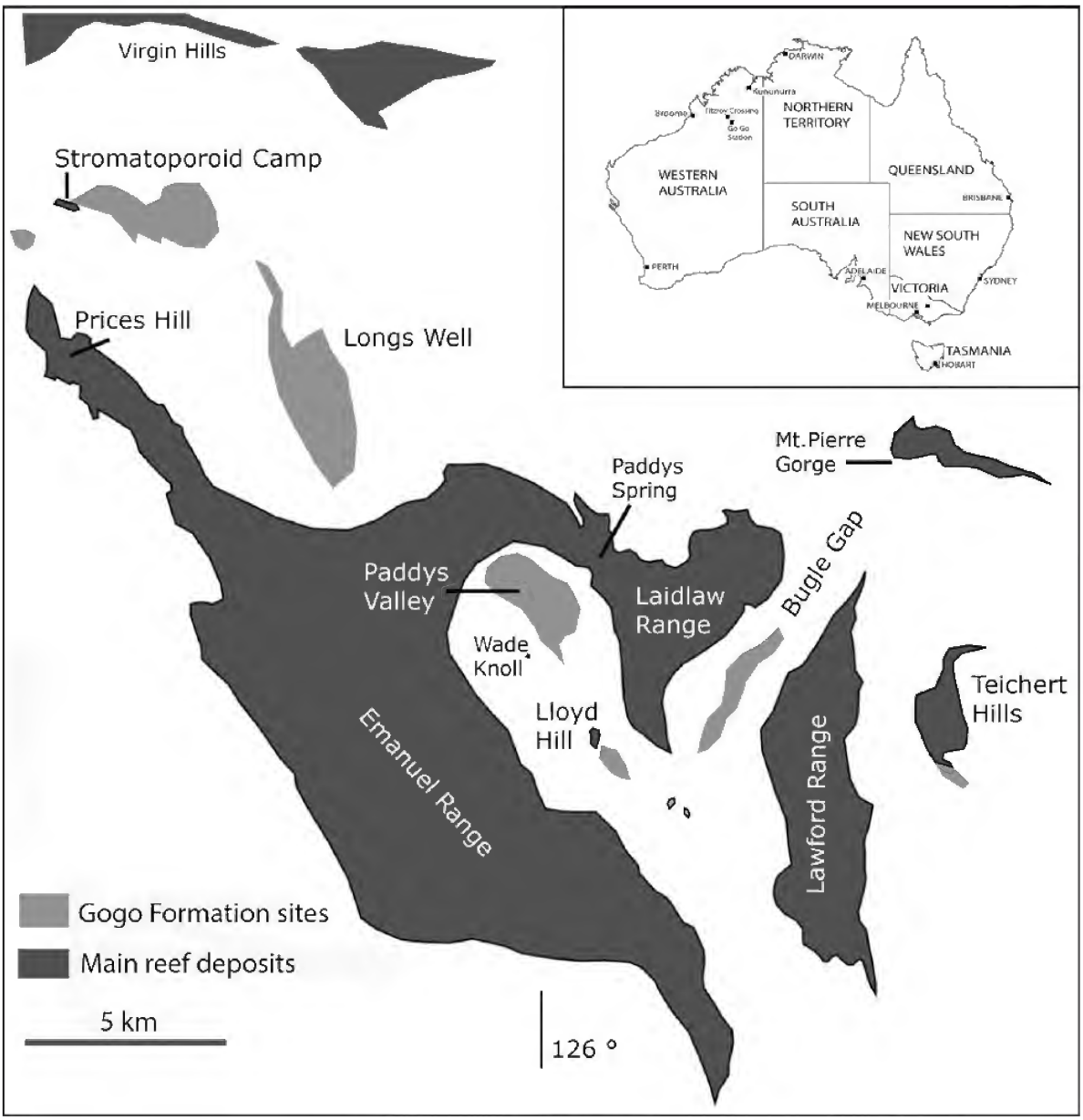

Figure 1. Map showing area covering the Gogo Formation site localities (geology taken from Long and Trinajstic, 2010, figure 1).

produced large numbers of published pages. As scientific papers can range from a one-page abstract to several hundred page monographs, the number of scientific publications on the fossil fauna and/or flora of a site is here considered of far less importance than the total numbers of peer-reviewed pages published. Finally, like routine academic performance, a high citation rate from papers produced around a site can be expressed as an h-index (numbers of publications having equal or greater numbers of citations) for each site. In palaeontology, unlike other mainstream science disciplines, there is a smaller pool of active academics (compare with say medicine or biology in general), so overall citation rates tend to be low.

A fossil site is used here is in the broader context to contain all individual sites from similar formation defined as follows: a set of sites within a contained area that is linked by having fossils of similar preservation coming from the same geological

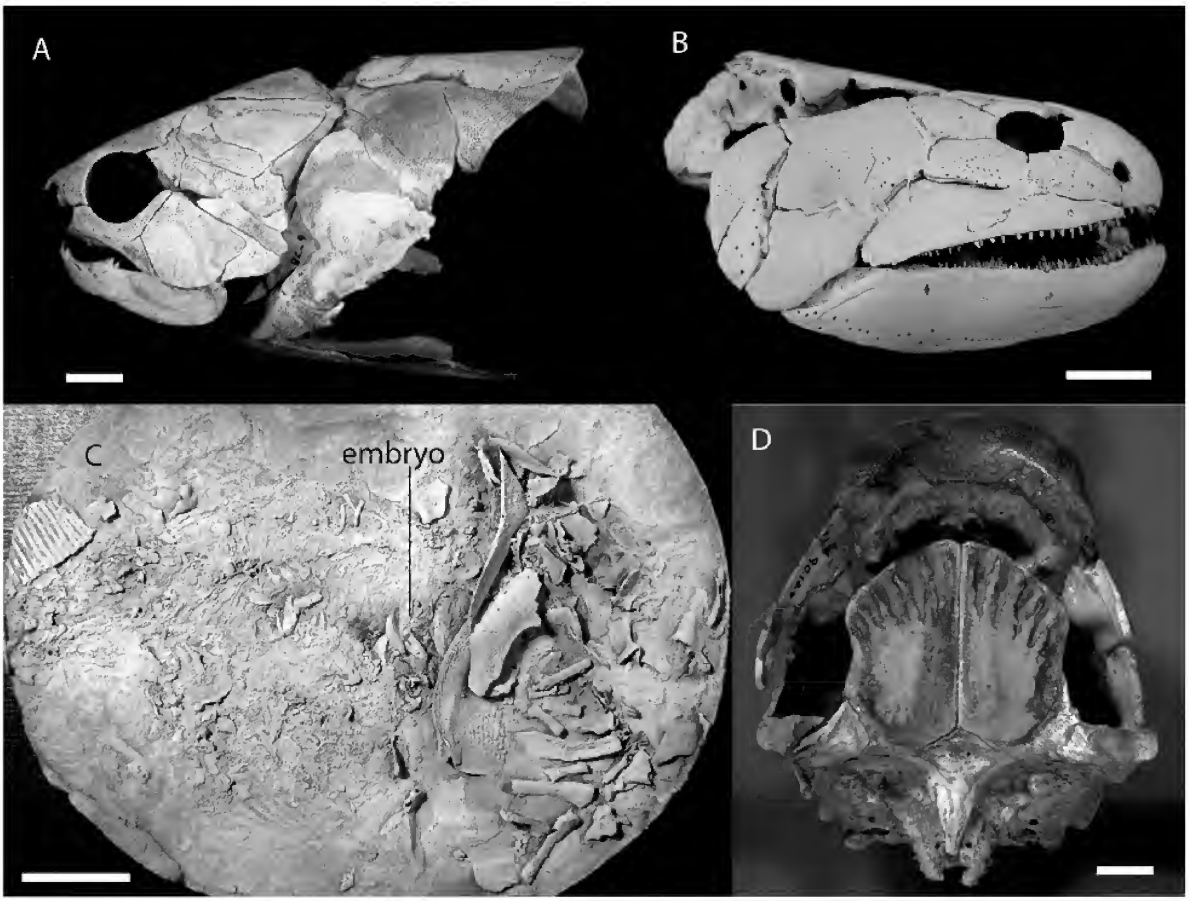

Figure 2. Examples of Gogo fish preservation (WAM = Western Australian Museum; NMV P = Museum Victoria Palaeontology Collection). A, eubrachythoracid placoderm *Mcnamaraspis kaprios*, the state fossil emblem of Western Australia (WAM 86.9.676, from Long, 1995). B, The tetrapodomorph fish *Gogonasus andrewsae* (NMV P221807). C, the ptyctodontid placoderm *Austroptyctodus gardineri* which has 3 embryos preserved inside it (WAM 86.9.662). D, palatal view of the lungfish *'Chirodipterus' australis* (most likely a new genus). WAM 90.10.8. Scale bars are 1 cm.

formation, of approximate same stratigraphic age, and same palaeoenvironment. The Gogo sites comprise a large number of individual sites across an area of about 200km^2, so the term "Gogo fossil sites" refers to a suite of sites containing well-preserved fossils all found from surface limestone concretions derived from exposures of the Gogo Formation (fig. 1). Most of the better known sites are listed by Miles (1971). The sites comprises one of only 6 recognised Lägerstatten (sites of exceptional quality fossil preservation), designated for the known fossil fish sites of this age globally, as listed in the supplementary information (Anderson et al., 2011).

In this paper the measure of that significance is discussed with respect to factors that apply to measuring academic outputs in terms of both quantitative (numbers of significant specimens as a corollary of numbers of significant scientific papers) and qualitative measures (quality of preservation, disparity of species variation also translating into a diversity of scientific papers). The metrics applied are provided in Supplementary Appendix 1. Natural History collections can be evaluated in a similar way, as shown by Winkler and Withrow (2013). By creating a Google Scholar profile for the bird collections at the University of Alaska Fairbanks Museum, they were able to show that the body of work supported by the collection had a profile h-index of 42, equivalent to that of an average Nobel Laureate in Physics. Similarly the Louisiana Museum of Natural History bird collections have their own Google scholar page that now records an h index of 69 (based on 25,469 citation as of December 1st, 2014). These measures thus send a positive message of how significant these collections are by virtue of how well used and cited is the work on its specimens. A similar approach is proposed in this paper to show how well utilised the scientific papers generated from a particular fossil site can be applied to give an indication of the site's scientific significance.

It is important to be able to quantifiably measure the relative significance of a fossil site for varying applications: assessing heritage status for local conservation planning, for issuing permits for collecting for scientific work in national parks (or when sites fall under the auspices of local shire land management); and for potential future nominations for national heritage registers and international recognition including potential future world heritage nominations.

Previously fossil sites have been assessed for the old register of national estate (national heritage listings) based on how expert assessors with specialist knowledge of the site and its fauna position them within an arbitrary framework relative to other known sites. The problem with this is that the individual specialist who knows a particular site well may not necessarily be familiar with the full body of scientific literature on other sites of different age and faunal composition. This informal placement of sites as 'highly significant' or extremely important lacks a quantitative approach that can be used to argue that other sites that are potentially above the average local or national significance, and thus help target future sites in need of some form of legislative protection against site damage by non-professional collectors or fossil dealers (see Long, 2002, for case examples). The Gogo sites have been chosen as the case study in this work mainly because of the author's familiarity with the site, having collected at the localities for the past 30 years and worked on its vertebrate fauna for the past 30 years, and from being familiar with its extensive scientific and popular literature.

The Gogo Fossil Sites and Inferred Scientific Significance

The significance of the Gogo Fossil sites were recognised in the 1960s when the acetic acid preparation technique was refined at the Natural History Museum, London by Harry Toombs (Toombs, 1948). Toombs was able to prepare 3-D skeletons of Devonian fishes out of limestone, revealing perfect 3-D shape and form. Furthermore, in recent years preservation of fossil impressions of soft tissues including muscle fibres (Trinajstic et al., 2007, 2013), nerve cells (Trinasjtic et al., 2007), umbilical structures and embryos (Long et al., 2008, 2009, Trinajstic et al., 2014; also see fig 2C) and alimentary structures (Long and Trinajstic, 2010) have been identified. Examples of the 3-D preservation of Gogo fishes and embryos is shown in figure 2. Biomarkers have recently been identified in Gogo crustaceans preserving proteins only found in living crustaceans (Melendez et al., 2013). The real utilisation of the Gogo fossil fish fauna though is due to the clear unambiguous preservation of the bony skeletons. It has been widely utilised for detailed histological studies of early vertebrate tissues (e.g. Smith, 1977; Smith & Campbell, 1987 etc.), as well as inclusion in major phylogenetic papers analysing character distributions (Miles and Dennis, 1979; Miles and Young, 1977, Long et al., 2014). The landmark paper on transformed cladistics by Rosen et al. (1981) utilised Gogo lungfish material to press home certain points about the homology of the tetrapod choana. Today this paper has been cited nearly 400 times (Google Scholar) and remains a seminal work on the topic.

In terms of non-quantifiable highlights of the Gogo fauna's significance, this includes a series of world first or unique occurrences of species, genera and families. The Gogo fauna contains a mostly endemic fauna of around 90% unique genera and species. It contains the world's only known record of camuropiscid and inscisoscutid arthrodires. It also contains the highest diversity of lungfishes (c. 12 spp.) and actinopterygians (c. 5 spp.) for any site of similar age. In its high diversity of vertebrates (c. 50 spp.) it is well above any other site of similar age, including the World Heritage Miguasha site in Canada (20 fish species; Cloutier, 2010). From a purely intuitional perspective one can sense the value and degree of scientific significance of such a uniquely well-preserved, diverse and endemic fauna is obviously high. The question is how do we measure this?

Gogo Sites: Actual Measures of Scientific Significance

The premise of this work implies that the diversity of a fauna is reflected in the numbers of papers on the fauna, and the numbers of pages of peer-reviewed publications. Works of monographic stature indicate seminal papers that are widely cited as the key reference for the study group (e.g., Gardiner's 1984 monograph on Gogo actinopterygians has 250 citations). Thus sites of high scientific significance would be expected to generate not only a lot of papers, but large descriptive papers and therefore highly cited papers. Large monographic works are amongst some of the most highly cited works in palaeontology, and on-line journals like *Paleontologia Electronica* still publish such works without charge to authors. A good measure for the total significance of a body of work centred around a topic is the cumulative impact factor points of the journals they have been published in. The academic website ResearchGate uses this approach by adding up the impact factor points for an individual's body of work to give a total tally. Using this approach we find that the Gogo sites have an impact factor points tally of around 611. The method used in the scoring was to assign low ranking journals (IF=0-1) as a score of 1, and then round up or down any other impact factors to the nearest whole numbers.

Assessing very significant fossil specimens. A fossil that solves a major evolutionary problem or bridges a major morphological boundary as a key transitional form will attract high numbers of citations. For example the discovery of *Tiktaalik*, which was found to be the immediate ancestor of all living tetrapods, was published in the journal N*ature* as two back-to-back articles in April 2006 (it was also the cover story). To date these two papers on *Tiktaalik*, now one of the most well-known and iconic fossil discoveries of the 20th century, have received 255 citations (Daeschler et al., 2006) and 188 citations (Shubin et al., 2006) respectively. Yet a third paper on *Tiktaalik*, also published in *Nature* (Downes et al., 2008), has only received 25 citations. Another example is the discovery of *Homo floresiensis,* the so-called 'hobbit'. The initial paper announcing the discovery by Brown et al. (2004) in *Nature* has now received around 609 citations. Using these as a reasonable basis for comparison, we see that the Gogo fauna's most highly cited descriptive papers (Miles, 1977, 188 citations; Gardiner, 1984, 250 citations),

though not published in high impact journals, still yield high citations directly comparable to the original *Tiktaalik* papers.

Very High Impact Papers. One measure of the international significance of fossil specimens is whether they are valuable in solving a major phylogenetic or biogeographic problem, or provide new information about evolutionary biology deemed highly significant. In such cases the work is occasionally accepted in the highest ranking interdisciplinary science journals like *Nature* or *Science*. Of course, this is not always the case as some very significant discoveries get routinely rejected by such journals. Nonetheless, as these journals publish only a handful of palaeontological papers each year (e.g., *Nature* published about 10 palaeontological papers in 2014), each paper is judged to be a highly significant breakthrough worthy of high impact publication by both the board of editors and reviewers of these papers. These are thus here given special attention as 'very high impact papers' (impact factor as of 2013 > 30; Nature, IF=42; Science IF=31).

A measure of international significance for a site can therefore be also gauged by the total number of very high impact papers (VHIP) published on its fossil materials. For the Gogo sites, this amounts to 10 such papers (9 on primary materials, plus one review paper on the site's significance, Ahlberg, 1989; see Supplementary Appendix 1). This is more VHIPs than any other fossil site in Australia (for comparison, Riversleigh World Heritage fossil mammal site has 4 VHIPs, Victoria's Early Cretaceous vertebrate sites have 4 VHIPs, Ediacara c. 3 VHIPs). Excluding African hominid sites, the only other fossil sites in the world that immediately come to mind to have 10 or more VHIPs published on their faunas would include the Jehol Biota of China (Liaoning sites, covering a very wide range of sites and stratigraphic horizons), and the Burgess Shale sites in Canada.

Numbers of papers/pages published. This gives an overall estimate of the quantity, but not quality, of peer-reviewed work published from a site. Naturally a large number of papers reflect either a diverse fauna, or that continuous new data is being described from a site. This suggests the site hasn't yet peaked in terms of yielding scientifically significant new specimens. In some cases work might be published as a series of monographs, which limits the overall numbers of papers published but increases the total number of pages of published work. For Gogo this is a large number: 4389 pages. This excludes any books that are not specifically on the Gogo fossil fauna. This doesn't include papers on the geology of the site, but only papers that primarily describe Gogo fossils (fishes plus invertebrates and microfossils) or figure Gogo specimens in elucidating the descriptions of other early vertebrate specimens.

Other measures of the cultural and scientific significance of a site

Books and popular magazine articles published. Both technical and popular books centred around the fossil biota of a site can be used to gauge its significance as only books that publishers see worthy of competing in the market will be published by mainstream or academic publishers. In other words a site yielding information that is a consumable product for the general public rather than just for a specific scientific audience will get published by major publishers (excluding self-published projects). In such cases, we can also corroborate publication about the site in a number of popular science magazine publications (e.g., *New Scientist, Scientific American, Discover, Cosmos, Australasian Science* etc.) as well as being subject material for popular books for the adult lay audience. This has been achieved for the Gogo fauna, with many articles appearing in the international popular science journals (eg *New Scientist*, April 1989; *Scientific American,* cover story for January 2011). This includes books written about the evolution of fishes featuring Gogo specimens (Long, 1995, 2011a), as well as a history and significance of the Gogo fossil discoveries (Long, 2006), a book telling the story of the origins of copulation (Long, 2011b, 2012b) and a children' s book about the story of Gogo fish becoming a state fossil emblem (Long, 2004).

Media Focus on the Site. The international significance of a fossil site can also be measured in terms of how much national and international media coverage the site has generated through inclusion in general documentary programs covering broad topics like vertebrate evolution or the prehistory of a country. The Gogo sites featured in David Attenborough's 1979 series *Life on Earth* (episode 4, fishes), and in recent years featured on other local documentaries made about Australia's prehistoric past (e.g., Richard Smith's Australia: Time Traveller series, ABC TV, 2012). Gogo fish fossils have also been the topic of 3 features screened on the ABC TV's science program *Catalyst* (formerly called '*Quantum*'). Social media could be another way to measure impact or visibility of a site, using popular web blog sites like 'The Conversation' to highlight the significance of certain sites. Altmetrics from such sites record numbers of hits, tweets and media pick-ups on each article.

Tourism. The amount of tourism to a site (e.g., annual number of visitors), funds raised by visitations, sales, and so on could also be applied if the site was open to the public (e.g., Naracoorte Caves world heritage site). These metrics really only apply to the sites that can capture such visitations and their associated funding.

A Proposed Site Significance Index (SSSI)

One way of generating a usable index of scientific significance is to arbitrarily combine all the metrics discussed above into a formula that smooths out the very high numbers with the low but significance indices.

Ppr=pages published (peer-reviewed) is a large number for Gogo, so Ppr/100 gives 4389/100 =43.89, rounded up to 44.

Ip=Impact points 611 is also a large number so Ip/10 gives 611/10=61.

Cn=Total citations is also a large number, so Cn/100 gives 4009/100=40 (rounded).

VHIP=very high impact papers is always a relative low number so needs to be multiplied by 10 for a reasonable comparison with other sites where VHIP might regularly be less than 5. For Gogo this gives 10x10=100. This measure is seen to be highly significant as an index of globally significant papers.

The suggested formula for assessing site significance that brings these factors into account would be: SSSI=(Ppr/100)+(Cn/100)+(Ip/10)+(VHIP x10).

For the Gogo sites as assessed at the time of submission of this work, this score is

SSSI=44+40+61+100=245.

The meaning of such a score can only be assessed when further work is completed on other significant fossil sites to measure and compare the same metrics. As this paper was intended primarily to be a generator of discussion, I hope that this will incite other researchers to score other fossil sites they have worked on, particularly those who have focussed on a special fossil site for most of their working careers so that the body of published information on the site is captured. This will enable other fossil sites to be eventually compared with one another using the metric approach here outlined. It is also hoped that further discussion on this topic will be generated by this paper to determine if the parameters chosen herein are suitable enough or if other factors need be scored and added into the mix to give a more meaningful assessment of a fossil site's scientific significance.

Acknowledgements

This paper is dedicated to Dr Thomas H. Rich who has been one of the most inspirational mentors towards my early career development. Tom dedicated many years of his life working the Victorian Cretaceous fossil sites in search of our country's oldest mammals, and he eventually found them after many years of hard searching. He has taught me and many of my colleagues the value of persistence in working a site year after year until the very significant fossils are eventually found. The MS has benefitted from discussions with Erich Fitzgerald, Gavin Prideaux, Gavin Young and Kate Trinajstic.

References

Ahlberg PE. 1989. Fossil fishes from Gogo. *Nature* 337: 511-512.

Anderson, P., Friedman, M., Brazeau, M. and Rayfield, E.J. 2011. Initial radiation of jaws demonstrated stability despite faunal and environmental change. *Nature* 476: 206-209.

Brown, P., Sutikna, T., Morwood, M.J., Soejono, R.P., Jatmiko, Saptomo E.W., and Due, R.A. 2004. A new small-bodied hominin from the Late Pleistocene of Flores, Indonesia. *Nature* 431: 1055-1061.

Cloutier, R. 2010. The late Devonian Biota of the Miguasha national park UNESCO world heritage site. AAAP Search and Discovery Article #90172, GeoConvention, Calgary, Alberta, May 10–14. Ppl-4 (on-line).

Daeschler, E.B., Shubin, N.H., and Jenkins, F.A. 2006. A Devonian tetrapod-like fish and the evolution of the tetrapod body plan. *Nature* 440: 757-763.

Downes, J., Daeschler, E.B., Jenkins, F.A. and Shubin, N.H. 2008. The cranial endoskeleton of *Tiktaalik rosae*. *Nature* 455: 925-929.

Gardiner, B.G. 1984. Relationships of the palaeoniscoid fishes, a review based on new specimens of *Mimia* and *Moythomasia* from the Upper Devonian of Western Australia. *Bulletin of the British Museum of Natural History (Geology)* 37: 173-428.

Long, J.A. 1995. *The Rise of Fishes, 500 Million years of Evolution.* UNSW Press, Johns Hopkins University Press, 224 pp.

Long, J.A. 2002. *The Dinosaur Dealers: mission, to uncover international fossil smuggling.* Allen & Unwin, Sydney, 220 pp.

Long, J.A. 2004. *Gogo Fish! The story of the state fossil emblem of Western Australia.* The Western Australian Museum, Perth. 48 pp.

Long, J.A. 2011a. *The Rise of Fishes, 500 Million years of Evolution.* 2nd ed. UNSW Press, Johns Hopkins University Press, 288 pp.

Long, J.A. 2011b. *Hung like an Argentine duck: a journey back in time to the origins of sexual intimacy.* Fourth Estate, HarperCollins, Sydney. 278 pp.

Long, J.A. 2012a. Case Studies of Intangible Natural Heritage from Museum Collections. Pp. 43-55 *in Intangible Natural Heritage: New Perspectives on Natural Objects,* E. Dorfman (ed.), Routledge Press, New York.

Long, J,A, 2012b. *Dawn of the Deed: the prehistoric origins of sex.* University of Chicago Press, Illinois. 278 pp.

Long, J.A. and Trinajstic, K. 2010. The Late Devonian Gogo Formation Lägerstatte –Exceptional preservation and Diversity in early Vertebrates. *Annual Reviews of Earth and Planetary Sciences* 38: 665-680.

Long, J.A., Trinajstic, K.M. and Johanson, Z. 2009. Devonian arthrodire embryos and the origin of internal fertilization in vertebrates. *Nature* 457: 1124-112.

Long, J.A., Trinajstic, K.M., Young, G.C. and Senden, T. 2008. Live birth in the Devonian period. *Nature* 453: 650-652.

Long, J.A., Mark-Kurik, E., Johanson, Z., Lee, M.S.Y., Young, G.C., Zhu, M., Ahlberg, P.E., Newman, M., Jones, R., den Blaauwen, J., Choo, B., and Trinajstic, K. 2015. Copulation in antiarch placoderms and the origin of gnathostome internal fertilization. *Nature* 517: 196–199.

Melendez, I., Grice, K., Trinajstic, K., Ladjavardi, M., Greenwood, P., and Thompson, K. 2013. Biomarkers reveal the role of photic zone euxinia in exceptional fossil ptreservation: an organic geochemical perspective. *Geology* 41: 123-126.

Miles, R.S. 1971. The Holonematidae (placoderm fishes): a review based on new specimens of *Holonema* from the Upper Devonian of Western Australia. *Philosophical Transactions of the Royal Society of London* 263B: 101-234.

Miles, R.S. 1977. Dipnoan (lungfish) skulls from the Upper Devonian of Western Australia. *Zoological Journal of the Linnean Society* 61: 1-328.

Miles, R.S. and Dennis, K. 1979. A primitive eubrachythoracid arthrodire from Gogo, Western Australia. *Zoological Journal of the Linnean Society* 66: 31-62

Miles, R.S. and Young, G.C. 1977. Placoderm interrelationships reconsidered in the light of new ptyctodontids from Gogo Western Australia. *Zoological Journal of the Linnean Society, Symposium Ser*ies 4: 123-198.

Pena dos Reis, R. and Henriques, M.H. 2009. Approaching an integrated qualification and evaluation system for geological heritage. *Geoheritage* 1: 1–10.

Rich, P.V. and Archbold, N.W. 1991. Squatters, priests and professors: a brief history of vertebrate palaeontology in *Terra Australis.* Ch.1 in: *The Vertebrate Palaeontology of Australasia,* P.V. Rich, J. Monaghan, R.F. Baird & T. Rich, (eds), Pioneer Design Studios, Lilydale: pp. 1-44.

Rosen, D.E., Forey, P.L., Gardiner, B.G. and Patterson, C. 1981. Lungfishes, tetrapods, palaeontology and plesiomorphy. *Bulletin of the American Museum of Natural History* 167: 159-276.

Shubin, N.H., Daeschler, E.B. and Jenkins, F.A. 2006. The pectoral fin of *Tiktaalik rosae* and the origin of the tetrapod limb. *Nature* 440: 764-771.

Smith, M.M. 1977. The microstructure of the dentition and dermal ornament of three dipnoans from the Devonian of Western Australia: a contribution towards dipnoan interrelations, and morphogenesis, growth and adaptation of the skeletal tissues. *Philosophical Transactions of the Royal Society of London* 281B: 29-72.

Smith, M.M., and Campbell, K.S.W. 1987. Comparative morphology, histology and growth of dental plates of the Devonian dipnoan *Chirodipterus*. *Philosophical Transactions of the Royal Society of London* 317B: 329-363.

Toombs, H. A. 1948. The use of acetic acid in the development of vertebrate fossils. *Museums Journal* 48: 54-55.

Trinajstic, K., Boisvert, C., Long, J., Masimenko, A. and Johanson, Z. 2014. Pelvic and reproductive structures in placoderms (stem gnathostomes). Biological Reviews DOI: 10.1111/brv.12118. 35 pp.

Trinajstic, K., Marshall, C., Long, J.A.and Bifield, K. 2007. Exceptional preservation of nerve and muscle tissues in Late Devonian placoderm fish and their evolutionary implications. *Biology Letters* 3: 197-200.

Winkler, K. and Withrow, J.J. 2013. Natural history: small collections make a big impact. Nature 493. doi:10.1038/493480b (published online 23 Jan, 2013).

Supplementary Appendix 1.

Gogo Fossil publications (palaeontology only, papers primarily concerned with palaeontology or fossil preservation/ diagenesis, not primarily geology or background information). Includes page numbers, impact factors, and citations. Impact factors (IF) based on 2013 scores rounded up or down to nearest full number (eg 2.34=2, 2.56 =3), journals with no recorded impact factor or those lower than 1 are here allocated an arbitrary score of '1'; citations from google scholar (cn, as of Nov 20-21, 2014). Incudes primary references on Gogo fossils, major review papers on Gogo fossils, plus peer-reviewed papers illustrating Gogo specimens to assist with morphological interpretation of other materials. Only publications which have citation and or impact factor metrics are recorded.

VERY HIGH IMPACT PAPERS (IF>30)
(full references cited below).

1. Rolfe1966 (Nature)
2. Ahlberg 1989 (Nature)
3. Smith & Johanson 2003 (Science)
4. Long 2006 (Nature)
5. Long et al 2008 (Nature)
6. Long et al 2009 (Nature)
7. Ahlberg et al 2009 (Nature)
8. Rucklin et al 2012 (Nature)
9. Trinajstic et al 2013 (Science)
10. Long et al 2014 (Nature)

TOTAL Impact factor points added as scored by system defined above= 611.

TOTAL pages published (peer-reviewed papers only) –c (less popular books) = 4389pp.

*Including popular books featuring a lot of Gogo material: Rise of Fishes 2nd ed. 288pp, Dawn of the Deed, 278pp. Rise of Fishes 1 (188pp), Swimming in Stone (320pp) = 4384 plus 1074 = 5458 pp.

TOTAL citations, google scholar = 4009 citations.

Gogo Site h factor =33

Papers with citations=>32

1. Andrews et al 2006 (cn=34); 2. Campbell Barwick 1983 (cn=41); 3. Campbell, Barwick 1987 (cn=87); 4. Campbell, Barwick 1988b (cn=37); 5. Dennis Miles 1979a (cn=36); 6. Dennis Miles 1981 (cn=43); 7. Dennis-Bryan 1987 (cn=64); 8. Druce 1976 (cn=77); 9. Gardiner 1973 (cn=57); 10. Gardiner 1984 (cn=250); 11. Gardiner & Bartram 19977 (cn=39); 12. Glenister 1958 (cn=51); 13. Glenister, Klapper 1966 (cn=124); 14. Long 1995 (cn= 121); 15. Long 1997 (cn=36); 16. Long et al. 1997 (cn=64); 17. Long et al 2009 (cn=40); 18. Long et al. 2008 (cn=52); 19. Long et al. 2006 (cn=66); 20. Marshall et al.1986 (cn=39); 21. Miles 1971 (cn=80); 22. Miles 1977 (cn=188); 23. Miles Dennis 1979 (cn=45); 24. Miles & Young 1977 (cn=55); 25. Nazarov et al. 1982 (cn=48); 26. Nicoll 1977 (cn=42); 27. Rosen et al.1981 (cn=392); 28. Smith 1977(cn=48); 29. Smith 1979 (cn=48); 30. Young 1984 (cn=43); 31. Young 1986- 94; 32. Sanchez et al 2012 -33; 33. Trinajstic et al 2007- 34

BIBLIOGRAPHY OF GOGO FOSSIL PAPERS

Not inclusive of primarily geological papers. As mentioned above, the list below contains primary references on Gogo fossils, major review papers on Gogo fossils, plus peer-reviewed papers illustrating Gogo specimens to assist with morphological interpretation of other materials.

Ahlberg PE. 1989. Fossil fishes from Gogo. *Nature* 337, 511-512. (IF=42, cn=6, pp=3).

Ahlberg PE, Smith MM, Johanson Z. 2006. Developmental plasticity and disparity in early dipnoan (lungfish) dentitions. *Evol. Devel.* 8:331-349 (IF= 3, cn=32, pp=19)

Ahlberg PE, Trinajstic K, Johnason Z, Long, JA. 2009. Pelvic claspers confirm chondrichthyan-like internal fertilisation in arthrodires. *Nature* 459: 888-889 (IF =42; cn=21, pp=2).

Anderson P. 2008. Shape variation between arthrodire morphotypes indicates possible feeding niches. *J. Vert. Paleontol.* 28:961-969 (IF=2, cn=8, pp=9).

Andrews SM, Long J, Ahlberg P, Barwick R, Campbell K. 2006. The structure of the sarcopterygian *Onychodus jandemarrai* n.sp. from Gogo, Western Australia: with a functional interpretation of the skeleton. *Trans. R. Soc. Edinb. (Earth Sci.)* 96: 197-307 (IF=1; cn=34, pp=110).

Barwick R, Campbell KSW. 1996. A Late Devonian dipnoan, *Pillararhynchus,* from Gogo, Western Australia, and its relationships. *Palaeontograph.* 239A: 1-42 (IF=1, cn=18, pp=42). Cn= 129

Briggs DEG, Rolfe I. 1983. New Concavicarida (new order:?Crustacea) from the Upper Devonian of Gogo, Western Australia, and the palaeoecology and affinities of the group. *Spec. Pap. Palaeont.* 30: 249-276 (IF=2; cn=26, pp=28).

Brunton CHC, Miles RS, Rolfe WDI. 1969. Gogo Expedition 1967. *Proc. Geol. Soc. Lond.* 1655: 79-83 (IF=1, cn=1, pp =5).

Burrow, C. J., Trinajstic, K. & Long, J.A. 2012. First acanthodian from the Upper Devonian (Frasnian) Gogo Formation of Western Australia. *Historical Biology,* ifirsDOI:10.1080/08912963.2012.660150, 1-9. (IF=1, cn=2, pp=9)

Campbell KSW. 1981. Lungfishes - alive and extinct. *Field Mus. Nat. Hist. Bull.* Sept. 1981: 3-5. (no IF, cn=5, pp=2).

Campbell KSW, Barwick RE. 1982. The neurocranium of the primitive dipnoan *Dipnorhynchus sussmilchi* (Etheridge). *J. Vert. Paleontol.* 2: 286-327 (IF=2, cn=30, pp=32).

Campbell KSW, Barwick RE. 1983. Early evolution of dipnoan dentitions and a new species *Speonesydrion. Mems. Ass. Australas. Palaeontols* 1: 17-49 (IF=2, cn=41, pp=33). 230

Campbell KSW, Barwick RE. 1984a. The choana, maxillae, premaxillae and anterior bones of early dipnoans. *Proc. Linn. Soc. N.S.W.* 107: 147-170 (IF=1, cn=25, pp=24).

Campbell KSW, Barwick RE. 1987. Palaeozoic lungfishes - a review. *J. Morph. Suppl.* 1: 93-131. (IF=2, cn=87, pp=38).

Campbell KSW, Barwick RE. 1988a. Geological and palaeontological information and phylogenetic hypotheses. *Geol. Mag.* 125: 207-227 (IF=2, cn=27, pp=20).

Campbell KSW, Barwick RE. 1988b. *Uranolophus:* a reappraisal of a primitive dipnoan. *Mems. Ass. Australas. Palaeontols* 7: 87-144 (IF=1, cn=37, pp=61).

Campbell KSW, Barwick RE. 1990. Palaeozoic dipnoan phylogeny: functional complexes and evolution without parsimony. *Paleobiol.* 16: 143-169 (IF=3. cn=55, pp=27).

Campbell KSW, Barwick RE. 1991. Teeth and tooth plates in primitive lungfish and a new species of *Holodipterus*. In *Early vertebrates and related problems of evolutionary biology,* ed. MM Chang, Liu, YH, Zhang GR, pp. 429-440. Beijing: Science Press. (no IF; cn=15, pp=12).

Campbell KSW, Barwick RE. 1995. The primitive dipnoan dental plate. *J. Vert. Palaeontol.* 15: 13-27 (IF=2, cn=14, pp=14).

Campbell KSW, Barwick RE. 1998. A new tooth-plated dipnoan from the Upper Devonian Gogo Formation and its relationships. *Mems. Queensl. Mus.* 42: 403-437 (no IF, cn=23, pp=33). 513

Campbell KSW, Barwick RE. 1999. Dipnoan fishes from the Late Devonian Gogo Formation of Western Australia. *Recs. West. Aust. Mus., Suppl.* 57: 107- 138 (IF=1, cn=18, pp=32).

Campbell KSW, Barwick RE. 2002. The axial postcranial structure of *Griphognathus whitei* from Gogo; comparisons with other Devonian dipnoans. *Recs. West. Aust. Mus.* 21:167-201 (IF=1, cn=6, pp=35

Campbell, K. S. W. & Barwick, R. E. 2006. Morphological innovation through gene regulation: an example from Devonian Onychodontiform fish. *International Journal of Developmental Biology* 50: 371-375 (IF=3, cn =9, pp=5).

Campbell KSW, Barwick RE, JL den Blaauwen. 2006. Structure and function of the shoulder girdle in dipnoans: new material from *Dipterus valenciennesi. Senckenberg. Leth.* 86:77–91 (IF=1, cn=4, pp=15).

Campbell KSW, Smith MM. 1987. The Devonian dipnoan *Holodipterus:* dental variation and remodelling growth mechanisms. *Recs. Aust. Mus.* 38: 131-67 (IF=1; cn=20, pp=37).

Cheng H. 1989. On the tubuli in Devonian lungfishes. *Alcheringa* 13: 153-166 (IF=1; cn=6, pp=14).

Choo, B. 2011. Revision of the actinopterygian genus *Mimipiscis* (=*Mimia*) from the Upper Devonian Gogo Formation of Western Australia and the interrelationships of the early Actinopterygii. *Earth and Environmental Science Transactions of the Royal Society of Edinburgh* 102: 1-28 (IF=1, cn=10, pp=28).

Choo, B. 2015., A new species of the Devonian actinopterygian *Moythomasia* from Bergisch-Gladbach, Germany and fresh observations on *M. durgaringa* from the Gogo Formation of Western Australia. *Journal of Vertebrate Paleontology.*35: 1-20 (IF=2.0, cn =0, pp=20)

Choo B, Long J, Trinajstic K. 2009. A new genus and species of basal actinopterygian fish from the Upper Devonian Gogo Formation of Western Australia *Act. Zool.* 90: 194-210 (IF=1; cn=12, pp=17). 592

Clement, A., Long, J.A. 2010. *Xeradipterus hatcheri*, a new dipnoan from the late Devonian (Frasnian) Gogo Formation, Western Australia, and other new holodontid material. *Journal of Vertebrate Paleontology* 30: 681-695. (IF=2, cn=2, pp=15).

Clement, A. 2012. A new species of long-snouted lungfish from the Late Devonian of Australia, and its functional and biogeographical implications. Palaeontology 55, 51-71 (IF=2, cn=0, pp=20).

Clement, A. & Long, J.A. 2010. Air-breathing adaptation in a marine Devonian lungfish. *Biology Letters* 6:509-512 (IF=3, cn=15, pp=4).

Dennis KD, Miles RS. 1979a. A second eubrachythoracid arthrodire from Gogo, Western Australia. *Zool. J. Linn. Soc.* 67: 1-29 (IF=3, cn=36, pp=29).

Dennis KD, Miles RS. 1979b. Eubrachythoracid arthrodires with tubular rostral plates from Gogo, Western Australia. *Zool. J. Linn. Soc.* 67: 297-328 (IF=3, cn=29, pp=32).

Dennis KD, Miles RS. 1980. New durophagous arthrodires from Gogo, Western Australia. *Zool. J. Linn. Soc.* 69: 43-85 (IF=3; cn=28, pp=43).

Dennis KD, Miles RS 1981. A pachyosteomorph arthrodire from Gogo, Western Australia. *Zool. J. Linn. Soc.* 73: 213-258 (IF=3, cn=43, pp=46).

Dennis KD, Miles RS. 1982. A eubrachythoracid arthrodire with a snub-nose from Gogo, Western Australia. *Zool. J. Linn. Soc.* 75: 153-166 (I IF=3, cn=15, pp=14).

Dennis-Bryan K. 1987. A new species of eastmanosteid arthrodire (Pisces: Placodermi) from Gogo, Western Australia *Zool. J. Linn. Soc. Society* 90: 1-64 (IF=3, cn=40, cn=64, pp=64).

Dennis-Bryan, K. Miles RS. 1983. Further eubrachythoracid arthrodires from Gogo, Western Australia. *Zool. J. Linn. Soc.* 77: 145-173 (IF=3, cn=23, pp=28). 947

Druce EC. 1976. Conodont biostratigraphy of the Upper Devonian reef complexes of the canning basin, Western Australia. *Bur. Min. Res. Aust. Bull.* 158: 1-303 (no IF, cn=77, pp=303). 1024

Forey PL, Gardiner BG.1986. Observations on *Ctenurella* (Ptyctodontida) and the classification of placoderm fishes. *Zool. J. Linn. Soc.* 86: 43-74 (IF=3, cn=29, cn=26, pp=34).

Freidman M. 2007a. The interrelationships of Devonian lungfishes (Sarcopterygii; Dipnoi) as inferred from neurocranial evidence and new data from the genus *Soederberghia* Lehman 1959. *Zool. J. Linn. Soc.* 151:115–171 (IF=3, cn=26, pp= 56).

Friedman M. 2007c. Cranial structure in the Devonian lungfish *Soederberghia groenlandica* and its implications for the interrelationships of 'rhynchodipterids". *Trans. R. Soc. Edinb. (Earth Sci.)* 98: 179-198 (IF=1, cn=4, pp=20).

Gardiner BG. 1973. Interrelationships of teleostomes. In *Interrelationships of Fishes*, ed. PH Greenwood, RS Miles, C Patterson. *Zool. J. Linn. Soc.* 52 (supplement): 105-135 (IF=3, cn=57, pp=31).

Gardiner BG. 1984. Relationships of the palaeoniscoid fishes, a review based on new specimens of *Mimia* and *Moythomasia* from the Upper Devonian of Western Australia. *Bull. Brit. Mus.. Nat. Hist. (Geol.)* 37: 173-428 (no IF, cn=250, pp=256).

Gardiner BG, Bartram AWH.1977. The homologies of ventral cranial fissures in osteichthyans. In *Problems in early vertebrate evolution* ed. SM Andrews, RS Miles, AD Walker, pp. 227-245. London: Academic Press (no IF, cn=39, pp=19).

Gardiner BG, Miles RS. 1975. Devonian fishes of the Gogo Formation, Western Australia. *Coll. internat. C.N.R.S.* 218: 73-79 (no IF, cn=25, pp=7). 1454

Gardiner BG, Miles RS. 1990. A new genus of eubrachythoracid arthrodire from Gogo,Western Australia. *Zool. J. Linn. Soc* 99: 159-204 (IF=3, cn=27, pp=46).

Gardiner BG, Miles RS. 1994. Eubrachythoracid arthrodires from Gogo, Western Australia. *Zool. J. Linn. Soc.*112: 443-477 (IF=3, cn=24, pp=35).

Glenister BF. 1958. Upper Devonian ammonoids from the *Manticoceras* zone. Fitzroy Basin, Western Australia. *J. Paleont* 32: 58-96 (IF=1, cn=51, pp=39).

Glenister BF, Klapper G. 1966. Upper Devonian conodonts from the Canning Basin, Western Australia. J. Paleont. 40: 777-842 (IF=1, cn=124, pp=66). 1680

Grey K. 1992. Miospore assemblages from the Devonian reef complexes, Canning Basin, Western Australia. *Geol. Surv. West. Aust. Bull.* 140: 1-139 (no IF, cn=15, pp=139).

Holland, T. 2014. The endocranial anatomy of Gogonasus andrewsae Long 195 revaled through micro-CT scanning. *Earth and Environmental Science Transactions of the Royal Society of Edinburgh* 105, 9-34 (IF=1, cn=0, pp=25)

Holland T, Long .A. 2009. On the phylogenetic position of *Gogonasus andrewsae* Long 1985, within the Tetrapodamorpha. *Acta Zool.* 90: 285-296 (IF=1, cn=7, pp=12). 1702

Johanson Z. 2003. Placoderm branchial and hypobranchial muscles and origins in jawed vertebrates. *J. Vert. Paleont.* 23: 735-749 (IF=2, cn=20, pp=15).

Johanson, Z, Trinasjtic, K. 2014. Fosisl ontogenies: the contribution of placoderm ontogeny to our understanding of the evlution of eraly gnathostomes. Palaeontology 57: 505-516. (IF=2, cn=0, pp=12).

Long JA. 1985b. A new osteolepidid fish from the Upper Devonian Gogo Formation, Western Australia. *Rec. West. Aust. Mus.* 12: 361-367 (IF= 1, cn=18, pp=7).

Long JA. 1987b. Late Devonian fishes from the Gogo Formation, Western Australia, new discoveries. *Search* 18: 203-205 (no IF, cn=4, pp=3) 1744

Long JA. 1988a. New information on the Late Devonian arthrodire *Tubonasus* from Gogo, Western Australia. *Mems. Ass. Australas. Palaeontols.* 7:81-85 (IF=1, cn=5, pp=5). 1749

Long JA. 1988b. A new camuropiscid arthrodire (Pisces: Placodermi) from Gogo, Western Australia. *Zool. J. Linn. Soc.* 94: 233-258 (IF=3; cn=16, pp=26).

Long JA. 1988c. Late Devonian fishes from the Gogo Formation, Western Australia. *Nat. Geog. Res.* 4: 436-450 (no IF; cn=24, pp=15). 1789

Long JA. 1988d. The extraordinary fishes of Gogo. *New Scientist* 1639: 41-45 (IF=1; cn=4, pp=5).

Long JA. 1988e. 360 million-year-old Gogo fishes. *Geo, Austral. Geograph. Mag.* 11 (3):102-113 (no IF, cn=0, pp=12).

Long JA. 1990b. Two new arthrodires (placoderm fishes) from the Upper Devonian Gogo Formation, Western Australia. *Mems. Qld. Mus.* 28: 51-63 (IF=1, cn=9, pp=13).

Long JA. 1991. Arthrodire predation by *Onychodus* (Pisces, Crossopterygii) from the Late Devonian Gogo Formation, Western Australia. *Rec. West. Aust. Mus.* 15: 479-482 (IF=1, cn=6, pp=4).

Long JA. 1992a. *Gogodipterus paddyensis* gen. nov., a new chirodipterid lungfish from the Late Devonian Gogo Formation, Western Australia. *The Beagle, N.T. Mus.* 9: 11-20 (no IF, cn=12, pp=10). 1820

Long JA. 1994. A second incisoscutid arthrodire from Gogo, Western Australia. *Alcheringa* 18: 59-69 (IF=1, cn=7, pp=11).

Long JA. 1995. A new plourdosteid arthrodire from the Upper Devonian Gogo Formation of Western Australia. *Palaeontology* 38: 39-62 (IF=2, cn=20, pp=33). 1847

Long JA. 1995. *The Rise of Fishes-500 million years of evolution.* Baltimore: Johns Hopkins University Press. 188pp (no IF, cn =121, pp=188).

Long JA. 1997. Ptyctodontid fishes from the Late Devonian Gogo Formation, Western Australia, with a revision of the European genus *Ctenurella* Ørvig 1960. *Geodiversitas* 19: 515-555 (IF =1, cn=36, pp=41).

Long JA. 2001. On the relationships of *Onychodus* and *Psarolepis. J. Vert. Paleontol.* 21: 815-820 (IF=2, cn=23, pp=6).

Long JA. 2006. *Swimming in Stone –The amazing Gogo fossils of the Kimberley.* Perth: Fremantle Press. 320pp (no IF, cn=16, p=320).

Long JA. 2010.Holodontid lungfishes from the Late Devonian Gogo Formation of Western Australia. In *Fossil fishes and related Biota: Morphology, Phylogeny and Paleobiogeography –In honour of Chang Meeman*, ed.Yu X, Maisey J, Miao D. Berlin:Verlag Pfeil, pp. 277-299. (no IF, cn=3, pp=23)

Long JA, Barwick RE, Campbell KSW. 1997. Osteology and functional morphology of the osteolepiform fish, *Gogonasus andrewsae* Long, 1985, from the Upper Devonian Gogo Formation, Western Australia. *Rec. West. Aust. Mus. Suppl.* 53: 1-90 (IF=1, cn=64, pp=90).

Long JA, Trinajstic KM. 2000. Devonian microvertebrate faunas from Western Australia. *Courier-Forsch. Senckenberg* 223: 471-486 (IF=1, cn=14, pp=15).

Long, J.A. & Trinajstic, K. 2010. The Late Devonian Gogo Formation Lägerstatte –Exceptional preservation and Diversity in early Vertebrates. *Annual Reviews of Earth and Planetary Sciences* 38: 665-680 (IF=9, cn =31, pp=26). 2356

Long JA, Trinajstic KM, Johanson Z. 2009. Devonian arthrodire embryos and the origin of internal fertilization in vertebrates. *Nature* 457:1124-1127 (IF=42, cn=40, pp=4 +SI).

Long JA, Trinajstic KM, Young GC, Senden T. 2008. Live birth in the Devonian period. *Nature* 453: 650-652 (IF=42, cn=52, pp=3 +SI).

Long JA, Young GC, Holland T, Senden T, Fitzgerald EMG. 2006. An exceptional Devonian fish shed slight on tetrapod evolution. *Nature* 444: 199-202 (IF=42, cn=66, pp=4 + SI).

Marshall CR. 1986. Lungfish: Phylogeny and Parsimony. *J. Morph. Suppl.* 1:151-162 (IF=2, cn= 39, pp=12). 2553

McNamara KJ, Long JA, Brimmell K. 1991. Catalogue of type fossils in the Western Australian Museum. *Recs. West. Aust. Mus. Suppl.* 39: 1-106 (IF=1, cn=0, pp=106).

Melendez, I., Grice, K., Trinajstict, K., Ladjavardi, M., Greenwood, P. & Thompson, K. 2013. Biomarkers reveal the role of photic zone euxinia in exceptional fossil ptreservation: an organic geochemical perspective. *Geology* 41: 123-126 (IF=5, cn=12, pp=4).

Miles RS. 1971. The Holonematidae (placoderm fishes): a review based on new specimens of *Holonema* from the Upper Devonian of Western Australia. *Phil. Trans. R. Soc. Lond.* 263B: 101-234 (IF= 3, cn=80, pp=133).

Miles RS. 1977. Dipnoan (lungfish) skulls from the Upper Devonian of Western Australia. *Zool. J.. Linn. Soc.* 61: 1-328 (IF=3, cn=188, pp=328).

Miles RS, Dennis K. 1979. A primitive eubrachythoracid arthrodire from Gogo, Western Australia. *Zool. J. Linn. Soc* 66: 31-62 (IF=3 cn=45, pp=32).

Miles RS, Young GC. 1977. Placoderm interrelationships reconsidered in the light of new ptyctodontids from Gogo Western Australia. *Linn. Soc. Symp. Ser.* 4: 123-198 (IF=3, cn=55, pp=7748

Nazarov BB, Cockbain AE, Playford PE. 1982. Late Devonian Radiolaria from the Gogo Formation, canning basin, Western Australia. *Alcheringa* 6: 161-174 (IF=1, cn=40, pp=14). 2973

Nazarov BB, Ormiston AR. 1984. Upper Devonian (Frasnian) radiolarian fauna from the Gogo Formation, Western Australia. *Micropal.* 29: 454-466 (IF=1, cn=48, pp=13).

Nicoll RS. 1977. Conodont apparatuses in Upper Devonian palaeoniscoid fish from the Canning basin, Western Australia. *Bur. Min. Res. J. Aust. Geol. Geophys.* 2: 217-228 (no IF, cn=42, pp=12).

Pridmore PA, Barwick RE. 1993. Post-cranial morphologies of the Late Devonian dipnoans *Griphognathus* and *Chirodipterus* and locomotor implications. *Mems. Australas. Ass. Palaeontols.* 15: 161-182 (IF=1, cn=15, pp=21). 3078

Pridmore P A, Campbell KSW, Barwick RE. 1994. Morphology and phylogenetic position of the holodipteran dipnoans of the Upper Devonian Gogo Formation of northeastern Australia. *Phil. Trans. R. Soc. Lond. B.* 344: 105-164 (IF=3, cn=18, pp=60).

Rolfe, WDI. 1966. Phyllocarid crustaceans of European aspect from the Devonian of Western Australia. *Nature* 209: 192 (IF=42, cn=12, pp=1).

Rolfe, WDI 1995. Form and function in Thylacocpehala, Conchyliocarida and Concavicarida (?Crustacea): aproblem of interpretation. *Trans. Royal Society of Edinburgh* 76: 391-399. (IF =1, cn=19, pp=9).

Rosen DE, Forey PL, Gardiner BG, Patterson C. 1981. Lungfishes, tetrapods, palaeontology and plesiomorphy. *Bull. Amer. Mus.. Nat. Hist.* 167: 159-276 (IF =1, cn=392, pp=117). 3519

Rucklin, M., Donoghue, P.C.J., Trinajstic, K., Marone, F. & Stampanoni. M. 2012. Development of teeth and jaws in the the earliest jawed vertebrates. *Nature* 491: 888-892. (IF=42, cn=21, pp=5).

Sanchez, S., Ahlberg, P.E., Trinasjtic, K.M., Mirone, A., Tafforeau, P. 2012. Three-dimesnional synchrotron virtual paleohistology: a new insight into the world of fossil bone microstructures. *Microscopy and Microanalysis* 18: 1095-1105. (IF=2, cn=33, pp=11). 3573

Smith MM. 1977. The microstructure of the dentition and dermal ornament of three dipnoans from the Devonian of Western Australia: a contribution towards dipnoan interrelations, and morphogenesis, growth and adaptation of the skeletal tissues. *Phil. Trans. R. Soc. Lond. B* 281: 29-72 (IF =3, cn=48, pp=43).

Smith MM.1979. SEM of the enamel layer in oral teeth of fossil and extant crossopterygian and dipnoan fishes. *Scan. Elec. Micros.* 2: 483-90 (IF=3, cn=48, pp=8).

Smith MM. 1984. Petrodentine in extant and fossil dipnoan dentitions: microstructure, histogenesis and growth. *Proc. Linn. Soc. N.S.W.* 107: 367-407 (IF=1, cn=33, pp=40).

Smith MM, Campbell KSW. 1987. Comparative morphology, histology and growth of dental plates of the Devonian dipnoan *Chirodipterus*. *Phil. Trans. R. Soc. Lond. B* 317: 329-363 (IF=3; cn=27, pp=34).

Tetlie OE, Braddy SJ, Butler PD, Briggs DE. 2004. A new eurypterid (Chelicerata: Eurypterida) from the Upper Devonian Gogo Formation of Western Australia, with a review of the Rhenopteridae. *Palaeontology* 47: 801-809 (IF=2, cn=20, pp=9). 3701

Trinajstic K. 1995. The role of heterochrony in the evolution of the eubrachythoracid arthrodires with special reference to *Compagospiscis croucheri* and *Incisoscutum ritchiei* from the Late Devonian Gogo Formation, Western Australia. *Geobios, Mem. Spec.* 19: 125-128 (IF=1, cn=4, pp=4).

Trinajstic K. 1999. New anatomical information on *Holonema* (Placodermi) based on material from the Frasnian Gogo Formation and the Givetian-Frasnian Gneudna Formation, Western Australia. *Geodiversitas* 21: 69-84 (IF=1; cn=4, pp=16).

Trinajstic K. 1999b. Scales of palaeoniscoid fishes (Osteichthyes: Actinopterygii) from the Late Devonian of Western Australia. *Rec. West. Aust. Mus. Suppl.* 57: 93-106 (IF=1, cn=7, pp=14).

Trinajstic K. 1999c. Scale morphology of the Late Devonian palaeoniscoid *Moythomasia durgaringa* Gardiner and Bartram 1977. *Alcheringa* 23: 9-19 (IF=1, cn=13, pp=11).

Trinajstic, K., Boisvert, C., Long, J., Masimenko, A. Johanson, Z. 2014. Pelvic and reproductive structures in placoderms (stem gnathostomes). Biological reviews DOI: 10.1111/brv.12118. (If=10, cn=2, pp=35)

Trinajstic K, Dennis-Bryan K. 2009. Phenotypic plasticity, polymorphism and phylogeny within placoderms. *Acta Zoologica*. 90: 83-102 (IF=1; cn=10, pp=20).

Trinajstic KM, George AD. 2009. Microvertebrate biostratigraphy of Upper Devonian (Frasnian) carbonate rocks in the Canning and Carnarvon Basins of Western Australia. *Palaeontology* 52: 642-659 (IF=2; cn=7, pp=17).

Trinajstic K, Hazelton M. 2007. Ontogeny, phenotypic variation and phylogenetic implications of arthrodires from the Gogo Formation, Western Australia. *J. Vert. Paleontol.*27: 571-583 (IF=2; cn=11, pp=13). 3759

Trinajstic K, Long JA. 2009. A new genus and species of Ptyctodont (Placodermi) from the Late Devonian Gneudna Formation, Western Australia, and an analysis of ptyctodont phylogeny *Geol. Mag.* 146: 743-760 (IF=2; cn=4, pp=18).

Trinajstic K, Marshall C, Long JA, Bifield,, K. 2007. Exceptional preservation of nerve and muscle tissues in Late Devonian placoderm fish and their evolutionary implications. *Biol. Lett.* 3: 197-200 (IF=3; cn=34, pp=14)

Trinajstic K, McNamara KJ. 1999. Heterochrony in the Late Devonian arthrodiran fishes *Compagopiscis* and *Incisoscutum. Rec. West. Aust. Mus. Suppl.* 57: 77-92 (IF=1, cn=8, pp=15). 3805

Trinajstic, K., Sanchez, S., Dupret, V., Tafforeau, P..Long, J., Young, G., Senden, T., Boisvert, C., Power, N. & Ahlberg, P.E. 2013. Fossil musculature of the most primitive jawed vertebrates. *Science* 341: 160-164 (IF=31, cn=5, pp=5).

Young GC. 1984c. Reconstruction of the jaws and braincase in the Devonian placoderm fish *Bothriolepis*. *Palaeontology* 27: 625-661 (IF=2; cn=43, pp=38).

Young GC. 1986b. The relationships of placoderm fishes. *Zool. J. Linn. Soc.* 88: 1-57 (IF=3, cn=.94, pp=57). 3942

Young GC, Barwick RE, Campbell KSW. 1990. Pelvic girdles of lungfishes (Dipnoi). In *Pathways in Geology*- Essays in honour of E.S. Hills, ed. RW Le Maitre, pp.59-75. Melbourne: Blackwell Press. (Book Chapter, no IF, cn=8, pp=17

PART B: POPULAR PUBLICATIONS CITING GOGO FISHES

Long, J.A. 2004. *Gogo Fish! The story of the Western Australian State fossil emblem.* The Western Australian Museum, Perth. 48pp.

Long, J.A. 2011. *Hung Like an Argentine Duck-the prehistoric origins of intimate sex.* Sydney: Fourth Estate, Harper Collins. 278pp.

Long, J.A. 2011. *The Rise of Fishes -500 Million years of Evolution*. 2nd ed. Johns Hopkins University Press, Baltimore, and University of New South Wales Press, UNSW, +288pp.

Long, J.A. 2012. *The Dawn of the Deed –The Prehistoric Origins of Sex.* Chicago: University of Chicago Press. 288pp.

Long, J.A. 2014.The Fossil Files –The placoderm renaissance *Australasian Science*, 35(7): p.42

Long, J.A., Trinajstic, K. 2014. The first vertebrate sexual organs evolved as an extra piar of legs. The Conversation, https://theconversation.com/the-first-vertebrate-sexual-organs-evolved-as-an-extra-pair-of-legs-27578

Trinajstic, K. 2013. From bone to brawn: ancient fish show off their muscles. The Conversation, https://theconversation.com/from-bone-to-brawn-ancient-fish-show-off-their-muscles-15098.

Memoirs of Museum Victoria 74: 17–28 (2016) Published 2016

ISSN 1447-2546 (Print) 1447-2554 (On-line)
http://museumvictoria.com.au/about/books-and-journals/journals/memoirs-of-museum-victoria/

Cretaceous marine amniotes of Australia: perspectives on a decade of new research

Benjamin P. Kear

Museum of Evolution, Uppsala University, Norbyvägen 18, SE-752 36 Uppsala, Sweden (banjamin.kear@em.uu.se)

Abstract

Kear, B.P. 2016. Cretaceous marine amniotes of Australia: perspectives on a decade of new research. *Memoirs of Museum Victoria* 74: 17–28.

Cretaceous marine amniote fossils have been documented from Australia for more than 150 years, however, their global significance has only come to the fore in the last decade. This recognition is a product of accelerated research coupled with spectacular new discoveries from the Aptian–Albian epeiric sequences of the Eromanga Basin – especially the opal-bearing deposits of South Australia and vast *lagerstätten* exposures of central-northern Queensland. Novel fragmentary records have also surfaced in Cenomanian and Maastrichtian strata from Western Australia. The most notable advances include a proliferation of plesiosaurian taxa, as well as detailed characterization of the 'last surviving' ichthyosaurian *Platypterygius*, and some of the stratigraphically oldest protostegid sea turtles based on exceptionally preserved remains. Compositionally, the Australian assemblages provide a unique window into the otherwise poorly known Early Cretaceous marine amniote faunas of Gondwana. Their association with freezing high latitude palaeoenvironments is also extremely unusual, and evinces a climate change coincident diversity turnover incorporating the nascent radiation of lineages that went on to dominate later Mesozoic seas.

Keywords

Plesiosauria, *Platypterygius*, Protostegidae, Mosasauroidea, Aptian-Albian, Cenomanian, Maastrichtian.

Introduction

Although Australia has anecdotal Triassic (Kear, 2004; Kear and Hamilton-Bruce, 2011) and rare Jurassic (Kear, 2012) marine amniote fossil occurrences, virtually all of its currently documented Mesozoic record is Cretaceous in age. The earliest historical publications date from the late 19th century (McCoy, 1867a, 1867b, 1869; Owen, 1882; Etheridge 1888, 1897), with only sporadic reports appearing between 1900–1940 (Etheridge, 1904; Longman, 1915, 1922, 1924, 1930, 1932, 1935, 1943; White, 1935; Teichert and Matheson, 1944), and in the last decades of the 20th Century (Romer and Lewis, 1959; Lundelius and Warne, 1960; Persson, 1960, 1982; McGowan, 1972; Gaffney, 1981; Murray, 1985, 1987; Wade, 1984, 1985, 1990; Molnar, 1991; Thulborn and Turner, 1993; Cruickshank and Long, 1997; Long and Cruickshank, 1998; Cruickshank et al., 1999; Choo, 1999). Kear (2003) provided the first comprehensive overview confirming the presence of elasmosaurid, possible cryptoclidid, polycotylid, rhomaleosaurid, and pliosaurid plesiosaurians, the ubiquitous ophthalmosaurian ichthyosaurian *Platypterygius*, protostegid sea turtles, and enigmatic mosasaurids (fig. 1). Since then, a decade of intensive study has anatomically clarified and phylogenetically redefined many of these taxa, and added a plethora of new discoveries that emphasize the global palaeoecological and palaeobiological significance of the Australian Cretaceous assemblages. This paper provides both an updated summary and bibliography of these finds, with the purpose of stimulating further investigation into this dynamic field of antipodean vertebrate palaeontology over the decade to come.

Institutional abbreviations

AM, Australian Museum, Sydney, Australia; AOD, Australian Age of Dinosaurs Museum, Winton, Australia; NMV, Museum Victoria, Melbourne, Australia; NTM, Northern Territory Museum and Art Gallery, Darwin, Australia; QM, Queensland Museum, Brisbane, Australia; SAM, South Australian Museum, Adelaide, Australia; UWA, University of Western Australia, Perth, Australia; WAM, Western Australian Museum, Perth, Australia.

Plesiosaurians

Australian Cretaceous plesiosaurian fossils are abundant, and in several rock units, exceptionally well preserved. Those from the Aptian opal-bearing strata of the Bulldog Shale at Coober Pedy and Andamooka in South Australia, and Wallumbilla Formation at White Cliffs, as well as the Albian Griman Creek Formation in New South Wales (fig. 2), are perhaps the most unusual because they manifest diagenetic replacement of the bony tissue by opaline hydrated silica. Kear (2005a, 2006a, 2006b) revised the existing specimens and

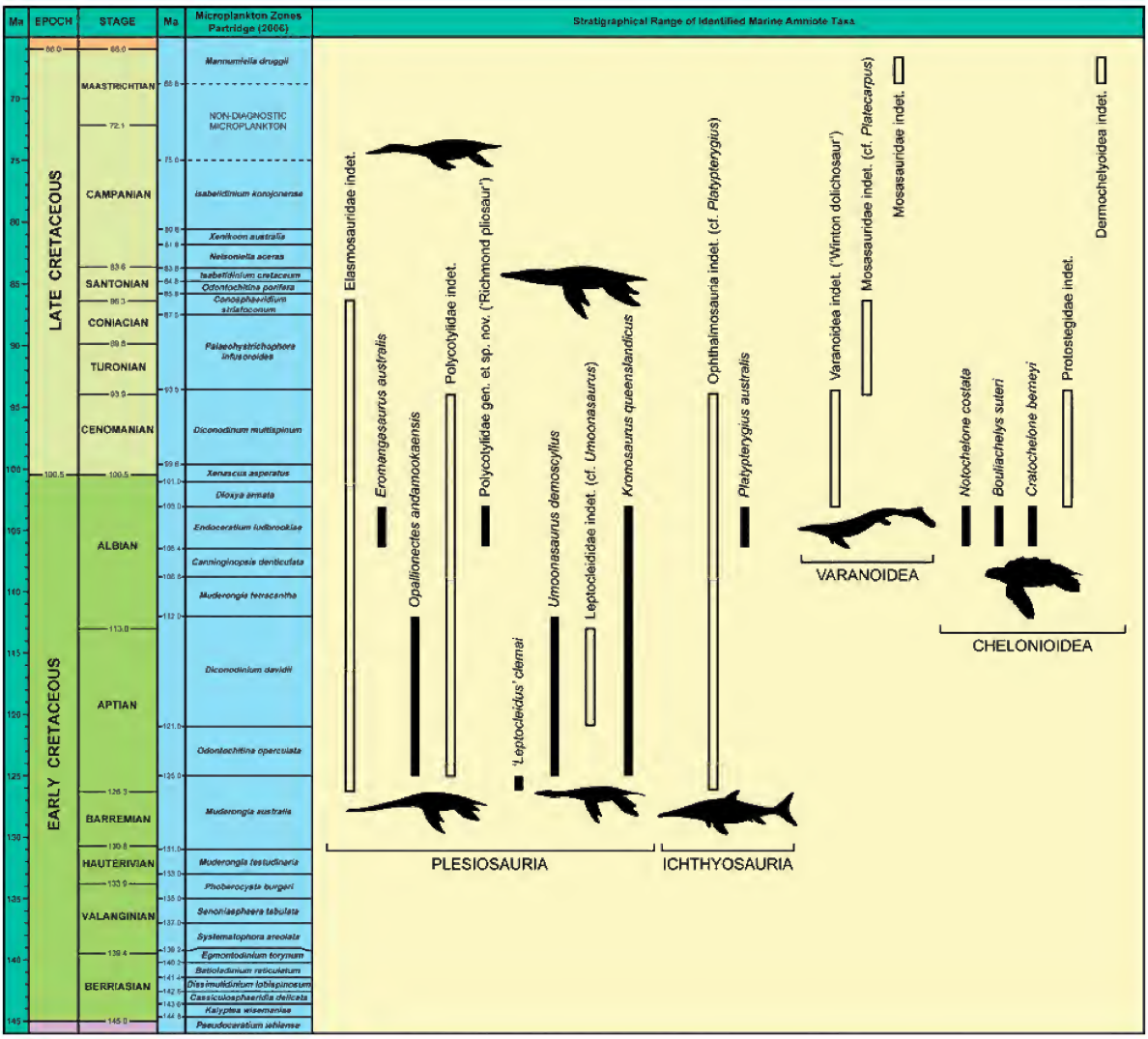

Figure 1. Stratigraphical distribution of Australian Cretaceous marine amniote taxa updated from Kear (2003). Australian standard microplankton (dinoflagellate) zonation is modified from Partridge (2006) to accommodate the emended geological timescale of Gradstein et al. (2012). Taxon ranges indicate named species (black bars) or indeterminate occurrences assigned to higher-level taxa (open bars).

recognized a diversity of taxa. These included indeterminate elasmosaurids, some of which were osteologically immature and of surprisingly small body-size – the most diminutive being less than 2 m in estimated maximum length (AM F9639–F9928: see Kear, 2002a). Their vertebral morphology showed characteristics of other Gondwanan elasmosaurids. For example, the lack of a pronounced ventral notch on the articular faces of the cervical centra (Kear, 2002a, p. 672, fig. 1) is typical of the Early Cretaceous *Callawayasaurus colombiensis* (Welles, 1962) from Colombia, as well as *Eromangasaurus australis* (Sachs, 2005) and the *nomen dubium Woolungasaurus glendowerensis* Persson, 1960 (Sachs, 2004) from Australia. Furthermore, the centrum proportions of these 'juvenile' elasmosaurids (Kear, 2002a, p. 673, table 1) are reminiscent of the austral high-latitude *Aristonectes parvidens* Cabrera, 1941 and *Kaiwhekia katiki* Cruickshank and Fordyce, 2002 (see O'Gorman et al., 2014) from Patagonia-Antarctica and New Zealand respectively. Note, though, that elasmosaurid cervical centrum proportions are intraspecifically variable and of uncertain taxonomic significance (O'Keefe and Hiller, 2006; Sachs et al., 2013).

Kear (2005b, 2007a) and Sachs (2005) reported on cranial material of *E. australis* from the middle–upper Albian Toolebuc Formation near Maxwelton in Queensland (fig. 2).

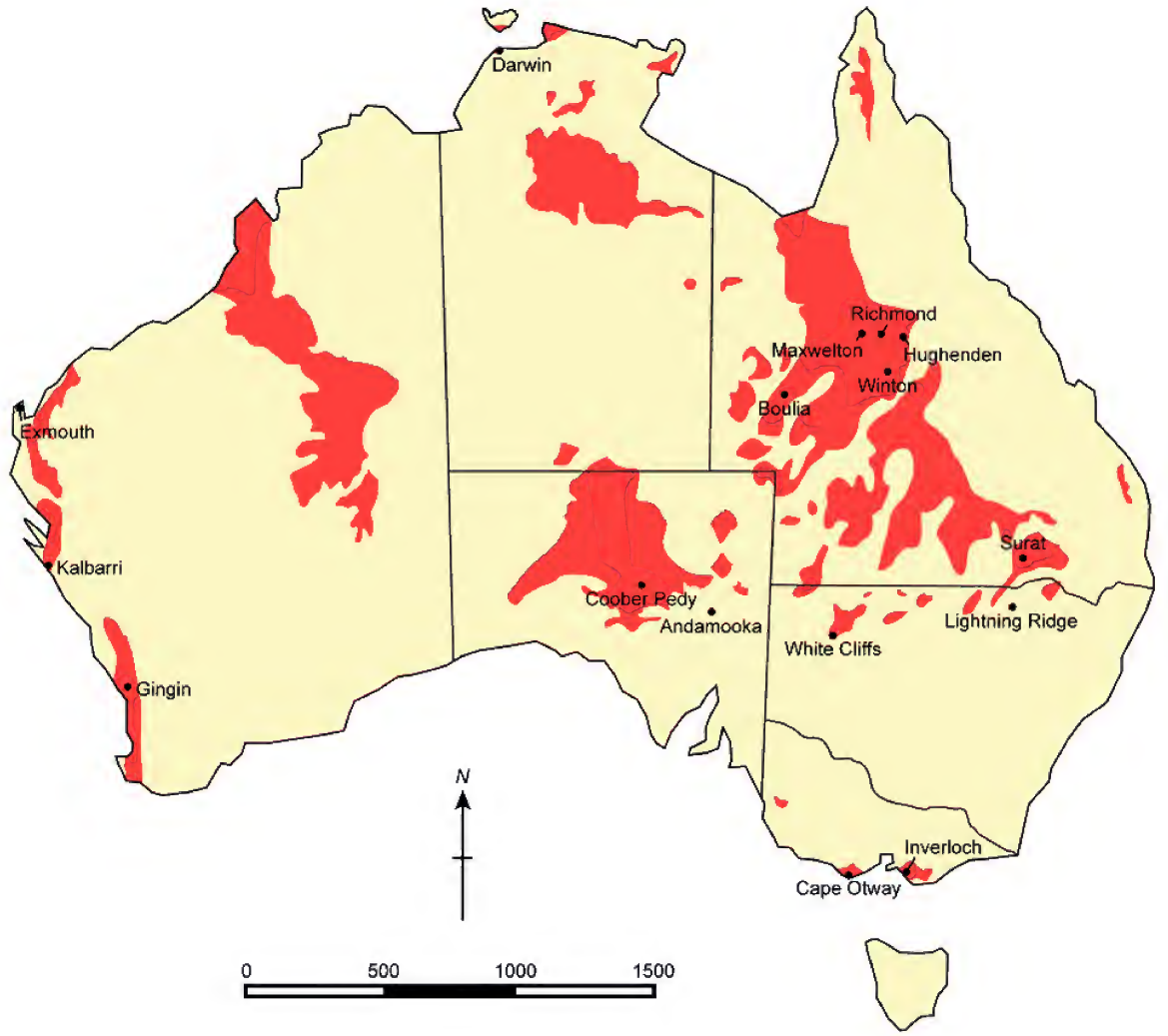

Figure 2. Diagrammatic map of Cretaceous rock outcrops on the Australian continent with state borders and specific locality references for fossil occurrences discussed in the text (developed from Kear and Hamilton-Bruce, 2011).

The Toolebuc Formation and overlying Allaru Mudstone are lagerstätten sequences that have yielded some of the most spectacular Early Cretaceous marine amniote fossils found worldwide. The holotype skull of *E. australis* (QM F11050: Kear, 2005b, p. 794, fig. 2A–C) is a classic example. It bears a series of depression fractures and crushing attributed to a bite from a gigantic predatory pliosauroid (Thulborn and Turner, 1993). Moreover, its phylogenetic character states include circular (non-compressed) tooth cross-sections and the possible presence of a pineal foramen, which suggest a basal position within Elasmosauridae (Benson and Druckenmiller, 2014), although, its topology within this clade is ambiguous (Sachs and Kear, 2015). Several other fragmentary elasmosaurid skulls have also been found in the Toolebuc Formation (e.g. AM F87826: Kear, 2001a), one of which has a well-preserved premaxillary palate exposing the intracranial sinuses (SAM P40510: fig. 3A). A number of articulated elasmosaurid postcranial skeletons await adequate preparation and study. In addition, indeterminate isolated vertebrae occur in the Aptian Birdrong Sandstone (WAM 94.7.6), lower Albian Windalia Radiolarite (WAM 05.2.1), as well as the Cenomanian upper Gearle Siltstone (WAM 15.2.1) in Western Australia. McHenry et al. (2005) reported on a remarkable elasmosaurid specimen (QM F33037) from the Wallumbilla Formation (referred to as the Blackdown or Doncaster Formation in the Walsh Creek region of Queensland) that preserved an

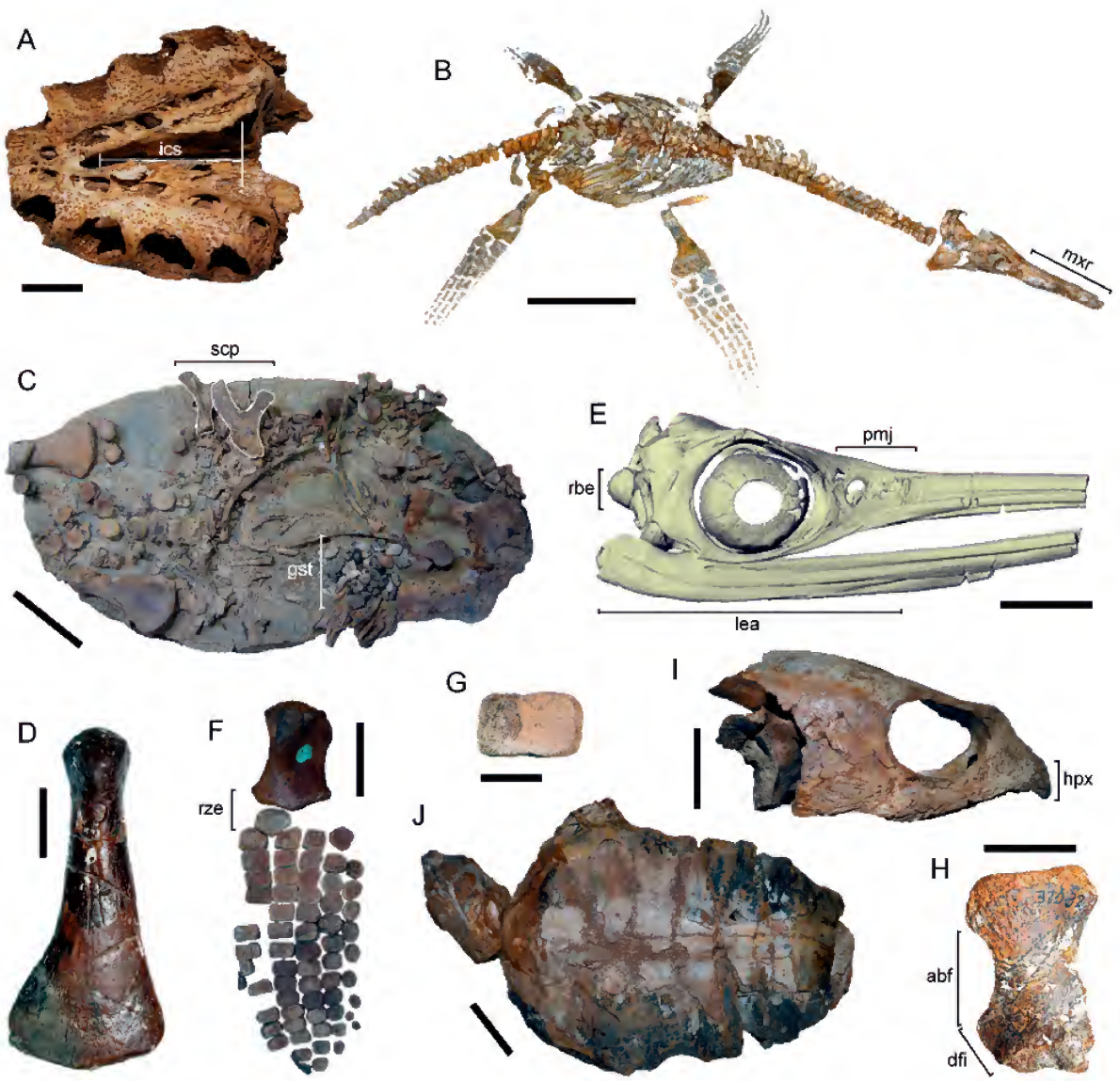

Figure 3. Marine amniote fossils from Cretaceous strata in Australia. A, elasmosaurid premaxillary palate (SAM P40510) exposing the vomerine contact and intracranial sinus. B, spectacular mounted skeleton (QM F18041) of the new polycotylid popularly dubbed the 'Richmond pliosaur'. C, partially disarticulated 'juvenile' postcranium referred to *Umoonasaurus demoscyllus*. Both scapulae (outlined) and an in situ gastrolith mass are indicated. D, '*Umoonasaurus*-like' propodial from the late Aptian Darwin Formation, Northern Territory. E, CT rendering of an exceptionally preserved 'juvenile' *Platypterygius australis* cranium and mandible (AM F98273). Image compilation: Ben Hill (Adelaide). F, articulated humerus and distal forelimb elements (AM F107444) of a 'juvenile' *Platypterygius australis*. G, ophthalmosaurian phalanx (WAM 99.1.4) from the late Cenomanian Geale Siltstone, Western Australia. Image: Mikael Siversson (Western Australian Museum). H, mosasaurid ulna (UWA 37092) with antebrachial foramen and intermedium contact indicated. I, cranium of *Bouliachelys suteri* (SAM P41106) in lateral view. J, articulated cranium and carapace of *Bouliachelys suteri* (SAM P40525) in dorsal view. Scale bars represent 20 mm in A, G, H; 500 mm in B; 100 mm in C, J; and 50 mm in D–F, I. Abbreviations: abf – antebrachial foramen; dfi – distal facet for the intermedium; ics – intracranial sinus; gst – gastrolith mass; hpx – hooked premaxillae; lea – lateral exposure of angular; pmj – premaxillary, maxillary, and jugal contacts; rbe – reduced basioccipital extracondylar area; rze – position of radial zeugopodial element; scp – scapulae.

associated bromalite comprising belemnites and a high proportion of benthic bivalves and gastropods. This implied a propensity for bottom feeding, a habit advocated elsewhere from bite marks on bivalve shells (Kear and Godthelp, 2008).

Perhaps the most enigmatic Australian plesiosaurian named in recent years is *Opallionectes andamookaensis* Kear, 2006a from the Aptian Bulldog Shale of Andamooka. This taxon was identified from a single skeleton (SAM P24560), but an isolated tooth (privately owned) has since been found in coeval strata at Coober Pedy. Kear (2006a) noted features of the vertebrae, including craniocaudally short/broad cervical centra, the lack of a longitudinal ridge, and platycoelous to shallowly amphocoelous articular faces that might be homologous with those of the Late Cretaceous aristonectine elasmosaurids *Aristonectes* spp. and *K. katiki* (O'Gorman et al., 2013; O'Gorman et al., 2014). The absence of an intercoracoid embayment on the pectoral girdle (see Kear, 2006a, p. 843, fig. 3B), however, clearly differentiates *O. andamookaensis* from remains referred to *Aristonectes* (O'Gorman et al., 2013; Otero et al., 2014). Furthermore, a combination of its prominent caudolateral coracoid cornuae, distally expanded propodials, pre- and post-xial accessory ossicles in the epipodial row, and small labiolingually compressed teeth that lack enamel ridges is alternatively consistent with Late Jurassic – Early Cretaceous cryptoclidids – e.g. *Kimmerosaurus langhami* Brown, 1981, *Tatenectes laramiensis* (Knight, 1900) (O'Keefe and Street, 2009), and *Abyssosaurus nataliae* Berezin, 2011.

Australian polycotylids are contentious and might incorporate the oldest stratigraphical exemplar of the group: a fragmentary opalized skeleton (AM F6266–F6298) from the Aptian Wallumbilla Formation at White Cliffs. Persson (1960) first mooted the polycotylid affinity of this specimen, a conclusion supported by Kear (2005a) based on its characteristically slender, homodont teeth and cervical centra that were shorter than high with sharp mid-ventral keels and constricted lateral sides (see O'Keefe, 2004; Druckenmiller and Russell, 2008a; Schmeisser, McKean, 2012). Other features such as laterally flared dorsal apices on the neural spines (see Kear, 2005a, p. 775, fig. 4C) compare well with *Dolichorynchops herschelensis* Sato, 2005. Craniad swelling of the median ventral edge of the articular facet rim is diagnostic for Polycotylidae (Sato and Storrs, 2000) but also resembles the prominent 'lip' described in the leptocleidian *Hastanectes valdensis* Benson, Ketchum, Naish and Turner, 2013a.

Polycotylid-like elements have been recovered in the Aptian Bulldog Shale (SAM P36356: Kear, 2006a), middle–late Albian Toolebuc Formation (SAM P41967), latest Albian–Cenomanian Mackunda Formation in Queensland (e.g. AOD F336), and late Cenomanian upper Gearle Siltstone (WAM 14.10.3.1–11). However, the only unequivocally diagnostic skeleton (QM F18041: fig. 3B) is the 'Richmond pliosaur' from the Allaru Mudstone of Richmond, Queensland (fig. 2). This sensational specimen represents one of the most complete Gondwanan plesiosaurian fossils yet discovered, and comprises a skull with characteristically elongate maxillary rostrum and symphyseal region of the mandible, incorporating a caudal extension of the splenial to the eighth tooth position. The splenial alternatively projects beyond the 10th tooth position in most Late Cretaceous polycotylids (Carpenter, 1996; Arkhangelsky et al., 2007). The palate of QM F18041 displays distinctively convex (= "dished" sensu O'Keefe, 2001) lateral palatal pterygoid surfaces bordering the posterior interpterygoid vacuities. Loss of the pineal foramen serves to differentiate QM F18041 from the only other named Early Cretaceous polycotylid *Edgarosaurus muddi* Druckenmiller, 2002. Conspicuous ornamentation of ridges and grooves along the snout and mandible is further reminiscent of the Patagonian Campanian–Maastrichtian *Sulcusuchus erraini* Gasparini and Spalletti, 1990, and might have housed a dermal sensory system (O'Gorman and Gasparini, 2013; Foffa et al., 2014).

A second osteologically immature polycotylid skeleton (QM F12719) from the Toolebuc Formation near Hughenden in Queensland (fig. 2) was considered a new leptocleidid by Glen and McHenry (2007) but is morphologically indistinguishable from QM F18041 and thus probably conspecific.

Cruickshank and Long (1997) named the first Australian leptocleidid plesiosaurian *Leptocleidus clemai* Cruickshank and Long, 1997 based on several partial skeletons (WAM 92.8.1, WAM 94.1.6) from the Aptian Birdrong Sandstone of Kalbarri in Western Australia (fig. 2). These were phylogenetically re-evaluated by Kear and Barrett (2011), who failed to resolve *L. clemai* with other *Leptocleidus* spp., and noted that the only discrete character state diagnosing the species – epipodials broader than long – was ubiquitous amongst polycotylids and other Cretaceous plesiosaurians. Cruickshank and Long (1997) listed a 30% size increase relative to the type species *Leptocleidus superstes* Andrews, 1922 as another specifically differential feature, but failed to offer an explicit case for their generic referral to *Leptocleidus* (Kear and Barrett, 2011). Little else remains to distinguish *Leptocleidus clemai* except perhaps its robust propodials, which have a noticeably sigmoidal profile like polycotylids (e.g. Albright et al., 2007; O'Keefe, 2008) and *L. superstes* (Kear and Barrett, 2011); although, the articular surface on the humeral head exhibits pronounced lateral flaring unlike the more cylindrical capitulum of *L. superstes* (compare Kear, 2003, p. 294, fig. 6A, B with Kear and Barrett, 2011, p. 673, fig. 4F–I).

Kear (2006b) documented isolated small pliosauroid bones and teeth that were similar to those of leptocleidids but occurred in non-marine strata of the Aptian-Albian Eumeralla Formation from Cape Otway to Inverloch in Victoria, and in the early-middle Albian Griman Creek Formation of Lightning Ridge, New South Wales and Surat in Queensland (fig. 2). New plesiosaurian elements from the Eumeralla Formation were figured by Benson et al. (2013b, p. 3, fig. 2), including NMV P198945, a large broken tooth (45 mm high) missing most of its enamel surface (Benson et al., 2013b, p. 2, fig. 1). Benson et al. (2013b) argued for plesiosaurian affinity based on remnants of three incomplete and irregularly spaced enamel ridges (the remaining intact surface was otherwise smooth), conical tooth shape, and the apparent absence of carinae. While these traits are certainly compatible with plesiosaurians, they are likewise similar to spinosaurid theropods (also recovered from the Eumeralla Formation: Barrett et al., 2011), which can express smooth or fluted enamel, conical tooth form, and reduced carinae (e.g. Dal Sasso et al., 2005; Medeiros, 2006; Richter et al., 2013).

The best-known leptocleidan taxon from Australia is *Umoonasaurus demoscyllus* Kear, Schroeder and Lee, 2006a from the Aptian Bulldog Shale of Coober Pedy. A number of skeletons have been discovered, including multiple small-bodied 'juveniles', one of which (SAM P15980; originally identified as cf. *Leptocleidus* sp. by Kear, 2007b) was proportionately scaled to the 2.5 m long holotype (AM F99374) and thereby estimated to be only 700 mm in maximum body length (Kear, 2007b). Another 'juvenile' specimen (SAM P33915) was also probably less than 1 m long and includes an in situ gastrolith accumulation, together with complete scapulae that display lateral shelves – a key leptocleidid synapomorphy (fig. 3C). Originally classified with Jurassic rhomaleosaurids (Kear et al., 2006a) or polycotylids (Druckenmiller and Russell, 2008a), the leptocleidid affinity of *U. demoscyllus* has been iterated by recent phylogenies (Ketchum and Benson, 2010; Benson and Druckenmiller, 2014), but relies upon few states including the presence of a lateral shelf on the scapula (disparately occurring in Jurassic taxa: Sato et al., 2003; Sachs et al., 2014), and a triangular fossa extending from the pineal foramen to the sagittal crest on the dorsal surface of the parietal; evident elsewhere in the disputed leptocleidids *Nichollssaura borealis* (Druckenmiller and Russell, 2008b) and *Brancasaurus brancai* Wegner, 1914 (Benson et al., 2013a). The skull of *U. demoscyllus* is, however, unique in its development of thin, high crests along the midline of the snout and above the orbits on the frontals (see Kear et al., 2006a, p. 617, fig. 1b). The function of these is unclear but they potentially represent display structures that might have been sexually dimorphic (Kear et al., 2006a).

Kear (2002b) reported on leptocleidid remains from the late Aptian Darwin Formation near Darwin in the Northern Territory (fig. 2). Further assessment of this material has revealed propodials (e.g. NTM P998-6; fig. 3D) and associated vertebrae that are indistinguishable from those of *U. demoscyllus* (see Kear, 2006a, supplemental fig. S7f, g) and might evidence this, or another closely related species inhabiting the Australian continental margin during the Early Cretaceous.

The gigantic pliosauroid *Kronosaurs queenslandicus* Longman, 1924 is the largest and most stratigraphically widespread plesiosaurian taxon thus far documented from Australia. Its conspicuous remains have been recovered from Aptian units throughout the Eromanga Basin, including the Bulldog Shale at Coober Pedy (Kear, 2006a), and the Wallumbilla Formation at both White Cliffs (Kear, 2005a) and near Richmond; this was the source of the famous Harvard University skeleton (MCZ 1285: Romer and Lewis, 1959). The holotype (QM F1609), however, derived from the Albian Toolebuc Formation at Hughenden, with a second flattened skull (QM F2446) that is thought to represent a separate species (Molnar, 1991). In contrast, McHenry (2009) considered all of the Australian *Kronosaurus* remains coherent with a monospecific morphotype, and thus presented a composite reconstruction of the cranium and mandible (see McHenry, 2009, p. 349, fig. 5-35) incorporating parts of a 10 m long skeleton (QM F10113) from the Toolebuc Formation near Hughenden.

Phylogenetic determinations have placed *K. queenslandicus* as a derived member of the Brachaucheninae (Benson and Druckenmiller, 2014), a Cretaceous pliosauroid radiation notably characterised by loss of the subcentral foramina on the cervical vertebrae. Cranial modelling and inferred gastric residues also suggest that *K. queenslandicus* might have favoured smaller prey particularly marine turtles, elasmosaurid plesiosaurians, and possibly sharks (McHenry, 2009).

Ichthyosaurians

Australian Cretaceous ichthyosaurian fossils have been intensively studied. Wade (1984) compiled a seminal review, recognizing a single species *Platypterygius australis* (McCoy, 1867a). Subsequent uncertainty over the holotype led to taxonomic conflict (Wade, 1990). However, Zammit (2010) resolved these issues with a reassessment of the original specimens described by McCoy (1869). These included a partial skull (MV P12989: Zammit, 2010, p. 6, fig. 2A), probably associated with the type vertebrae (Wade, 1985), that supported referral to the genus *Platypterygius* (via a reduced extracondylar area on the basioccipital: McGowan and Motani, 2003), and conformed with other exemplars of *P. australis* (which exhibit exclusion of the lacrimal from the external bony nasal aperture and the presence of accessory caudodorsal nasal foramina: Kear, 2005c). Fossils of *P. australis* are otherwise prolific and often excellently preserved, especially in the middle–late Albian Toolebuc Formation and Allaru Mudstone of Queensland. This unprecedented quantity and quality of material has facilitated comprehensive appraisals of craniodental (Kear, 2005c; Maxwell et al., 2011) and postcranial anatomy (Zammit et al., 2010) that are now a comparative standard for Cretaceous ichthyosaurian remains worldwide (e.g. Maxwell and Kear, 2010; Maxwell et al., 2012; Fischer et al., 2014). Moreover, functional analyses and feeding traces have permitted reconstruction of locomotory modes (Zammit et al., 2014), jaw musculature and sense organs (Kear, 2005c), and dietary specialisation towards small-bodied prey including bony fish (Wretman and Kear, 2014) and aquatic amniotes (e.g. hatchling turtles: Kear et al., 2003). Pathological elements have further afforded evocative glimpses into ichthyosaurian disease (dental caries: Kear, 2001b) and intraspecific behavioural interactions (Zammit and Kear, 2011). Exceptionally preserved foetal remains also infer a K-selection reproductive strategy favouring large young (around one meter long at parturition) that were born 'tail first' and probably precocial (Kear and Zammit, 2014).

The precise phylogenetic relationships of *P. australis* are ambiguous, but the taxon is undoubtedly an advanced ophthalmosaurian because of the restricted basicoccipital extracondylar area, extensive lateral exposure of the angular, and extra pre-radial zeugopodial element/digit articulating with the humerus (McGowan and Motani, 2003: fig. 3E, F). Kear and Zammit (2014) identified additional ontogenetically stable autapomorphies that were consistently expressed through an *in-utero* to osteologically mature 'adult' growth trajectory: premaxillary *processus supranarialis* having minimal contact with the bony nasal aperture; premaxillary *processus subnarialis* of subequal length to the *processus supranarialis* and extending across the external face of the maxilla; a well sutured jugal-maxilla contact; and absence of a squamosal (fig. 3E).

Other Australian *Platypterygius* occurrences are known from the Aptian Bulldog Shale, Wallumbilla Formation, Darwin Formation, and Birdrong Sandstone (Kear, 2002b, 2003, 2005a, 2006a), as well as the late Albian–Cenomanian Alinga Formation and Molecap Greensand of Western Australia (Choo, 1999; Kear 2003). Novel discoveries have extended this range into the mid-late Cenomanian upper-most Gearle Siltstone. This was based on an isolated phalanx (WAM 99.1.4: fig. 3G) from the Murchison River region west of Kalbarri, which is important because it could represent the stratigraphically youngest ichthyosaurian fossil thus far documented from the southern hemisphere (see Sachs and Grant-Mackie, 2003; Zammit, 2012).

Aquatic squamates

Kear et al. (2005) summarized the Australian marine squamate record noting the presence of various indeterminate mosasaurids. These incorporated an ulna and phalanx (UWA 37092) which Lundelius and Warne (1960, p. 1216) thought similar to either *Platecarpus* Cope, 1869 or *Clidastes* Cope, 1868, but "perhaps closer to *Platecarpus*". The ulna (fig. 3H) certainly has a compact shaft with shallowly concave edges suggesting an oval antebrachial foramen. However, the distal extremity appears to be offset for contact with the intermedium, which is more like *Clidastes* (Russell, 1967). UWA 37092 derived from the Molecap Greensand near Gingin (fig. 2), a slumped sequence of Cenomanian–Coniacian strata associated with a buried Cretaceous impact crater (Mory et al., 2005). Some mosasaurid dorsal vertebrae have been documented from this unit (WAM 98.7.1–10), and other mosasaurid vertebrae are known from the early Maastrichtian Korojon Calcarenite (UWA 133937), and late Maastrichtian Miria Formation (WAM 91.8.16) of Western Australia (see Kear et al., 2005, p. 309, fig. 2G–O).

Scanlon and Hocknull (2008) mentioned the surprising occurrence of a 'dolichosaur-like' presacral vertebra (QM F52673) in the non-marine latest Albian–Turonian Winton Formation at Winton in Queensland (fig. 2). The tapered centrum shape, "moderately prominent" synapophyses, and apparent absence of pachyostosis (evident in various aquatic varanoids: Houssaye et al., 2008) were advocated to support this assignment. The oval outline and cranial inclination of the cotyle (see Scanlon and Hocknull, 2008, p. 133, fig. 1F) are otherwise similar to varanids as well as basal mosasauroids (Carroll and De Braga, 1992; Makádi et al., 2012), yet the badly eroded condyle seems to lack a varanid-like precondylar constriction (Scanlon and Hocknull, 2008). The affinities of QM F52673 are thus unclear and the specimen is probably best interpreted as an indeterminate varanoid.

Marine Turtles

Marine turtle fossils are frequently discovered in Australia, but are at present stratigraphically restricted to only a few units including the middle–late Albian Toolebuc Formation and Allaru Mudstone (Kear, 2003), together with the late Albian–Cenomanian Mackunda Formation (e.g. AOD F795), and late Maastrichtian Miria Formation (Kear and Siverson, 2010). Molnar (1991, p. 618) reported a possible marine, "or at least aquatic" turtle (listed as a "tortoise" by Molnar, 1991, p. 612) from an unspecified locality northwest of Winton (fig. 2) that was mapped within the non-marine Winton Formation. This specimen (QM F12413) consists of an internal cast of the carapace (Molnar, 1991, p. 690, pl. 1), but seems to show reduced costal plates and fontanellization consistent with Chelonioidea (Wood et al., 1996; Lehman and Tomlinson, 2004). All other identifiable Winton Formation turtle remains pertain to chelids (Hocknull et al., 2009). However, the lower-most Albian section of the Winton Formation does produce typically marine vertebrates (e.g. ichthyodectiform teleosts: Berrell et al., 2014), and was deposited by a tidal fluvial system that could have accommodated euryhaline organisms.

Most Australian Cretaceous marine turtles are referred to the cosmopolitan clade Protostegidae, which might represent either a basal chelonioid lineage (Hirayama, 1998; Hooks, 1998; Kear and Lee, 2006; Bardet et al., 2013), or a more archaic radiation of marine cryptodires (Joyce, 2007). Three endemic Australian taxa have been named from the middle–late Albian Toolebuc Formation, and are amongst the oldest protostegids documented worldwide. Owen (1882) described the partial carapace and plastron (AM F67326) of *Notochelys costata* Owen, 1882, from an unknown location on the Thomson River in Queensland (see De Vis, 1911). Lydekker (1889) subsequently replaced the epithet '*Notochelys*' with *Notochelone* Lydekker, 1889 because of synonymy, and De Vis (1911) referred additional elements that Kear (2003) used to compile an emended diagnosis. Kear and Lee (2006) listed the jugal-quadrate contact, extension of the pterygoid onto the articular condyle of the quadrate, and incorporation of the vomer into the upper triturating surface as states distinguishing *N. costata* from the larger-bodied (around 50%) coeval taxon *Bouliachelys suteri* Kear and Lee, 2006. This is known from several spectacular skulls (e.g. SAM P41106: fig. 3I) found near Boulia in Queensland (fig. 2). Kear and Lee (2006) phylogenetically placed both *N. costata* and *B. suteri* as basal protostegids. Parham and Pyenson (2010) further correlated the distinctive hooked premaxillae and poorly developed secondary palate of *B. suteri* with 'shear' feeding (as opposed to durophagy), and proposed protostegid convergence upon extant herbivorous cheloniids. Interestingly, Kear (2006c) identified both gastrolites/cololites and coprolites within multiple '*Notochelone*-like' specimens that contained dense accumulations of *Inoceramus* bivalve shell. These were processed orally, implying benthic 'grazing' and an invertebrate-based diet in the earliest protostegids (Kear, 2006c).

Despite obvious character state differentiation, Myers (2007) suggested that *N. costata* and *B. suteri* might be synonymous because of proportional similarities in their crania. This warrants further exploration especially relative to their postcranial elements, which now include several articulated skeletons under preparation and study (e.g. SAM P40525: fig 3J).

The holotype (QM F14550: Kear, 2006d, p. 781, fig. 2A–R) and only specimen of the colossal (around four meters in length) Toolebuc Formation protostegid *Cratochelone berneyi* Longman, 1915 discovered near Hughenden, was re-evaluated

by Kear (2006d), and found to possess highly vascular limb bone surfaces compatible with the advanced protostegids *Archelon* Wieland, 1896 and *Protostega* Cope, 1872. Comparable microstructures occur in Australia's only Late Cretaceous chelonioid fossil, a dermochelyoid scapula (WAM 03.3.37: Kear and Siverson, 2010, p. 4, fig. 2E) from the late Maastrichtian Miria Formation southwest of Exmouth in Western Australia (fig. 2), and suggest that complex metabolic physiology repeatedly coupled with body size (see Rhodin, 1985) and perhaps pelagic lifestyles throughout marine turtle evolution.

Conclusions and Future Research

Australian Cretaceous marine amniote fossils represent a significant resource for exploring the enigmatic vertebrate biodiversity of Gondwana. The astounding taxonomic richness, preservation quality, and sheer productivity of the documented source units, particularly those from the Aptian–Albian strata of the Eromanga Basin in Queensland and South Australia (Kear, 2003), mark them as some of the most important (although as yet under-popularized) Mesozoic marine vertebrate *lagerstätten* known worldwide. Their association with Early Cretaceous freezing high latitude palaeoenvironments is also unique, and has been linked with climate change coincident dispersals and cladogenic events that shaped later Cretaceous faunas (Kear et al., 2006b). Clearly this offers an exciting focus for on-going research, especially given the recent advances in quantitative modeling (e.g. Benson et al., 2010a), geochemical analyses (e.g. Bernard et al., 2010), bone microstructure visualization (e.g. Houssaye, 2013), and soft tissue reconstruction (e.g. Lindgren et al., 2014) that are changing the perspectives on Mesozoic marine amniote evolution. Nevertheless, such innovative approaches would not be possible without the pioneering studies undertaken over the last decade. These have provided not only a fundamental systematic framework but also posed an intriguing experimental question that can be used to frame future investigations – did Australia's Cretaceous marine amniotes experience high-latitude thermal isolation and low-temperature adaptation concomitant with the coeval continental record of inimitable relics (e.g. Thulborn and Turner, 2003; Smith and Kear, 2013), regional immigrants (e.g. Rich and Vickers-Rich, 2003; Smith et al., 2008; Hocknull et al., 2009; Rich et al., 2009; Agnolin et al., 2010; Benson et al., 2010b; Kellner et al., 2010; Barrett et al., 2011; Benson et al., 2012; Fitzgerald et al., 2012; Poropat et al., 2014; Poropat et al., 2015; Rich et al., 2014), and endemic progenitors (e.g. Pridmore et al., 2005; Salisbury et al., 2006; Rowe et al., 2008; Smith, 2010) whose descendants are still extant on the Australian landmass today?

Acknowledgements

This article is dedicated to Dr Thomas H. Rich, whose outstanding contributions to Australian vertebrate palaeontology have inspired generations of young scientists to follow in his footsteps. Thanks to Erich Fitzgerald for the invitation to contribute to this festschrift volume. Mary-Anne Binnie (South Australian Museum), Gavin Dally (Museum & Art Gallery of the Northern Territory), David Pickering (Museum Victoria), R. John Reeve (University of Western Australia), Mikael Siversson (Western Australian Museum), Kristen Spring and Andrew Rozefelds (Queensland Museum), and Yong Yi Zhen (Australian Museum) assisted with access to specimens and collection information. The Australian Research Council, Swedish Research Council, National Geographic Society, Sir Mark Mitchell Research Fund, South Australian Museum, Umoona Opal Mine and Museum, Uppsala University and other private patrons provided financial support for the research.

References

Agnolin, F.L., Ezcurra, M.D., Pais, D.F., and Salisbury, S.W. 2010. A reappraisal of the Cretaceous non-avian dinosaur faunas from Australia and New Zealand: Evidence for their Gondwanan affinities. *Journal of Systematic Palaeontology* 8: 257–300.

Albright, L.B. III, Gillette, D.D., and Titus, A.L. 2007. Plesiosaurs from the Upper Cretaceous (Cenomanian–Turonian) tropic shale of southern Utah, part 2: polycotylidae. *Journal of Vertebrate Paleontology* 27: 41–58.

Arkhangelsky, M.S., Averianov, A.O., and Pervushov, E.M. 2007. Short-necked plesiosaurs of the Family Polycotylidae from the Campanian of the Saratov Region. *Paleontological Journal* 41: 656–660.

Bardet, N., Jalil, N.E., de Broin, F.D.L., Germain, D., Lambert, O., and Amaghzaz, M. 2013. A giant chelonioid turtle from the Late Cretaceous of Morocco with a suction feeding apparatus unique among tetrapods. *PloS ONE* 8(7), e63586.

Barrett, P.M., Benson, R.B.J., Rich, T.H., and Vickers-Rich, P. 2011. First spinosaurid dinosaur from Australia and the cosmopolitanism of Cretaceous dinosaur faunas. *Biology Letters* 7: 933–936.

Benson, R.B.J., and Druckenmiller, P.S. 2014. Faunal turnover of marine tetrapods during the Jurassic-Cretaceous transition. *Biological Reviews* 89: 1–23.

Benson, R.B.J., Butler, R.J., Lindgren, J., and Smith, A.S. 2010a. Mesozoic marine tetrapod diversity: mass extinctions and temporal heterogeneity in geological megabiases affecting vertebrates. *Proceedings of the Royal Society of London, Series B* 277: 829–34.

Benson, R.B.J., Barrett, P.M., Rich, T.H., and Vickers-Rich, P. 2010b. A southern tyrant reptile. *Science* 327: 1613.

Benson, R.B.J., Rich, T.H., Vickers-Rich, P., and Hall, M. 2012. Theropod fauna from southern Australia indicates high polar diversity and climate-driven dinosaur provinciality. *PloS ONE* 7(5): e37122.

Benson, R.B.J., Ketchum, H.F., Naish, D., and Turner, L.E. 2013a. A new leptocleidid (Sauropterygia, Plesiosauria) from the Vectis Formation (Early Barremian–early Aptian; Early Cretaceous) of the Isle of Wight and the evolution of Leptocleididae, a controversial clade. *Journal of Systematic Palaeontology* 11: 233–250.

Benson, R.B.J., Fitzgerald, E.M.G., Rich, T.H., and Vickers-Rich, P. 2013b. Large freshwater plesiosaurian from the Cretaceous (Aptian) of Australia. *Alcheringa* 37: 1–6.

Berezin, A.Y. 2011. A new plesiosaur of the Family Aristonectidae from the Early Cretaceous of the center of the Russian platform. *Paleontological Journal* 45: 648–660.

Bernard, A., Lécuyer, C., Vincent, P., Amiot, R., Bardet, N., Buffetaut, E., Cuny, G., Fourel, F., Martineau, F., Mazin, J.-M., and Prieur, A. 2010. Regulation of body temperature by some Mesozoic marine reptiles. *Science* 328: 1379–1382.

Berrell, R.W., Alvarado-Ortega, J., Yabumoto, Y., and Salisbury, S.W. 2014. First record of the ichthyodectiform fish *Cladocyclus* from eastern Gondwana: An articulated skeleton from the Early Cretaceous of Queensland, Australia. *Acta Palaeontologica Polonica*. 59: 903–920.

Brown, D.S. 1981. The English Upper Jurassic Plesiosauroidea (Reptilia) and a review of the phylogeny and classification of the Plesiosauria. *Bulletin of the British Museum (Natural History) Geological Series* 35: 253–347.

Cabrera, A. 1941. Un plesiosaurio nuevo del Cretáceo del Chubut. *Revista del Museo de La Plata* 2: 113–130.

Carpenter, K. 1996. A review of the short-necked plesiosaurs from the Cretaceous of the Western Interior, North America. *Nues Jahrbuch für Geologie und Paläontologie, Abhandlungen* 201: 259–287.

Choo, B. 1999. Cretaceous ichthyosaurs from Western Australia. *Records of the Western Australian Museum, Supplement* 57: 207–218.

Cope, E.D. 1868. On new species of extinct reptiles. *Proceedings of the Academy of Natural Sciences of Philadelphia* 20: 181.

Cope, E.D. 1869. On the reptilian orders Pythonomorpha and Streptosauria. *Boston Society of Natural History Proceedings* 12: 250–266

Cope, E.D. 1872. A description of the genus *Protostega*, a form of extinct Testudinata. *Proceedings of the American Philosophical Society* 12: 422–433.

Cruickshank, A.R.I., and Long, J.A. 1997. A new species of pliosaurid reptile from the Early Cretaceous Birdrong Sandstone of Western Australia. *Records of the Western Australian Museum* 18: 263–276.

Cruickshank, A.R.I., and Fordyce, R.E. 2002. A new marine reptile (Sauropterygia) from New Zealand: further evidence for a Late Cretaceous austral radiation of cryptoclidid plesiosaurs. *Palaeontology* 45: 557–575.

Cruickshank, A.R.I., Fordyce, R.E., and Long, J.A. 1999. Recent developments in Australasian sauropterygian palaeontology (Reptilia: Sauropterygia). *Records of the Western Australian Museum, Supplement* 57: 201–205.

Carroll, R.L., and Debraga, M. 1992. Aigialosaurs: mid-Cretaceous varanoid lizards. *Journal of Vertebrate Paleontology* 12: 66–86.

Dal Sasso, C., Maganuco, S., Buffetaut, E., and Mendez, M.A. 2005. New information on the skull of the enigmatic theropod *Spinosaurus*, with remarks on its size and affinities. *Journal of Vertebrate Paleontology* 25: 888–896.

De Vis, C.W. 1911. On some Mesozoic fossils. *Memoirs of the Queensland Museum* 10: 1–11.

Druckenmiller, P.S. 2002. Osteology of a new plesiosaur from the Lower Cretaceous (Albian) Thermopolis Shale of Montana. *Journal of Vertebrate Paleontology* 22: 29–42.

Druckenmiller, P.S., and Russell, A.P. 2008a. A phylogeny of Plesiosauria (Sauropterygia) and its bearing on the systematic status of *Leptocleidus* Andrews, 1922. *Zootaxa*, 1863: 1–120.

Druckenmiller, P.S., and Russell, A.P. 2008b. Skeletal anatomy of an exceptionally complete specimen of a new genus of plesiosaur from the Early Cretaceous (Early Albian) of northeastern Alberta, Canada. *Palaeontographica A*, 283: 1–33.

Etheridge, R. Jr 1888. On additional evidence of the genus *Ichthyosaurus* in the Mesozoic rocks ('Rolling Downs Formation') of north-eastern Australia. *Proceedings of the Linnean Society of New South Wales* 2: 405–409.

Etheridge, R. Jr 1897. An Australian sauropterygian (*Cimoliasaurus*), converted into precious opal. Records of the Australian Museum 3: 21–29.

Etheridge, R. Jr 1904. A second sauropterygian converted to opal, from the Upper Cretaceous of White Cliffs, New South Wales. *Records of the Australian Museum* 5: 306–316.

Fischer, V., Arkhangelsky, M.S., Naish, D., Stenshin, I.M., Uspensky, G.N., and Godefroit, P. 2014. *Simbirskiasaurus* and *Pervushovisaurus* reassessed: implications for the taxonomy and cranial osteology of Cretaceous platypterygiine ichthyosaurs. *Zoological Journal of the Linnean Society* 171: 822–841.

Fitzgerald, E.M.G., Carrano, M.T., Holland, T., Wagstaff, B.E., Pickering, D., Rich, T.H., and Vickers-Rich, P. 2012. First ceratosaurian dinosaur from Australia. *Naturwissenschaften* 99: 397–405.

Foffa, D., Sassoon, J., Cuff, A.R., Mavrogordato, M.N., and Benton, M.J. 2014. Complex rostral neurovascular system in a giant pliosaur. *Naturwissenschaften* 101: 453–456.

Gaffney, E.S. 1981. A review of the fossil turtles of Australia. *American Museum Novitates* 2720: 1–38.

Gasparini, Z., and Spalletti, L.A. 1990. Un nuevo crocodilo en los depósitos mareales maastrichtianos de la Patagonia noroccidental. *Ameghiniana* 27: 141–150.

Glen, C., and McHenry, C. 2007. Preliminary report on a plesiosaur from the early Cretaceous of central Queensland, Australia. *Journal of Vertebrate Paleontology* 27: 82A–82A.

Gradstein, F.J., Ogg, J.G., Schmitz, M.D., and Ogg, G.M. 2012. *The Geologic Time Scale 2012. Volume 2*. Elsevier: Amsterdam, 1144 pp.

Hirayama, R. 1998. Oldest known sea turtle. *Nature* 392: 705–708.

Hocknull, S.A., White, M.A., Tischler, T.R., Cook, A.G., Calleja, N.D., Sloan, T., and Elliott, D.A. 2009. New mid-Cretaceous (latest Albian) dinosaurs from Winton, Queensland, Australia. *PLoS ONE* 4(7): e6190.

Hooks, G.E. III 1998. Systematic revision of the Protostegidae, with a redescription of *Calcarichelys gemma* Zangerl, 1953. *Journal of Vertebrate Palaeontology* 18: 85–98.

Houssaye, A. 2013. Bone histology of aquatic reptiles: what does it tell us about secondary adaptation to an aquatic life? *Biological Journal of the Linnean Society* 108: 3–21.

Houssaye, A., De Buffrenil, V., Rage, J.C., and Bardet, N. 2008. An analysis of vertebral 'pachyostosis' in *Carentonosaurus mineaui* (Mosasauroidea, Squamata) from the Cenomanian (early Late Cretaceous) of France, with comments on its phylogenetic and functional significance. *Journal of Vertebrate Paleontology* 28, 685–691.

Joyce, W.G. 2007. Phylogenetic relationships of Mesozoic turtles. *Bulletin of the Peabody Museum of Natural History* 48: 3–102.

Kear, B.P. 2001a. Elasmosaur (Reptilia: Plesiosauria) basicranial remains from the Early Cretaceous of Queensland. *Records of the South Australian Museum* 34: 127–133.

Kear, B.P. 2001b: Dental caries in an Early Cretaceous ichthyosaur. *Alcheringa* 25: 387–390.

Kear, B.P. 2002a. Reassessment of the Early Cretaceous plesiosaur *Cimoliasaurus maccoyi* Etheridge, 1904 (Reptilia: Sauropterygia) from White Cliffs, New South Wales. *Australian Journal of Zoology* 50: 671–685.

Kear, B.P. 2002b. Darwin Formation (Early Cretaceous, Northern Territory) marine reptile remains in the South Australian Museum. *Records of the South Australian Museum* 35: 33–47.

Kear, B.P. 2003. Cretaceous marine reptiles of Australia: a review of taxonomy and distribution. *Cretaceous Research* 24: 277–303.

Kear, B.P. 2004. Biogeographic and biostratigraphic implications of Australian Mesozoic marine reptiles. *Australian Biologist* 17, 4–22.

Kear, B.P. 2005a. Marine reptiles from the Lower Cretaceous (Aptian) deposits of White Cliffs, southeastern Australia: implications of a high-latitude cold water assemblage. *Cretaceous Research* 26: 769–782.

Kear, B.P. 2005b. A new elasmosaurid plesiosaur from the Lower Cretaceous of Queensland, Australia. *Journal of Vertebrate Paleontology* 25: 792–805.

Kear, B.P. 2005c. Cranial morphology of *Platypterygius longmani* Wade, 1990 (Reptilia: Ichthyosauria) from the Lower Cretaceous of Australia. *Zoological Journal of the Linnean Society* 145: 583–622.

Kear, B. P. 2006a. Marine reptiles from the Lower Cretaceous of South Australia: elements of a high-latitude cold water assemblage. *Palaeontology* 49: 837–856.

Kear, B.P. 2006b. Plesiosaur remains from Cretaceous high-latitude non-marine deposits in southeastern Australia. *Journal of Vertebrate Paleontology* 26: 196–199.

Kear, B.P. 2006c. First gut contents in a Cretaceous sea turtle. *Biology Letters* 2: 113–115.

Kear, B.P. 2006d. Reassessment of *Cratochelone berneyi* Longman, 1915, a giant Early Cretaceous sea turtle from Australia. *Journal of Vertebrate Paleontology* 26: 779–783.

Kear, B.P. 2007a. Taxonomic clarification of the Australian elasmosaurid *Eromangasaurus*, with reference to other austral elasmosaur taxa. *Journal of Vertebrate Paleontology* 27: 241–246.

Kear, B.P. 2007b. A juvenile pliosauroid plesiosaur from the Lower Cretaceous of South Australia. *Journal of Paleontology* 81: 154–162.

Kear, B.P. 2012. A revision of Australia's Jurassic plesiosaurs. *Palaeontology* 55: 1125–1138.

Kear, B.P., and Lee, M.S.Y. 2006. A primitive protostegid from Australia and early sea turtle evolution. *Biology Letters* 2: 116–119.

Kear, B.P., and Siverson, M. 2010. First evidence of a Late Cretaceous sea turtle from Australia. *Alcheringa* 34: 265–272.

Kear, B.P., and Barrett, P.M. 2011. Reassessment of the Lower Cretaceous (Barremian) pliosauroid *Leptocleidus superstes* Andrews, 1922 and other plesiosaur remains from the non-marine Wealden succession of southern England. *Zoological Journal of the Linnean Society* 161: 663–691.

Kear, B.P., and Godthelp, H. 2008. Inferred vertebrate bite marks on an Early Cretaceous unionoid bivalve from Lightning Ridge, New South Wales, Australia. *Alcheringa* 32: 65–71.

Kear, B.P., and Hamilton-Bruce, R.J. 2011. *Dinosaurs in Australia. Mesozoic Life from the Southern Continent.* CSIRO Publishing: Melbourne, 190 pp.

Kear, B.P., and Zammit, M. 2014. In utero foetal remains of the Cretaceous ichthyosaurian *Platypterygius*: ontogenetic implications for character state efficacy. *Geological Magazine* 151: 71–86.

Kear, B.P., Boles, W.E., and Smith, E.T. 2003. Unusual gut contents in a Cretaceous ichthyosaur. *Proceedings of the Royal Society of London, Series B* 270: S206–S208.

Kear, B.P., Long, J.A., and Martin, J.E. 2005. A review of Australian mosasaur occurrences. *Netherlands Journal of Geosciences* 84: 307–313.

Kear, B.P., Schroeder, N.I., and Lee, M.S.Y. 2006a. An archaic crested plesiosaur in opal from the Lower Cretaceous high latitude deposits of Australia. *Biology Letters* 2: 615–619.

Kear, B.P., Schroeder, N.I., Vickers-Rich, P., and Rich, T.H. 2006b. Early Cretaceous high latitude marine reptile assemblages from southern Australia. *Paludicola* 5: 200–205.

Kellner, A.W., Rich, T.H., Costa, F.R., Vickers-Rich, P., Kear, B.P., Walters, M., and Kool, L. 2010. New isolated pterodactyloid bones from the Albian Toolebuc Formation (western Queensland, Australia) with comments on the Australian pterosaur fauna. *Alcheringa* 34: 219–230.

Ketchum, H.F., and Benson, R.B.J., 2010. Global interrelationships of Plesiosauria (Reptilia, Sauropterygia) and the pivotal role of taxon sampling in determining the outcome of phylogenetic analyses. *Biological Reviews* 85: 361–392.

Knight, W. C. 1900. Some new Jurassic vertebrates. *American Journal of Science, Fourth Series* 10 (160): 115–119.

Lehman, T.M., and Tomlinson, S.L., 2004. *Terlinguachelys fischbecki*, a new genus and species of sea turtle (Chelonioidea: Protostegidae) from the Upper Cretaceous of Texas. *Journal of Paleontology* 78: 1163–1178.

Lindgren, J., Sjövall, P., Carney, R.M., Uvdal, P., Gren, J.A., Dyke, G., Schultz, B.P., Shawkey, M.D., Barnes, K.R., and Polcyn, M.J. 2014. Skin pigmentation provides evidence of convergent melanism in extinct marine reptiles. *Nature* 506: 484–488.

Long, J.A., and Cruickshank, A.R.I. 1998. Further records of plesiosaurian reptiles of Jurassic and Cretaceous age from Western Australia. *Records of the Western Australian Museum* 19: 47–55.

Longman, H.A. 1915. On a giant turtle from the Queensland Lower Cretaceous. *Memoirs of the Queensland Museum* 3: 24–29.

Longman, H.A. 1922. An ichthyosaurian skull from Queensland. *Memoirs of the Queensland Museum* 7: 246–256.

Longman, H.A. 1924. A new gigantic marine reptile from the Queensland Cretaceous, *Kronosaurus queenslandicus* new genus and species. *Memoirs of the Queensland Museum* 8: 26–28.

Longman, H.A. 1930. *Kronosaurus queenslandicus*. A gigantic Cretaceous pliosaur. *Memoirs of the Queensland Museum* 10: 1–7.

Longman, H.A. 1932. Restoration of *Kronosaurus queenslandicus*. *Memoirs of the Queensland Museum* 10: 98.

Longman, H.A. 1935. Palaeontological notes. *Memoirs of the Queensland Museum* 10: 236–239.

Longman, H.A. 1943. Further notes on Australian ichthyosaurs. *Memoirs of the Queensland Museum* 12: 101–104.

Lundelius, E., and Warne, S.St.J. 1960. Mosasaur remains from the Upper Cretaceous of Western Australia. Journal of Paleontology 34: 1215–1217.

Lydekker, R. 1889. Catalogue of the Fossil Reptilia and Amphibia in the British Museum (Natural History). Part III. Order Chelonia. British Museum (Natural History): London, 309 pp.

Makádi, L., Caldwell, M.W., and Ősi, A. 2012. The first freshwater mosasauroid (Upper Cretaceous, Hungary) and a new clade of basal mosasauroids. *PloS ONE* 7(12): e51781.

Maxwell, E.E., and Kear, B.P. 2010. Postcranial anatomy of *Platypterygius americanus* (Reptilia: Ichthyosauria) from the Cretaceous of Wyoming. *Journal of Vertebrate Paleontology* 30: 1059–1068.

Maxwell, E.E., Caldwell, M.W., and Lamoureux, D.O. 2011. Tooth histology in the Cretaceous ichthyosaur *Platypterygius australis*, and its significance for the conservation and divergence of mineralized tooth tissues in amniotes. *Journal of Morphology* 272: 129–135.

Maxwell, E.E., Zammit, M., and Druckenmiller, P.S. 2012. Morphology and orientation of the ichthyosaurian femur. *Journal of Vertebrate Paleontology* 32: 1207-1211.

McCoy, F. 1867a. On the occurrence of *Ichthyosaurus* and *Plesiosaurus* in Australia. *Annals and Magazine of Natural History, Third Series* 19: 355–356.

McCoy, F. 1867b. On the discovery of the Enaliosauria and other Cretaceous fossils in Australia. *Transactions and Proceedings of the Royal Society of Victoria* 8: 41–42.

McCoy, F. 1869. On the fossil eye and teeth of the *Ichthyosaurus australis* (M'Coy), from the Cretaceous formations of the source of the Flinder's River; and on the palate of *Diprotodon*, from the Tertiary limestone of Limeburner's Point, near Geelong. *Transactions and Proceedings of the Royal Society of Victoria* 2: 77–78.

McGowan, C. 1972. The systematics of Cretaceous ichthyosaurs with particular reference to the material from North America. *Contributions to Geology, University of Wyoming* 11: 9–29.

McGowan, C., and Motani, R. 2003. *Ichthyopterygia. Handbuch der Paleoherpetologie Part* 8. Verlag Dr. Friedrich Pfeil: München. 175 pp.

McHenry, C.R. 2009. *'Devourer of gods'. The palaeoecology of the Cretaceous pliosaur Kronosaurus queenslandicus*. Ph.D. Thesis, University of Newcastle: Newcastle. 616 pp.

McHenry, C.R., Cook, A.G., and Wroe, S. 2005. Bottom-feeding plesiosaurs. *Science* 310: 75.

Medeiros, M.A. 2006. Large theropod teeth from the Eocenomanian of northeastern Brazil and the occurrence of Spinosauridae. *Revista brasileira de Paleontologia* 9: 333–338.

Molnar, R.E. 1991. Fossil reptiles in Australia. Pp. 605–702 in: Vickers-Rich, P., Monaghan, J.M., Baird, R.F., and Rich, T. H. (eds). *Vertebrate Palaeontology of Australasia*. Pioneer Design Studio, Monash University: Melbourne, 1437 pp.

Mory, A.J., Haig, D.W., McLoughlin, S., and Hocking, R.M. 2005. Geology of the northern Perth Basin, Western Australia—a field guide. *Geological Survey of Western Australia Record* 9: 1–71.

Murray, P.F., 1985. Ichthyosaurs from Cretaceous Mullaman Beds near Darwin, Northern Territory. *The Beagle* 2: 39–55.

Murray, P.F. 1987. Plesiosaurs from Albian aged Darwin Formation siltstones near Darwin, Northern Territory, Australia. *The Beagle* 4: 95–102.

Myers, T. 2007. Osteological morphometrics of Australian chelonioid sea turtles. *Zoological Science* 24: 1012–1027.

O'Gorman, J.P., and Gasparini, Z., 2013. Revision of *Sulcusuchus erraini* (Sauropterygia, Polycotylidae) from the Upper Cretaceous of Patagonia, Argentina. *Alcheringa* 37: 161–174.

O'Gorman, J. P., Otero, R. A., and Hiller, N. 2014. A new record of an aristonectine elasmosaurid (Sauropterygia, Plesiosauria) from the Upper Cretaceous of New Zealand: implications for the Mauisaurus haasti Hector, 1874 hypodigm. *Alcheringa* 38: 504–512.

O'Gorman, J. P., Gasparini, Z. B., and Salgado, L. 2013. Postcranial morphology of *Aristonectes* (Plesiosauria, Elasmosauridae) from the Upper Cretaceous of Patagonia and Antarctica. *Antarctic Science* 25: 71–82.

O'Keefe, F.R. 2001. A cladistic analysis and taxonomic revision of the Plesiosauria (Reptilia, Sauropterygia). *Acta Zoologica Fennica* 213: 1–63.

O'Keefe, F.R. 2004. On the cranial anatomy of the polycotylid plesiosaurs, including new material of *Polycotylus latipinnis* Cope, from Alabama. *Journal of Vertebrate Paleontology* 24: 326–340.

O'Keefe, F.R. 2008. Cranial anatomy and taxonomy of *Dolichorhynchops bonneri* new combination, a polycotylid (Sauropterygia, Plesiosauria) from the Pierre Shale of Wyoming and South Dakota. *Journal of Vertebrate Paleontology* 28: 664–676.

O'Keefe, F. R., and Hiller, N. 2006. Morphologic and ontogenetic patterns in elasmosaur neck length, with comments on the taxonomic utility of neck length variables. *Paludicola* 5: 206–229.

O'Keefe, F. R., and Street, H. P. 2009. Osteology of the cryptocleidoid plesiosaur *Tatenectes laramiensis*, with comments on the taxonomic status of the Cimoliasauridae. *Journal of Vertebrate Paleontology* 29: 48–57.

Otero, R. A., Soto-Acuña, S., O'Keefe, F. R., O'Gorman, J. P., Stinnesbeck, W., Suárez, M. E., Rubilar-Rogers, D., Salazar, C., and Quinzio-Sinn, L. A. 2014. *Aristonectes quiriquinensis*, sp. nov., a new highly derived elasmosaurid from the upper Maastrichtian of central Chile. *Journal of Vertebrate Paleontology* 34: 100–125.

Owen, R. 1882. On an extinct chelonian reptile (*Notochelys costata*, Owen) from Australia. *Quarterly Journal of the Geological Society of London* 38: 178–183.

Parham, J.F., and Pyenson, N.D. 2010. New sea turtle from the Miocene of Peru and the iterative evolution of feeding ecomorphologies since the Cretaceous. *Journal of Paleontology* 84: 231–247.

Persson, P.O. 1960. Early Cretaceous plesiosaurians (Reptilia) from Australia. *Lunds Universitets Årsskrift* 56: 1–23.

Persson, P.O. 1982. Elasmosaurid skull from the Lower Cretaceous of Queensland (Reptilia, Sauropterygia). *Memoirs of the Queensland Museum* 20: 647–655.

Poropat, S.F., Mannion, P.D., Upchurch, P., Hocknull, S.A., Kear, B.P., & Elliott, D.A. 2014. Reassessment of the non-titanosaurian somphospondylan *Wintonotitan wattsi* (Dinosauria: Sauropoda: Titanosauriformes) from the mid-Cretaceous Winton Formation, Queensland, Australia. *Papers in Palaeontology* 1: 59–106.

Poropat, S.F., Upchurch, P., Mannion, P.D., Hocknull, S.A., Kear, B.P., Sloan, T., Sinapius, G.H.K., and Elliott, D.A. 2015. Revision of the sauropod dinosaur *Diamantinasaurus matildae* Hocknull et al. 2009 from the mid-Cretaceous of Australia: Implications for Gondwanan titanosauriform dispersal. *Gondwana Research* 27: 995–1033.

Pridmore, P.A., Rich, T.H., Vickers-Rich, P., and Gambaryan, P.P. 2005. A tachyglossid-like humerus from the Early Cretaceous of south-eastern Australia. *Journal of Mammalian Evolution* 12: 359–378.

Rhodin, A.G. 1985. Comparative chondro-osseous development and growth of marine turtles. *Copeia* 1985: 752–771.

Rich, T.H., and Vickers-Rich, P. 2003. Diversity of Early Cretaceous mammals from Victoria, Australia. *Bulletin of the American Museum of Natural History* 285: 36–53.

Rich, T.H., Vickers-Rich, P., Flannery, T.F., Kear, B.P., Cantrill, D., Komarower, P., Kool, L., Pickering, D., Trussler, P., Morton, S., Van Klaveren, N., and Fitzgerald, E.M.G. 2009. An Australian multituberculate and its palaeobiogeographical implications. *Acta Palaeontologica Polonica* 54: 1–6.

Rich, T.H., Kear, B.P., Sinclair, R., Chinnery, B., Carpenter, K., McHugh, M.L. and Vickers-Rich, P. 2014. *Serendipaceratops arthurcclarkei* Rich & Vickers-Rich, 2003 is an Australian Early Cretaceous ceratopsian. 38: 456–479.

Richter, U., Mudroch, A., and Buckley, L.G. 2013. Isolated theropod teeth from the Kem Kem beds (early Cenomanian) near Taouz, Morocco. *Paläontologische Zeitschrift* 87: 291–309.

Romer, A.S., and Lewis, A.D. 1959. A mounted skeleton of the giant plesiosaur *Kronosaurus*. *Breviora* 112: 1–15.

Rowe, T., Rich, T.H., Vickers-Rich, P., Springer, M., and Woodburne, M.O. 2008. The oldest platypus and its bearing on divergence timing of the platypus and echidna clades. *PNAS* 1054: 1238–1242.

Russell, D.A. 1967. Systematics and morphology of American mosasaurs (Reptilia: Sauria). *Bulletin of the Peabody Museum of Natural History, Yale University* 23: 1–240.

Sachs, S. 2004. Redescription of *Woolungasaurus glendowerensis* (Plesiosauria: Elasmosauridae) from the Lower Cretaceous of Northeast Queensland. *Memoirs of the Queensland Museum* 49: 713–731.

Sachs, S. 2005. *Tuarangisaurus australis* sp. nov. (Plesiosauria: Elasmosauridae) from the Lower Cretaceous of Northeastern Queensland, with addional notes on the phylogeny of the Elasmosauridae. *Memoirs of the Queensland Museum* 50: 425–440.

Sachs, S., and Grant-Mackie, J.A. 2003. An ichthyosaur fragment from the Cretaceous of Northland, New Zealand. *Journal of the Royal Society of New Zealand* 33: 307–314.

Sachs, S. and Kear, B.P. 2015. Postcranium of the paradigm elasmosaurid plesiosaurian *Libonectes morgani* (Welles, 1949). *Geological Magazine* 152: 649-710.

Sachs, S., Kear, B.P., and Everhart M.J. 2013. Revised vertebral count in the "longest-necked vertebrate" *Elasmosaurus platyurus* Cope 1868, and clarification of the cervical-dorsal transition in Plesiosauria. *PLoS ONE* 8(8): e70877.

Sachs, S., Schubert, S., and Kear, B.P. 2014. Note on a new plesiosaur (Reptilia: Sauropterygia) skeleton from the upper Pliensbachian (Lower Jurassic) of Bielefeld, northwest Germany. *Berichte Naturwissenschaftlicher Verein für Bielefeld und Umgegend* 52: 26–35.

Salisbury, S.W., Molnar, R.E., Frey, E., and Willis, P.M. 2006. The origin of modern crocodyliforms: new evidence from the Cretaceous of Australia. *Proceedings of the Royal Society, Series B* 273: 2439–2448.

Sato, T. 2005. A new polycotylid plesiosaur (Reptilia: Sauropterygia) from the Upper Cretaceous Bearpaw Formation of Saskatchewan, Canada. *Journal of Palaeontology* 79: 969–980.

Sato, T., and Storrs, G.W. 2000. An early polycotylid plesiosaur (Reptilia, Sauropterygia) from the Cretaceous of Hokkaido, Japan. *Journal of Paleontology* 74: 907–914.

Sato, T., Li, C., and Wu, X.C. 2003. Restudy of *Bishanopliosaurus youngi* Dong 1980, a freshwater plesiosaurian from the Jurassic of Chongqing. *Vertebrata PalAsiatica* 41: 18-33.

Scanlon, J.D., and Hocknull, S.A. 2008. A dolichosaurid lizard from the latest Albian (mid-Cretaceous) Winton Formation, Queensland, Australia. Pp. 131-136 in: Everhart, M.J. (ed). Proceedings of the Second Mosasaur Meeting. *Transactions of the Kansas Academy of Science, Fort Hays Studies Special Issue* 3, 172 pp.

Schmeisser McKean, R. 2012. A new species of polycotylid plesiosaur (Reptilia: Sauropterygia) from the Lower Turonian of Utah: extending the stratigraphic range of *Dolichorhynchops*. *Cretaceous Research* 34: 184–199.

Smith, E.T. 2010. Early Cretaceous chelids from Lightning Ridge, New South Wales. *Alcheringa* 34: 375–384.

Smith, E.T., and Kear, B.P. 2013. *Spoochelys ormondea* gen. et sp. nov., an archaic meiolaniid-like turtle from the Lower Cretaceous of Lightning Ridge, Australia. Pp. 277-287 in: Brinkman, D., Holroyd, P., and Gardner, J. (eds), Morphology and Evolution of Turtles. Springer, Dordrecht: The Netherlands, 577 pp.

Smith, N.D., Makovicky, P.J., Agnolin, F.L., Ezcurra, M.D., Pais, D.F., and Salisbury, S.W. 2008. A *Megaraptor*-like theropod (Dinosauria: Tetanurae) in Australia: support for faunal exchange across eastern and western Gondwana in the Mid-Cretaceous. *Proceedings of the Royal Society B* 275: 2085–2093.

Teichert, C., and Matheson, R. 1944. Upper Cretaceous ichthyosaurian and plesiosaurian remains from Western Australia. *Australian Journal of Science* 6: 167–178.

Thulborn, T., and Turner, S. 1993. An elasmosaur bitten by a pliosaur. *Modern Geology* 18: 489–501.

Thulborn, T., and Turner, S. 2003. The last dicynodont: an Australian Cretaceous relict. *Proceedings of the Royal Society of London, Series B* 270: 985–993.

Wade, M. 1984. *Platypterygius australis*, an Australian Cretaceous ichthyosaur. *Lethaia* 17: 93–113.

Wade, M. 1985. *Platypterygius australis* (McCoy) 1867: a Cretaceous marine reptile. Pp. 137–142 in: Rich, P., and Van Tets, G. (eds), Kadimakara. Princeton University Press: Princeton, 284 pp.

Wade, M. 1990. A review of the Australian Cretaceous longipinnate ichthyosaur *Platypterygius* (Ichthyosauria, Ichthyopterygia). *Memoirs of the Queensland Museum* 28: 115–137.

Welles, S.P. 1962. A new species of elasmosaur from the Aptian of Colombia, and a review of the Cretaceous plesiosaurs. *University of California Publications in Geological Sciences* 44: 1–96.

White, T.E. 1935. On the skull of *Kronosaurus queenslandicus* Longman. *Occasional Papers of the Boston Society of Natural History* 8: 219–228.

Wieland, G.R. 1896. *Archelon ischyros*: a new gigantic cryptodire testudinate from the Pierre Cretaceous of South Dakota. *American Journal of Science* 2: 399–412.

Wood, R., Grove, C.J., Gaffnet, E.S., and Maley, K.F. 1996. Evolution and phylogeny of leatherback turtles (Dermochelydae), with descriptions of new fossil taxa. *Chelonian Conservation and Biology* 2: 266–286.

Wretman, L., and Kear, B.P. 2014. Bite pathologies on an ichthyodectiform fish skull from Australia: evidence of trophic interaction in an Early Cretaceous marine ecosystem. *Alcheringa* 38: 170–176.

Zammit, M. 2010. A review of Australasian ichthyosaurs. *Alcheringa* 34: 281–292.

Zammit, M. 2012. Cretaceous ichthyosaurs: dwindling diversity, or the empire strikes back? *Geosciences* 2: 11–24.

Zammit, M., and Kear, B.P. 2011. Healed bite marks on a Cretaceous ichthyosaur. *Acta Palaeontologica Polonica* 56: 859–863.

Zammit, M., Norris, R., and Kear, B.P. 2010. The Australian Cretaceous ichthyosaur *Platypterygius australis*: a description and review of postcranial remains. *Journal of Vertebrate Paleontology* 30: 1726–1735.

Zammit, M., Kear, B.P., and Norris, R. 2014. Locomotory capabilities in the Early Cretaceous ichthyosaur *Platypterygius australis* based on osteological comparisons with extant marine mammals. *Geological Magazine* 151: 87–99.

Memoirs of Museum Victoria 74: 29–48 (2016) Published 2016

ISSN 1447-2546 (Print) 1447-2554 (On-line)
http://museumvictoria.com.au/about/books-and-journals/journals/memoirs-of-museum-victoria/

A new specimen of *Valdosaurus canaliculatus* (Ornithopoda: Dryosauridae) from the Lower Cretaceous of the Isle of Wight, England

Paul M. Barrett

Department of Earth Sciences, The Natural History Museum, Cromwell Road, London SW7 5BD, UK
(p.barrett@nhm.ac.uk)

Abstract

Barrett, P.M. 2016. A new specimen of *Valdosaurus canaliculatus* (Ornithopoda: Dryosauridae) from the Lower Cretaceous of the Isle of Wight, England. *Memoirs of Museum Victoria* 74: 29–48.

The anatomy of *Valdosaurus canaliculatus* is incompletely known and until recently was based exclusively upon the holotype femora. Additional discoveries from the Wessex Formation (Barremian) of the Isle of Wight during the past decade have considerably expanded the amount of material available and offered insights into the morphology of the vertebral column and pelvis. However, all of these specimens consist primarily of hind limb material. Here, I describe a newly discovered individual of this taxon, the most complete yet found, which was found in articulation and includes a partial dorsal series, an almost complete tail, pelvic material, and both hind limbs. Although the specimen is partially crushed it offers new information on the anatomy of *Valdosaurus*, facilitating comparisons with other dryosaurid taxa.

Keywords

Wealden, Dinosauria, Wessex Formation, Barremian

Introduction

The Wessex Formation of the Isle of Wight (UK) has yielded a rich Early Cretaceous (Barremian) dinosaur fauna (Martill and Naish, 2001) that includes four well-established ornithopod taxa: the non-iguanodontian *Hypsilophodon foxii* (Huxley, 1869), the dryosaurid *Valdosaurus canaliculatus* (Galton, 1975) and the ankylopollexians *Mantellisaurus atherfieldensis* (Hooley, 1925) and *Iguanodon bernissartensis* Boulenger in Beneden, 1881. It is possible that other taxa, represented by isolated but potentially distinctive material, were also present (Galton, 2009) and other names have been proposed for Wessex Formation iguanodontian taxa (e.g. Hulke, 1879, 1882; Lydekker, 1888; Paul, 2008; Carpenter and Ishida, 2010), but these are currently regarded either as nomina dubia or as junior synonyms of the aforementioned taxa (Norman, 2004, 2012; McDonald, 2012).

Hypsilophodon, *Mantellisaurus* and *Iguanodon* are known on the basis of complete or near-complete specimens from the Isle of Wight and other Early Cretaceous strata in the UK and elsewhere in western Europe: each has been the focus of numerous studies, including comprehensive monographs (e.g. Hulke, 1882; Hooley, 1925; Galton, 1974; Norman, 1980, 1986). By contrast, *Valdosaurus* is relatively poorly known. This taxon was established on the basis of an associated pair of small femora (Galton, 1975), but the collection of new specimens and reinterpretation of historical collections has expanded both the amount and quality of material available (Galton, 2009; Barrett et al., 2011) to comprise four previously reported partial skeletons. Other dryosaurid material is also known from the Wessex Formation of the Isle of Wight and the Tunbridge Wells Sands Formation (Valanginian) and Weald Clay Subgroup (Barremian) of southern England, some of which may be referable to *Valdosaurus* (Blows, 1998; Naish and Martill, 2001; Galton, 2009; Barrett et al., 2011; pers. obs.). Unusually, all previously described specimens consist almost exclusively of hind limb elements, with sporadic preservation of material from the axial column and pelvic girdle (Barrett et al., 2011: BELUM K17051; IWCMS 2007.4; MIWG.6438, MIWG.6879; NHMUK PV R184, R185). Here, I describe a new specimen of *Valdosaurus* from the Wessex Formation of the Isle of Wight, the most complete yet found, and discuss its implications.

Institutional abbreviations

BELUM, Ulster Museum (National Museums of Northern Ireland), Belfast, UK; BMB, Booth Museum, Brighton, UK; IWCMS (formerly MIWG, note that both sets of abbreviations still in use), Dinosaur Isle, Sandown, UK; MUCPv, Universidad Nacional del Comahue, Paleovertebrate Collection, Lago Barreales, Argentina; NHMUK, Natural History Museum, London, UK; NMV, Museum Victoria, Melbourne, Australia.

Material

The specimen (IWCMS 2013.175) was discovered by Mr Nick Chase in October 2012, in a plant debris bed (sensu Sweetman and Insole, 2010) cropping out from a cliff on a National Trust owned property in Compton Bay, on the southwest coast of the Isle of Wight. As other dinosaur material was discovered nearby, the exact locality details are withheld to prevent theft from the site, but are held on file at IWCMS. The skeleton was excavated from the Wessex Formation (Lower Cretaceous: Barremian; Allen and Wimbledon, 1991; Rawson, 2006), a sequence of terrestrial mudstones and sandstones deposited by rivers and lakes on a seasonally arid floodplain that was subject to seasonal wildfires (Martill and Naish, 2001).

IWCMS 2013.175 comprises a partial postcranial skeleton representing the hindquarters of a single individual. The specimen was found in situ within the plant debris bed and in articulation (fig. 1). It consists of six middle-posterior dorsal vertebrae (the only part of the specimen found weathered out at the surface), the sacrum, an articulated series of 45 caudal vertebrae (including chevrons in the anterior part of the tail), both pelvic girdles, and both hind limbs (lacking many of the pedal phalanges, but otherwise complete). Ossified tendons are also present in the sacral and caudal regions. Although surface collected, the proximity and characteristics of the dorsal vertebrae clearly demonstrate that they pertain to the same individual. Most parts of the skeleton have been fully prepared, but matrix has been retained around the sacroiliac block, obscuring many details of the sacrum and the medial surfaces of the ilia. In addition, as the pelvic girdles and proximal parts of the femora are articulated, these elements often overlie each other preventing full description.

As the hind limb anatomy of *Valdosaurus* has already been described in detail on the basis of several other specimens (Galton, 1975, 2009; Barrett et al., 2011: BELUM K17051; IWCMS 2007.4; MIWG.6438, MIWG.6879; NHMUK PV R184, R185), and as those of IWCMS 2013.175 are rather poorly preserved in spite of their completeness, the following description focuses on those areas of the anatomy that were previously unknown or poorly documented for *Valdosaurus*, primarily the axial column and pelvic girdle.

The specimen can be referred to *Valdosaurus canaliculatus* on the basis of the following femoral characters, which are currently regarded as either autapomorphic or part of a unique character combination for the taxon (Barrett et al., 2011): the anterior trochanter extends dorsally to almost the same level as the greater trochanter; and the left femur possesses an anterior intercondylar groove that is broad, parallel-sided and 'U'-shaped (although crushing has partially closed the groove). Moreover, the combined presence of a proximally placed fourth trochanter and of a deep anterior intercondylar groove is unique for *Valdosaurus* among the ornithopods currently known from the Wealden Group of the UK (Galton, 1975, 2009; Barrett et al., 2011).

All measurements for IWCMS 2013.175 can be found in Tables 1–5.

Description

Dorsal Vertebrae. A series of six middle-posterior dorsal (D) vertebrae is present, all of which are completely prepared and visible in all views. With the exception of two conjoined vertebrae, they were not found in articulation, but can be arranged into a series on the basis of size that suggests they did originally form a natural sequence. The following numbering scheme labels each of the vertebrae from 1 (anterior-most) to 6 (posterior-most), as arranged in the exhibition mount. There are no indications of any tendons along the dorsal series, but this observation is tentative due to the fragmentary nature of the neural arches and the exposure of the vertebrae at the surface prior to collection.

None of the vertebrae are complete, although each centrum is present (see table 1 for measurements). All six dorsals have been sheared and somewhat distorted, with the neural arch (where present) rotated relative to the centrum. The left-hand sides of all six centra are damaged: those of D1 and 2 bear indentations on their left lateral surfaces, whereas in D3–6 this entire surface is either crushed inward or poorly preserved. Some parts of the centra in D4–6 are missing. All of the dorsals preserve small parts of the neural arch. The position of the neurocentral junction can be seen in several of the vertebrae, but it is unclear whether it was open or partially fused. As D1 is the best preserved of the series most of the following description is derived from this vertebra, but this has been augmented with details from the other dorsals where possible (fig. 2).

D1 consists of a complete centrum, with a partial neural arch that is lacking all of the processes (fig. 2A–F). The arch has been rotated relative to the centrum, so that it is displaced to the right. The course of the neurocentral suture is clearly visible on the right-hand side though it is not clear if it is still open or partially fused. In anterior view, the articular surface has a subcircular outline, with a straight dorsal margin and rounded lateral and ventral margins that meet along a continuous smooth curve. The articular surface is shallowly concave and bordered by a raised rim on all sides. In lateral view, the centrum is elongate, approximately 1.9 times as long as it is high and has a ventral margin that is gently concave dorsally. The lateral surface of the centrum is anteroposteriorly concave and dorsoventrally convex and is pierced by a small

Table 1. Measurements (in mm) of the dorsal (D) vertebrae of *Valdosaurus canaliculatus* (IWCMS 2013.175). Abbreviations: ACH, anterior centrum height ACW, anterior centrum width; CL, centrum length; PCH, posterior centrum height; PCW, posterior centrum width. '*' indicates that the measurement as been affected by deformation.

	ACW	ACH	CL	PCW	PCH
D1	35	31	58	32	32
D2	39	34	58	39	39
D3	41	37	60	38*	42
D4	38*	41*	64	41*	47*
D5	47*	42*	59	46	50
D6	44*	44*	58*	49*	56*

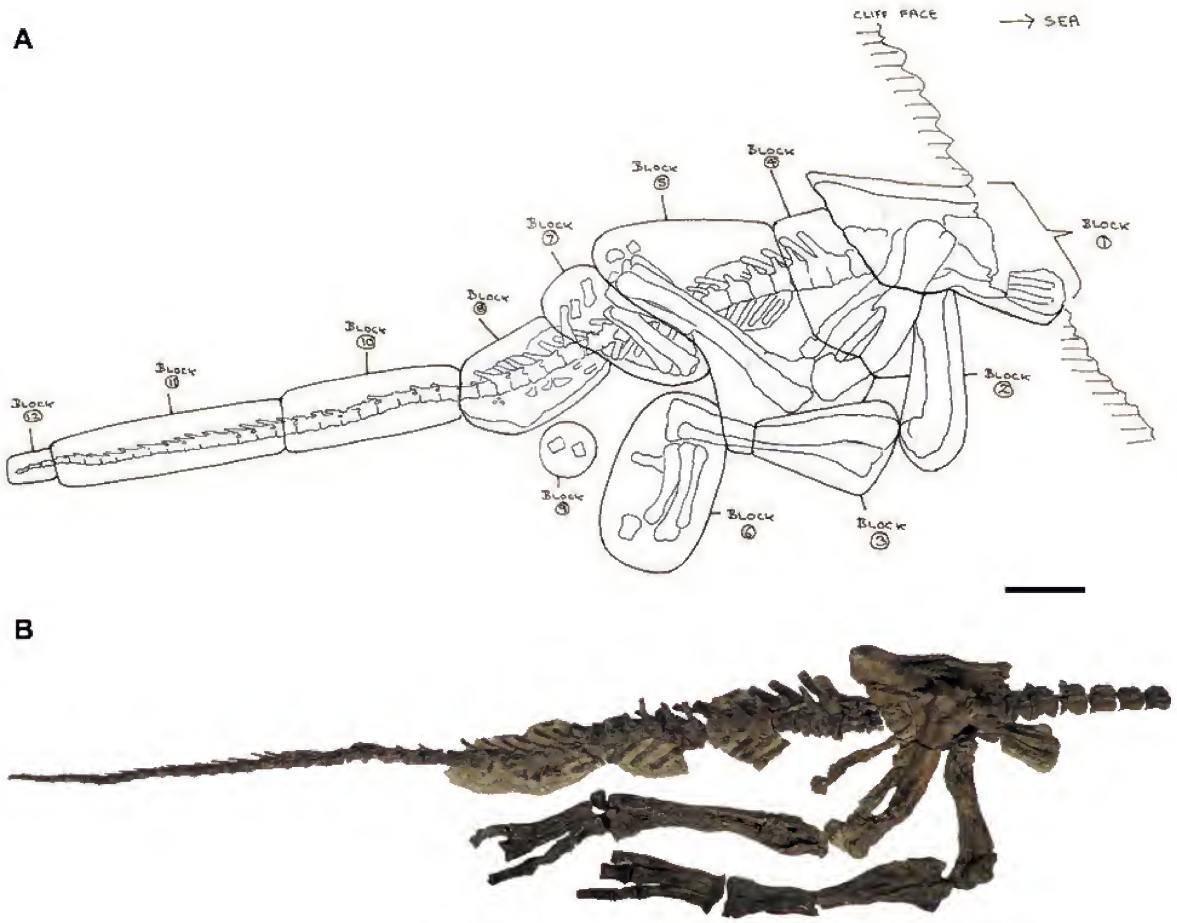

Figure 1. New specimen of *Valdosaurus canaliculatus* (IWCMS 2013.175). A, field map of the discovery showing the position of the skeleton in situ and the blocks in which the elements were originally excavated. Drawn by N. Chase, original on file at IWCMS. B, skeleton following preparation, as displayed in Dinosaur Isle, in left lateral view. Scale bars = 200 mm.

elliptical nutrient foramen at midlength. The lateral surfaces merge smoothly with the ventral surface and there is no distinct break of slope or ridge to separate them. In ventral view, the centrum is hourglass-shaped: there is some suggestion of a ventral keel, but this has probably been accentuated by mild crushing. Prominent longitudinally oriented striations extend along the lateral and ventral surfaces of the centrum from their junctions with the anterior and posterior surfaces. The posterior articular surface is also subcircular in outline, though the articular surface is flat, rather than concave.

The neural arch extends for almost the full length of the centrum. Crushing and breakage obscure much of the morphology of the processes and of the neural canal outline. However, it can be determined that a thin lamina extended posteriorly from the lateral margin of the prezygapophysis towards the diapophysis (prezygodiapophyseal lamina: PRDL; lamina terminology follows Wilson, 1999). The PRDL and anterior centrodiapophyseal lamina (ACDL) together frame a deep, anterolaterally facing prezygopophyseal centrodiapophyseal fossa (prcdf; fossa terminology follows Wilson et al., 2011) with a subelliptical outline in lateral view. There is no sign of a parapophysis on the centrum or on the ACDL, so this structure must have merged with the (missing) diapophysis. A thick, buttress-like posterior centrodiapophyseal lamina (PCDL) is also present, which with the ACDL frames a shallow, laterally facing and extensive centrodiapophyseal fossa (cdf). The PCDL merges with the base of the diapophysis to give the latter a triangular cross-section, whose apex points ventrally. A very small, elliptical spinoprezygapophyseal fossa (sprf) is present at the base of the anterior surface of the neural spine. The broken base of the neural spine indicates that it was mediolaterally compressed and plate-like. A postzygodiapophyseal lamina

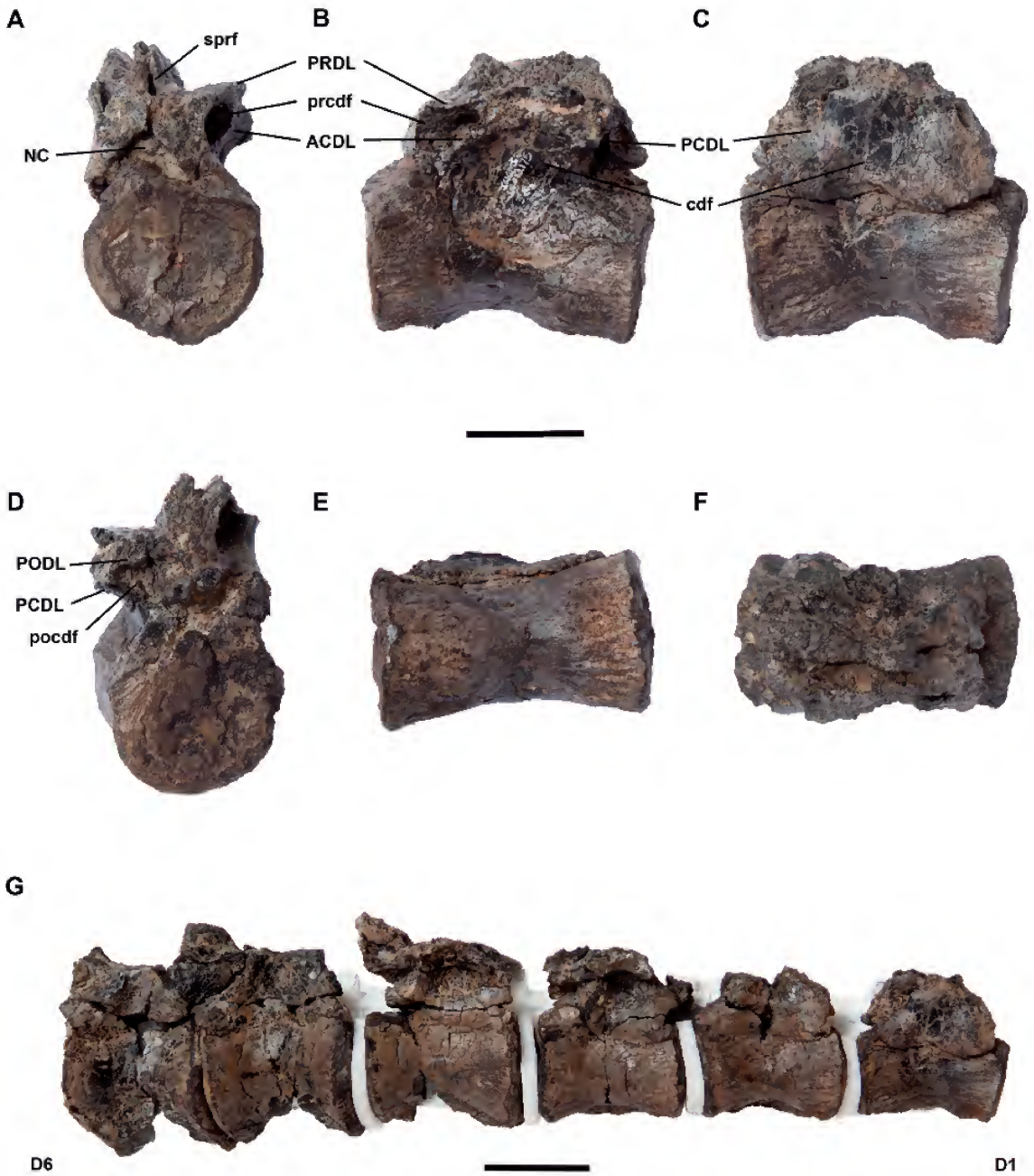

Figure 2. Dorsal vertebrae of *Valdosaurus canaliculatus* (IWCMS 2013.175). A–F, dorsal 1 in A, anterior, B, left lateral, C, right lateral, D, posterior, E, ventral, and F, dorsal views. G, dorsals 1–6 in articulation in left lateral view. Abbreviations: ACDL, anterior centrodiapophyseal lamina; cdf, centrodiapophyseal fossa; NC, neural canal; PCDL, posterior centrodiapophyseal lamina; pocdf, postzygopophyseal centrodiapophyseal fossa; PODL, postzygodiapophyseal lamina; prcdf, prezygopophyseal centrodiapophyseal fossa; PRDL, prezygodiapophyseal lamina; sprf, spinoprezygapophyseal fossa. Scale bars = 25 mm (A–F) and 50 mm (G).

Table 2. Measurements (in mm) of the caudal (Cd) vertebrae of *Valdosaurus canaliculatus* (IWCMS 2013.175). Abbreviations: ACH, anterior centrum height ACW, anterior centrum width; CL, centrum length; PCH, posterior centrum height; PCW, posterior centrum width. '*' indicates that the measurement as been affected by deformation. Many measurements are missing as obscured by articulation or matrix or too deformed to be useful (all measurements in the cases of Cd13–14 and Cd18).

	ACW	ACH	CL	PCW	PCH
Cd1	40*	45*	60	48*	49*
Cd2	-	-	54*	-	-
Cd3	49*	53*	50*	52*	50*
Cd4	49*	51*	54*	34	45
Cd5	36*	-	46*	-	57
Cd6	-	44	52	-	44
Cd7	-	39	60*	32*	42*
Cd8	-	-	56	-	-
Cd9	-	-	54	-	-
Cd10	-	-	50	-	-
Cd11	-	-	47	-	-
Cd12	-	-	48	-	-
Cd13	-	-	-	-	-
Cd14	-	-	-	-	-
Cd15	-	27	45	-	-
Cd16	-	30	53	-	-
Cd17	-	32	52	-	-
Cd18	-	-	-	-	-
Cd19	-	-	47	-	-
Cd20	-	27	49	-	-
Cd21	33	30	52	31	31
Cd22	32	30	52	35	32
Cd23	32	29	52	32	29
Cd24	32	27	50	33	27
Cd25	32	26	49	37*	33*
Cd26	35	28	52	34	27
Cd27	32	24	50	32	26
Cd28	29	24	49	31	25
Cd29	30	24	48	30	25
Cd30	30	25	48	29	24
Cd31	30	23	45	29	23
Cd32	31	21	45	29	22
Cd33	21	20	43	22	21
Cd34	27	20	43	25	21
Cd35	27	18	41	25	19
Cd36	23	20	42	24	19
Cd37	22	17	43	21	17
Cd38	22	16	40	21	18
Cd39	21	16	40	20	16
Cd40	19	14	38	17	14
Cd41	17	14	39	16	14
Cd42	15	15	36	16	13
Cd43	12	12	36	13	11
Cd44	14	13	34	13	13
Cd45	14	13	34	12	13

(PODL) also appears to have been present, framing a posterolaterally opening postzygopophyseal centrodiapophyseal fossa (pocdf) with the PCDL. Although broken, the posterior part of the arch dorsal to the neural canal bears a small inverted 'Y'-shaped process that extends ventral to the broken bases of the postzygapophyses.

D2 consists of the centrum and a poorly preserved, incomplete neural arch that lacks any indications of processes or laminae other than the right PCDL (fig. 2G). As far as can be determined, D2 is identical to D1 in almost every respect, although the anterior articular surface is flat rather than concave. D3 consists of a complete centrum and partial neural arch. Deformation of the centrum is severe and the entire left-hand side is crushed inward, which has created a pseudo-keel along the ventral surface. As far as can be determined, the centrum and neural arch is identical to that of D1 and 2. As in D1, the ACDL and PCDL are present and frame a shallow cdf. There is some evidence for a PODL that frames a posteriorly opening and deep pocdf with the PCDL. The bases of both diapophyses are present, which are angled dorsolaterally with respect to the centrum, but the angle between them has been exaggerated by deformation. D4 is almost identical to D3 in terms of the parts preserved and the features that can be assessed.

D5 and 6 each consists of a centrum and partial neural arch (fig. 2G). The vertebrae are larger than the preceding ones and are less elongate (length to height ratio of ~1.3). The longitudinal striations on the lateral surfaces of the centra are less prominent than in the earlier dorsals. In all other respects, however, the centra are similar to those of the other dorsals (with flat articular surfaces, no keel, an hourglass-shaped outline in ventral view, no distinct separation between the lateral and ventral surfaces, single small nutrient foramen, etc.). D5 and 6 possess a buttress-like ACDL that is less distinct that those of earlier dorsals, whereas the PCDL remains a clear and distinct lamina in all preserved dorsals. Their prominent PCDL forms the posterior margin of a deep subtriangular cdf and the anterior margin of a smaller, but deep pocdf posteriorly. The dorsal margin of the pocdf is provided by a prominent PODL. The postzygapophyses of D5 are partially preserved but are largely obscured by the overlapping prezygapophyses of D6. They appear to be very steeply inclined forming an angle of almost 80° with the horizontal plane in anterior view. The prezygapophyses of D6 only overlap the postzygapophyses of D5 for a short distance and have narrow triangular transverse cross-sections.

Sacrum. Although the sacrum is present and likely complete, it is largely obscured by matrix and the adjacent ilia. In ventral view, a dorsosacral is exposed on the anterior part of the pelvic block and the posterior margin of a posterior sacral and the anterior part of the caudosacral (and associated sacral rib) can be seen posterior to the ischia. The posterior part of the caudosacral is articulated with the first caudal vertebra and is thus preserved separately from the pelvic block. The number of sacral vertebrae cannot be determined, but on the basis of the lengths of those that are visible it seems likely that at least five and potentially six were present (including those vertebrae identified as the dorso- and caudosacrals). As each vertebra is only partially visible in ventral view, the amount of anatomical

information is limited. All three vertebrae have transversely convex ventral surfaces that lack keels and longitudinal grooves. The dorsosacral is identified as such as it bears a short, anteroposteriorly narrow diapophysis that differs from the expanded morphology that would be expected in 'true' sacral ribs. This diapophysis extends laterally to contact the medial surface of the preacetabular process of the ilium. By contrast, a large, fan-shaped sacral rib is borne by the posterolateral corner of the exposed posterior sacral and the anterolateral corner of the caudosacral. The medial part of the rib is anteroposteriorly narrow, but flares within a short distance to form a broad, subtriangular and dorsally convex sheet whose scalloped lateral margin articulates with the ilium along almost the full length of the brevis shelf.

Caudal vertebrae. Forty-five caudal (Cd) vertebrae are present and it seems likely that almost the whole tail was preserved, with the loss of only a few (if any) very small distal-most vertebrae (see table 2 for measurements). Some of the vertebrae have been fully prepared (Cd1–4), while others are partially embedded in blocks of matrix and exposed in one view only. The proximal caudals (Cd1–4) have suffered the most deformation, mainly mild crushing and mediolateral shearing, and have crazed bone surfaces. Nevertheless, they are largely complete and the middle and posterior caudals are very well preserved. Many of the vertebrae are still in articulation: consequently, some individual details are obscured by the presence of other vertebrae in the series.

Cd1 and 2 are in the same block as the posterior part of the caudosacral (fig. 3A, B). As a result the posterior surface of the caudosacral and the anterior and posterior articular surfaces of Cd1 and the anterior surface of Cd2 are obscured. The right-hand sides of the vertebrae are obscured by the overlying posterior process of the left ilium, which is adhered to this block and separated from the rest of the left ilium.

The centra have ventrally concave margins in lateral view and the lateral surfaces are anteroposteriorly concave and dorsoventrally convex. The longitudinal striations present on the lateral surfaces of the dorsal vertebrae are absent, but the crazed bone surface prevents determination of the presence/absence of nutrient foramina. The lateral surfaces are distinctly separated from the ventral surfaces by a break in slope and there is some indication of a ventral groove on both Cd1 and 2. The visible parts of the articular surfaces suggest that they were very shallowly convex. Poor preservation prevents identification of the neurocentral sutures. There is no evidence for a chevron facet on Cd1, but a posterior facet is present on Cd2. This chevron facet is a flat, subtrapezoidal surface, which is indented on the ventral midline.

The neural arches are reasonably complete, but some details are obscured by matrix, deformation and the apposition of the ilium and caudosacral. The prezygapophyses of Cd2 (missing in Cd1) are short, stout triangular processes that only extend a short distance beyond the anterior margin of the centrum. In both Cd1 and 2, the caudal ribs are broken, with only the remnants of the bases present. The neural spines are inclined posteriorly and dorsally, so that their posterior margins form an angle of approximately 45° with the horizontal. They are mediolaterally compressed, maintain the same mediolateral thickness along their entire length, are anteroposteriorly short, and are taller (as measured from the level of postzygapophyses to the tip of the spine) than their respective centra are long. They are slightly constricted in lateral view just above the level of the postzygapophyses and expand again slightly anteroposteriorly above this point. In lateral view, the neural spine of Cd1 extends to terminate posterior to the anterior margin of Cd3: the overlap between the neural spine and the next two vertebrae in the series continues throughout the proximal and middle sections of the tail. The spine of Cd1 is more expanded anteroposteriorly in its distal part than that of Cd2. The neural spine summits are gently rounded in lateral view. In contrast to the dorsal series, neural arch laminae are absent. Postzygapophyses are present in Cd1 (missing from Cd2) and are short, robust and have squat subtriangular transverse cross-sections.

Cd3 and 4 are in articulation, but their neural arches are slightly detached from their respective centra (fig. 3C). Deformation makes it difficult to assess the morphology, but there is some evidence that the lateral surfaces met along a grooved midline keel and there is no evidence for a distinct ventral surface. Both vertebrae possess a large posterior chevron facet (and the chevrons associated with Cd3 and 4 are preserved on the next block in the sequence). No obvious anterior chevron facets are present due to damage. In all other respects, the centra of Cd3 and 4 are identical to those of Cd1 and 2.

The neural arches are also identical to those of Cd1 and 2, but are better preserved. In lateral view, the neural spines expand slightly anteroposteriorly towards their apices and are more strongly posteriorly inclined than in Cd1 and 2 (at around 30° from the horizontal), but this orientation may have been accentuated by crushing. Both the pre- and postzygapophyses are small, subtriangular in cross-section, almost vertically inclined, and short so that neither extends far beyond the margins of the centrum. The caudal ribs are preserved but deformed: they appear to have been inclined laterally, dorsally and slightly posteriorly. All are incomplete distally, but the caudal ribs were dorsoventrally flattened plates that were anteroposteriorly short and tapered slightly as they extended laterally. The anterior margin of the caudal rib is thickened relative to its posterior margin. At the base of the caudal rib this thickening is more marked and helps to define a shallow excavation on its proximoventral surface. This thickened leading edge could be regarded as an ACDL as it is continuous with the centrum.

Cd5–7 are visible in left lateral view only as they are embedded in a block, although the anterior and posterior surfaces of Cd5 and Cd7, respectively, are exposed (fig. 3C). The same block also includes the chevrons for Cd3–6. As in Cd1–4, the caudals are deformed due to mediolateral shear and torsion and their surfaces are crazed, but the shearing is less marked than in Cd1–4, so more details are visible. The centra are essentially identical to those in the preceding vertebrae, but are better preserved and only minor differences are noted here. The visible articular surfaces of the centra are subelliptical (but deformed) and shallowly concave. In contrast to earlier caudals, the neurocentral sutures are visible and appear to be open. A small anterior and large posterior chevron facet is present in Cd6 and 7. The very narrow ventral surface is separated from the lateral surfaces by a distinct break in slope and bears a marked

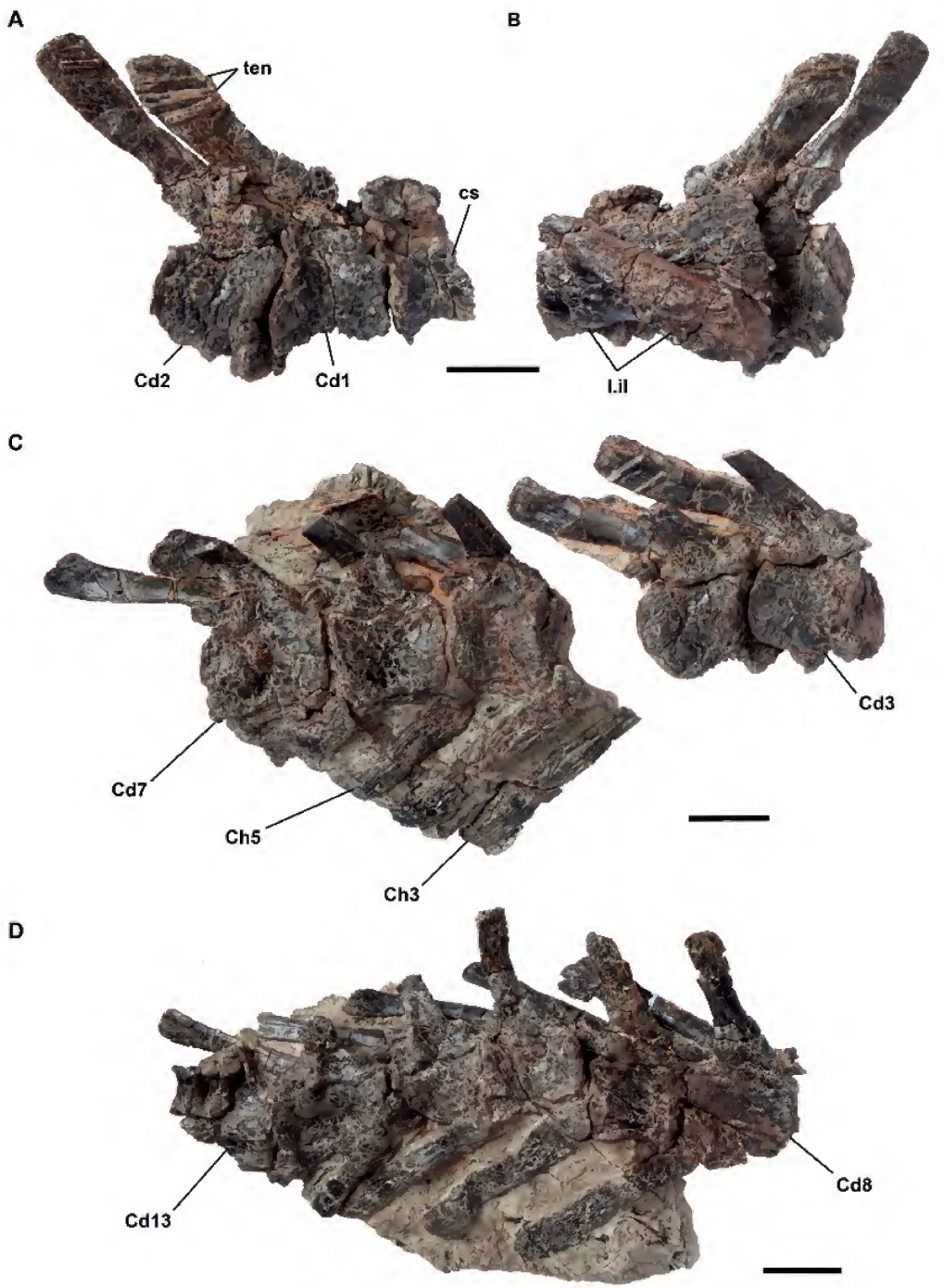

Figure 3. Proximal caudal vertebrae of *Valdosaurus canaliculatus* (IWCMS 2013.175). A–B, caudosacral plus caudals 1 and 2 in right (A) and left (B) lateral views. Note that the postacetabular process of the left ilium is attached to caudals 1 and 2. C, caudal vertebrae 3–7 in right lateral view. D, caudal vertebrae 8–13 in right lateral view. Abbreviations: Cd, caudal vertebra; Ch, chevron; Cs, caudosacral vertebra; l.il, left ilium; ten, ossified tendons. Scale bars = 50 mm.

Figure 4. Middle caudal vertebrae of *Valdosaurus canaliculatus* (IWCMS 2013.175). A, caudal vertebrae 14–20 in right lateral view. B–G, caudal vertebra 21 in right lateral (B), left lateral (C), anterior (D), posterior (E), ventral (F) and dorsal (G) views. Abbreviations: Cd, caudal vertebra; Ch, chevron. Scale bars = 50 mm (A) and 25 mm (B–G).

longitudinal groove. There are no significant differences in the morphology of the neural arches between Cd1–4 and Cd5–7 that cannot be accounted for by deformation or damage.

The next block in the caudal sequence contains Cd8–13 (though only the anterior part of Cd13, which is poorly preserved, with the remainder of this vertebra in the next block in the caudal sequence) (fig. 3D). In terms of overall morphology, these vertebrae are smaller versions of Cd5–7 and only differences from the latter are noted here. Cd8–13 are mainly visible in left lateral view and have suffered crushing so that the caudal ribs have been rotated upwards to extend parallel to the neural spines. The left caudal ribs of Cd8 and Cd10 are complete, demonstrating that they terminate in bluntly squared-off distal tips. The fossae present on the proximoventral surfaces of the caudal ribs of Cd1–8 become less prominent from Cd9 onwards and are absent from Cd12 and all subsequent caudal vertebrae. Ventral grooves on the centra are present in Cd8–10, but their presence/absence in Cd11–13 is not determinable due to the orientation in which these vertebrae are preserved.

A clear break in morphology occurs between Cd12/13 and Cd14/15 and the Cd13/14 boundary is regarded here as the transition point from the proximal to the middle caudal series. Cd14–20 are preserved in sequence in lateral view within a single block of matrix (with the posterior part of Cd13 at its anterior end), although Cd14 is not well preserved and Cd18 is slightly disarticulated from the other vertebrae, with its anterior end extending into the block (fig. 4A). Cd15–20 are much better preserved than any of the preceding caudals. An isolated phalanx from the right pes is also present in this block, overlying the chevron associated with Cd14.

Figure 5. Middle caudal vertebrae of *Valdosaurus canaliculatus* (IWCMS 2013.175). A–C, caudal vertebrae 22–25 in right lateral (A), ventral (B) and dorsal (C) views (caudal 22 is to the right in each case). D–F, caudal vertebrae 26–29 in right lateral (D), ventral (E) and dorsal (F) views (caudal 26 is to the right in each case). G, detail of caudal vertebrae 27 and 28 in left lateral view showing bundles of ossified tendons. Abbreviation: Cd, caudal vertebra. Scale bars = 50 mm.

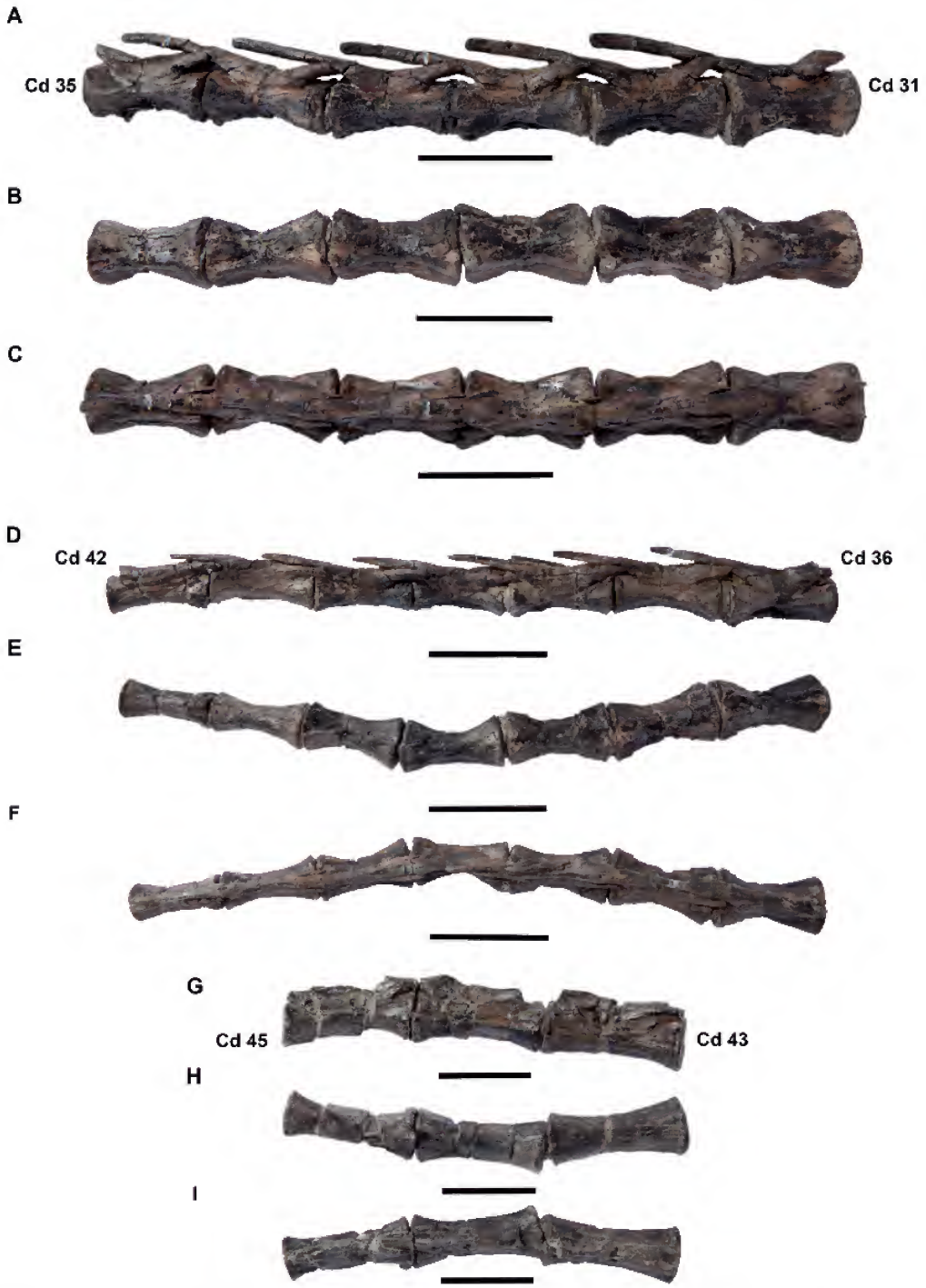

Figure 6. Distal caudal vertebrae of *Valdosaurus canaliculatus* (IWCMS 2013.175). A–C, caudal vertebrae 30–35 in right lateral (A), ventral (B) and dorsal (C) views (caudal 30 is to the right in each case). D–F, caudal vertebrae 36–42 in right lateral (D), ventral (E) and dorsal (F) views (caudal 36 is to the right in each case). G–I, caudal vertebrae 43–45 in right lateral (G), ventral (H) and dorsal (I) views (caudal 43 is to the right in each case). Abbreviation: Cd, caudal vertebra. Scale bars = 25 mm.

The centra of Cd14–20 are more elongate and spool-like than those of the preceding caudals (ratio of centrum length to height >1.6 in middle caudals whereas in proximal caudals this ratio is <1.6 and often closer to 1.0). The lateral surfaces are longitudinally concave and dorsoventrally convex, but the ventral, anterior and posterior surfaces are generally obscured and many details are not visible. Well-defined, but small, posterior chevron facets are present, but the anterior chevron facets are harder to distinguish. Cd19–20 exhibit an incipient longitudinal ridge, which extends along the full length of the centrum lateral surface, at centrum midheight.

The neural arches of the middle caudals differ from those of proximal caudals in several respects. For example, caudal ribs appear to be completely absent from Cd14 onwards. Also, the prezygapophyses of Cd14–20 are reduced in length and no longer extend beyond the anterior margins of the centrum. The postzygapophyses are no longer separate processes, but have become small facets that are positioned on the base of the neural spine. In contrast to the preceding vertebrae, the neural spines become almost parallel-sided in lateral view (whereas there is some anteroposterior expansion in the distal part of the spine in proximal caudals), and curve dorsally along their length. Together with the short prezygapophyses the neural spines form a unified, curved and scimitar-shaped structure in lateral view.

Cd21 is fully prepared out and separated from the rest of the caudals (fig. 4B–G); Cd22–25 and Cd26–29 are also fully prepared, but as two articulated series (fig. 5). Cd21–29 are well preserved and are either complete or missing only small parts of the neural spine summit. All of these vertebrae share most of the features seen in Cd14–20, but exhibit new anatomical details and/or reveal morphological trends along the tail. The centra of Cd27–29 are more elongate than those preceding, with centrum length/height ratios of >2.0. Where exposed, anterior and posterior articular surfaces of Cd21–25 are shield-shaped, shallowly concave and subequal in their mediolateral and dorsoventral dimensions. However, in Cd26–29 the anterior and posterior articular surfaces have a more hexagonal outline. This change is due to stronger development of the longitudinally extending ridges on the lateral surfaces of the centra in the latter vertebrae. These lateral ridges, which were incipiently present in Cd19–20, exhibit a progressive increase in prominence from Cd21–29. They divide the lateral surfaces of Cd21–29 into separate dorsal and ventral excavations. In Cd21 the lateral ridge is at centrum midheight, but the position of the ridge moves dorsally in Cd22–29 to a position around one-third of the distance from the dorsal margin of the centrum. A small, elliptical nutrient foramen is variably present on the lateral surfaces of the centra in Cd21–29. In addition, all of these vertebrae also bear faint longitudinal striations that extend for short distances along the lateral surfaces from their junctions with the anterior and posterior articular surfaces. In ventral view, the centra are spool-like and constricted at midlength. A distinct groove is present along the ventral midline, bounded by low, sharp ridges. A remnant of the anterior chevron facet is present in Cd21, represented by a small bevelled surface, but is absent from Cd22 onward. A distinct posterior facet is present in Cd21–29, but reduces in size through the series. The posterior chevron facet is bifurcated ventrally by the ventral midline groove giving it a 'W'-shaped outline.

The neural arches of Cd21–29 are almost identical to those of Cd14–20 and the neural spines remain very elongate, although from Cd23 onwards the orientation of the spine changes, to form an angle of only ~15° with the horizontal (in contrast to ~30° in the preceding caudals). From Cd22 onward, the postzygapophyses are reduced to indistinct facets on the neural spine.

Cd30–45 represent the distal caudals (fig. 6). They are all fully prepared and generally well preserved (although Cd43–45 lack neural spines) and are grouped into several articulated series (Cd30–35, Cd36–42 and Cd43–45). Although similar to the middle caudals in many respects, they can be distinguished from them on the basis of several features. For example, the trend toward vertebral elongation continues, with centrum length/height ratios of ~2.7–3.0 in the posterior-most vertebrae (e.g. Cd42–45). The ventral groove present on the centra of the middle caudals is present in Cd30–35, but is reduced to a short notch that bifurcates the ventral margin of the posterior chevron facet from Cd36–40. Posterior chevron facets and ventral grooves are both absent from Cd41 onward. Cd36–40 retain the hexagonal transverse cross-section and particular surface outlines present in the middle caudal vertebrae, but the lateral ridge extending along the centrum reduces in prominence and disappears from Cd41 onward. As a result, the centra of Cd41–45 possess a simplified, spool-like morphology in which the lateral and ventral surfaces are smoothly excavated and continuous with each other.

Perhaps the most obvious difference between the middle and distal caudal vertebrae is a progressive reduction in the length and prominence of the neural spine: from Cd30 onward, the neural spine extends no further posteriorly than the posterior margin of the successive vertebra (rather than extending beyond this point, as in the more anterior caudals: see above). In Cd36–42 this trend continues, with the neural spine terminating at a point only halfway along the next caudal in the series. As the prezygapophyses and neural spines are present as distinct processes in Cd43–45, it is likely that several more distal vertebrae would have been present in vivo, as in other dinosaurs with complete tails the terminal vertebra lacks neural arch structures and tapers to a blunt point lacking an articular surface (Hone, 2012).

Chevrons. With the exceptions of those associated with Cd4 and Cd8 (which are visible in anterior view), the chevrons articulated with the proximal caudals (Cd3–13) are visible in lateral view only (fig. 3D). The chevron for Cd14 is too poorly preserved to offer any useful information. Measurements of selected chevrons are provided in table 3. In anterior view, the chevrons have a 'Y'-

Table 3. Measurements (in mm) of selected chevrons (Ch) of *Valdosaurus canaliculatus* (IWCMS 2013.175). '*' indicates that the measurement as been affected by breakage.

	Chevron length
Ch8	116
Ch9	111
Ch15	51
Ch16	37*

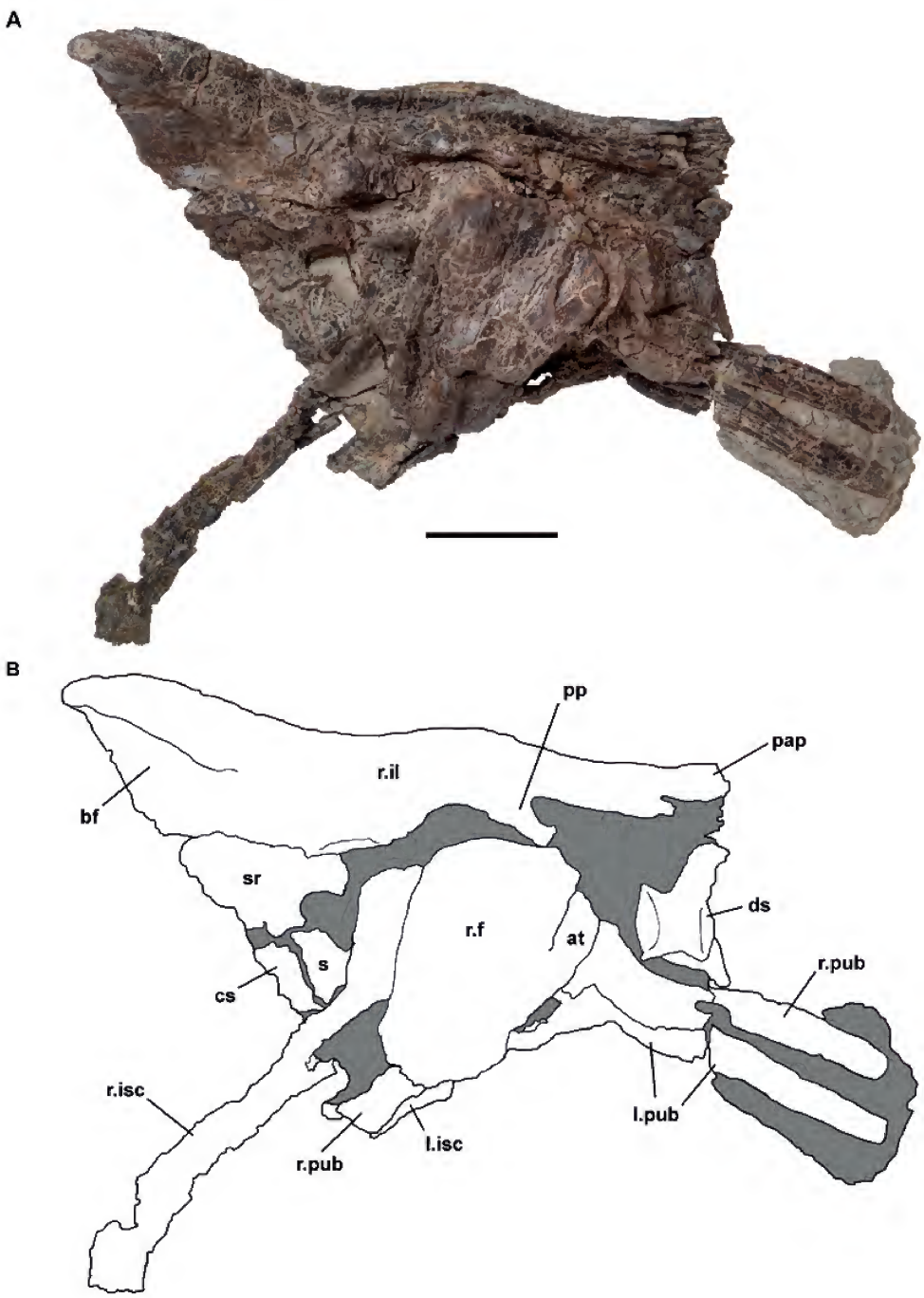

Figure 7. Partially articulated pelvic girdle of *Valdosaurus canaliculatus* (IWCMS 2013.175) in right lateral view. Note that majority of the right femur and adhered left ischium have been removed for clarity. Photograph (A) and interpretative diagram (B). Abbreviations: at, anterior trochanter; bf, brevis fossa; cs, caudosacral; ds, dorsosacral; l.isc, left ischium; l.pub, left pubis; pap, preacetabular process; pp, pubic peduncle; r.f, right femur; r.il, right ilium; r.isc, right ischium; r.pub, right pubis; s, sacral vertebra; sr, sacral rib. Scale bar = 100 mm.

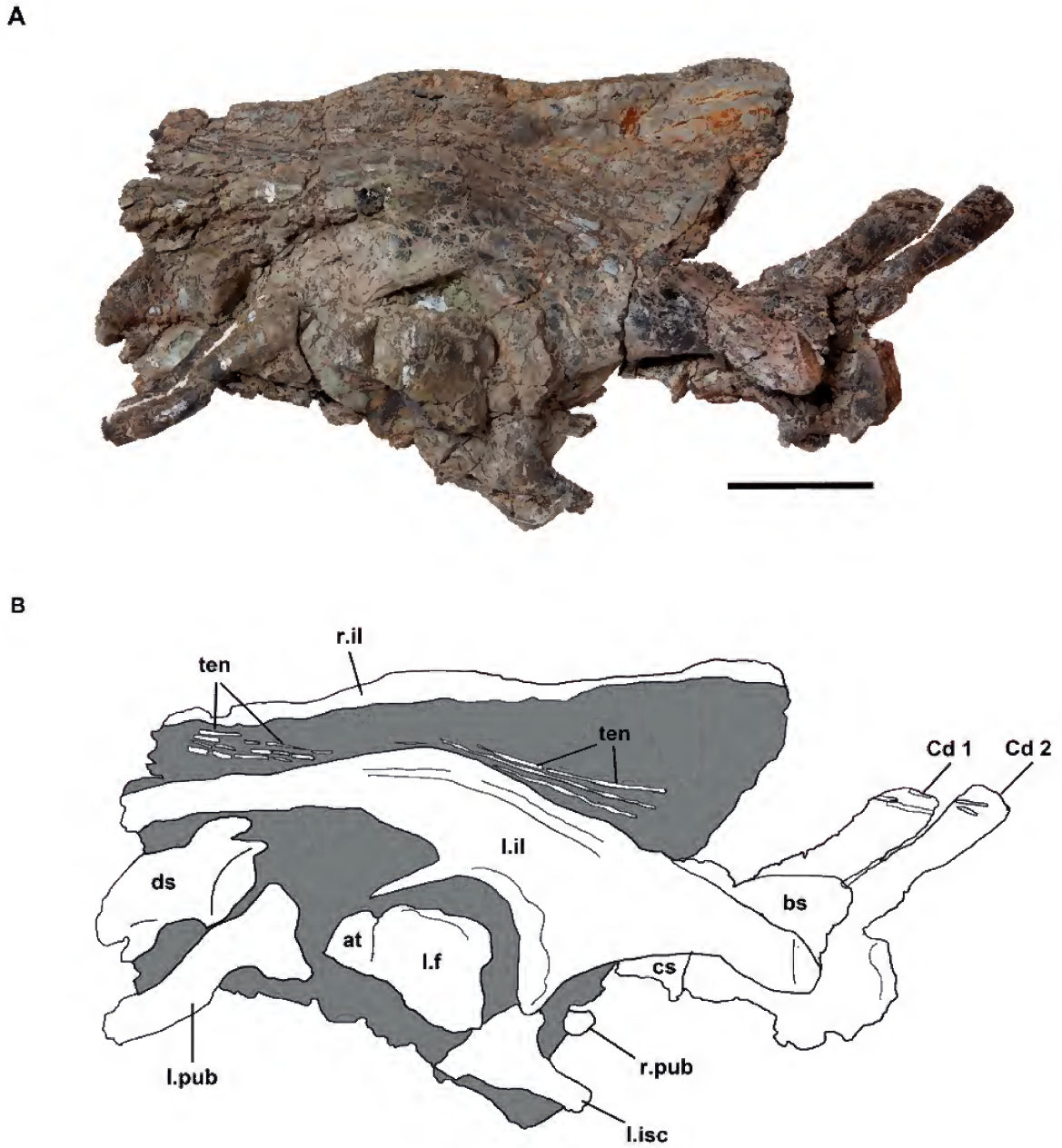

Figure 8. Left pelvic girdle and articulated proximal caudal vertebrae of *Valdosaurus canaliculatus* (IWCMS 2013.175) in left lateral view. Note that majority of the left femur has been removed for clarity. Photograph (A) and interpretative diagram (B). Abbreviations: at, anterior trochanter; bs, brevis shelf; Cd, caudal vertebra; cs, caudosacral; ds, dorsosacral; l.f, left femur; l.il, left ilium; l.isc, left ischium; l.pub, left pubis; r.il, right ilium; r.pub, right pubis; ten, ossified tendons. Scale bar = 100 mm.

shaped morphology, with the proximal branches enclosing a short, narrow and triangular haemal canal that is closed dorsally. The haemal canal is recessed within a shallow fossa that extends for approximately 30% of total chevron length. Ventral to the haemal canal the chevron shaft extends as a thin vertical strut. In dorsal view, the articular surface of the chevron has a dumbbell-shaped outline that is mediolaterally concave.

In lateral view, the chevrons associated with Cd3–11 are straight, parallel-sided rods, whose shafts possess no constrictions or expansions along their length and that terminate in bluntly rounded ventral margins. They are very elongate, reaching up to 2.0 times the length of their associated centrum where complete (e.g. those associated with Cd8–9). The chevrons articulated with Cd12–13 possess a subtly different morphology in lateral view, in which the distal-most end of the shaft becomes slightly expanded anteroposteriorly relative to the rest of the shaft.

Chevrons associated with the middle caudal series (Cd15–18: the chevron for Cd17 is missing) differ in morphology from those in the proximal part of the tail (fig. 4A). In lateral view, they are reduced in length relative to the proximal caudals and are approximately equal in length to their respective centra. The distal ends of the chevron shafts are anteroposteriorly expanded relative to their proximal portions: most of this expansion occurs posteriorly to form an asymmetrical distal flange with a subtriangular outline. Numerous fine striations are present on the ventrolateral surfaces of these expanded flanges. No chevrons are preserved posterior to Cd18, but the presence of posterior chevron facets up to Cd40 indicates they were present for most of the length of the tail.

Ossified tendons. Fragments of numerous ossified tendons are either adhered to the neural spines of the caudal vertebrae or found in the matrix adjacent to the tail along its entire length. These vary between 1.5 and 5 mm in diameter and some have a circular cross-section, while that of others is flattened (figs. 3A, 5G). Those tendons that are preserved in their natural orientations (e.g. those preserved alongside Cd26–29) extend subparallel to each other, and the overlapping trellis-like arrangement seen in ankylopollexian ornithopods (e.g. Norman, 1980, 1986) was absent.

Ilium. Both ilia are substantially complete and preserved in articulation with the sacrum and femoral heads, though each is only visible in lateral view (figs. 7, 8). The right ilium is lacking the anterior-most part of the preacetabular process, has been slightly crushed, and its brevis fossa has been artificially enlarged by plastic deformation (fig. 7). By contrast, the left ilium is well preserved and undeformed, but has been broken so that its postacetabular process is associated with Cd1 and 2 and is not currently attached to the sacral block (fig. 8).

The ilium is long and low, with the dorsoventral distance between the dorsal rim of the acetabulum relatively short in comparison to overall iliac length (ratio of height above acetabulum to total length of the left ilium is 0.17). The dorsal margin of the ilium is slightly sinuous in outline, due to the downturning of the preacetabular process in combination with a dorsally convex margin over the pubic peduncle, a slightly concave margin over the ischiadic peduncle, and a strongly concave dorsal margin of the postacetabular process. The preacetabular process extends almost anteriorly in the right ilium, but anteroventrally in the left ilium: as the latter is less deformed this is considered to be closer to the original morphology. The preacetabular process is strap-like in lateral view, and has parallel dorsal and ventral margins. It is incomplete anteriorly in both ilia. The ventral margin of the preacetabular process and the anterior margin of the pubic peduncle are separated by a deep, concave sulcus.

The pubic peduncle has a thin, elongate subtriangular outline in lateral view and is anteroposteriorly narrow. It has a subtriangular transverse cross-section, with the apex of this triangle pointing laterally and is considerably smaller than the ischiadic peduncle. The lateral surface of the iliac body dorsal to the acetabulum was shallowly concave both dorsoventrally and anteroposteriorly, with this concavity accentuated by deformation in the right ilium. Neither ilium possesses a distinct supraacetabular flange. In lateral view, the dorsal margin of the acetabulum describes a low, gentle curve and is not strongly arched. The ischiadic peduncle has a stout subtriangular outline and is pyramidal in shape. Both the pubic and ischiadic peduncles appear to have extended for the same distance ventrally.

The postacetabular process is elongate and bears an extensive brevis fossa, which faces ventrally in the left ilium and ventrolaterally in the deformed right ilium. The fossa is separated from the lateral surface of the postacetabular process by a robust anteroventrally extending ridge that merges with the posterior margin of the ischiadic peduncle. The fossa was not visible in lateral view in the left ilium, but has been exposed by deformation in the right ilium. In ventral view, the brevis fossa is very strongly flared laterally and expands posteriorly to form an equilateral triangle-shaped flange in ventral view. In lateral view, the dorsal margin of the iliac body is slightly thickened mediolaterally, but it is not folded to form an antitrochanter. This area bears numerous short striations indicative of muscular attachment (for the M. iliotibialis: e.g. Norman, 1986; Maidment and Barrett, 2011). A shallow groove extends parallel to the dorsal margin of the ilium along the central part of the iliac body in lateral view. It is not clear if this groove is a natural feature or due to deformation, but it is present in both ilia.

A large and well-preserved bundle of ossified tendons is present in the matrix between the ilia, which extend parallel to each other and do not form a trellis-like arrangement (fig. 8). Measurements of both ilia are presented in table 4.

Table 4. Selected measurements (in mm) of the pelvic elements of *Valdosaurus canaliculatus* (IWCMS 2013.175). Abbreviations: L, left; R, right. '*' indicates damaged or deformed.

Ilium	
Total ilium length	410 (L) 390* (R)
Height of iliac body above acetabulum	70 (L) 52* (R)
Length of postacetabular process	135 (L) 170* (R)
Maximum transverse width of postacetabular process	90 (L) 120* (R)
Pubis	
Length of prepubic process (as preserved)	195 (L) 220 (R)

Figure 9. Selected hind limb elements of *Valdosaurus canaliculatus* (IWCMS 2013.175). A, left femur in lateral view (proximal end missing as attached to pelvic block). B, articulated left tibia, fibula, astragalus and calcaneum in posterior view. C, right calcaneum in lateral view. D, right metatarsus in anterior view. E, left metatarsus in anterior view. Scale bars = 100 mm (A, B, D, E) and 25 mm (C).

Pubis. The proximal parts of each pubis are present, but it is unclear how much of the postpubic processes might extend into the matrix that encases most of the sacral block. The prepubic processes are elongate, strap-like and extended beyond the anterior margin of the preacetabular process of the ilium in lateral view (see table 4 for measurements) (figs. 7, 8). They have subparallel dorsal and ventral borders and do not expand distally, but end in a bluntly rounded terminus. The prepubic processes are mediolaterally-compressed plates, with rounded dorsal and ventral margins in transverse cross-section. Prominent depressions that extend along the lateral surface of the right prepubis and medial surface of the left prepubis are probably due to crushing. More posteriorly, the prepubes curve ventrally then dorsally as they merge into the main body of the pubis, but this may be a preservational artefact.

The pubic body is expanded relative to the plate-like prepubis, is anteroposteriorly short and block-like and bears a strongly convex surface for articulation with the ischium and ilium. The pubic contribution to the acetabulum was relatively small. An open obturator notch was present, but was partially enclosed posteriorly by a ventral projection from the posterior articular surface of the pubic body. The proximal part of the postpubic rod is cylindrical in cross-section.

Ischium. Both ischia are present, but the proximal ends are obscured by the overlying femora and by matrix and the shafts are friable and poorly preserved (figs. 7, 8). The left ischial shaft is attached to the right femur, whereas the right ischial shaft is free. The right ischium has a fan-shaped proximal plate, whose iliac articulation is visible in lateral and dorsal views. The articular surface is oval in outline and mediolaterally expanded relative to the rest of the exposed part of the proximal plate. The shaft arises from the posteroventral corner of the proximal plate. There is no indication of a groove along the dorsal margin of the proximal part of the shaft, which is smooth and rounded. The presence/absence of an obturator process cannot be determined due to breakage. In lateral view, the ischial shafts are straight, extend posteroventrally from the proximal plate and have parallel dorsal and ventral margins. There is no sign of any ventral curvature, although both ischia are incomplete distally so its absence might be artefactual. The shafts are mediolaterally compressed. It is not possible to determine the extent of any symphysis between them due to breakage and poor surface preservation.

Table 5. Selected measurements (in mm) of the hind limb elements of *Valdosaurus canaliculatus* (IWCMS 2013.175). Abbreviations: L, left; R, right. '*' indicates damaged or deformed.

Femoral length	460* (L)	499* (R)
Tibia length	562* (L)	555* (R)
Distal width of tibia	102 (L)	121* (R)
Fibula length	510* (L)	505* (R)
Length of fibula proximal end	88 (L)	– (R)
Fibula midshaft diameter	20 (L)	21 (R)
Mediolateral width of astragalus	83 (L)	90 (R)
Dorsoventral height of calcaneum	- (L)	51 (R)
Mediolateral width of calcaneum	- (L)	24 (R)
Metatarsal II length	199 (L)	200 (R)
Metatarsal II proximal width	27 (L)	26 (R)
Metatarsal II midshaft diameter	14 (L)	12 (R)
Metatarsal II distal width	29 (L)	29 (R)
Metatarsal III length	239 (L)	247 (R)
Metatarsal III proximal width	- (L)	46* (R)
Metatarsal III midshaft diameter	34 (L)	43* (R)
Metatarsal III distal width	52 (L)	52 (R)
Metatarsal IV length	195 (L)	221* (R)
Metatarsal IV proximal width	57* (L)	29 (R)
Metatarsal IV midshaft diameter	35 (L)	35 (R)
Metatarsal IV distal width	29 (L)	28 (R)

Hind limb. Although they are almost complete, the hind limbs of IWCMS 2013.175 provide no new anatomical information. Some elements, such as the femora, tibiae and fibulae are crushed, deformed and possess poor surface preservation, although the proximal tarsals, metatarsi and pedal elements are well preserved (fig. 9). As far as can be determined, all of these elements are identical to those of other recently described specimens of *Valdosaurus* (see Barrett et al., 2011). Measurements for all hind limb elements are presented in table 5.

Both femora are complete, but each is preserved in two parts, with the proximal part of the bone in articulation with each acetabulum (figs. 7, 8) and the distal part prepared separately (fig. 9A). The right femur is adhered to the left ischial shaft. *Valdosaurus* possesses several diagnostic femoral characteristics: 1) a deep cleft between the anterior and greater trochanters that is visible in both medial and anterior views; 2) a scar for the M. caudofemoralis that is placed close to the base of the fourth trochanter; 3) a 'U'-shaped anterior intercondylar groove that is deeply incised into the femur with near parallel sides; and 4) the proximal end of the anterior trochanter of the femur is level with, or only slightly ventral to, the proximal end of the greater trochanter (Barrett et al., 2011). Unfortunately, it is not possible to assess the presence or absence of characters 1) and 2) in IWCMS 2013.175 due to damage, but characters 3) and 4) are present, supporting referral to *Valdosaurus canaliculatus* (see above). It appears that the anterior intercondylar groove was partially closed by a lip of bone arising from the medial condyle, as occurs in other large individuals (Galton, 2009; Barrett et al., 2011).

The tibiae are also complete, but preserved in several sections. The left tibia is preserved in two parts (fig. 9B): a proximal part comprising the proximal expansion and two-thirds of the shaft and a distal part consisting of the rest of the shaft, which articulated with the distal part of the left fibula, the left astragalus and a fragment of the left calcaneum. The right tibia is also preserved in two sections: the small proximal section is in articulation with the proximal region of the right fibula, while the larger distal section, comprising around three-quarters of the length of the bone, is articulated with the distal fibula shaft and the right astragalus. The proximal ends of both tibiae are very poorly preserved: that of the right tibia is

flattened, while that of the left tibia has experienced both crushing and strong torsion, although all three of the major proximal processes (cnemial crest, inner and outer condyles) can be identified. Torsion has caused the cnemial crest of the left tibia to extend laterally rather than anteriorly.

Both fibulae are almost complete and each is preserved in two sections with small sections of the shaft missing. The proximal end of the left fibula is generally well preserved, but has been crushed mediolaterally, whereas the distal part of the shaft is extensively cracked and warped. By contrast, the proximal end of the right fibula is poorly preserved and extensively crushed, but the shaft is more three-dimensional. A small contact was present between the distal fibula and the astragalus.

In general, the proximal tarsals are well preserved and undeformed. Both astragali are present and in articulation with their respective tibiae. The left calcaneum is also in articulation with the left tibia, but is broken and incomplete, whereas the complete right calcaneum has become separated from the rest of the right ankle (fig. 9C). The only differences between these elements and those previously described for *Valdosaurus* are that the medial surfaces of the calcanea, which form the articulation for the astragalus, are strongly rugose and that the articular surfaces for the distal tarsals for both the astragali and calcanea are slightly corrugated, in contrast to the smooth surfaces present in other specimens referred to this taxon (Barrett et al., 2011).

Both metatarsi, comprising metatarsals (Mt) 2–4, are preserved in articulation and each metatarsal is complete (fig. 9D, E). The left metatarsus has suffered some minor deformation, but has good surface preservation; the right is slightly crushed, but also in good condition. A distal tarsal is articulated with the proximal surface of the left metatarsus and positioned primarily over Mt3, but also partially overlaps the proximal surfaces of Mt2 and Mt4. It has an elliptical outline and concave proximal surface. Mt2 and Mt3 are closely appressed along their entire lengths, whereas Mt4 is kinked laterally at a point about halfway along its length so its distal end diverges slightly from that of Mt3 (both conditions are present in both metatarsi). There is no evidence for the presence of a first or fifth metatarsal in either foot.

Several non-ungual phalanges are preserved, though they were not found in articulation with the metatarsals. Several are very well preserved and are uncracked and undistorted: it is possible that these are associated with the similarly well-preserved left metatarsus. Conversely, the other more heavily cracked and crushed phalanges might pertain to the slightly crushed right metatarsus. Preserved phalanges (Ph) include both PhII.1 and one PhIII.1. Several other phalanges are also present, but their positions within the pes cannot be determined.

Discussion

The anatomy of dryosaurids is poorly known: all known taxa are represented by either isolated femora (*Callovosaurus*, *Elrhazosaurus*), partial skeletons (*Dryosaurus*, *Eousdryosaurus*, *Kangnasaurus*, *Valdosaurus*), or bonebed material that is disarticulated and lacks some key skeletal elements (*Dysalotosaurus*) (see Janensch, 1955; Shepherd et al., 1977; Galton, 1975, 1981, 1983, 1989, 2009; Galton and Taquet, 1982; Cooper, 1985; Blows, 1998; Ruiz-Omeñaca et al., 2007; Hübner and Rauhut, 2010; Barrett et al., 2011; Escaso et al., 2014). Thus, the new specimen reported herein not only increases the amount of anatomical information available for *Valdosaurus*, but also provides some information that might be more generally applicable for the clade as a whole.

IWCMS 2013.175 confirms the validity of a previously proposed autapomorphy for *Valdosaurus*: the presence of an open obturator notch on the pubis (Barrett et al., 2011). Other dryosaurids for which the pubis is known (*Dryosaurus*, *Dysalotosaurus*) have a closed notch (Janensch, 1955; Galton, 1981). One new feature of the tail is proposed herein as a potential autapomorphy of *Valdosaurus*: the presence of elongate neural spines in the middle of the caudal series that extend to reach over more than one subsequent vertebra (fig. 5D). This condition appears to be absent in *Kangnasaurus* (although on the basis of fragmentary material: Cooper, 1985) and is absent in non-iguanodontian ornithopods like *Hypsilophodon* (NHMUK OR28707; NHMUK PV R196), *Tenontosaurus* (Forster, 1990), rhabdodontids (Weishampel et al., 2003) and ankylopollexians (Norman, 1986). It is difficult to assess this character in *Dryosaurus* due to damage, but the orientation of the preserved bases of the neural spines suggests that they might have been more vertically inclined and thus might not have extended beyond the posterior margin of the succeeding vertebra (Galton, 1981). Unfortunately this feature cannot be assessed in *Callovosaurus*, *Dysalotosaurus*, *Elrhazosaurus* or *Eousdryosaurus* due to incomplete preservation (Janensch, 1955; Galton and Taquet, 1982; Ruiz-Omeñaca et al., 2007; Escaso et al., 2014).

IWCMS 2013.175 enables comparisons with other taxa that were not previously possible. With the exception of the potentially autapomorphic middle caudal neural spines, the preserved axial column of IWCMS 2013.175 is generally similar to that of *Dryosaurus*, *Dysalotosaurus*, *Eousdryosaurus* and *Kangnasaurus* (Janensch, 1955; Galton, 1981; Cooper, 1985; Escaso et al., 2014). The neural arches of the proximal caudal vertebrae in *Eousdryosaurus* possess small, anteriorly projecting, "thorn-like" processes that have been proposed as diagnostic for this taxon (Escaso et al., 2014: 1104): these processes are absent in *Valdosaurus*. The distal ends of the middle caudal chevrons of *Valdosaurus* are anteroposteriorly expanded in lateral view (fig. 4A): although comparative material is lacking for other dryosaurids, similar chevrons are known in *Gasparinisaura* (Coria and Salgado, 1996; MUCPv-212), *Leaellynasaura* (NMV P185992, NMV P186047) and *Tenontosaurus* (Forster, 1990). Fortuitously, IWCMS 2013.175 possesses the most complete tail of any dryosaurid specimen described to date and demonstrates that *Valdosaurus* is likely to have possessed no more than 46–50 caudal vertebrae (fig. 1B). This number is similar to that seen in many other ornithopods (Norman, 2004; Norman et al., 2004), but much lower than those recorded for the exceptionally long tails of *Leaellynasaura* (>70 caudal vertebrae; Herne, 2009) and *Tenontosaurus* (60–65 caudal vertebrae: Forster, 1990).

The overall shape of the ilium in *Valdosaurus* (IWCMS 2013.175) falls within the range of variation seen in *Dryosaurus* and *Dysalotosaurus* (Janensch, 1955; Galton, 1981). In *Eousdryosaurus* the brevis fossa is exposed in lateral view (Escaso et al., 2014), but that of *Valdosaurus* is largely obscured and faces posteroventrally (fig. 8: the right ilium of IWCMS 2013.175 has a laterally open brevis fossa, but this has resulted from plastic deformation: see above). The ilia of *Eousdryosaurus*, some *Dryosaurus* individuals and of an indeterminate dryosaurid from the Tunbridge Wells Sands Formation of Cuckfield, UK (NHMUK OR2132) possess a straight dorsal margin in lateral view (Escaso et al., 2014). By contrast, those of *Dysalotosaurus*, *Valdosaurus* and two other indeterminate dryosaurid specimens from the Tunbridge Wells Sands Formation (BMB 004274; NHMUK OR2150) are gently sinuous (Janensch, 1955; Galton, 2009; see above). In *Valdosaurus*, BMB 00472 and NHMUK OR2150 the postacetabular processes are posterodorsally inclined (BMB 004274; NHMUK OR2150; Galton, 2009), whereas in NHMUK OR2131, this process extends posteriorly.

Escaso et al. (2014) proposed that the calcaneum of *Eousdryosaurus* could be distinguished from those of other dryosaurids on the basis of the rounded (rather than more sharply triangular) 'proximal projection', which comprises the triangular process that divides the facets for the tibia and fibula in lateral view. However, this process is similarly rounded in IWCMS 2013.175 (fig. 9C) and hence, this feature cannot be regarded as a reliable autapomorphy for *Eousdryosaurus*. Moreover, Escaso et al. (2014) also proposed that the calcaneum of *Valdosaurus* differed from that of other dryosaurids in possessing a distinct offset between the facets for the tibia and fibula in lateral view (with the tibia facet positioned more ventrally), whereas in other dryosaurids the facets were at the same level. However, this is not the case: if the calcanea are figured in their 'natural' orientations (i.e. as if in articulation with the distal tibia) the fibula facets in all of these taxa (including *Eousdryosaurus*) would be positioned somewhat dorsally relative to the level of the tibia facets, reflecting the shorter length of the fibula relative to the tibia in dryosaurids (Galton, 1981; Barrett et al., 2011; Escaso et al., 2014).

Finally, IWCMS 2013.175 enables the scoring of several phylogenetic characters for *Valdosaurus* that were unknown from other specimens and scored as missing data in the analyses of McDonald et al. (2010), Barrett et al. (2011) and Escaso et al. (2014). For example, it reveals the longitudinal (rather than basket-like) arrangement of ossified tendons along the vertebral column (McDonald et al., 2010: character 95[0]). Several iliac characters can also be scored: the preacetabular process of the ilium was not twisted along its length (McDonald et al., 2010: character 110[0]); the dorsal margin of the main iliac body is only slightly sinuous, rather than displaying the extreme sinuosity seen in more derived iguanodontians (McDonald et al., 2010: character 111[0]); and the dorsal margin of the iliac body dorsal to the ischial peduncle is smooth and lacks the development of any prominent processes (McDonald et al., 2010: character 112[0]). All of these character scores are identical to those present in *Dryosaurus* and *Dysalotosaurus* (McDonald et al., 2010; Barrett et al., 2011).

Conclusions

IWCMS 2013.175 is the most complete individual of *Valdosaurus canaliculatus* yet found and offers new information on the axial skeleton and pelvis of this poorly known iguanodontian ornithopod. Its discovery highlights the fact that *Valdosaurus* was a more common component of the Wessex Formation dinosaur fauna than usually thought. Frustratingly, all known individuals are represented by their hindquarters only, limiting comparisons with other dryosaurids. Additional discoveries of specimens that include both hind limb material and elements from the presacral region are now critical to enable further integration of *Valdosaurus* into both phylogenetic and palaeoecological scenarios.

Acknowledgements

This paper is dedicated to Thomas Rich in recognition of his work on the dinosaurs of the Australian Early Cretaceous, which were roaming Victoria around the time that *Valdosaurus* lived in the Northern Hemisphere. Tom has been generous with his time and material and has done much to illuminate the previously poorly known Cretaceous ecosystems in this region.

Numerous individuals and organisations contributed to the collection and preparation of the specimen, and I would like to express my sincere thanks to the following: the National Trust (owners of the locality) for donating the specimen to Dinosaur Isle; Nick Chase for his discovery of the specimen, leading role in its excavation and initial preparation; Steve Hutt, Penny Newbury and Jeremy Lockwood for their involvement in the excavation; and Gary Blackwell and Martin New for preparation of the specimen. I am extremely grateful to Alex Peaker for his continued assistance and hospitality at Dinosaur Isle, as well the provision of key information on the specimen. Martin Munt is thanked for bringing the specimen to my attention and for logistical support while working on the Isle of Wight. In addition to those already listed, a number of curators provided access to material in their care, including S. Hutt, J. Porfiri, M. Simms and T. Rich. Photographs were taken by Kevin Webb (NHM Image Resources) and the NHM Earth Sciences Departmental Investment Fund provided funding for travel. I thank referees Susannah Maidment and Andrew McDonald and editor Erich Fitzgerald for their helpful comments and the editor for the invitation to contribute to this volume.

References

Allen, P., and Wimbledon, W.A. 1991. Correlation of NW European Purbeck-Wealden (nonmarine Lower Cretaceous) as seen from the English type-areas. *Cretaceous Research* 12: 511–526.

Barrett, P.M., Butler, R.J., Twitchett, R.J., and Hutt, S. 2011. New material of *Valdosaurus canaliculatus* (Ornithischia: Ornithopoda) from the Lower Cretaceous of southern England. *Special Papers in Palaeontology* 86: 131–163.

Beneden, P.-J. van 1881. Sur l'arc pelvien chez les dinosauriens de Bernissart. Bulletins de l'Académie Royale des Sciences, des Lettres et des Beaux-Arts de Belgique, Classe des Sciences (Series 3) 1: 600–608.

Blows, W.T. 1998. A review of Lower and middle Cretaceous dinosaurs of England. *New Mexico Museum of Natural History and Science, Bulletin* 14: 29–38.

Carpenter, K., and Ishida, Y. 2010. Early and "middle" Cretaceous iguanodonts in time and space. *Journal of Iberian Geology* 36: 145–164.

Cooper, M.R. 1985. A revision of the ornithischian dinosaur *Kangnasaurus coetzeei* Haughton, with a classification of Ornithischia. *Annals of the South African Museum* 95: 281–317.

Coria, R.A., and Salgado, L. 1996. A basal iguanodontian (Ornithischia: Ornithopoda) from the Late Cretaceous of South America. *Journal of Vertebrate Paleontology* 16: 445–457.

Escaso, F., Ortega, F., Dantas, P., Malafaia, E., Silva, B., Gasulla, J.M., Mocho, P., Narváez, I., and Sanz, J.L. 2014. A new dryosaurid ornithopod (Dinosauria, Ornithischia) from the Late Jurassic of Portugal. *Journal of Vertebrate Paleontology* 34: 1102–1112.

Forster, C.A. 1990. The postcranial skeleton of the ornithopod dinosaur *Tenontosaurus tilletti*. *Journal of Vertebrate Paleontology* 10: 273–294.

Galton, P.M. 1974. The ornithischian dinosaur *Hypsilophodon* from the Wealden of the Isle of Wight. *Bulletin of the British Museum (Natural History), Geology* 25: 1–152.

Galton, P.M. 1975. English hypsilophodontid dinosaurs (Reptilia: Ornithischia). *Palaeontology* 18: 741–752.

Galton, P.M. 1981. *Dryosaurus*, a hypsilophodontid dinosaur from the Upper Jurassic of North America and Africa. Postcranial skeleton. *Paläontologische Zeitschrift* 55: 271–312.

Galton, P.M. 1983. The cranial anatomy of *Dryosaurus*, a hypsilophodontid dinosaur from the Upper Jurassic of North America and East Africa, with a review of hypsilophodontids from the Upper Jurassic of North America. *Geologica et Palaeontologica* 17: 207–243.

Galton, P.M. 1989. Crania and endocranial casts from ornithopod dinosaurs of the families Dryosauridae and Hypsilophodontidae (Reptilia: Ornithischia). *Geologica et Palaeontologica* 23: 217–239.

Galton, P.M. 2009. Notes on Neocomian (Lower Cretaceous) ornithopod dinosaurs from England – *Hypsilophodon*, *Valdosaurus*, "*Camptosaurus*", "*Iguanodon*" – and referred specimens from Romania and elsewhere. *Revue de Paléobiologie* 28: 211–273.

Galton, P.M. and Taquet, P. 1982. *Valdosaurus*, a hypsilophodontid dinosaur from the Lower Cretaceous of Europe and Africa. *Geobios* 15: 147–159.

Herne, M. 2009. Postcranial osteology of *Leaellynasaura amicagraphica* (Dinosauria: Ornithischia) from the Early Cretaceous of Southeastern Australia. *Journal of Vertebrate Paleontology* 29 (3, Supplement): 113A.

Hone, D.W.E. 2012. Variation in the tail length of non-avian dinosaurs. *Journal of Vertebrate Paleontology* 32: 1082–1089.

Hooley, R.W. 1925. On the skeleton of *Iguanodon atherfieldensis* sp. nov., from the Wealden Shales of Atherfield (Isle of Wight). *Quarterly Journal of the Geological Society of London* 81: 1–61 + pls 1–2.

Hübner, T.R., and Rauhut, O.W.M. 2010. A juvenile skull of *Dysalotosaurus lettowvorbecki* (Ornithischia: Iguanodontia), and implications for cranial ontogeny, phylogeny, and taxonomy in ornithopod dinosaurs. *Zoological Journal of the Linnean Society* 160: 366–396.

Hulke, J.W. 1879. *Vectisaurus valdensis*, a new Wealden dinosaur. *Quarterly Journal of the Geological Society of London* 35: 421–424 + pl. 21.

Hulke, J.W. 1882. Description of some Iguanodon remains indicating a new species, *I. seeleyi*. *Quarterly Journal of the Geological Society of London* 38: 135–144 + pl. 4.

Huxley, T.H. 1869. On *Hypsilophodon*, a new genus of Dinosauria. *Abstracts of the Proceedings of the Geological Society of London* 204: 3–4.

Janensch, W. 1955. Der Ornithopode *Dysalotosaurus* der Tendaguruschichten. *Palaeontographica, Supplement* 7: 105–176 + pls 9–14.

Lydekker, R. 1888. *Catalogue of the fossil Reptilia and Amphibia in the British Museum. Part I. Containing the orders Ornithosauria, Crocodilia, Dinosauria, Squamata, Rhynchocephalia and Proterosauria*. British Museum of Natural History: London. xii + 309 pp.

Maidment, S.C.R., and Barrett, P.M. 2011. The locomotor musculature of basal ornithischian dinosaurs. *Journal of Vertebrate Paleontology* 31: 1265–1291.

Martill, D.M., and Naish, D. 2001. The geology of the Isle of Wight. Pp. 25–43 in: Martill, D.M. and Naish, D. (eds), *Dinosaurs of the Isle of Wight (Palaeontological Association Field Guides to Fossils, 10)*. Palaeontological Association: London. 433 pp.

McDonald, A.T., Barrett, P.M., and Chapman, S.D. 2010. A new basal iguanodont (Dinosauria: Ornithischia) from the Wealden of England. *Zootaxa* 2569: 1–43.

McDonald, A.T. 2012. The status of *Dollodon* and other basal iguanodonts (Dinosauria: Ornithischia) from the Lower Cretaceous of Europe. *Cretaceous Research* 33: 1–6.

Naish, D., and Martill, D.M. 2001. Ornithopod dinosaurs. Pp. 60–132 in: Martill, D.M. and Naish, D. (eds), *Dinosaurs of the Isle of Wight (Palaeontological Association Field Guides to Fossils, 10)*. Palaeontological Association: London. 433 pp.

Norman, D.B. 1980. On the ornithischian dinosaur *Iguanodon bernissartensis* of Bernissart (Belgium). *Mémoire de l'Institut Royal des Sciences Naturelles de Belgique* 178: 1–104.

Norman, D.B. 1986. On the anatomy of *Iguanodon atherfieldensis* (Ornithischia: Ornithopoda). *Bulletin de l'Institut Royal des Sciences Naturelles de Belgique* 56: 281–372.

Norman, D.B. 2004. Basal Iguanodontia. Pp. 413–437 in: Weishampel, D.B., Dodson, P., and Osmólska, H. (eds), *The Dinosauria* (Second Edition). University of California Press: Berkeley. 861 pp.

Norman, D.B. 2012. Iguanodontian taxa (Dinosauria: Ornithischia) from the Lower Cretaceous of England and Belgium. Pp. 174–212 in: Godefroit, P. (ed.), *Bernissart dinosaurs and Early Cretaceous terrestrial ecosystems*. Indiana University Press: Bloomington and Indianapolis. 629 pp.

Norman, D.B., Sues, H.-D., Witmer, L.M., and Coria, R.A. 2004. Basal Ornithopoda. Pp. 393–412 in: Weishampel, D.B., Dodson, P., and Osmólska, H. (eds), *The Dinosauria* (Second Edition). University of California Press: Berkeley. 861 pp.

Paul, G.S. 2008. A revised taxonomy of the iguanodont dinosaur genera and species. *Cretaceous Research* 29: 192–216.

Rawson, P.F. 2006. Cretaceous: sea levels peak as the North Atlantic opens. Pp. 365–393 in: Brenchly, P.J., and Rawson, P.F. (eds), *The geology of England and Wales* (Second Edition). The Geological Society: London. 559 pp.

Ruiz-Omeñaca, J.I., Pereda Suberbiola, X., and Galton, P.M. 2007. *Callovosaurus leedsi*, the earliest dryosaurid dinosaur (Ornithischia: Euornithopoda) from the Middle Jurassic of England. Pp. 3–16 in: Carpenter, K. (ed.), *Horns and beaks: ceratopsian and ornithopod dinosaurs*. Indiana University Press: Bloomington and Indianapolis. xi + 369 pp.

Shepherd, J.D., Galton, P.M., and Jensen, J.A. 1977. Additional specimens of the hypsilophodontid dinosaur *Dryosaurus altus* from the Upper Jurassic of western North America. *Brigham Young University Geology Studies* 24: 11–15.

Sweetman, S.C., and Insole, A.N. 2010. The plant debris beds of the Early Cretaceous (Barremian) Wessex Formation of the Isle of Wight, southern England: their genesis and palaeontological significance. *Palaeogeography, Palaeoclimatology, Palaeoecology* 292: 409–424.

Weishampel, D.B., Jianu, C.-M., Csiki, Z., and Norman, D.B. 2003. Osteology and phylogeny of *Zalmoxes* (n. g.), an unusual euornithopod dinosaur from the latest Cretaceous of Romania. *Journal of Systematic Palaeontology* 1: 65–123.

Wilson, J.A. 1999. A nomenclature for vertebral laminae in sauropods and other saurischian dinosaurs. *Journal of Vertebrate Paleontology* 19: 639–653.

Wilson, J.A., D'Emic, M.D., Ikejiri, T., Moacdieh, E.M., and Whitlock, J.A. 2011. A nomenclature for vertebral fossae in sauropods and other saurischian dinosaurs. *PLoS ONE* 6(2): e17114 (doi:10.1371/journal.pone.0017114).

Memoirs of Museum Victoria 74: 49–61 (2016) Published 2016

ISSN 1447-2546 (Print) 1447-2554 (On-line)
http://museumvictoria.com.au/about/books-and-journals/journals/memoirs-of-museum-victoria/

Phylogenetic relationships of the Cretaceous Gondwanan theropods *Megaraptor* and *Australovenator*: the evidence afforded by their manual anatomy

Fernando E. Novas[1,2,*], Alexis M. Aranciaga Rolando[1] and Federico L. Agnolín[1,3]

[1] Museo Argentino de Ciencias Naturales, Avenida Ángel Gallardo 470, 1405DJR Buenos Aires, Argentina
[2] CONICET, Consejo Nacional de Investigaciones Científicas y Técnicas, Argentina
[3] Fundación de Historia Natural "Félix de Azara", Universidad Maimónides, Hidalgo 775, 1405BDB, Buenos Aires, Argentina
* To whom correspondence should be addressed. E-mail: fernovas@yahoo.com.ar

Abstract

Novas, F.E., Aranciaga Rolando, A.M. and Agnolín, F.L. 2016. Phylogenetic relationships of the Cretaceous Gondwanan theropods *Megaraptor* and *Australovenator*: the evidence afforded by their manual anatomy. *Memoirs of Museum Victoria* 74: 49–61.

General comparisons of the manual elements of megaraptorid theropods are conducted with the aim to enlarge the morphological dataset of phylogenetically useful features within Tetanurae. Distinctive features of *Megaraptor* are concentrated along the medial side of the manus, with metacarpal I and its corresponding digit being considerably elongated. Manual ungual of digit I is characteristically enlarged in megaraptorids, but it is also transversely compressed resulting in a sharp ventral edge. We recognize two derived characters shared by megaraptorans and coelurosaurs (i.e., proximal end of metacarpal I without a deep and wide groove continuous with the semilunar carpal, and metacarpals I and II long and slender), and one derived trait similar to derived tyrannosauroids (i.e., metacarpal III length <0.75 length of metacarpal II). However, after comparing carpal, metacarpal and phalangeal morphologies, it becomes evident that megaraptorids retained most of the manual features present in *Allosaurus*. Moreover, *Megaraptor* and *Australovenator* are devoid of several manual features that the basal tyrannosauroid *Guanlong* shares with more derived coelurosaurs (e.g., *Deinonychus*), thus countering our own previous hypothesis that Megaraptora is well nested within Tyrannosauroidea.

Keywords

Dinosauria, Theropoda, Megaraptoridae, Cretaceous, Argentina, Australia, morphology.

Introduction

Megaraptoridae is a Cretaceous theropod family including several taxa recorded from different regions of Gondwana (Novas et al., 2013). The best known megaraptorids are *Megaraptor namunhuaiquii* (Novas, 1998; Calvo et al., 2004; Porfiri et al., 2014), *Orkoraptor bukei* (Novas et al., 2008), and *Aerosteon riocoloradensis* (Sereno et al., 2008), coming from different formations of Turonian through Santonian age of Argentina; and *Australovenator wintonensis* (Hocknull et al., 2009; White et al., 2012, 2013), from Cenomanian rocks of Australia.

The megaraptorids and their sister taxon *Fukuiraptor kitadaniensis* (Azuma and Currie, 2000), from Barremian beds of Japan, constitutes the clade Megaraptora, originally coined by Benson et al. (2010a). After a comprehensive phylogenetic analysis, these authors considered megaraptorans as allosauroids closely related with carcharodontosaurid theropods, an interpretation subsequently followed by later authors (Carrano et al., 2012; Zanno and Makovicky, 2013). However, recent studies conducted by some of us (e.g., Novas et al., 2013; Porfiri et al., 2014) have suggested that megaraptorans are not representative of archaic allosauroid tetanurans, but instead argued that megaraptorans are coelurosaurs, and representatives of a basal tyrannosauroid radiation in particular (Novas et al., 2013). Recent discovery of cranial remains of a juvenile specimen of *Megaraptor namunhuaiquii* (Porfiri et al., 2014) offered novel anatomical information that supported this phylogenetic interpretation.

The fossil record of megaraptorids in Gondwana has increased over the last few years. Additional evidence of the presence of megaraptorids in regions of South America other than Argentina comes from Brazil, from which isolated caudal vertebrae have been described (Mendez et al., 2013). Cretaceous formations of Australia have yielded several isolated elements referred to Megaraptoridae, including *Rapator ornitholestoides* (Huene, 1932; Agnolín et al., 2010; White et al., 2012), an isolated ulna closely similar to that of *Megaraptor* and *Australovenator* (Smith et al., 2008), more than one hundred isolated teeth (Benson et al., 2012), and probably an isolated astragalus (Molnar et al., 1981; Fitzgerald et al., 2012), and paired pubes originally described as tyrannosauroid (Benson et al., 2010b; Novas et al., 2013).

Available information demonstrates that megaraptorans were a diverse and relatively abundant clade of large predatory dinosaurs in the southern landmasses (Novas, 1998, 2008; Calvo et al., 2004; Benson et al., 2010a; Novas et al., 2013), sharing with abelisauroids and carcharodontosaurids the role of top predators.

We offer here a comparative survey of the manual bones of *Megaraptor* and *Australovenator* with the aim to recognize anatomical features characterizing these theropods. Also, we briefly discuss the distribution of some manual features among theropods that may inform the phylogenetic relationships of megaraptorid among Tetanurae.

Institutional abbreviations

AODF, Australian Age of Dinosaurs Fossil, Winton, Australia; BMNH, British Museum of Natural History, London, England; IVPP, Institute of Vertebrate Paleontology and Paleoanthropology, Beijing, China; MUCPv, Museo de la Universidad Nacional del Comahue, Neuquén, Argentina; UUVP, University of Utah Vertebrate Paleontology, Utah, USA; YPM, Yale Peabody Museum, New Haven, USA.

Materials and Methods

Material examined. A comparative study of the holotype and referred specimens of *Megaraptor namunhuaiquii* (MUCPv 595, MUCPv 1353, and MUCPv 341), *Australovenator wintonensis* (AODF 604), and cast of *Rapator ornitholestoides* (cast of BMNH R3718) was conducted. The following specimens were also studied: *Guanlong wucaii* (IVPP V14531), *Allosaurus fragilis* (cast of UUVP 6000), *Deinonychus antirrhopus* (cast of YPM 5205), *Xuanhanosaurus qilixiaensis* (cast of IVPP V6729), *Coelurus fragilis* (cast of YPM 2010), and *Ornitholestes hermanni* (cast of AMNH 619).

Comparative Anatomy

Megaraptor and *Australovenator* are currently the only megaraptorans in which the forelimb bones are fairly well documented (Calvo et al., 2004; Hocknull et al., 2009; White et al., 2012). Specimen MUCPv 341 of *Megaraptor namunhuaiquii* preserves articulated forearm bones (i.e., ulna and radius) and manus, but no humerus (fig. 3). However, the recent discovery of a juvenile specimen of *M. namunhuaiquii* (Porfiri et al., 2014) documents for the first time the humeral morphology in this genus. Although the humerus does not preserve complete proximal and distal ends, it offers reliable information to calculate humeral proportions in this Patagonian taxon. The type specimen of *Australovenator* preserves most of the forelimb except metacarpal III and some manual phalanges.

Humerus. The humerus of *Megaraptor* (Porfiri et al., 2014) and *Australovenator* (White et al., 2012) resembles basal tetanurans (e.g., *Allosaurus, Acrocanthosaurus, Piatnitzkysaurus*; Madsen, 1976; Currie and Carpenter, 2000; Bonaparte, 1986) and basal coelurosaurs (e.g., *Coelurus, Ornitholestes, Guanlong;* Osborn, 1903; Carpenter, 2005; Xu et al., 2006; fig. 1) in being sigmoid-shaped in anterior and lateral views, with a prominent deltopectoral crest. These characters are absent in non-coelurosaurian theropods like *Xuanhanosaurus* (Dong, 1984), *Ceratosaurus* (Madsen and Welles, 2000), *Torvosaurus* (Galton and Jensen, 1979), *Baryonyx* (Charig and Milner, 1997), and some coelurosaurs including ornithomimids (Kobayashi and Lü, 2003; Nichols and Russel, 1985), and tyrannosaurids (Brochu, 2002) (fig. 1). The internal tuberosity also resembles basal tetanurans in being conical-shaped (e.g., Bonaparte et al., 1990). However, the humerus of both *Megaraptor* and *Australovenator* exhibits a deep longitudinal furrow that runs on the medial surface of the shaft, distally to the internal tuberosity, a feature also present in *Fukuiraptor* and some coelurosaurs (*Deinonychus*, tyrannosaurids; Ostrom, 1969; Brochu, 2002). This character is absent in other coelurosaurs like *Chilantaisaurus*, *Ornitholestes, Coelurus,* oviraptorosaurs (Benson and Xu, 2008; Osborn, 1903; Carpenter, 2005; Lu, 2002), and non-coelurosaurian tetanurans (e.g. *Allosaurus, Acrocanthosaurus, Piatnitzkysaurus;* Madsen, 1976; Currie and Carpenter, 2000; Bonaparte 1986) (fig. 1). Furthermore the entire distal end bends anteriorly, showing a sigmoid shape in lateral view. Notably, the distal humeral condyles of *Australovenator* (White et al., 2012) are well-defined and much more rounded anteriorly than those of *Allosaurus, Acrocanthosaurus* or *Xuanhanosaurus* (Madsen 1976; Currie and Carpenter, 2000; Dong 1984) (fig. 2), and are separated by deep extensor and flexor grooves not present in non-celurosaurian tetanurans. In this regards, the distal end of the humerus of *Australovenator* (White et al., 2012) resembles coelurosaurs like *Coelurus, Ornitholestes* (Carpenter, 2005), *Guanlong* (IVPP IVPP V14531), *Deinonychus* (Novas, 1996) (fig. 2) and Aves, and may suggest a more complex folding system than in basal theropods, a hypothesis that needs to be tested properly. Apart from the similarity with some coelurosaurs described for the distal end, the robust construction of the humerus in *Megaraptor* and *Australovenator* is closer to *Allosaurus* (width:length ratio approximately 40; Madsen, 1976; Hocknull et al., 2009; Porfiri et al., 2014) than the elongate and more gracile humeral proportions of *Guanlong* and *Deinonychus* (width:length ratio approximately 30; pers. obs.).

Ulna. As already noted by previous authors (e.g., Novas, 1998; Calvo et al., 2004; Smith et al., 2008; Agnolin et al., 2010; Benson et al., 2010a; Hocknull et al., 2009; White et al., 2012; Novas et al., 2013), the megaraptorid ulna exhibits a transversally compressed blade-like olecranon process, and a robust and dorsoventrally extended lateral tuberosity. These two features are absent in the remaining theropods, including the basal megaraptoran *Fukuiraptor*, thus they have been interpreted as unambiguous synapomorphies of Megaraptoridae (Novas et al., 2013). The megaraptorid ulna narrows distally, a condition similar to that of *Allosaurus* (e.g., Madsen, 1976) or basal coelurosaurs (e.g. *Guanlong, Ornitholestes, Coelurus;* Ornithomimids; Nichols and Russel, 1985; Xu et al., 2006; Osborn, 1903; Carpenter, 2005). But absent in megalosauroids (Dong, 1984; Charig and Milner, 1997) and derived coelurosaurs (e.g. *Deinonychus*; Ostrom, 1969).

Remarkable features characterizing megaraptorids correspond to the manus, in particular the formidable development of the manual unguals of digits I and II, and the

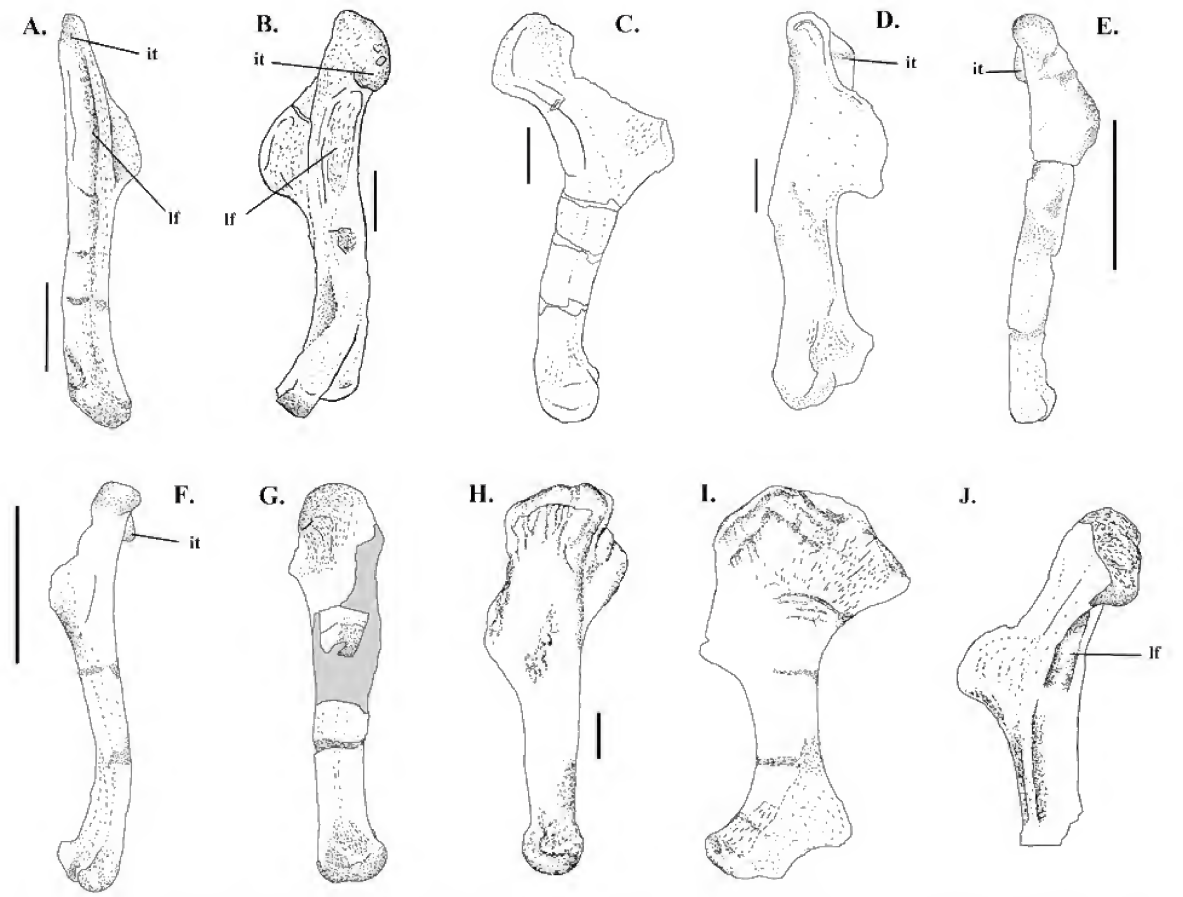

Figure 1. Humerus in lateral (C-I) and medial (A-B,J) views of: A, *Megaraptor* (MUCPv 341), B, *Australovenator*, C, *Allosaurus*, D, *Acrocanthosaurus*, E, *Coelurus*, F, *Ornitholestes*, G, *Xuanhanosaurus*, H, *Torvosaurus*, and I, *Baryonyx*. J, *Fukuiraptor*. B, modified from White et al. (2012). D, modified from Currie and Carpenter (2000). H, modified from Galton and Jensen (1979). I, modified from Charing and Milner (1997). Scale bar: 5cm. **Abbreviations**: it, internal tuberosity; lf, longitudinal furrow.

transverse compression and ventral sharpness of the ungual of digit I (Calvo et al., 2004; Novas et al., 2013).

Carpus. In *Megaraptor* (Calvo et al., 2004) and *Australovenator* (White et al., 2012) two carpal elements are documented: a disk-shaped radiale, and an enlarged distal carpal described as distal carpal 1 by White et al. (2012). Because the homology of this bone among theropods is difficult to interpret (e.g., Xu et al., 2006, 2009, 2014), we will informally describe it as a "semilunate carpal", based on its proximally arched profile in dorsal view.

Semilunate carpals of *Megaraptor* and *Australovenator* resemble *Allosaurus* (Madsen, 1976) in being gently convex proximally (figs. 3, 4, 5). As in the latter taxon, the semilunate carpal is in contact with most of the proximal end of metacarpal I, and also the medial half of the proximal end of metacarpal II. The semilunate carpal of megaraptorids bears a pair of distal projections for articulation with metacarpal bones, also present in *Allosaurus*, *Acrocanthosaurus* and the basal coelurosaur *Guanlong* (Madsen, 1976; Currie and Carpenter, 2000; Xu et al., 2006). One of these projections is visible in ventral view, and wedges between metacarpals I and II. The other projection is seen in dorsal view, and lodges into a socket on the proximal end of metacarpal I. Such interlocking among the semilunate carpal and metacarpals I and II probably constitutes a tetanuran feature, apomorphically lost among derived coelurosaurs (e.g., oviraptorosaurs, paravians) in which the distal surface is flat or slightly concave, without projecting between metacarpals I and II (Rauhut, 2003).

Aside from the general similarities noted with *Allosaurus*, the semilunate carpal of megaraptorids exhibits a proximodistally deep profile, mainly due to the bulged condition of the distal projection that lodges into the proximal end of metacarpal I. In this regard, the semilunate carpal of *Megaraptor* and *Australovenator* differs from the

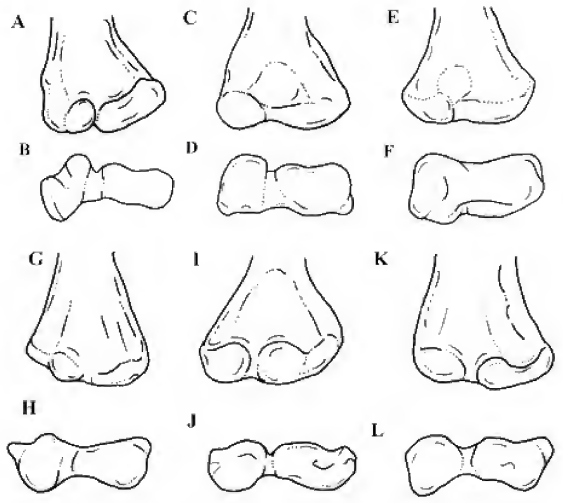

Figure 2. Distal end of humerus in anterior (A,C,E,G,I,K,) and distal (B,D,F,H,J,L) views of *Australovenator* (A,B), *Allosaurus* (C,D), *Xuanhanosaurus* (E,F), *Chilantaisaurus* (G,H), *Guanlong* (I,J), and *Coelurus* (K,L). Not to scale. A,B, modified from White et al. (2012). G,H, modified from Benson and Xu (2008).

proximodistally shallower semilunate carpal of basal tetanurans (e.g., *Allosaurus, Acrocanthosaurus*) and basal coelurosaurs, such as *Tanycolagreus* (Carpenter et al., 2005), *Sinosauropteryx* (Currie and Chen, 2001), *Scipionyx* (Dal Sasso and Maganuco, 2011), *Coelurus*, and ornithomimosaurs (Kobayashi and Lü, 2003).

In sum, megaraptorids retained a carpal morphology diagnostic at the level of Tetanurae. No derived features shared with coelurosaurs are identified. The distally convex condition of the semilunate carpal probably represents a synapomorphic feature for Megaraptoridae.

Metacarpus. Comparing the forearms of *Megaraptor* with those of *Allosaurus* and *Acrocanthosaurus* (equaling the length of the ulna), permits recognition that the manus of the first taxon is much more elongate and slender than in those basal tetanurans. In particular, metacarpal I of *Megaraptor* is less massive than the block-like Metacarpal I of *Allosaurus, Acrocanthosaurus,* and *Torvosaurus* (figs. 3, 6; Madsen, 1976; Galton and Jensen, 1979; Currie and Carpenter, 2000). In *Megaraptor* the ratio between transverse diameter and total length of the metacarpal I results in, approximately 40, whereas in *Allosaurus* the same ratio is of 50 (Novas, 1998). Digits II and III of *Megaraptor* are considerably elongate, in particular their respective ungual phalanges. The exception is digit III, which is not proportionally longer with respect to *Allosaurus*. In this regard, the shortness of digit III was considered as a derived feature shared by megaraptorids and tyrannosaurids (Novas et al., 2013). Moreover, the ungual phalanx of digit III of *Megaraptor* is less curved and trenchant than its homologue in *Allosaurus*. *Australovenator* also exhibits slender metacarpals as in *Megaraptor*, as well as an enlarged ungual on digit I. However, proportions of the remaining phalanges are intermediate between those of *Allosaurus* and *Megaraptor*.

Metacarpal I. As pointed out by Rauhut (2003), metacarpal I in most coelurosaurs is much longer than broad. Rauhut (2003) proposed that a length:width ratio greater than 2.2 is diagnostic for derived coelurosaurs (e.g., *Ornitholestes,* troodontids, oviraptorids, dromaeosaurids), and that was <2 in other theropods. Metacarpal I of megaraptorids exhibits slender proportions resembling those of coelurosaurs, contrasting with most non-coelurosaurian theropods in which the metacarpal is approximately as broad as long (e.g., *Allosaurus, Torvosaurus, Acrocanthosaurus*; fig. 7). In megaraptorids the metacarpal I has a length:width ratio of 1.85 for *Megaraptor,* and 2 for *Australovenator*. This contrasts with non-coelurosaurian theropods, such as *Allosaurus, Acrocanthosaurus,* and *Xuanhanosaurus,* in which the relationship between length:width is 1.52, 1,24 and 1,67 respectively (Madsen, 1976; Dong, 1984; Currie and Carpenter, 2000). In addition, the elongation of metacarpal I is also shared by the Australian *"Rapator"* (see White et al., 2013). On the other hand, in coelurosaurians like *Deinonychus* and *Guanlong*, the ratio is 1,89 and 1,86 respectively (Ostrom, 1076; obs. pers.), resembling in this aspect the megaraptoran condition.

As already said, the proximal end of metacarpal I bears a deep embayment to lodge the semilunate carpal. This proximal concavity of metacarpal I is also present in basal tetanurans (e.g., *Allosaurus*) as well as basal tyrannosauroids (e.g., *Guanlong*), but in megaraptorids it is emphasized by the presence of a prominent proximal projection on the medial corner of the bone. Huene (1932), in the original description of *Rapator ornitholestoides,* pointed out the peculiar proximomedial process of metacarpal I (figs. 7, 8). This feature was usually considered as a probable autapomorphic trait diagnostic for this taxon (e.g., Molnar, 1980, 1990). However, Agnolín et al. (2010) recognized that a similar process is also present in *Australovenator* and *Megaraptor,* thus suggesting that it may constitute a synapomorphy of Megaraptoridae (see also White et al., 2012). The proximal concavity on metacarpal I and its associated proximomedial process are less well developed in basal coelurosaurs (e.g., *Scipionyx*; Dal Sasso and Maganuco, 2011), basal tyrannosauroids (e.g., *Tanycolagreus*; Carpenter, Miles and Cloward, 2005), and paravians (e.g., *Deinonychus*; Ostrom, 1976), in which the proximal margin of metacarpal I is almost straight and a proximomedial process is lacking. The only possible exception among basal coelurosaurs is the compsognathid *Sinosauropteryx*, which appears to posseses a metacarpal I that is proximally notched and bears an associated proximomedial process (Figure 6; Currie and Chen, 2001).

In the Australian megaraptorids *Australovenator* and *"Rapator"* the lateral margin of metacarpal I is straight (in dorsal and ventral views), and the lateral surface for articulation with metacarpal II is slightly faced dorsally (fig. 8). This morphology resembles metacarpal I of basal tyrannosauroids (e.g., *Guanlong*; Xu et al., 2006) and derived coelurosaurs (e.g., *Deinonychus*; Ostrom, 1969), and differs from basal tetanurans (e.g., *Torvosaurus, Allosaurus, Acrocanthosaurus*; Madsen, 1976; Currie and Carpenter, 2000; Galton and Jensen,

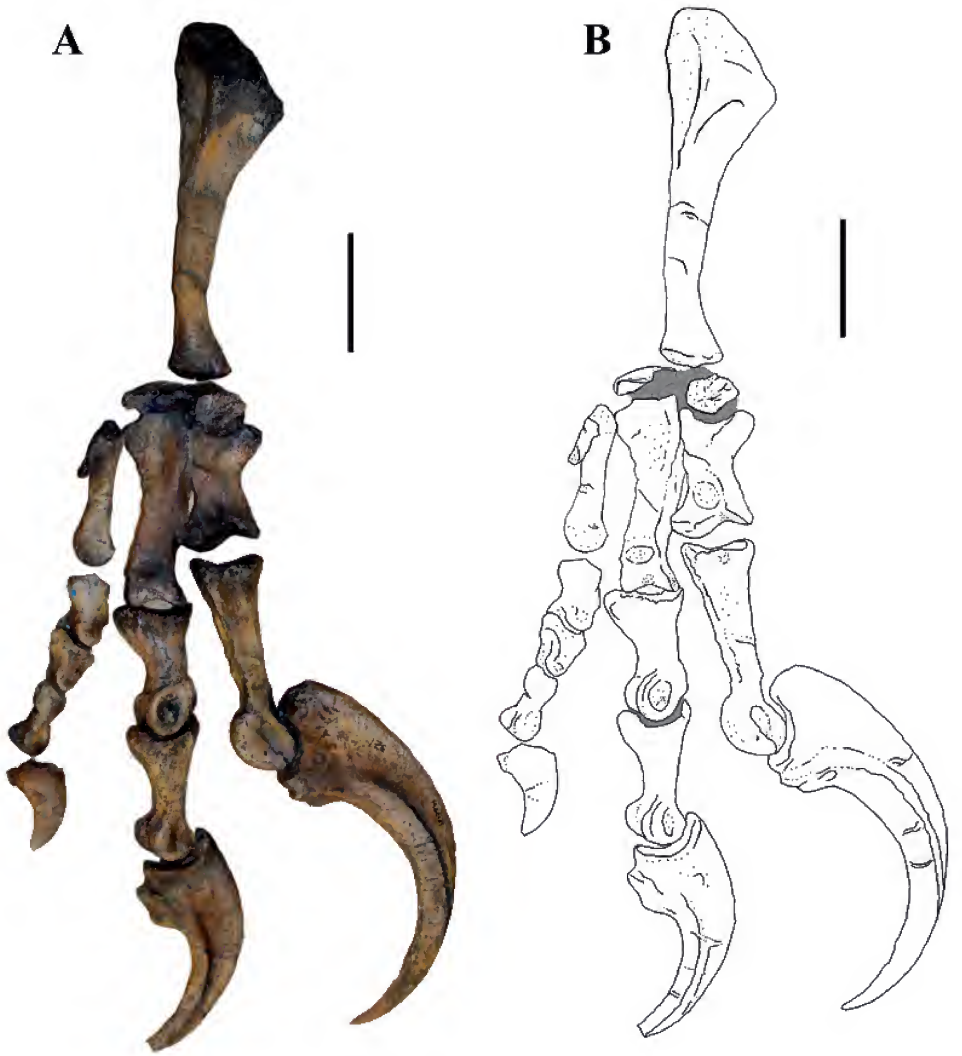

Figure 3. Left manus of *Megaraptor namunhuaiquii* (MUCPv 341) in dorsal view (A) and schematicrepresentation (B) . Scale bar: 1 cm.

1979) in which metacarpal I possesses a well-developed posterolateral surface (also partially faced proximally) for articulation with metacarpal II. The latter bone has a transversely expanded its proximal head, embracing metacarpal I ventrally. The morphology of the proximolateral portion of metacarpal I and the way it articulates with metacarpal II is not uniform among megaraptorids, as shown by *Megaraptor* in which the proximolateral corner of metacarpal I is truncated in a similar condition to that described for *Allosaurus* (Madsen, 1976). In other words, *Megaraptor* exhibits the ancestral tetanuran condition, but its close relative *Australovenator* developed an articulation of metacarpal I that is morphologically closer to that of coelurosaurian theropods. This suggests that character transformation within Megaraptoridae has been more complex than we expected.

In megaraptorids (i.e., *Australovenator, Megaraptor, "Rapator"*) the medial edge of metacarpal I is transversely rounded and dorsoventrally deep (as seen in proximal view; fig. 8). This prominent medial margin resembles *Allosaurus*, being different from the dorsoventrally depressed and sharp medial margin present in some coelurosaurs, such as *Guanlong* and *Deinonychus* (Ostrom, 1976; Xu et al., 2006).

In megaraptorids (e.g., *Megaraptor, Australovenator, "Rapator"*) the medial distal condyle of metacarpal I is more distally placed than in other theropods (Calvo et al, 2004;

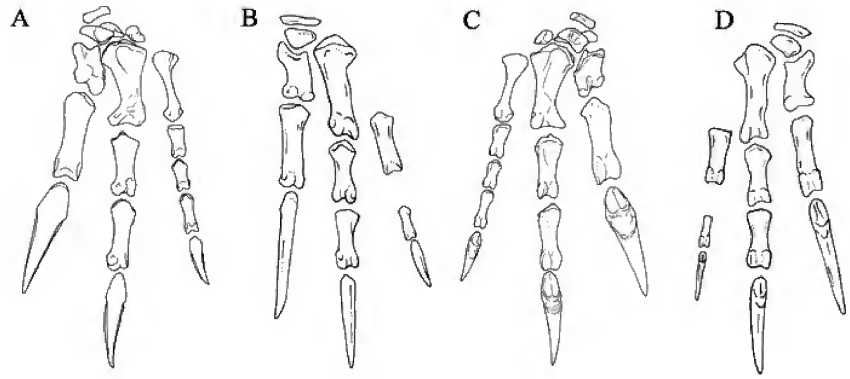

Figure 4. Left manus of (A,C), *Allosaurus fragilis*, and (B,D), *Australovenator wintonensis* in (A,B) dorsal, and (C,D) ventral views. Not to scale. B,D, mofied from White et al. (2012).

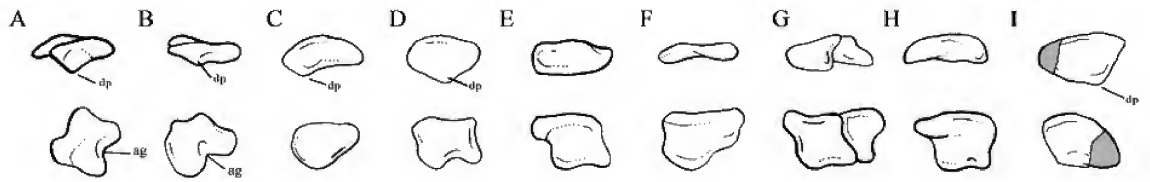

Figure 5. Left "semilunate" carpal in proximal (upper row) and dorsal (lower row) of A, *Allosaurus*, B, *Acrocanthosaurus* (modified from Currie and Carpenter, 2000); C, *Megaraptor*; D, *Guanlong* (modified from Xu et al., 2014); E, *Ornitholestes* (mofiied from Carpenter et al., 2005); F, *Tanycolagreus* (modified from Carpenter et al., 2005); G, *Alxasaurus* (modified from Xu et al., 2014); H, *Deinonychus* (modified from Ostrom, 1969); and I, *Australovenator* (modified from White et al., 2012). Not to scale. **Abbreviations**: ag, anterior groove; dp, distal projections.

White et al., 2012; fig. 8). In addition, the distal end of metacarpal I in megaraptorids is distally oriented, lacking a medial tilting (Calvo et al., 2004; Agnolin et al., 2010; White et al., 2012, 2013). This morphology results in a metacarpal I that is distally less asymmetrical than in other theropods, with the exception of derived paravians, including *Archaeopteryx,* dromaeosaurids and troodontids, in which the distal end lacks the medial twisting present in other theropods (Rauhut, 2003).

In most saurischians, including theropods, the distal end of the first metacarpal I shows asymmetrically developed articular condyles, in which the lateral condyle is larger than the medial condyle (Galton, 1971). This pattern is also present in all known megaraptorids (Calvo et al., 2004; White et al., 2012, 2013). However, the distal end of metacarpal I shows some minor distinctions among megaraptorids: in *Megaraptor* metacarpal I differs from *Allosaurus* and *Australovenator* in the presence of a greatly developed lateral distal condyle, which is ventrally wider than in the above mentioned taxa. In *Australovenator*, the medial distal condyle is prominently projected ventrally (as seen in distal view; see White et al., 2012, fig.13C), constituting a condition hitherto unreported among theropods, with the exception of of *Guanlong* in which the medial condyle projects incipiently ventrally. Differences between *Megaraptor* and *Australovenator* may reveal subtle variations in the way digit I functioned. Contrasting with *Acrocanthosaurus* and *Allosaurus* (Madsen, 1976; Currie and Carpenter, 2000), *Megaraptor* has a metacarpal I that bears distal articular condyles that are little-developed dorsally and lack the globe-shaped morphology characteristic of the aforementioned allosauroids. In the same way, *Xuahanosaurus* has a poorly developed distal articular surface in both views (Dong, 1984). The extensor ligament pit of metacarpal I in *Megaraptor* is roughly triangular in outline, unlike the transversely elongate and elliptical form of this feature *Acrocanthosaurus* and *Allosaurus* (Madsen, 1976; Currie and Carpenter, 2000; fig. 7). *Guanlong* has a similar condition to *Megaraptor* (Xu et al., 2014).

The dorsal surface of metacarpal I in non-coelurosaurian theropods (e.g., *Allosaurus, Acrocanthosaurus, Torvosaurus;* Madsen, 1976; Galton and Jensen, 1979; Currie and Carpenter, 2000) is longitudinally grooved. This groove is contiguous with a similar trough on the dorsal surface of the semilunate carpal (fig. 5). By contrast, in coelurosaurs (e.g., *Scipionyx, Tyrannosaurus, Falcarius, Gallimimus*, *Deinonychus*; Ostrom, 1979; Brochu, 2003; Zanno, 2010; Dal Sasso and Maganuco, 2011) the dorsal surface of metacarpal I and its

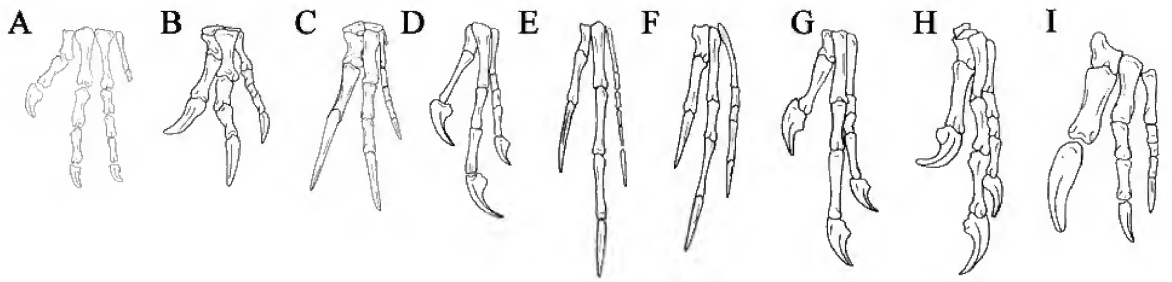

Figure 6. Left manus in dorsal view of A, *Dilophosaurus* (modified from Welles, 1980); B, *Allosaurus*; C, *Megaraptor*; D, *Sinocalliopteryx*; E, *Tanycolagreus* (modified from Carpenter et al., 2005); F, *Deinonychus* (modified from Ostrom, 1969); G, *Scipionyx* (modified from Dal Sasso and Maganuco, 2011); H, *Guanlong* (modified from Xu et al., 2009); and I, *Sinosauropteryx* (modified from Currie and Chen, 2001). Not to scale.

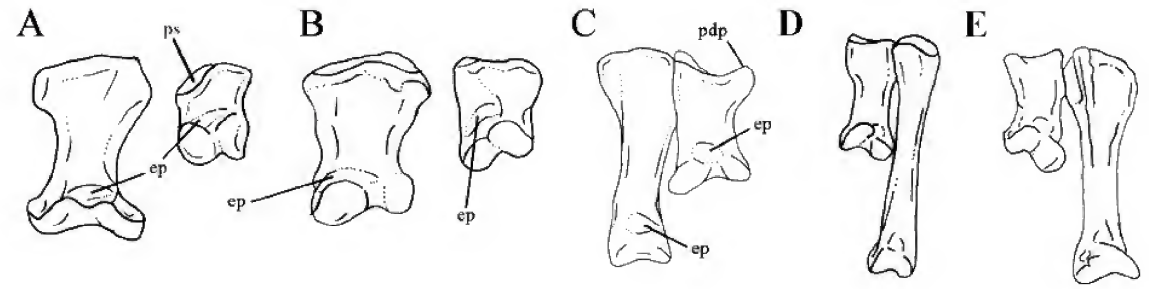

Figure 7. Right metacarpals II and I in dorsal view of A, *Acrocanthosaurus* (modified from Currie and Carpenter, 2000); B, *Torvosaurus* (modified from Galton and Jensen, 1979); C, *Megaraptor*; D, *Deinonychus* (modified from Ostrom, 1969); E, *Guanlong* (modified from Xu et al., 2009). Not to scale. **Abbreviations**: ep, extensor pit; pdp, proximomedial process; ps, proximolateral surface.

corresponding carpal is almost flat or slightly concave. In *Australovenator* the dorsal surfaces of both metacarpal I and the semilunate carpal are almost flat, resembling the condition described for coelurosaurs. In *Megaraptor* the metacarpal I is slightly concave, and although the semilunar carpal is damaged, its dorsal surface is flattened. A similar condition to *Megaraptor* is retained in other basals coelurosaurs like *Guanlong, Ornitholestes* and *Tanycolagreus* which possesses a deep groove in dorsal view (Carpenter et al., 2005; Xu et al., 2006). In sum, the absence of a continuous proximodistal groove on metacarpal I and semilunate carpal may constitute a sinapomorphic trait uniting megaraptorids with coelurosaurs retained in some basals coelurosaurs.

Metacarpal II. In *Megaraptor* and *Australovenator* the metacarpal II is long and slender, with a distal ginglymoid transversely narrower than the proximal end of the bone. This condition differs from that of *Syntarsus, Dilophosaurus, Allosaurus*, and *Acrocanthosaurus*, in which the distal end of metacarpal II bears a prominent ginglymus that flares on both sides, with a transverse diameter equals to that of the proximal end. The just condition described for megaraptorids resembles that of *Compsognathus* (Ostrom, 1969) and *Sinocalliopteryx* (Ji et al., 2007). An intermediate step between the allosauroid and the megaraptorid condition is seen in *Guanlong* (Xu et al., 2006). Scaled at the same size, the distal ginglymoid of metacarpal II of *Megaraptor* is considerably narrower than that of *Allosaurus*, representing half the transverse diameter of the latter taxon's metacarpal II. Another condition is seen in derived coelurosaurids *(Deinonychus;* Ostrom, 1969) which has a slender metacarpal I with equally developed extremities. In congruence with the narrow condition of distal ginglymus, the extensor ligament pit of metacarpal II in *Megaraptor* has a proximodistally extended sub-triangular contour, similar to *Sciurumimus* (Rauhut et al., 2012), but different from the proximodistally short and transversely wide ligament pit of *Allosaurus* (Madsen, 1976).

As mentioned above, in *Megaraptor* the proximal head of metacarpal II is medially expanded, ventrally embracing metacarpal I. This condition differs from that of most coelurosaurs, including *Compsognathus,* tyrannosauroids (e.g., *Guanlong, Tanycolagreus, Tyrannosaurus;* Xu et al., 2009; Carpenter et al., 2005; Brochu, 2003), and more crownward forms (e.g., *Ornitholestes, Deinonychus, Velociraptor*; Carpenter et al., 2005; Ostrom, 1976), in which

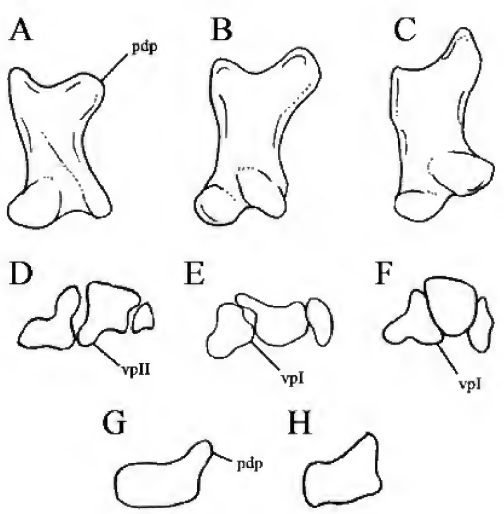

Figure 8. A-C, left first metacarpal in dorsal view of A, *Megaraptor*, B, *Australovenator*, and C, *Rapator*; D-F, proximal view of left metacarpus of D, *Guanlong* (modified from Xu et al.,2009), E, *Tanycolagreus* (modified from Carpenter et al., 2005), and F, *Deinonychus* (modified from Ostrom, 1969); G-H, proximal view of right first metacarpal of G, *Rapator*, and H, *Australovenator*. Not to scale. **Abbreviations**: pdp, proximomedial process; vpI, ventral process of metacarpal I; vpII, ventral process of metacarpal II.

the lateroventral margin of metacarpal I is laterally projected, thus embracing the ventral surface of metacarpal II.

Metacarpal III. Among megaraptorans, this bone has been solely recorded in *Megaraptor*. Calvo et al. (2004) described the metacarpal III of *Megaraptor* as transversally compressed, its distal end being narrower than its proximal end. This condition is also present in most tyrannosaurids (e.g., *Daspletosaurus, Tyrannosaurus, Albertosaurus*; Russell, 1970; Lipkin and Carpenter, 2008), in which metacarpal III is extremely slender. This condition has been interpreted as diagnostic of advanced tyrannosauroids (Holtz, 2004).

The reduction of metacarpal III is correlated with the reduction of the entire digit III. In *Megaraptor* the phalanges of digit III are proximodistally shortened and transversely compressed, thus resulting in a digit III shorter and more slender than in basal tetanurans (e.g., *Allosaurus, Acrocanthosaurus*; Madsen, 1976; Currie and Carpenter, 2000). This peculiar morphology may be regarded as autapomorphic for *Megaraptor*.

In *Megaraptor*, the length of metacarpal III represents 71% of metacarpal II, a ratio that matches that of specialised tyrannosauroids (Russell, 1970; Barsbold, 1982; Rauhut, 2003; Holtz, 2004). This proportion, as well as the short length of the entire digit III may be a condition shared between both groups.

Megaraptor retained a small and rod-like metacarpal IV, and no evidence of phalanges of digit IV have been found in the preserved manus (Calvo et al., 2004), thus it is probable that digit IV was completely lost. The only available specimen of *Australovenator* does not preserve metacarpal IV (Hocknull et al., 2009; White et al., 2012). Presence of metacarpal IV in *Megaraptor* is here interpreted as an apomorphic reversal from the neotetanuran ancestral state, in which metacarpal IV is absent (e.g., *Sciurumimus, Allosaurus, Acrocanthosaurus;* Rauhut, 2003). This conclusion agrees with Rauhut et al. (2012) who recognized a high level of homoplasy in this characteristic, given that the basal allosauroid *Sinraptor* (Currie and Zhao, 1993) and the basal tyrannosauroid *Guanlong* (Xu et al., 2006) retained a rudimentary fourth metacarpal.

Manual phalanges. In *Megaraptor* and *Australovenator*, manual phalanges exhibit shallow and triangular-shaped extensor ligament pits, which lack well-defined margins and are not proximally delimited by a transverse ridge (fig. 7). Rauhut (2003) pointed out that coelurosaurs lack well-defined extensor pits on manual phalanges. In contrast, in non-coelurosaurian theropods, extensor ligament pits are deep and transversely extended, as shown for example in *Eoraptor, Dilophosaurus, Syntarsus, Xuanhanosaurus, Torvosaurus, Allosaurus, Acrocanthosaurus, Sinraptor,* and *Baryonyx* (Raath, 1969; Madsen, 1976; Galton and Jensen, 1979; Welles, 1984; Dong, 1984; Currie and Zhao, 1993; Sereno et al., 1993; Charig and Milner, 1997; Currie and Carpenter, 2000; Rauhut, 2003). In contrast most coelurosaurian theropods have shallow or absent extensor pits (e.g. *Deinonychus, Nothronychus, Tyrannosaurus, Troodon*; Ostrom, 1969; Currie and Russel, 1987; Bochu, 2003; Zanno et al., 2009; Zanno, 2010).

Phalanges of digit I. Megaraptor is distinguished from the remaining theropods, including *Australovenator*, in the remarkable elongation of the internal bones of the manus (i.e., metacarpal I, phalanx 1.I, and especially the ungual phalanx). The tip of digit I ungual ends at the level of the mid-length of the second ungual digit (fig. 3).

Phalanx 1 of digit I of *Megaraptor* exhibits a proximodorsal lip. In most basal theropods (e.g., coelophysoids, *Torvosaurus, Spinosaurus, Allosaurus, Acrocanthosaurus;* Rauhut, 2003; Ibrahim et al., 2014) the phalanx I.1 bears a transversely wide proximodorsal lip on phalanx 1 of digit I. Such a wide lip appears to be related with a transversely extended, deep, and well-defined extensor ligament pit on distal metacarpal I, a condition regarded as plesiomorphic among theropods (Sereno et al., 1993; Rauhut, 2003). However, among coelurosaurs (e.g., *Tanycolagreus, Guanlong, Tyrannosaurus, Gallimimus, Deinonychus*; Ostrom, 1976; Brochu, 2003; Carpenter et al., 2005; Xu et al., 2006) the proximodorsal lip of phalanx 1 is narrower. In *Megaraptor* and *Australovenator* the proximal surface of the proximal phalanx presents a pointed proximodorsal lip, which is different from the condition described for the remaining theropods. This pointed process appears to be related with a reduction in the distal extensor pits of the metacarpals, as diagnostic of coelurosaurs (Rauhut, 2003).

In *Megaraptor* and *Australovenator* the proximal end of phalanx I.1 is sub-quadrangular in outline (fig. 9). It shows robust and thickened lateral, medial, and dorsal margins, conforming to an expanded articular surface for metacarpal I. The lateral margin is even more thickened than the medial one and is strongly proximally expanded. This set of features

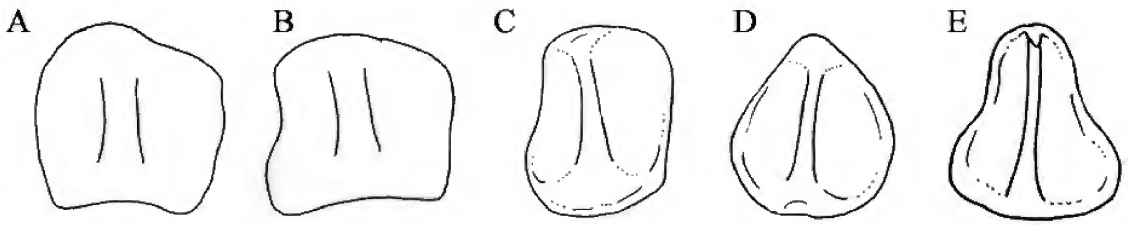

Figure 9. Proximal end of right phalanx I.1 of A, *Megaraptor*; B, *Australovenator*; C, *Allosaurus*; D, *Tyrannosaurus* (modified from Brochu, 2003); and E, *Deinonychus* (modified from Ostrom, 1969). Not to scale.

appears to be unique to megaraptorids: in other theropods, the proximal end is transversely narrow and dorsoventrally deep, being sub-rectangular in shape (e.g., *Allosaurus, Acrocanthosaurus, Torvosaurus, Tyrannosaurus*; Galton and Jensen, 1979; Madsen, 1976; Currie and Carpenter, 2000; Brochu, 2003) or subtriangular in outline (as in *Guanlong* and *Deinonychus*; Ostrom, 1976; Xu et al., 2006). Furthermore, in *Megaraptor* the proximal articular surface is transversely wider dorsally than ventrally (Novas, 1998). This condition is unknown in other theropods, including *Australovenator* (White et al., 2012), in which the proximal end is transversely wider on its ventral margin than on its dorsal edge.

Phalanx 1 of digit I in *Megaraptor* shows a deep and wide furrow along its ventral surface (Novas, 1998). As a result, both lateral and medial margins of this surface acquired the form of sharp longitudinal ridges (fig. 10). These features are also documented in *Australovenator* (White et al., 2012). In other theropods, phalanx 1.I is ventrally excavated, but the furrow is restricted on the proximal half of the bone, and it is not as deep as in megaraptorids. No longitudinal ridges are present. It is interesting to note that in megaraptorids, the ventral margin of the proximal articular surface of phalanx 1.I is concave, reflecting the deep furrow present along the ventral surface of the bone. This is in contrast with other theropods, in which this margin is straight (e.g., *Allosaurus*; Madsen, 1976) or convex (e.g., *Guanlong, Deinonychus*; Ostrom, 1976; Xu et al., 2006).

The distal ginglymus of phalanx 1.I of *Megaraptor* is dorsoventrally deeper and transversely narrower than in other theropods (including *Australovenator*), and the dorsoventral sulcus is much more incised.

Megaraptor is well-known by its extremely large and elongate manual ungual on digit I (Calvo et al., 2004), which is subequal in length to the ulna. This condition is unusual among theropods, being absent among basal tetanurans (e.g., *Allosaurus*; Madsen, 1976), basal coelurosaurs (e.g., *Scipionyx, Tanycolagreus, Chilantaisaurus*; Dal Sasso and Maganuco, 2011; Carpenter et al., 2005; Benson and Xu, 2008), ornithomimosaurs (e.g., *Gallimimus*), oviraptorosaurs, basal therizinosaurs (e.g., *Falcarius, Nothronychus*; Zanno, 2010; Zanno et al., 2009), and paravians (e.g., *Deinonychus*; Ostrom, 1969). Furthermore, in the megaraptorans *Australovenator* and *Fukuiraptor*, the ungual of digit I is much shorter than the ulna, representing approximately half of its length. Basal tetanurans that evolved an enlarged ungual in manual digit I are the compsognathid *Sinosauropteryx* (Currie and Chen, 2001), and the megalosauroids *Baryonyx* and *Torvosaurus* (Galton and Jensen, 1979; Charig and Milner, 1997).

In the original description of *Megaraptor* (Novas, 1998), it was remarked that the ungual phalanx bore a sharp longitudinal ventral keel. This trait was later considered as a synapomorphy of Megaraptoridae (Novas et al., 2013). In *Megaraptor*, towards the proximal end of the claw, the ventral keel gradually displaces laterally, joining the lateral margin of the claw on its most proximal portion, a condition also reported in *Australovenator* (White et al., 2012; fig. 11). Other theropods, including *Fukuiraptor* (Azuma and Currie, 2000), basal tyrannosauroids (e.g., *Guanlong*; Xu et al., 2006), megalosauroids (e.g., *Baryonyx, Torvosaurus*; Galton and Jensen, 1979; Charig and Milner, 1997) and the problematic *Chilantaisaurus* (Benson and Xu, 2008) have unguals with a transversely rounded expanded ventral surface, without traces of a ventral keel. In sum, such a transverse compression of the enlarged ungual constitutes a distinctive feature of Megaraptoridae.

In addition, the manual ungual I of *Megaraptor* and *Australovenator* share very deep and well-defined flexor facets on the lateral and medial surfaces of the flexor tubercle. These facets are deep, wide, and more well-defined than in other theropods, including *Allosaurus, Baryonyx* and *Torvosaurus* (Madsen, 1976; Galton and Jensen, 1979; Charig and Milner, 1997). Furthermore, in *Megaraptor* such facets are delimited by acute ridges of bone (Figure 12). It is worth nothing that similar facets were described for *Fukuiraptor* (Azuma and Currie, 2000).

Digit II. In *Megaraptor*, phalanx 1.II is shorter than phalanx 2.II, a condition similar to that of some allosauroids, such as *Allosaurus* (Gilmore, 1920; Madsen, 1976) and *Acrocanthosaurus* (Currie and Carpenter, 2000), and selected coelurosaurs, as for example *Sinocalliopteryx* (Ji et al., 2007), *Sinosauropteryx* (Currie and Chen, 2001), *Scipionyx* (Dal Sasso and Maganuco, 2011), *Guanlong* and *Deinonychus*. Distribution of this feature (i.e., length ratio of pre-ungual phalanges of digit II) is not uniform among tetanurans. For example, in the megaraptorid *Australovenator* and the basal tyrannosauroid *Tanycolagreus* (Carpenter et al., 2005), phalanges 1 and 2 of

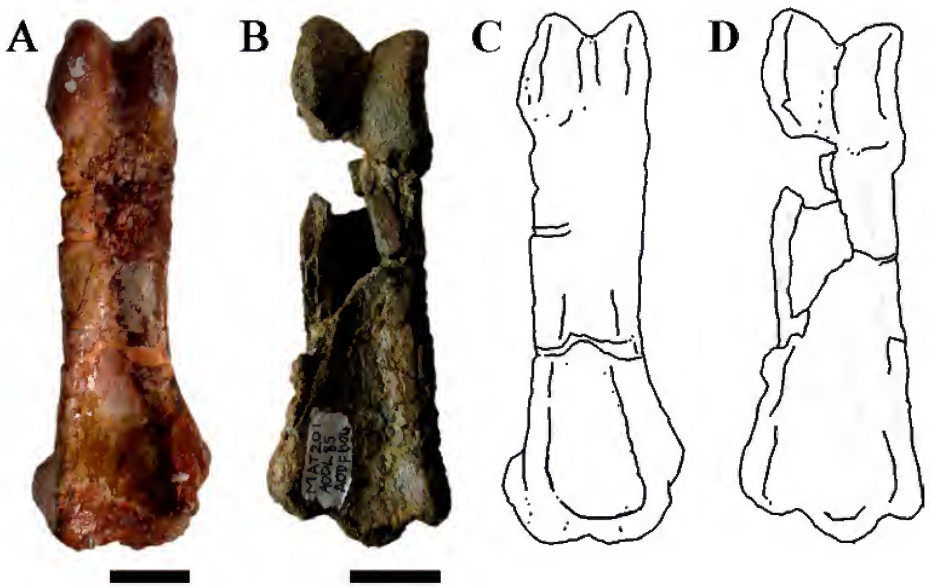

Figure 10. Right manual phalanx 1 of digit I in ventral view and schematic representations of *Megaraptor* (A, C), *Australovenator* (B,D). Scale bar: 2 cm. Note the well-developed longitudinal ventral furrow.

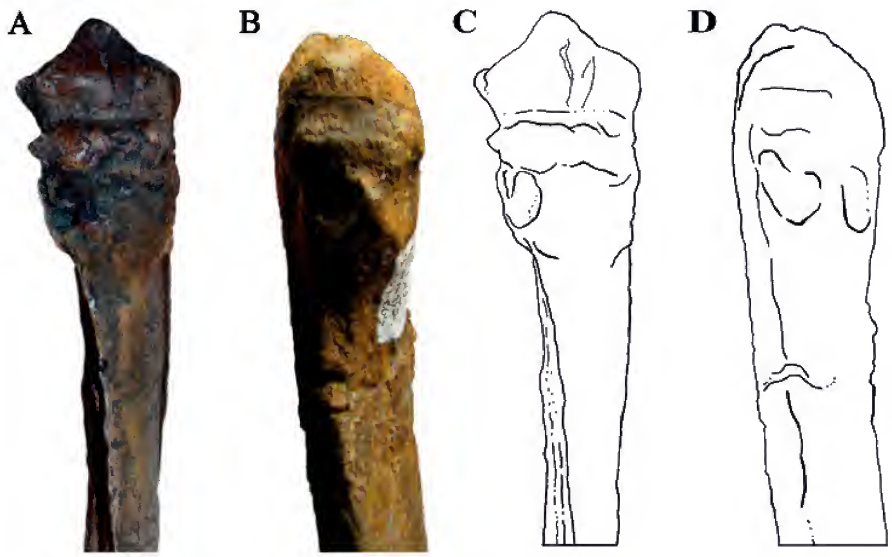

Figure 11. Right manual ungual phalanx of digit I in ventral view and schematic representation of *Megaraptor* (A,C); and *Australovenator* (B,D). Not to scale.

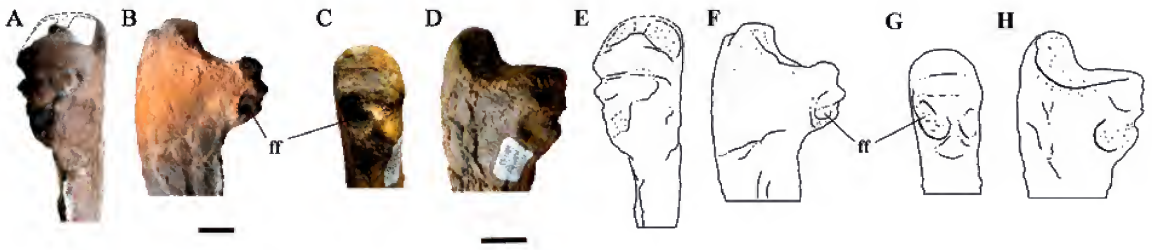

Figure 12. Right manual ungual phalanx of digit I in A,C, ventral, and B,D, lateral views. A-B, *Megaraptor*; C-D, *Australovenator* and schematic representation in E,G, ventral, and F,H, lateral views. E-F, *Megaraptor;* G-H, *Australovenator.* Scale bar: 2 cm. **Abbreviations**: ff, flexor facets.

digit II are subequal in length, and the megalosauroid *Sciurumimus* (Rauhut et al., 2012) shows coelurosaur-like proportions, with phalanx 1.II shorter than phalanx 2.II.

In *Megaraptor*, the proximal articular surface of phalanx 1.II describes a dorsoventrally deep ovoid contour. Its ventral margin bears a rounded process that projects proximomedially, a feature shared with *Australovenator* (White et al., 2012) and *Fukuiraptor* (Azuma and Currie, 2000). This results in a relatively narrow ventral margin of the proximal end of phalanx 1.I. This shape is in contrast with other theropods, such as *Allosaurus* and *Tyrannosaurus* (Madsen, 1976; Brochu, 2003), in which the ventral margin is straight. Furthermore, in *Megaraptor*, and probably also in *Australovenator* and *Fukuiraptor*, the proximal articular surface phalanx 1.II is obliquely oriented with respect to the distal articular trochlea, a condition unknown in other theropods, in which the main axes of both proximal and distal ends are sub-parallel.

In *Megaraptor*, metacarpal II and its corresponding non-ungual phalanges have respective distal articular trochleae with a medial condyle more ventrally projected than the lateral one. In probable correlation with this shape, it is seen that non-unguals of digit II exhibit a longitudinal keel that runs along their ventromedial margins. Such strong asymmetry of distal condyles and longitudinal ridges appear to be absent in other theropods, including *Australovenator*, although in the available phalanx 1.II of *Fukuiraptor* (Azuma and Currie, 2000) a similar ventromedial ridge seems to be present.

Digit III. In *Megaraptor* phalanges of this digit look similar in proportions to those of *Allosaurus* (Gilmore, 1920; Madsen, 1976), except for the ungual, which is proportionally shorter and smaller. The pre-ungual phalanx of digit III of *Megaraptor* is longer than phalanges 1 and 2 of the same digit, as generally occurs among tetanurans, although it does not reach the elongation that characteristically occurs in coelurosaurs (e.g., *Sinocalliopteryx, Dilong, Guanlong, Deinonychus*; Ostrom, 1976; Xu et al., 2006; Ji et al., 2007).

Conclusions

Shared presence of a longitudinal groove along the medial side of humeral shaft in megaraptorans and tyrannosaurids conforms a novel feature supporting close relationships between these theropod families. Comparison of the manus in *Megaraptor* and *Australovenator* allowed the recognition of several features that may shed light on the phylogenetic relationships of megaraptorids. The manus of *Megaraptor* exhibits the following unique traits that are not present in other theropods, and are here interpreted as autapomorphies of this genus: 1) metacarpal I with an acute medial condyle on distal gynglimus; 2) phalanges of digit II with ventromedial ridges; and 3) an extremely elongate manual ungual on digit I, approximating the length of the ulna.

Manual characters here interpreted as diagnostic of Megaraptoridae include: symmetrical-shaped metacarpal I, proximal end of phalanx 1.I transversally expanded, phalanx 1.I with a longitudinal ventral furrow, and ungual phalanx of digit I with a laterally displaced sharp ventral margin. Manual characters diagnostic of Megaraptora are more difficult to recognize because the manus of the basal megaraptoran *Fukuiraptor* is poorly known. Nevertheless, two possible derived features have been identified: asymmetrical phalanx 1. II; and first digit ungual with deep facets on the flexor tubercle.

After comparing carpal, metacarpal and phalangeal morphology, it becomes evident that megaraptorids retained several of the manual features present in basal tetanurans, such as *Allosaurus*. In this regard, *Megaraptor* and *Australovenator* are devoid of several manual features that the basal tyrannosauroid *Guanlong* shares with more derived coelurosaurs (e.g., *Deinonychus*). However, there are some manual characters that support Megaraptora as members of Coelurosauria, including the elongate and slender shaft of metacarpals I and II, and the presence of separated flexor and extensor distal end of the humerus, and the absence of a longitudinal furrow on the dorsal surface of metacarpal I, and a semilunar carpal. Furthermore, megaraptorans are similar to specialised members of Tyrannosauroidea in having a transversely narrow metacarpal III that represents 0.75 the length of metacarpal II, a set of features previously interpreted as synapomorphies uniting both clades (Novas et al., 2013; Porfiri et al., 2014).

Acknowledgements

The senior author wishes to thank deeply Tom and Pat Rich for their genereous invitation to visit Australia, and for allowing the study of the valuable Cretaceous theropod materials they collected in Victoria. Scott Hocknull and his crew kindly facilitated access to the specimen of *Australovenator*. Xu

Xing allowed access to several theropod specimens under his care. Special thanks to Steve Brusatte and an anonymous reviewer that made clever observations that improved the quality of the manuscript.

References

Agnolín, F.L., Ezcurra, M.D., Pais, D.F. and Salisbury, S.W. 2010. A reappraisal of the Cretaceous non-avian dinosaur faunas from Australia and New Zealand: evidence for their Gondwanan affinities. Journal of Systematic Palaeontology 8; 257–300.

Azuma, Y. and Currie, P.J. 2000. A new carnosaur (Dinosauria: Theropoda) from the Lower Cretaceous of Japan. Canadian Journal of Earth Sciences 37; 1735–1753.

Benson, R.B.J., Carrano, M.T. and Brusatte, S.L. 2010a. A new clade of archaic large-bodied predatory dinosaurs (Theropoda: Allosauroidea) that survived to the latest Mesozoic. Naturwissenschaften 97; 71–78.

Benson, R.B.J., Barrett, P.M., Rich, T.H., Vickers-Rich, P., 2010b. A southern tyrant reptile. Science 327, 1613.

Benson, R.B.J., Rich, T.H., Vickers-Rich, P. and Hall, M. 2012. Theropod fauna from Southern Australia indicates high Polar Diversity and Climate-Driven dinosaur provinciality. PlosOne 7(5), e37122.

Benson, R.B.J. and Xu X. 2008. The anatomy and systematic position of the theropod dinosaur *Chilantaisaurus tashuikouensis* Hu, 1964 from the Early Cretaceous of Alashan, People´s Republic of China. Geological Magazine 145; 778–789.

Brochu, C.A., 2003. Osteology of *Tyrannosaurus rex*: insights from a nearly complete skeleton and high-resolution computed tomographic analysis of the skull. Society of Vertebrate Paleontology Memoir 7; 1–138.

Bonaparte, J. 1986. Les Dinosaures (Carnosaures, Allosaurides, Sauropodes, Cetiosaurides) du Jurassique moyen de Cerro Condor (Chubut, Argentine). Annales de Pateontologie, 72; 247–289, 326–386.

Calvo, J.O., Porfiri, J.D., Veralli, C., Novas, F.E. and Poblete, F. 2004. Phylogenetic status of *Megaraptor namunhuaiquii* Novas based on a new specimen from Neuquén, Patagonia, Argentina. Ameghiniana 41; 565–575.

Carpenter, K., Miles, C. and Cloward, K. 2005. New small theropod from the Upper Jurassic Morrison Formation of Wyoming. In: Carpenter, K. (ed), The Carnivorous Dinosaurs. Indiana University Press, Bloomington, pp. 23–48.

Charig, A.J. and Milner, A.C. 1997. *Baryonyx walkeri*, a fish-eating dinosaur from the Wealden of Surrey. Bulletin of the Natural History Museum of London 53; 11–70.

Currie, P.J. and Zhao, X. 1993. A new carnosaur (Dinosauria, Theropoda) from the Jurassic of Xinjiang, People´s Republic of China. Canadian Journal of Earth Sciences 30; 2037–2081.

Currie, P.J. and Carpenter, K. 2000. A new specimen of *Acrocanthosaurus atokensis* (Theropoda, Dinosauria) from the Lower Cretaceous Antlers Formation (Lower Cretaceous, Aptian) of Oklahoma, USA. Geodiversitas 22; 207–246.

Currie, P.J. and Chen, P.J. 2001. Anatomy of *Sinosauropteryx prima* from Liaoning, northeastern China. Canadian Journal of Earth Sciences 38; 705–727.

Currie, P.J. and Russell, D. A. 1988. Osteology and relationships of *Cirosrenotes pergracilis* (Saurischia, Theropoda) from the Judith River (Oldman) Formation of Alberta, Canada. *Canadiall Journal of Earth Sciences, 25*; 972–986.

Dal Sasso, C. and Maganuco, S. 2011. *Scipionyx samniticus* (Theropoda: Compsognathidae) from the Lower Cretaceous of Italy. Osteology, ontogenetic assessment, phylogeny, soft tissue anatomy, taphonomy and palaeobiology. Memorie Della Societa Italiana de Scienze Naturali e del Museo Civico di Storia Naturale di Milano 37; 1–281.

Dong, Z., 1984. A new theropod dinosaur from the Middle Jurassic of Sichuan Basin. Vertebrata PalAsiatica 22; 213–218. [In Chinese].

Fitzgerald, E.M.G., Carrano, M.T., Holland, T., Wagstaff, B.E., Pickering, D., Rich, T.H. and Vickers-Rich, P. 2012. First ceratosaurian dinosaur from Australia. Naturwissenschaften 99: 397–405.

Galton, P.M. 1971. Manus movements of the coelurosaurian dinosaur *Syntarsus* and opposability of the theropod hallux. Arnoldia 15: 1–8.

Galton, P.M. and Jensen, J. A. 1979. A new large theropod dinosaur from the Upper Jurassic of Colorado. Brigham Young University Geology Studies 26; 1–12.

Gilmore, C.W. 1920. Osteology of the carnivorous Dinosauria in the United States National Museum, with special reference to the genera *Antrodemus* (*Allosaurus*) and *Ceratosaurus*. Bulletin of the United States National Museum 110, 1–154.

Hocknull, S.A., White, M.A., Tischler, T.R., Cook, A.G., Calleja, N.D., Sloan, T. and Elliott, D.A. 2009. New Mid-Cretaceous (Latest Albian) Dinosaurs from Winton, Queensland, Australia. PLoS ONE 4, e6190.

Holtz, T.R. Jr. 2004. Tyrannosauroidea. In: Weishampel, D.B., Dodson, P., Osmólska, H. (eds), The Dinosauria, Second Edition. University of California Press, pp. 111–136.

Huene, F. von., 1932. Die fossile Reptil-Ordnung Saurischia, ihre Entwicklung und Geschichte. Monographie fur Geologie und Palaontologie 4; 1–361.

Ibrahim, N., Sereno, P. C., Dal Sasso, C., Maganuco, S., Fabbri, M., Martill, D. M., Zouhri, S., Myhrvold, N. and Iurino, D. A. 2014. Semiaquatic adaptations in a giant predatory dinosaur. Science, doi:10.1126/science.1258750

Ji, S., Ji, Q., Lu J. and Yuan, C. 2007. A new giant compsognathid dinosaur with long filamentous integuments from Lower Cretaceous of Northeastern China. Acta Geologica Sinica 81; 8–15.

Kobayashi, Y. and Lü, J.-C. 2003. A new ornithomimid dinosaur with gregarious habits from the Late Cretaceous of China. Acta Palaeontologica Polonica 48; 235–259.

Lipkin, C. and Carpenter, K. 2008. Looking again at the forelimb of *Tyrannosaurus rex*. In: Larson P.L., Carpenter K. (eds) *Tyrannosaurus rex*, the tyrant king. Indiana University Press, pp. 167–192.

Lu, J., 2002. A new oviraptorosaurid (Theropoda: oviraptorosauria) from the late Cretaceous of southern of China. Journal of Vertebrate Paleontology 22(4):871-875.

Madsen, J.H., Jr. 1976. *Allosaurus fragilis*: a revised osteology. Utah Geological and Mineralogical Survey Bulletin 109; 3–163.

Madsen, J.H. and Welles, S.P. 2000. *Ceratosaurus* (Dinosauria, Theropoda). A revised osteology. Utah Geological Survey. Miscellalleous Publicatioll, 00-2, 80 pp.

Molnar, R.E., 1980. Australian Late Mesozoic terrestrial tetrapods: some implications. Mémoires de la Société Géologique de France 139; 131–143.

Molnar, R.E., 1990. Problematic Theropoda: "Carnosaurs". In: Weishampel, D.B., Dodson, P., and Osmólska, H. (eds). The Dinosauria. University of California Press, Berkeley, pp. 306–317.

Molnar, R.E., Flannery, T.F. and Rich, T.H.V. 1981. An allosaurid theropod dinosaur from the Early Cretaceous of Victoria, Australia. Alcheringa 5: 141–146.

Nichols, E.L. and Russel, A.P. 1985. Structure and function of the pectoral girdle and forelimb of *Struthiomimus altus* (Theropoda: ornithomimidae). Palaeontology 28; 643–677.

Novas, F.E. 1998. *Megaraptor namunhuaiquii* gen. et. sp. nov., a large-clawed, Late Cretaceous Theropod from Argentina. Journal of Vertebrate Paleontology 18: 4–9.

Novas, F.E., Ezcurra, M.D. and Lecuona, A. 2008. *Orkoraptor burkei* nov.gen. et sp., a large theropod from the Maastrichtian Pari Aike Formation, Southern Patagonia, Argentina. Cretaceous Research 29; 468–480.

Novas, F.E., Agnolin, F.L., Ezcurra, M.D., Porfiri, J. and Canale, J.I. 2013. Evolution of the carnivorous dinosaurs during the Cretaceous: the evidence from Patagonia. Cretaceous Research 45; 174–215.

Osborn, H.F. 1903.*Ornitholestes hermanni*, a new compsognathoid dinosaur from the upper Jurassic. Bulletin American Museum of Natural History 19; 459–464.

Ostrom, J.H. 1969. Osteology of *Deinonychus antirrhopus*, an unusual theropod from the Lower Cretaceous of Montana. Bulletin of the Peabody Museum of Natural History 30; 1–165.

Porfiri, J.D., Novas, F.E., Calvo, J.O., Agnolin, F.L., Ezcurra, M.D. and Cerda, I.A. 2014. Juvenile specimen of *Megaraptor* (Dinosauria, Theropoda) sheds light about tyrannosauroid radiation. Cretaceous Research 51; 35–55.

Raath. M.A. 1969. A new coelurosaurian dinosaur from the Forest Sandstone of Rhodesia. Amoldia, 4, 1–25. 1985. The theropod Syntarsus and ilS bearing on the origin of birds. 219-227. In Hecht. M. K., Ostrom.J. H., Viohl. G., and Wellnhofer. P. (ed). The beginning of birds. Freunde des Jura Museums, Eichsliitt, 382 pp.

Rauhut, O.W.M. 2003. Interrelationships and evolution of basal theropod dinosaurs. Special Papers in Palaeontology 69; 1–215.

Rauhut, O.W.M. Foth, C., Tischlinger, H. and Norell, M.A. 2012. Exceptionally preserved juvenile megalosauroid theropod dinosaur with filamentous integument from the Late Jurassic of Germany. Proceedings of the National Academy of Sciences of the United States of America 109; 11746–11751.

Russell, D.A. 1970. Tyrannosaurs from the Late Cretaceous of western Canada. National Museum of Natural Sciences Publications in Paleontology 1; 1–34.

Sereno, P.C. and Novas, F.E. 1993. The skull and neck of the basal theropod Herrerasaurus ischigualastensis. Journal of Vertebrate Paleontology 13; 451–476.

Sereno, P.C., Martínez, R.N., Wilson, J.A., Varricchio, D.J. and Alcober, O.A. 2008. Evidence for avian intrathoracic air sacs in a new predatory dinosaur from Argentina. Plos One 3, e3303.

Smith, N.D., Makovicky, P.J., Agnolín, F.L., Ezcurra, M.D., Pais, D.F. and Salisbury, S.W. 2008. A *Megaraptor*-like theropod (Dinosauria: Tetanurae) in Australia: support for faunal exchange across eastern and western Gondwana in the Mid-Cretaceous. Proceedings of the Royal Society of London 275; 2085–2090.

Welles, S.P. 1984. *Dilophosaurus wetherilli* (Dinosauria, Theropoda). Osteology and comparisons. *Palaeontographica* A. 185; 85–180.

White, M.A., Cook, A.G., Hocknull, S.A., Sloan, T., Sinapius, G.H.K. and Elliott, D.A. 2012. New forearm elements discovered of holotype specimen *Australovenator wintonensis* from Winton, Queensland, Australia. Plos One 7 (6), e39364.

White, M.A., Falkingham, P.L., Cook, A.G., Hocknull, S.A. and Elliott, D.A. 2013. Morphological comparisons of metacarpal I for *Australovenator wintonensis* and *Rapator ornitholestoides*: implications for their taxonomic relationships. Alcheringa 37; 1-7.

Xu, X., Clark, J.M., Forster, C.A., Norell, M.A., Erickson, G.M., Eberth, D.A., Ji, A.C. and Zhao, Q. 2006. A basal tyrannosauroid dinosaur from the Late Jurassic of China. Nature 439; 715–718.

Xu, X., Clark, J.M., Mo, J., Choiniere, J., Forster, C.A., Erickson, G.M., Hone, D.W.E., Sullivan, C., Eberth, D.A., Nesbitt, S., Zhao, Q., Hernandez, R., Jia, C.-K., Han, F.-L. and Guo, Y. 2009. A Jurassic ceratosaur from China helps clarify avian digital homologies. Nature 459; 940–944.

Xu, X., Han, F. and Zhao, Q. 2014. Homologies and homeotic transformation of the theropod "semilunate" carpal. Scientific Reports 4, 6042.

Zanno, L.E., Gillette, D. D., Albright L. B. and Titus, L. A. 2009. A new North American therizinosaurid and the role of herbivory in 'predatory' dinosaur evolution. Proceedings of the Royal Society 276; 3505–3511.

Zanno, L.E. 2010. Osteology of *Falcarius utahensis* (Dinosauria: Theropoda): characterizing the anatomy of basal therizinosaurs. Zoological Journal of the Linnean Society 158; 196–230.

Zanno, L.E. and Makovicky, P.J. 2013. Neovenatorid theropods are apex predators in the Late Cretaceous of North America. Nature Communications 3827; 1–9.

Memoirs of Museum Victoria 74: 63–71 (2016) Published 2016

ISSN 1447-2546 (Print) 1447-2554 (On-line)
http://museumvictoria.com.au/about/books-and-journals/journals/memoirs-of-museum-victoria/

A close look at Victoria's first known dinosaur tracks

Anthony J. Martin

Department of Environmental Sciences, Emory University, Atlanta, Georgia 30322 USA (geoam@emory.edu)

Abstract

Martin, A.J. 2016. A close look at Victoria's first known dinosaur tracks. *Memoirs of Museum Victoria* 74: 63–71.

Lower Cretaceous (Aptian-Albian) rocks of Victoria, Australia are well known for their dinosaur body fossils, but not so much for their trace fossils. For example, the first known dinosaur track from the Eumeralla Formation (Albian) of Knowledge Creek, Victoria, was not discovered until 1980. This specimen, along with two more Eumeralla tracks found at Skenes Creek in 1989, constituted all of the dinosaur tracks recognised in Lower Cretaceous strata of southern Australia until the late 2000s. Unfortunately, none of these first-known dinosaur tracks of Victoria were properly described and diagnosed. Hence, the main purpose of this study is to document these trace fossils more thoroughly. Remarkably, the Knowledge Creek and one of the Skenes Creek tracks are nearly identical in size and form; both tracks are attributed to small ornithopods. Although poorly expressed, the second probable track from Skenes Creek provides a search image for less obvious dinosaur tracks in Lower Cretaceous strata of Victoria. The Skenes Creek tracks were also likely from the same trackway, and thus may represent the first discovered dinosaur trackway from Victoria. These tracks are the first confirmed ornithopod tracks for Victoria, augmenting abundant body fossil evidence of small ornithopods ('hypsilophodontids') in formerly polar environments during the Early Cretaceous.

Keywords

Cretaceous, dinosaur, footprint, ichnology, ornithopod, trace fossil, track.

Introduction

Victoria is world famous for its dinosaur body fossils, which reflect the best-documented polar-dinosaur assemblage in the Southern Hemisphere (Rich et al., 2002; Rich and Vickers-Rich, 2003; Kear and Bruce, 2011; Benson et al., 2012). The first known dinosaur body fossil in Victoria, a theropod ungual from the Wonthaggi Formation (Aptian) found by William Ferguson in 1903, was also the first Australian dinosaur fossil known to science (Rich and Vickers-Rich, 2000; Rich and Vickers-Rich, 2003). However, dinosaur trace fossils, such as tracks, nests, burrows, and other direct evidence of dinosaur behavior in the Cretaceous rocks of Victoria remained unnoticed by palaeontologists until 1980, 77 years after the first recognised body fossil. This ichnological drought ended when Thomas H. Rich and Patricia Vickers-Rich discovered and collected a dinosaur track from the Eumeralla Formation (Albian) at Knowledge Creek, Victoria (Rich and Vickers-Rich, 2000) (fig. 1).

Another eight years passed before two more dinosaur tracks were noticed in a Eumeralla Formation stratum at Skenes Creek in early 1989. In 2006, I recognized two large theropod tracks in the Wonthaggi Formation at the Flat Rocks ("Dinosaur Dreaming") dinosaur dig site, near Inverloch, Victoria; Tyler Lamb then found another at the same site in 2007 (Martin et al., 2007). Three years later, the largest assemblage of polar-dinosaur tracks in the Southern Hemisphere – made by small- to moderate-sized theropods – was discovered in the Eumeralla Formation at Milanesia Beach (Martin et al., 2012). Recently, closely associated tridactyl and tetradactyl tracks were described from Dinosaur Cove, and were interpreted as non-avian theropod and avian in origin, respectively (Martin et al., 2014). Otherwise, the only other trace fossils ascribed to non-avian dinosaurs in Lower Cretaceous strata of Victoria include possible burrows (Martin, 2009). Nests, toothmarks, gastroliths, coprolites and other such trace fossils apparently have not yet been discovered (Martin, 2014).

The Knowledge Creek track has been figured in numerous publications, and was much reproduced for educational purposes (Rich and Vickers-Rich, 2000, 2003). However, it and the Skenes Creek tracks have not been described nor interpreted in detail. Thus the main purposes of this study are to: (1) thoroughly document these tracks; (2) interpret their dinosaur makers and preservational modes; (3) assess the palaeontological importance of the tracks; and (4) suggest how this information might be used to prospect for more such tracks in Lower Cretaceous strata of Victoria.

Methods

The three specimens are in the Museum Victoria Palaeontology Collection (NMV P); thus they are available for further study by qualified researchers. I measured the tracks with Mitutoyo digital calipers, using minimum-outlines for track widths, lengths, and other parameters (fig. 2). Digit-impression lengths

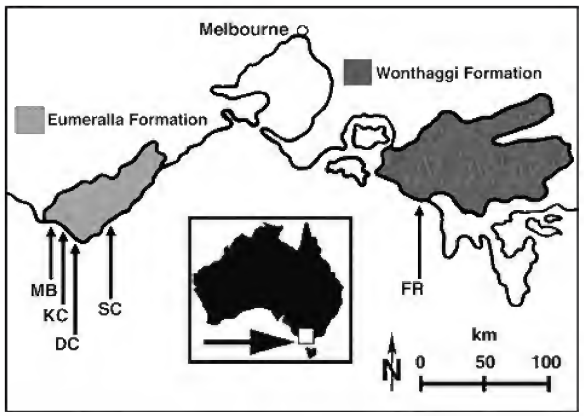

Figure 1. Locality and outcrop map for Early Cretaceous dinosaur tracks found thus far in Victoria, with the three tracks described in this study coming from Knowledge Creek and Skenes Creek. Key and latitude-longitude coordinates for each of the tracksites, from east to west: Flat Rocks (FR), S38° 45.3', E145° 40.9'; Skenes Creek (SC), S38° 42.9', E143° 44.4'; Dinosaur Cove (DC), S38° 46.9', E143° 24.3'; Knowledge Creek (KC), S38° 45.3', E143° 20.9'; Milanesia Beach (MB), S38° 45.3', E143° 19.3'.

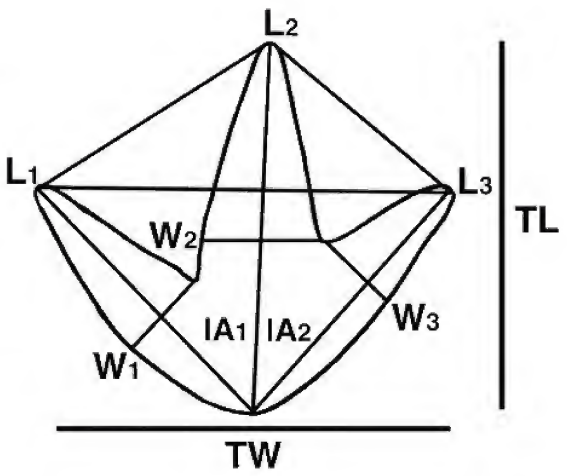

Figure 2. Track parameters measured in this study. Key: TW = total width; TL = total length; L1-L3 = digit lengths; W1-3 = digit widths; IA1-IA2 = interdigital angles. Anterior triangle defined by total track width (base of the triangle) and middle-digit length measured from that base.

were measured from the midline of each digit, and digit-impression widths were taken perpendicular to this midline and medially along the length of each impression. Interdigital angles were measured with a circular protractor, using a digit-impression axis radiating from a single point on the rear margin of the track, as depicted by Thulborn (1990, fig. 4.5). The anterior triangle length:width ratio (*sensu* fig. 2 in Lockley, 2009) was derived from measuring the base of a triangle, defined by the width between the lateral digit impressions and the length of the middle digit impression from that base. Semiquantitative and qualitative information, such as the host lithology and other descriptive traits of the tracks, were also noted. All data are provided here and summarized (table 1) so that future investigators may examine, test, or otherwise attempt to correct the results reported here.

Descriptions

Knowledge Creek Track. On December 18, 1980, Thomas Rich and Patricia Vickers-Rich discovered the Knowledge Creek track, cataloged as NMV P159790 (fig. 3, Appendix I). The track was located on a marine platform just above sea level and about 100 m east of Knowledge Creek. Rich and Vickers-Rich used hand chisels and rock hammers to extract and collect the track, which they brought to the museum.

The track is in a very fine-fine lithic arenite, although the track itself is filled with fine-coarse, moderately sorted quartz and lithic sand held together with hematitic cement. The bed is 36-47 mm thick and horizontally laminated in cross section, with no apparent disruptions of bedding by bioturbation. The area surrounding the track is flat, and lacks other physical or biogenic sedimentary structures on this surface. The track is preserved as a nearly flat but positive-relief (raised) epichnion, rather than a depression. It was weathered such that its form is expressed in nearly full relief.

The track is tridactyl and mesaxonic. It is almost equant in length and width: 106 mm long and 118 mm wide, with a length:width ratio of 0.90. The anterior triangle length:width ratio is 0.40, with a base (width) of the triangle of 118 mm and length from that base of 47 mm. Outermost digit impressions were 90 mm and 84 mm long (left and right, respectively), and the central impression is also the length of the track, 106 mm. Medial thicknesses of the three digit impressions, measured perpendicular to the long axis of each digit, are from left to right: 25 mm, 31 mm, and 30 mm. Using an average of 29 mm, digit-impression widths are about 27% of footprint length. Divarication between the outermost digit impressions is 85°, which combines an angle of 47° between the left and middle, and 38° between the right and middle. All three impressions are outlined completely. Digit impressions narrow distally, but are subrounded at their ends. The track bears three small, oval protuberances, two on the middle digit impression and one on the left. These structures on the middle impression are 4 x 8 mm wide (toward the distal end) and 4 x 5 mm wide (at the right intersection with the right impression), whereas the one on the left impression is 5 x 5 mm (outer edge). Each structure is labeled as "B" (for "burrow") on fig. 3b.

The sand fill varies from 4 mm thick at the posterior "heel" (proximal) end of the track to 8-10 mm thick at the anterior (distal) ends of each digit impression (fig.3c,d). Thus a longitudinal profile of the track would show a gradual thickening of the sand fill from posterior to anterior. A 1-mm thick, slightly curved thread-like structure, filled with the same reddish sand as the track, cross-cuts the grey lithic arenite below the right posterior portion of the track (fig. 3c).

Table 1. Measurements of dinosaur tracks from: Knowledge Creek (KC1), specimen P.159790; and Skenes Creek (SC1 and SC2), specimen P.208232. Key: L = length, W = width, L:W = length:width, IA1 = left-middle interdigital angle, IA2 = middle-right interdigital angle, D = divarication (interdigital angle between left and right), L1 = left digit length, L2 = middle digit length (same as track length), L3 = right digit length, W1 = left digit width, W2 = middle digit width, W3 = right digit width, at-L = anterior triangle length, at-W = anterior triangle width, at-L:W = anterior triangle length:width, n/a = not applicable. All measurements are in millimeters except for IA1, IA2, and D, which are in degrees.

Track	L	W	L:W	IA1	IA2	D	L1	L2	L3	W1	W2	W2	at-L	at-W	at-L:W
KC1	106	118	0.90	47°	38°	85°	90	106	84	25	31	30	47	118	0.40
SC1	106	115	0.92	37°	46°	83°	91	106	87	n/a	34	36	43	115	0.37
SC2	127	138	0.92	44°	27°	71°	102	127	103	n/a	n/a	n/a	43	138	0.31

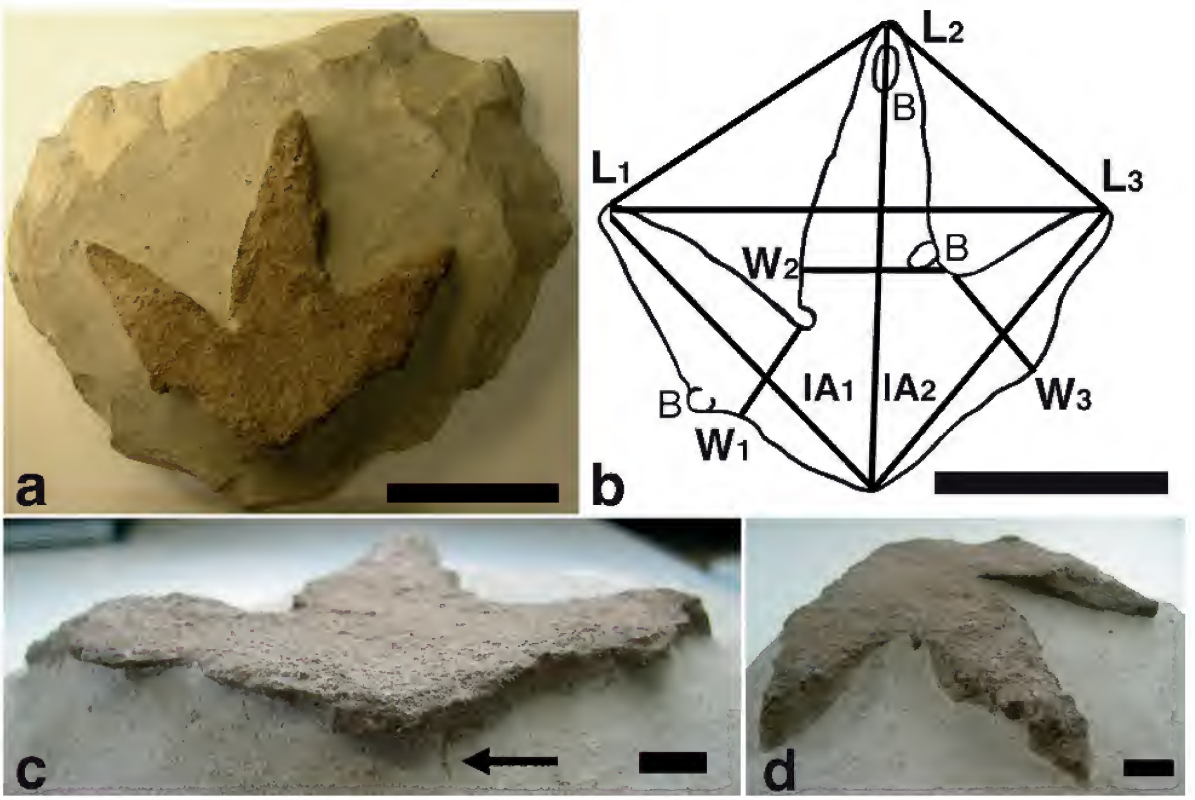

Figure 3. Knowledge Creek track, NMV P159790. a. Overall top view of track in collected slab, with bedding and chisel marks evident along edge; scale = 5 cm. b. Outline of track and parameters measured, with anterior triangle indicated (see Figure 2 for key), B = invertebrate burrows; scale = 5 cm. c. Posterior-edge view of track, showing full relief of track, thin fill of coarse sand, and possible small burrow below (arrow); scale = 1 cm. D. Anterior-oblique view of track, showing gradually thicker sand fill toward distal ends of digits; scale = 1 cm.

Skenes Creek Track 1. Helmut Tracksdorf, a local citizen and geologist from the Skenes Creek area, discovered two dinosaur footprints there in January 1989, with both cataloged as NMV P208232 (figs. 4-5, Appendix I). Tracksdorf alerted Museum Victoria about them, and personnel from the Museum collected the tracks on March 18, 1989. Although no additional information is available about who collected or cataloged these tracks, the exact field location of the tracks was just recently verified, having come from the supratidal marine platform of rock exposed between Skenes Creek and Browns Creek (Appendix II).

The most clearly defined of the two tracks (herein designated Skenes Creek Track 1) is in a 16 x 20 cm cut slab of very fine-fine, well-sorted lithic arenite. The bed is 25-41 mm thick, with seven parallel and symmetrical ripples sharing the top surface with the track. Assuming an arbitrary "north"

Figure 4. Skenes Creek Track 1, NMV P208232. a. Overall top view of track in collected slab, with rock saw cuts evident on three sides, as well as symmetrical and parallel ripple marks below track; scale = 5 cm. b. Close-up of track, showing raised relief and thin, laminated "platform" above ripple marks; scale = 5 cm. c. Outline of track and parameters measured, with anterior triangle indicated (see Figure 2 for key); scale = 5 cm.

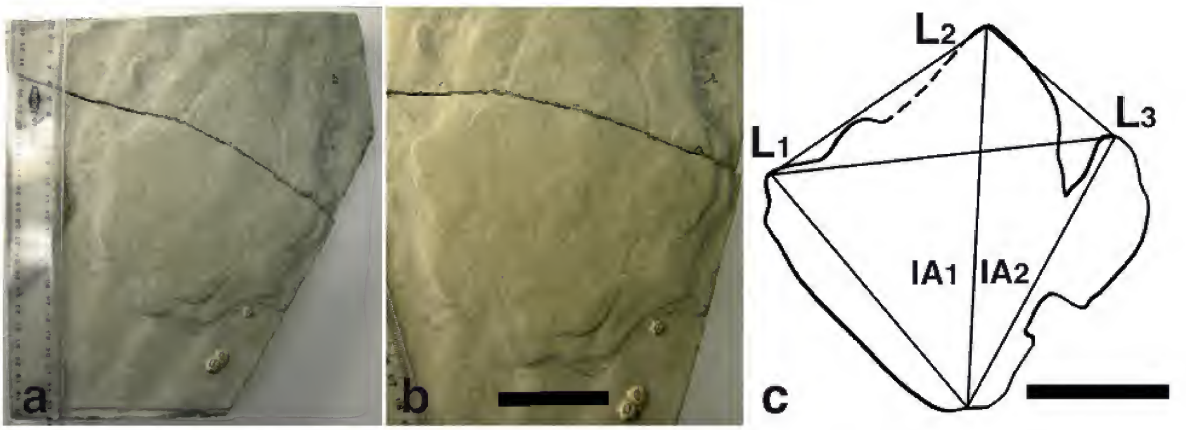

Figure 5. Skenes Creek Track 2, NMV P208232 (shared with Track 1). a. Overall top view of track in collected slab, with rock saw cuts evident on five sides and fracture cutting across anterior part of track; scale (left) in centimetres and millimetres. b. Close-up of track, showing raised relief and thin, laminated "platform" above ripple marks; scale = 5 cm. c. Outline of track and parameters measured, with anterior triangle indicated (see Figure 2 for key); scale = 5 cm.

defined by the axis of the middle digit impression, ripple-crests trend "northeast-southwest." Ripples have amplitudes of 4-7 mm and wavelengths of 30-40 mm; ripple bedding was also evident in cross-section. The track is preserved as a nearly flat, 1-2 mm thick positive-relief (raised) epichnion, but is filled with sand texturally and compositionally identical to the main host lithology. It is circumscribed and somewhat mimicked in outline by a 4-8 mm thick quadrilateral platform between it and the rippled surface. Bedding in the track and its platform is mostly planar and laminated, although slight variations in surface topography synch with underlying ripples.

The track is tridactyl, mesaxonic, and nearly equant in length and width, at 106 mm long and 115 mm wide; this results in a length:width ratio of 0.92. Outermost digit impressions were 91 mm and 87 mm long (left and right, respectively), and the central impression is the length of the track, 106 mm. The right impression has a seemingly complete outline, whereas the left is apparently expressed partially. The anterior triangle length:width ratio is 0.37, with a base (width) at 115 mm and length measured from that base of 43 mm. Medial thicknesses of the two complete digit impressions are, from middle to right, 34 and 36 mm. With an average of 35 mm, digit-impression widths are about 33% of footprint length. Divarication between the outermost impressions is 83°, which combines an angle of 37° between the left and middle, and 46° between the right and middle. Both the middle and right digit impressions narrow distally, but are subrounded at their ends. An unidentified modern barnacle is attached to the lower right-side edge of the track.

Skenes Creek Track 2. This probable dinosaur track (herein called Skenes Creek Track 2) was also cataloged as part of NMV P208232 (fig. 5, Appendix I). Based on its same specimen

number and having many identical sedimentary traits as the Skenes Creek Track 1, I conclude that it was also discovered by Helmut Tracksdorf in 1989, then later collected from the same marine-platform bedding plane by Museum of Victoria personnel at the same time as Skenes Creek Track 1. This supposition is supported by two adjacent rock-saw cuts at the probable discovery site, which were relocated by Helmut Tracksdorf in 2013 and Mike Cleeland in 2014 (Appendix II).

The track is in a pentagonal slab (cut by a rock saw) with long dimensions of 24 x 21 cm; a fracture runs transversely across the track (fig. 5a). The lithology is identical to that hosting the Skenes Creek Track 1, consisting of a very fine-fine, well-sorted lithic arenite, with a bed thickness of 30-40 mm. The top surface of the bed has six parallel, symmetrical, and low-amplitude ripples underneath the track. Using an arbitrary "north-south" defined by the medial axis of the track, ripple-crests trend "northeast-southwest." Ripples have amplitudes of 5-7 mm and wavelengths of 25-40 mm; ripple bedding was visible in cross-section. Also like Skenes Creek Track 1, it is preserved as an almost-flat, positive-relief epichnion, filled with sand texturally and compositionally identical to that of its host rock. The track is circumscribed by two levels, one about 5 mm above the rippled surface and another inner and topmost level that is about 2 mm thick. Again, like Skenes Creek Track 1, bedding in both upper levels is mostly planar and laminated, with variations in surface topography corresponding with underlying ripples.

Skenes Creek Track 2 is apparently tridactyl, with three rounded points opposite another rounded end, which are assumed as the anterior and posterior parts of the track, respectively. Using this configuration, track length was 127 mm, whereas the width was 138 mm, resulting in a length:width ratio of 0.92. Owing to vague outlines of presumed digit impressions, width measurements were not attempted, but lengths could be measured, yielding 102 mm for the left digit impression and 103 mm for the right. Assuming this configuration, the interdigital angles were 44° (left-middle) and 27° (middle-right), for a divarication of 71°. The anterior triangle length:width ratio was also calculable, yielding a value of 0.31, with the base (width) the same as track width (138 mm) and length measured from that base of 43 mm. The posterior part of the track is slightly indented along its margin, and the lower-level outline just below the measured part of the track is bilobed. Three unidentified modern barnacles are attached on the lowermost bedding surface, all to the lower right of the track, but with one proximal and two more distal.

Interpretations and Discussion

The two most completely preserved tracks from Knowledge Creek and Skenes Creek (Track 1) were very likely pes impressions made by small 'hypsilophodontid' ornithopods akin to *Atlascopcosaurus*, *Fulgurotherium*, or *Leaellynasaura*, all of which are in the Eumeralla Formation (Rich and Vickers-Rich, 1999; Rich et al., 2010). These trace fossils thus constitute the first ornithopod footprints discovered in Lower Cretaceous rocks of Victoria; all others found since the 1980s have been attributed to theropods (Martin et al., 2007, 2012, 2014). The interpretation of tracks as ornithopod tracks is based on track forms, sizes, and their preservation in strata chronologically close to those containing the skeletal remains of these ornithopods in the Eumeralla Formation (Rich and Vickers-Rich, 2003; Kear and Bruce-Hamilton, 2011). The second probable dinosaur track from Skenes Creek (Track 2), although less definite in outline, is also likely from a small ornithopod and comes from the same bed as the other track. Furthermore, it may have been part of the same trackway as the more completely defined track.

The two comparable tracks from Knowledge Creek and Skenes Creek Track 1 are remarkably similar in size and form (Figure 6). Both tracks are tridactyl, presumably reflecting digits II-IV, with digit II-IV divarications of 85° (Knowledge Creek) and 83° (Skenes Creek Track 1). Their lengths and widths are nearly identical, their digit-impression widths vary by only a few millimeters, and middle digit-impression widths (digit III) are 27% and 33% of footprint length (Knowledge Creek and Skenes Creek Track 1, respectively). Moreover, their anterior triangle length:width ratios are nearly convergent, at 0.40 for the Knowledge Creek track and 0.37 for Skenes Creek Track 1. Their expression as positive-relief epichnia, along with the other less completely preserved Skenes Creek ichnite, is also noteworthy, implying their preservational conditions may have been similar as well. However, because the tracks are nearly symmetrical and do not show any pressure-release structures related to movement (*sensu* Martin et al., 2012), I cannot identify digit impressions II or IV in either tracks, nor state with certainty whether either represents a right or left footprint.

Both quantitative and qualitative traits indicate the Knowledge Creek and Skenes Creek Track 1 trace fossils are ornithopod tracks. Length:width ratios of about 0.9, digit II-IV divarications of 83-85°, anterior-triangle length-width ratios of about 0.4, relatively thick digits, and rounded (blunt) ends on digit impressions are all consistent with ornithopod tracks (Moratallo et al., 1988; Lockley, 2009; Mateus and Milàn, 2010; Martin et al., 2012; Farlow et al., 2012). Relatively small sizes of the tracks also agree with assessments of Eumeralla Formation dinosaur assemblages, which are dominated by small 'hysilophodontids' (Rich and Vickers-Rich, 1999; Rich et al., 2002). A possibly comparable ichnogenus in size and form to these tracks is *Dinehichnus* isp. (*sensu* Gierliński et al, 2009, fig. 7), reported from the Late Jurassic of Poland and North America, and interpreted as that of a small ornithopod (Lockley and Foster, 2006; Foster, 2007; Gierliński et al., 2009; Lockley et al., 2009). Furthermore, the Victoria tracks resemble *Iguanodontipus*, which has been attributed to Early Cretaceous iguanodontids (Sarjeant et al., 1998; Cobos and Gascó, 2012), although these are often much larger (Castanera et al., 2013). In Australia, *Wintonopus* of the Lower Cretaceous Winton Formation (Queensland) is another small ornithopod track comparable to the Victoria specimens (Thulborn and Wade, 1984; Romilio et al., 2013). In short, similarities between the Victoria tracks and these ichnogenera affirm that their likely tracemakers were small ornithopods. The tracks can be further used to estimate tracemaker size via a footprint formula of 4.0 x footprint length = hip height (Alexander, 1976; Henderson,

Figure 6. Skenes Creek Track 1 (left) and Knowledge Creek track (right) together, allowing for a side-by-side comparison. The slab holding the Knowledge Creek track is slightly thicker (~10 mm) than the Skenes Creek slab, hence they are not being viewed on exactly the same horizon; scale = 10 cm.

2003). Using this formula, the Knowledge Creek and Skenes Creek (Track 1) ornithopod tracemakers had hip heights of about 42 cm (based on 10.6 x 4.0 = 42.4 cm). Owing to its poor definition, the hip height of the trackmaker for Skenes Creek Track 2 was not calculated, but if it does indeed belong to the same trackway, it can be assumed as similar to that of Track 1.

Other dinosaur tracemakers that could have made tridactyl tracks include small theropods, such as those interpreted from the Eumeralla Formation dinosaur tracksite at Milanesia Beach (Martin et al., 2012) or a single non-avian theropod track from Dinosaur Cove (Martin et al., 2014). However, the Milanesia and Dinosaur Cove theropod tracks were "thin-toed," with middle digit widths of only 5-16% of footprint lengths. In contrast, digits of the Knowledge Creek and Skenes Creek tracks were more than twice as thick, at 27 and 33% of footprint lengths (respectively). Furthermore, most of the Milanesia Beach tracks had thin (sharp) clawmarks, which are also characteristic of theropods (Martin *et al.*, 2012, and references therein). Avian theropods (birds) were also discounted as possible tracemakers for the Knowledge Creek and Skenes Creek tracks for the same reasons, as well as for having digital divarications of 83-85°; bird tracks more typically have divarications of 95-120° (Lockley et al., 1992; Falk et al., 2011; Martin et al., 2014). Both tracks also lack evidence of a digit I impression, a trait noted in two similarly sized avian tracks from the Eumeralla Formation at Dinosaur Cove (Martin et al., 2014).

The positive-relief (raised) expression of all three tracks, yet on bed tops as epichnia, is unusual for most fossil tracks. Fossil tracks are normally preserved either as depressions (negative-relief epichnia) or as natural casts on bed bottoms (positive-relief hypichnia) (Lockley, 1991; Farlow et al., 2012). Because all three specimens were recovered from marine platforms eroded by tides and waves, their positive-relief preservation implies that sediment filling the tracks was better cemented – and hence more resistant to weathering – than their host rocks. This differential cementation and weathering that resulted in convex dinosaur tracks on bed tops was also noted for large theropod tracks in the Wonthaggi Formation (Aptian) at the Flat Rocks ("Dinosaur Dreaming") dig site (Martin et al., 2007). An uneven fill and cementation probably contributed to the vague definition of Skenes Creek Track 2, in which the "true track" is buried below the outwardly expressed positive epichnion.

Track surfaces are mainly uniform, but the Knowledge Creek track contained three oval-outlined protuberances, which I interpret as cross-sections of invertebrate burrows (figs. 3a,b). The burrows would have been made in an originally thicker bed composed of the same medium-coarse sand that filled the track. A thin vertical structure with the same sand fill underneath and toward the rear of the track is also likely a burrow, but one in the underlying host lithology and passively filled by sand from above. Owing to insufficient details, ichnotaxa were not assigned to these burrows.

Skenes Creek Track 2, despite its larger dimensions and less definite outline, is similar enough to its companion track from the same site that it is also interpreted as a dinosaur track, and probably that of a small ornithopod. This supposition is based on its tridactyl form, rounded ends to the probable digit impressions, a length:width ratio of 0.92, and an anterior-triangle length:width ratio of 0.31, which again are consistent with ornithopod tracemakers (Lockley, 2009). One of the "interdigital" angles on Skenes Creek Track 2 roughly corresponded with that of Track 1 (44° versus 46°, respectively); however, divarication was notably different (71° versus 83°, respectively). As mentioned before, the original depressions ("true track") for both Tracks 1 and 2 are likely underneath the currently expressed positive-relief outline, filled with sand that later cemented differently from the

surrounding substrate. These depressions may even cut across the ripples underneath the track or deformed surrounding sediments so that the subsequent fill and cementation of that fill affected the outward appearance and weathering of the tracks on the same marine platform.

Although no information was recorded about the spatial relationship of the Skenes Creek tracks on the marine platform when and where they were recovered in 1989, the rock-saw cuts corresponding to their locations were found by Helmut Tracksdorf in June 2014, which was confirmed by Michael Cleeland in February 2015 (Appendix II). Interestingly, the rectangular outlines of the rock-saw cuts are directly aligned and in a sandstone bed with low-amplitude ripples, with ripple crests oriented obliquely relative to the outlines. Furthermore, both tracks have similar forms and are atop ripples oriented the same with respect to footprint directions, i.e., "northeast-southwest" with tracks pointing toward an arbitrary "north." Consequently, these tracks likely belong to the same trackway and were made by the same individual ornithopod. If so, these would constitute the first discovered dinosaur trackway in Victoria, usurping a small-theropod trackway discovered at Milanesia Beach in 2010 (Martin et al., 2012). To test this preliminary interpretation, the exact distance between incisions will need to be measured, and rock-saw outlines should be compared to the shapes and orientations of the two recovered slabs. Conversely, if the tracks are not aligned (e.g., point in opposite directions) and the collected slabs do not correspond to the outlines, they can be reasonably attributed to separate trackways made by similar tracemakers.

Unfortunately, all three tracks are isolated specimens taken out of context from their original field exposures in 1980 (Knowledge Creek) and 1989 (Skenes Creek). Thus very little additional information can be said about the palaeoenvironments trodden by their ornithopod tracemakers. The Eumeralla Formation is interpreted as a series of fluvial channel-fill, overbank, and floodplain facies deposited in circumpolar rift valleys, with less common alluvial or lacustrine facies (Bryan et al., 1997; Tosolini et al., 1999; Vickers-Rich et al., 1999). Given this broad framework, the most probable palaeoenvironments for dinosaurs making preservable tracks would have been point bars or floodplains, which are common sites for dinosaur track preservation (Martin, 2014). If the Skenes Creek trackmaker was walking on a floodplain, ripples underneath these tracks might have been current ripples, exposed after water flowed over that surface. Similar modern occurrences of current ripples later cross-cut by vertebrate tracks, providing a possible analogue for the Skenes Creek tracks, were described from a Arctic point bar in Alaska (Martin, 2009b). The largest assemblage of dinosaur tracks from the Eumeralla Formation – found at Milanesia Beach and described from two separate slabs of the same sandstone bed – was also in what were likely floodplain sandstones (Martin et al., 2012). Indeed, the circumpolar setting of these river valleys during the Early Cretaceous meant that dinosaur tracks might have been made and preserved only seasonally, from spring through fall (Martin et al., 2012). If so, this limiting factor may account for the relative rarity of dinosaur tracks and other trace fossils in Lower Cretaceous strata of Victoria (Martin et al., 2012).

Conclusions

The first known dinosaur tracks from Victoria may be small and few, but nonetheless carry useful information about Early Cretaceous dinosaurs in Victoria. For one, the Knowledge Creek and Skenes Creek tracks are from localities where no dinosaur bones are yet known, therefore confirming a dinosaurian presence at each of these places. Secondly, the tracks demonstrate that dinosaurs – specifically small ornithopods – actually lived in the palaeoenvironments of these places. In contrast, most dinosaur body fossils in Victoria, such as those from the Flat Rocks ("Dinosaur Dreaming") site at Inverloch and Dinosaur Cove, were likely transported and deposited in fluvial channels (Rich and Vickers-Rich, 2000; Rich et al., 2003). Lastly, these tracks are the first discovered Early Cretaceous ornithopod tracks from Victoria, and the Skenes Creek tracks may represent the first discovered dinosaur trackway in Victoria. These finds thus supplement comparatively abundant body fossils of 'hypsilophodontids' in the Wonthaggi and Eumeralla Formations.

The preservation of these small ornithopod tracks as positive-relief epichnia, as well as those of large theropod tracks in the Wonthaggi Formation (Martin et al., 2007), also may be typical modes of preservation for dinosaur tracks in Lower Cretaceous strata of Victoria. Hence future researchers scanning bedding planes of the Wonthaggi and Eumeralla Formations might adjust their search images for raised tracks on bed tops, rather than just depressions. Furthermore, less definite forms of dinosaur, such as that of Skenes Creek Track 2, should not be so easily ignored or dismissed once found. Given all of these insights, I have every confidence that more dinosaur tracks will be discovered, whether from ornithopods, theropods, or other tetrapod taxa whose trace fossil records are not yet known from this otherwise palaeontologically well-studied area of Australia.

Acknowledgements

I am extremely grateful to Thomas (Tom) Rich and Patricia (Pat) Vickers-Rich for their guidance, mentorship, and friendship over the years, starting with a sabbatical I enjoyed at Monash University in 2006 and visits to Australia since then. I thank Erich Fitzgerald (Museum Victoria) for asking me to write this manuscript, as well as Lisa Buckley and Anthony Romilio for their insightful and helpful reviews. Appreciation is extended to David Pickering, Lesley and Gerry Kool, Michael and Naomi Hall, and Michael Cleeland for their time in the field with me, as well as educating this inexperienced Yank whenever he dropped in for a too-brief glance at their lovely Lower Cretaceous rocks. Helmut Tracksdorf and Michael Cleeland also were invaluable in helping to document the original discovery site of the Skenes Creek tracks. The Emory University Faculty Travel Fund and the Center for International Programs Abroad assisted with some of my travel expenses during various visits. Last but not least, I am indebted to my wife, Ruth, nicknamed "Lefty" by her fellow southpaw Tom, for her sinistral support during much of the research.

References

Alexander, R.M. 1976 Estimates of speeds of dinosaurs. *Nature* 262: 129-130.

Benson, R.B., Rich, T.H., Vickers-Rich, P. and Hall, M. 2012. Theropod fauna from Southern Australia indicates high polar diversity and climate-driven dinosaur provinciality. *PLoS ONE* 7(5): e37122.

Bryan, S.E., Constantine, A.E., Stephens, C.J., Ewart, A., Schön, R.W., and Parianos, J. 1997. Early Cretaceous volcano-sedimentary successions along the eastern Australian continental margin: implications for the break-up of eastern Gondwana. *Earth and Planetary Science Letters* 153: 85–102.

Castanera, D., Pascual, C., Razzolini, N.L., Vila, B., Barco, J.L., and Canudo, J.I. 2013. Discriminating between medium-sized tridactyl trackmakers: Tracking ornithopod tracks in the base of the Cretaceous (Berriasian, Spain). PLoS ONE 8(11): e81830.

Cobos, A. and Gascó, F. 2012 Presencia del icnogénero *Iguanodontipus* en el Cretácico Inferior de la provincia de Teruel (España). *Geogaceta* 52: 185-188.

Farlow, J.O., Chapman, R.E., Breithaupt, B., and Matthews, N. 2012. The scientific study of dinosaur footprints. Pp. 713–759 in: Brett-Surman, M.K., Holtz, T.R., Jr., and Farlow, J.O. (eds), *The Complete Dinosaur* (2nd Edition). Indiana

University Press: Bloomington, Indiana. 1112 pp.

Foster, J.R. 2007. *Jurassic West: The Dinosaurs of the Morrison Formation and Their World*. Indiana University Press. Bloomington, Indiana. 389 pp.

Gierliński, G.D., Niedźwiedzki, G. and Nowacki, P. 2009. Small theropod and ornithopod tracks in the Jurassic of Poland. *Acta Geologica Polonica* 59: 221-234.

Henderson, D.M. 2003. Footprints, trackways, and hip heights of bipedal dinosaurs: testing hip height predictions with computer models. *Ichnos* 10: 99–114.

Kear, B.P., and Hamilton-Bruce, R.J. 2011. *Dinosaurs in Australia: Mesozoic Life from the Southern Continent*. CSIRO Publishing: Collingwood, Victoria. 190 pp.

Lockley, M.G. 1991. *Tracking Dinosaurs: A New Look at an Ancient World*. Cambridge University Press: Cambridge, U.K. 264 pp.

Lockley, M.G., and Foster, J.R. 2006. Dinosaur and turtle tracks from the Morrison Formation (Upper Jurassic) of Colorado National Monument, with observations on the taxonomy of vertebrate swim tracks. Pp. 193-198 in: Foster, J.R., and Lucas, S.G. (eds), Paleontology and Geology of the Upper Jurassic Morrison Formation, *New Mexico Museum of Natural History and Science Bulletin*, 36: 249 pp.

Lockley, M.G., Yang, S.Y., Matsukawa, M., Fleming, F. and Lim, S K. 1992. The track record of Mesozoic birds: evidence and implications. *Philosophical Transactions of the Royal Society of London* 336: 113–134.

Lockley, M.G. 2009. New perspectives on morphological variation in tridactyl footprints: clues to widespread convergence in developmental dynamics. *Geological Quarterly* 53: 415–432.

Martin, A.J., 2009a. Dinosaur burrows in the Otway Group (Albian) of Victoria, Australia, and their relation to Cretaceous polar environments. *Cretaceous Research* 30: 1223–1237.

Martin, A.J., 2009b. Neoichnology of an Arctic fluvial point bar, North Slope, Alaska. *Geological Quarterly* 53: 383–396.

Martin, A.J. 2014. *Dinosaurs Without Bones: Dinosaur Lives Revealed by Their Trace Fossils*. Pegasus Press: New York. 460 pp.

Martin, A.J., Vickers-Rich, P., Rich, T.H. and Kool, L. 2007. Polar dinosaur tracks in the Cretaceous of Australia: though many were cold, few were frozen. *Journal of Vertebrate Paleontology* 27 (Supplement 3): 112A.

Martin, A.J., Rich, T.H., Hall, M., Vickers-Rich, P. and Vazquez-Prokopec, G. 2012. A polar dinosaur-track assemblage from the Eumeralla Formation (Albian), Victoria, Australia. *Alcheringa* 36: 171–188.

Martin, A.J., Vickers-Rich, P., Rich, T.H., and Hall, M. 2014. Oldest known avian footprints from Australia: Eumeralla Formation (Albian), Dinosaur Cove, Victoria. *Palaeontology* 57: 7–19.

Mateus, O., and Milán, J. 2010. A diverse Upper Jurassic dinosaur ichnofauna from central-west Portugal. *Lethaia* 43: 245–257.

Moratalla, J.J., Sanz, S.L., and Jiminez, S., 1988. Multivariate analysis on Lower Cretaceous dinosaur footprints: discrimination between ornithopods and theropods. *Geobios* 21: 395–408.

Rich, T.H., and Rich, P.V. 1989. Polar dinosaurs and biotas of the Early Cretaceous of southeastern Australia. *National Geographic Research* 5: 15–53.

Rich, T.H., and Vickers-Rich, P. 1999. The Hypsilophodontidae from southeastern Australia. Pp. 167–180 in: Tomada, Y., Rich, T.H., and Vickers-Rich (eds.), Proceedings of the Second Gondwana Dinosaur Symposium. *National Science Museum Monographs* 15. 296 pp.

Rich, T.H., and Vickers-Rich, P. 2000. *Dinosaurs of Darkness*. Indiana University Press: Bloomington, Indiana. 222 pp.

Rich, T.H., and Vickers-Rich, P. 2003. *A Century of Australian Dinosaurs*. Queen Victoria Museum and Art Gallery: Launceston, Tasmania. 124 pp.

Rich, T.H., Vickers-Rich, P., and Gangloff, R.A. 2002. Polar dinosaurs. *Science* 295: 979–980.

Rich, T.H., Galton, P.M., and Vickers-Rich, P. 2010. The holotype individual of the ornithopod dinosaur *Leaellynasaura amicagraphica* Rich & Rich, 1989 (late Early Cretaceous, Victoria, Australia). *Alcheringa* 34: 385–396.

Rich, P.V., Rich, T.H., Wagstaff, B.E., McEwen-Mason, J., Douthitt, C.B., Gregory, R.T., and Felton, E.A. 1988. Evidence for low temperatures and biologic diversity in Cretaceous high latitudes of Australia. *Science* 242: 1403–1406.

Romilio, A., Tucker, R.T., and Salisbury, S.W. 2013. Reevaluation of the Lark Quarry dinosaur Tracksite (late Albian–Cenomanian Winton Formation, central-western Queensland, Australia): no longer a stampede? Journal of Vertebrate Paleontology 33: 102-120.

Sarjeant, W.A.S., Delair, J.B., and Lockley, M.G. 1998. The footprints of *Iguanodon*: A history and taxonomic study. *Ichnos* 6: 183-202.

Thulborn, R.A. 1990. *Dinosaur Tracks*. Chapman & Hall: London. 410 pp.

Thulborn, R.A., and Wade. M. 1984. Dinosaur trackways in the Winton Formation (Mid-Cretaceous) of Queensland. *Memoirs of the Queensland Museum* 21: 413-517.

Tosolini, A.-M.P., McLoughlin, A., and Drinnan, A.N. 1999. Stratigraphy and fluvial sedimentary facies of the Neocomian lower Strzelecki Group, Gippsland Basin, Victoria. *Australian Journal of Earth Sciences* 46: 951-970.

Vickers-Rich, P., Rich, T.H., and Constantine, A. 1999. Environmental setting of the polar faunas of southeastern Australia and adaptive strategies of the dinosaurs. Pp. 181–195 in: Tomada, Y., Rich, T.H., and Vickers-Rich (eds), Proceedings of the Second Gondwana Dinosaur Symposium, *National Science Museum Monographs* 15. 296 pp.

Appendices

Appendix I. Specimen Label Information

Specimen label information for Knowledge Creek track: P.159790; Dinosaur track, Otway Group, Knowledge Creek, Victoria on wave platform about 100 m east of mouth of

Knowledge Creek. T. Rich Exp., 18-12-1980 [December 18, 1980]

Specimen Label Information for Skenes Creek tracks: P.208232; T.H. Rich Exp., 18-3-1989 [March 18, 1989] Skenes Creek (Catalog 149). Locality: Shore platform, Skenes Creek.

Appendix II. Discovery of the Skenes Creek Tracks

The specimen label for the two Skenes Creek tracks does not credit their original discoverer, and repeated inquiries posed to personnel at Museum Victoria and long-time volunteers did not result in anyone taking credit for finding them. So I was gratified to learn in 2013 that credit for their discovery should go to Helmut Tracksdorf, a geologist who lived in Victoria near Skenes Creek at the time of their discovery.

In October 2013, Mr. Tracksdorf read a blog post written by me referring to the track. Mr. Tracksdorf sent me an e-mail message, received on October 20, 2013, revealing that he was the person who found the tracks. According to his message, he then reported these tracks and their location to Museum Victoria personnel. Several months after reporting them, he did not receive a confirmation from Museum Victoria on whether or not the tracks were recovered. However, he later visited the site and saw where they had been cut out of the marine platform. The e-mail message was sent by Helmut Tracksdorf and received by me (Anthony J. Martin) at 5:43 p.m. on October 20, 2013. The full, verbatim text of the e-mail is available for reading with permission of both Mr. Tracksdorf and myself.

Later, on July 9, 2014, Trackdorf contacted me again via e-mail with more information about the probable original location of the tracks; he copied Thomas Rich, David Pickering, Lesley Kool, and Michael Cleeland onto this message. In this message, he described the rock-saw cuts on the marine platform as 50-100 m west of Browns Creek (east of both Skenes Creek and Petticoat Creek) and about 50 m south of the Great Ocean Road. Along with this description, Tracksdorf provided a Google Earth image of the locality, as well as photographs of the site and rock-saw cuts in the marine platform, with the photos taken in June, 2014 by Trackdorf's brother (name not given). These descriptions aided me in figuring the approximate latitude-longitude coordinates of the tracks. On February 17, 2015, Cleeland and his wife (Pip) stopped by the location to look for the rock-saw cuts on the marine platform, relocated them, and photographed the rock-saw cuts; these were aligned with one another and in a rippled sandstone very similar to those of the Skenes Creek tracks (NMV P208232). On March 2, 2015, he sent these photographs to Rich, Pickering, Kool, Trackdorf, and me. Given this confirmation, we were satisfied that this is indeed the discovery site of the tracks.

In deference to their long-established nickname as the "Skenes Creek tracks," I recommend retaining this location designation, rather than adopting the more geographically appropriate "Browns Creek tracks." I also suggest that future researchers searching for more such dinosaur tracks in this area might concentrate their efforts on rippled sandstones in the marine platform between Petticoat Creek and Browns Creek.

Memoirs of Museum Victoria 74: 73–79 (2016) Published 2016

ISSN 1447-2546 (Print) 1447-2554 (On-line)
http://museumvictoria.com.au/about/books-and-journals/journals/memoirs-of-museum-victoria/

Organic geochemistry of a high-latitude Lower Cretaceous lacustrine sediment sample from the Koonwarra Fossil Beds, South Gippsland, Victoria, Australia

Michael L. Tuite*, David T. Flannery and Kenneth H. Williford

NASA Jet Propulsion Laboratory, California Institute of Technology, Pasadena, California, USA
* To whom correspondence should be addressed. E-mail: mtuite@jpl.nasa.gov

Abstract

Tuite, M.L., Flannery , D.T., and Williford, K.H. 2016. Organic geochemistry of a high-latitude Lower Cretaceous lacustrine sediment sample from the Koonwarra Fossil Beds, South Gippsland, Victoria, Australia. *Memoirs of Museum Victoria* 74: 73–79.

The Koonwarra Fossil Beds are widely recognized for their high-fidelity preservation of freshwater/terrestrial vertebrate and invertebrate fossils. A preliminary investigation suggests that organic biomarkers are also exceptionally well preserved and could contribute significantly to understanding the ecology of this ancient lake system. Solvent-extractable organic matter was collected from a single feldspathic siltstone/mudstone sample and analyzed using gas chromatography-mass spectrometry (GC-MS). The distribution of n-alkanes suggests a significant input of terrestrial plant material into the lake. The very low ratio of eukaryotic steranes to bacterial hopanes may reflect the decomposition of abundant plant material in the lake. Polycyclic aromatic hydrocarbons may record wildfire activity in the surrounding watershed.

Keywords

Koonwarra fossil beds, Cretaceous, paleolimnology, biomarkers.

Introduction

The Lower Cretaceous Koonwarra Fossil Beds in South Gippsland, Victoria, Australia (fig. 1), were discovered during road works in 1961 (Jell and Duncan, 1986). They are thought to be a freshwater lacustrine deposit of Barremian-Aptian age based on plant and animal fossils, palynology, and fission track dating (Douglas, 1969, 1974; Dettmann, 1986; Drinnan and Chambers, 1986; Jell and Duncan, 1986). Paleogeographic reconstructions place southern Australia well within the Antarctic Circle at this time, and the $\delta^{18}O$ values of early diagenetic carbonate concretions imply mean annual temperatures of ~5°C, despite a generally warm Cretaceous climate (Embleton and McElhinny, 1982; Rich et al., 1988).

The Koonwarra Fossil Beds are known for high-fidelity preservation of freshwater/terrestrial fossils, including several fish groups, insects, crustaceans, bird feathers and a freshwater xiphosuran (e.g. Riek, 1970; Riek and Gill, 1971; Jell and Duncan, 1986; Vickers-Rich, 1991; Krzemiński et al., 2015). Waldman (1971) interpreted varves and multiple horizons of fish fossils to be the result of winter ice covering a shallow lake and causing anoxia, mass fish kills, and the settling of clay from suspension (which would have further prevented the decomposition of covered carcasses). Warmer conditions during the spring might also be expected to cause decomposition and re-floatation of fish carcasses in a shallow-water environment (Wilson, 1977). Alternatively, Elder and Smith (1988) proposed a stratified lake model, wherein fish carcasses sunk to deep, cold waters, where scavenging and decomposition were inhibited by oxygen depletion. The formation of the fish beds could also be related to toxic summer algal blooms, as suggested by McGrew (1975) for the Eocene Green River Formation.

In this brief report, we present the results of a preliminary study of the organic geochemistry of a sediment sample collected from the Koonwarra Fossil Beds in early 2013. The sample analysed here was collected from the fossil fish beds; approximately 5 m from the bottom of the unit. It is a feldspathic siltstone/mudstone laminated on a mm-cm scale. Fish fossils are abundant in this zone (fig. 2). Our results reveal a well-preserved biomarker record in the Koonwarra deposit and suggest that further geochemical investigation is likely to yield significant insights into Cretaceous paleolimnology and the exceptional taphonomy at Koonwarra. These data also suggest that terrigenous organic matter, deriving both from higher plants and perhaps soil bacteria, was an important supplement to aquatic primary production as a trophic resource for lake consumers.

Materials and Methods

Geochemical analyses were performed in the Astrobiogeochemistry Laboratory (abcLab) at the Jet Propulsion Laboratory. A sample without visible macrofossils was powdered using an alumina grinding dish in a model 8530 Shatterbox (SPEX Sample Prep). A ~0.5 g aliquot was

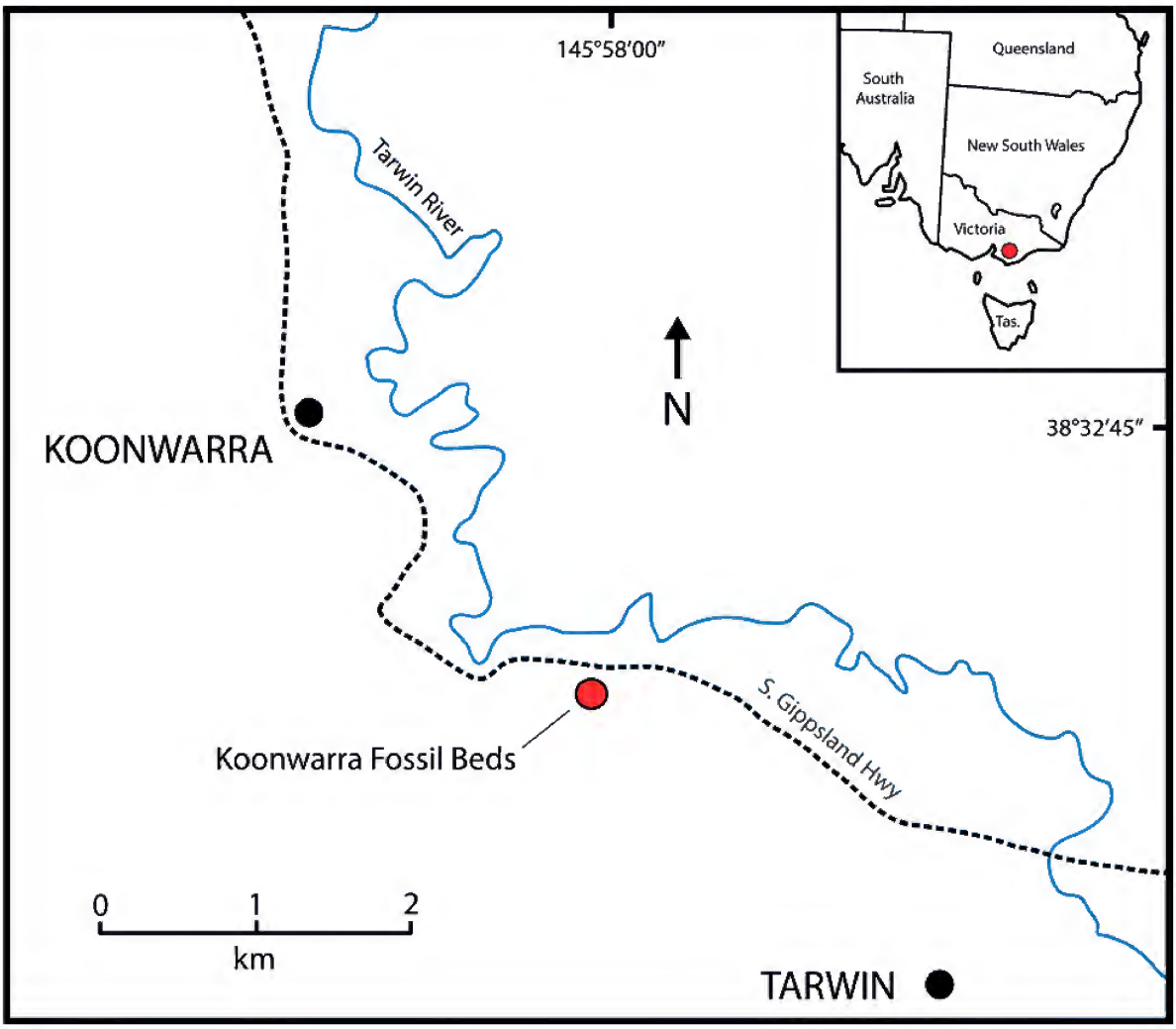

Figure 1: Location of the Lower Cretaceous Koonwarra Fossil Beds in South Gippsland, Victoria, Australia

decarbonated with excess 1N HCl, washed to neutrality with ultrapure (<18 MΩ) deionized water, and dried at 50°C for 48 hours. For determination of total organic carbon (TOC), approximately 30 mg of dried sample was weighed in a tin capsule and combusted at 980°C in a Costech 4010 elemental analyzer. The resulting CO_2 was chemically dried and transferred via He carrier flow to a Delta V Plus (Thermo) isotope ratio mass spectrometer. The mass of organic C was determined by comparison of the area of the mass 44 chromatogram of the sample with the regression of a series of acetanilide standards of known C content ($r^2 = 0.999$).

Thirty grams of the powdered sample were extracted for 48 hours using a soxhlet apparatus in a DCM:methanol (9:1 v:v) mixture. The extraction yielded 0.57 mg of total lipid extract that was subsequently separated into saturate, aromatic, and polar fractions using small column chromatography (Bastow et al., 2007). The three fractions were eluted using *n*-hexane, *n*-hexane:DCM (7:3 v:v), and DCM:methanol (1:1 v:v), respectively. Saturate and aromatic fractions were analyzed via gas chromatography-mass spectrometry (GC-MS) using a Trace GC Ultra (Thermo) connected to an ISQ Series quadrupole MS (Thermo).

Results

The TOC value of the sample is 0.4% and the yield of extractable lipids is 0.02 mg per gram of sample or 4.75 mg per gram TOC. The saturate fraction total ion chromatogram (fig. 3) has a small, unresolved complex mixture (C_{15}–C_{23})

Figure 2: An uncommon example of disarticulation of a fish carcass, collected during an excavation of the Koonwarra Fossil Beds led by Tom Rich in 2013. This specimen was collected approximately 5 m from the bottom of the unit (defined here as the first > 20 cm thick unit of green siltstone/mudstone; the underlying rocks are predominantly cross-bedded, fluviatile arkosic sandstone).

above the baseline suggesting that biodegradation of the fossil organic matter has been minimal. The *m/z* 85 mass chromatogram reveals a stepwise increase in the abundance of short-chained *n*-alkanes (C_{15}–C_{22}) with increasing molecular weight likely associated with aquatic sources such as algae. The longer chained *n*-alkanes (C_{23}–C_{31}) that are indicative of terrestrial higher-plant input (Bourbonniere and Meyers, 1996) show a clear odd-over-even carbon number predominance (OEP = 1.48 where 1.0 means no predominance) (Scalan and Smith, 1970). The OEP preserves a distribution characteristic of terrestrial plant epicuticular waxes and indicates that thermal alteration of the sample that would have diminished the uneven distribution has been minimal (Peters et al., 2005).

A measure of the relative contributions of terrestrial and aquatic organic matter sources is the terrestrial/aquatic ratio (TAR; Bourbonniere and Meyers, 1996) calculated using *n*-alkane peak areas:

$$TAR = (C_{15} + C_{17} + C_{19}) / (C_{27} + C_{29} + C_{31}).$$

Although the ratio is most useful when comparing changes in organic matter sources along a stratigraphic series of samples, the value we determined (TAR = 4.7) indicates a significant higher-plant contribution to the total carbon flux to the sediment. This is supported by the ratio of the regular isoprenoids pristane (Pr) and phytane (Ph) that are usually understood to have derived from the phytol tail of the chlorophyll molecule (Brooks et al., 1969). The ratio is influenced by the source organic matter as well as by the redox state of the environment of deposition. The value for Pr/Ph for this sample of 3.1 is diagnostic of a predominantly terrestrial organic matter source deposited under oxic conditions (Peters et al., 2005).

Hopanes are pentacyclic triterpenoids that are derived predominantly from cell wall lipids of prokaryotes (Ourisson et al., 1979). Steranes derive from lipids found only in eukaryotes including microbial photoautotrophs and metazoans (Chapman and Schopf, 1983). A sterane/hopane ratio of 0.03 was calculated using the summed peak areas of 17α-hopane isomers and C_{27}, C_{28}, and C_{29} sterane isomers (fig. 4). Low sterane/hopane ratios are typically indicative of either a dominantly terrigenous organic matter source or biodegradation of organic matter (Tissot and Welte, 1984; Peters et al., 2005). The small contribution of unresolved complex mixture to the saturate fraction indicates that post-

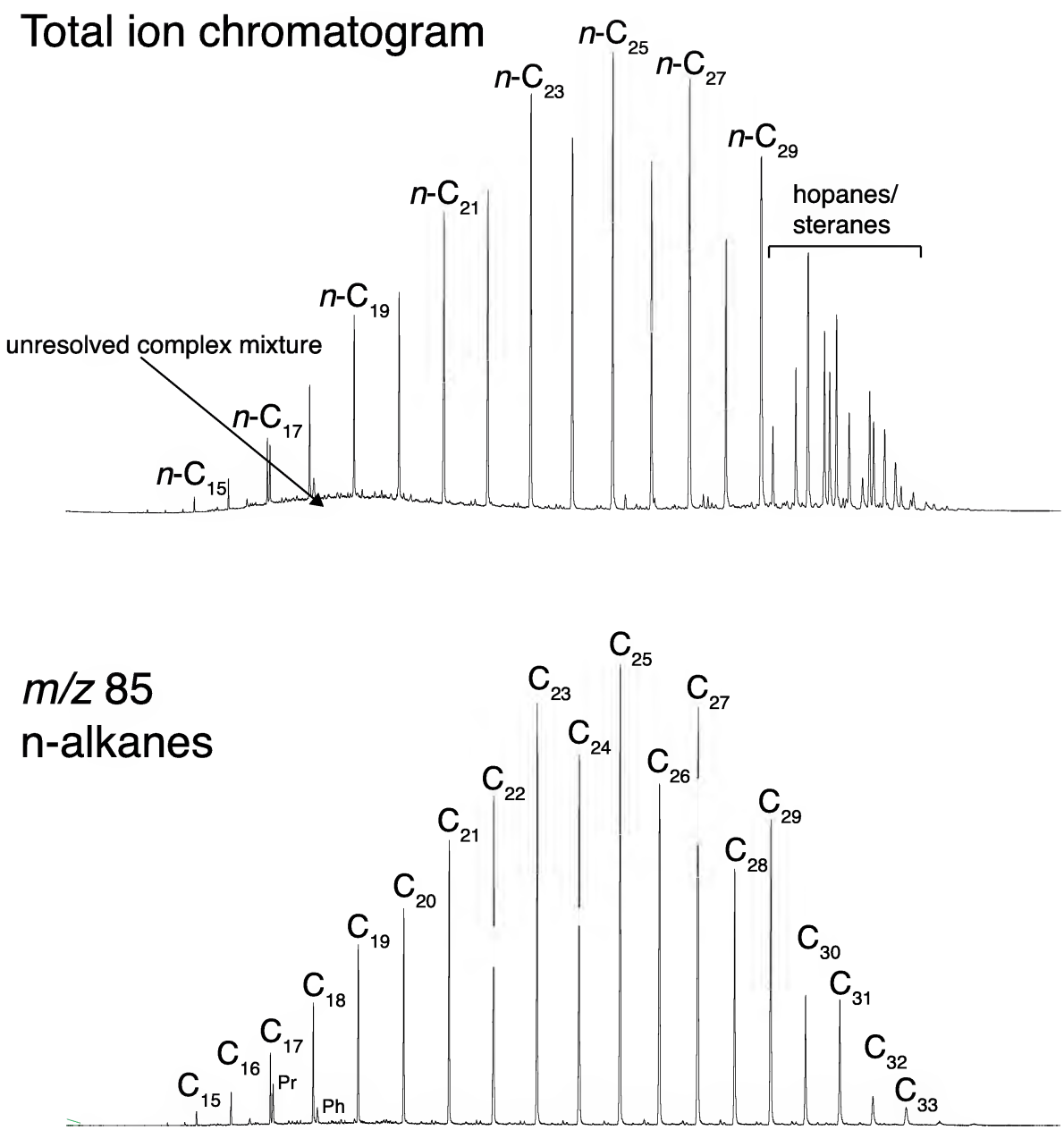

Figure 3: Saturate fraction total ion chromatogram and *m/z* 85 mass chromatogram showing distribution and relative abundances of *n*-alkanes and isoprenoids pristane and phytane.

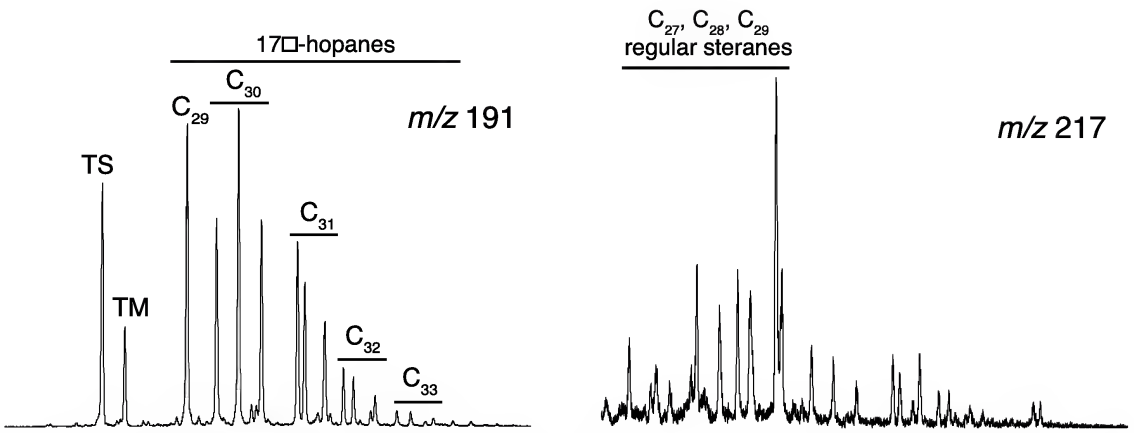

Figure 4: Partial *m/z* 191 and 217 mass chromatograms used in calculation of sterane/hopane ratio. A ratio of 0.03 indicates that a very significant proportion of overall biomass in the lake was derived from bacteria.

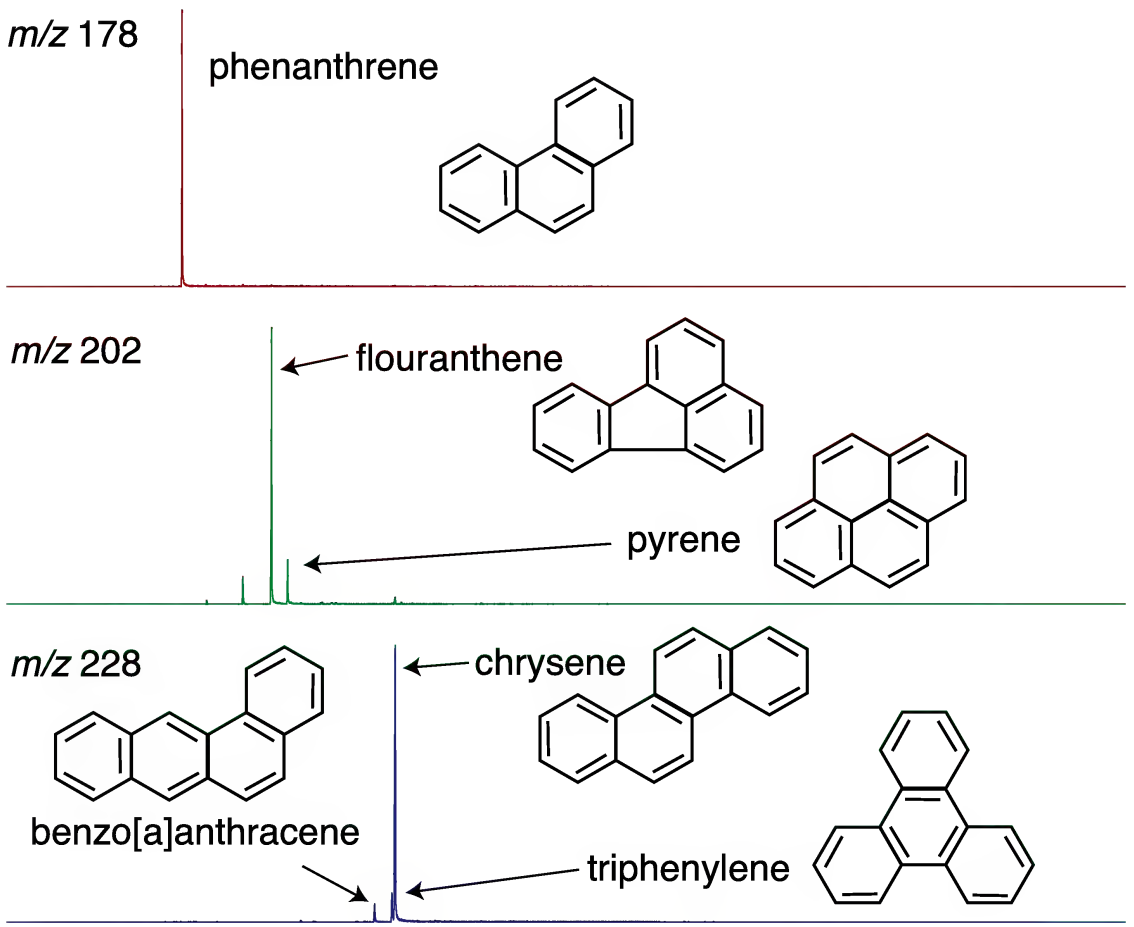

Figure 5: Partial *m/z* 178, 202 and 228 mass chromatograms showing the distribution of common polycyclic aromatic hydrocarbons (PAH) in the aromatic fraction.

depositional biodegradation was probably not significant. Possible sources of the abundant hopanes include soil bacteria from the surrounding watershed and the aquatic bacterial heterotrophs responsible for the decomposition of terrestrial plant matter.

The aromatic organic fraction contains a range of polycyclic aromatic hydrocarbons (PAH). PAHs in sediments may derive from incomplete combustion of wood and plant matter (Blumer and Youngblood, 1975) or from diagenesis of organic precursors (Jiang et al., 1998). Figure 5 shows three mass/charge-specific chromatograms that illustrate the presence of potentially combustion-related PAHs phenanthrene, fluoranthene, pyrene, and benzo[a]anthracene, chrysene, and triphenylene. Venkatesan and Dahl (1989) observed high concentrations of these and other pyrosynthetic PAHs at a variety of Cretaceous/Tertiary boundary sites that they interpreted as evidence of extensive wildfires. Similar distributions of PAHs at the Permian/Triassic boundary also suggest that wildfires were unusually common at the time of the end-Permian extinction (Nabbefeld et al., 2010).

Conclusions

The Koonwarra beds provide fossil evidence of a complex, high latitude lacustrine ecosystem. Organic geochemical evidence suggests that supplementation of aquatic trophic resources by terrigenous organic matter in the form of soil bacteria and plant tissues washed into the lake may have played an important role in sustaining that ecosystem. This supplementation may have been particularly significant given the impact of the high annual variability of solar insolation on aquatic primary production at high latitudes. The presence of combustion-related PAHs indicates an atmospheric pO_2 capable of sustaining combustion and confirms the presence of forested land cover and soils in the vicinity of the lake.

In addition to illuminating the environmental context of the extensive fossil record at Koonwarra, the sample also clearly indicates that the state of organic matter preservation in the unit is highly conducive to further integration of paleontological and geochemical evidence in assembling a comprehensive understanding of an exceptionally well-preserved ecosystem. Further work is likely to yield insights into redox conditions and other environmental factors that led to the high-fidelity preservation of fossils.

Acknowledgements

We are foremost indebted to Tom Rich, who introduced us to the Koonwarra Fossil Beds and led the excavations in 2013. Simon George provided a thoughtful and thorough review. David Flannery thanks Abigail Allwood for supporting his interest in this area. The research was carried out at the Jet Propulsion Laboratory, California Institute of Technology, under a contract with the National Aeronautics and Space Administration.

References

Bastow, T.P., van Aarssen, B.G.K., and Lang, D. 2007, Rapid small-scale separation of saturate, aromatic and polar components in petroleum. *Organic Geochemistry* 38(8): 1235–50.

Blumer, M., and Youngblood, W.W. 1975. Polycyclic Aromatic-Hydrocarbons In Soils And Recent Sediments. *Science* 188(4183): 53–5.

Bourbonniere, R.A., and Meyers, P.A. 1996. Sedimentary geolipid records of historical changes in the watersheds and productivities of Lakes Ontario and Erie. *Limnology and Oceanography* 41(2): 352–9.

Brooks, J.D., Gould, K., and Smith, J.W. 1969. Isoprenoid Hydrocarbons in Coal and Petroleum *Nature* 222(5190): 257–259.

Chapman, D.J., and Schopf, J.W. 1983. Biological and biochemical effects of an aerobic environment. Pp. 302-320 in: Schopf, J.W. (ed), Earth's *Earliest Biosphere*. Princeton University Press, Princeton, NJ.

Dettmann, M.E. 1986. Early Cretaceous palynoflora of subsurface strata correlative with the Koonwarra Fossil Bed, Victoria. *Association of Australasian Palaeontologists, Memoir* 3: 79–110.

Douglas, J.G. 1969. The Mesozoic floras of Victoria, Parts 1 and 2. *Geological Survey of Victoria Memoire* 28: 1–310.

Douglas, J.G. 1974. The Mesozoic floras of Victoria, Part 3. *Geological Survey of Victoria Memoire* 28:1–185.

Drinnan, A.N., and Chambers, T.C. 1986. Flora of the Lower Cretaceous Koonwarra Fossil Bed (Korumburra Group), South Gippsland, Victoria. *Association of Australasian Palaeontologists, Memoir* 3: 1–77.

Elder, R.L., and Smith, G.R. 1988. Fish taphonomy and environmental inference in paleolimnology. *Palaeogeography, Palaeoclimatology, Palaeoecology* 62.1: 577–592.

Embleton, B.J., and McElhinny, M.W. 1982. Marine magnetic anomalies, palaeomagnetism and the drift history of Gondwanaland. *Earth and Planetary Science Letters* 58(2): 141–150.

Jell, P.A., and Duncan, P.M. 1986. Invertebrates, mainly insects, from the freshwater Lower Cretaceous, Koonwarra Fossil Bed (Korumburra Group), South Gippsland, Victoria. *Association of Australasian Palaeontologists, Memoir* 3: 111–205.

Jiang, C.Q., Alexander, R., Kagi, R.I., and Murray, A.P. 1998. Polycyclic aromatic hydrocarbons in ancient sediments and their relationships to palaeoclimate, *Organic Geochemistry* 29(5-7): 1721–35.

Krzemiński, W., et al. 2015. Revision of the unique Early Cretaceous Mecoptera from Koonwarra (Australia) with description of a new genus and family. *Cretaceous Research* 52:501-506.

McGrew, P. O. 1975. Taphonomy of Eocene fish from Fossil Basin, Wyoming. *Fieldiana* 33(14): 257–270.

Nabbefeld, B., Grice, K., Summons, R.E., Hays, L.E., and Cao, C. 2010. Significance of polycyclic aromatic hydrocarbons (PAHs) in Permian/Triassic boundary sections. *Applied Geochemistry* 25: 1374–1382.

Ourisson, G., Albrecht, P., and Rohmer, M. 1979. Hopanoids - Palaeochemistry and Biochemistry of a Group of Natural-Products. *Pure and Applied Chemistry* 51(4): 709–29.

Peters, K.E., Walters, C.C., and Moldowan, J.M. 2005. The Biomarker Guide: Biomarker and Isotopes in Petroleum Exploration and Earth History. Cambridge University Press, New York.

Rich P.V., Rich, T.H., Wagstaff, B.E., Mason, J.M., Douthitt, C.B., Gregory, R.T., and Felton, E.A. 1988. Evidence for low temperatures and biologic diversity in Cretaceous high latitudes of Australia. *Science* 242: 1403–6.

Riek, E.F. 1970. Lower Cretaceous fleas. *Nature* 227: 746–747.

Riek, E. F., and Gill, E.D. 1971. A new xiphosuran genus from Lower Cretaceous freshwater sediments at Koonwarra, Victoria, Australia. *Palaeontology* 14.2: 206–210.

Scalan, R.S., and Smith, J.E. 1970. An Improved Measure of Odd-Even Predominance in Normal Alkanes of Sediment Extracts and Petroleum. *Geochimica et Cosmochimica Acta* 34(5): 611–620.

Tissot, B.P., and Welte, D.H. 1984. *Petroleum Formation and Occurrence*. Springer-Verlag, New York.

Venkatesan, M.I., and Dahl, J. 1989. Organic Geochemical Evidence for Global Fires at the Cretaceous Tertiary Boundary, *Nature* 338(6210): 57–60.

Vickers-Rich, P. 1991. The Mesozoic and Tertiary history of birds on the Australian Plate. Pp. 721–808 in: Rich, P.V., Monaghan, J.M., Baird, R.F., and Rich, T.H. (eds.), *Vertebrate Palaeontology of Australasia*. Pioneer, Victoria.

Waldman, M. 1971. Fish from the freshwater Lower Cretaceous of Victoria, Australia, with comments on the paleo-environment. *Special Papers Palaeontology* 9(1): 1–124.

Wilson, M.V.H. 1977. Paleoecology of Eocene lacustrine varves at Horsefly, British Columbia. *Canadian Journal of Earth Sciences* 14: 953–962.

Memoirs of Museum Victoria 74: 81–91 (2016) Published 2016

ISSN 1447-2546 (Print) 1447-2554 (On-line)
http://museumvictoria.com.au/about/books-and-journals/journals/memoirs-of-museum-victoria/

Morphological variation of stratigraphically important species in the genus *Pilosisporites* Delcourt & Sprumont, 1955 in the Gippsland Basin, southeastern Australia

Doris E. Seegets-Villiers[1*] and Barbara E. Wagstaff[2]

[1] School of Earth, Atmosphere and Environment, Monash University, Clayton Campus, Victoria 3800, Australia (doris.seegets-villiers@monash.edu)
[2] School of Earth Sciences, The University of Melbourne, Victoria 3010, Australia (wagstaff@unimelb.edu.au)
* To whom correspondence should be addressed. E-mail: doris.seegets-villiers@monash.edu

Abstract

Seegets-Villiers, D.E. and Wagstaff, B.E. 2016. Morphological variation of stratigraphically important species in the genus *Pilosisporites* Delcourt & Sprumont, 1955 in the Gippsland Basin, southeastern Australia. *Memoirs of Museum Victoria* 74: 81–91.

Three hundred and ninety eight mudstone samples of Early Cretaceous age from the onshore part of the Gippsland Basin in southeastern Australia were used to ascertain the morphological variation in three species of spores in the genus *Pilosisporites*. In Australia all species of *Pilosisporites* are biostratigraphically useful and this study confirms that in the Gippsland Basin the ranges of *Pilosisporites notensis*, *Pilosisporites parvispinosus* and *Pilosisporites grandis* are as defined by some previous authors. Morphological variations of these three taxa from the published descriptions are discussed. In the case of *P. grandis* and *P. parvispinosus* the main variation was in the size of specimens, however *P. notensis* showed sculpture variations in regard to element size, type and distribution. Two distinct types of this species were defined with only one occurring in the youngest part of the section. Modern fern species can exhibit similar spore sculpture and size variations as a result of polyploidy. This could possibly be the cause of the variations in all three species of *Pilosisporites* and also their short-lived, in geological terms, species ranges.

Keywords

palynology, Early Cretaceous, Gippsland Basin, *Pilosisporites*, palynostratigraphy.

Introduction

In Australia all four species in the Early Cretaceous spore genus *Pilosisporites* Delcourt and Sprumont, 1955 are biostratigraphically important. The endemic Western Australian species *Pilosisporites ingramii* Backhouse, 1988 is the oldest representative of the genus in Australia and ranges through the Berriasian *Biretisporites enneabbaensis* Zone in that state (Backhouse, 1988). The remaining species *Pilososporites notensis* Cookson and Dettmann, 1958 *Pilosisporites parvispinosus* Dettmann, 1963 and *Pilosisporites grandis* Dettmann, 1963 have first and last appearance datums that play critical roles in defining spore-pollen zones in eastern Australia. Originally, the endemic Western Australian species, later defined as *P. ingramii* (Backhouse, 1988), was identified as *P. notensis* (Backhouse, 1978). The confusion over what constituted the species *P. notensis* led to Morgan's (1980) conclusion that the species had a climate-controlled migration across the continent. As such *P. notensis* was regarded as exhibiting different ranges in the east and west of the continent (Morgan, 1980; Helby et al., 1987). However, the recognition of *P. ingramii* as a separate species, endemic to Western Australia (Backhouse, 1988) meant that such discussion became irrelevant and Partridge (2006) set in place the biostratigraphic usefulness of all four Australian species.

Two species of *Pilosisporites*, *P. notensis and P. parvispinosus*, first described from Australia, have subsequently been recorded in Early Cretaceous strata in other continents. Pestchevitskaya (2007) used the first appearance of *P. parvispinosus* as a biostratigraphically important datum in the late Berriasian in Siberia, and *P. notensis* just above the early/late Hauterivian boundary and at the base of the Barremian in different regions in Siberia (Pestchevitskaya, 2007, 2008). In the Athgarh Basin in eastern India both *P. notensis* and *P.* cf. *P. notensis* were recorded (Goswami et al., 2008), whereas in the Rajmahal Basin further north Tiwari and Tipathi (1995) noted the absence of *P. notensis* and *P. parvispinosus* from the Lower Cretaceous sections as being of interest. Zhang et al. (2008) listed *P. notensis* in the Lower Cretaceous of northeast China. The type species of the genus, *Pilosisporites trichopapillosus* has never been recorded in Australia but has been recorded globally in North and South America, Europe, Africa and Asia (Alroy, 2014).

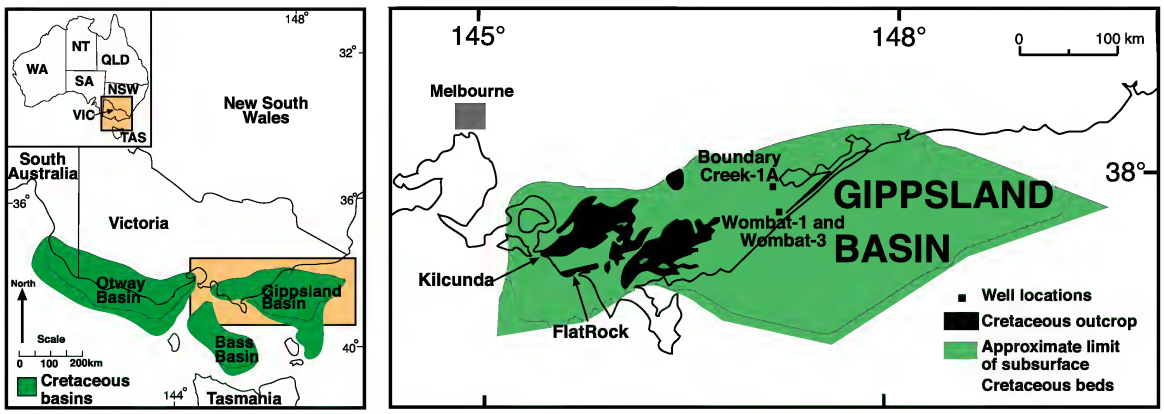

Figure 1. Gippsland Basin map showing the distribution of exposed and subsurface Cretaceous sediments and the locations of petroleum exploration wells mentioned in text (redrawn from Douglas 1988 and Tosolini *et al.*, 1999).

Morphological variations exhibited by the illustrated holotypes of the four Australian species of *Pilosisporites* (Backhouse, 1988; Dettmann, 1963; Cookson and Dettmann, 1958) are distinctive and should not present any difficulty in identifying the spores. However, extensive studies on lower Cretaceous surface and subsurface sedimentary successions in the Gippsland Basin in Victoria have shown that the eastern Australian species of *Pilosisporites*, i.e. *P. notensis*, *P. parvispinosus,* and *P. grandis*, all exhibit morphological variations that are not included in the original descriptions.

Study location, lithology and age

All samples used in this study were from the Lower Cretaceous Strzelecki Group in the Gippsland Basin, Victoria, Australia (fig. 1). This basin was formed during the Early Cretaceous as a result of rifting between Australia and Antarctica (Duddy, 2003), with an approximately NW to SE basin axis (Willcox et al., 1992). Continuous separation, accompanied by progressive subsidence, resulted in the accumulation of vast sedimentary successions, the sediment source of which was contemporaneous volcanism from the active volcanic arc of the Tasman Rise (Bryan et al., 1997). The rift valley floor was a vast floodplain crossed by massive westward flowing (O'Sullivan et al., 2000) primarily braided river systems (Vickers-Rich et al., 1997) with subordinate lacustrine conditions (Dettmann, 1986; Waldman, 1971). The resultant lithologies are dominated by sandstone, mudstone and to a lesser extent conglomerate and coals (Wagstaff and McEwen Mason, 1989). Coastal outcrop sections of these rocks were used for the oldest part of the Early Cretaceous (*Foraminisporis wonthaggiensis*-lowest *Cyclosporites hughesii* zones/ Hauterivian-early Aptian age) and samples from exploration wells provided the lowest part (upper *Crybelosporites striatus* to *Coptospora paradoxa* zones/Albian age). The wells used in this study form part of Lakes Oil N.L. tight gas exploration program in the onshore Gippsland Basin, Victoria, Australia. Wombat-1 (Lat 38°21'15"S Long 147°09'32"E) and Wombat-3 (Lat 38°21'33"S Long 147°08'57"E) wells are located in the Wombat Gas field and the shallow (total depth 366 m) Boundary Creek-1A sidetrack bore (Lat 38°11'25"S Long 147°07'54"E). Due to lack of outcrop and core there is a gap in the section examined between the upper part of the *C. hughesii* and the lower part of the *C. striatus* zones therefore encompassing most of the Aptian.

Materials and methods

Core, cuttings and outcrop samples used had been collected over a period of 30 years by the authors of this study to undertake a range of different research objectives including palynostratigraphic dating, assessing vegetation abundance changes through time and environmental interpretation. This resulted in a total data set of 398 samples.

Samples used. At most of the outcrop localities only low-resolution sampling had been carried out for the exposed succession (a maximum of two or four samples) focusing on mudstone beds. Two outcrop sites included in this study however, involved high-resolution sampling. At the Flat Rocks (Lat 38°39'39"S Long 145°40'52"E) vertebrate fossil locality (fig. 1) near Inverloch, rock platform and cliffs had been sampled to provide 70 samples through the stratigraphic section. At Kilcunda (Lat 38°33'04"S Long 145°28'13"E) 38 samples had been taken at regular intervals through the mudstones in a cliff section (fig. 1). One hundred and nineteen samples were used from the Boundary Creek-1A sidetrack core between 203.03–366.5 m. Forty-four samples were from Wombat-1 between 1485–1971 m. They included eight unwashed cuttings samples and 36 samples from washed cuttings. Fifty-four washed cuttings samples were examined in the section in Wombat-3 between 1386–2169 m. This study also involved the re-examination of the type specimens of *P. parvispinosus*, *P. notensis* and *P. grandis.*

Table 1 Summary of the processing and mounting mediums used for all samples in this study.

Location/Well	Number of samples	Hydrochloric acid	Hydrofluoric acid	Oxidation	Heavy liquid separation	Sieving	Mounting medium
Western coastal outcrop (San Remo to Black Head)	14	√	√	Nitric acid	Zinc bromide	10μm	acrylic resin
	19	√	√	Schulze solution	Zinc bromide	none	acrylic resin
Kilcunda cliff	38	√	√	Schulze solution	Zinc bromide	none	silicone oil
Eastern coastal outcrop (Harmers Haven to Inverloch)	23	√	√	Nitric acid	Zinc bromide	10μm	acrylic resin
	17	√	√	Schulze solution	Zinc bromide	none	acrylic resin
Flat Rocks	31	√	√	Schulze solution	Sodium polytungstate	10μm	glycerine jelly
	39	√	√	Nitric acid	Zinc bromide	10μm	acrylic resin
Wombat-1	44	√	√	Nitric acid	Zinc bromide	10μm	acrylic resin
Wombat-3	54	√	√	Nitric acid	Zinc bromide	10μm	acrylic resin
Boundary Creek-1A	24	√	√	Nitric acid	Zinc bromide	10μm	acrylic resin
	95	√	√	Schulze solution	Zinc bromide	none	acrylic resin

Sample processing. Thirty-one samples from the Flat Rocks site and all the samples (38) from Kilcunda were processed by the authors in the laboratory of the School of Geography and Environmental Science at Monash University. Morgan Palaeo Associates processed the remaining 39 samples from the Flat Rocks site. Laola Pty. Ltd. (subsequently Core Laboratories Australia Pty. Ltd.) in Western Australia processed 37 outcrop samples, the remainder being processed by Global Geolab in Calgary, Canada. Core Laboratories Australia Pty. Ltd. in Western Australia processed all samples from Wombat-1 and Wombat-3 plus 24 samples from Boundary Creek-1A sidetrack bore. Global Geolab in Calgary Canada processing all other samples from this bore. Table 1 summarises the chemical and physical processing of all samples. Although the slides were initially examined and counted on a range of microscopes the work for this paper was undertaken on a Zeiss Axioscope A1 microscope in the School of Earth Sciences at the University of Melbourne and all photographs were taken on a Jentopik ProgRes CT3 camera using ProgRes Mac CapturePro 2.7 software. All illustrated specimens and the type slides are housed in the palaeontological collection of Museum Victoria and have registered numbers in the collection (prefixed "P").

The authors acknowledge that the different mounting mediums may have an effect on the size of the fossils. Faegri and Iverson (1975) considered the effects on pollen grains mounted in glycerine jelly, indicating that the grains had a tendency to swell in the medium. They (Faegri and Iverson, 1975) noted that this is more serious for large grains rather than small ones. However, Faegri and Iverson (1975) also noted that in silicone oil the size of the pollen grain does not change with storage. Sluyter (1997) investigated the effects of using silicone oil, glycerine jelly and acrylic resin on pollen grain size and determined conversion factors to account for the increase of grain sizes in the latter two mounting mediums. Sluyter (1997) also determined that glycerine jelly progressively increases the size of the grains and that measurements should be made immediately after grain mounting. However, there is no discussion anywhere in the literature on either the processing or the mounting medium altering the sculptural elements or their distribution on spores. As stated by Large and Braggins (1990), exine morphology is relatively unaffected by the various chemical treatments. Table 1 summarises the processing and mounting media used in this study.

Results

Biostratigraphic outcomes. Due to the size of the Australian continent, spore-pollen biostratigraphic schemes were initially developed that related to the present day geographical location of the basins studied and the palynologists involved. This resulted in distinctive spore-pollen biostratigraphies for the Early Cretaceous in Western Australia (Backhouse, 1978, 1988; Balme, 1957, 1964), northeastern Australia (Burger 1973, 1986; Norvick and Burger, 1975) and southeastern Australia (Dettmann, 1986; Dettmann and Douglas, 1976; Dettmann and Playford, 1969; Morgan et al., 1995). Although the stratigraphic distribution of many key taxa is the same Australia-wide, the ranges of many other species that are biostratigraphically

useful, as noted by Morgan et al. (1995), vary. The pan-Australian Mesozoic palynostratigraphy published by Helby et al. (1987), and its latest update by Partridge (2006), acknowledged some of these range variations, but did not utilise others. Also, of importance for this study is the fact that the order of stratigraphic occurrences of some taxa in Partridge (2006) varies when compared to the most recent biostratigraphic scheme of Dettmann (1986) for Victoria. Recently, Wagstaff et al. (2012) defined subzones of the *Coptospora paradoxa* Zone, the youngest zone in this study.

In this study, the coastal outcrop sections examined encompassed the *Foraminisporis wonthaggiensis* Zone to just above the base of the overlying *Cyclosporites hughesii* Zone of Helby et al. (1987). The first appearance of the indicator of the base of this zone, i.e. *Foraminisporis asymmetricus* and/or the first appearance of the angiosperm species *Clavatipollenites hughesii* (this study), marks the top of the coastal section. The wells examined encompass a section that starts with the upper part of the *Crybelosporites striatus* Zone and almost reaches the top of the overlying *Coptospora paradoxa* Zone. Although this study does not cover the entire Lower Cretaceous in the Gippsland Basin, due to lack of continuous stratigraphic section, enough section has been examined to allow some conclusions to be drawn in relation to the spore-pollen ranges and the biostratigraphic usefulness of taxa. This study confirms the order of first appearances of *P. notensis* and *P. parvispinosus* in the Gippsland Basin as indicated by Dettmann (1986) and *P. grandis* as shown in Dettmann and Douglas (1976). Using the zones of Helby et al. (1987), *P. notensis* first appears at the base of the *Foraminisporis wonthaggiensis* Zone, and *Pilosisporites parvispinosus* first appears within this zone. The first appearance of *P. grandis* defines the base of the *P. grandis* Subzone (Wagstaff et al., 2012) of the *Coptospora paradoxa* Zone while both *P. notensis* and *P. parvispinosus* become extinct, in the Gippsland Basin, just above this event. This study has confirmed that the order of first and last occurrences up section is as shown in figure 2, and as such rejects some of the suggestions of Partridge (2006) for the Gippsland Basin.

Taxonomic outcomes. The diagnosis of *P. grandis* and *P. parvispinosus* basically conform to those of Dettmann (1963), except for minor variations as discussed below. However, *P. notensis* shows a range of sculptural variations (size, type, distribution of sculptural elements) in which the holotype is only representative of one morphological variant. It is enigmatic as to why these variations have not been described before as a close inspection of the type slide P17611 as used by Cookson and Dettmann (1958) revealed that some of these variations were present on specimens that occur in this slide, but were not included in the original description. Also, an examination of the descriptions and the photo plates in the literature suggests that previous workers had encountered this variation, as evidenced by published images representing these different types.

The species of *Pilosisporites* are discussed in geochronologic order from oldest to youngest.

Genus *Pilosisporites* Delcourt and Sprumont, 1955

TYPE SPECIES (by original designation): *Pilosisporites trichopapillosus* (Thiergart, 1949) Delcourt and Sprumont, 1955 (Early Cretaceous, Germany).

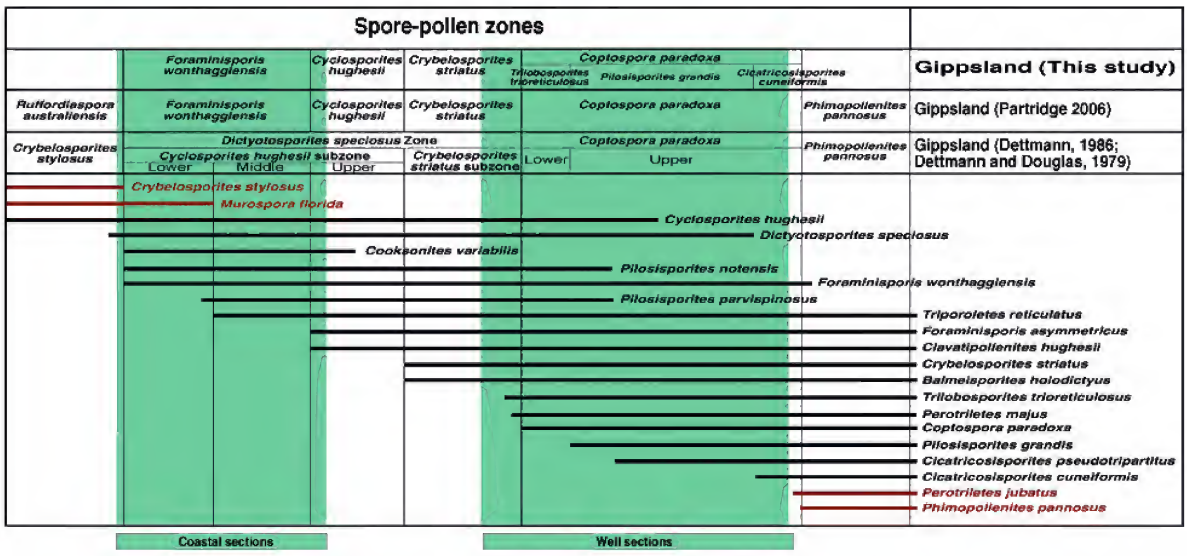

Figure 2. Spore-pollen zones and age indicator species in the Gippsland Basin. Green shaded areas represent the stratigraphy recorded in this study, with the ranges of taxa encountered shown in black and the ranges of taxa not recorded shown in brown. Some ranges are inferred from previous work of Dettmann (1986) and Dettmann and Douglas (1979).

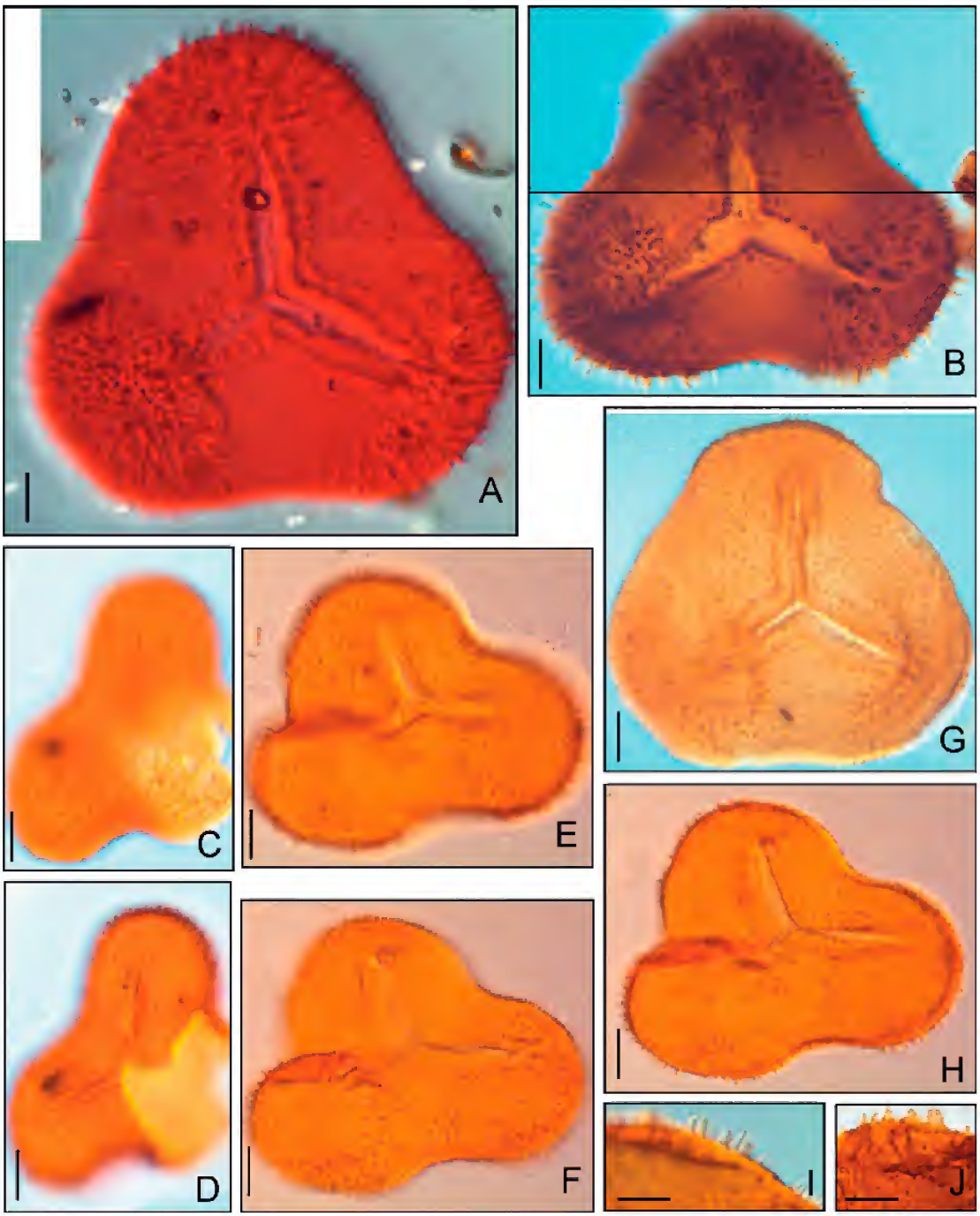

Figure 3. Scale bar Figs A–H = 10 µm; Figs I–J = 12 µm, EFR = England Finder Reference, DIC = Differential interference contrast. A *Pilosisporites notensis* Holotype Slide P1761 EFR Q37/4. Photograph taken using DIC. B *Pilosisporites notensis* Flat Rocks Slide P252131 EFR T31/1. Specimen with long apical spines. Photograph taken using DIC. C, D *Pilosisporites notensis* Wombat-3 Slide P252136 #2 EFR P28/0. E, F, H *Pilosisporites notensis* Shack Bay Slide P252135 EFR H21/1. G *Pilosisporites notensis* Flat Rocks Slide P252132 EFR H37/1 Photograph taken using DIC. I *Pilosisporites notensis* Flat Rocks Slide P252132 EFR F39/4. Sculpture predominantly spines. Photograph taken using DIC. J *Pilosisporites notensis* Flat Rocks P252133 EFR E21/1. Sculpture cones and curved spines.

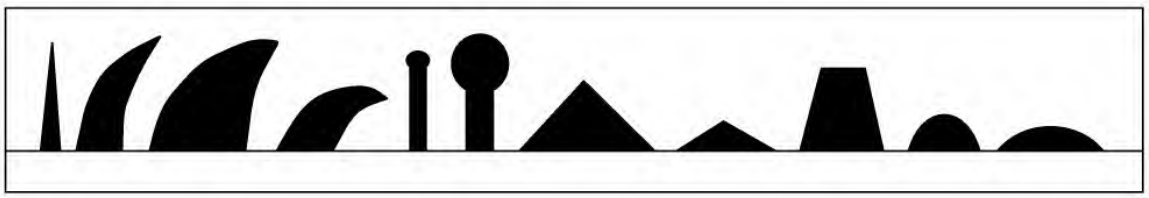

Figure 4. Range of sculptural elements recorded in *Pilosiporites notensis*.

Pilosisporites notensis Cookson and Dettmann, 1958 emend.

Figure 3 A–J

Synonymy: 1958 *Pilosisporites notensis* Cookson and Dettmann, p. 102, pl. 15, figs 1, 3

1963 *Pilosisporites notensis* Cookson and Dettmann; Dettmann, p. 37–38, pl. 4, figs 1–5; p. 33 fig 4D

1964 *Pilosisporites notensis* Cookson and Dettmann; Balme, p.74, pl. VII, fig. 10

1969 *Pilosisporites notensis* Cookson and Dettmann; Dettmann and Playford, pl. 11, fig. 2

1973 *Pilosisporites notensis* Cookson and Dettmann; Burger, pl. 2, fig. 1

1974 *Pilosisporites notensis* Cookson and Dettmann; Burger, pl. 13 fig 11

1976 *Pilosisporites notensis* Cookson and Dettmann; Norvick and Burger, pl. 18, fig 17

non 1978 *Pilosisporites notensis* Cookson and Dettmann; Backhouse, p.18, Pl. 2, fig. 1

1980 *Pilosisporites notensis* Cookson and Dettmann; Burger, p. 52, pl. 6, fig. 5

1986 *Pilosisporites notensis* Cookson and Dettmann; Dettmann, fig. 6M

1987 *Pilosisporites notensis* Cookson and Dettmann; Helby et al., fig. 20N

1988 *Pilosisporites notensis* Cookson and Dettmann; Backhouse, pl.15 fig. 2

2012 *Pilosisporites notensis* Cookson and Dettmann; Wagstaff et al., pl.II fig. 2

Emended diagnosis: Trilete spores, with strongly convex distal and almost flat proximal surface. Amb triangular with concave to nearly straight sides and broadly rounded apices. Laesurae straight, length $^{2}/_{3}$ to $^{3}/_{4}$ of spore radius, with raised, membraneous lips. Exine 1.5–3.5 μm thick, ornamented by straight-sided or curved cones and/or spines (*sensu* Punt et al., 1994) of 0.5–3.5 μm basal diameter and 1–6.5 μm height. This sculpture co-occurs with rare other sculpture types including baculae, clavae, pilae, tuberculae and verrucae (fig. 4). Sculptural elements consistently arranged along laesurae margins and either covering the entire spore surface or restricted to the apical areas. Sculpture elements of equal size and distribution on proximal and distal surface.

Size: Equatorial diameter 52 (80) 125 μm (136 specimens), polar diameter 52 (71) 91 μm (14 specimens).

Remarks and comparison: Specimens generally conform to the original descriptions (Cookson and Dettmann, 1958; Dettmann, 1963). However, observations on a large number of specimens in this study have revealed differences regarding the distribution and type of sculptural elements (figs. 3, 4). The most common morphological extreme of *P. notensis* exhibits short sculptural elements (up to 3 μm high) and base diameters of between 0.5–3 μm. This group shows sculpture distributed either over the entire spore surface as illustrated by Backhouse (1988) or mainly restricted to apical areas where they are closely packed (fig. 3G). The second morphological extreme, shows elongate sculptural elements (up to 6.5 μm), with a narrow basal diameter of as little as 1 μm. Sculptural elements are either distributed over the entire distal and proximal surface (figs. 3E, F, H) or primarily restricted to and closely packed together in the apical areas of the spore (fig. 3B) as in the original description of *P. notensis* by Cookson and Dettmann (1958) and as occurs in the holotype (fig. 3A).

The specimens of *P. notensis* with long apically distributed spines, superficially resemble *P. ingramii* Backhouse (1988) in that they possess long spines, and in some instances, a single row of small spines on the laesurae. However, the grain size in general exceeds that of *P. ingramii* and sculptural elements are in general shorter. Between each morphological end member there is a continual spectrum of distribution of sculptural elements on the amb of the spores ranging from primarily the apex with rare inter-apical occurrences, to increasing frequency of elements inter-apically to spores in which the sculpture extends over the entire surface of the amb. Sculptural element size and distribution is independent of the overall size of the grain.

Two other species of *Pilosisporites* bear a resemblance to *P. notensis*. *Pilosisporites trichopapillosus* (Thiergart) Delcourt and Sprumont, 1955 is recorded as also having sculpture variation in which the long spines were restricted to apical areas or covering the entire surface of the grain (Couper, 1958). However, there is no suggestion that there are any sculptural elements other than spines on this species (e.g. Couper, 1958; Singh, 1964; Archangelsky and Llorens, 2005). *Pilosisporites verus* (Delcourt and Sprumont) emend. Archangelsky and Llorens, 2005 has sculptural elements that include spines with broad bases and acute apices that are sometimes curved, with lesser numbers of cones, bacula, granules and mameliform processes. The sculptural elements are often concentrated at the apical areas (Singh, 1964) but the spines in *P. verus* are longer, i.e. 5.5–11 µm (Archangelsky and Llorens, 2005), than those that occur in *P. notensis*. The equatorial diameter of both these species is also within the lower end of the size of *P. notensis*.

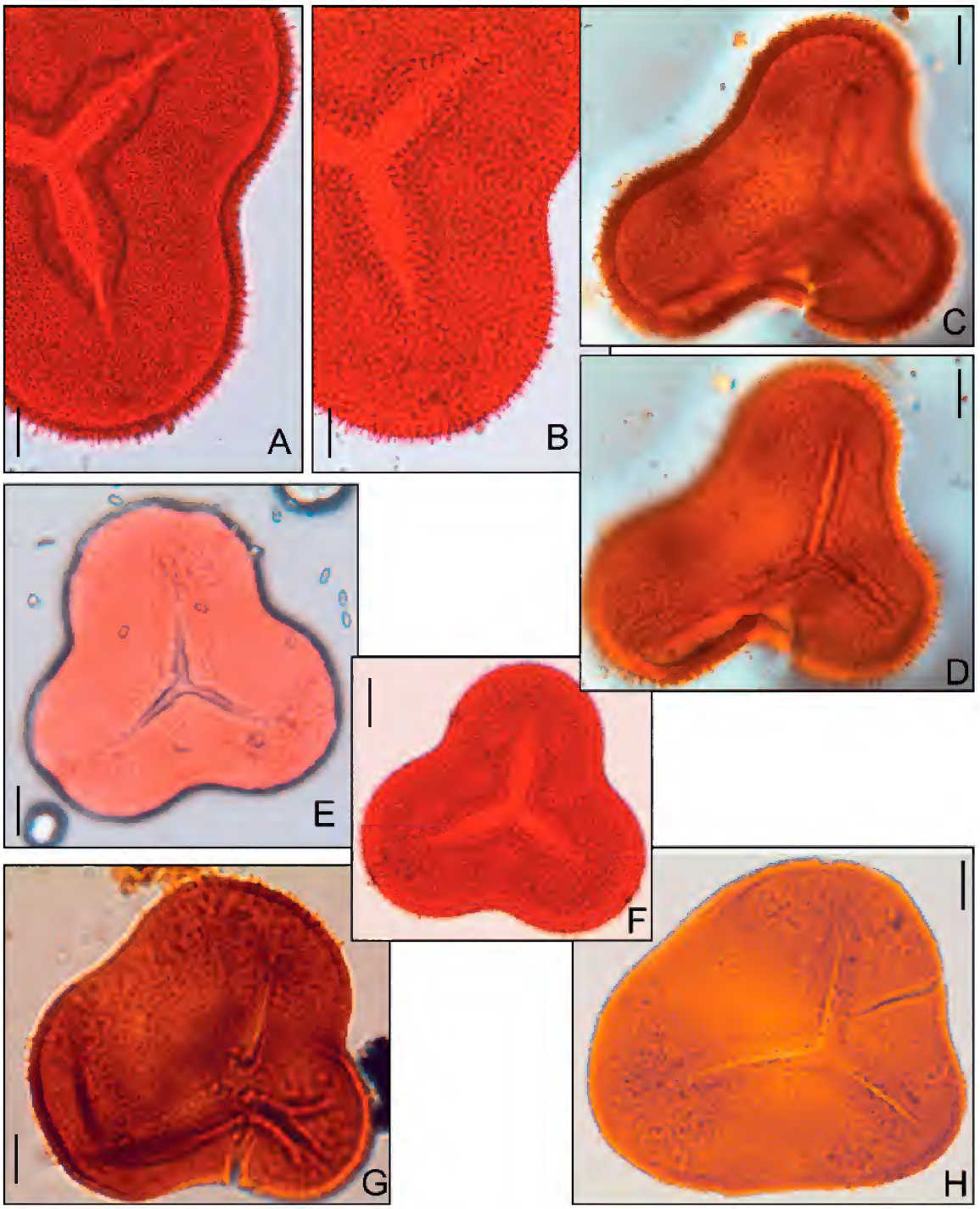

Figure 5. Scale bar Figs A–E and G–H = 10 µm; Fig. F=25 µm, EFR = England Finder Reference. A, B, F *Pilosisporites grandis* Holotype Slide P22098 EFR N20/0. C, D *Pilosisporites grandis* Boundary Creek -1A core 285.5m Slide P252137 EFR Q14/4. E *Pilosisporites parvispinosus* Holotype Slide P21997 EFR E37/3. G *Pilosisporites parvispinosus* Flat Rocks Slide P252134 EFR L41/3. H *Pilosisporites parvispinosus* Flat Rocks Slide P252134 EFR Q31/1.

Distribution (this study): Base of the *Foraminisporis wonthaggiensis* Zone to within the lower part of the *P. grandis* subzone of the *C. paradoxa* Zone. This study found that both end members co-occur in the older part of the succession with their First Appearance Datum (FAD) at the base of the *F. wonthaggiensis* Zone. However, in the uppermost part of the range of *P. notensis*, i.e. in the *C. striatus* and *C. paradoxa* zones, only the shorter spined forms occur (figs. 3C, D). *P. notensis* is never abundant or common in the upper part of its range.

Pilosisporites parvispinosus Cookson and Dettmann, 1958

Figure 5E, G, H

Synonymy 1958 *Pilosisporites notensis* Cookson and Dettmann, p. 102, pl. XV fig. 2

1963 *Pilosisporites parvispinosus* Dettmann, p. 38, pl. IV figs. 6–8; p. 33 fig 4F

1980 *Pilosisporites parvispinosus* Dettmann; Burger, p. 52, pl. 5 fig 9; pl. 6 figs 1–3

non 2012 *Pilosisporites parvispinosus* Dettmann; Lebedeva and Pestchevitskaya, pl. 1 fig. 7

2012 *Pilosisporites parvispinosus* Dettmann; Wagstaff et al., pl. II fig. 7

Diagnosis: see Dettmann (1963).

Size: Equatorial diameter 78 (85) 106 μm (11 specimens).

Remarks: Representatives of this species usually conform to the diagnosis by Dettmann (1963), but show, in rare cases, a slightly thicker exine (2–3.5 μm compared to Dettmann's (1963) 2–3 μm). The spinulate sculpture occasionally has spinules with a wider base diameter (1–2 μm) compared to Dettmann's 1 μm) and a sculpture height of (1–2.5 μm). Rarely present are longer apical sculptural elements.

Distribution (this study): Upper part of the *Foraminisporis wonthaggiensis* Zone to *Coptospora paradoxa* Zone, specifically the lower part of the *Pilosisporites grandis* subzone.

Pilosisporites grandis Dettmann, 1963

Figures 5A–D, F

Synonymy: 1963 *Pilosisporites grandis* Dettmann, pp. 38–39, pl. V, figs 1–3; p. 33 fig 4E

1969 *Pilosisporites grandis* Dettmann; Dettmann and Playford, pl.11 fig. 1

1980 *Pilosisporites grandis* Dettmann; Burger, p. 52, pl. 6, fig. 4

2012 *Pilosisporites grandis* Dettmann; Wagstaff et al., p. 69, pl. 2 fig. 2

non 2014 *Pilosisporites grandis* Dettmann; Takeshi and Vijaya, fig. 5E

Size: Equatorial diameter 85 (92) 100 μm. (4 specimens).

Remarks: As discussed in Wagstaff et al. (2012) the grains encountered in the Gippsland Basin are smaller than those originally described by Dettmann (1963) from the Great Artesian and Otway Basins. Dettmann (1963) gave the equatorial diameter of the species as 100 (117) 142 μm. The specimen illustrated by Burger (1980) from the Surat Basin (Burger, 1980, plate 6, fig. 4) is also smaller (appearing to be approximately 90 μm) than the size range given by Dettmann (1963). We accept the statement of Burger (1980) in the plate (pl. 6, fig. 4) description that the species is primarily identified by its "dense and regular distribution of spines on the exine".

Distribution (this study): *Coptospora paradoxa* Zone, specifically *Pilosisporites grandis* to *Cicatricosisporites cuneiformis* subzones.

Discussion

The genus *Pilosisporites* is unique in Australian palynology in that all four species of the genus are biostratigaphically useful. In spite of the morphological diversity of *P. notensis*, and the size variations of *P. grandis* and *P. parvispinosus*, this fact is not altered. However, this variation is, in the case of *P. notensis*, so extreme that it warrants further investigation.

Hughes (1989) made an in-depth critique of the concept of species and indicated that over time the addition of new specimens identified as a species can cause the original definition of the species to become broader causing the taxon to become an ever larger cluster with irregular limits rather than the neat concept of its generator. This is due to more specimens being examined that encompass a greater span of geologic time, geography (other localities) or both. Hughes (1989, p. 12) also stated that "From the moment of publication, it is customary for appropriate other newly discovered material to be 'identified with', or attributed to, the existing species as far as possible, because new species are in general erected with caution and even with reluctance." This leads over time to the alteration of the meaning or scope of definition of the totality of specimens included in the species under the name. This seems to be the case for *P. notensis* where an examination of the published images from across eastern Australia from different localities and different spore-pollen zones, shows a variation in morphology. However, temporal and geographic components cannot be the only reasons for the variation in the current study. The Flat Rocks and Kilcunda localities are both small stratigraphic sections that were sampled (70 and 38 respectively) with high resolution. At each locality the full range of morphological variation of *P. notensis* occurred, even in many instances in a single sample. As such, the variation cannot be attributed to geologic time or geographic differences and needs to be explained.

Dettmann (1963, 1986) suggested no modern equivalents for the Victorian *Pilosisporites* spore species, but did consider them to be produced by ferns. Variation of the spore sculpture within a species is not unknown in extant ferns. Parks et al. (2000) found that the monolete fern spore *Cystopteris fragilis* (L.) Bernhardi 1805 that occupied different microclimates and substrates in Scotland had three distinctive sculptural types: echinate, rugose and a "smooth" type that appeared to be slightly granular using SEM. The plants producing these distinctive spore types occupied different microclimates and substrates (Parks et al., 2000). Parks et al. (2000) concluded that the fern *C. fragilis* was polyploid with several populations of variants. Beck et al. (2011) indicated that ploidy level could

also control the size of spores with diploids, triploids, and tetraploids of fern species in the genus *Astrolepis,* Benham and Windham 1992 having statistically different and non-overlapping spore diameter distributions. Diverse ploidy levels were also used to explain marked spore size differences in the tropical American fern genus *Stigmatopteris* Christensen 1909 (Tryon and Tryon, 1982). These morphological variations pose an interesting dilemma for palynologists as Otto and Whitten (2000) estimate that the frequency of polyploidy is particularly high in extant ferns (41.7%).

Polyploidy is the existence of genetically related taxa (Thompson and Lumaret, 1992) with three or more basic chromosome sets in their cell nuclei as opposed to the usual two (Bennet, 2004). Polyploidy is heritable (Comai, 2005) and allows homosporous ferns to create and maintain genetic variation in spite of the effects of self-fertilisation due to their monoecious gametophtye stage (Klekowski and Baker, 1966). Klekowski and Baker (1966) further suggested that polyploidy provides selective advantages to homosporous ferns allowing them to maintain, create and release genetic variability in spite of producing homozygous sporophytes. Page (2002) indicates that the entire process of polyploidy in ferns results in the creation of morphological and ecological novelty providing a rapid route for species evolution and adaption and increasing the plants' vigour. The resulting taxa have the ability to adapt to a broader range of ecological conditions compared to their parents and in an actively evolving flora in a changing environment higher ploidy derivatives more often find niches for ecological success. Comai (2005) provided evidence that polyploidy increases the diversity and plasticity of a species, and contributes to its adaptive potential in the arctic where polyploids are able to rapidly adapt to new niches and are able to efficiently invade newly deglaciated areas due to hybrid vigour. However, these polyploids are often considered to be static entities in which gene silencing results in isolated populations (Haufler, 2008). Thus, the picture for polyploids is not favourable in the long term. Their ability to establish and flourish during periods of environmental change when new niches are opened is well recognised, but polyploids face evolutionary difficulties as gene selection is inefficient due to the multiple copies and they are often evolutionary dead-ends (Arrigo and Barker, 2012).

High levels of niche variablity would be a major feature of the Early Cretaceous of the Gippsland Basin. The evolving rift between Australia and Antarctica (Duddy, 2003) and its fast flowing braided river system (Vickers-Rich et al., 1997) would have been a dynamic unstable landscape. The palaeogeographic setting of southeastern Australia was significant in that it was near or inside the Antarctic Circle (Rich and Vickers-Rich, 2000; Wagstaff et al., 2013). Therefore, in spite of the high carbon dioxide levels characteristic of the Cretaceous Greenhouse, and warm and equable global climates (Spicer and Corfield, 1992), it is suggested that in the Aptian-Albian this region would still have been cold (Gregory et al., 1989) and in winter would have experienced months of darkness.

The short biostratigraphic ranges of the species of *Pilosisporites* that occur in the Cretaceous successions in Australia suggest each species is very intolerant of climate/environmental variability. The inability of *P. ingramii* to migrate from Western Australia to the east implies high levels of endemism, as does the inability of *P. parvispinosus*, *P. notensis* and *P. grandis* to migrate into Western Australia. As the climate became drier in the Gippsland Basin (Wagstaff et al., 2013) the extinction of both *P. parvispinosus* and *P. notensis* in the Albian and the evolution of *P. grandis* just prior to this event, seems to suggest that the two former species could not cope with these changed conditions. The variation that occurs in the morphology of *P. notensis* could represent a fern species that had undergone polyploidy thus allowing it to inhabit a range of niches in an unstable braided fluvial setting. The fact that the full range of morphotypes can occur in one sample appears to indicate that the fern is occasionally abundant/diverse in a riparian setting that encompasses a range of sub-environments.

Conclusions

This study on spores in the genus *Pilosisporites* in Lower Cretaceous strata in the Gippsland Basin has three outcomes. The biostratigraphic usefulness of the three species is confirmed with the following ranges. *Pilosisporites notensis* first appears at the base of the *Foraminisporis wonthaggiensis* Zone, and *Pilosisporites parvispinosus* within the zone. The first appearance of *Pilosisporites grandis* defines the base of the *P. grandis* subzone of the *Coptospora paradoxa* Zone while both *P. notensis* and *P. parvispinosus* become extinct just above this event. Taxonomically, the descriptions of *P. grandis* and *P. parvispinosus* have extended size ranges compared to the original descriptions. *P. notensis* shows not only variation in size from the original description but also a division into shorter and longer sculptural element types, and within these, variation in the distribution of the sculpture on the amb. This study suggests that the inability of the eastern and western Australian species of *Pilosisporites* to migrate across the continent, in combination with their short geological ranges and the size and sculptural variation exhibited by the three species examined from the Gippsland Basin, may be evidence of polyploid reproductive strategies in the ferns of this genus.

Acknowledgements

We would like to thank Professor Patricia Vickers-Rich and Dr Thomas Rich who funded the majority of the research on the outcrop samples. BHP Billiton funded the research at Kilcunda. We would like to thank Lakes Oil N.L. for providing some of the samples from Wombat-3. The Department of Primary Industries allowed sampling of the wells and we would particularly like to thank Terry Smith for providing help with accessing the cuttings and core. We would like to thank David Pickering from Museum Victoria for locating and loaning us the type slides from their collection. We appreciate the comments provided by the editor and two anonymous reviewers that helped improve the text. ARC Linkage Grant LP0989203 funded the research on the well sections with industry partners Lakes Oil N.L., Nexus Energy and Geotrack International.

References

Alroy, J. 2014. Taxonomic occurrences of *Pilosisporites trichopapillosus* recorded in the Paleobiology Database. Fossilworks. http://fossilworks.org.

Archangelsky A., Llorens, M., 2005. Palinología de la Formación Kachaike, Cretácico Inferior de la Cuenca Austral, provincia de Santa Cruz. II Esporas. *Ameghiniana* 42(2): 311–328.

Arrigo, N., Barker, M.S., 2012. Rarely successful polyploids and their legacy in plant genomes. *Current Opinion in Plant Biology* 15: 1–7.

Backhouse, J., 1978. Palynological zonation of the Late Jurassic and Early Cretaceous sediments of the Yarragadee Formation central Perth Basin, Western Australia. *Geological Survey of Western Australia Report* 7: 1–52.

Backhouse, J., 1988. Late Jurassic and Early Cretaceous palynology of the Perth Basin, Western Australia. *Geological Survey of Western Australia Bulletin* 135: 1–233.

Balme, B.E., 1957. Spores and pollen grains from the Mesozoic of Western Australia. *Commonwealth Scientific and Industrial Research Organization Coal Research Section, Technical Communication* 25: 1–48.

Balme, B.E., 1964. The palynological record of Australian pre-Tertiary floras. Pp.49–80. in: Cranwell, L.M., (ed). *Ancient Pacific Floras*. University of Hawaii Press, Honolulu.

Bennet, M.D., 2004. Perspectives on polyploidy in plants – ancient and neo. *Biological Journal of the Linnean Society* 82: 411–423.

Beck, J.B., Windham, M.D., Pryer, K.M., 2011. Do asexual polyploidy lineages lead short evolutionary lives? A case study from the fern genus *Astrolepis*. *Evolution* 65: 3217–3229.

Bryan, S.E., Constantine, A.E., Stephens, C.J., Ewart, A., Schön, R.W., Parianos, J., 1997. Early Cretaceous volcano-sedimentary successions along the eastern Australian continental margin: Implications for the break-up of eastern Gondwana. *Earth and Planetary Science Letters* 153: 85–102.

Burger, D., 1973. Spore-zonation and sedimentary history of the Neocomian, Great Artesian Basin, Queensland. *Special Publications Geological Society of Australia* 4: 87–118.

Burger, D., 1980. Palynology of the Lower Cretaceous in the Surat Basin. *Australian Bureau of Mineral Resources Bulletin* 189: 1–106.

Burger, D., 1986. Palynology, cyclic sedimentation, and palaeoenvironments in the late Mesozoic of the Eromanga Basin. Pp. 53–70. in: Gravestock, D.I., Moore, P.S., Pitt, G.M., (eds). *Contributions to the Geology and Hydrocarbon Potential of the Eromanga Basin*. Special Publication Geological Society of Australia 12. Geological Society of Australia, Sydney.

Clarke, L.J., Jenkyns, H.C., 1999. New oxygen isotope evidence for long-term climatic change in the Southern Hemisphere. *Geology* 27(8): 699–702.

Comai, L., 2005. The advantages and disadvantages of being polyploid. *Nature Reviews Genetics* 6: 836–846.

Cookson, I. Dettmann, M. E., 1958. Some trilete spores from Upper Mesozoic deposits in the eastern Australian region. *Proceedings of the Royal Society of Victoria* 70: 95–128.

Couper, R.A., 1958. British Mesozoic microspores and pollen grains: A systematic and stratigraphic study. *Palaeontographica Abt. B* 103: 75–179.

Dettmann, M.E., 1963. Upper Mesozoic microfloras from south-eastern Australia. *Proceedings of the Royal Society of Victoria* 77: 1–148.

Dettmann, M.E., 1986. Early Cretaceous palynoflora of subsurface strata correlative with the Koonwarra Fossil Bed, Victoria. *Memoir of the Association of Australasian Palaeontologists* 3: 79–110.

Dettmann, M.E., Douglas, J.G., 1976. Mesozoic palaeontology. *Special Publications Geological Society of Australia* 5: 164–169. in: Douglas, J.G., Ferguson, J.A. (eds), Geology of Victoria

Dettmann, M.E., Playford, G, 1969. Palynology of the Australian Cretaceous: a review. Pp. 174–210. in: Campbell, K.S.W. (ed). Stratigraphy and Palaeontology, *Essays in Honour of Dorothy Hill*. Australian National University Press, Canberra.

Duddy, I.R., 2003. Mesozoic. Pp. 239–286. in Birch, W.D., (ed). *Geology of Victoria*. Special Publication Geological Society of Australia 23.

Faegri, K.,Iverson, J., 1975. *Textbook of Pollen Analysis*. Munksgaard, Copenhagen, Denmark. 295 pp.

Frakes, L.A., Francis, J.E., Syktus, J.I., 1992. *Climate Modes of the Phanerozoic*. Cambridge University Press. 274pp.

Goswami, S., Meena, K.L., Das, M., Guru, B.C., 2008. Upper Gondwana palynoflora of Mahanadi Master Basin, Orissa, India. *Acta Palaeobotanica* 48(2): 171–181.

Gregory, R T, Douthitt, C.B., Duddy, I.R., Rich, P.V., Rich, T.H., 1989 Oxygen isotopic composition of carbonate concretions from the Lower Cretaceous of Victoria, Australia: implications for the evolution of meteoric waters on the Australian continent in a paleopolar environment. *Earth and Planetary Science Letters* 92(1): 27–42.

Helby, R., Morgan, R., Partridge, A.D., 1987. A palynological zonation of the Australian Mesozoic. *Memoir of the Association of Australasian Palaeontologists* 4: 1–94.

Hughes, N.F., 1989. *Fossils as Information: New Recording and Stratal Correlation Techniques*. Cambridge University Press, Cambridge, UK. 136 pp.

Haufler, C.H., 2008. Species and speciation. Pp 303–331. in: Ranker, T.A., Haufler, C.H. (eds), *Biology and Evolution of Ferns and Lycophytes*, Cambridge University Press, Cambridge, UK.

Klekowski, E.J., Baker, H.G., 1966. Evolutionary significance of polyploidy in the Pteridophya. *Science* 153: 305–307.

Morgan, R. 1980. Palynostratigraphy of the Australian Early and Middle Cretaceous. *Memoirs of the Geological Survey of New South Wales, Palaeontology* 18: 1–153.

Morgan, R., Alley, N.F., Rowett, A.I., White, M.R., 1995. Chapter 6— Biostratigraphy. Pp. 95–101 in: Morton, J.G.G., Drexel, J.F. (eds), *The Petroleum Geology of South Australia: Vol. 1: Otway Basin. Mines and Energy South Australia Report 95/12*.

Norvick, M.S., Burger, D., 1975. Palynology of the Cenomanian of Bathurst Island, Northern Territory, Australia. *Bureau of Mineral Resources Geology and Geophysics Bulletin* 151: 1–169.

O'Sullivan, P.B., Mitchell, M.M., O'Sullivan, A.J., Kohn, B.P., Gleadow, A.J.W., 2000. Thermotectonic history of the Bassian Rise, Australia: implication for the breakup of eastern Gondwana along Australia's southeastern margins. *Earth and Planetary Science Letters* 182: 31–47.

Otto, S.P., Whitten, J., 2000. Polyploid incidence and evolution. *Annual Review of Genetics* 34:401–37.

Page, C.N., 2002. Ecological strategies in fern evolution: a neotropical overview. *Review of Palaeobotany and Palynology* 119: 1–33.

Parks, J.C., Dyer, A.F., Lindsay, S., 2000. Allozyme, spore and frond variation in some Scottish populations of the ferns *Cystopteris dickieana* and *Cystopteris fragilis*. *Edinburgh Journal of Botany* 57(1): 83–105.

Partridge, A.D., 2006. Jurassic – Early Cretaceous spore-pollen and dinocyst zonations for Australia. in: Monteil, E. (co-ord), Australian Mesozoic and Cenozoic Palynology Zonations – updated to the 2004 Geologic Time Scale. *Geoscience Australia Record 2006/23* (CD only).

Pestchevitskaya, E.B., 2007. Lower Cretaceous biostratigraphy of northern Siberia: palynogical units and their correlation significance. *Russian Geology and Geophysics* 48: 941–959.

Pestchevitskaya, E.B., 2008. Lower Cretaceous palynostratigraphy and dinoflagallate cyst palaeoecology in the Siberian palaeobasin. *Norwegian Journal of Geology* 88: 279–286.

Punt, W., Blackmore, S., Nilsson, S., Le Thomas, A., 1994. Glossary of pollen and spore terminology. *LPP Contributions Series No.1*, Utrecht.

Rich, T.H., Vickers-Rich, P., 2000. *The Dinosaurs of Darkness*. University of Indiana Press, Bloomington. 222 pp.

Royer, D.L., 2006. CO_2-forced climate thresholds during the Phanerozoic. *Geochiemica et Cosmochimica Acta* 70: 5665–5675.

Singh, C., 1964. Microflora of the Lower Cretaceous Mannville Group, East Central Alberta. *Alberta Research Council Bulletin* 15: 1–239.

Sluyter, A., 1997. Analysis of maize (*Zea mays* subsp. *mays)* pollen normalizing the effects of microscope-slide mounting media on diameter determinations. *Palynology* 21: 35–39.

Spicer, R.A., Corfield, R.M., 1991. A review of terrestrial and marine climates in the Cretaceous with implications for modelling the "Greenhouse Earth." *Geological Magazine* 129(2): 169–180.

Thompson, J.D., Lumaret, R., 1992. The evolutionary dynamics of polyploidy plants: origins, establishment and persistence. *Tree* 7(9): 302–307.

Tiwari, R.S., Tipathi, A., 1995. Palynological assemblages and absolute age relationship of Intertrappean beds in the Rajmahal Basin, India. *Cretaceous Research* 16: 53–72.

Tryon, R.M., Tryon, A.F., 1982. Ferns and Allied Plants with Special Reference to Tropical America Springer-Verlag, New York, USA. 857 pp.

Vickers-Rich, P., Rich, T. H., Constantine, A., 1997. The polar dinosaurs of southeastern Australia. Pp. 253–257. in: Wolberg, D. L., Stump, E., Rosenberg, G. D. (eds), Dinofest International Proceedings. Academy of Natural Sciences, Philadelphia.

Wagstaff, B.E., McEwen Mason, J., 1989. Palynological dating of Lower Cretaceous coastal vertebrate localities, Victoria, Australia. *National Geographic Research* 5(1): 54–63.

Wagstaff, B.E., Gallagher, S.J., Norvick, M.S., Cantrill, D.J., Wallace, M.W., 2013. High latitude Albian climate variability: Palynological evidence for long-term drying in a greenhouse world. *Palaeogeography, Palaeoclimatology, Palaeoecology* 386: 501–511.

Wagstaff, B.E., Gallagher, S.J., Trainor, J.K., 2012. A new subdivision of the Albian spore-pollen zonation of Australia. *Review of Palaeobotany and Palynology* 171: 57–72.

Waldman, M., 1971. Fish from the Lower Cretaceous of Victoria, Australia with some comments palaeoenvironement. *Special Papers in Palaeontology* 9: 1–124.

Willcox, J. B., Colwell, J. B., Constantine, A., 1992. New ideas on Gippsland Basin regional tectonics. Pp. 93–110. in: Barton, C. M., Hill, K. A., Abele, C., Foster, J., Kempton, N. (eds), Energy, Economics and Environment: Gippsland Basin Symposium. Australian Institute of Mining and Metallurgy.

Zhang, J., Liu, H-t, Wu, B-w, 2008. Early Cretaceous spore and pollen assemblages from the Zhangqiang Depression in the Zhangwu Basin, Liaoning Province. *Acta Micropalaeontologica Sinica* 2008 (Issue 2): 196–203.

Memoirs of Museum Victoria 74: 93–96 (2016) Published 2016

ISSN 1447-2546 (Print) 1447-2554 (On-line)
http://museumvictoria.com.au/about/books-and-journals/journals/memoirs-of-museum-victoria/

What is 'Pseudo' in Pseudotribosphenic Teeth?

Alistair R. Evans[1,2]

[1] School of Biological Sciences, Monash University, VIC 3800, Australia (alistair.evans@monash.edu)
[2] Geosciences, Museum Victoria, Melbourne, VIC 3001, Australia

Abstract

Evans, A.R. 2016. What is 'Pseudo' in Pseudotribosphenic Teeth? *Memoirs of Museum Victoria* 74: 93–96.

The discovery of a 'pseudotribosphenic' lower tooth row in 1982, with a basin anterior to the trigonid rather than posterior, caused a large stir in mammalian palaeontology. This indicated that a tooth shape of equivalent complexity to the tribosphenic tooth form could evolve more than once. The upper tooth predicted to occlude with the pseudotribosphenic molar was reconstructed with a 'pseudoprotocone' to occlude with the pseudotalonid basin. Here I discuss the relative merits of naming the major upper lingual cusp of pseudotribosphenic molars as 'protocone' due to its likely similar developmental and functional relations as the protocone of tribosphenic molars. The use of a different name implies greater morphological distance between tribosphenic and pseudotribosphenic upper molars than is perhaps warranted, and likely exaggerates the perception of the difficulty in evolving both tribospheny and pseudotribospheny. The choice between the evolution of the alternative forms of tribospheny may in fact be related to the degree of anterior-posterior bias in lower molar development – tribospheny with a posterior bias, while pseudotribospheny with an anterior one.

Keywords

tribosphenic, pseudotribosphenic, *Shuotherium*, protocone, pseudoprotocone.

Introduction

'Tribosphenic' was the term Simpson (1936) coined for the basal tooth type of all extant therian mammals, from its dual functions of grinding ('tribo') and shearing (wedge or 'sphen'). The key structures of this tooth form are the occluding blades leading from the main cusps (forming a W-shaped ectoloph on the upper molar, and a disconnected W on the lower molar), and the mortar-and-pestle crushing of the protocone on the lingual side of the upper molar into the talonid basin that sits at the posterior of the lower molar behind the elevated trigonid (fig. 1a). For decades, the complexity and intimate relationships between these teeth led workers to the conclusion that it would be 'almost inconceivable' that such a tooth shape could have evolved more than once in the history of mammals (Simpson, 1936:797). After Simpson's work, Patterson (1956) outlined the stages of evolution of the tribosphenic molar. Based on a functional analysis of occluding crests, Crompton (1971) detailed a scenario for the evolution of the tribosphenic dentition from pre-tribosphenic forms. The importance of the tribosphenic form in the evolutionary history of mammals was emphasised by Tom Rich's graduate advisor, Malcolm McKenna (1975), using it to diagnose a clade of crown therians (Tribosphenida).

The single origin of the tribosphenic form began to look more doubtful with the discovery of *Shuotherium dongi* by Chow and Rich (1982), in which a small basin was positioned at the anterior of the elevated, triangular trigonid of the lower molars (fig. 1b). Chow and Rich (1982) termed this basin the pseudotalonid, in analogy to the shape and function of the true talonid. For this to be analogous to the talonid, it must be a crushing basin that receives a protocone-like structure. Chow and Rich (1982) predicted that the upper molars of *Shuotherium* would have such a cusp, which they termed the 'pseudoprotocone'. This prediction was borne out by the discovery by Wang et al. (1998) of an upper molar of *Shuotherium* with a lingual cusp in general agreement with the predicted position and shape.

The purpose of this short note is to discuss the usefulness of the conventions currently used for naming cusps in the pseudotribosphenic dentition, and the potential for names to colour our interpretation of evolutionary scenarios. Here I will consider what does 'pseudo' mean, and which parts of teeth may consistently be called 'pseudo'?

Cusp Development

In an embryo, the future tooth surface begins as the interface between epithelium and mesenchyme cell layers in the tooth germ. Soon after the initiation of the tooth germ, the primary enamel knot forms. The enamel knot is the main signalling centre of the tooth, expressing dozens of genes. Certain gene products of the enamel knot prevent proliferation of the epithelium adjacent to the knot, and the proliferation of surrounding epithelium continues. This differential proliferation bends the epithelium-mesenchyme interface, creating a local topological maximum that is the site of a

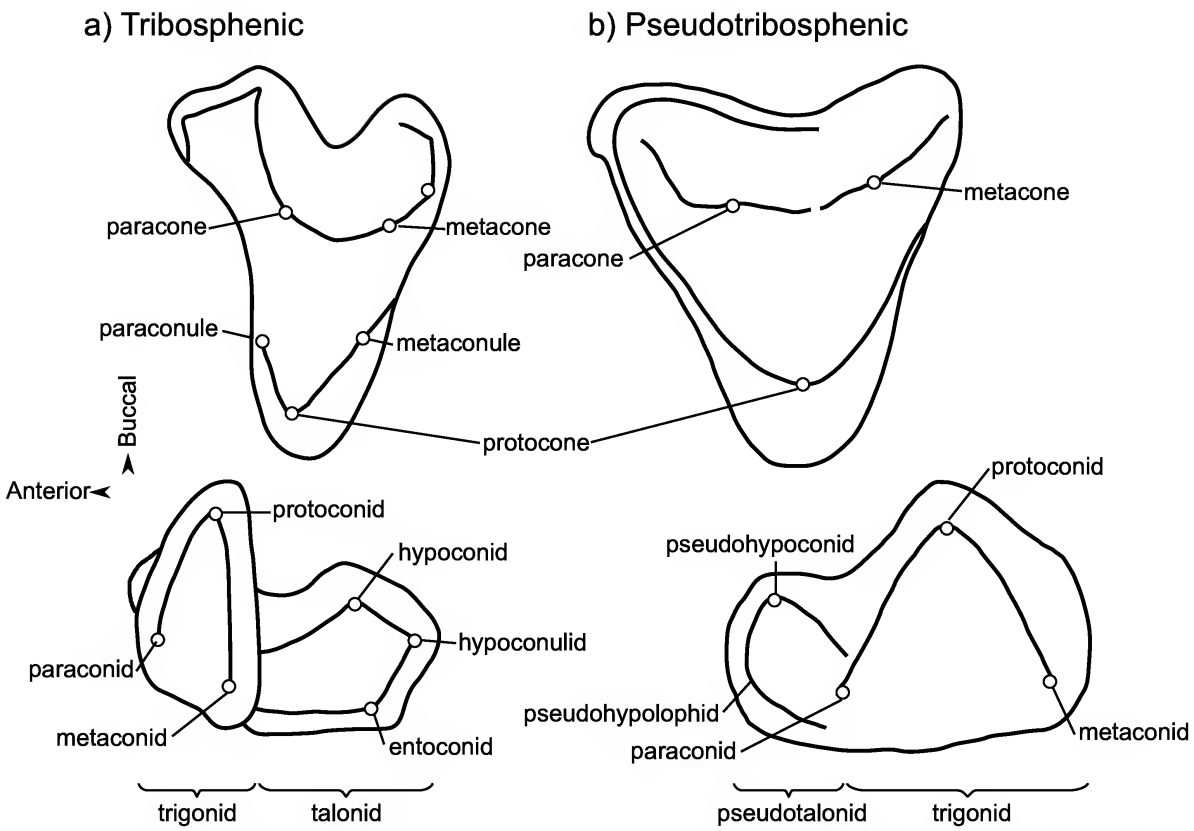

Fig. 1. Comparison of tribosphenic (a) and pseudo-tribosphenic (b) morphology for upper (top) and lower (bottom) molars, with basins and cusps labelled according to the nomenclature proposed here. The main upper cusps of both forms are labelled protocone, paracone and metacone, while the structures associated with the pseudotalonid basin on the lower are suffixed with 'pseudo'. (a) upper is *Peramus* and lower is unidentified lower from Crompton (1971), redrawn from Wang et al. (1998); (b) upper and lower are based on *Pseudotribos*, redrawn from Luo et al. (2007).

future cusp. At some distance from the primary enamel knot, additional knots can form, called secondary enamel knots, that also produce local maxima in the folded interface. The result is the general topography of the tooth represented by the epithelial-mesenchyme interface. After folding at each cusp is completed, mineralisation commences, starting at the cusp tip, with dentine deposited from the interface towards the interior of the tooth, and enamel on the outer surface.

While it is conceivable that the developmental-genetic process may exist such that tooth cusps are in some way encoded in a gene or genes, there are no unique gene signatures in any single cusp that has been investigated. In fact, because of the pleiotropy of genes (the effect of a gene on many phenotypic features) and the network nature of gene expression and signalling pathways, most tooth features including cusps are interlinked in development by shared genes and signalling pathways. In this sense, the cusps are not independent at the level of developmental processes (Kangas et al., 2004). The spacing and timing of each enamel knot controls the relative position and height of the resulting cusps. This mechanism appears to be conserved among therian mammals (placentals: Jernvall and Thesleff, 2000; marsupials: Moustakas et al., 2011). Therefore, we cannot identify a cusp based on any particular gene or specific combination of genes, i.e., there is no 'protocone gene'. However, there may be a gene or genes that control aspects such as lingual bias in growth of the upper tooth. The increase in such a signal may produce sufficient space for a cusp, which would then be called a 'protocone'.

Some genes are known to affect cusp formation. *Ectodysplasin* (*Eda*) is a tumor necrosis factor (TNF) gene that is expressed in the developing tooth (Kangas et al., 2004; Harjunmaa et al., 2014). When the EDA protein is absent, as is the case in the spontaneous null mutant in the mouse called Tabby, the molars are simpler and smaller, but when EDA is overexpressed in the epithelium, they are more complex compared to the wild type (Kangas et al., 2004; Harjunmaa et al., 2012). Fine-tuning of the amount of ectodysplasin generates intermediate tooth shapes, and replicates the order in which these cusps appeared in evolution (Harjunmaa et al., 2014).

Cusp Homology

The lack of specific genes for each cusp and the lability of the developing tooth to changes in gene products such as EDA appear to be somewhat at odds with the palaeontological perspective, which tends to view the positioning and relative size of major cusps as highly conserved and very stable. Evolutionary change appears very gradual compared to the havoc that can be wreaked by the modification in a single gene like *Eda*. This implicit view has led to the use of presence/absence or shape of tooth features as cladistics characters for phylogenetic reconstruction. If the developmental process were so labile, then there would be no phylogenetic signature in tooth cusp patterns at all. The phylogenetic signature in teeth at high taxonomic level is relatively low, presumably due to high degrees of homoplasy (such as the repeated evolution of the hypocone; Jernvall et al., 1996), but still can be informative at lower levels.

The use of tooth characteristics in phylogenetic reconstruction assumes homology among cusps. Homologies of cusps among tooth forms, and even between upper and lower teeth, have been proposed for over a century (Osborn, 1888). While it is now clear that it is very unlikely that there is a simple relationship of 'homology' among cusps, naming conventions have at least in part been based on criteria of homology. Wang et al. (1998) proposed these to be morphology, topographic position and occlusal relationships. Based on differences in topographic position, the lower basins of tribosphenic and pseudotribosphenic teeth are justified in their divergent names.

Protocone and the Meaning of 'Pseudo'

The major lingual cusp on upper molars of pseudotribosphenic dentitions has been analogised to the protocone, given its similarity in position, shape and inferred function to the protocone in tribosphenic dentitions. However, because it occludes with the basin on the anterior of the lower, the prefix 'pseudo' has been used to indicate that it is in some way different from the standard protocone.

Comparisons between the position and shape of the protocone and pseudoprotocone reveal a reasonable concordance between them (fig. 1; see also Wang et al., 1998, fig. 6). They both fulfil the same function of supporting crests that occlude with the lingual crests of the talonid basin. Wang et al. (1998) suggest that *Shuotherium* was not able to closely approximate the buccal surface of the pseudoprotocone with the lingual surface of the pseudotalonid basin, and so may not be able to 'crush' or 'grind' as many, but not all, tribosphenic molars can do (Crompton and Sita-Lumsden, 1970). Regardless, their overall functional relationships remain the same, although they are mirrored in the anterior-posterior axis. In what ways are these lingual cusps different? Since we currently understand that there is not a unique gene signature that could distinguish these two, and they are in the same position of the tooth with approximately the same shape, we could conclude that there is no major difference in their development or function. Therefore, I propose that there is no need to use the qualifier of 'pseudo' for the large lingual cusp on the upper molars of pseudotribosphenic teeth, and that it be called 'protocone'.

In the hypothetical upper pseudotribosphenic molar, Chow and Rich (1982) named the posterobuccal cusp metacone, using the same topological convention as tribosphenic molars (as did Luo et al., 2007 for the new pseudotribosphenic mammal *Pseudotribos robustus*). Wang et al. (1998) label this cusp the 'pseudometacone', which occludes between the pseudohypoconid of the opposing lower tooth and the protoconid of the tooth posterior to it. The 'pseudometacone' of the pseudotribosphenic teeth has an equivalent position and shape to the metacone of tribosphenic teeth. The justification for the 'pseudo' designation is likely because of its different occlusal relationships with the lower compared to the tribosphenic metacone, which occludes in the space between the hypoconid and protoconid of the same lower tooth. An equivalent difference in occlusal relationships exists for the paracone, and so following the same convention it would be the 'pseudoparacone'. This shows an inconsistent use of the 'pseudo' prefix in exactly what is different or 'pseudo' about the feature. I propose here that the 'pseudo' be used only for the new topographical structure, the anterior basin of the lower molar, and its associated cusps and crests, such as the pseudohypoconid and pseudohypolophid (fig. 1b).

Importance of Names

Why is it important to reconsider the naming of this cusp, in what looks like a purely nomenclatural discussion? The term pseudoprotocone implies some substantive difference from the protocone, and suggests major developmental and/or functional distinctions between these cusps.

In order to evolve a tribosphenic-like tooth from a basal reversed-triangle tooth, three features must be added: a basin on the lower tooth, a lingual cusp on the occluding upper, and an additional buccal cusp (either paracone or metacone) also on the upper. The biggest difference between evolving a tribosphenic tooth and a pseudotribosphenic tooth is whether the basin is anterior or posterior. This will affect the shape of the protocone, paracone and metacone, but the protocone and two buccal cusps must still be present. From a developmental perspective, then, the protocone is essentially the same for the two tooth forms.

Anterior-posterior Bias

Using 'pseudo' gives the impression of substantial difference in shape and function from tribosphenic, while in fact the differences are relatively minor. It is likely only the anterior-posterior bias in the lower molar that makes the difference. Recent developmental experiments show an inherent bias in the morphogenesis of mouse molars, such that a posterior extension is more likely than an anterior one (Harjunmaa et al., 2014; Luo, 2014). It is likely that such a bias existed in the ancestor to all modern toothed mammals. This begs the question of whether pseudotribosphenic mammals had an anterior bias rather than a posterior one. How labile may this anterior-posterior bias be? Could a switch in the bias have

changed several times in the history of mammals? Depending on the postulated evolutionary relationships among tribosphenic and pseudotribosphenic mammals, this switch may have occurred once or several times (Luo et al., 2007; Rich and Vickers-Rich, 2010).

The origin and evolution of anterior-posterior developmental bias in lower molar development relative to the upper appears to be a bigger question than the convergence of the tribosphenic-like form itself. If a lower molar has a posterior bias in producing a basin, then it can occlude with a nascent lingual cusp that can later evolve to become a protocone. A basin produced by an anterior developmental bias can also occlude with a nascent protocone.

Currently there are no obvious molecular signals that may produce this anterior-posterior differential bias in tooth development, but this is a significant line of enquiry for future research.

Conclusion

While the tribosphenic tooth is an intricate, precisely-occluding device (Evans and Sanson, 2003; Evans and Sanson, 2006), equivalent structures have evolved a number of times, at least in tribosphenic and pseudotribosphenic mammals. But the difficulty of evolving such a shape may have been overestimated, and is perhaps exaggerated by the 'pseudoprotocone' terminology.

Acknowledgements

I would like to thank Tom Rich for his enthusiasm and dedication to Mesozoic mammal research in Australia, and inspiration to generations of Australian palaeontologists and biologists. I also thank Erich Fitzgerald for inviting me to contribute to this volume to honour Tom Rich's contributions to vertebrate palaeontology. Thanks to Zhe-Xi Luo and an anonymous reviewer for suggestions that refined the ideas presented here and improved the manuscript.

References

Chow, M., and Rich, T.H.V. 1982. *Shuotherium dongi*, n. gen. and sp., a therian with pseudo tribosphenic molars from the Jurassic of Sichuan, China. *Australian Mammalogy* 5: 127–142.

Crompton, A.W. 1971. The origin of the tribosphenic molar. Pp. 65–87 in: Kermack, D.M. and Kermack, K.A. (eds), *Early Mammals*. Academic Press: London.

Crompton, A.W., and Sita-Lumsden, A. 1970. Functional significance of the therian molar pattern. *Nature* 227: 197-199.

Evans, A.R., and Sanson, G.D. 2003. The tooth of perfection: functional and spatial constraints on mammalian tooth shape. *Biological Journal of the Linnean Society* 78: 173–191.

Evans, A.R., and Sanson, G.D. 2006. Spatial and functional modeling of carnivore and insectivore molariform teeth. *Journal of Morphology* 267: 649–662.

Harjunmaa, E., Kallonen, A., Voutilainen, M., Hamalainen, K., Mikkola, M.L., and Jernvall, J. 2012. On the difficulty of increasing dental complexity. *Nature* 483: 324–327.

Harjunmaa, E., Seidel, K., Hakkinen, T., Renvoise, E., Corfe, I.J., Kallonen, A., Zhang, Z.-Q., Evans, A.R., Mikkola, M.L., Salazar-Ciudad, I., Klein, O.D., and Jernvall, J. 2014. Replaying evolutionary transitions from the dental fossil record. *Nature* 512: 44–48.

Jernvall, J., and Thesleff, I. 2000. Reiterative signaling and patterning during mammalian tooth morphogenesis. *Mechanisms of Development* 92: 19–29.

Jernvall, J., Hunter, J.P., and Fortelius, M. 1996. Molar tooth diversity, disparity, and ecology in Cenozoic ungulate radiations. *Science* 274: 1489–1492.

Kangas, A.T., Evans, A.R., Thesleff, I., and Jernvall, J. 2004. Nonindependence of mammalian dental characters. *Nature* 432: 211–214.

Luo, Z.-X. 2014. Tooth structure re-engineered. *Nature* 512: 36–37.

Luo, Z.X., Ji, Q., and Yuan, C.X. 2007. Convergent dental adaptations in pseudo-tribosphenic and tribosphenic mammals. *Nature* 450: 93–97.

McKenna, M.C. 1975. Toward a phylogenetic classification of the Mammalia. Pp. 21–46 in: Luckett, W.P. and Szalay, F.S. (eds), *Phylogeny of the Primates*. Plenum Publishing Corporation: New York.

Moustakas, J.E., Smith, K.K., and Hlusko, L.J. 2011. Evolution and development of the mammalian dentition: insights from the marsupial *Monodelphis domestica*. *Developmental Dynamics* 240: 232–239.

Osborn, H.F. 1888. The evolution of mammalian molars to and from the tritubercular type. *American Naturalist* 22: 1067–1079.

Patterson, B. 1956. Early Cretaceous mammals and the evolution of mammalian molar teeth. *Fieldiana Geology* 13: 1–105.

Rich, T., and Vickers-Rich, P. 2010. Pseudotribosphenic: the history of a concept. *Vertebrata PalAsiatica* 48: 336–347.

Simpson, G.G. 1936. Studies of the earliest mammalian dentitions. *Dental Cosmos* 78: 791-800, 940–953.

Wang, Y.Q., Clemens, W., Hu, Y.M., and Li, C.K. 1998. A probable pseudo-tribosphenic upper molar from the late Jurassic of China and the early radiation of the Holotheria. *Journal of Vertebrate Paleontology* 18: 777-787.

Memoirs of Museum Victoria 74: 97–105 (2016) Published 2016

ISSN 1447-2546 (Print) 1447-2554 (On-line)
http://museumvictoria.com.au/about/books-and-journals/journals/memoirs-of-museum-victoria/

The upper dentition and relationships of the enigmatic Australian Cretaceous mammal *Kollikodon ritchiei*

Rebecca Pian[1,2,3], Michael Archer[1,*], Suzanne J. Hand[1], Robin M.D. Beck[1,4] and Andrew Cody[5]

[1] PANGEA Research Centre, School of Biological, Earth and Environmental Sciences, University of New South Wales, Sydney, New South Wales 2052, Australia (m.archer@unsw.edu.au)
[2] Division of Paleontology, American Museum of Natural History, New York, NY 10024, USA (rpian@amnh.org)
[3] Department of Earth and Environmental Sciences, Columbia University, New York, NY 10026 USA
[4] School of Environment & Life Sciences, University of Salford, Salford M5 4WT, England
[5] The National Opal Collection, 119 Swanston St, Melbourne, Victoria 3000, Australia
*To whom correspondence should be addressed. E-mail: m.archer@unsw.edu.au

Abstract

Pian, R., Archer, M., Hand, S.J., Beck, R.M.D. and Cody, A. 2016. The upper dentition and relationships of the enigmatic Australian Cretaceous mammal *Kollikodon ritchiei*. *Memoirs of Museum Victoria* 74: 97–105.

Mesozoic mammals from Australia are rare, so far only known from the Early Cretaceous, and most are poorly represented in terms of dentitions much less cranial material. No upper molars of any have been described. *Kollikodon ritchiei* is perhaps the most bizarre of these, originally described on the basis of a dentary fragment with three molars. Here we describe a second specimen of this extremely rare taxon, one that retains extraordinarily specialised upper cheekteeth (last premolar and all four molars). Each molar supports rows of bladeless, rounded cuspules many of which exhibit apical pits that may be the result of masticating hard items such as shells or chitin. Reanalysis of the phylogenetic position of this taxon suggests, based on a limited number of apparent synapomorphies, that it is an australosphenidan mammal and probably the sister group to Monotremata. This reanalysis also supports the view that within Monotremata, tachyglossids and ornithorhynchids diverged in the early to middle Cenozoic.

Keywords

New South Wales, Mesozoic, Albian, Australosphenida, Monotremata, Ausktribosphenidae.

Introduction

Mesozoic mammals from Australia were unknown until the description in 1985 of the holotype and only known specimen of the monotreme *Steropodon galmani* (Archer et al., 1985), a partial right dentary with all three molars, from the Early Cretaceous (Albian) Griman Creek Formation at Lightning Ridge, New South Wales. This was followed by discovery at Lightning Ridge of *Kollikodon ritchiei* (Flannery et al., 1995), known from a single partial right dentary with three molars *in situ* and alveoli for the posterior two premolars and a fourth molar. Since then, additional Early Cretaceous mammals have been described from sites in southern Victoria and New South Wales. These include: from the Aptian Flat Rocks locality in Victoria, the ausktribosphenids *Ausktribosphenos nyktos* (Rich et al., 1997) and *Bishops whitmorei* (Rich et al., 2001a), the monotreme *Teinolophos trusleri* (Rich et al., 1999, 2001b), and the multituberculate *Corriebaatar marywaltersae* (Rich et al., 2009); from the Albian Dinosaur Cove locality in Victoria, the partial humerus of (the possible monotreme) *Kryoryctes cadburyi* (Pridmore et al., 2005); and from Lightning Ridge in New South Wales a very large, mammal-like isolated tooth (Clemens et al., 2003). Most recent phylogenetic analyses have placed ausktribosphenids and monotremes within a larger Gondwanan radiation termed Australosphenida (Luo et al., 2001, 2002, 2007a; Martin and Rauhut, 2005; Rougier et al., 2011; Wood and Rougier, 2005), together with the early Jurassic (Toarcian) (Cúneo et al., 2013) South American *Asfaltomylos* (Rauhut et al., 2002) and *Henosferus* (Rougier et al., 2007), and the middle Jurassic (Bathonian) *Ambondro mahabo* (Flynn et al., 1999) from Madagascar. Some authors, however, have questioned the inclusion of monotremes within Australosphenida (Pascual et al., 2002; Rich et al., 2002; Rowe et al., 2008; Woodburne, 2003).

Archer et al. (1985) described *Steropodon galmani* as a plesiomorphic, toothed monotreme in the monotypic family Steropodontidae, an assignation that has been widely accepted (Kielan-Jaworowska et al., 1987; Musser, 2006; Phillips et al., 2009). Inclusion of *Teinolophos trusleri* within Monotremata is also uncontested, despite some debate over placement within the stem or crown group (Phillips et al., 2009; Rich et al., 2001b; Rowe et al., 2008). Flannery et al., (1995) described *Kollikodon ritchiei* as a possible monotreme, placing it in its own monotypic family, the Kollikodontidae. This assignation has proved more controversial, with suggestions that it may be a basal

mammaliaform rather than a monotreme and as such more appropriately placed outside crown-group Mammalia (Musser, 2003). This controversy rejects in part the limited morphological information available on the basis of the previously only known specimen, a partial dentary with three highly autapomorphic, bunodont molars. Discovery of an additional specimen of *K. ritchiei*, a partial maxilla with one premolar and four molars, now provides significant additional information about the structure and likely evolutionary relationships of this enigmatic taxon. This specimen also represents the first maxilla with teeth known for any Australian Mesozoic mammal.

Here we describe this specimen and test the evolutionary relationships of *K. ritchei* via phylogenetic analysis based on a comprehensive morphological character matrix.

Materials and Methods

Measurements of the specimen were taken to the nearest 0.01 mm using a Leica M205 C microscope and integrated Leica DFC290 camera. Tooth lengths were measured along the long axis of the molar row. Widths were measured from the widest transverse points across the tooth, perpendicular to the long axis.

Kollikodon ritchiei was added to a revised version of the character matrix of Luo et al. (2011), which is in itself a modified version of earlier matrices (Luo et al., 2001, 2002, 2007b; Luo & Wible, 2005). Revisions to the matrix were made on the basis of corrections and criticisms by Woodburne et al. (2003), Rougier et al. (2007), Rowe et al. (2008) and Phillips et al. (2009). The final matrix included 104 taxa and 438 characters. 62 multistate characters representing plausible morphoclines were ordered. The topologies of the consensus trees derived through the ordered and unordered analyses were very similar, and as such only the ordered analyses are included here (Wiens, 2001).

Maximum parsimony analyses were conducted using the computer program PAUP* (Phylogenetic Analysis Using Parsimony and Other Methods) version 4.0b10 (Swofford, 2002). 1,000 heuristic replicates were initially carried out, saving 10 trees per replicate, followed by a second heuristic search within the trees obtained from the first search. Zero-length branches were then collapsed. Strict and 50% majority-rule consensus trees were derived from the most parsimonious trees recovered for each analysis. Bootstrap analysis was used to assess nodal support. To calculate bootstrap values, 250 bootstrap replicates were run, with a time limit of 60 seconds per replicate.

Bayesian analyses were conducted using Lewis's (2001) Mk likelihood model for discrete morphological data in the program MrBayes 3.2.1 (Ronquist et al., 2012). Applied assumptions included scoring of only parsimony informative characters and gamma distribution that permits rate variation across different characters. Two independent runs of four Monte Carlo Markov chains (one cold and three heated) were run for 5,000,000 generations with trees sampled every 500 generations. Convergence was confirmed by average standard deviation of split frequencies of less than 0.05. The first 25% of samples were discarded as "burn-in" and remaining samples used to construct the 50% majority-consensus.

Systematic Palaeontology

Mammalia Linnaeus, 1758

Australosphenida Luo, Cifelli and Kielan-Jaworowska, 2001

Kollikodontidae Flannery, Archer, Rich and Jones, 1995

Kollikodon Flannery, Archer, Rich and Jones, 1995

Kollikodon ritchiei Flannery, Archer, Rich and Jones, 1995

Holotype. AM F96602 (Australian Museum Palaeontological Collection, Sydney, Australia,), right dentary fragment preserving m1-3 and alveoli for two premolars and m4.

Referred specimen. Opalised right skull fragment preserving part of the maxilla, which retains the posterior premolar (possibly P4) and M1-4, and possibly also part of the palatine (Figs 1–2). A 35μm voxel Xradia microCT data file of the specimen has been lodged with the Museum of Victoria in Melbourne. Detailed 3D prints of this specimen can be made from the scan data. Solid casts taken from a mould of the complete upper dentition are also available; one (AM F140201) is registered in the collections of the Australian Museum. Although the original specimen, which is a natural glass cast without internal structure of any kind, is less informative than the microCT scan data (given that it reveals structures in undercut areas not visible via conventional microscopy) and no more informative than 3D prints and hard casts, this specimen is available for further examination as part of the National Opal Collection, on application to its Director, Andrew Cody (andrew@codyopal.com).

Locality and age. Griman Creek Formation; Early Cretaceous (Middle Albian) (Flannery et al., 1995). The type locality is claim 30226, Moonshine area of the Cocoran opal field, Lightning Ridge, New South Wales, Australia (Flannery et al., 1995). The new skull fragment described here comes from an unnamed mine on the Cocoran opal field.

New diagnosis of clade containing Kollikodon *and monotremes. Kollikodon ritchiei* and definitive monotremes (ornithorhynchids, tachyglossids, *Steropodon* and *Teinolophos*) differ from other groups variously regarded as australosphenidans (ausktribosphenids, *Ambondro*, *Asfaltomylos* and shuotheriids), in so far as they are known, in having no paraconid on the first lower molar, an extremely abrupt discontinuity in size between the ultimate premolar and the first molar in the upper and lower dentitions, and in the presence of an enlarged dentary canal.

Revised specific diagnosis. Kollikodon ritchiei is a large (by Mesozoic standards) mammal (estimated body mass approximately 1935 g based on m1 area (Legendre, 1986)) that differs from definitive monotremes that retain a functional dentition in exhibiting the following combination of features: bunodont molars with no vertical blades (lophs or crests) of any kind; broadly crescentic upper molars with unique cusp arrangement; reduced or absent posterior cingula/cingulids on all molars; markedly convex curve of the buccal edge of the upper and (to a lesser extent) lower molar rows.

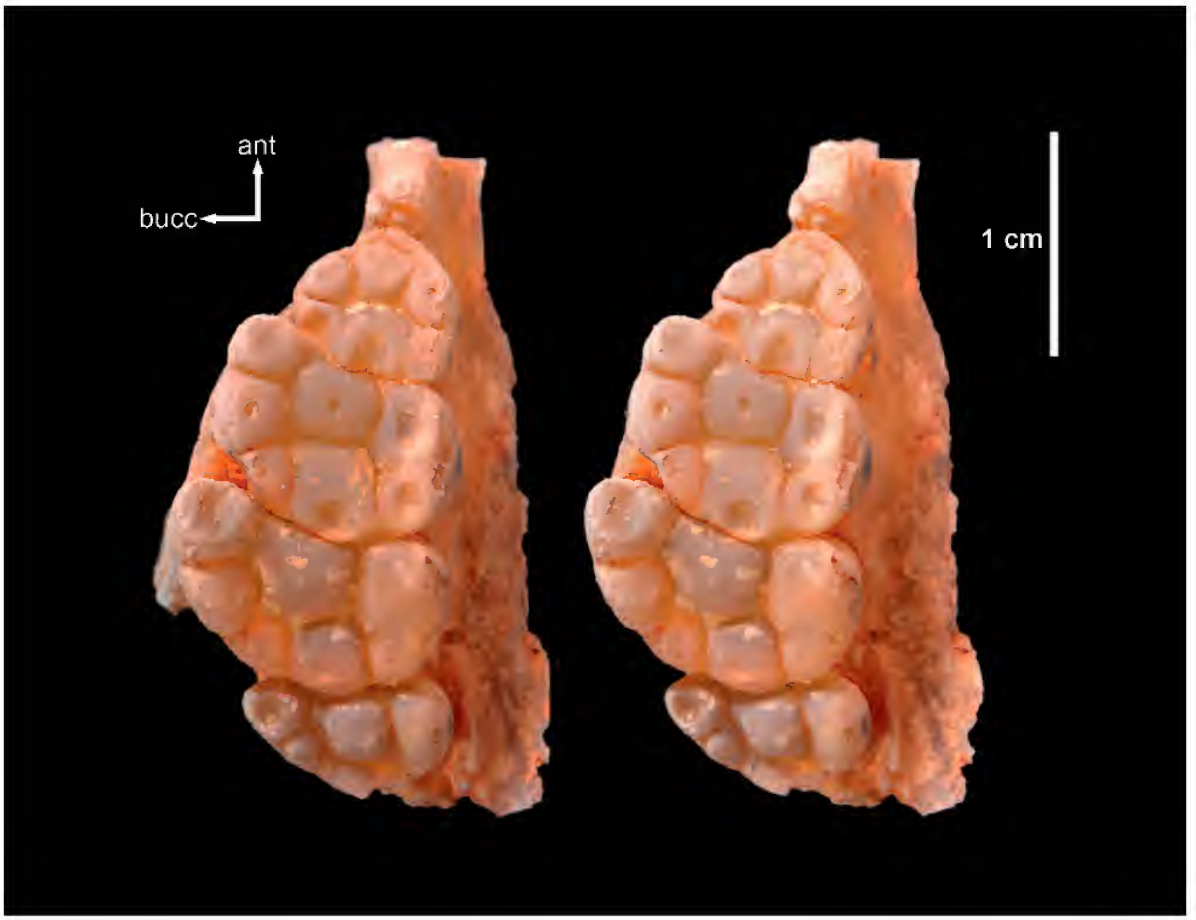

Figure 1. *Kollikodon ritchiei* right maxillary fragment and molar row preserving Px, M1, M2, M3 and RM4. Stereopair occlusal view. ant, anterior; bucc, buccal.

Description of the upper dentition and cranial fragment

The new specimen is a right cranial fragment comprising part of the maxilla and possibly part of the palatine (Figs 1–2). The maxilla preserves the root of the zygomatic arch and part of the palatal shelf. The palatine may form part of the posterior section of this shelf, although no sutures are evident. The infraorbital canal is exposed on the anterodorsal edge of the broken maxilla. No complete edges can be identified around the preserved portion of the palate.

Within the maxilla, the posterior premolar (actual homology with other mammalian premolars is unknown) and all four upper molars, M1-4, are preserved in situ. No inference can be made about teeth anterior to the posterior premolar because the maxilla is missing anterior to that point. As in the lower dentition, there is a stark discontinuity in size between the premolar and the molar row. The double-rooted, comparatively simple premolar aligns with the median row of cusps on the molars. The four fully bunodont molars are characterized by rows of low, rounded, dome-like cusps that are separated from each other by arcuate grooves of varying depth. None of the cusps is subtended by blades although the enamel edges of pits in the apices of many of the cusps may have provided horizontal arcuate blades that assisted in segmenting food during transverse mastication.

The occlusal plane of the upper molar row is anteroposteriorly convex, corresponding to the concavity of the occlusal plane of the lower molar row. Although the lingual margin of the upper tooth row is more or less rectilinear, the buccal margin is strongly convex, reflecting differences in the width of the individual molars, with M2-3 being the widest. When the holotype is placed in centric occlusion with the upper dentition, the buccal margins of the upper molars markedly overhang the buccal margin of the lower molars, resulting in a strongly anisodontic bite. Considering the molars, M3 has the largest total occlusal surface followed in descending order by M2, M4 and M1 (Table 1).

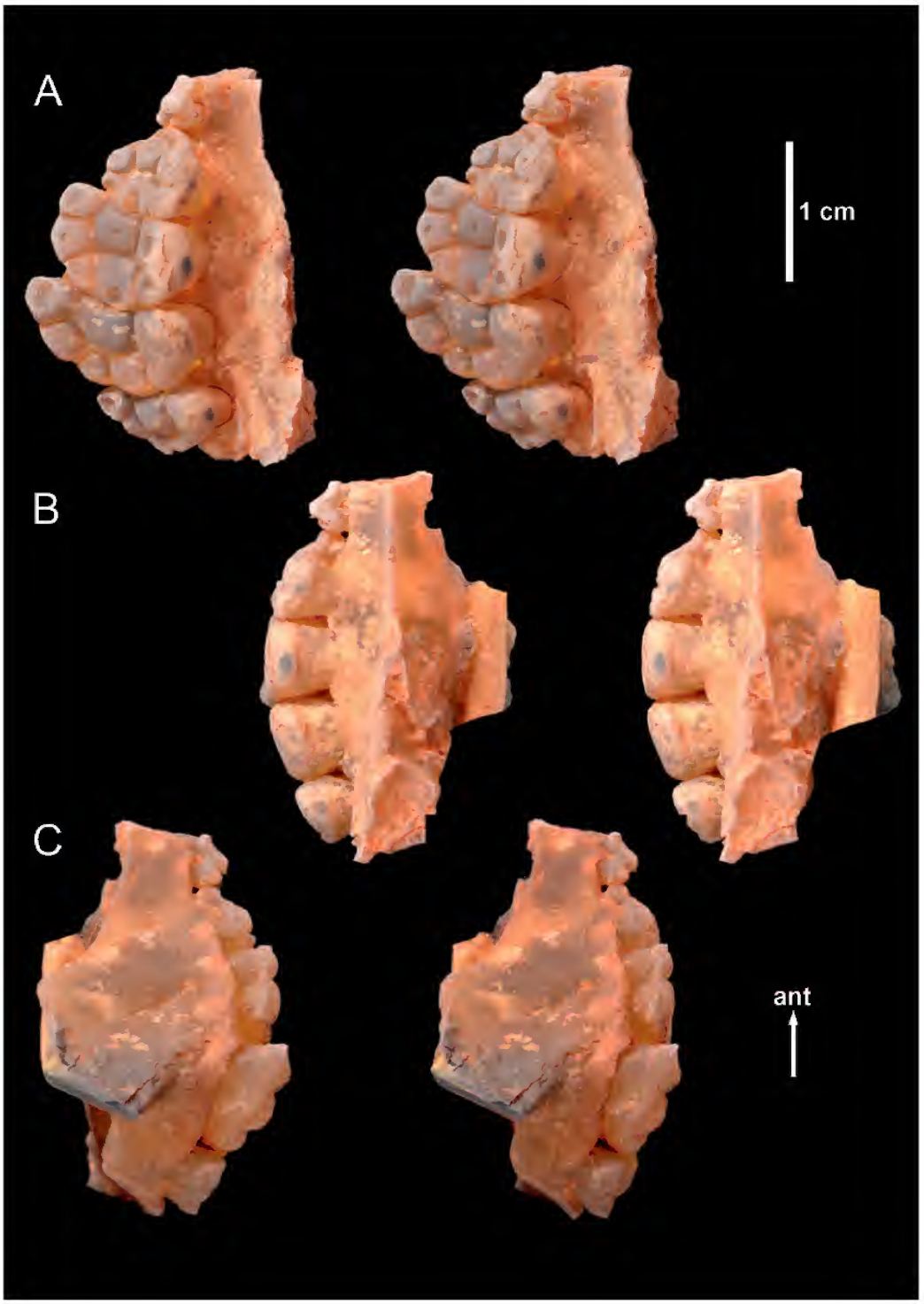

Figure 2. *Kollikodon ritchiei* right maxillary fragment and molar row preserving Px, M1, M2, M3 and M4. (A) Stereopair oblique-occlusal view. (B) Stereopair lingual view. (C) Stereopair buccal view. ant, anterior.

Although each molar is distinctly different from the others, there are common features and meristic trends that progress posteriorly along the molar row. The molars are transversely wide. Many of the cusps have pits or depressions at their apices. The arrangement of cusps on each molar could be interpreted as forming either a series of two arcuate transverse rows of cusps, three variably-longitudinal rows of cusps, or two central anteromedial cusps ringed by a perimeter of 2 to 3 buccal cusps and 1 to 2 lingual cusps. Given the morphological distinctiveness of each molar, none of these interpretations applies equally well to all of the individual teeth.

On M2-4 the anterobuccal and anterolingual corner cusps are anteriorly displaced compared to the anteromedial cusp, resulting in a concave anterior margin and a convex posterior margin of the crown. In contrast, M1 has convex margins on both the anterior and posterior sides of the crown making it unlike the otherwise crescentic M2-4. The distinction between the lingual cusps becomes less evident posteriorly such that in M4 only one anteroposteriorly elongate lingual cusp is apparent. M1 is the only molar that exhibits a basal anterior cingulum. In contrast to the holotype in which it can be clearly seen that each lower molar is double-rooted, the number of roots for each upper molar and the internal structure of the maxilla are unclear. There appears to be no preservation of any anatomical feature within the glass structure of the maxilla.

The apical pits invite speculation that these may have originally been areas of thin or even absent enamel that, once breached to expose softer dentine, served to increase the transverse cutting capacity of the otherwise blade-less molars. Functionally they would have acted as entrapment devices to help immobilize items being transversely sheared. Unfortunately, the amorphous glass constituency of the crowns does not enable differentiation of enamel and dentine hence this possibility cannot be tested. Alternatively the pits may be the result of apical concussive pressure caused by compression against wide, flat, hardened surfaces such as mollusc shells or crustacean chitin. If the result of compression, it is perhaps surprising that all except two (the hemicircular pits in the posterobuccal and posteromedial cusps of M1) are nearly circular even at the extreme buccal edge of the dentition such as the anterobuccal cusp of M4. If the two hemicircular pits at the posterior margin of M1 were also originally circular, interproximal wear could have removed the posterior halves of these pits. However, if this is the explanation for the hemicircularity, the lack of corresponding loss of tooth material from the anterior flank of M2 as well as the lack of posterior wear on the posterior premolar invite a more detailed analysis of potentially unique occlusal mechanics in this strange group of mammals.

Phylogenetic Analysis

Maximum parsimony analysis of our morphological character matrix, with selected multistate characters ordered, recovered 6048 most parsimonious trees (tree length = 2339; consistency index = 0.35). A simplified 50% majority-rule consensus is given in Fig. 3A, with dotted lines indicating nodes that collapse in the strict consensus. In the 50% majority-rule consensus tree, *Kollikodon ritchiei* is placed within Australosphenida, forming a polytomy with the monotreme *Teinolophos trusleri* and another monotreme clade comprising *Steropodon galmani, Tachyglossus aculeatus, Obdurodon dicksoni* and *Ornithorhynchus anatinus*. The *K. ritchiei*/monotreme clade is weakly supported, with a bootstrap value of 53% and it collapses in the strict consensus. There is, however, strong support (bootstrap value 80%) for the clade comprising *S. galmani*, *Ta. aculeatus, Ob. dicksoni* and *Or. anatinus*. Under strict consensus the australosphenidan clade collapses, as does the clade placing *K. ritchiei* and *Te. trusleri* with the other monotremes. When *K. ritchiei* is excluded from analyses, however, Australosphenida is retained in the strict consensus and is reasonably well supported compared to other higher-level clades, with a bootstrap value of 69%; monophyly of the monotremes is also strongly supported, with a bootstrap value of 86%.

Table 1. Dimensions of the upper right dentition of the original specimen of *Kollikodon ritchiei* represented by AM F140201 (in mm).

Tooth	Length	Width
Px	4.49	3.58
M1	6.86	8.77
M2	8.33	13.24
M3	7.74	15.20
M4	5.74	12.01

Bayesian analysis of the same matrix using the Mk model and a gamma distribution to model rate heterogeneity between characters (Fig. 3B) resulted in a similar topology to the maximum parsimony analysis; specifically, *K. ritchiei* is placed within Australosphenida as sister to monotremes. Bayesian posterior probability (BPP) support for a monotreme/*Kollikodon* clade was moderate at 0.83. Support for Australosphenida was considerably stronger, with a BPP of 0.95. Unlike in the maximum parsimony analysis, the position of *Te. trusleri* was retained in the Bayesian analysis, with a support value of 0.75. Strikingly, in contrast to the maximum parsimony tree, *Or. anatinus* and *Ta. aculeatus* were sister-taxa to the exclusion of *Ob. dicksoni*, with relatively high BPP of 0.94.

The monotreme/*Kollikodon* clade (as resolved in the maximum parsimony analysis) is supported by a single synapomorphy that can be scored for *K. ritchiei*: the abrupt disjunction in size between premolars and molars, with the molars being significantly larger than the premolars in both groups (character 448: 0 => 1). This character state change optimizes as a synapomorphy of this clade regardless of whether accelerated or delayed transformation is assumed, and occurs along no other branch on the tree (i.e. it has a consistency index of 1).

Comparisons with other putative australosphenidans are equally difficult because the molar morphology of *K. ritchiei* is so autapomorphic with no resemblance to any of the tribosphenic or pseudotribosphenic morphologies exhibited by species of *Ambondro*, *Henosferus*, *Asfaltomylos*, *Ausktribosphenos*, *Bishops*, *Pseudotribos* or *Shuotherium*. On the other hand, features noted above that appear to group *K.*

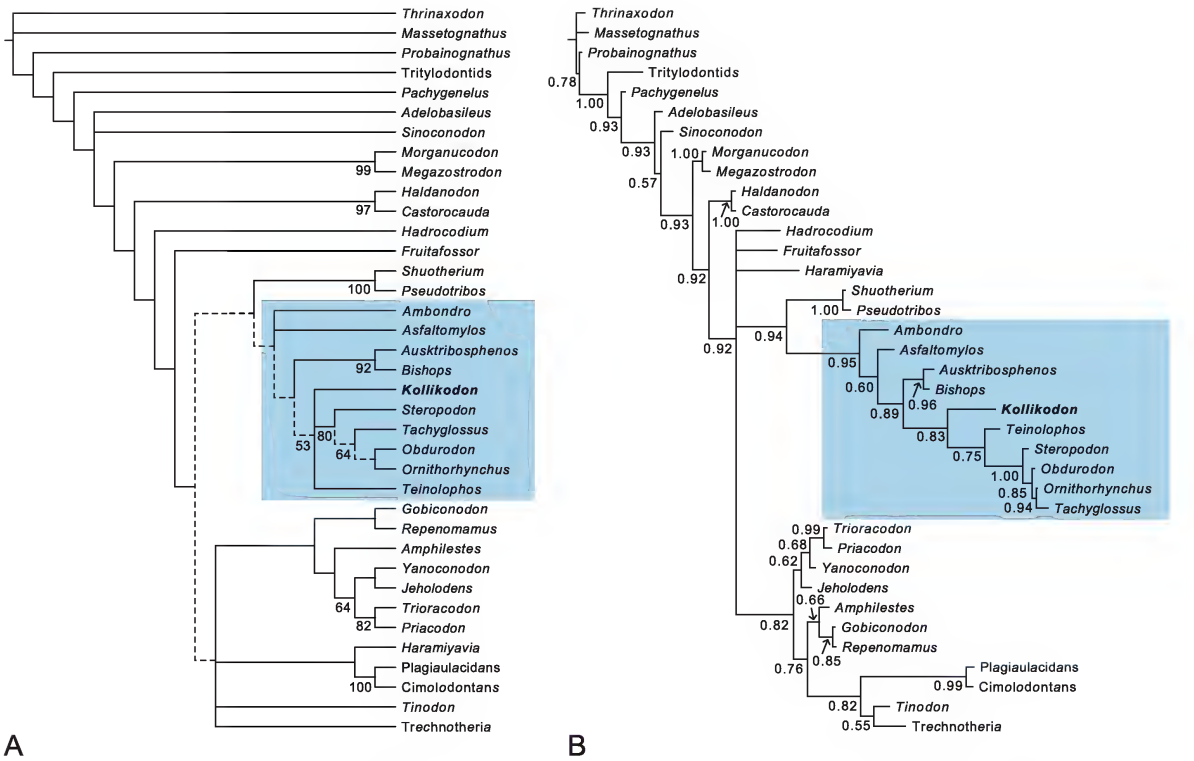

Figure 3. Results of phylogenetic analyses of 104 taxa and 438 characters, including 62 ordered characters. *Kollikodon ritchiei* is highlighted in bold, Australosphenida is indicated by blue shading. 68 taxa are collapsed in the clade Trechnotheria. (A) Maximum parsimony analysis 50% majority-rule consensus. Dashed lines indicate nodes that collapse under strict consensus of 6048 most parsimonious trees, each with a tree length of 2336 and consistency index (CI) of 0.35. Numbers below branches indicate bootstrap values (only those above 50% reported). (B) Bayesian analysis 50% majority-rule consensus of the post burn-in trees. Nodal support values indicate Bayesian posterior probabilities above 50%.

ritchiei with monotremes are not shared with species in these other australosphenidan taxa.

Discussion

The specimen described here represents the first maxillary dentition of any Australian Mesozoic mammal. It can be confidently referred to *Kollikodon ritchiei* on the basis of similarities in the bunodont dentition and other aspects of molar crown morphology, compatible size, and a close occlusal fit with the holotype. This specimen confirms that *K. ritchiei* is highly autapomorphic and in fact even more unusual than originally appreciated, with the crescent-shaped upper molars and cusp arrangement being unique among mammaliaforms known to date. The original description suggested that *K. ritchiei* had at least four lower molars (Flannery et al., 1995). Based on the presence of four molars in the upper dentition, four molars were probably also present in the lower dentition.

The numerous apical pits present on the upper molars combined with the highly bunodont morphology, curvature of the cusp rows on each crown and marked convexity of the molar row as a whole suggest an unusual form of occlusion. None of the cusps is subtended by primary blades, suggesting that whatever food was eaten was probably crushed although the circular pits, however they were formed, may have helped immobilize hard food items that were being masticated in whichever direction comminution took place.

The known material of *K. ritchiei* preserves very few features that are phylogenetically informative and this taxon is therefore scored for only 26 of 438 characters in our matrix. The upper and lower cheektooth dentition is well preserved, as are some aspects of mandibular morphology, but the material composition of the maxilla (transparent glass with no internal features preserved) and its missing margins have resulted in retention of very little additional information about cranial morphology. Many dental characters in the modified matrix of Luo et al. (2011) relate to the presence or absence of specific cusps, as well as their relative position and sizes (if present). The majority of these characters cannot be scored for *K. ritchiei* because the homologies of most of the cusps (particularly on the upper molars) are unclear. The difficulties of applying tribosphenic terminology to even tribosphenic-like monotreme teeth is also an ongoing point of contention (Woodburne, 2003). A further stumbling block is the limited

fossil record of other Mesozoic australosphenidans, because no upper dentitions or maxillae have yet been published. Nevertheless maximum parsimony and Bayesian methods of phylogenetic analysis support the inclusion of *K. ritchiei* within crown-group Mammalia, in contrast to recent suggestions that it may have been a stem-mammaliaform (Musser, 2003). Both methods also place *K. ritchiei* as sister group to definitive monotremes within Australosphenida, albeit with varying degrees of support.

It should be emphasized that only one feature was recovered as synapomorphic for a *Kollikodon*/monotreme clade in all analyses: the marked disjunction in size between the posterior premolar and the first molar. This feature occurs in all toothed monotremes that are represented by adequate fossils, i.e. *Steropodon galmani* (Archer et al., 1985) and the Miocene ornithorhynchid *Obdurodon dicksoni* (Archer et al., 1992), in addition to *K. ritchiei*. As such it appears to be an unambiguous, uncontradicted synapomorphy for this clade. The same condition appears to be present in the extant platypus *Ornithorhynchus anatinus* (Green, 1937) but, because of significant uncertainties about its vestigial dentition, it was scored as unknown in our matrix. Presence of an enlarged mandibular canal was also identified in the original description of *K. ritchiei* (Flannery et al., 1995) as an apomorphy linking this taxon with definitive monotremes, possibly indicating sensory elaboration at the front of the face such as occurs in ornithorhynchids which have many electroreceptors in the dermis covering the bill.

In contrast to the autapomorphic and extremely bunodont *K. ritchiei*, all known toothed monotremes show remarkable similarity in molar morphology spanning a significant period of time from the Early Cretaceous *S. galmani* and *T. trusleri* to the Paleocene *Monotrematum sudamericanum* and the three Oligocene/Miocene species of *Obdurodon* (Musser, 2006; Pascual et al., 2002; Pian et al., 2013). The only molar features that have been identified as characteristic of monotremes that are also present in *K. ritchei* include the presence of very large and wide talonids, and absence of a cusp in the paraconid position on the first lower molar (Long et al., 2002). Definitive monotremes that retain an adult dentition share a number of additional dental apomorphies, including prominent shelf-like anterior and posterior cingulids on the lower molars and high transverse, loph-like blades on the trigonids and talonids present as either a single blade or as a V-shaped blade. In definitive monotremes for which the upper dentition is known, this pattern is mimicked on the upper molars with transverse V-shaped blades. Although the dentition of *Or. anatinus* is vestigial and deciduous, the same pattern appears to be present in the molar remnants found in juveniles (Green, 1937; Woodburne & Tedford, 1975).

In contrast, *Kollikodon ritchiei* lacks any traces of vertical transverse blades, cingula or cingulids. Furthermore, although the cusps of the lower molars of *K. ritchiei* can be tentatively homologised with those of toothed monotremes (Flannery et al., 1995), we are unable to do this with any confidence for the cusps of the upper molars. However, it is possible that the bunodont form of the molars in *K. ritchiei* evolved from a relatively more plesiomorphic transverse blade system of the kind seen in species of *Steropodon*, *Teinolophus*, *Monotrematum* and *Obdurodon*. Based on the results of our formal phylogenetic analyses and pending discovery of morphologically annectant taxa, we suggest the most parsimonious hypothesis is that *K. ritchiei* is a highly autapomorphic sister-taxon to definitive monotremes.

While in both the maximum parsimony and Bayesian analyses, *Kollikodon* fell outside crown-group Monotremata, it was closer to definitive monotremes than other australosphenidans. Whether *Kollikodon* itself should be considered a monotreme is ultimately dependent on how the clade Monotremata is defined. A *Kollikodon* plus definitive monotreme clade is supported by the following apomorphies: presence of a partially enlarged mandibular canal, the marked disjunction in size between the last premolar and the first molar, large and wide talonids, and absence of a cusp in the position of a paraconid on the first lower molar. Tentatively we suggest that, despite these potential synapomorphies, the otherwise highly autapomorphic and character-ambiguous *Kollikodon* should be regarded as a sister group of Monotremata.

One striking difference between our maximum parsimony and Bayesian analyses is the relationships suggested between the living platypus *Ornithorhynchus anatinus*, the fossil platypus species of *Obdurodon*, and the living short-beaked echidna *Tachyglossus aculeatus*. The maximum parsimony analysis weakly supported an *Ornithorhynchus* plus *Obdurodon* clade to the exclusion of *Tachyglossus*, whereas the Bayesian analysis recovered a strongly supported *Ornithorhynchus* plus *Tachyglossus* clade to the exclusion of *Obdurodon*. The latter topology implies that tachyglossids evolved from a semi-aquatic, billed platypus-like ancestor, potentially relatively late in the Cenozoic. Further evidence in support of this hypothesis comes from molecular-based divergence dates, which estimate that *Ornithorhynchus* and tachyglossids diverged 19–48 million years ago (Meredith et al., 2011; Phillips et al., 2009), and also from estimates of myoglobin net surface charge in *T. aculeatus* which suggest an amphibious ancestry (Mirceta et al., 2013). To date, the fossil record has provided little additional data bearing on this issue because all known fossil tachyglossids are edentulous and obviously 'echidna-like'. There are no pre-Pleistocene cranial remains of tachyglossids known with the exception of *Megalibgwilia robustus* (also known as "*Zaglossus*" *robustus*; see Flannery and Groves, 1998; Griffiths et al., 1991; Musser, 2006). The single specimen of *M. robustus* is commonly presumed to be Miocene in age. However, there is significant uncertainty about this dating and a Pliocene age may be more likely (Musser, 2006). If the latter is the case, there are no pre-Pliocene tachyglossids known. The phylogenetic analyses presented here also support this hypothesis in that *Obdurodon*, *Tachyglossus* and *Ornithorhynchus* form a clade to the exclusion of *Steropodon* and *Teinolophos*, although the precise relationships within this clade differ depending on the method of analysis. No support was found for the recent hypothesis (Rowe et al., 2008) that *T. trusleri* and *S. galmani* are crown-group monotremes closer to *Ornithorhynchus* than to tachyglossids.

Acknowledgements

We thank Dr Chris Telford for assistance in providing advice about appropriate molding materials that have enabled us to produce casts of the specimen that is the focus of this research. We also thank two anonymous referees for their helpful suggestions about how to improve this contribution.

References

Archer, M., Flannery, T. F., Ritchie, A. and Molnar, R. E. 1985. First Mesozoic mammal from Australia - an Early Cretaceous monotreme. *Nature* 318 (6044): 363–366. doi:10.1038/318363a0.

Archer, M., Jenkins Jr, F. A., Hand, S. J., Murray, P. and Godthelp, H. 1992. Description of the skull and non-vestigial dentition of a Miocene platypus (*Obdurodon dicksoni* n. sp.) from Riversleigh, Australia and the problem of monotreme origins. Pp.15-27 in: Augee, M. (ed.), *Platypus and Echidnas*. Royal Zoological Society of New South Wales: Sydney.

Clemens, W. A., Wilson, G. P. and Molnar, R. E. 2003. An enigmatic (synapsid?) tooth from the Early Cretaceous of New South Wales, Australia. *Journal of Vertebrate Paleontology* 23: 232–237.

Cúneo, R., Ramezani, J., Scasso, R., Pol, D., Escapa, I., Zavattieri, A. M. and Bowring, S.A. 2013. High-precision U–Pb geochronology and a new chronostratigraphy for the Cañadón Asfalto Basin, Chubut, central Patagonia: Implications for terrestrial faunal and floral evolution in Jurassic. *Gondwana Research* 24: 1267–1275. doi:10.1016/j.gr.2013.01.010.

Flannery, T. F., Archer, M., Rich, T. H. and Jones, R. 1995. A new family of monotremes from the Cretaceous of Australia. *Nature* 377 6548: 418–420. doi:10.1038/377418a0.

Flannery, T. F. and Groves, C. P. 1998. A revision of the genus *Zaglossus* (Monotremata, Tachyglossidae), with description of new species and subspecies. Mammalia 62: 367–396. doi:10.1515/mamm.1998.62.3.367.

Flynn, J. J., Parrish, J. M., Rakotosamimanana, B., Simpson, W. F. and Wyss, A. R. 1999. A Middle Jurassic mammal from Madagascar. *Nature* 401: 57–60.

Green, H. L. H. H. 1937. The development and morphology of the teeth of *Ornithorhynchus*. *Philosophical Transactions of the Royal Society B: Biological Sciences* 228: 367–420. doi:10.1098/rstb.1937.0015.

Griffiths, M., Wells, R. T. and Barrie, D. J. 1991. Observations on the skulls of fossil and extant echidnas (Monotremata: Tachyglossidae). *Australian Mammalogy* 14: 87–101.

Kielan-Jaworowska, Z., Crompton, A. W. and Jenkins Jr, F. A. 1987. The origin of egg-laying mammals. *Nature* 326: 871–873.

Legendre, S. 1986. Analysis of mammalian communities from the Late Eocene and Oligocene of southern France. *Palaeovertebrata* 16: 191–212.

Lewis, P. 2001. A likelihood approach to estimating phylogeny from discrete morphological character data. *Systematic Biology* 50: 913–925.

Long, J. A., Archer, M., Flannery, T. F. and Hand, S. J. 2002. *Prehistoric mammals of Australia and New Guinea: one hundred million years of evolution*. University of New South Wales Press: Sydney.

Luo, Z.-X., Chen, P., Li, G. and Chen, M. 2007a. A new eutriconodont mammal and evolutionary development in early mammals. *Nature* 446: 288–293. doi:10.1038/nature05627.

Luo, Z.-X., Cifelli, R. L. and Kielan-Jaworowska, Z. 2001. Dual origin of tribosphenic mammals. *Nature* 409: 53–7. doi:10.1038/35051023.

Luo, Z.-X., Ji, Q. and Yuan, C.-X. 2007b. Convergent dental adaptations in pseudo-tribosphenic and tribosphenic mammals. *Nature* 450: 93–97. doi:10.1038/nature06221.

Luo, Z.-X., Kielan-Jaworowska, Z. and Cifelli, R. L. 2002. In quest for a phylogeny of Mesozoic mammals. *Acta Palaeontologica Polonica* 47: 1–78.

Luo, Z.-X. and Wible, J. R. 2005. A Late Jurassic digging mammal and early mammalian diversification. *Science* 308: 103–107. doi:10.1126/science.1108875

Luo, Z.-X., Yuan, C.-X., Meng, Q.-J. and Ji, Q. 2011. A Jurassic eutherian mammal and divergence of marsupials and placentals. *Nature*, 476: 442–445. doi:10.1038/nature10291

Martin, T. and Rauhut, O. W. M. 2005. Mandible and dentition of *Asfaltomylos patagonicus* (Australosphenida, Mammalia) and the evolution of tribosphenic teeth. *Journal of Vertebrate Paleontology* 25: 414–425.

Meredith, R. W., Janečka, J. E., Gatesy, J., Ryder, O. A, Fisher, C. A, Teeling, E. C., … Murphy, W. J. 2011. Impacts of the Cretaceous terrestrial revolution and KPg extinction on mammal diversification. *Science* 334: 521–524. doi:10.1126/science.1211028.

Mirceta, S., Signore, A. V, Burns, J. M., Cossins, A. R., Campbell, K. L., and Berenbrink, M. 2013. Evolution of mammalian diving capacity traced by myoglobin net surface charge. *Science* 340: 1234192. doi:10.1126/science.1234192.

Musser, A. M. 2003. Review of the monotreme fossil record and comparison of palaeontological and molecular data. *Comparative Biochemistry and Physiology Part A* 136: 927–942. doi:10.1016/S1095-6433.

Musser, A. M. 2006. Furry egg-layers: monotreme relationships and radiations. Pp. 927–942 in: Merrick, J.R., Archer, M., Hickey, G.M. and Lee, M. S. Y. (eds), *Evolution and Biogeography of Australasian Vertebrates*. Auscipub: Oatlands. 942 pp.

Pascual, R., Goin, F. J., Balarino, L. and Udrizar Sauthier, D. D. 2002. New data on the Paleocene monotreme *Monotrematum sudamericanum*, and the convergent evolution of triangulate molars. *Acta Palaeontologica Polonica* 47: 487–492.

Phillips, M. J., Bennett, T. H. and Lee, M. S. Y. 2009. Molecules, morphology, and ecology indicate a recent, amphibious ancestry for echidnas. *Proceedings of the National Academy of Sciences of the United States of America* 106: 17089–17094. doi:10.1073/pnas.0904649106.

Pian, R., Archer, M. and Hand, S. J. 2013. A new, giant platypus, *Obdurodon tharalkooschild*, sp. nov. (Monotremata, Ornithorhynchidae), from the Riversleigh World Heritage Area, Australia. *Journal of Vertebrate Paleontology* 33: 1255–1259. doi:10.1080/02724634.2013.782876.

Pridmore, P. A., Rich, T. H. Vickers-Rich, P., and Gambaryan, P. P. 2005. A tachyglossid-like humerus from the Early Cretaceous of south-eastern Australia. *Journal of Mammalian Evolution* 12: 359–378. doi:10.1007/s10914-005-6959-9.

Rauhut, O. W. M., Martin, T., Ortiz-Jaureguizar, E. and Puerta, P. 2002. A Jurassic mammal from South America. *Nature* 416: 165–168. doi:10.1038/416165a.

Rich, T. H., Flannery, T. F., Trusler, P., Kool, L., van Klaveren, N. A. and Vickers-Rich, P. 2001a. A second tribosphenic mammal from the Mesozoic of Australia. *Records of the Queen Victoria Museum* 110: 1–9.

Rich, T. H., Flannery, T. T. F., Trusler, P., Kool, L., van Klaveren, N. A. and Vickers-Rich, P. 2002. Evidence that monotremes and ausktribosphenids are not sistergroups. *Journal of Vertebrate Paleontology* 22: 466–469.

Rich, T. H., Vickers-Rich, P., Constantine, A., Flannery, T. F., Kool, L. and van Klaveren, N. 1997. A tribosphenic mammal from the Mesozoic of Australia. *Science* 278: 1438–1442. doi:10.1126/science.278.5342.1438.

Rich, T. H., Vickers-Rich, P., Constantine, A., Flannery, T. F., Kool, L. and van Klaveren, N. 1999. Early Cretaceous mammals from Flat Rocks, Victoria, Australia. *Records of the Queen Victoria Museum* 106: 1–35.

Rich, T. H., Vickers-Rich, P., Flannery, T. F., Kear, B. P., Cantrill, D. J., Komarower, P., Kool, L., Pickering, D., Trusler, P., Morton, S., van Klaveren, N. and Fitzgerald, E. M. G. 2009. An Australian multituberculate and its palaeobiogeographic implications. *Acta Palaeontologica Polonica* 54: 1–6. doi:10.4202/app.2009.0101.

Rich, T. H., Vickers-Rich, P., Trusler, P., Flannery, T. F., Cifelli, R., Constantine, A., Kool, L., van Klaveren, N. 2001b. Monotreme nature of the Australian Early Cretaceous mammal *Teinolophos*. *Acta Palaeontologica Polonica* 46: 113–118.

Ronquist, F., Teslenko, M., van der Mark, P., Ayres, D. L., Darling, A., Höhna, S., Larget, B., Lui, L., Suchard, M. A. and Huelsenbeck, J. P. 2012. MrBayes 3.2: efficient Bayesian phylogenetic inference and model choice across a large model space. *Systematic Biology* 61: 539–542. doi:10.1093/sysbio/sys029.

Rougier, G. W., Apesteguía, S. and Gaetano, L. C. 2011. Highly specialized mammalian skulls from the Late Cretaceous of South America. *Nature* 479: 98–102. doi:10.1038/nature10591.

Rougier, G. W., Martinelli, A. G., Forasiepi, A. M. and Novacek, M. J. 2007. New Jurassic mammals from Patagonia, Argentina: a reappraisal of australosphenidan morphology and interrelationships. *American Museum Novitates* 3566: 1–54. doi:10.1206/0003-0082(2007)507[1:njmfpa]2.0.co;2.

Rowe, T., Rich, T. H., Vickers-Rich, P., Springer, M. and Woodburne, M. O. 2008. The oldest platypus and its bearing on divergence timing of the platypus and echidna clades. *Proceedings of the National Academy of Sciences of the United States of America* 105: 1238–1242. doi:10.1073/pnas.0706385105.

Swofford, D. L. 2002. *PAUP*. Phylogenetic Analysis Using Parsimony (*and Other Methods)*. Sinauer Associates: Sunderland, Massachusetts.

Wiens, J. J. 2001. Character analysis in morphological phylogenetics: problems and solutions. *Systematic Biology* 50: 689–699.

Wood, C. B. and Rougier, G. W. 2005. Updating and recoding enamel microstructure in Mesozoic mammals: in search of discrete characters for phylogenetic reconstruction. *Journal of Mammalian Evolution* 12: 433–460.

Woodburne, M. 2003. Monotremes as pretribosphenic mammals. *Journal of Mammalian Evolution* 10: 195–248. doi:10.1023/B:JOMM.0000015104.29857.f0.

Woodburne, M. O., Rich, T. H. and Springer, M. S. 2003. The evolution of tribospheny and the antiquity of mammalian clades. *Molecular Phylogenetics and Evolution* 28(2): 360–385. doi:10.1016/S1055-7903(03)00113-1.

Woodburne, M. O. and Tedford, R. H. 1975. The first Tertiary monotreme from Australia. *American Museum Novitates* 2588: 1–12.

Memoirs of Museum Victoria 74: 107–116 (2016) Published 2016

ISSN 1447-2546 (Print) 1447-2554 (On-line)
http://museumvictoria.com.au/about/books-and-journals/journals/memoirs-of-museum-victoria/

Mysticetes baring their teeth: a new fossil whale, *Mammalodon hakataramea*, from the Southwest Pacific

R. Ewan Fordyce[1,2,*] (http://zoobank.org/urn:lsid:zoobank.org:author:311048BF-4642-412E-B5DA-E01B8C03B802) and Felix G. Marx[1,3] (http://zoobank.org/urn:lsid:zoobank.org:author:1791C478-33A7-4C75-8104-4C98C7B22125)

[1] Department of Geology, University of Otago, PO Box 56, Dunedin 9054, New Zealand (ewan.fordyce@otago.ac.nz)
[2] Departments of Vertebrate Zoology and Paleobiology, National Museum of Natural History, Smithsonian Institution, Washington DC 20560, USA
[3] Department of Geology and Palaeontology, National Museum of Nature and Science, Tsukuba, Japan (felix.marx@otago.ac.nz)
* To whom correspondence should be addressed. E-mail: ewan.fordyce@otago.ac.nz

http://zoobank.org/urn:lsid:zoobank.org:pub:7A2CAF55-70DC-4561-AA3D-86FA72C721E6

Abstract

Fordyce, R.E. and Marx, F.G. 2016. Mysticetes baring their teeth: a new fossil whale, *Mammalodon hakataramea*, from the Southwest Pacific. *Memoirs of Museum Victoria* 74: 107–116.

A small, toothed fossil cetacean from Hakataramea Valley (South Canterbury, New Zealand) represents a new Late Oligocene species, *Mammalodon hakataramea*. The new material is from the Kokoamu Greensand (Duntroonian Stage, about 27 Ma, early to middle Chattian) of the Canterbury Basin, and thus about 2 Ma older than the only other species included in this genus, *Mammalodon colliveri* (Late Oligocene, Victoria, Australia). The anterior pedicle of the tympanic bulla is not fused to the periotic and resembles that of Delphinidae in basic structure. The teeth show extreme attritional and/or abrasive wear, which has obliterated the crowns. Like *Mammalodon colliveri*, *M. hakataramea* was probably raptorial or a benthic suction feeder.

Keywords

systematics, evolution, stratigraphy, anatomy, New Zealand, *Osedax*.

Introduction

New Zealand is a notable source of fossil cetaceans (whales, dolphins) in the Southwest Pacific, with specimens ranging in age from late Middle Eocene to Pleistocene. Rocks of the southern Canterbury Basin (Field et al., 1989), in particular, have produced rare Eocene and more common Late Oligocene to earliest Miocene cetaceans. These mid-Cenozoic fossils include representatives of the archaeocete family Basilosauridae, putative stem neocetes (Kekenodontidae) and diverse odontocetes, such as kentriodontids and other putative delphinoids, waipatiids (e.g. *Otekaikea* Tanaka and Fordyce, 2014, 2015), squalodontids and *Squalodelphis*-like taxa. Mysticetes are represented by a diverse assemblage comprising Eomysticetidae (e.g. *Tohoraata* Boessenecker and Fordyce, 2014a), basal Balaenopteroidea, and enigmatica (e.g. *Horopeta* Tsai and Fordyce, 2015). The key cetacean-bearing units – the Kokoamu Greensand (see below) and the Otekaike Limestone – and the localities in and around the Waitaki Valley that expose them were reviewed in the aforementioned articles.

Here, we name and describe a new species of the toothed mysticete *Mammalodon*, based on specimen OU 22026 from the southern Canterbury Basin. The fossil is distinct from the hitherto monotypic *Mammalodon colliveri* (Late Oligocene, ~23.9-25.7 Ma) of Victoria, Australia (Fitzgerald, 2010), and is probably close to 27 Ma. Of note, the fossil includes a tympanic bulla with a well-preserved anterior pedicle, otherwise poorly described for archaeocetes and archaic Neoceti.

Specimen OU 22026 was listed by Fordyce (1991: 1312) as *Mammalodon* sp. and was later mentioned, but not named, in an abstract (Fordyce and Marx, 2011). Recently, we included OU 22026 in a total-evidence phylogenetic analysis of extant and fossil Mysticeti (Marx and Fordyce 2015: fig. 2; see fig. 4 here), which identified it as sister to *Mammalodon colliveri*, with *Janjucetus hunderi* immediately adjacent (basal). Together, these three species form an expanded Mammalodontidae, which in turn are closely related to a diverse range of aetiocetids described only from the North Pacific. OU 22026 was also sampled for isotopes by Clementz et al. (2014), who reported $\delta^{13}C$ and $\delta^{18}O$ values for structural bone carbonate from the bulla that are inconsistent with (filter-)feeding low in the food chain.

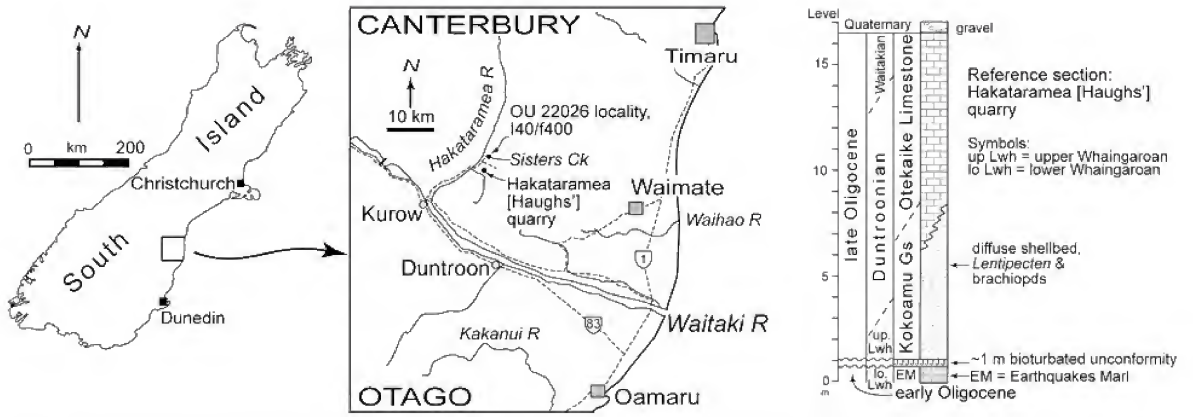

Fig. 1, Locality map and stratigraphy of the Sisters Creek-Homestead Creek area of Hakataramea Valley. The stratigraphic column, right, is modified from that of Tsai and Fordyce (2015) for "Haughs' Quarry", which provides the nearest detailed column to Sisters Creek. *Mammalodon hakataramea* came from about the horizon identified as the diffuse shellbed with *Lentipecten hochstetteri* and brachiopods.

Definitions and terminology

Anatomical terminology follows Mead and Fordyce (2009), unless indicated.

Methods

All elements were uncovered by hand scraping from soft matrix. The bulla was recovered fractured but still naturally associated; it was cleaned and consolidated with cyanoacrylate region by region. For photography, the bulla, teeth and skull roof of *M. hakataramea* and the bulla of *Mammalodon colliveri* were coated with sublimed ammonium chloride. Images of the bulla of *M. hakataramea* are composites, stacked (using Adobe Photoshop) from multiple shots at varying foci. Photography used a Nikon 105 mm micro lens with a D700 or D800 (*M. hakataramea*) or D70 (*M. colliveri*) camera body.

Institutional abbreviations

NMV P, Museum Victoria Palaeontology Collection, Melbourne, Australia. OU, fossil collection in Geology Museum, University of Otago, Dunedin, New Zealand.

Systematic Palaeontology

Cetacea Brisson, 1762

Neoceti Fordyce and Muizon, 2001

Mysticeti Gray, 1864

Mammalodontidae Mitchell, 1989

Mammalodon Pritchard, 1939

Emended diagnosis of Mammalodon. Small-sized mysticetes differing from chaeomysticetes in having teeth. Differ from all toothed mysticetes except *Janjucetus* in having a foreshortened, dorsoventrally tall rostrum, a linguiform anterior border of the supraorbital process, a triangular wedge of the frontal separating the ascending process of maxilla from the posterolateral margin of the nasal, a roughly horizontal dorsal profile of the braincase (relative to the lateral edge of the rostrum) and posteriorly reclined mandibular cheek teeth; further differ from all other toothed mysticetes except *Janjucetus* and *Chonecetus* in having a distinctly V-shaped fronto-parietal suture in dorsal view; from *Llanocetus* and two previously coded, undescribed archaic mysticetes (ChM PV4745; OU GS10897) in having both relatively and absolutely smaller posterior cheek teeth with proximally fused roots, and an inner posterior prominence of the tympanic bulla that is subequal to the outer prominence in posterior view; from all aetiocetids in having a more elongate intertemporal region and an anteroposteriorly broader coronoid process of the mandible; from *Aetiocetus* and *Fucaia* in lacking a medially expanded lacrimal and a dorsoventrally constricted mandible, and in having more robust cheek teeth with distally separate roots; from *Chonecetus* in having a broader, less anteriorly-thrust supraoccipital bearing a well-developed external occipital crest, and in lacking a parasagittal cleft on the dorsal surface of the parietal; from *Aetiocetus* in having a clearly heterodont dentition and closely-spaced posterior cheek teeth with well-developed enamel ridges on both the labial and lingual sides of the crown; from *Morawanocetus* in having a much more robust postorbital process of the frontal; from *Ashorocetus* in having a less steeply inclined supraoccipital shield and a somewhat more anteromedially oriented basioccipital crest; and from the enigmatic *Willungacetus* in having a clearly marked orbitotemporal crest extending posteriorly on to the intertemporal constriction and a rounded (rather than triangular), less anteriorly-thrust supraoccipital bearing a well-developed external occipital crest. Finally, *Mammalodon* differs from the only other described mammalodontid, *Janjucetus*, in having a rostrum with a bluntly rounded apex and a gently convex lateral profile in dorsal view,

coalesced alveoli for the upper incisors, a gracile, foreshortened and dorsoventrally flattened premaxilla, an anteriorly expanded nasal, a transversely narrow, linguiform ascending process of the maxilla extending posteriorly as far as the nasal, a more anteriorly directed orbit, a more laterally oriented postorbital process, a transversely convex dorsal profile of the parietals with no salient sagittal crest, a more laterally oriented nuchal crest, a broadly rounded apex of the supraoccipital shield in dorsal view, an anterior portion of the tympanic bulla that is squared (rather than obliquely truncated) in ventral view, an inner posterior prominence of the tympanic bulla that is subequal to the outer prominence in posterior view, a straight and comparatively gracile mandible bearing large mental foramina, and three upper and four lower molars, all of which (at least in adult specimens) are affected by heavy occlusal wear.

Remarks. Comparisons of *Mammalodon* with *Ashorocetus eguchii*, *Willungacetus aldingensis* and *Chonecetus sookensis* are currently hampered by the poor state of preservation of the available material; none of the latter, for example, includes the tympanic bulla or teeth. *Ashorocetus* is currently known only from the posterior portion of a braincase preserving little surface detail (Barnes et al. 1995). *Willungacetus* and *Chonecetus sookensis* are based on somewhat more complete, but still highly fragmentary crania having lost their rostra, most or all of the ear bones and much of the (basicranial) surface detail (Pledge, 2005; Russell, 1968). Until the discovery of better material, the comparisons made here are necessarily provisional. The use of occlusal wear as a potential diagnostic character may be queried, as this feature may primarily correlate with age or the foraging environment. Nevertheless, the extreme wear present in the two species of *Mammalodon* is unusual amongst fossil cetaceans as a whole, and highly so in the context of toothed mysticetes in particular. If tooth wear in *Mammalodon* is primarily linked to the manner of occlusion and/or food preferences, it may record a valid character that can be used for diagnostic and cladistic purposes. Without evidence to the contrary, we therefore retain it here as part of the diagnosis.

Mammalodon hakataramea Fordyce and Marx sp. nov.

Zoobank LSID. http://zoobank.org/urn:lsid:zoobank.org:act:6D960230-3799-4597-BAAD-2537772B99A6

Figs. 2, 3

Holotype. OU 22026 – dorsal part of braincase, comprising much of the supraoccipital and parts of the parietals and squamosals, preserved with the original dorsal surface down, and the bioeroded ventral surface upwards; left tympanic bulla lacking the posterior process; five teeth with little or no remnants of the crown. All elements were closely associated, with no other fossil cetacean remains nearby.

Type locality. Open flat bed of Sisters Creek, 70-80 m downstream from a prominent limestone bank directly north of Riverside farmhouse, McHenrys Road, Hakataramea Valley, South Canterbury (Fig. 1). Field number REF 13-10-87-2. Grid reference: latitude 44 deg 38 min 30.5 sec, longitude 170 deg 38 min 45.0 sec, or NZMS260 map I40: 232 158. The Geoscience Society of New Zealand fossil record number is I40/f400. The locality is 2 km NNW of the informally-named "Haughs' Quarry," as shown by Tanaka and Fordyce (2015).

Horizon and age. OU 22026 is from a massive, bioturbated, calcareous section of the Kokoamu Greensand, where it was associated with sparse macrofossils including scattered pectinids (*Lentipecten hochstetteri*) and terebratulid brachiopods. *Lentipecten hochstetteri* and the benthic foraminiferan *Notorotalia spinosa* indicate the Duntroonian Stage. Judging from a comparable section in the Greensand at Haughs' Quarry, about 2 km to the SSE (fig. 1, right; also, see Tsai and Fordyce, 2015), the diffuse shellbed of pectinids and brachiopods is low in the Duntroonian, probably near the base. The Duntroonian is dated as 25.2–27.3 Ma (Raine et al. 2015) and OU 22026 is presumed close to 27 Ma, or early Chattian (Vandenberghe et al., 2012).

Diagnosis. Differs from *M. colliveri* in having smaller teeth, an anteroposteriorly longer supraoccipital and a parabolic nuchal crest that lacks an abrupt anterolateral curve in dorsal view, as well as in having a tympanic bulla with a more distinct interprominential notch, a straight medial margin, an anterolaterally more inflated outer lip, and a deeper involucrum bearing less developed oblique sulci (without adjacent nodules).

Etymology. Hakataramea, a Maori name for the valley where the holotype was collected. Haka, a dance; taramea, a sharp-spined herb, "spear-grass" (Apiaceae: *Aciphylla squarrosa*), with sweet-smelling gum from the flower stalks. The name may commemorate a specific incident (Reed and Dowling, 2010).

Description

Ontogenetic stage. The specimen is probably a mature adult because of the extreme wear that has mostly obliterated the tooth crowns (fig. 1A–E). The parieto-occipital suture is open along parts of the nuchal crest, but this condition is also seen in adult modern baleen whales (e.g. *Balaenoptera acutorostrata*, Miller, 1924: plate 4; *Balaenoptera borealis*, Andrews, 1916: plate 41; *Megaptera novaeangliae*, True 1904: plates 29, 32).

Skull roof. The dorsal roof of the skull (fig. 2 F, G; table 1) is represented by the ventrally eroded, thin parietals, the supraoccipital and, at the posterolateral margins, probably the dorsalmost portions of both squamosals. There is no distinct

Table 1. Measurements of the skull roof of OU 22026, +/- 0.5 mm.

Skull roof, anteriormost parietal to posteriormost supraoccipital, midline	+134.5
Length of parietals on vertex	+45.0
Length of supraoccipital, midline	+94.0
Width, outer margins of nuchal crest, posteriormost preserved points (= posterolateral extremities of skull roof)	+154.5

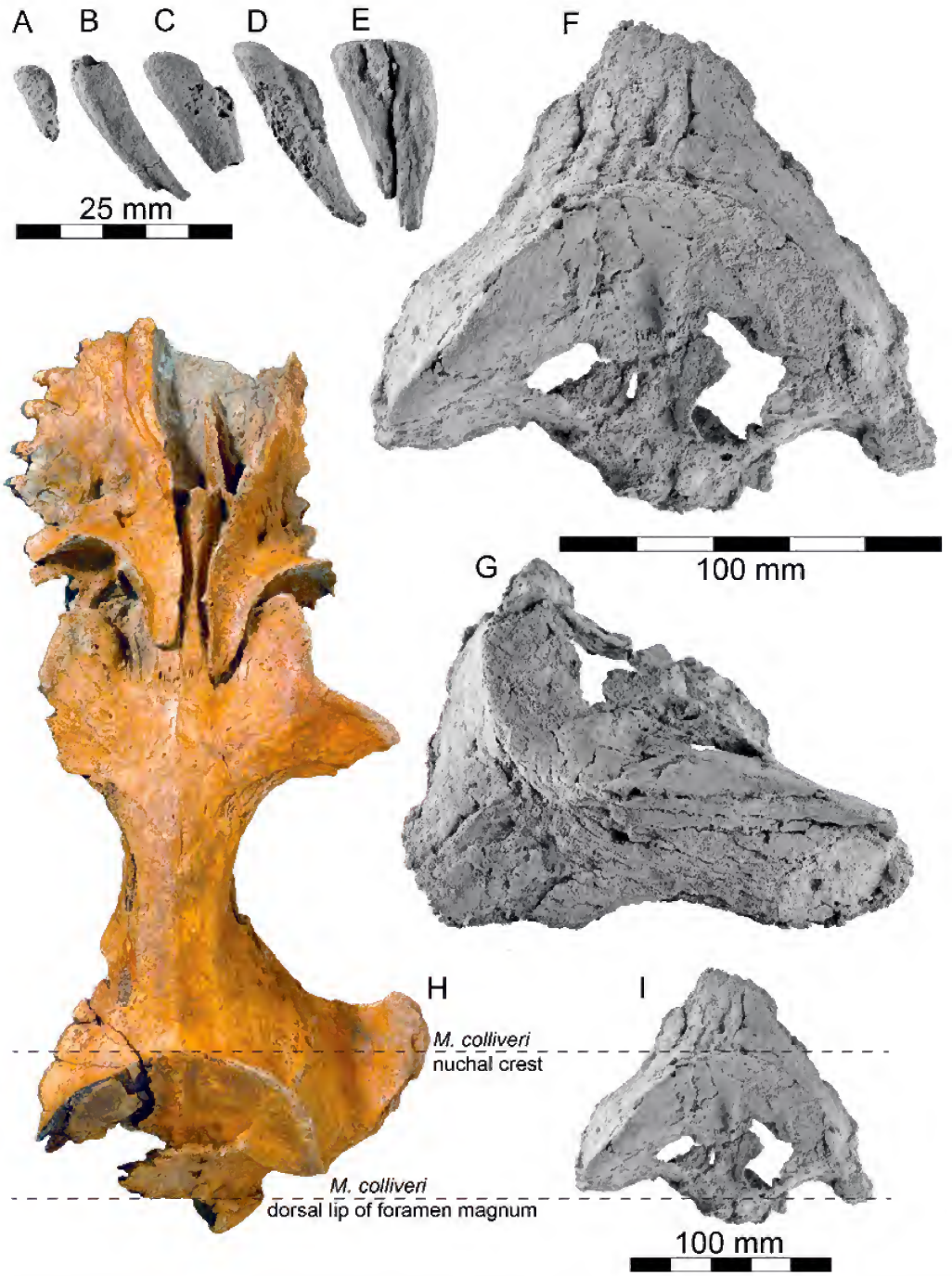

Fig. 2. A-G, I, holotype of *Mammalodon hakataramea*, OU 22026; all material coated with sublimed ammonium chloride and lit from upper left. A-E, individual isolated teeth in labial or lingual view. F, G, I, holotype skull roof of *Mammalodon hakataramea*. F, I, dorsal view, anterior towards the top; G, oblique dorsolateral view from the left, anterior towards the lower left. H, holotype skull of *Mammalodon colliveri* Pritchard, NMV P199986, dorsal view, not coated with sublimed ammonium chloride. H and I are shown at the same scale to compare the differences in size and profile between the two *Mammalodon* species. The two dashed lines show the position of the apex of the nuchal crest and the dorsal lip of the foramen magnum in *M. colliveri*; *M. hakataramea* is aligned with the upper line.

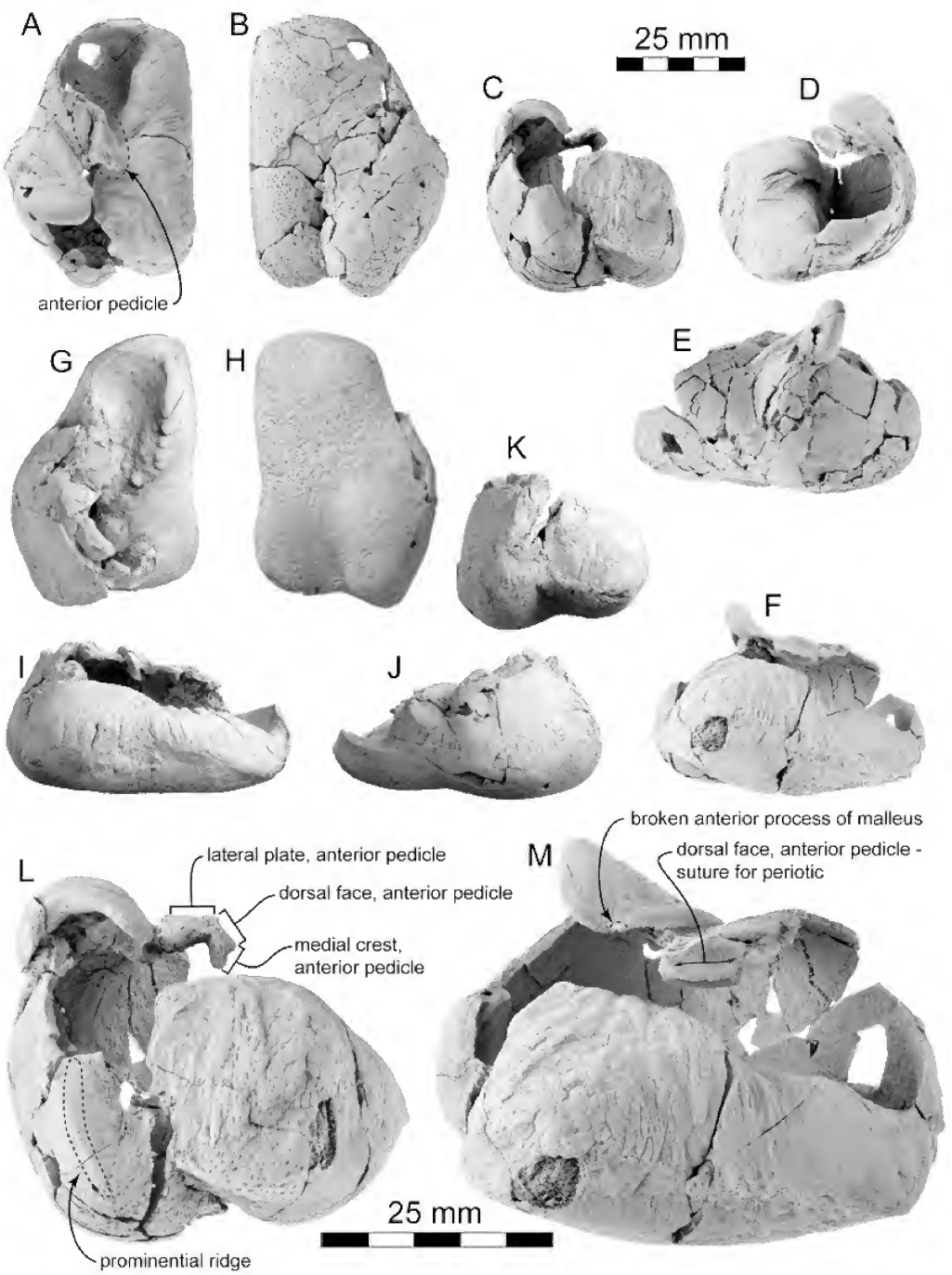

Fig. 3. A-F, L, M, holotype left tympanic bulla of *Mammalodon hakataramea*, OU 22026; all views show the bulla coated with sublimed ammonium chloride and lit from upper left. A, dorsal. B, ventral. C, posterior. D, anterior. E, lateral. F, medial. G-K, holotype right tympanic bulla of *Mammalodon colliveri* Pritchard, NMV P199986, with views mirrored for ease of comparison with *M. hakataramea*; bulla is coated with sublimed ammonium chloride and mirrored views show lighting from upper right. G, dorsal. H, ventral. I, medial. J, lateral. K, posterior. L, M, enlarged views of left tympanic bulla of *Mammalodon hakataramea* to show anterior pedicle. L, slightly dorsomedial posterior view. M, slightly posterior dorsomedial view.

interparietal. The dorsal periosteal surfaces are damaged by patchy bioerosion, which in two places has also led to the perforation of the supraoccipital. Enough remains to see that the supraoccipital is longer, from its apex to the margin of foramen magnum, than in *M. colliveri* (fig. 2H, I). The gently concave supraoccipital is raised little (~ 3 mm) above the parietals, and forms a thin-edged nuchal crest with a parabolic profile and a smoothly rounded apex in dorsal view (fig. 2F, G). By contrast, the crest in *M. colliveri* is more robust, with abruptly curved anterolateral corners that markedly overhang the parietals (fig. 2H). A lateral or oblique view (fig. 2G) shows the nuchal crest gently convex anteriorly but markedly steepening posteriorly, as if descending toward the posterior margin of the temporal fossa. Anteriorly, the supraoccipital has a small, flattened dorsal apex, passing backwards into a short but well-developed external occipital crest. Posteriorly, the supraoccipital is raised and thickened in the midline, with the adjacent surfaces steepening bilaterally; in *M. colliveri*, such features are developed near the foramen magnum.

What remains of the parietals suggests that the fused bones form a wide and smoothly rounded intertemporal region without any salient sagittal or parasagittal crests, contrasting with the narrower, dorsally tabular, condition in *M. colliveri*. Irregular parasagittal grooves could result from bioerosion, but are more likely to be sulci associated with parietal foramina. Poorly-preserved irregularities in the bone surface posteriorly (fig. 2G) may represent the parieto-squamosal sutures.

Tympanic bulla (fig. 3A–F, L–M; table 2). The left bulla is slightly crushed, with the outer lip a little compressed ventrally. The anterior pedicle has been distorted post-mortem and rotated ventromedially, so that the suture for the anterior bullar facet of the periotic is steeply dipping, rather than sub-horizontal. The posterior process, conical process and the anterolateral crest of the outer lip are lost.

In dorsal view (fig. 3A), the bulla has a straight medial profile, a bluntly rounded, slightly squared apex and an inflated outer lip, with the bone attaining its greatest width at the level of the sigmoid process. The two posterior prominences or lobes are separated by the conspicuous, near-perpendicular interprominential notch (fig. 3A, B). In dorsal or ventral view, the outer prominence is sharp, passing dorsally into a marked prominential ridge (*sensu* Tsai and Fordyce, 2015). The inner prominence is more smoothly rounded and does not extend as far posteriorly, which may indicate an anteromedial *in situ* orientation of the long axis of the bulla as seen, for example, in *Janjucetus hunderi*. In posterior view (fig. 3C, L) a strong, slightly oblique ridge crosses the inner prominence to reach the interprominential notch; there is no ridge on the outer prominence. Ventrally (fig. 3B), the interprominential notch passes into a median furrow 22–23 mm long, about half the length of the bulla.

Table 2. Measurements of left bulla of OU 22026, +/- 0.5 mm

Length, apex adjacent to Eustachian outlet to apex of outer posterior prominence	56.5
Length, parallel with medial face	55.5
Width, maximum, immediately below sigmoid cleft	38.0
Depth of involucrum, maximum, at anterior margin of broken base of inner posterior pedicle	25.5
Depth, tip of sigmoid process to ventral surface with bulla sitting in stable position	38.0
Length, apex adjacent to Eustachian outlet to apex of sigmoid process	38.5

The Eustachian outlet forms a shallow, anteromedially oriented notch (fig. 3A, M). The adjacent portion of the involucrum is obliquely flat medially and excavated laterally. Posteriorly, the involucrum rises and widens via an abrupt, obliquely oriented step at mid-length. Oblique striae that cross the involucrum are finer than in *M. colliveri* (fig. 3F) and not separated by tubercles laterally. The otherwise smooth dorsal surface anteriorly on the involucrum was probably covered by a lobe of the peribullary sinus; this smooth bone extends posteriorly 20+ mm, at least to the oblique "step" in the dorsal profile, and possibly to the level of the prominent sub-vertical postmortem crack (fig. 3M). Further posteriorly, the elevated involucral surface is considerably rougher, suggesting that the peribullary sinus may not have extended over the involucrum here. In medial view, the involucrum has a horizontal zone of irregular fine creases, probably marking tendinous connections to the basioccipital crest (fig. 3F, M). A large irregular depression on the posteriormost portion of the involucrum (fig. 3M) is probably a collapsed cluster of galleries formed by the osteophagous siboglinid worm *Osedax* (see Boessenecker and Fordyce, 2014b for similar occurrences in other New Zealand Oligocene Cetacea). In posterior view, the involucrum is more prolonged in a dorsolateral-ventromedial plane than the sub-cylindrical involucrum of *M. colliveri* (compare figs. 3C, D and 3K). An oblique (slightly lateral) dorsal view, not figured here, shows a slight concavity in the medial profile of the involucrum – much less than in *M. colliveri*, in which this concavity is pronounced.

The outer lip preserves a sharp crest at the Eustachian outlet and becomes anterolaterally inflated as it passes back towards the anterior pedicle. The anterolateral corner of the tympanic bulla formed by this inflated portion is more rounded than in *M. colliveri* (compare fig. 3B, H). The crest of the outer lip is broken to reveal the tympanic cavity in dorsal view. The floor of the latter is smooth and has a marked transverse saddle about level with the anterior pedicle, behind which the tympanic cavity deepens markedly, and narrows. The cavity both undercuts the involucrum and, at its posterior limit, rises dorsally to excavate it below the inner posterior pedicle.

The anterior pedicle has a narrow, anteroposteriorly long junction with the outer lip (fig. 3A, M). The junction is cracked, and it is uncertain if a groove for the chorda tympani nerve was present. In dorsal or dorsomedial view (fig. 3A, M), the anterior pedicle has three elongate faces roughly perpendicular to each other. The original structure and orientations are interpreted thus: a lateral plate that descends to the outer lip; an elongate sub-oval dorsal face with a shallow grooved suture for the periotic; and a descending medial crest, with a groove that presumably contributes to the origin of the tensor tympani

muscle (following Tsai and Fordyce 2015). A posterior view (fig. 3L) shows the silhouetted cross section of the pedicle, with the three surfaces bounding an elongate V- to U-shaped ventral groove. On the dorsal face, the suture for the anterior bullar facet of the periotic is a long, shallow groove (fig. 3L, M); accordingly, the fovea epitubaria was probably shallow and flat, rather than saddle-shaped. The dorsal face of the pedicle does not show any clear region of fusion with the anterior margin of the mallear fossa, although the lateral edge of the posterior apex has lost a sub-mm area of surface bone which might indicate fusion.

Adjacent to the anterior pedicle, the outer lip bears a shallow vertical groove, but no obvious lateral furrow (fig. 3E). The mallear ridge is prominent, oriented obliquely and most raised at its mid-length. Posteriorly, at the inner margin of the sigmoid process, the ridge passes into a tiny projection representing the broken anterior process of the malleus (fig. 3M). In anterior or posterior view (fig. 3D, L), the dorsal profile of the sigmoid process has three indistinctly separate faces: a medial one, probably marking the proximity of the malleus; a dorsal one, possibly apposing the sigmoid fossa of the squamosal; and a lateral one. The enrolled posterior lip of the sigmoid process overhangs a sigmoidal cavity (*sensu* Tsai and Fordyce, 2015) delimited by a low oblique ridge presumably for the tympanic sulcus (fig. 3L). In lateral view (fig. 3E), the sigmoid process is bounded ventrally by a damaged, anteroventrally oblique sigmoid cleft. The conical process is lost. A strong prominential ridge (*sensu* Tsai and Fordyce, 2015) lateral to the elliptical foramen is matched by a thickened ridge within the tympanic cavity. Judging from well-preserved thin flanges, the elliptical foramen was patent as a narrow opening about 5 mm deep.

Teeth (fig. 2A–E; table 3). Five teeth are represented by roots, with one tooth (fig. 2B) retaining a tiny possible dentine remnant of the crown. The other four teeth are worn, exposing sections through the infilled pulp cavity. The worn, sub-ovate surfaces curve down both labiolingually and mesiodistally. Wear exposes lines of arrested growth (growth-layer groups, as commonly used for Cetacea), marked by alternating lighter and darker coloured bands in the outer biomineral, which is presumed to be cementum. Occlusal surfaces were examined under high magnification, but no wear patterns (grooves, striations) were apparent. Tooth A of Figure 2 is laterally compressed and conical. Tooth B is conical, with a double distal tip, perhaps representing two fused roots. Tooth C is laterally compressed. Tooth D is grooved on the labial and lingual faces, perhaps representing two fused roots. Tooth E has two closely approximated large roots that taper and converge distally, with a small third root between the two larger adjacent to the occlusal surface. Tooth E is the only one that can reasonably be identified to position, as a posterior premolar or molar.

Discussion

Mammalodon hakataramea is one of relatively few toothed mysticetes to be formally described, and only the third member of the highly unusual and seemingly rather localised mammalodontids (fig. 4). Bianucci et al. (2011), however, mentioned a potential record of this family from the Mediterranean. *Mammalodon hakataramea* is also the first new species of archaic toothed mysticete from the New Zealand region to be formally named as such. Other New Zealand Oligocene Cetacea likely also represent archaic Mysticeti, but have either been misidentified or remain undescribed. One example of such material is "*Squalodon*" *serratus* Davis, 1888, an isolated cheek tooth that may have belonged to an aetiocetid (Fordyce, 2008). Another is an Early Oligocene specimen described by Keyes (1973) as a "proto-squalodont", but identified as a basal mysticete by Marx and Fordyce (2015) based on as-yet undescribed portions of the skull (OU GS10897). Nevertheless, toothed mysticetes from New Zealand are rare, and only a handful of potential candidates have been recovered during Fordyce's field programme of 30 years.

The holotype of *Mammalodon hakataramea* shows two features that are noteworthy in terms of structure and/or function. First, the anterior pedicle of the bulla reveals details rarely preserved in basal mysticetes: the long, thin lateral plate merging with the outer lip, the dorsal face with the suture for the anterior bullar facet of the periotic and the medial crest, all of which bound a ventral groove. These structures are readily homologised with the anterior pedicle, or accessory ossicle, in extant Delphinidae, e.g. *Tursiops truncatus* and *Globicephala melas*. In the delphinids, the lateral plate descends to the groove for the chorda tympani. The dorsal face (with a faintly grooved suture for the periotic) is short and arched anteroposteriorly to match the saddle-shaped fovea epitubaria. The medial plate is inflated and nodular (thus partly closing the ventral groove), and contributes to the origin for the tensor tympani (see Mead and Fordyce, 2009: fig. 25W). A ventrally-grooved anterior pedicle and unfused bulla/periotic contact also occur in at least one kekenodontid and one eomysticetid at OU, albeit in pedicles broken from the bulla. In the putative gulp-feeding Late Oligocene mysticetes *Mauicetus parki* and *Horopeta umarere* (both Chaeomysticeti), the dorsal face of the anterior pedicle is partly fused posteriorly to the periotic. In addition, the medial ridge is not developed in these taxa, but extends dorsally up the medial face of the periotic. Accordingly, there is no ventral groove.

Table 3. Measurements of teeth of OU 22026, +/- 0.5 mm

Tooth of Fig. 2A, maximum length of root	9.5
Tooth of Fig. 2A, maximum diameter	4.0
Tooth of Fig. 2B, maximum length of root	21.0
Tooth of Fig. 2B, maximum diameter	5.5
Tooth of Fig. 2C, maximum length of root	16.5
Tooth of Fig. 2C, maximum diameter	7.0
Tooth of Fig. 2D, maximum length of root	26.0
Tooth of Fig. 2D, maximum diameter	7.0
Tooth of Fig. 2E, maximum length of root	23.5
Tooth of Fig. 2E, maximum diameter, mesiodistal	11.0

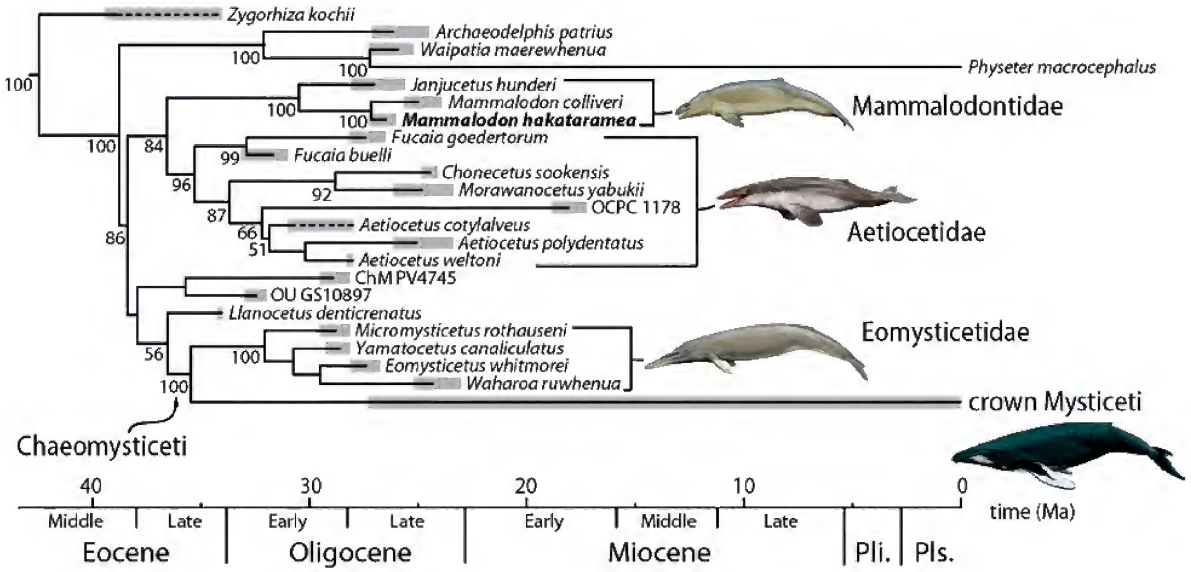

Fig. 4. Relevant detail of phylogeny from Marx and Fordyce (2015: Fig. 2), showing relationships of *Mammalodon hakataramea* and other Mysticeti basal to the crown group. Pli., Pliocene; Pls., Pleistocene.

Secondly, the worn occlusal surfaces of the teeth curve down on to the mesiodistal and labiolingual faces of the roots. The similar shape and surface detail amongst the teeth suggest that the wear is not post-mortem bioerosion, but was likely caused by abrasion. Phylogenetic bracketing (fig. 4) implies that *M. hakataramea* actually had functional tooth crowns on robust teeth in a short rostrum, like its sister taxon *M. colliveri*. The rounded worn surfaces in *M. hakataramea* contrast with the more clearly planar wear characterising the cheek tooth crowns in the holotype of *M. colliveri* (see Fitzgerald, 2010). Nevertheless, planar attrition cannot be ruled out as a factor earlier in the ontogeny of OU 22026, and it is possible that the rounded wear surfaces reflect old age. Extensive attritional wear might have removed much of the tooth crown, as in *M. colliveri*, until proper occlusion, and thus further attrition, became impossible. Abrasive wear, conversely, could have continued through on-going contact of the teeth with food or ingested sediment.

That OU 22026 survived despite having lost functional tooth crowns argues against tooth-assisted filter feeding, as was also argued by Fitzgerald (2010). This conclusion is consistent with the isotopic values reported by Clementz et al. (2014), which indicate that *M. hakataramea* fed higher in the food chain than typical filter feeding mysticetes. We agree with Fitzgerald (2010) that the extensive wear in *Mammalodon* is more easily reconciled with suction feeding than with raptorial feeding, which depends on functional teeth for grasping and/or processing large prey; nevertheless, facultative durophagy or raptorial sarcophagy cannot be ruled out.

Cetacean ecology during the Oligocene was rather different from today. Modern seas are dominated by one clade of mysticetes – the gulp-feeding rorquals (Balaenopteridae) – and two clades of echolocating odontocetes: the deep-diving, suction-feeding beaked whales (Ziphiidae) and the ecologically rather plastic dolphins (Delphinidae). Like the modern species, some of New Zealand's Late Oligocene baleen whales (e.g. *Mauicetus parki, Horopeta umarere*), probably filter-fed by skimming or gulping. The long- and narrow-jawed eomysticetids, with no modern equivalents, could have been skimmers or suction feeders, but probably not gulp feeders. The small-toothed mysticetes from the wider Australasian region were rather disparate, and probably included both raptorial and (benthic) suction feeders, such as *Mammalodon colliveri*. Given their overall similarity and shared extreme tooth wear, *M. colliveri* and *M. hakataramea* were perhaps suction feeders. Late Oligocene odontocetes were all echolocators, with assemblages dominated by platanistoid dolphins in contrast to the dominant delphinids of modern seas. These platanistoids included both clearly heterodont taxa, such as shark-toothed dolphins with a robust dentition suitable for crushing food, and near-homodont forms that – like modern dolphins – probably swallowed with minimal processing. Remarkably, kekenodontid archaeocetes coexisted, until about 26 Ma, with cetaceans of "modern" feeding habit, presumably snap-feeding raptorially and without the benefit of echolocation.

Acknowledgements

This work has its origins in a chance meeting between Thomas H. Rich and R. Ewan Fordyce in 1974, in the office of GA Tunnicliffe at Canterbury Museum. Fordyce was then a

student, considering New Zealand-based postgraduate studies in some mix of zoology and geology; Rich was assessing the potential to find fossil terrestrial mammals in New Zealand. Unsurprisingly, Rich raised the topic of vertebrate palaeontology and, further, he persisted by letter to encourage Fordyce. In turn, Fordyce started doctoral studies on New Zealand fossil Cetacea, and ultimately took a job at University of Otago where he developed a vertebrate palaeontology research programme, leading to finds such as that reported here. Thank you, Tom Rich. We also thank the following for their help in this project: Michael Brosnan, landowner, for allowing excavation; the McKenzie family for field accommodation; Andrew Grebneff and Craig Jones for field work; Andrew Grebneff for preparing the specimen; O.P. Singleton and Neil Archbold for access to *Mammalodon colliveri*; Erich Fitzgerald for discussions on *Mammalodon*. We thank the reviewers, Travis Park and Erich Fitzgerald, for their constructive critiques. Research was supported by a University of Otago PhD scholarship and a Japan Society for the Promotion of Science postdoctoral scholarship to FG Marx, by National Geographic Society field grants 3542-87 and 3657-87 to RE Fordyce, and by a Monash University Postdoctoral Fellowship which supported Fordyce's early study on *Mammalodon colliveri*.

References

Andrews, R. C. 1916. Monographs of the Pacific Cetacea. II. The sei whale (*Balaenoptera borealis* Lesson). 1. History, habits, external anatomy, osteology, and relationship. Memoirs of the American Museum of Natural History 1:289–388.

Barnes, L. G., Kimura, M., Furusawa, H. and Sawamura, H. 1995. Classification and distribution of Oligocene Aetiocetidae (Mammalia; Cetacea; Mysticeti) from western North America and Japan. Island Arc 3:392-431.

Bianucci, G., M. Gatt, R., Catanzariti, S., Sorbi, C. G., Bonavia, R., Curmi, and A. Varola. 2011. Systematics, biostratigraphy and evolutionary pattern of the Oligo-Miocene marine mammals from the Maltese Islands. Geobios 44: 549-585.

Boessenecker, R. W., and Fordyce, R. E., 2014a. A new eomysticetid (Mammalia: Cetacea) from the Late Oligocene of New Zealand and a reevaluation of *'Mauicetus' waitakiensis*. Papers in Palaeontology doi: 10.1002/spp2.1005: 1-34.

Boessenecker, R. W. and Fordyce, R. E. 2014b. Trace fossil evidence of predation upon bone-eating worms on a baleen whale skeleton from the Oligocene of New Zealand. Lethaia DOI:10.1111/let.12108.

Brisson, M. J. 1762. Regnum animale in classes IX distributum sive synopsis methodica. Editio altero auctior; Theodorum Haak, Leiden, Netherlands.

Clementz, M. T., Fordyce, R. E., Peek, S. L. and Fox, D. L. 2014. Ancient marine isoscapes and isotopic evidence of bulk-feeding by Oligocene cetaceans. Palaeogeography, Palaeoclimatology, Palaeoecology 400:28-40.

Davis, J. W. 1888. On fossil fish remains from the Tertiary and Cretaceo-Tertiary formations of New Zealand. Transactions of the Royal Dublin Society, series 2 4:1-56.

Field, B. D., Browne, G.H. and Davy, B. W. 1989. Cretaceous and Cenozoic sedimentary basins and geological evolution of the Canterbury Region, South Island, New Zealand. New Zealand Geological Survey basin studies 2:1-94.

Fitzgerald, E. M. G. 2010. The morphology and systematics of *Mammalodon colliveri* (Cetacea: Mysticeti), a toothed mysticete from the Oligocene of Australia. Zoological Journal of the Linnean Society 158:367-476.

Fordyce, R. E. 1991. A new look at the fossil vertebrate record of New Zealand; pp. 1191-1316 in P. V. Rich, J. M. Monaghan, R. F. Baird, and T. H. Rich (eds), Vertebrate palaeontology of Australasia. Pioneer Design Studio and Monash University, Melbourne.

Fordyce, R. E. 2008. Fossil mammals; pp. 415-428 in Winterbourn, M. J., Knox, G. A., Burrows, C. J. and Marsden, I. (eds), Natural history of Canterbury. University of Canterbury Press, Christchurch.

Fordyce, R. E., and Marx, F.G. 2011. Toothed mysticetes and ecological structuring of Oligocene whales and dolphins from New Zealand. Geological Survey of Western Australia, Record 2011/9:33.

Fordyce, R. E., and Muizon, C. de. 2001. Evolutionary history of whales: a review; pp. 169-234 in Mazin, J.-M. and Buffrenil, V. de (eds), Secondary adaptation of tetrapods to life in water. Proceedings of the international meeting, Poitiers, 1996. Verlag Dr Friedriech Pfeil, München.

Gray, J. E. 1864. On the Cetacea which have been observed in the seas surrounding the British Islands. Proceedings of the Zoological Society of London 1864 (2): 195-248.

Keyes, I. W. 1973. Early Oligocene squalodont cetacean from Oamaru, New Zealand. New Zealand Journal of Marine and Freshwater Research 7:381-390.

Marx, F. G., and Fordyce, R.E. 2015. Baleen boom and bust: a synthesis of mysticete phylogeny, diversity and disparity. Royal Society Open Science 2:DOI 10.1098/rsos.140434.

Mead, J. G., and Fordyce, R.E. 2009. The therian skull: a lexicon with emphasis on the odontocetes. Smithsonian Contributions to Zoology 627:1-248.

Miller, G. S. 1924. A pollack whale from Florida presented to the National Museum by the Miami Aquarium Association. Proceedings of the United States National Museum 66(9): 1-15.

Mitchell, E. D. 1989. A new cetacean from the Late Eocene La Meseta Formation, Seymour Island, Antarctic Peninsula. Canadian Journal of Fisheries and Aquatic Science 46:2219-2235.

Pledge, N. S. 2005. A new species of early Oligocene cetacean from Port Willunga, South Australia. Memoirs of the Queensland Museum 51:123-133.

Pritchard, G. B. 1939. On the discovery of a fossil whale in the older tertiaries of Torquay, Victoria. The Victorian Naturalist 55:151-159.

Raine, J. I., Beu, A.G., Boyes, A.F., Campbell, H.J., Cooper, R.A., Crampton, J.S., Crundwell, M.P., Hollis, C.J., and Morgans, H.E.G. 2015. Revised calibration of the New Zealand Geological Timescale: NZGT2015/1. GNS Science Report 2012/39: 1-53.

Reed, A. W., and Dowling, P. 2010. Place names of New Zealand. Penguin, Auckland, 502 pp.

Russell, L. S. 1968. A new cetacean from the Oligocene Sooke Formation of Vancouver Island, British Columbia. Canadian Journal of Earth Science 5:929-933.

Tanaka, Y., and Fordyce, R.E. 2014. Fossil dolphin *Otekaikea marplesi* (latest Oligocene, New Zealand) expands the morphological and taxonomic diversity of Oligocene cetaceans. PLoS One 9(9): e107972.

Tanaka, Y., and Fordyce, R.E. 2015. A new Oligo-Miocene dolphin from New Zealand: *Otekaikea huata* expands diversity of the early Platanistoidea. Palaeontologia electronica 18.2.23A: 1-71.

True, F. W. 1904. The whalebone whales of the western North Atlantic compared with those occurring in European waters with some observations on the species of the North Pacific. Smithsonian contributions to knowledge 33: 1-332.

Tsai, C.-H., and Fordyce, R.E. 2015. The earliest gulp-feeding mysticete (Cetacea: Mysticeti) from the Oligocene of New Zealand. Journal of Mammalian Evolution: DOI 10.1007/s10914-015-9290-0.

Vandenberghe, N., Hilgen, F.J., Speijer, R.P., Ogg, J.G., Gradstein, F.M., Hammer, O., Hollis, C.J., and Hooker, J. J. 2012. Chapter 28 - The Paleogene Period; pp. 855-921 in Gradstein, F.M., Ogg, J.G., Schmitz, M., and Ogg, G. (eds), The Geologic Time Scale. Elsevier, Boston.

Memoirs of Museum Victoria 74: 117–136 (2016) Published 2016

ISSN 1447-2546 (Print) 1447-2554 (On-line)
http://museumvictoria.com.au/about/books-and-journals/journals/memoirs-of-museum-victoria/

A late Oligocene waipatiid dolphin (Odontoceti: Waipatiidae) from Victoria, Australia

Erich M.G. Fitzgerald[1,2]

[1] Geosciences, Museum Victoria, GPO Box 666, Melbourne, Victoria 3001, Australia (efitzgerald@museum.vic.gov.au)
[2] Department of Vertebrate Zoology, National Museum of Natural History, Smithsonian Institution, Washington DC 20560, USA

Abstract

Fitzgerald, E.M.G. 2016. A late Oligocene waipatiid dolphin (Odontoceti: Waipatiidae) from Victoria, Australia. *Memoirs of Museum Victoria* 74: 117–136.

A partial odontocete skeleton comprising isolated teeth, forelimb elements, ribs, and vertebrae is described from the upper Oligocene (Chattian) Jan Juc Marl of Jan Juc, Victoria, southeast Australia. Its dental and forelimb characters most closely resemble those of the late Oligocene *Waipatia* and *Sulakocetus* from New Zealand and the Caucasus, respectively; thus the Jan Juc odontocete is referred to an indeterminate species in the family Waipatiidae (Platanistoidea). This specimen represents the first report of Waipatiidae in Australia, expands the taxonomic diversity of Australian Oligocene Cetacea, and shows that Waipatiidae occurred in the Chattian cetacean assemblages of both Australia and New Zealand.

Keywords

Platanistoidea, Waipatiidae, dolphin, Paleogene, fossil, systematics, taxonomy.

Introduction

The fossil record of Cetacea (whales and dolphins) in Australia is meager: not through lack of Cenozoic marine rock outcrop, which is widespread in southern Australia, but rather a limited history of systematic research (Fitzgerald, 2004; Fordyce, 2006). Yet, the potential for improving this meager record, and gaining broader insights into cetacean evolution, have long been recognized by Thomas H. Rich (Rich, 1976, 1999; Vickers-Rich and Rich, 1993; Rich in Warne et al., 2003). Rich developed an awareness of the potential for research on Australasian fossil Cetacea, first in New Zealand during National Geographic Society-funded fieldwork (Rich, 1975; Rich and Rich, 1982), and then in Australia at the beginning of his career as Curator at the National Museum of Victoria (now Museum Victoria) in 1974. In both instances, this nascent attention paid to fossil Cetacea was encouraged by Dr Frank C. Whitmore, Jr., a United States Geological Survey marine mammal palaeontologist assigned to the National Museum of Natural History (Eshelman and Ward, 1994). By November 1975, Rich had produced a comprehensive inventory of the fossil Cetacea in the Palaeontology Collection of Museum Victoria.

The following year (1976), Rich with the assistance of Ian R. Stewart, collected a partially articulated incomplete fossil cetacean skeleton from the Upper Oligocene Jan Juc Marl at Jan Juc Beach, Victoria (Figs. 1 and 2). This specimen was registered in 1978 as Museum Victoria Palaeontology Collection (NMV P) 48861 and identified as a "squalodontoid?" On 7 October 1987, F. C. Whitmore, Jr. examined some of the homodont anterior teeth of NMV P48861, identifying the specimen as a "delphinoid". It was not until 2003 that the preparation of NMV P48861 was commenced by the author, resulting in a third (preliminary) attempt at identifying this fossil as "?Eurhinodelphinidae" (Fitzgerald, 2004: 191).

The aims of this paper are to describe the informative parts of the skeleton of NMV P48861, resolve its phylogenetic relationships, and interpret its biogeographic significance. Until now, the described late Oligocene cetacean assemblage from Australia has consisted of a probable kekenodontid archaeocete ('*Squalodon*' *gambierensis* Glaessner, 1955), two species of toothed mysticete in the family Mammalodontidae (*Mammalodon colliveri* Pritchard, 1939 and *Janjucetus hunderi* Fitzgerald, 2006), and isolated teeth referred to the enigmatic odontocete genus *Prosqualodon* (Fordyce, 1982; Fitzgerald, 2004). In addition, unnamed odontocete remains tentatively attributed to the Eurhinodelphinidae have been described from the fluvio-lacustrine ~Upper Oligocene Namba Formation of northeast South Australia (Fordyce, 1983; Fitzgerald, 2004). The allocation of NMV P48861 to the odontocete clade Waipatiidae marks the first record of this family in Australia, thereby increasing the family-level diversity of cetaceans known locally from the Paleogene, and expanding the record of Australian fossil Cetacea.

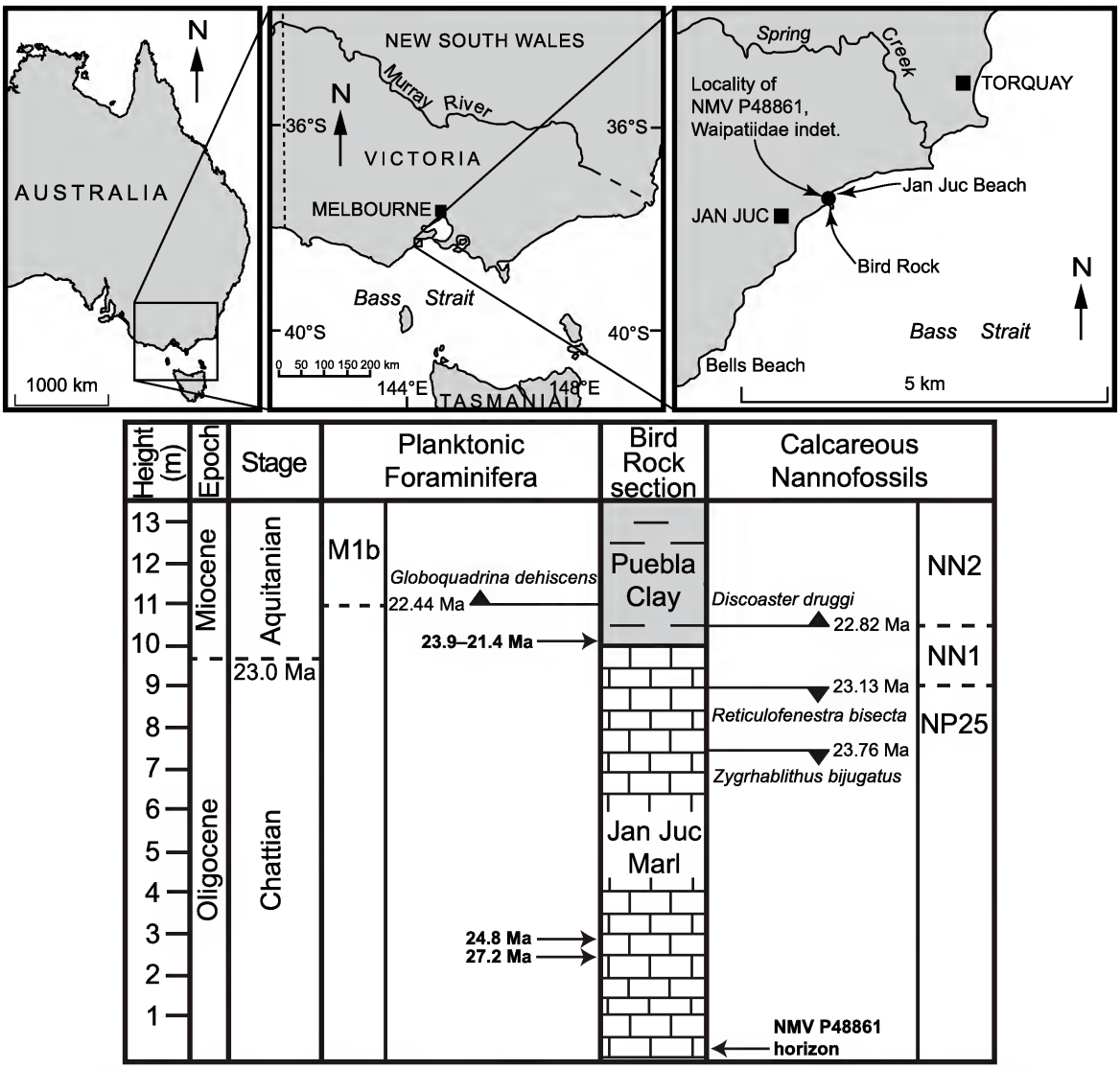

Figure 1. Locality map and stratigraphic section of the locality of NMV P48861, Waipatiidae gen. et sp. indet. Dates in bold text are based on measured $^{87}Sr/^{86}Sr$ ratios in McLaren et al. (2009). Planktonic foraminiferal and calcareous nannofossil stratigraphy, and geochronology are based on Gradstein et al. (2012). Planktonic foraminiferal data from Li et al. (1999), and calcareous nannofossil data from Siesser (1979). The measured section at Bird Rock is based on McLaren et al. (2009).

Material and Methods

Preparation. Material was prepared at Melbourne Museum primarily using pneumatic engravers and pin vises fitted with tungsten carbide rod. Dilute (10%) acetic acid was used to remove concretionary carbonate surrounding some bones. Limited areas of resistant matrix were removed using an air-abrasive machine. Bone was glued with cyanoacrylate and/or 40% Paraloid B-72 ethyl-methacrylate copolymer dissolved in acetone. A dilute (3%) solution of Paraloid B-72 in acetone was used as a consolidant.

Photography and measurement. Prior to preparation, archival photographs showing the exposed bones in the sediment were made using a 35 mm film Nikon EL SLR. A digital composite of scans of these photographs is depicted in Fig. 2. All other photographs were taken with a Nikon D90 DSLR camera and a 60 mm micro lens. All measurements were made with vernier calipers.

Anatomical terminology. Because all teeth were found isolated their precise position in the tooth row is unknown, therefore each tooth is numbered with Roman numerals (I–IX) in ascending order to indicate its estimated relative position in the tooth row from most anterior (I) to most posterior (IX). Due to uncertain homology with the cusps of other mammals, the term denticle is used instead of cusp for each major projection on the crown. Denticles (d) are coded as main (md), anterior (a, numbered away from the md: ad1, ad2, etc.), or posterior (p, numbered away from the md: pd1, pd2, etc.) following Marx et al. (2015: 16). Postcranial terms follow Flower (1885) and Schaller (2007).

Institutional abbreviations. LACM, Natural History Museum of Los Angeles County, Los Angeles; MLP, Museo de La Plata, La Plata, Argentina; NMV C, Mammalogy Collection, Museum Victoria, Melbourne; NMV P, Palaeontology Collection, Museum Victoria, Melbourne; OU, Geology Museum, University of Otago, Dunedin; USNM, National Museum of Natural History, Washington, DC.

Systematic Palaeontology

Cetacea Brisson, 1762

Odontoceti Flower, 1865, sensu Flower, 1867

Platanistoidea Gray, 1863, sensu Muizon, 1987

Waipatiidae Fordyce, 1994

Gen. et sp. indet.

"...a primitive eurhinodelphinid odontocete." (Fitzgerald, 2004: 184)

Referred material. NMV P48861, incomplete skeleton consisting of: nine isolated teeth; fragments of one cervical and 12 thoracic vertebrae; parts of 16 ribs; left incomplete scapula, humerus, radius, ulna, two metacarpals, and phalanx; right (fragmentary) scapula, humerus, radius, ulna, metacarpal, and phalanx; and fragments of two presumed carpals plus three phalanges (Figs. 2–11; Tables 1–2). Collected by Thomas H. Rich and Ian Stewart, 1976.

Locality. Shore platform in intertidal zone, immediately north of Bird Rock (a prominent stack), western end of Jan Juc Beach, Jan Juc, Victoria, southeast Australia; near latitude 38° 20' 58" S, longitude 144° 18' 10" E (Fig. 1).

Horizon and age. NMV P48861 was collected as a single large block (dimensions ~850×520×300 mm) of massive light grey friable silty sandy glauconitic marl forming the lowermost ~2 m of the Jan Juc Marl exposed at Bird Rock (Unit BR 1 in Section 4 of Abele, 1979: 23–25) (Fig 1). The sparse associated macrofossils include molluscs (*Dosinia*, *Limopsis chapmani*, *Notocallista*, *Ennucula*, cf. *Tellina*, and Turritellidae indet.: T. A. Darragh, pers. comm. 3 July 2015), bryozoans (*Otionellina* and cf. *Lunulites rutella*: R. Schmidt, pers. comm. 3 July 2015), and teleost fish bones.

Table 1. Measurements in mm of NMV P48861, Waipatiidae gen. et sp. indet.: teeth.

Tooth	crown height	crown anteroposterior length	crown labiolingual width	maximum root length
I	10.4+	6.6	5.8	36.6+
II	7.3+	5.9	4.7	31.8+
III	14.0	6.0	5.0	43.0
IV	12.0	5.7	5.2	27.8+
V	8.2+	5.9	4.0	22.3+
VI	10.1+	6.2	4.5	23.9+
VII	10.1+	9.1	4.7	21.4+
VIII	8.5+	10.3	6.5	23.2
IX	8.4+	10.4	6.2	21.0

Table 2. Measurements in mm of NMV P48861, Waipatiidae, gen. et sp. indet.: forelimb elements. Dimensions adapted from Uhen (2004). Measurements rounded to nearest 0.5 mm. + symbol denotes measurements of the preserved dimension of an incomplete element.

Scapula	left	right
maximum preserved height	134.0+	–
maximum preserved length	183.0+	–
neck of scapula width	46.0	–
depth of glenoid fossa	8.0	–
Humerus	**left**	**right**
maximum length	147.0	150.0
maximum width of proximal end	66.0+	65.5+
maximum width of shaft	56.0	56.0
minimum width of shaft	40.0	42.0
maximum width of distal end	38.0	37.0
maximum transverse diameter of proximal end	69.0	–
transverse diameter of shaft at mid-length	28.0	28.0
transverse diameter of distal end	26.0	25.0
Ulna	**left**	**right**
maximum length	141.0+	172.0+
shaft length	99.0+	122.5
olecranon length	68.0+	75.0+
maximum width across olecranon	70.0	64.5+
width of shaft at mid-length	34.0	33.0
maximum width of distal end	41.5+	42.5
Radius	**left**	**right**
maximum length	143.0	–
shaft length	118.0	–
maximum width of proximal end	28.0+	29.0+
width of shaft at mid-length	35.0	–
maximum width of distal end	33.5+	–

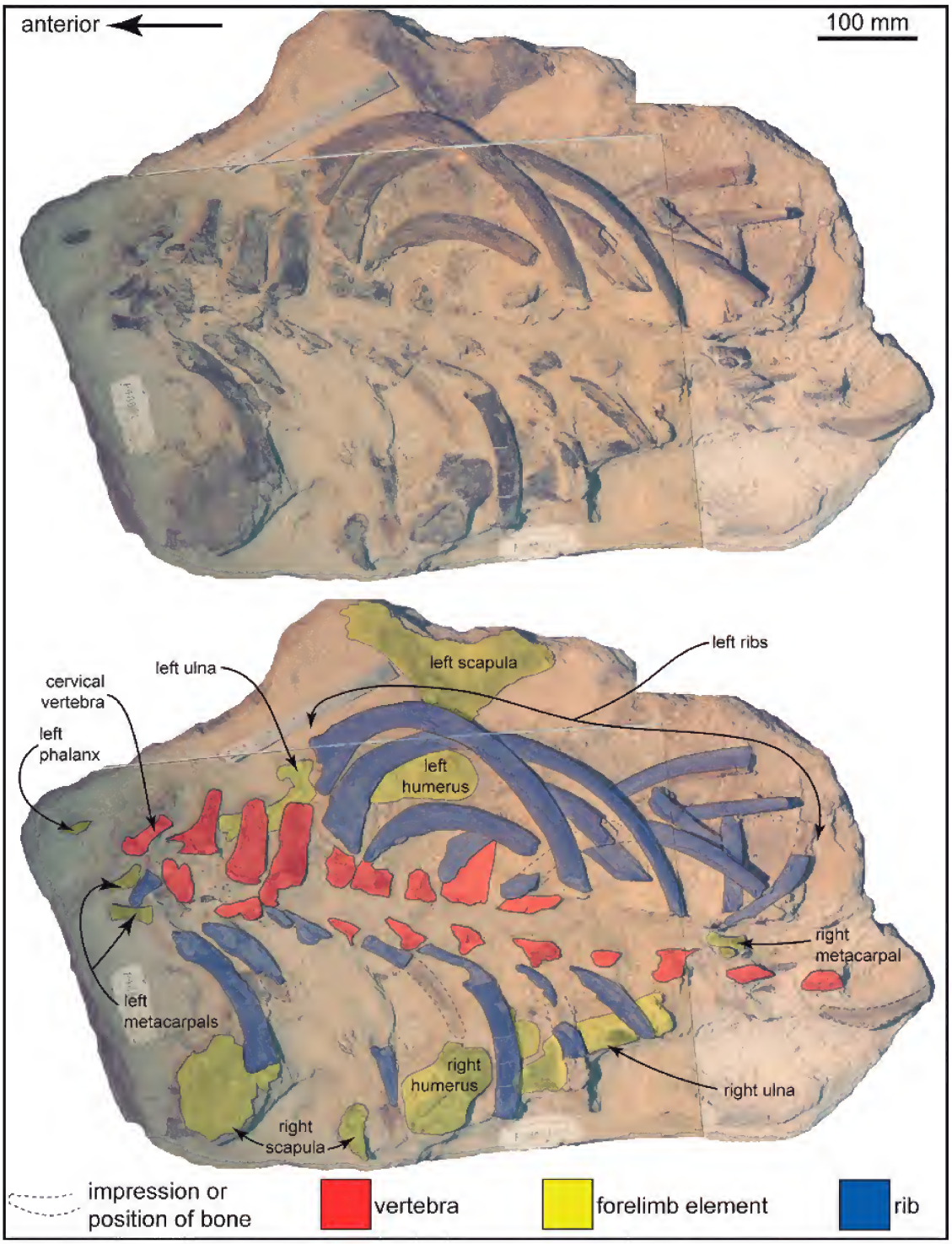

Figure 2. The original distribution of elements in matrix prior to preparation, NMV P48861, Waipatiidae gen. et sp. indet. **Top**, block of matrix enclosing bones as collected in field, prior to preparation. **Bottom**, tracing of bone outlines in matrix prior to preparation.

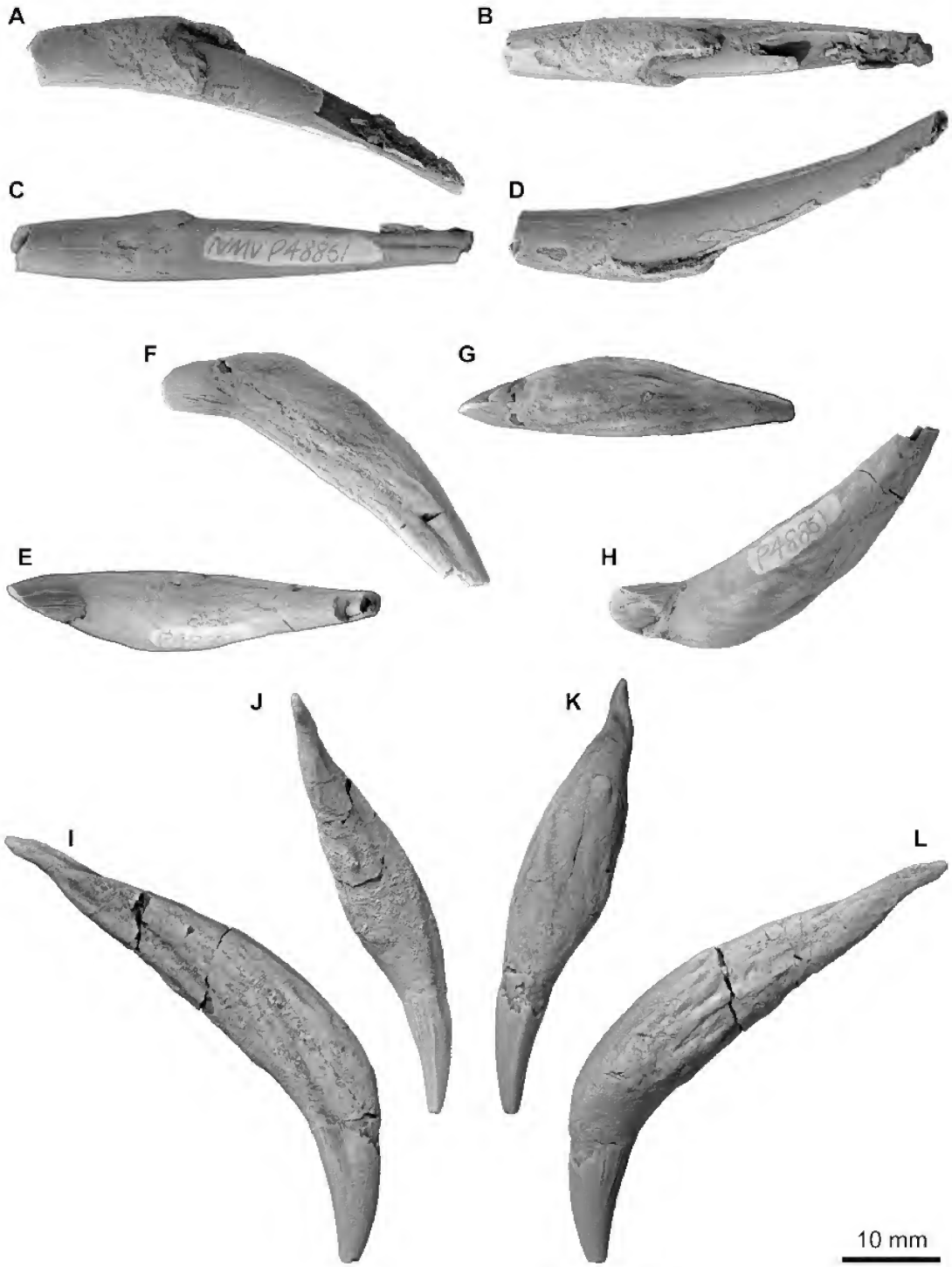

Figure 3. Anterior teeth I–III of NMV P48861, Waipatiidae gen. et sp. indet. Tooth I, presumed procumbent incisor in: **A**, labial; **B**, anterior; **C**, posterior; and **D**, lingual views. Tooth II, anterior tooth in: **E**, posterior; **F**, labial; **G**, anterior; and **H**, lingual views. Tooth III, right upper anterior tooth in: **I**, labial; **J**, posterior; **K**, anterior; and **L**, lingual views. Specimens whitened with ammonium chloride.

Figure 4. Right upper anterior/anterior cheek teeth IV–VI of NMV P48861, Waipatiidae gen. et sp. indet., in labial (A, E, I), lingual (B, F, J), anterior (C, G, K), and posterior (D, H, L) views. **A–D**: tooth IV. **E–H**: tooth V. **I–L**: tooth VI. Specimens whitened with ammonium chloride.

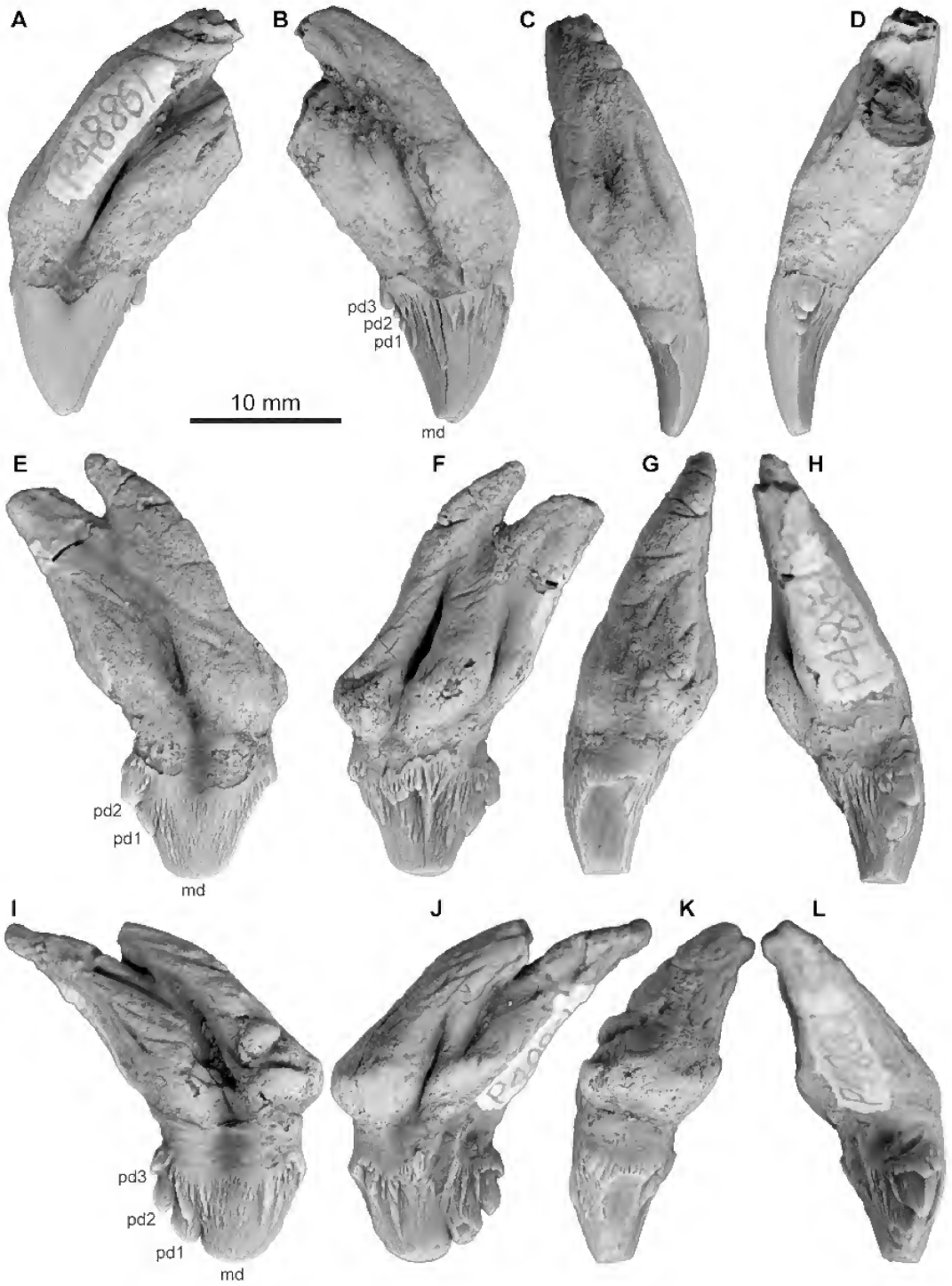

Figure 5. Upper cheek teeth VII–IX of NMV P48861, Waipatiidae gen. et sp. indet., in labial (A, E, I), lingual (B, F, J), anterior (C, G, K), and posterior (D, H, L) views. **A–D**: tooth VII, left upper anterior cheek tooth. **E–H**: tooth VIII, right upper posterior cheek tooth. **I–L**: tooth IX, right upper posterior cheek tooth. See Material and Methods for abbreviations. Specimens whitened with ammonium chloride.

Figure 6. Ribs of NMV P48861, Waipatiidae gen. et sp. indet. in anterior view. **1**: first right rib. **2**: second left rib. **3**: third left rib.

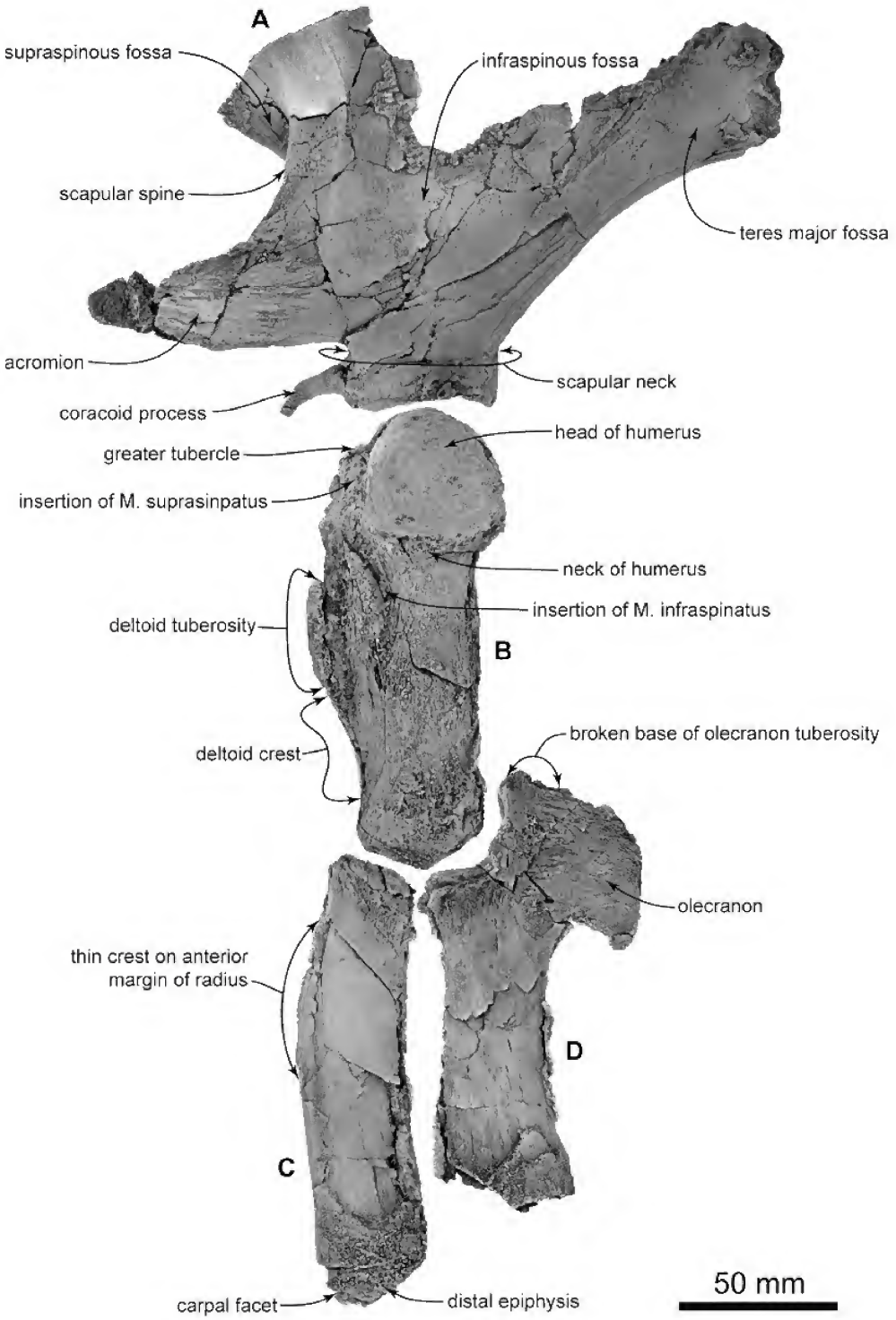

Figure 7. The left forelimb bones of NMV P48861, Waipatiidae gen. et sp. indet. in lateral view. **A**: scapula. **B**: humerus. **C**: radius. **D**: ulna. Specimens whitened with ammonium chloride.

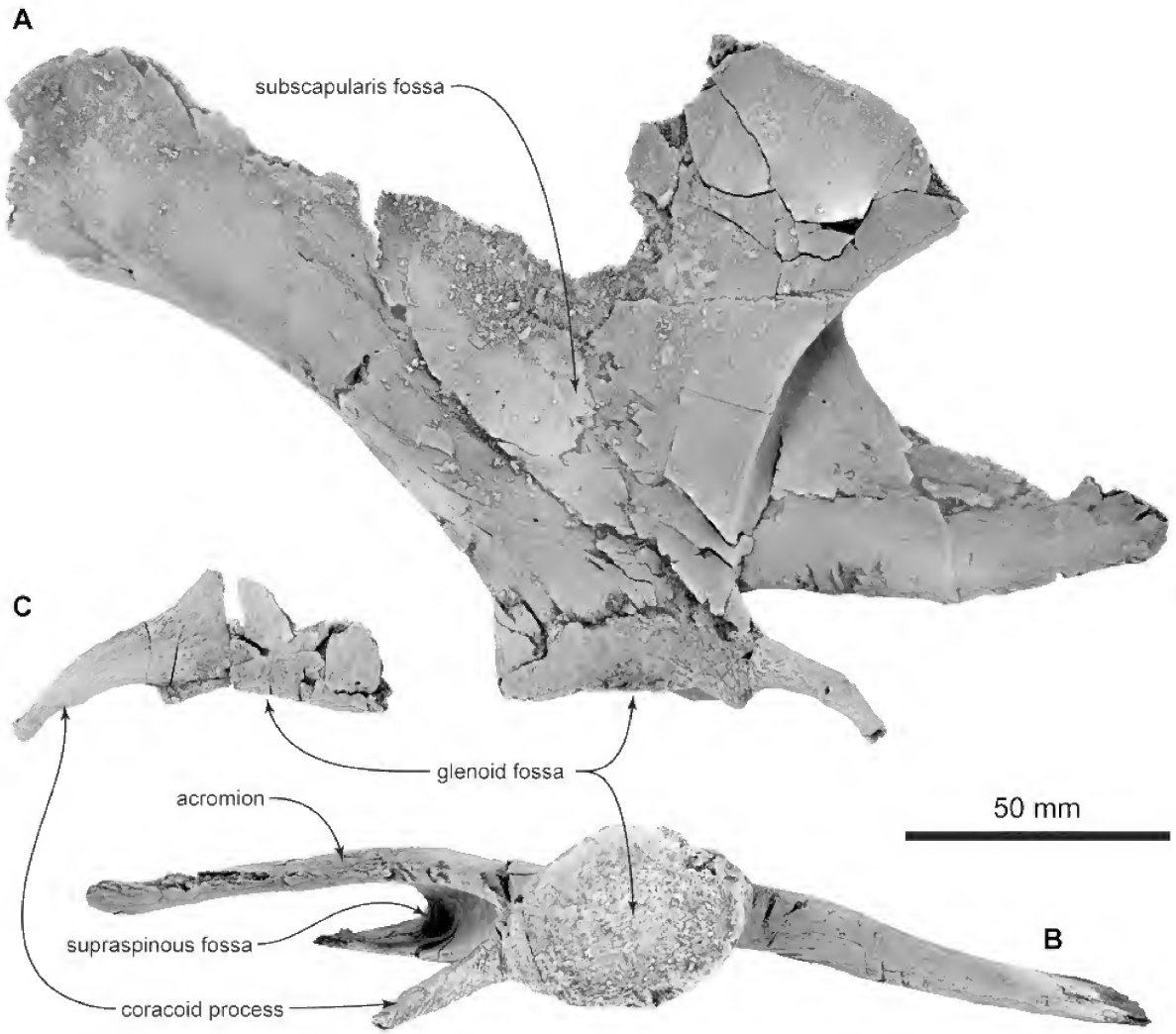

Figure 8. Scapulae of NMV P48861, Waipatiidae gen. et sp. indet. Left scapula in: **A**, medial; and **B**, distal views. **C**: glenoid region of right scapula in medial view. Specimens whitened with ammonium chloride.

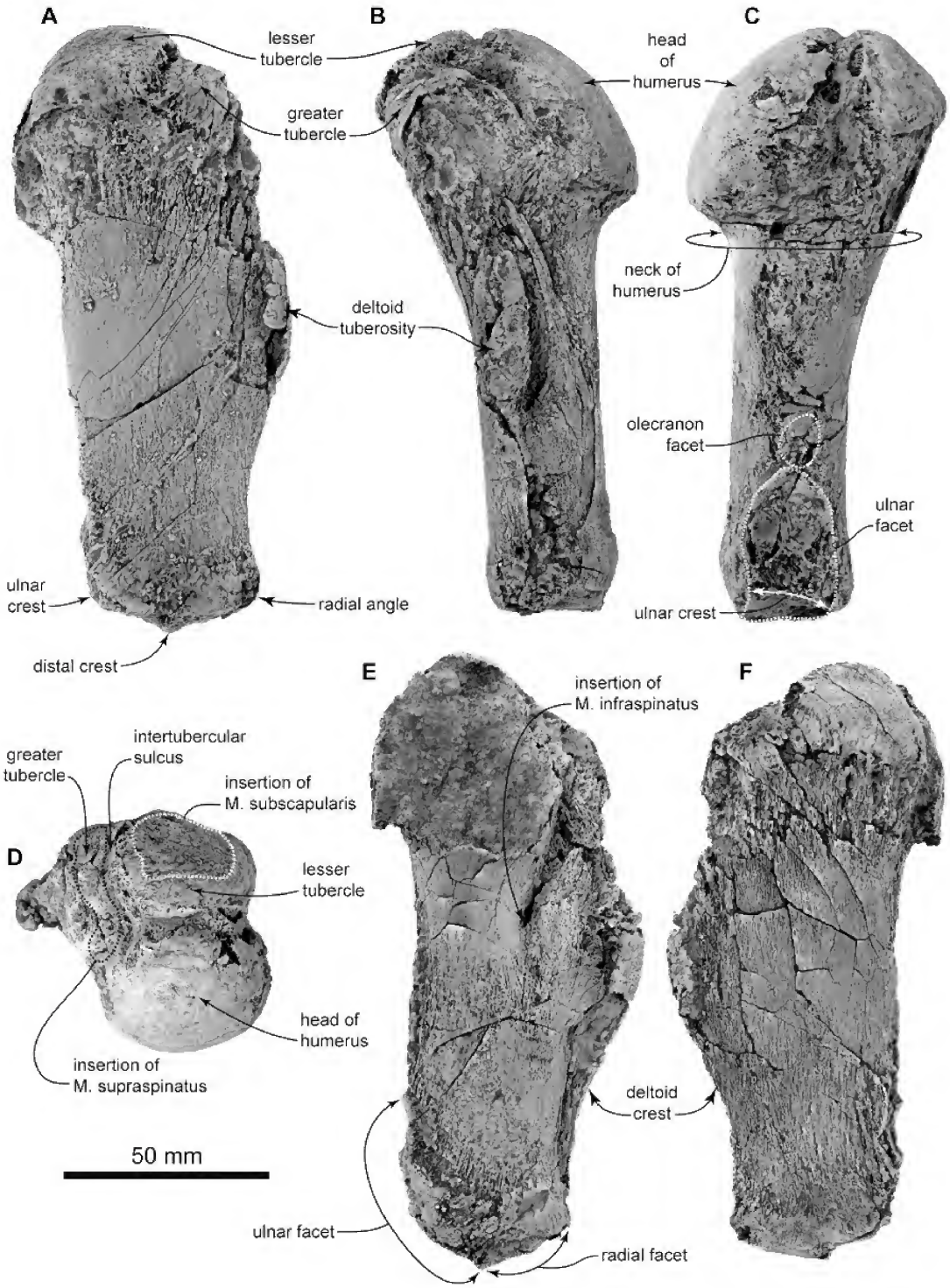

Figure 9. Humeri of NMV P48861, Waipatiidae gen. et sp. indet. Left humerus in: **A**, medial; **B**, anterior; **C**, posterior; and **D**, proximal views. Right humerus in: **E**, lateral; and **F**, medial views. Specimens whitened with ammonium chloride.

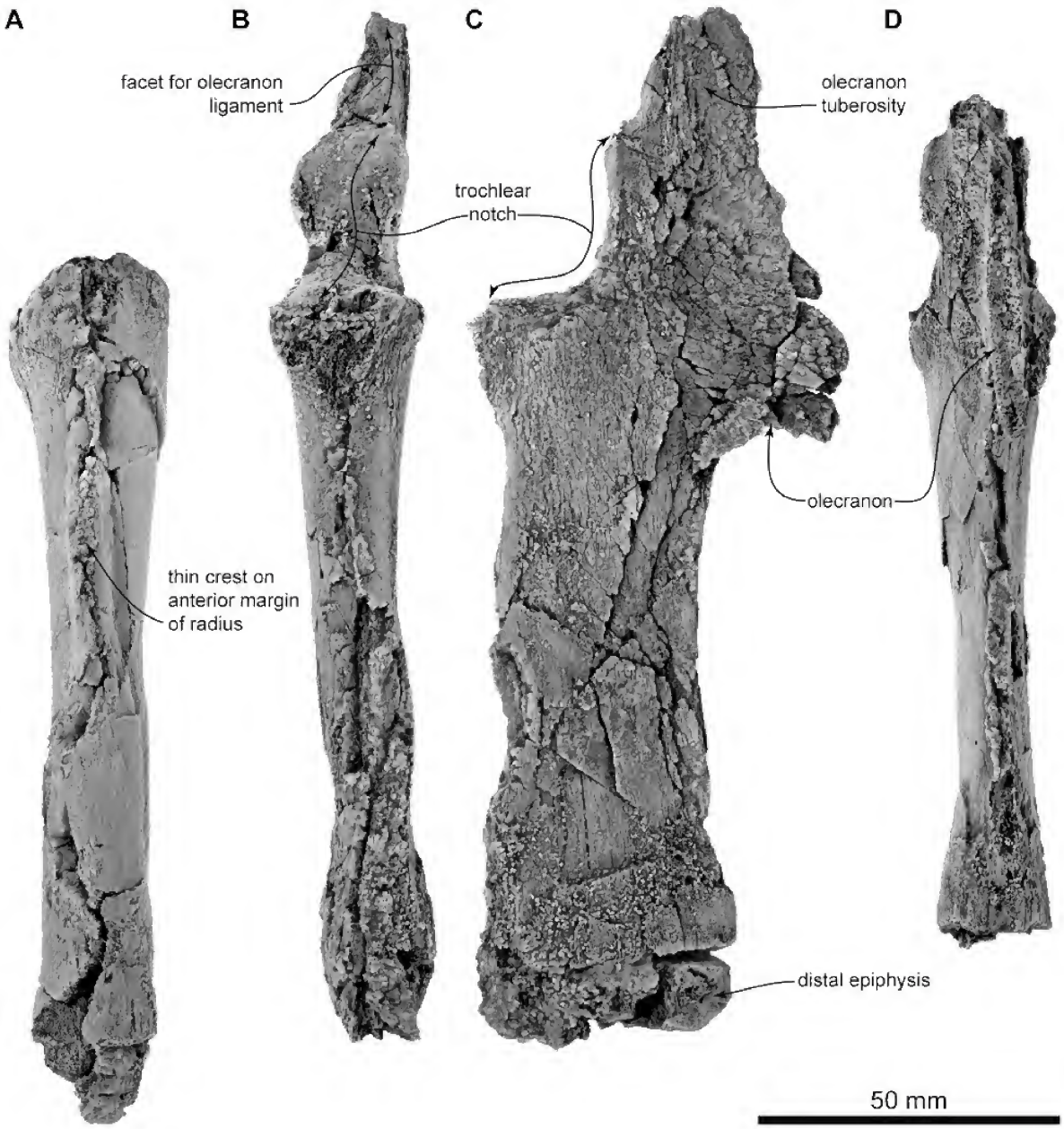

Figure 10. Radius and ulnae of NMV P48861, Waipatiidae gen. et sp. indet. **A**: left radius in anterior view. **B**: right ulna in anterior view. **C**: right ulna in medial view. **D**: left ulna in posterior view. Specimens whitened with ammonium chloride.

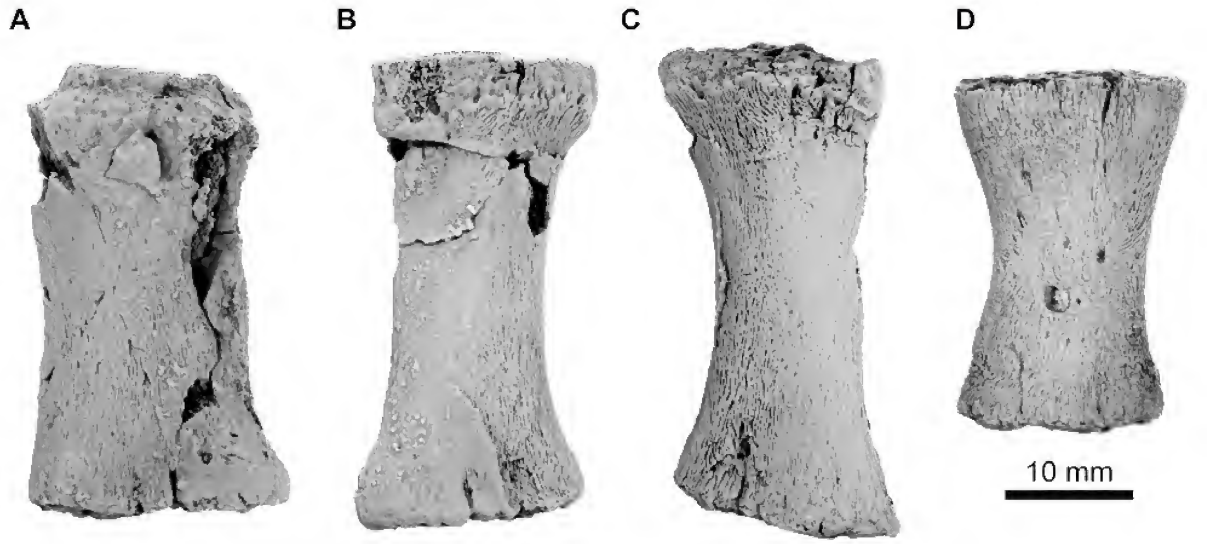

Figure 11. Metacarpals and phalanx of NMV P48861, Waipatiidae gen. et sp. indet. **A**: left metacarpal. **B**: left metacarpal. **C**: right metacarpal. **D**: left phalanx in lateral view. Specimens whitened with ammonium chloride.

Although planktonic foraminifera are rare in the Jan Juc Marl and rarely age-diagnostic (Li et al., 1999), maximum and minimum age constraints are available. $^{40}Ar/^{39}Ar$ dating of Angahook Formation basalts underlying the Point Addis Limestone (laterally equivalent to the Jan Juc Marl) at Aireys Inlet gave an age of 28.7 ± 0.2 Ma (McLaren et al., 2009). The oldest age of the Jan Juc Marl based on $^{87}Sr/^{86}Sr$ ratios measured in brachiopods from the lowest 3 m of the Bird Rock section is 27.2 Ma (McLaren et al., 2009). *Sphenolithus ciperoensis* occurs in the basal beds of the Jan Juc Marl at Bird Rock, marking the base of calcareous nannofossil zone NP24 and therefore an age of <29.62 Ma (Siesser, 1979; Gradstein et al., 2012). Together, these data suggest the Jan Juc Marl in outcrop is no older than the Rupelian–Chattian boundary, 28.1 Ma (McLaren et al., 2009).

The contact between the Jan Juc Marl and conformably overlying Puebla Clay has long been considered to approximate the Oligocene–Miocene boundary (Abele, 1979; Li et al., 1999; McLaren et al., 2009). *Zygrhablithus bijugatus* is absent from the top ~2.5 m of Jan Juc Marl in the Bird Rock section (Siesser, 1979), its last appearance datum within calcareous nannofossil zone NP25 at 23.76 Ma (Gradstein et al., 2012). Siesser (1979) also reported the last occurrence of *Reticulofenestra bisecta* about 1 m below the Jan Juc Marl/Puebla Clay contact; the last appearance datum of this species marking the top of zone NP25 at 23.13 Ma (Gradstein et al., 2012). The first appearance datum of *Discoaster druggi* marks the boundary between calcareous nannofossil zones NN1 and NN2 (22.82 Ma), and this species is first recorded in the beds above the Jan Juc Marl/Puebla Clay contact (Siesser, 1979; Gradstein et al., 2012) (Fig. 1). The planktonic foram *Globoquadrina dehiscens*, the first occurrence of which marks the base of zone M1b (22.44 Ma) in southern Australia, is first recorded in the basal Puebla Clay (Li et al., 1999; McGowran et al., 2004; Gradstein et al., 2012). The evidence from biostratigraphy shows that the Jan Juc Marl/Puebla Clay contact is between 23.13 and 22.82 Ma, straddling the Oligocene–Miocene boundary at 23.03 Ma (McLaren et al., 2009) (Fig. 1). This is corroborated by $^{87}Sr/^{86}Sr$ ratios from the basal Puebla Clay, which give a range of possible ages from 23.89–21.39 Ma (McLaren et al., 2009).

The age of the exposed Jan Juc Marl is therefore most rigorously constrained to between about 28.10 and 22.82 Ma, Chattian to earliest Aquitanian. NMV P48861 was collected from the lowest beds in the Bird Rock section of the Jan Juc Marl, stratigraphically below the last occurrence of *Zygrhablithus bijugatus*, which has a last appearance datum of 23.76 Ma (Fig. 1). This constrains the age of NMV P48861 to between about 28.1 and 23.7 Ma, and therefore within the Chattian.

Diagnosis. An odontocete with: heterodont dentition including at least one pair of procumbent apical teeth and small double-rooted posterior cheek teeth with triangular crowns bearing two or three posterior denticles; a small rod-like coracoid process of the scapula; an elongated humerus bearing a strongly salient deltoid tuberosity continuous with a distally-elongated crest, and a distal end that is distinctly narrower (anteroposteriorly) than the proximal end of the shaft; a long and anteroposteriorly narrow radius bearing a transversely thin crest on its anterior edge; and a well-developed hatchet-shaped olecranon of the ulna. None of these characters represent unambiguous synapomorphies of Waipatiidae, but this combination of characters is found only in taxa assigned to that clade (see Comparisons below).

Remarks on Platanistoidea. The concept of Platanistoidea used here is that of Muizon (1987) with emendments by Fordyce (1994) and Tanaka and Fordyce (2015a); namely that Platanistoidea includes the living family Platanistidae plus the extinct clades

Squalodelphinidae, Waipatiidae, *Otekaikea*, and Squalodontidae. This definition and taxonomic content of Platanistoidea has been questioned (Lambert et al., 2014: 988): some recent analyses posit both Squalodontidae and Waipatiidae as stem odontocetes (Geisler et al., 2011, 2014; Lambert et al., 2014, 2015; Sanders and Geisler, 2015); or platanistoids (Murakami et al., 2012; Tanaka and Fordyce, 2015a); or exclude squalodontids from Platanistoidea, but include Waipatiidae in the latter (Tanaka and Fordyce, 2014). The taxonomic content and phylogenetic position of Squalodontidae (and the potentially related *Prosqualodon*) are enduring problems in cetacean systematics recently reviewed by Tanaka and Fordyce (2014: 27). Their hypothesis for the content of Squalodontidae is followed here. For reviews of the taxonomic content and phylogenetic position of other putative platanistoid clades (i.e. Allodelphinidae, Dalpiazinidae) see Muizon (1988, 1991, 1994), Fordyce (1994), Barnes (2006), Barnes and Reynolds (2009), and Lambert et al. (2014).

Description

Ontogenetic age. The ossified and smooth articular surfaces on the scapula and humerus, twinned with the distal epiphyses of the radius and ulna not being fused, suggests that NMV P48861 represents at least a sexually mature but physically immature adult (Class V) according to the qualitative developmental categories established by Perrin (1975) for the delphinid *Stenella attenuata*.

Teeth. NMV P48861 is a heterodont odontocete, with evidence of at least one pair of procumbent tusk-like anterior teeth. Six single-rooted teeth (teeth I–VI: Figs. 3–4) and three double-rooted teeth (teeth VII–IX: Fig. 5) are preserved in isolation. The relative position of each tooth is identified with reference to *Waipatia maerewhenua* (Fordyce, 1994; cast of the holotype OU 22095). All teeth apart from a presumed tusked incisor (tooth I) and conical anterior tooth (tooth II) are interpreted as upper teeth on the basis of their strong lingual recurvature. The tusked incisor (tooth I: Figs. 3A–D) has a broken crown exposing dentine and a patent pulp cavity. The enamel-covered crown is subcircular in cross section, lacks keels, and bears enamel with longitudinal ridges on its lingual/posterolingual surface. The anterolingual surface of the crown has a small pyriform wear facet (Fig. 3D). The enamelocementum boundary extends further basally on the lingual/posterolingual side of the crown. The elongate and gently recurved root is missing most of its cementum, exposing dentine.

A conical anterior tooth (tooth II: Figs. 3E–H) has a crown with an oval cross section, and an oblique apical wear facet on its lingual aspect. When complete, the crown was probably relatively short compared to the elongated root. The labial surface of the crown is smooth, with a keeled posterior edge, and fine ridges on its preserved posterolingual surface. Immediately basal to the crown, the single root is slightly waisted, but then becomes inflated in the anteroposterior and labiolingual planes before tapering towards the root apex. The labial surface of the apical one-quarter of the root has a median groove.

Two upper right caniniform anterior teeth (teeth III and IV: Figs. 3I–L and 4A–D, respectively) bear a crown with a single conical denticle and a worn crown apex. The crown is recurved lingually and is somewhat labiolingually inflated at its base. The anterior and posterior edges are strongly keeled, and there are fine longitudinal ridges on the labial side of the crown base. The lingual surface of the crown in tooth III has diffuse longitudinal ridges (Fig. 3L). The single root immediately basal to the crown is waisted such that there is a distinct 'neck'. Further towards the root apex the root is labiolingually inflated, then tapers towards the root apex.

An upper right anterior tooth (tooth V: Figs. 4E–H) has a crown with a single triangular denticle and a worn crown apex. The relatively small crown is recurved lingually, bears a strongly keeled posterior edge, and has fine ridges on its posterolabial and posterolingual surfaces. The enamelocementum boundary extends further basally at the posterior ends of both labial and lingual sides of the crown. In labial and lingual views there is a distinct 'neck' immediately basal to the crown. The single root is strongly labiolingually inflated and bears a median groove on the labial surface of its preserved apex (Fig. 4E).

An upper right anterior tooth (tooth VI: Figs. 4I–L) has a crown with a single triangular denticle and a worn crown apex. The crown is recurved lingually, bears strongly keeled anterior and posterior edges, and fine ridges on its posterolabial and lingual surfaces. The enamelocementum boundary extends further basally at the anterior ends of both labial and lingual sides of the crown. The crown of this tooth closely approximates the morphology of the right upper anterior cheek teeth of *Waipatia maerewhenua*. The incomplete (presumed) single root is labiolingually inflated.

A double-rooted upper left anterior cheek tooth (tooth VII: Figs. 5A–D) has a crown with a high triangular main denticle (md) bearing keeled anterior and posterior edges, an incipiently papillate anterolingual cingulum, three tiny posterior denticles (pd1–3: Fig. 5B), indistinct ridges along the base of its labial surface, and strong longitudinal ridges along the base of its lingual surface. A distinct 'neck' occurs basal to the enamelocementum boundary. The two parallel roots are fused along their entire preserved length, recurved posterodorsally, and labiolingually inflated at approximately mid-length. The anterior root tapers strongly towards its apex such that its preserved apical end is about half the diameter of the posterior root.

A double-rooted upper right posterior cheek tooth (tooth VIII: Figs. 5E–H) has a crown with a relatively low triangular md and two small posterior denticles (pd1–2: Fig. 5E). The md is heavily worn on its anterior edge and apex. The posterior denticles are worn on their apices. The posterior edges of all denticles bear strong keels. The labial surface of the crown bears indistinct fluted ornament, whereas enamel on the lingual surface is heavily ornamented with longitudinal ridges and wrinkles arising from a basal papillate cingulum. A distinct 'neck' basal to the enamelocementum boundary can be seen in labial and lingual views. The two parallel roots are fused for about three-quarters of their length, recurved posterodorsally (at an angle of ~60° to the axis of the crown), and strongly labiolingually inflated in their basal half. Both roots taper towards their apex, although the apical end of the anterior root is less than half the diameter of the posterior root. A prominent elongate swelling on the lingual aspect of the posterior root probably represents a vestigial fused third root (Fig. 5F).

A double-rooted upper right posterior cheek tooth (tooth IX: Figs. 5I–L) has a crown with a low triangular md and three posterior denticles (Fig. 5I). The posterior denticles decrease in size away from the md (anteroposterior diameter = 5.4 mm): pd1 anteroposterior diameter = 2.2 mm; pd3 anteroposterior diameter = 1.3 mm. The main denticle plus pd1 and pd2 have heavily worn apices. Additionally, the anterior edge of the md is worn (Fig. 5K). A distinct shear wear facet occurs on the lingual surface of the crown at the level (anteroposteriorly) of the notch between the md and pd1 (Fig. 5J). The posterior edges of all denticles are keeled. The labial surface of the crown bears distinct ridged and fluted ornament. The enamel on the lingual surface of the crown is more heavily ornamented with longitudinal ridges and wrinkles arising from a strongly papillate basal cingulum. This cingulum wraps around the anterior and posterior edges of the crown base and on to the antero- and posterolabial corners of the basal crown. The crown of this tooth resembles the morphology of the third-to-last upper cheek teeth of *Waipatia maerewhenua*. A clear 'neck' occurs basal to the enamelocementum boundary. The two parallel roots are fused for about two-thirds of their length, recurved posterodorsally (at an angle of ~50° to the axis of the crown), and strongly labiolingually inflated in their basal half. There is a prominent anterior bulge at the base of the anterior root, and both roots are strongly tapered towards their apices.

Vertebrae. The fragmentary spinous processes, right halves of the vertebral arch, and transverse processes of one cervical (probably the seventh), and twelve thoracic vertebrae (first to twelfth) are preserved (Fig. 2). Thoracic vertebrae 1–3 have high and transversely flat spinous processes, with the spinous process of thoracic vertebra 1 being approximately half the width of those of thoracic vertebrae 2 and 3. The rest of the preserved parts of the vertebrae are uninformative.

Ribs. Parts of 16 ribs, five right, eight left (five of which are double-headed), and three indeterminate, are preserved (Fig. 6). A partial right rib 1 has a wide and flat shaft (29 mm maximum and 10 mm minimum diameter proximally), which increases in width distally (34 mm maximum diameter at preserved distal end). Three left double-headed ribs (damaged ventrally) are interpreted as ribs 2, 3, and a mid-series rib (based on position in the sediment relative to the vertebral column and comparisons with modern odontocetes, e.g., *Platanista gangetica* NMV C27417 and *Delphinus delphis* NMV C24964), and are 262+, 322+, and 284+ mm in chord length, respectively. Left ribs 2 and 3 are anteroposteriorly flat and wide along their length (rib 2, 25 mm maximum and 11 mm minimum diameter at mid-shaft; rib 3, 19 mm maximum and 9 mm minimum diameter at mid-shaft). The left mid-series rib is narrower and more ovoid in cross-section (18 mm maximum and 11.5 mm minimum diameter at mid-shaft).

Scapula. Both left and right scapulae are incomplete: the left scapula lacks the dorsal margin (Figs. 7, 8A), and the right scapula is represented by an uninformative fragment of dorsal margin (Fig. 2) plus the coracoid process and approximately half of the glenoid (Fig. 8C). Orientation of the scapula follows Tanaka and Fordyce (2015a: 32) whereby the glenoid fossa is ventral. The scapula is: fan-shaped, its anterior and posterior edges forming an angle of about 100°; transversely thin (especially in the middle of the infraspinous fossa); and, by analogy with other odontocete scapulae (e.g., Benke, 1993; Muizon, 1994), probably longer than high. Anteriorly, there are two projections: the acromion and coracoid process.

Viewed laterally (Fig. 7), the long (80+ mm) acromion projects anteroventrally, has a dorsoventrally high base, and does not expand distally. In distal view (Fig. 8B), the acromion curves gently laterally at its base, but more distally curves anteromedially. The rod-like coracoid process arises from a robust base (8.5 mm width, 12 mm height) ventromedial to the acromion. The coracoid process is strongly recurved ventromedially, and long relative to its transverse diameter (32 mm long; minimum and maximum diameters of 5.7 mm and 7.6 mm, respectively, at mid-length). Viewed distally, the angle between the coracoid process and acromion is about 40°. The coracoid process is distinctly waisted about 10 mm from its distal apex, which is slightly globular (Fig. 8C). The scapular neck is constricted. Distally, the glenoid fossa has an oval outline, longer than wide (47 mm length, 35 mm width).

In lateral view (Fig. 7), the base of the acromion is continuous posterodorsally with the scapular spine, which curves anterodorsally. Anteriorly, the preserved supraspinous fossa is anteroposteriorly narrow. It is separated from the anteroposteriorly broad infraspinous fossa by a ridge with a tabular lateral surface (anteroposterior diameter 19 mm). The infraspinous fossa has a smoothly undulating surface. Its posterior edge is formed by a subtle convexity for the border between the infraspinous and teres major fossae. The posterior edge of the scapula has a gently concave profile in lateral view (angle between posterior edge of the scapula and neck of the scapula is ~140°). The medial surface of the scapular blade is dominated by the broad V-shaped subscapularis fossa (Fig. 8A).

Humerus. The left humerus is nearly complete (Figs. 7, 9A–D), but the head of the right humerus is eroded (Fig. 9E). Surface detail on both humeri is generally well preserved. The humerus is relatively elongated (length >250% of maximum width), and has a slightly transversely flattened shaft (minimum width of shaft ~140% of its transverse diameter) (Table 2). The distal end of the humerus is significantly narrower than the proximal end (width of distal end of humerus ~57% of its proximal end).

The locations of some muscle attachments on the humerus differ between odontocete families, and in some cases depart from their homologues in terrestrial mammals. Notable here is the insertion for M. deltoideus, which in terrestrial mammals is a distinct deltoid tuberosity and/or crest (Flower, 1885; Schaller, 2007). However, in odontocetes the deltoid tuberosity varies in its relative size and position, and indeed may not be present at all, hence M. deltoideus inserts on: a distinct deltoid tuberosity and adjacent crest of humerus in *Physeter* (Berzin, 1972) and *Kogia* (Schulte and Smith, 1918); lateral surface of the distal end of the humerus in *Inia* (Klima et al., 1980), *Pontoporia* (Strickler, 1978), *Neophocaena* (Howell, 1927), and *Phocoena* (Smith et al., 1976); anterior edge and lateral surface of the humerus in *Monodon* (Howell, 1930); and the

anteroventral edge and adjacent lateral surface of the humerus in *Tursiops* and *Stenella* (Benke, 1993). For this study, muscle attachments are identified using a combination of the aforementioned literature on odontocete myology, plus artiodactyls (Nickel et al., 1986; Schaller, 2007).

The proximal end of the humerus is dominated by a smooth, rounded, head that has a hemi-elliptical outline in lateral view (Fig. 7), and represents about 30% of the length of the humerus. Viewed proximally, the head of the humerus is approximately the same size as the tubercles, from which it is separated by a deep sulcus (Fig. 9D). In anterior and posterior views the proximal edges of the head and lesser tubercle are at approximately the same level, and a distinct neck separates the head from the body of the humerus (Figs. 9B–C). Medial to the head, the proximal surface of the lesser tubercle has a distinct flattened region for insertion of the M. subscapularis. A distinct intertubercular sulcus separates the lesser tubercle from the anteriorly adjacent and relatively small greater tubercle, which has a flattened area on its proximomedial aspect for insertion of M. supraspinatus that marks a steep step between the proximal surfaces of the two tubercles. The insertion of the M. supraspinatus continues posterolaterally into a deep pit and ventrolaterally angled flattened area. Further distally, on the lateral surface of the humerus and below the anterior edge of the head, is a proximodistally long fossa for the insertion of M. infraspinatus, which terminates in a deep pit (but not a patent foramen) at the level of the proximal one-third of shaft length (Fig. 9E). The anterior edge of the humerus is transversely thin and sigmoidal in lateral/medial view. A strongly developed and proximodistally long (~40 mm length) deltoid tuberosity occupies about half of the length and the maximum width of the shaft. The apex of the deltoid tuberosity is located within the proximal 65% of the humerus. The deltoid crest of the humerus runs distally from the deltoid tuberosity, becoming indistinct proximal to the radial angle (Figs. 9E–F). Distally, the radial and ulnar facets have gently undulating surfaces, are separated by a sharp distal crest, and form an obtuse angle in lateral view (Fig. 7). A low ulnar crest marks the transition from the distal part of the ulnar facet to its pentagonal part on the posterior aspect of the humerus (Fig. 9C). Proximomedial to the latter feature is a small, flattened olecranon facet for attachment of the olecranon ligament.

Radius. The left and right radii are nearly complete, but somewhat crushed mediolaterally; and the right radius is corroded and lacks some of its external surface (Figs. 7, 10A). The shaft is narrow and elongated, in lateral view having a gently convex anterior edge and slightly concave posterior edge (Fig. 7). The distal epiphysis is incompletely fused to the shaft. Proximally, the fovea of the head of the radius has a quadrangular outline with a distinct concavity at its anteromedial corner. The surface of the fovea (articular face for the radial facet of the humerus) is posteromedially-tilted (Fig. 10A). Anteriorly, the shaft bears a thin crest that extends from the head of the radius distally to the shaft's mid-length (Fig. 10A). The distal half of the radius widens gradually towards the distal epiphysis, which is wider than the proximal end. The carpal facet has an angular distal profile in lateral view (Fig. 7).

Ulna. The left ulna is nearly complete, lacking the anteroproximal region of the olecranon and part of the distal end (including epiphysis) (Figs. 7, 10D). The right ulna lacks the posterior edge of the olecranon, but is otherwise virtually complete (Figs. 10B–C). The proximal and distal ends of the ulna are robust (23 mm and 19 mm transverse diameter, respectively) with the shaft being transversely thin at its mid-length (~11 mm); giving the shaft of the ulna a subtly hourglass-shaped outline in anterior and posterior views (Figs. 10B, D). The olecranon projects proximally and posteriorly as a transversely thin blade. Anteriorly, the olecranon bears a rugose and proximodistally elongated facet for the olecranon ligament, located proximal to the hourglass-shaped trochlear notch (Fig. 10B). Posteriorly, the outer edge of the olecranon has a rugose surface (Fig. 10D). In lateral view, the trochlear notch forms a nearly 90° angle, with its vertical part being transversely narrower (18 mm maximum transverse diameter) than the horizontal part (22 mm maximum transverse diameter) (Figs. 7, 10C). Anterodistal to the trochlear notch is a small tuberosity that fits a notch in the posteroproximal edge of the radius (Fig. 7). The distal half of the lateral surface of the shaft bears numerous nutrient foramina of uncertain homology (Fig. 7). The interosseous and posterior borders of the shaft gradually diverge towards the distal end, to which the ellipsoid epiphysis is not fused.

Carpals. Two bone fragments (presumed carpals) are uninformative and are not described.

Metacarpals. Three metacarpals were found in the sediment during preparation of NMV P48861: two close to the distal end of the left antebrachium (hence identified as left metacarpals), and one close to the distal end of the right antebrachium (hence identified as a right metacarpal) (Figs. 2, 11A–C). Each metacarpal has: an approximately rhomboid outline, with concave anterior and posterior edges; transversely convex lateral surface; and a transversely flattened palmar surface. The shorter left metacarpal (Fig. 11A) is relatively wide (20.5 mm maximum width, 36 mm length) and ellipsoid in cross section (6 mm transverse diameter, 16 mm wide at mid-length). The longer left metacarpal (Fig. 11B) is elongated (18 mm maximum width, 39 mm length) and more ovoid in cross section (8 mm transverse diameter, 12 mm wide at mid-length). The right metacarpal (Fig. 11C) is nearly identical in size and shape to the longer left metacarpal. It is not possible to accurately identify which position each metacarpal occupied in the manus.

Phalanges. Four phalanges were found in the sediment during preparation of NMV P48861, although only one phalanx is complete enough to merit description (Fig. 11D). It was found close to the distal end of the left antebrachium (Fig. 2), and is hence identified as a left phalanx. It is flattened transversely (5 mm transverse diameter, 12 mm wide at mid-length), and relatively long (28.5 mm long, 18 mm width at proximal end). This elongated form, and possession of a wider proximal than distal (16 mm) end, suggests that this is a proximal phalanx. It is hourglass-shaped in lateral/plantar views, with flat proximal and distal ends.

Discussion

Comparisons. NMV P48861 differs from archaeocetes by having relatively tiny heterodont cheek teeth and a humerus that lacks a trochleated distal end, instead possessing distinct radial and ulnar facets. NMV P48861 differs from mysticetes (including toothed stem taxa) (e.g., *Fucaia goedertorum* (Barnes and Furusawa in Barnes et al., 1995), LACM 131146; Kellogg, 1965; Benke, 1993; Boessenecker and Fordyce, 2015a) by having an elongated and narrow rod-like coracoid process of the scapula, and a humerus that is longer than the antebrachium. NMV P48861 can be further differentiated from the toothed mysticete clades: Llanocetidae and Mammalodontidae by having smaller and lower-crowned cheek teeth lacking strongly developed ridges on both labial and lingual surfaces of the crown; and Aetiocetidae by having posterior cheek teeth with more strongly developed ornament on the labial surface of the crown. NMV P48861 is not a xenorophid, simocetid, mirocetid, or agorophiid odontocete, differing by having smaller posterior cheek teeth. In addition, the humerus of NMV P48861 is more specialized than that of *Mirocetus riabinini* Mchedlidze, 1970 (Sanders and Geisler, 2015) by having: a less laterally-projecting head; a less prominent deltoid crest distal to the deltoid tuberosity; and distinct radial and ulnar facets on the distal end. NMV P48861 differs from *Prosqualodon* by having: relatively small posterior cheek teeth that lack strong nodular crown ornament; an elongated coracoid process on the scapula; a humerus with a straight posterior edge (viewed laterally) and a strongly developed deltoid tuberosity; and a more elongated antebrachium. NMV P48861 differs from crown odontocetes other than Platanistoidea in lacking: homodont conical posterior teeth, a distal end of the humeral shaft with an anteroposterior width ≥ to that of the proximal end of the shaft, and a strongly developed coracoid process that enlarges distally. Although the coracoid process of the scapula is reduced in eurhinodelphinids to a rod-like form (*Xiphiacetus bossi* Kellogg, 1925, USNM 11867, Muizon, 1994), NMV P48861 further differs from this family by lacking a distinct crest between the infraspinatus fossa and teres major fossa on the scapula.

Based on these comparisons and the character combinations described above, NMV P48861 is assigned to the Platanistoidea. Within Platanistoidea, NMV P48861 differs from all taxa other than Squalodontidae and Waipatiidae in having heterodont dentition and double-rooted posterior cheek teeth. However, it differs from Squalodontidae by lacking large robust teeth. NMV P48861 lacks the two scapular characters proposed as synapomorphies of Platanistoidea: the acromion positioned on the leading (anterior) edge of the scapula, resulting in loss of the supraspinous fossa; and absence of the coracoid process (e.g., Muizon, 1987, 1994). However, several taxa hypothesized to be platanistoids possess both a supraspinous fossa and a distinct coracoid process on the scapula: the squalodontid *Phoberodon arctirostris* Cabrera, 1926 (Cozzuol and Humbert-Lan, 1989; Cozzuol, 1996; MLP 5-4); *Otekaikea* spp. (Tanaka and Fordyce, 2014, 2015a); and *Sulakocetus dagestanicus* Mchedlidze, 1976 (Mchedlidze, 1984; Muizon, 1987). Hence, the scapular characters of Muizon (1987) may be synapomorphies of a more exclusive clade within Platanistoidea (i.e. Squalodelphinidae + Platanistidae) and/or evolved independently in *Prosqualodon* and *Squalodon*. NMV P48861 shares tusk-like anterior teeth and a rod-like morphology of the coracoid process with *Otekaikea*, but differs from that genus by having: more strongly heterodont cheek teeth with lower, less conical crowns bearing salient posterior denticles; a scapula with a posteroventral border forming a 45° angle with the horizontal in lateral view (cf. ~15° in *Otekaikea*); a more elongated humerus (minimum anteroposterior width of shaft is <30% humerus length); the dorsal edge of the head of the humerus approximately level with the dorsal edge of the lesser tubercle; an infraspinous fossa that does not terminate distally in a distinct ovoid pit on the lateral surface of the humeral shaft; and a longer antebrachium (length of radius is nearly equal to humerus length).

Amongst described platanistoids, NMV P48861 is most similar to *Waipatia* in having heterodont dentition including: tusk-like anterior teeth; and double-rooted posterior upper cheek teeth with small (<12 mm length) triangular crowns bearing two or three posterior denticles. NMV P48861 differs from *Waipatia maerewhenua* in its posterior upper cheek teeth having finer and more diffuse ridges on the labial surface of the crown. NMV P48861 differs from *W. hectori* (Benham, 1935) by having larger and less labiolingually inflated cheek teeth with shorter and more shallowly notched denticles. Neither described species of *Waipatia* are known from appendicular elements (Fordyce, 1994; Tanaka and Fordyce, 2015b), so it is unclear whether *Waipatia* possessed forelimb morphology similar to that of *Otekaikea* and NMV P48861. However, the holotype of *Sulakocetus dagestanicus*, which is probably a waipatiid (Fordyce, 1994, 2003; Fordyce and Muizon, 2001), includes much of the forelimb skeleton (Mchedlidze, 1984; Pilleri, 1986). NMV P48861 shares with *Sulakocetus*: small heterodont cheek teeth; coracoid process of the scapula present and apparently long and rod-like (Mchedlidze, 1984:43, Plate XVI); elongated humerus (minimum anteroposterior width of shaft is <30% humerus length); dorsal edge of the head of the humerus approximately level with the dorsal edge of the lesser tubercle; distinct intertubercular sulcus on humerus (Mchedlidze, 1984:43, Plate XII); strongly salient deltoid tuberosity with adjacent crest developed distally; a distal end of the humeral shaft with an anteroposterior width less than that of the proximal end of the shaft; and a radius with a transversely narrow crest on its anterior edge. NMV P48861 differs from *Sulakocetus* by having: somewhat larger humerus, radius and ulna; a head of the humerus subequal in size to the lesser tubercle; and a relatively longer and narrower radius. Because NMV P48861 possesses a combination of dental and forelimb characters only recorded in *Waipatia* or *Sulakocetus*, and lacks any synapomorphies that link this specimen with other odontocete clades, it is referred to an indeterminate species in the family Waipatiidae. A modern redescription and phylogenetic analysis of *Sulakocetus* (to test its relationship with *Waipatia*), plus discovery of forelimb bones referable to *Waipatia*, are required to test the relationships of NMV P48861 hypothesized here.

Biogeography. NMV P48861 represents the first evidence of Waipatiidae from Australia. Previously reported records of waipatiids include *Waipatia maerewhenua* and *W. hectori* from the late Chattian of New Zealand (Fordyce, 1994; Tanaka and Fordyce, 2015b), plus the potential waipatiids *Sulakocetus dagestanicus* from the late Chattian of Caucasus (Mchedlidze, 1976, 1984) and *Sachalinocetus cholmicus* Dubrovo in Siryk and Dubrovo, 1970 from the early Miocene of Sakhalin. In addition, rostral and mandibular fragments with teeth, as well as isolated periotics, referred to Waipatiidae were described from the early Miocene of Malta (Bianucci et al., 2011). Given this geographic and stratigraphic distribution, the occurrence of Waipatiidae in late Oligocene strata of southeast Australia is not surprising and indeed was anticipated by Fordyce (2006: 766).

Nevertheless, the waipatiid from the Jan Juc Marl is only the second odontocete taxon recognized from the Oligocene of Australia, the first, and hitherto only, recorded odontocete being *Prosqualodon* (represented by isolated teeth: Hall, 1911; Fordyce, 1982; Fitzgerald, 2004). Other cetaceans in this assemblage include a probable kekenodontid archaeocete (‘*Squalodon*’ *gambierensis*: Fordyce, 2004; Fitzgerald, 2004), and several small-bodied toothed mysticetes in the family Mammalodontidae (Fitzgerald, 2006, 2010, 2012). Each of these families also occurs in the late Oligocene of New Zealand (Fordyce, 1984, 1991, 2003; Fordyce and Marx, this volume), suggesting a generally similar cetacean fauna throughout the southwest Pacific that lacks confirmed records of taxa typical of Oligocene assemblages elsewhere, e.g., Aetiocetidae (North Pacific) and Xenorophidae (North Atlantic) (Fordyce, 2003). Despite the family-level taxonomic similarities between the late Oligocene cetacean assemblages of Australia and New Zealand, a notable disparity lies in the numerical dominance (and taxonomic richness) of toothed mysticete fossils in Australia versus the rarity of their remains in New Zealand (Fordyce and Marx, this volume). Furthermore, whereas fossils of Eomysticetidae and other Chaeomysticeti are relatively abundant and diverse in the late Oligocene of New Zealand (Boessenecker and Fordyce, 2015a–c; Tsai and Fordyce, 2015), they have not yet been recognized from southeast Australia. However, with continuing research, the absence in Australia of cetacean families recorded in the New Zealand Oligocene will likely become more apparent than real—as exemplified by the waipatiid described here.

Acknowledgements

T. Park, D. Pickering, A. Werner, and T. Ziegler are thanked for finishing preparation of NMV P48861. R. E. Fordyce and A. Grebneff (University of Otago) provided casts of OU 22095, the type specimen of *Waipatia maerewhenua*. L. Barnes and S. McLeod (Natural History Museum of Los Angeles County), D. Bohaska (National Museum of Natural History, Smithsonian Institution), I. von Lichtan (University of Tasmania), and M. Reguero (Museo de La Plata) are thanked for providing access to specimens in their care. Part of this research was carried out during a Smithsonian Postdoctoral Fellowship at the National Museum of Natural History. R. E. Fordyce and O. Lambert carefully and constructively reviewed the manuscript. Tom Rich encouraged the author’s interest in Australian fossil Cetacea, for which he is thanked.

References

Abele, C. 1979. Geology of the Anglesea area, central coastal Victoria. *Memoir of the Geological Survey of Victoria* 31: 1–71.

Barnes, L.G. 2006. A phylogenetic analysis of the superfamily Platanistoidea (Mammalia, Cetacea, Odontoceti). *Beiträge zur Paläontologie* 30: 25–42.

Barnes, L.G., and Reynolds, R.E. 2009. A new species of early Miocene allodelphinid dolphin (Cetacea, Odontoceti, Platanistoidea) from Cajon Pass, southern California, U.S.A. *Museum of Northern Arizona Bulletin* 65: 483–507.

Barnes, L.G., Kimura, M., Furusawa, H., and Sawamura, H. 1995. Classification and distribution of Oligocene Aetiocetidae (Mammalia; Cetacea; Mysticeti) from western North America and Japan. *The Island Arc* 3: 392–431. [For 1994.]

Benham, W.B. 1935. The teeth of an extinct whale, *Microcetus hectori* n. sp. *Transactions of the Royal Society of New Zealand* 65: 239–243.

Benke, H. 1993. Investigations on the osteology and the functional morphology of the flipper of whales and dolphins (Cetacea). *Investigations on Cetacea* 24: 9–252.

Berzin, A.A. 1972. *The Sperm Whale (Kashalot).* Israel Program for Scientific Translations, Jerusalem. 394 pp. [Translated from Russian.]

Bianucci, G., Gatt, M., Catanzariti, R., Sorbi, S., Bonavia, C.G., Curmi, R., and Varola, A. 2011. Systematics, biostratigraphy and evolutionary pattern of the Oligo-Miocene marine mammals from the Maltese Islands. *Geobios* 44: 549–585.

Boessenecker, R.W., and Fordyce, R.E. 2015a. A new genus and species of eomysticetid (Cetacea: Mysticeti) and a reinterpretation of ‘*Mauicetus*’ *lophocephalus* Marples, 1956: Transitional baleen whales from the upper Oligocene of New Zealand. *Zoological Journal of the Linnean Society* 175: 607–660.

Boessenecker, R.W., and Fordyce, R.E. 2015b. A new eomysticetid (Mammalia: Cetacea) from the late Oligocene of New Zealand and a re-evaluation of ‘*Mauicetus waitakiensis*’. *Papers in Palaeontology* 1: 107–140.

Boessenecker, R.W., and Fordyce, R.E. 2015c. Anatomy, feeding ecology, and ontogeny of a transitional baleen whale: a new genus and species of Eomysticetidae (Mammalia: Cetacea) from the Oligocene of New Zealand. *PeerJ* 3:e1129. DOI 10.7717/peerj.1129

Cabrera, A. 1926. Cetáceos fósiles del Museo de La Plata. *Revista Museo de La Plata* 29: 363–411.

Cozzuol, M.A. 1996. The record of the aquatic mammals in southern South America. Pp. 321–342 in: Arratia, G. (ed.), *Contributions of Southern South America to Vertebrate Paleontology.* Münchner Geowissenschaftliche Abhandlungen, Reihe A, Geologie und Paläontologie, 30.

Cozzuol, M.A., and Humbert-Lan, G. 1989. On the systematic position of the genus *Prosqualodon* Lydekker, 1893, and some comments on the odontocete family Squalodontidae. Abstracts of Papers and Posters, Fifth International Theriological Congress, Rome, 22–29 August 1989, 1: 483–484.

Eshelman, R.E., and Ward, L.M. 1994. Tribute to Frank Clifford Whitmore, Jr. *Proceedings of the San Diego Society of Natural History* 29: 3–10.

Fitzgerald, E.M.G. 2004. A review of the Tertiary fossil Cetacea (Mammalia) localities in Australia. *Memoirs of Museum Victoria* 61: 183–208.

Fitzgerald, E.M.G. 2006. A bizarre new toothed mysticete (Cetacea) from Australia and the early evolution of baleen whales. *Proceedings of the Royal Society B: Biological Sciences* 273: 2955–2963.

Fitzgerald, E.M.G. 2010. The morphology and systematics of *Mammalodon colliveri* (Cetacea: Mysticeti), a toothed mysticete from the Oligocene of Australia. *Zoological Journal of the Linnean Society* 158: 367–476.

Fitzgerald, E.M.G. 2012. Archaeocete-like jaws in a baleen whale. *Biology Letters* 8: 94–96.

Flower, W.H. 1885. *An Introduction to the Osteology of the Mammalia*. Third Edition. Macmillan and Co., London [reprinted by A. Asher and Co., Amsterdam (1966)]. 382 pp.

Fordyce, R.E. 1982. A review of Australian fossil Cetacea. *Memoirs of the National Museum of Victoria* 43: 43–58.

Fordyce, R.E. 1983. Rhabdosteid dolphins (Mammalia: Cetacea) from the Middle Miocene, Lake Frome area, South Australia. *Alcheringa* 7: 27–40.

Fordyce, R.E. 1984. Evolution and zoogeography of cetaceans in Australia. Pp. 929–948 in: Archer, M., and Clayton, G. (eds), Vertebrate Zoogeography and Evolution in Australasia. Hesperian Press: Perth. 1203 pp.

Fordyce, R.E. 1991. A new look at the fossil vertebrate record of New Zealand. Pp. 1191–1316 in: Vickers-Rich, P., Monaghan, J.M., Baird, R.F., and Rich, T.H. (eds), Vertebrate Palaeontology of Australasia. Pioneer Design Studio in cooperation with the Monash University Publications Committee: Melbourne. 1437.

Fordyce, R.E. 1994. *Waipatia maerewhenua*, new genus and new species (Waipatiidae, new family), an archaic Late Oligocene dolphin (Cetacea: Odontoceti: Platanistoidea) from New Zealand. *Proceedings of the San Diego Society of Natural History* 29: 147–176.

Fordyce, R.E. 2003. Cetacean evolution and Eocene-Oligocene oceans revisited. Pp. 154–170 in: Prothero, D.R., Ivany, L.C., and Nesbitt, E.A. (eds), From Greenhouse to Icehouse: The Marine Eocene-Oligocene Transition. Columbia University Press: New York. 541 pp.

Fordyce, R.E. 2004. The transition from Archaeoceti to Neoceti: Oligocene archaeocetes in the southwest Pacific. *Journal of Vertebrate Paleontology* 24 (Supplement to 3): 59A.

Fordyce, R.E. 2006. A southern perspective on cetacean evolution and zoogeography. Pp. 755–778 in: Merrick, J.R., Archer, M., Hickey, G.M., and Lee, M.S.Y. (eds), Evolution and Biogeography of Australasian Vertebrates. Auscipub: Oatlands. 942 pp.

Fordyce, R.E., and Marx, F.G. 2016. Mysticetes baring their teeth: a new fossil whale, *Mammalodon hakataramea*, from the southwest Pacific. *Memoirs of Museum Victoria* 74: in press.

Fordyce, R.E., and Muizon, C. de. 2001. Evolutionary history of cetaceans: a review. Pp. 169–233 in: Mazin, J.-M. and Buffrénil, V. de (eds), Secondary Adaptation of Tetrapods to Life in Water. Verlag Dr. Friedrich Pfeil: München. 367 pp.

Geisler, J.H., McGowen, M.R., Yang, G., and Gatesy, J. 2011. A supermatrix analysis of genomic, morphological, and paleontological data from crown Cetacea. *BMC Evolutionary Biology* 11: 112.

Geisler, J.H., Colbert, M.W., and Carew, J.L. 2014. A new fossil species supports an early origin for toothed whale echolocation. *Nature* 508: 383–386.

Glaessner, M.F. 1955. Pelagic fossils (*Aturia*, penguins, whales) from the Tertiary of South Australia. *Records of the South Australian Museum* 11: 353–372.

Gradstein, F.M., Ogg, J.G., Schmitz, M., and Ogg, G. 2012. *The Geologic Time Scale 2012*. Elsevier, Oxford. 1144 pp.

Hall, T.S. 1911. On the systematic position of the species of *Squalodon* and *Zeuglodon* described from Australia and New Zealand. *Proceedings of the Royal Society of Victoria* 23: 257–265.

Howell, A.B. 1927. Contribution to the anatomy of the Chinese finless porpoise, *Neomeris phocaenoides*. *Proceedings of the United States National Museum* 70: 1–43.

Howell, A.B. 1930. Myology of the narwhal (*Monodon monoceros*). *The American Journal of Anatomy* 46: 187–215.

Kellogg, A.R. 1925. On the occurrence of remains of fossil porpoises of the genus *Eurhinodelphis* in North America. *Proceedings of the United States National Museum* 66: 1–40.

Kellogg, A.R. 1965. Fossil marine mammals from the Miocene Calvert Formation of Maryland and Virginia: Part 1. A new whalebone whale from the Miocene Calvert Formation. *United States National Museum Bulletin* 247: 1–45.

Klima, M., Oelschläger, H.A., and Wünsch, D. 1980. Morphology of the pectoral girdle in the Amazon dolphin *Inia geoffrensis* with special reference to the shoulder joint and the movement of the flippers. *Zeitschrift für Säugetierkunde* 45: 288–309.

Lambert, O., Bianucci, G., and Urbina, M. 2014. *Huaridelphis raimondii*, a new early Miocene Squalodelphinidae (Cetacea, Odontoceti) from the Chilcatay Formation, Peru. *Journal of Vertebrate Paleontology* 34: 987–1004.

Lambert, O., Muizon, C. de, and Bianucci, G. 2015. A new archaic homodont toothed cetacean (Mammalia, Cetacea, Odontoceti) from the Early Miocene of Peru. *Geodiversitas* 37: 79–108.

Li, Q., Davies, P.J., and McGowran, B. 1999. Foraminiferal sequence biostratigraphy of the Oligo-Miocene Janjukian strata from Torquay, southeastern Australia. *Australian Journal of Earth Sciences* 46: 261–273.

Marx, F.G., Tsai, C.-H., and Fordyce, R.E. 2015. A new Early Oligocene toothed 'baleen' whale (Mysticeti: Aetiocetidae) from western North America: one of the oldest and the smallest. *Royal Society Open Science* 2: 150476. http://dx.doi.org/10.1098/rsos.150476

McGowran, B., Holdgate, G.R., Li, Q., and Gallagher, S.J. 2004. Cenozoic stratigraphic succession in southeastern Australia. *Australian Journal of Earth Sciences* 51: 459–496.

Mchedlidze, G.A. 1970. *Nekotorye Obshchie Cherty Istorii Kitoobraznykh*. Chast' I. Akademia Nauk Gruzinskoi S.S.R., Institut Paleobiologii, Metsniereba, Tbilisi. 112 pp. [In Russian.]

Mchedlidze, G.A. 1976. *Osnoynye Cherty Paleobiologicheskoi Istorii Kitoobraznykh*. Akademia Nauk Gruzinoskoi S.S.R., Institut Paleobiologii, Metsniereba, Tbilisi. 136 pp. [In Russian.]

Mchedlidze, G.A. 1984. *General Features of the Paleobiological Evolution of Cetacea*. Amerind Publishing Co. Pvt. Ltd., New Delhi. 139 pp. [English translation from Russian.]

McLaren, S., Wallace, M.W., Gallagher, S.J., Dickinson, J.A., and McAllister, A. 2009. Age constraints on Oligocene sedimentation in the Torquay Basin, southeastern Australia. *Australian Journal of Earth Sciences* 56: 595–604.

Muizon, C. de. 1987. The affinities of *Notocetus vanbenedeni*, an Early Miocene platanistoid (Cetacea, Mammalia) from Patagonia, southern Argentina. *American Museum Novitates* 2904: 1–27.

Muizon, C. de. 1988. Le polyphylétisme des Acrodelphidae, odontocètes longirostres du Miocène européen. *Bulletin du Muséum Nationale d'Histoire Naturelle (Paris)* (4)1, Sect. C 10: 31–88.

Muizon, C. de. 1991. A new Ziphiidae (Cetacea) from the Early Miocene of Washington State (USA) and phylogenetic analysis of the major groups of odontocetes. *Bulletin du Muséum Nationale d'Histoire Naturelle (Paris)* (4)3-4, Sect. C 12: 279–326. [For 1990.]

Muizon, C. de. 1994. Are the squalodonts related to the platanistoids? *Proceedings of the San Diego Society of Natural History* 29: 135–146.

Murakami, M., Shimada, C., Hikida, Y., and Hirano, H. 2012. A new basal porpoise, *Pterophocaena nishinoi* (Cetacea, Odontoceti, Delphinoidea), from the upper Miocene of Japan and its phylogenetic relationships. *Journal of Vertebrate Paleontology* 32: 1157–1171.

Nickel, R., Schummer, A., Seiferle, E., Frewein, J., Wilkens, H., and Wille, K.-H. 1986. *The Anatomy of the Domestic Animals. Volume 1. The Locomotor System of the Domestic Mammals.* Verlag Paul Parey, Berlin. 499 pp.

Perrin, W.F. 1975. Variation of spotted and spinner porpoise (genus *Stenella*) in the eastern Pacific and Hawaii. *Bulletin of the Scripps Institution of Oceanography of the University of California* 21: 1–206.

Pilleri, G. 1986. *Beobachtungen an den Fossilen Cetaceen des Kaukasus.* Hirnanatomisches Institut, Ostermundigen, Switzerland. 40 pp.

Pritchard, G.B. 1939. On the discovery of a fossil whale in the older Tertiaries of Torquay, Victoria. *The Victorian Naturalist* 55: 151–159.

Rich, T.H.V. 1975. Potential pre-Pleistocene fossil tetrapod sites in New Zealand. *Mauri Ora* 3: 45–54.

Rich, T.H. 1976. Recent fossil discoveries in Victoria. *Victorian Naturalist* 93: 198–206.

Rich, T.H. 1999. Australia: vertebrate paleontology. Pp. 140–149 in: Singer, R. (ed), Encyclopedia of Paleontology. Volume 1: A–L. Fitzroy Dearborn Publishers: Chicago. 687 pp.

Rich, T.H., and Rich, P.V. 1982. Search for fossils in New Zealand and Australia. *National Geographic Society Research Reports* 14: 557–568.

Sanders, A.E., and Geisler, J.H. 2015. A new basal odontocete from the upper Rupelian of South Carolina, U.S.A., with contributions to the systematics of *Xenorophus* and *Mirocetus* (Mammalia, Cetacea). *Journal of Vertebrate Paleontology* 35:1, e890107.

Schaller, O. 2007. *Illustrated Veterinary Anatomical Nomenclature.* Second Edition. Enke Verlag, Stuttgart. 614 pp.

Schulte, H. von W., and Smith, M. de Forest. 1918. The external characters, skeletal muscles, and peripheral nerves of *Kogia breviceps* (Blainville). *Bulletin of the American Museum of Natural History* 38: 7–72.

Siesser, W.G. 1979. Oligocene–Miocene calcareous nannofossils from the Torquay Basin, Victoria, Australia. *Alcheringa* 3: 159–170.

Siryk, I.M., and Dubrovo, I.A. 1970. Iskopayemyy Zubatyy Kit V Miotsenovykh Otlozheniyakh Yuzhnogo Sakhalina [Fossil toothed whale from the Miocene deposits of the south Sakhalin Island.]. *Geologija i geofizika, Novosibirsk* 1970 (9): 123–129. [In Russian.]

Smith, G.J.D., Browne, K.W., and Gaskin, D.E. 1976. Functional myology of the harbour porpoise, *Phocoena phocoena* (L.). *Canadian Journal of Zoology* 54: 716–729.

Strickler, T.L. 1978. Myology of the shoulder of *Pontoporia blainvillei*, including a review of the literature on shoulder morphology in the Cetacea. *American Journal of Anatomy* 152: 419–431.

Tanaka, Y., and Fordyce, R.E. 2014. Fossil dolphin *Otekaikea marplesi* (latest Oligocene, New Zealand) expands the morphological and taxonomic diversity of Oligocene cetaceans. *PLoS ONE* 9(9): e107972.

Tanaka, Y., and Fordyce, R.E. 2015a. A new Oligo-Miocene dolphin from New Zealand: *Otekaikea huata* expands diversity of the early Platanistoidea. *Palaeontologia Electronica* 18.2.23A: 1–71.

Tanaka, Y., and Fordyce, R.E. 2015b. Historically significant late Oligocene dolphin *Microcetus hectori* Benham 1935: a new species of *Waipatia* (Platanistoidea). *Journal of the Royal Society of New Zealand* DOI: 10.1080/03036758.2015.1016046.

Tsai, C.-H., and Fordyce, R.E. 2015. The earliest gulp-feeding mysticete (Cetacea: Mysticeti) from the Oligocene of New Zealand. *Journal of Mammalian Evolution* 22: 535–560.

Uhen, M.D. 2004. Form, function, and anatomy of *Dorudon atrox* (Mammalia, Cetacea): an archaeocete from the Middle to Late Eocene of Egypt. *University of Michigan Papers on Paleontology* 34: 1–222.

Vickers-Rich, P., and Rich, T.H. 1993. *Wildlife of Gondwana.* Reed, Chatswood. 276 pp.

Warne, M.T., Archbold, N.W., Bock, P.E., Darragh, T.A., Detmann, M.E., Douglas, J.G., Gratsianova, R.T., Grover, M., Holloway, D.J., Holmes, F.C., Irwin, R.P., Jell, P.A., Long, J.A., Mawson, R., Partridge, A.D., Pickett, J.W., Rich, T.H., Richardson, J.R., Simpson, A.J., Talent, J.A., and VandenBerg, A.H.M. 2003. Palaeontology: the biogeohistory of Victoria. Pp. 605–652 in: Birch, W.D. (ed), Geology of Victoria. Geological Society of Australia Special Publication 23, Geological Society of Australia (Victoria Division): Melbourne. 842 pp.

Memoirs of Museum Victoria 74: 137–150 (2016) Published 2016

ISSN 1447-2546 (Print) 1447-2554 (On-line)
http://museumvictoria.com.au/about/books-and-journals/journals/memoirs-of-museum-victoria/

Earliest known record of a hypercarnivorous dasyurid (Marsupialia), from newly discovered carbonates beyond the Riversleigh World Heritage Area, north Queensland

Michael Archer[1,*] (http://zoobank.org/urn:lsid:zoobank.org:author:F834D7C6-E2E5-47B3-9209-AF1820AF766B), Olivia Christmas[1], Suzanne J. Hand[1] (http://zoobank.org/urn:lsid:zoobank.org:author:632F42CF-93FF-48E2-A0BA-D2FA65639D98), Karen H. Black[1] (http://zoobank.org/urn:lsid:zoobank.org:author: 3DCED980-309C-44EE-8A79-7C2B7766FF19), Phil Creaser[1], Henk Godthelp[1], Ian Graham[1], David Cohen[1], Derrick A. Arena[1,2], Caitlin Anderson[1], Georgia Soares[1], Naomi Machin[1], Robin M. D. Beck[1,3], Laura A. B. Wilson[1], Troy J. Myers[1], Anna K. Gillespie[1], Bok Khoo[1], and Kenny J. Travouillon[4,5]

[1] PANGEA Research Centre, School of Biological, Earth & Environmental Sciences, UNSW, Sydney, NSW 2052, Australia
[2] Associated Scientific Ltd, Australia
[3] School of Environment & Life Sciences, Peel Building, University of Salford, Salford M5 4WT, UK
[4] School of Earth Sciences, University of Queensland, St Lucia, Queensland 4072, Australia
[5] Western Australian Museum, Locked Bag 49, Welshpool DC, WA 6986, Australia
* To whom correspondence should be addressed. E-mail: m.archer@unsw.edu.au

http://zoobank.org/urn:lsid:zoobank.org:pub:61B65B3D-6DC0-4763-83A7-7EA10DB105E7

Abstract

Archer, M., Christmas, O., Hand, S.J., Black, K.H., Creaser, P., Godthelp, H., Graham, I., Cohen, D., Arena, D.A., Anderson, C., Soares, G., Machin, N., Beck, R.M.D., Wilson, L.A.B., Myers, T.J., Gillespie, A.K., Khoo, B., and Travouillon, K.J. 2016. Earliest known record of a hypercarnivorous dasyurid (Marsupialia), from newly discovered carbonates beyond the Riversleigh World Heritage Area, north Queensland. *Memoirs of Museum Victoria* 74: 137–150.

Whollydooleya tomnpatrichorum gen. et sp. nov. is a new, highly specialised hypercarnivorous dasyuromorphian from a new mid-Cenozoic limestone deposit southwest of the Riversleigh World Heritage Area in northwestern Queensland. Dental dimensions suggest it may have weighed at least twice as much as the living Tasmanian devil (*Sarcophilus harrisii*). Although known only from a lower molar, it exhibits a plethora of carnivorous adaptations including a hypertrophied protoconid, tiny metaconid and a battery of vertical carnassial blades between most of the major cusps, most of which incorporate carnassial notches to immobilise materials being sheared. It is unique among dasyuromorphians in having a massive entoconid that closes the entire lingual side of the talonid. Comparison with previously known thylacinid and dasyurid hypercarnivores suggests its relationships are closer to dasyurids than thylacinids in the main because of the very large entoconid, a cusp that is relatively small to absent in all known thylacinids but commonly small to large in dasyurids. However, the extent of enlargement of the entoconid suggests that it is not closely related to previously known Cenozoic hypercarnivorous dasyurids in the genera *Dasyurus*, *Glaucodon*, *Sarcophilus* or any of the other previously described Cenozoic dasyurids. Although the early late Miocene *Ganbulanyi djadjinguli* is only known from an upper molar, the reduced area of its protocone suggests a correspondingly reduced rather than hypertrophied entoconid in its as-yet-unknown lower molars. Reconsideration of the structure of the talonid in species of *Sarcophilus* even suggests that within that Quaternary lineage, the entoconid may have been entirely lost, with the posteriorly displaced metaconid taking its functional place as an occlusal counterpart for the blades of the protocone. The large size of the new species signals the earliest indication within the dasyurid radiation of a late Cenozoic trend towards gigantism that became evident in many lineages of Australian marsupials. While the age is uncertain, on the basis of associated taxa such as species of *Ekaltadeta*, it is probably either mid or late Miocene in age. Geological features of the deposit suggest it was formed within a pool in a cave environment that periodically underwent desiccation. Some grains suggest an aeolian as well as an alluvial and pluvial origin for the deposit. This may relate to current understanding about environmental change that took place in the region following the mid Miocene climate oscillation.

Keywords

Dasyuridae; Dasyurinae; Thylacinidae; Riversleigh; Miocene; *Whollydooleya*; *Dasyurus*; *Sarcophilus*; *Glaucodon*; *Ganbulanyi*; *Thylacinus*

Introduction

In 2012, M. Archer, P. Creaser and H. Godthelp, with the assistance of the Queensland Parks and Wildlife Service, had the opportunity to explore a Cenozoic terrain approximately 1.2 km southeast of the southwestern border of the Riversleigh World Heritage Area but within the boundaries of Boodjamulla (Lawn Hill) National Park in northwestern Queensland. The purpose was to test an unpublished hypothesis developed by geologist Ned Stephenson. He had concluded (and speculatively mapped) on the basis of satellite data that Cenozoic freshwater limestone deposits similar to those contained within the World Heritage Area might occur within an equally vast region southwest of the known fossil deposits. A similar inference about the fossiliferous potential of the rocks in this same general area had previously been suggested by Rick Arena in 2009 on the basis of Google Earth imagery. One of the first ground-based discoveries that supported this hypothesis, made by P. Creaser, was a fossil deposit named Wholly Dooley Site on an isolated limestone knoll named Wholly Dooley Hill. Small samples of Wholly Dooley matrix were treated with acetic acid in the UNSW laboratory to obtain samples of the vertebrate fauna.

Among the first teeth recovered was a highly distinctive lower molar of a carnivorous marsupial, which is the subject of this paper. In 2013, the National Geographic Society provided research funding to M. Archer and colleagues to continue exploration in this remote region of northwestern Queensland. Additional new sites and faunal assemblages were discovered in 2013 and 2014 in the new area, now named New Riversleigh, but as yet none have produced additional specimens of this new carnivore.

Although several fossil Oligo-Miocene putative dasyurids or dasyurid-like taxa have already been described from the Riversleigh region (i.e., species of *Ganbulanyi*, *Barinya*, *Mayigriphus, Malleodectes* and *Joculusium*; Wroe, 1997a, 1998, 1999, 2001; Arena et al., 2011), these are significantly different from *Whollydooleya tomnpatrichorum* gen. et sp. nov. in terms of key structural features (see below in Comparisons). Although the only known specimen of *Ganbulanyi djadjinguli* Wroe, 1998 is a fractured, isolated upper molar with some features suggesting it was a hypercarnivore, in other features it too is clearly distinct as well as significantly smaller than the taxon described herein. Other distinctive Australian carnivorous marsupials previously described as late Oligocene dasyurids (e.g., *Ankotarinja*, *Keeuna*, *Wakamatha* and *Dasyulurinja* [Archer, 1976a, 1982; Archer and Rich, 1979] relegated by Wroe [1996, 1997b] to Dasyuromorphia *incertae sedis* and Godthelp et al. [1999] to Marsupialia *incertae sedis*), are tiny to small insectivores all of which lack the hypercarnivorous specialisations evident in *W. tomnpatrichorum*.

Abbreviations used in this paper include the following: QM F, Queensland Museum palaeontological collections; NMV P, Museum Victoria Palaeontology Collection; prd, protoconid; med, metaconid; hyd, hypoconid; end, entoconid; hyld, hypoconulid; co, cristid obliqua; mcd, metacristid; STB, stylar cusp B; STD, stylar cusp D. Molar morphology follows that used by Archer (1976b) or is self-explanatory or in common use. Thegotic terminology (e.g., alpha-scissorial) follows that used by Every (1970). Molar serial homology follows that used by Thomas (1888).

Systematics

Dasyuridae Goldfuss, 1820

?Dasyurinae Goldfuss, 1820

Whollydooleya Archer et al., gen. nov.

Generic diagnosis. Species of *Whollydooleya* differ from all other dasyuromorphians in having a massive (rather than blade-like, conical or reduced) entoconid that completely closes the lingual flank of the talonid.

Type species. *Whollydooleya tomnpatrichorum* Archer et al., 2015, sp. nov., by monotypy.

Whollydooleya tomnpatrichorum Archer et al., 2015, sp. nov.

Zoobank LSID. http://zoobank.org/urn:lsid:zoobank.org:act:9BAE184C-8E93-4E74-B10C-DB66EF882E82

Specific diagnosis. That of the genus until additional species are known.

Holotype. QM F57892, partial right lower molar, interpreted to be either M_2 or M_3.

Type locality. Wholly Dooley Site, Wholly Dooley Hill, the New Riversleigh area, southwest and adjacent to the Riversleigh World Heritage Area, northwestern Queensland. Wholly Dooley Site is one of several fossiliferous localities discovered by P. Creaser et al. on Wholly Dooley Hill in 2012. GPS coordinates for this site have been recorded with the Queensland Museum, Brisbane.

Etymology. The generic name refers to Wholly Dooley Site, which was discovered and named in 2012 by P. Creaser following preliminary analyses of satellite data by Ned Stephenson and Google Earth imagery by Rick Arena. The generic name is hereby given masculine gender. The species name honours Tom and Pat Rich for their years of research that included joint work on the mid-Cenozoic deposits of Riversleigh.

Geological context

The Wholly Dooley Site deposit (Fig. 1) shares a number of characteristics with other deposits at Riversleigh that indicate it represents an accumulation formed within a cave whose walls and ceiling have subsequently eroded away (Arena et al., 2014). The host micrite is dominated by calcite, with moderately common broken mollusc shell fragments and detrital quartz grains (Fig. 2A) and uncommon calcite pelloids and calcite rafts (Fig. 2B). The occurrence of calcite cave rafts is indicative of a quiescent pool of carbonate-rich water and suggests that these formed within a karst environment, possibly a small cave pool.

There is a clearly defined erosional contact between the host micrite and an overlying layer (layer 2; Fig. 2C). This layer comprises Fe-oxide (various mixtures of hematite and goethite), pelloids (Fig. 2D), detrital quartz grains and abundant late calcite-fill. Quartz in this later fill occurs as equant to prismatic,

Figure 1. Wholly Dooley Site, Wholly Dooley Hill, northwestern Queensland. The grey limestone massifs to the left are unfossiliferous Cambrian limestone and probably represent part of the western and southern walls of the original cave chamber. Fossiliferous Wholly Dooley matrix has been obtained from the excavated depression in the centre. About 7.2 km NE from this point is the approximate centre of the Riversleigh World Heritage Area; about 1.2 km NWN from this point is the southwestern boundary of the RWHA. Photo M. Archer.

subangular to well-rounded grains. Some of the quartz grains are highly fractured and coated in hematite/goethite, suggesting an aeolian origin. The abundance of goethite within this layer as fine colloidal aggregates and growths suggests a change in the environment, with drying-out of the cave system and evaporation of oxygen-rich cave waters, leading to *in situ* Fe-oxide precipitation. This drying-out of the environment is also indicated by the aeolian-derived detrital quartz grains. However, the lack of conspicuous desiccation cracks suggests that the sediment remained damp as it accumulated within the cave environment.

Layer 2 is unconformably overlain (erosional contact) by layer 3. Layer 3 comprises relatively abundant detrital quartz grains, and distinctly rhythmically banded goethite/calcite (Fig. 3A), with calcite also occurring as a void–fill phase (Fig. 3B). The layer also contains rare well-rounded subequant detrital tourmaline grains and cryptocrystalline silica as overgrowths around detrital quartz grains (Fig. 3C). Also within this layer is possible microbial-mediated goethite (Fig. 3D). The occurrence of rhythmically banded goethite/calcite suggests constantly changing water chemistry, from carbonate-rich waters to oxygen-rich waters, throughout crystallisation of this layer. The microbial-mediated goethite suggests that the system was exposed to at least periodic sunlight, and may indicate unroofing of the cave system.

The proposed paragenesis of Wholly Dooley Site is detrital quartz and tourmaline and fossil bone fragments, followed by calcite ($CaCO_3$), then rhythmic deposition of goethite (FeO(OH)) and calcite ($CaCO_3$). However the overall composition is highly variable, ranging from 10 to 30 modal% quartz, 20 to 40 modal% colloidal goethite and 30 to 70 modal% calcite cement. The size and shape of quartz grains are highly variable, ranging from subangular to well-rounded and equant to subprismatic in shape and the quartz grains are poorly sorted. There is also evidence of well-developed undulose extinction within many of

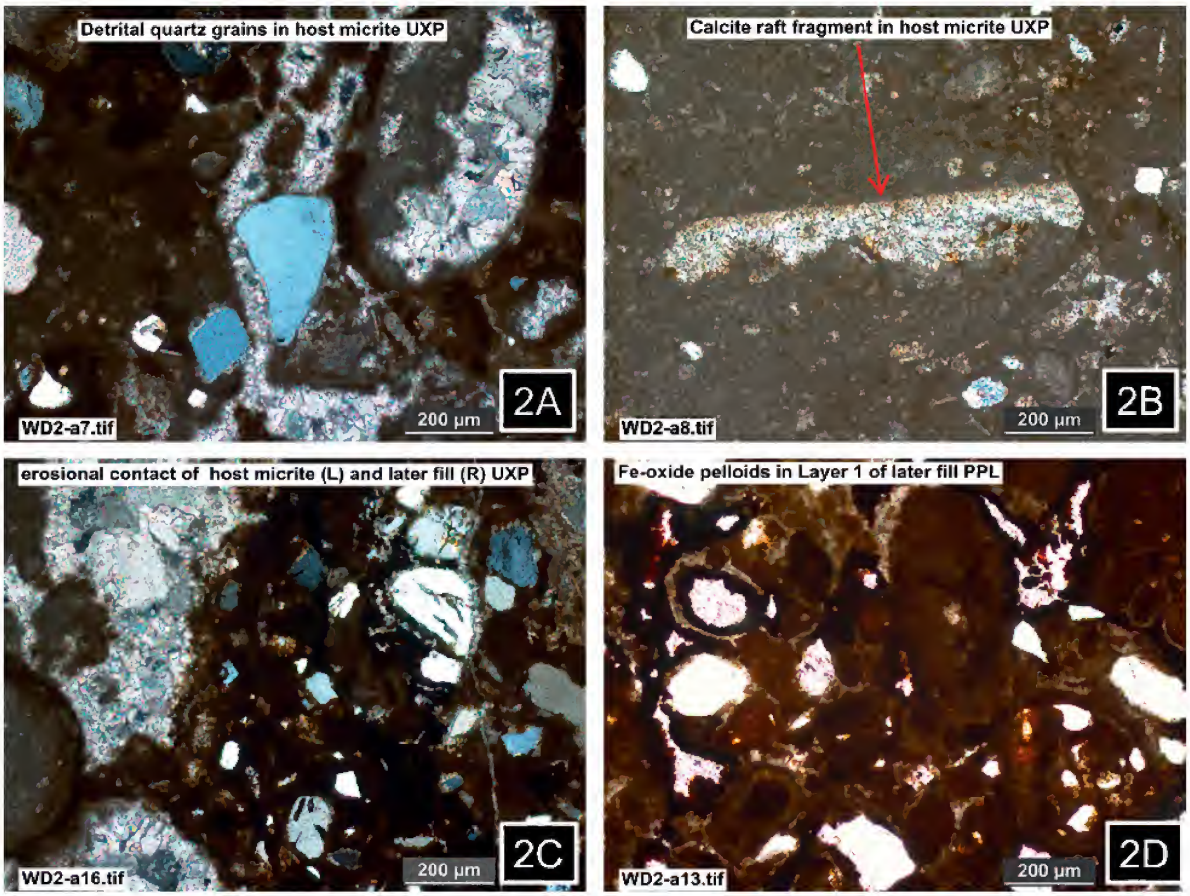

Figure 2. Photomicrographs of geological thin sections from Wholly Dooley Site. A, Detrital quartz grains within the host micrite UXP; B, calcite raft fragment within host micrite UXP; C, erosional contact between host micrite (left) and overlying layer 1 (right) showing abundant aeolian-derived quartz within layer 1 UXP; D, Fe-oxide pelloids and detrital quartz grains within layer 1 PPL. WD2 numbers refer to thin section images produced in the School of Biological, Earth & Environmental Sciences.

the quartz grains, along with uncommon recrystallised quartz grains. These features suggest that the detrital quartz grains are derived from at least three sources, including: 1, a proximal source via eluvial deposition (angular prismatic grains); 2, a more distal source via aeolian deposition (hematite-coated highly fractured equant-shaped well-rounded grains); and 3, a more distal source (subrounded to well-rounded equant to subprismatic grains) introduced via alluvial processes.

On balance, these sedimentological attributes suggest this deposit accumulated under somewhat different circumstances than those involved in accumulation of the previously known Oligo-Miocene fossil deposits from the Riversleigh World Heritage Area. The suggestion of intermittent desiccation may indicate accumulation during a younger, climatically drier period than those involved in triggering Depositional Phases 1–3 in the Riversleigh World Heritage Area (Creaser, 1997; Arena, 2004; Woodhead et al., 2014).

Description of the holotype

The holotype (Figs 4A–C, 5, 6, 9A-A'), which is comparable in size to the M_3 of the extant Tasmanian devil (*Sarcophilus harrisii*)[1], retains the entire talonid and broken posterior half of the trigonid. Partially repaired damage to the protoconid, from accidental breakage during preparation, has resulted in retention of a small displaced fracture that extends across the posterior face of the trigonid from the metaconid to the base of the protoconid. Structures missing from this tooth because of natural, taphonomic loss include the protocristid, paraconid and anterior cingulid.

1 There is uncertainty in the current literature about the nomenclatural relationship of *laniarius* Owen, 1838 and *harrisii* Boitard, 1841. Here we follow Dawson (1982) in using *harrisii* as the appropriate name for the living species on the interpretation that the larger extinct and smaller living Tasmanian Devils are neither clearly synonymous nor chronospecies.

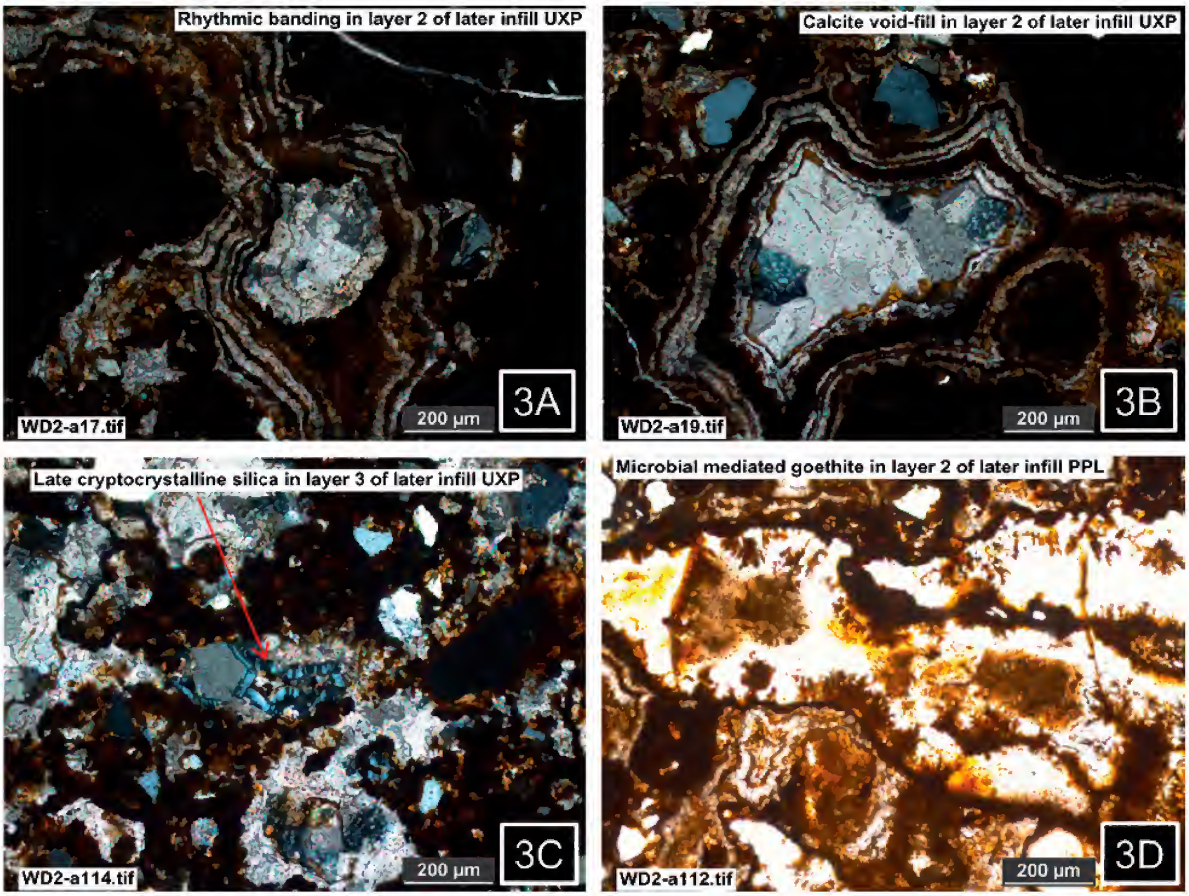

Figure 3. Photomicrographs of geological thin sections from Wholly Dooley Site later infills. A, Rhythmically banded calcite and goethite UXP; B, calcite filling void in layer 2 UXP; C, late cryptocrystalline silica (indicated by red arrow) filling fractures UXP; D, possible microbially mediated goethite precipitation (dendrites) in layer 2 PPL. WD2 numbers represent images of thin sections produced in the University of New South Wales.

The trigonid has a massive, well-developed protoconid and very small metaconid on the posterolingual flank of the protoconid. There is a rudimentary but distinct carnassial notch between the metaconid and metacristid at the point where the metaconid diverges from the posterolingual flank of the trigonid. There is a nearly vertical postmetacristid that descends from the metaconid to form the anterior half of a carnassial notch in a small, very steeply inclined lingual blade composed of the preentocristid and postmetacristid, as occurs in some dasyurids (e.g., species of *Dasyurus*).

The extremely steeply inclined metacristid, which is close to vertical in orientation, has sustained wear resulting from mastication that has breached the enamel on the lingual side of the trigonid with consequent production of a very sharp cutting edge along the shearing edge of this blade. The enamel exposed at the margins of this blade, and elsewhere over the entire crown, is very thin.

The posterior flank of the metacristid has been secondarily (during life) planed off by the preparacrista and preprotocrista of the corresponding upper molar producing a thegotic facette that covers most of the posterior flank of the trigonid trailing the dorsal leading edge of the metacristid blade, as occurs in all other dasyuromorphians. The wear striae on this facette are uniformly shallow, unidirectional and extend the length of the facette, features that are normal attributes of thegotic facettes (Every, 1970). This extensive facette also extends onto the posterobuccal apex of the metaconid after bridging rather than faceting the notch between the metaconid and metacristid. The tip of the protoconid, insofar as it is preserved, exhibits a very small apical wear facette, suggesting that this animal was relatively young at the time of death and that the extremely well-developed facette on the posterior flank of the metacristid is in fact primarily the result of tooth/tooth thegosis rather than mastication involving food. Nevertheless it is possible that the thegotic striations have

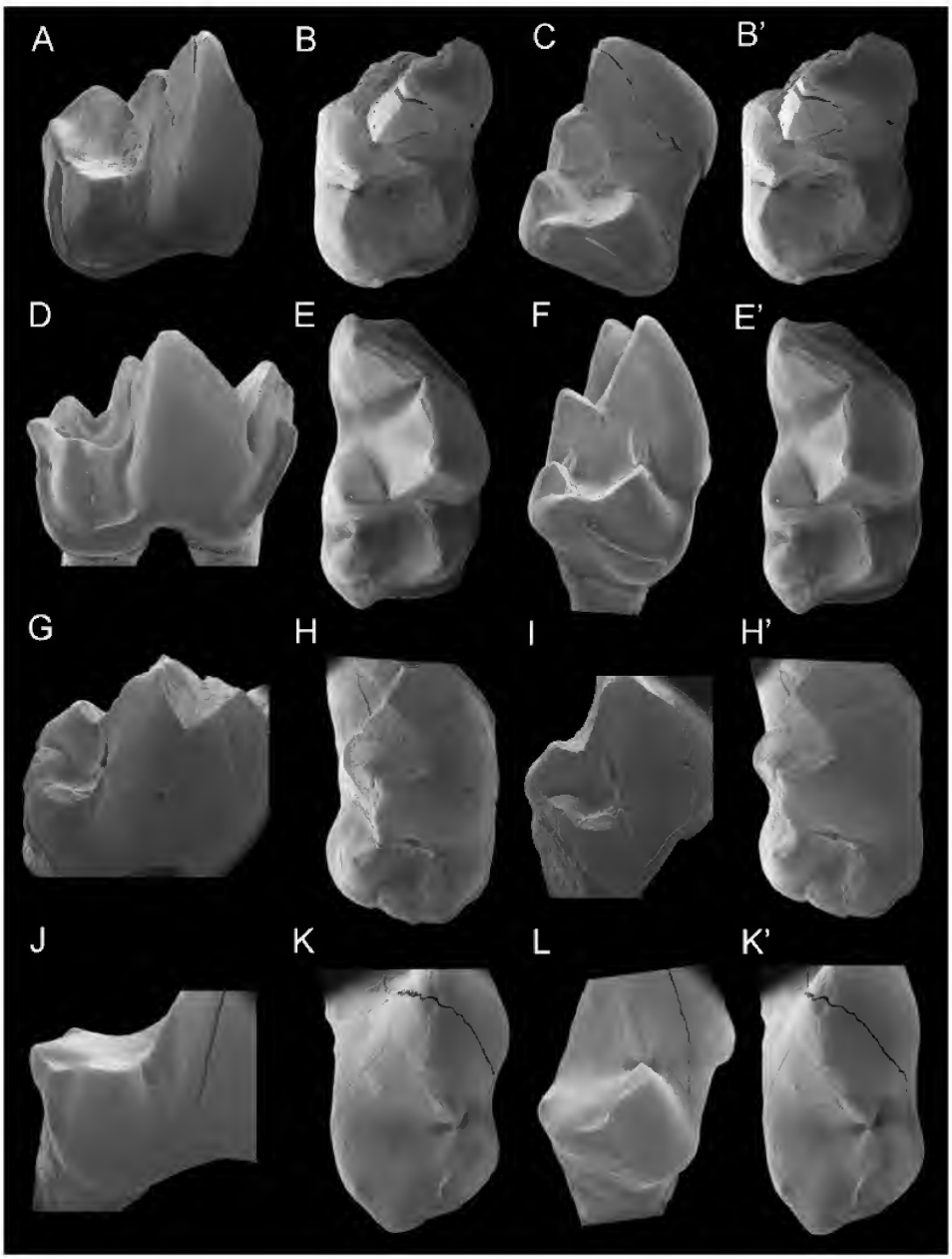

Figure 4. Comparison of the holotype of *Whollydooleya tomnpatrichorum* n. gen. et sp. QM F57892 with other hypercarnivorous dasyuromorphians (not to scale). A–C, *W. tomnpatrichorum*, QM F57892, m2 or m3. A, posterobuccal view; B-B', occlusal stereoview; C, oblique posterobuccal view. D–F, *Dasyurus maculatus*, AR21693, M_3. D, buccal view; E-E', occlusal stereoview; F, oblique posterobuccal view. G–I, *Sarcophilus harrisii*, AR21694, M_3. G, buccal oblique view; H-H', occlusal stereoview; I, oblique posterobuccal view. J–L, *Thylacinus cynocephalus*, AR21695, M_3 talonid (reversed from the LM_3). J, posterobuccal oblique view; K-K', occlusal stereoview; L, oblique posterobuccal view.

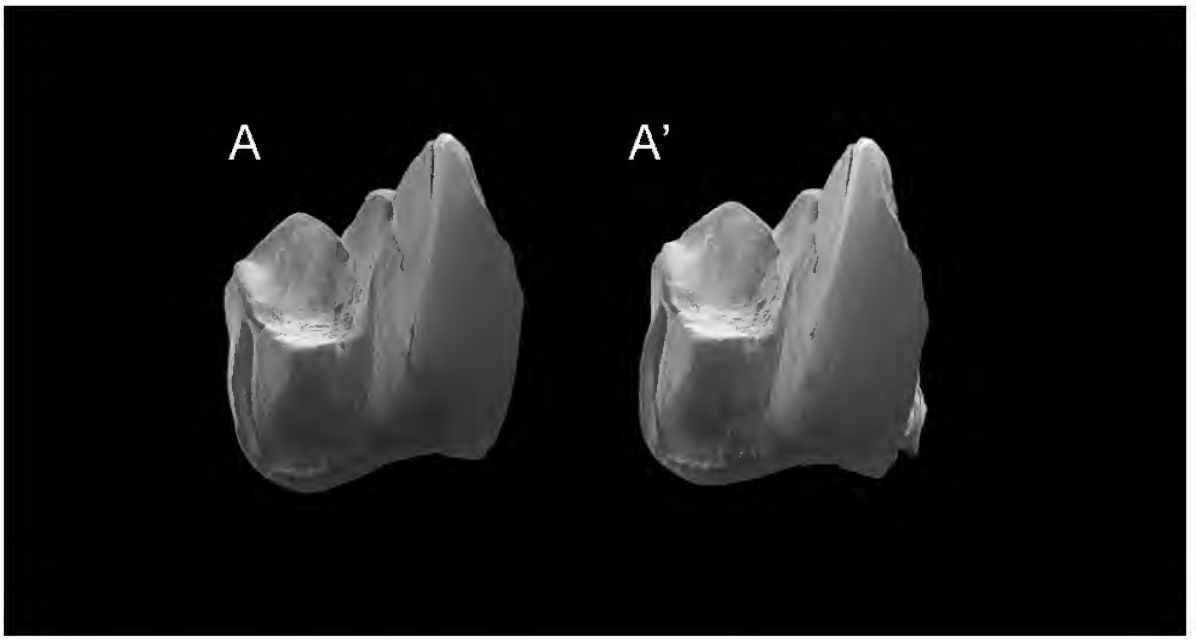

Figure 5. Stereoviews of the holotype of *Whollydooleya tomnpatrichorum* n. gen. et sp. QM F57892 from a buccal oblique view. The margin at the right represents the missing flank of the trigonid.

been overprinted on what may have been more irregular scorings resulting from mastication.

There is no buccal cingulum evident at the base of the protoconid, which is also characteristic of most dasyuromorphians (but not universal; e.g. species of *Dasyuroides* can exhibit better-developed buccal cingulids; Archer 1976b). However, the trigonid is broken, so structures that may have been present anterior to the widest point of the trigonid are unknown.

The talonid is wider than the trigonid and supports three cusps. The hypoconid is robust with a well-developed cristid obliqua and posthypocristid. The cristid obliqua appears to have extended towards the midpoint of the posterior flank of the trigonid, meeting the latter about midway up the height of the trigonid, although it is worn from the lowest point along this blade to the position of its attachment on the trigonid. There is a kink in the cristid obliqua at the low point, suggesting that there may have been a carnassial notch between the posterior descending and anterior ascending sections of the cristid obliqua, as occurs in most dasyuromorphians. On the anterior side of the junction between these two parts of the cristid obliqua, at the low point on the buccal side of the interface between the trigonid and talonid, there also appears to be a remnant of a small neomorphic cuspid. Wear of the cristid obliqua has produced a small carnassial notch that operates obliquely between this cuspid and the prehypocristid.

On the posterior flank of the hypoconid, subtending the posthypocristid blade, there is a distinctive thegotic facette that was produced by the premetacrista of the corresponding upper molar that parallels the far larger facette produced by the preparacrista of the upper molar on the posterior flank of the trigonid, hence both are the result of the same movement of the mandible. This facette similarly reveals fine, unidirectional oblique striations cut into the enamel. This posthypocristid facette extends ventrally across a small gap to include the buccal half of the ascending posterior cingulid, resulting in breached enamel and a dentine trough within the postcingulid (= the posterior cingulid). This part of the facette developed on the postcingulid was almost certainly caused by thegosis involving the apex of the metacone of the corresponding upper molar. There is also a wear facette on the anterior flank of the hypoconid subtending the prehypocristid that was produced by the postparacrista of the corresponding upper molar, a facette also commonly seen in dasyuromorphians, even in species of *Sarcophilus* that have undergone hypotrophy of the talonid.

The posthypocristid leading edge is notched along its length suggesting that it has been used to segment reasonably hard materials. While these notches could be the result of postmortem damage, given their restriction to the leading edge of this blade, it is more likely that they reflect use during the life of the animal. The posthypocristid terminates lingually before it includes or contacts the hypoconulid.

The hypoconulid is developed as a relatively (compared with the hypoconid and entoconid) small talonid cusp in the form of a short, imprecise, buccolingual vertical blade that is orientated in line with the posthypocristid and in effect extends that blade across a low gap between the two blades emanating from these cusps. Holistically, the hypoconulidcristid and the

posthypocristid form a combined transverse blade with a carnassial notch in effect developed by the low gap between the two blade segments. The buccal end of the hypoconulidcristid terminates at the junction of the lingual end of the posterior cingulid and the lingual end of the posthypocristid. Unlike the entoconid and hypoconid, there is no distinct high point on the hypoconulid; rather it is a small transverse ridge. It does not extend sufficiently posteriorly to have acted as an effective interlocking device inserted into the anterior cingulid of the succeeding molar. On its posterior flank there is a coarse wear facette indicating interdental abrasion with the anterior edge of the succeeding molar. The overall relationship between the hypoconid and hypoconulid is similar to that seen in some of the largest dasyurine dasyurids (species of *Glaucodon* and *Sarcophilus*) but differs from the condition seen in other dasyurids and in thylacinids where the hypoconulid of the M_2 is as large as or larger than the entoconid and projects posteriad to interlock within the anterior cingulid of M_3.

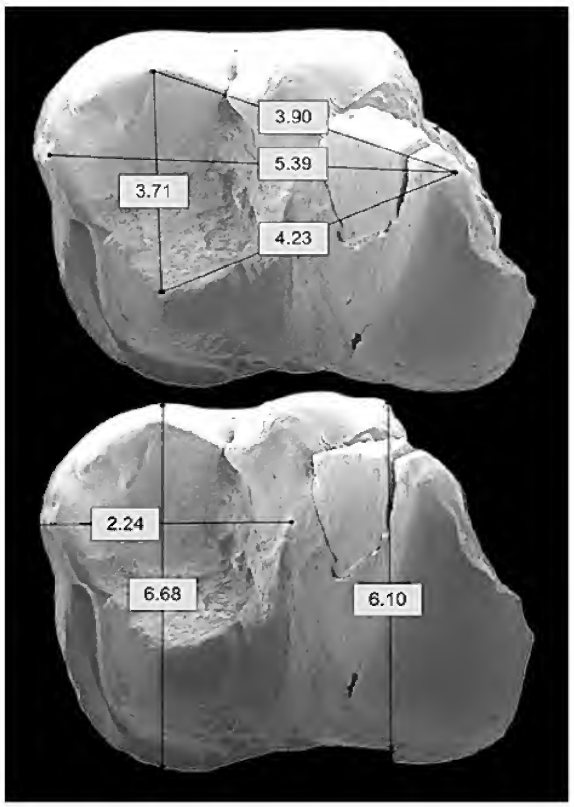

Figure 6. Measurements of the holotype of *Whollydooleya tomnpatrichorum* n. gen. et sp. QM F57892 in occlusal stereoview. In the upper figure, the sides of the triangle link: 1, protoconid to entoconid; 2, protoconid to hypoconid; and 3, entoconid to hypoconid. The longitudinal measure is the distance between the protoconid and the apex of the hypoconulid. In the lower figure, the measures are: talonid width through the entoconid and hypoconid; talonid length from the ascending extremity of the cristid obliqua against the posterior flank of the trigonid to the posterior extremity of the crown through the hypoconulid; and maximum width of the damaged trigonid.

The entoconid has a short preentocristid developed in relation to the postmetacristid, as noted above. Although the posterior as well as anterior flanks of the entoconid are relatively massive, there is no distinct postentocristid as such (although there is a poorly defined ridge descending its posterobuccal flank that is probably a vestigial homologue of this otherwise missing blade); as a result, there was a small open trough between the bases of the entoconid and hypoconulid such as occurs in most dasyuromorphians that have not reduced their talonids. Hence, there was no shearing activity provided by this specific region of the talonid.

The upper part of the buccal face of the entoconid exhibits a wear facette produced by the lingual face of the protocone of the corresponding upper molar. The intra-talonid bases of all talonid cusps facing each other across the talonid basin as well as the central part of the talonid basin itself, appear to be missing enamel. This may have been the result of attrition produced by occlusion with the corresponding protocone of the upper molar, but this seems improbable given the very limited masticatory wear on all cusps of this tooth. It is perhaps more likely that the enamel is missing because of chemical erosion resulting from some taphonomic process such as root-acid dissolution. Hence when cleaning the tooth, we stopped when the surface appeared to represent dentine.

The postcingulid descends from a distinct starting point about three-quarters of the way from the buccal side of the tooth, down around the base of the hypoconid and anteriorly as far as the posterobuccal base of the protoconid. On the buccal side, this cingulid is disrupted by small cuspids along its length. Seemingly similar cuspids, unattached to the basal cingulid, occur on the lowest anterobuccal flank of the prehypocristid portion of the cristid obliqua.

Comparisons

Based on overall morphology, there can be little doubt that *W. tomnpatrichorum* represents a dasyuromorphian. While definitive familial identification is uncertain given the lack of basicranial information (Wroe, 1999), the highly derived molar morphology including the plethora of vertical blades with carnassial notches (e.g., metacristid and preentocristid), hypotrophied metaconid and hypertrophied protoconid, strongly suggests that it represents this group. This overall conclusion is also supported by the argument of Voss and Jansa (2009) that while loss of the posterior cingulid (which is conspicuously present in *W. tomnpatrichorum*) is a synapomorphy of Marsupialia, secondary presence of this structure is a synapomorphy of dasyuromorphians.

Of the many different kinds of dasyuromorphians already known (e.g., Archer, 1982; Wroe, 2003), in its very reduced metaconid and hypertrophied protoconid it shares most derived features with dasyurine dasyurids and, to a lesser extent, thylacinids. Comparisons here have been made specifically with all of the largest and most specialised of the dasyurine dasyurids including the living Tiger Quoll (*Dasyurus maculatus*; Figs

Figure 7. NMV P207018, cast of a right dentary referred to *Glaucodon ballaratensis* by Gerdtz and Archbold (2003) that preserves the RC_1, P_{1-2} and M_{1-4}. Left upper, buccal view. Left lower, lingual view. Right, occlusal view of the dentition. Scale bar = 1 cm. Photographs by Darren Bellingham.

4D–F, 9B-B'), the early late Miocene *Gadbulanyi djadjinguli* (Wroe, 1998), the Pliocene *Glaucodon ballaratensis* (Figs 7, 9C-C'), the living Tasmanian Devil (*S. harrisii*; Figs 4G–I, 9E-E'), the early Pleistocene devil (*Sarcophilus moornaensis*; Figs 8, 9D-D'), and the Thylacine (*Thylacinus cynocephalus*; Figs 4J–L, 9F-F'). Juxtaposed M_3s of these taxa are presented in Figure 9. No lower molar is known for *G. djadjinguli*. Other mid to late Cenozoic dasyurid-like taxa known on the basis of molars from Riversleigh include species of *Barinya*, *Mayigriphus* and *Joculusium* but none of these have hypercarnivorous specialisations of the kind exhibited by *W. tomnpatrichorum*.

Comparisons here primarily involve M_2 and/or M_3 (Fig. 9). While position homology of the holotype of *W. tomnpatrichorum* is uncertain, the large talonid of the Wholly Dooley specimen means that it is highly likely that it is not M_4 given that the talonid of the posterior molar in all dasyuromorphians is much narrower than the trigonid. While it could be an M_1, this seems improbable because the hypoconid is very much lower in height than the protoconid. In the M_1 of larger dasyuromorphians, particularly the hypercarnivores, the hypoconid on M_1 is commonly almost half to three-quarters the height of the protoconid, while in the M_3 it is rarely more than a quarter the height of the protoconid—which is the condition seen in the holotype of *W. tomnpatrichorum*.

A buccal cingulid surrounding the base of the talonid, which is well-developed in *W. tomnpatrichorum* and all of the larger dasyurines including species of *Sarcophilus* (despite the latter having significantly hypotrophied talonids), is not present in the modern Thylacine (*T. cynocephalus*). It is present, however, in some Miocene thylacinids (e.g., *Badjcinus turnbulli*) and hence its absence in *T. cynocephalus* is almost certainly an autapomorphy.

The most striking feature of the talonid of *W. tomnpatrichorum* is the very large entoconid with well-developed, longitudinal pre-entocristids and poorly-developed postentocristid. These blades virtually enclose the whole of the lingual side of the talonid. This is in distinct contrast to all

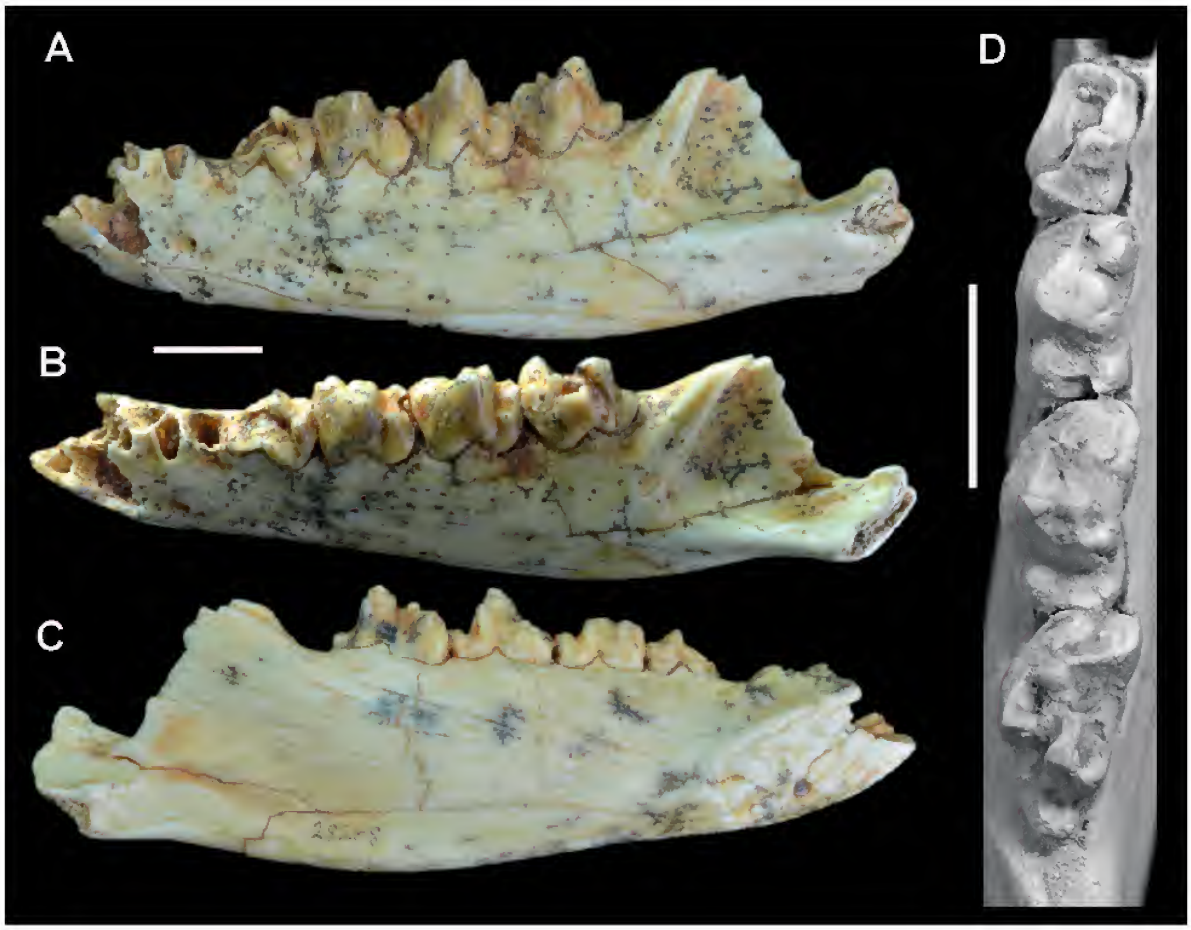

Figure 8. NMV P28684, right dentary of the holotype of *Sarcophilus moornaensis* preserving damaged M_{1-4}. A, Buccal view; B, buccal oblique view; C, lingual view; D, occlusal view of M_{1-4}. Photographs by Erich Fitzgerald.

known thylacinids, which have relatively small to almost absent entoconids that are also conical in shape without hypertrophy of any subtended longitudinal blades.

Considering entoconid development in dasyurines, none exhibit hypertrophy of this cusp remotely to the extent shown in *W. tomnpatrichorum*, although less specialised dasyurines such as species of *Dasyurus* have large (albeit much smaller than those in *W. tomnpatrichorum*) entoconids with distinct pre- and postentocristids. In *D. maculatus* (Figs 4D–F, 9B-B'), there is also a very well-developed carnassial notch, as in *W. tomnpatrichorum*, developed between the preentocristid and postmetacristid. In *D. maculatus*, however, the small, low postentocristid barely contacts the hypoconulid, which results in a failure of the entoconid and associated blades to effectively enclose the lingual side of the talonid; this contrasts with the condition in *W. tomnpatrichorum*, where the entire lingual side of the talonid is enclosed by these structures.

The largest of the dasyurines, the species of *Sarcophilus* and *Glaucodon*, have evolved in a different direction with extreme reduction of the entoconid and hypotrophy of the talonid as a whole. In the case of *S. harrisii* (Figs 4G–I, 9E-E'), this correlates with significant reduction of the protocone and other occlusal upper molar counterparts for talonid structures. In *G. ballaratensis* (structure of the M_3 in this species being based on the specimen described by Gerdtz and Archbold, 2003; Figs 7, 9C-C'), the entoconid is clearly present on the foreshortened talonid, but very small. In *S. moornaensis* (Figs 8, 9D-D'), it is even smaller to minuscule, although the talonid is less foreshortened than it is in *G. ballaratensis*. In *S. harrisii* something quite different has occurred (Figs 4G–I, 9E-E'): in conjunction with the far greater hypertrophy of the protoconid and coordinate posterior displacement of the metaconid, the talonid retains only two cusps and has become an 'appendage' at the base of the posterobuccal flank of the metacristid. The buccal-most of these cusps is the hypoconid but the homology

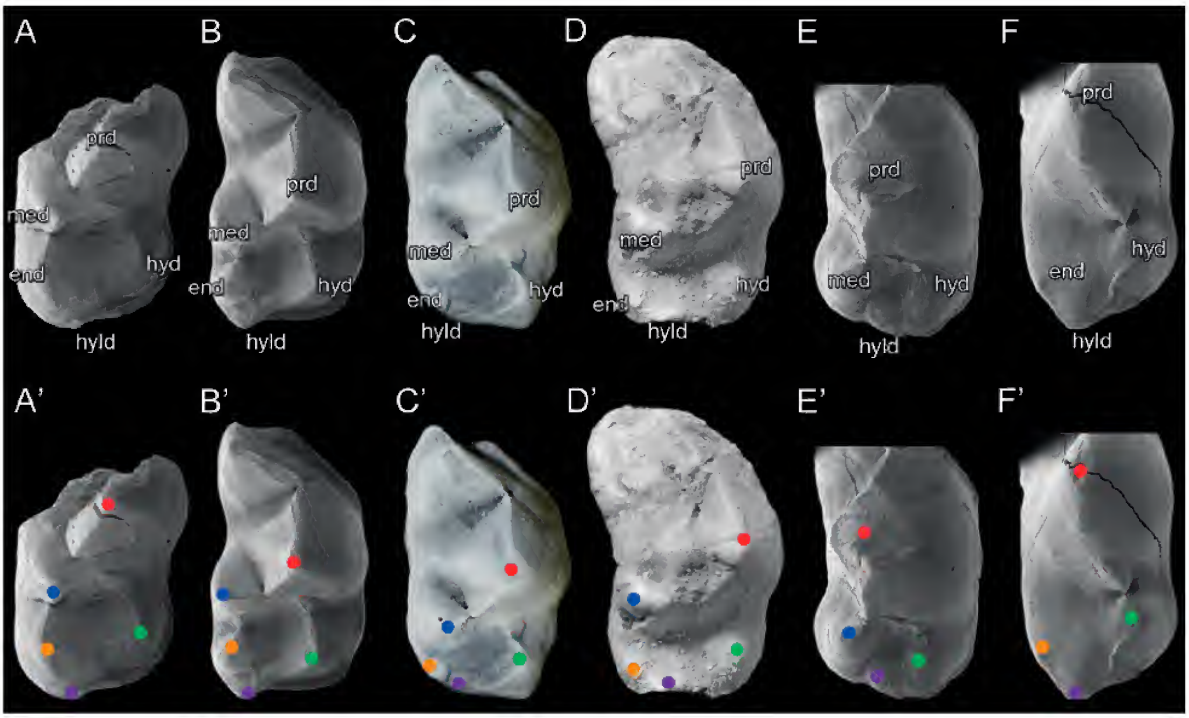

Figure 9. Comparison of the distribution of major cusps (in occlusal view) preserved in the *Whollydooleya tomnpatrichorum* holotype (QM F57892) with the RM_3 of representative extinct (†) and recent hypercarnivorous dasyuromorphians. A-A', *Whollydooleya tomnpatrichorum* (†); B-B', *Dasyurus maculatus*, AR21693; C-C', *Glaucodon ballaratensis*, P207018 (†); D-D', *Sarcophilus moornaensis*, NMV P28684 (†); E-E', *Sarcophilus harrisii*, AR21694; F-F', *Thylacinus cynocephalus*, AR21695 (image reversed from the LM_3) (†). Abbreviations: end, entoconid (orange dot); hyd, hypoconid (green dot); hyld, hypoconulid (purple dot); med, metaconid (blue dot); prd, protoconid (red dot). Not to scale.

of the other cusp is unclear. If the minuscule size of the entoconid in *S. moornaensis* presages changes leading to the condition seen in *S. harrisii*, then it would seem possible that the entoconid has been lost in *S. harrisii* and the cusp that remains is the hypoconulid. If this is the case, the most interesting consequence is that the posteriorly displaced metaconid may have replaced the function of the entoconid as the occlusal counterpart of the protocone, given that it now occurs directly lingual to the hypoconid and in the topographic position of the entoconid of other dasyurids. An arguably less plausible alternative, given the medial posterior position of the more lingual of the two talonid cusps in *S. harrisii*, would be that this is the entoconid and that the hypoconulid has been lost. Without annectant taxa bridging the transition between *Sarcophilus moornaensis* and *S. harrisii*, or perhaps a detailed analysis of occlusal relationships, the evolutionary fate of the entoconid in these large hypercarnivorous dasyurines is unclear. It is interesting to note that a similar argument has been made (Forasiepi et al., 2014) to explain what may have occurred on the other side of the world in relation to evolutionary reduction of the talonid in borhyaenids (Marsupialia, Sparassodonta) leaving uncertainty about the homology of the vestigial cusps in forms that retain talonid structures. There is even some uncertainty about the fate of the metaconid in more derived hypercarnivorous sparassodontans.

Although the modern Thylacine lacks a metaconid, presence in this Riversleigh taxon of a distinct (albeit reduced) metaconid does not exclude a more distant relationship to thylacinids given that that cusp is present in almost all of the Oligo-Miocene thylacinids. Reduction to loss of the metaconid is likely to be a convergent hypercarnivorous feature relating to hypertrophy of the protoconid and metacristid and longitudinal orientation and hypertrophy of the paracristid as the primary alpha-scissorial carnassial blade (Every, 1970) in derived thylacinids and dasyurids.

The hypoconulid in the M_{1-3} of dasyurids and thylacinids projects further posteriad than any other structure on the talonid and locks into the hypoconulid notch of the anterior cingulid of the following molar, thereby restricting differential transverse movement between adjacent teeth. Given the primarily alpha-scissorial function of the molars in these insectivorous/carnivorous marsupials, stability of posture for these molars during vertical shearing is aided by this interlocking system. For this reason, it is curious that the hypoconulid in *W. tomnpatrichorum* extends only just beyond the posterior flank of the talonid. This is also the case, however,

in species of *Glaucodon* (very small hypoconulid notch) and *Sarcophilus* (very small in M_2, absent in posterior molars), and may be a correlate of the larger, wider, potentially more laterally stable molar structure in species of these genera. It is uniquely developed in *W. tomnpatrichorum* more as an oblique transverse ridge (confluent with the posthypocristid, somewhat after the fashion seen in some peramelemorphians) than a discrete, posteriorly directed cuspid.

Of all the taxa noted above by way of comparison, the one that is the most enigmatic is the possibly early late Miocene *Ganbulanyi djadjinguli* from Encore Site at Riversleigh. The holotype, an isolated, incomplete, worn upper molar, was originally described by Wroe (1998) as probably conspecific with an isolated massive ovate premolar from the same deposit. Arena et al. (2011), in the course of describing *Malleodectes mirabilis*, suggested that the Encore molar and premolar represented different taxa and named the premolar *Malleodectes moenia*. They argued that both species of *Malleodectes* may have used their massive premolars to crush snail shells. Wroe's (1988) description of the holotype of *G. djadjinguli* suggests that this animal, based on the upper molar, was a hypercarnivore and hence it could possibly be related to *W. tomnpatrichorum*. Direct comparisons between the two teeth are, however, difficult because they are very different in size, exhibit markedly different degrees of wear and represent different tooth positions, the holotype of *W. tomnpatrichorum* being a lower molar while that of *G. djadjinguli* is an upper molar. Nevertheless, one of the key distinctive features of *D. djadjinguli* noted by Wroe (1998) is the relatively small occlusal area represented by the protocone. The very wide talonid and hypertrophied entoconid of *W. tomnpatrichorum* suggests an upper molar morphology that would have been significantly different with an uncharacteristically (for a hypercarnivorous dasyuromorphian) large protocone and associated blades. While tooth size alone clearly indicates that these taxa are not conspecific (the lower molar of *W. tomnpatrichorum* being wider than the upper molar of *G. djadjinguli*), the differences in protocone/talonid morphologies also suggest that the two taxa represent two quite distinct lineages of hypercarnivorous dasyurids. The nature of wear on the two specimens also suggests a significantly different life-style. In the case of the upper molar of *G. djadjinguli*, the wear is heavily apical resulting in conjoined paracone/STB and metacone/STD, wear patterns of a kind commonly seen in the molars of durophagous Tasmanian devils. In the lower molar of *W. tomnpatrichorum*, wear is clearly evident along the leading blade of the metacristid but there is very little apical wear evident on the protoconid and almost none on the hypoconid or entoconid, suggesting that this larger animal was nevertheless not a durophagous hypercarnivore.

Discussion

Whollydooleya tomnpatrichorum exhibits classic features of a marsupial hypercarnivore in being large (evidently larger than a modern Tasmanian Devil), in having a robust molar morphology with a hypertrophied protoconid, highly reduced metaconid and a plethora of vertical shearing blades with carnassial notches on both the trigonid and talonid. The uniformly fine, unidirectional striations on the posterior flank of the metacristid and posthypocristid indicate thegotic maintenance of the cutting edge of those blades. These features are shared by the larger dasyuromorphians such as species of *Dasyurus*, *Glaucodon*, *Sarcophilus* and some of the more plesiomorphic members of the Thylacinidae. This new species differs, however, from all thylacinids in having a very large entoconid and from the larger, later thylacinids in retaining a distinct metaconid. The massive entoconid distinguishes it additionally from all other dasyurids, including the largest dasyurine dasyurids to which it is otherwise most similar in terms of hypertrophy of the protoconid and reduction of the metaconid.

Until now, the oldest known hypercarnivorous dasyurids have been the dasyurine species of *Dasyurus* (earliest record being middle Pliocene; *Dasyurus dunmalli* Bartholomai, 1971; Wroe and Mackness, 1998; Archer, 1982), *Glaucodon* (only known from the Pliocene; *Glaucodon ballaratensis* Stirton, 1957; Gerdtz and Archbold, 2003) and *Sarcophilus* (first known from deposits interpreted to be Early Pleistocene in age; *Sarcophilus moornaensis* Crabb, 1982). Although the exact age of *W. tomnpatrichorum* is uncertain, it occurs with a suite of taxa that, at least at the generic level (e.g., *Ekaltadeta*, *Hypsiprymnodon*, cf. *Rhizophascolonus*), are broadly comparable but not identical to Miocene assemblages known from the Riversleigh World Heritage Area (Archer et al., 2006). Differences include, for example, a new species of *Hypsiprymnodon* that is abundantly present in the Wholly Dooley Local Fauna. We have therefore tentatively concluded that this faunal assemblage probably correlates with those from either Faunal Zone C or D in the Riversleigh World Heritage Area, which span approximately 16 to 13 Ma (Woodhead et al., 2014). However, it could be younger than this, possibly early late Miocene in age given the uncertain age of Encore Site, which has been estimated on the basis of biocorrelation to be early late Miocene (Black, 1997a, 1997b; Myers et al., 2001; Brewer et al., 2007; Black et al., 2012; Arena et al., 2014; Arena et al., 2015).

Wroe (2003) and Black et al. (2012) make the point, on the basis of the rich Riversleigh record in particular, that there appears to have been a gradual replacement of cat- and fox-sized thylacinids as the most abundant of the larger mammalian terrestrial carnivores in the late Oligocene to middle Miocene by comparable-sized dasyurids in the later Cenozoic.

Further, until now, few of the albeit rare dasyurids known from the Oligo-Miocene were large enough to qualify as hypercarnivores, *Ganbulanyi djadjinguli* being potentially the only other hypercarnivorous dasyurid. In contrast, *Whollydooleya tomnpatrichorum* was much larger than any of the other dasyurids and most of the thylacinids known to have been present during the Oligo-Miocene. Only late Miocene thylacinids (e.g., *Thylacinus potens* from the Alcoota Local Fauna in the Northern Territory) would have been larger. Using the regression equations for M_3 and M_2 widths published by Myers (2001; table 4; dasyuromorphian dataset), we estimate that a minimum mass for *W. tomnpatrichorum* may have been 20.3 kg if the holotype is an M_3 or 25.5 kg if it is an M_2. The average mass of living Tasmanian Devil males is 10–11 kg and of females is 7–8kg (Parks and Wildlife Service

Tasmania). Hence *W. tomnpatrichorum* may well have been at least twice the mass of living Devils, which are, currently, Australia's largest marsupial carnivore. Given Paddle's (2000) mass estimates for average-sized modern Thylacines (*Thylacinus cynocephalus*) of 29.5 kg, it is possible that *W. tomnpatrichorum* may have been as large as some of the smaller individuals of this recently extinct hypercarnivore.

Contemporaneity of other large hypercarnivorous dasyurids (e.g., species of *Dasyurus* and *Sarcophilus*) with a large thylacinid (*T. cynocephalus*) has been the situation in Australia since at least the Pliocene and persisted until Dingoes arrived on the Australian mainland in the mid Holocene and Europeans exterminated the Thylacine from Tasmania.

Wholly dooleya tomnpatrichorum, however, seems unlikely, on the basis of the hypertrophied entoconid, to have been on the direct line leading to the species of *Dasyurus*, *Glaucodon* or *Sarcophilus*. It is more likely to represent an independent, probably mid to late Miocene lineage of hypercarnivorous dasyurines that filled the niche occupied later, in the Pliocene to Holocene, by large hypercarnivorous dasyurines such as the living Tiger Quoll and Tasmanian Devil.

Appearance of this large hypercarnivorous dasyurid is the first indication of a trend towards gigantism within this family, which ultimately resulted in the largest known dasyurids of the late Cenozoic. Given that it does not appear to have been a member of the dasyurine lineage that includes *Glaucodon* and *Sarcophilus*, it had to represent a second lineage of dasyurids that underwent gigantism. If this was the case, it is possible that competition between the two could have led to loss of the lineage represented by *W. tomnpatrichorum*. That said, in terms of larger dasyurines, the only known *devil remains* are *in the detail* of the Pliocene and Quaternary record.

The presence in the deposit of what appear to be albeit rare aeolian-transported quartz grains and the indications of at least partial desiccation of the accumulating deposit may be a reflection of changing palaeoenvironments within the region. Following the late Oligocene and prior to the mid-Miocene climate oscillation, the faunal assemblages (Faunal Zones B and C) from the Riversleigh World Heritage area appear to suggest closed, biologically-rich forests (Archer et al., 1994, 1997; Travouillon et al., 2009; Black et al., 2012). While very few deposits from the Riversleigh World Heritage Area appear to represent post-Miocene oscillation assemblages, the few that do (e.g., Encore Site) suggest more open, drier forests (Myers et al., 2001, Travouillon et al. 2009). Wholly Dooley Site may have derived from a time when the region's palaeoenvironments were even drier, with potentially some wind-blown components becoming parts of the accumulating fossil deposit. Testing this possibility will involve ongoing research into other components of the Wholly Dooley Local Fauna as well as trying to radiometrically date speleothems that have been obtained from Wholly Dooley Hill.

Acknowledgements

Support for research at Riversleigh has come from Australian Research Council grants (LP100200486, DP1094569, DP130100197, DE130100467 and DE120100957 to M. Archer, S.J. Hand, K. H. Black, I. Graham and R.M.D. Beck at UNSW, Australia); XSTRATA Community Partnership Program (North Queensland); UNSW Australia; the National Geographic Society; P. Creaser and the CREATE Fund; the Queensland Parks and Wildlife Service; Environment Australia; the Waanyi Nation; the Queensland Museum; the Riversleigh Society Inc.; Outback at Isa; Mount Isa City Council; private supporters including Ken and Margaret Pettit, Elaine Clark, Margaret Beavis, and Martin Dickson; and the Waanyi people of northwestern Queensland. Assistance in the field has come from many hundreds of volunteers including those from the Geological Society of the Hunter Valley, the Waterhouse Club of South Australia, and the Riversleigh Society as well as staff and postgraduate students of the University of New South Wales. We thank Erich Fitzgerald of Museum Victoria for access to the holotype of *Sarcophilus moornaensis* and holotype as well as casts of the referred specimen of *Glaucodon ballaratensis*. Wayne Gerdtz provided advice about the origin of the referred specimen of *G. ballaratensis*. Ned Stephenson is thanked for his early recognition of the potential of the area now known as New Riversleigh to produce new fossil deposits. Jon Woodhead has developed the radiometric framework for dating speleothems from the Riversleigh World Heritage Area.

References

Archer, M. 1976a. Miocene marsupicarnivores (Marsupialia) from central South Australia, *Ankotarinja tirarensis* gen. et sp. nov., *Keeuna woodburnei* gen. et sp. nov., and their significance in terms of early marsupial radiations. *Transactions of the Royal Society of South Australia* 100: 53–73.

Archer, M. 1976b. The dasyurid dentition and its relationships to that of didelphids, thylacinids, borhyaenids (Marsupicarnivora) and peramelids (Peramelina: Marsupialia). *Australian Journal of Zoology Supplementary Series* 39: 1–34.

Archer, M. 1982. Review of the dasyurid (Marsupialia) fossil record, integration of data bearing on phylogenetic interpretation, and suprageneric classification. Pp. 397–443 in: Archer, M. (ed.), *Carnivorous Marsupials*. Surrey Beatty and Sons: Chipping Norton.

Archer, M. and Rich, T.H. 1979. *Wakamatha tasselli* gen. et sp. nov., a fossil dasyurid (Marsupialia) from South Australia convergent on modern *Sminthopsis*. *Memoirs of the Queensland Museum* 19: 309–317.

Archer, M., Hand, S.J., and Godthelp, H. 1994. *Riversleigh*. Reed Books Pty Ltd: Sydney. 264 pp.

Archer, M., Hand, S.J., Godthelp, H., and Creaser, P. 1997. Correlation of the Cainozoic sediments of the Riversleigh World Heritage Fossil Property, Queensland, Australia. Pp. 131–152 in: Aguilar, J-P., Legendre, S., and Michaux, J. (eds), *Actes du Congres BiocroM'97. Memoirs et Traveaux Ecole Pratique des Hautes Etudes*. Institut de Montpellier: Montpellier.

Archer, M., Arena, D.A., Bassarova, M., Beck, R.M.D., Black, K., Boles, W.E., Brewer, P., Cooke, B.N., Crosby, K., Gillespie, A., Godthelp, H., Hand, S.J., Kear, B.P., Louys, J., Morrell, A., Muirhead, J., Roberts, K.K., Scanlon, J.D., Travouillon, K.J., and Wroe, S. 2006. Current status of species-level representation in faunas from selected fossil localities in the Riversleigh World Heritage Area, northwestern Queensland. *Alcheringa: An Australasian Journal of Palaeontology* 30:1–17.

Arena, D.A. 2004. *The geological history and development of the terrain at the Riversleigh World Heritage Area during the middle Tertiary*. Unpublished Ph. D. Thesis, University of New South Wales, Sydney. 275 pp.

Arena, D.A., Archer, M., Godthelp, H., Hand, S.J., and Hocknull, S. 2011. Hammer-toothed 'marsupial skinks' from the Australian Cenozoic. *Proceedings of the Royal Society B* 278: 3529–3533.

Arena, D.A., Black, K.H., Archer, M., Hand, S.J., Godthelp, H., and Creaser, P. 2014. Reconstructing a Miocene pitfall trap: recognition and interpretation of fossiliferous Cenozoic palaeokarst. *Sedimentary Geology* doi:10.1016/j.sedgeo.2014.01.005.

Arena, D.A., Travouillon, K.J., Beck, R.M.D., Black, K.H., Gillespie, A.K., Myers, T.J., Archer, M., Hand, S.J. (2015). Mammalian lineages and the biostratigraphy and biochronology of Cenozoic faunas from the Riversleigh World Heritage Area, Australia. *Lethaia*, doi:10.1111/let.12131.

Bartholomai, A. 1971. *Dasyurus dunmalli*, a new species of fossil marsupial (Dasyuridae) in the upper Cainozoic deposits of Queensland. *Memoirs of the Queensland Museum* 16: 19–26.

Black, K. 1997a. A new species of Palorchestidae (Marsupialia) from the late middle to early late Miocene Encore Local Fauna, Riversleigh, northwestern Queensland. *Memoirs of the Queensland Museum* 41: 181–186.

Black, K. 1997b. Diversity and biostratigraphy of the Diprotodontoidea of Riversleigh, northwestern Queensland. *Memoirs of the Queensland Museum* 41: 187–192.

Black, K.H., Archer, M., Hand, S.J., and Godthelp, H. 2012. The rise of Australian marsupials: a synopsis of biostratigraphic, phylogenetic, palaeoecological and palaeobiogeographic understanding. Pp. 983–1078 in: Talent, J.A. (ed.), *Earth and Life: Global Biodiversity, Extinction Intervals and Biogeographic Perturbations through Time*. Springer Verlag: Dordrecht.

Brewer, P., Archer, M., Hand, S., Godthelp, H. 2007. A new species of the wombat *Warendja* from late Miocene deposits at Riversleigh, north-west Queensland, Australia. *Palaeontology* 50: 811–828.

Crabb, P.L. 1982. Pleistocene dasyurids (Marsupialia) from southwestern New South Wales. Pp. 511–16 in: Archer, M. (ed.) *Carnivorous Marsupials*. Surrey Beatty and Sons: Chipping Norton.

Creaser, P. 1997. Oligocene–Miocene sediments of Riversleigh: the potential significance of topography. *Memoirs of the Queensland Museum* 41: 303–314.

Dawson, L. 1982. Taxonomic status of fossil devils (*Sarcophilus*, Dasyuridae, Marsupialia) from late Quaternary eastern Australian localities. Pp. 517–25 in: Archer, M. (ed.) *Carnivorous Marsupials*. Surrey Beatty and Sons: Chipping Norton.

Every, R.G. 1970. Sharpness of teeth in man and other primates. *Postilla* 143: 1–30.

Gerdtz, W. and Archbold, N. 2003. *Glaucodon ballaratensis* (Marsupialia, Dasyuridae), a Late Pliocene 'Devil' from Batesford, Victoria. *Proceedings of the Royal Society of Victoria* 115: 35–44.

Forasiepi, A.M., Babot, M.J. and Zimicz, N. 2014. *Australohyaena antiqua* (Mammalia, Metatheria, Sparassodonta), a large predator from the late Oligocene of Patagonia. *Journal of Systematic Palaeontology*. doi:10.1080/14772019.2014.926403.

Godthelp, H., Wroe, S. and Archer, M. 1999. A new marsupial from the early Eocene Tingamarra Local Fauna of Murgon, southeastern Queensland: a prototypical Australian marsupial? *Journal of Mammalian Evolution* 6: 289–313.

Goldfuss, G.A. 1820. *Handbuch der Zoologie*. Nuremberg, 196 pp.

Myers, T.J. 2001. Prediction of marsupial body mass. *Australian Journal of Zoology* 49: 99–118.

Myers, T.J., Crosby, K., Archer, M. and Tyler, M. 2001. The Encore Local Fauna, a late Miocene assemblage from Riversleigh, northwestern Queensland. *Memoirs of the Association of Australasian Palaeontologists* 25: 147–154.

Owen, R. 1838. Fossil remains from Wellington Valley, Australia. Marsupialia. Pp 359–369 in: Appendix to Mitchell, T.L. (ed.), *Three expeditions into the interior of eastern Australia, with descriptions of the recently explored region of Australia felix, and of the present colony of New South Wales*. T. and W. Boone: London.

Parks and Wildlife Service Tasmania. No date. Tasmanian Devil—frequently asked questions. http://www.parks.tas.gov.au/?base=4756 accessed 25 June, 2015.

Paddle, R. 2000. *The Last Tasmanian Tiger: the History and Extinction of the Thylacine*. Cambridge University Press: Melbourne. 284 pp.

Stirton, R.A. 1957. Tertiary marsupials from Victoria, Australia. *Memoirs of the National Museum of Victoria* 21: 121–134.

Thomas, O. 1888. *Catalogue of the Marsupialia and Monotremata in the collection of the British Museum (Natural History)*. British Museum (Natural History): London. 401 pp.

Travouillon, K.J., Legendre, S., Archer, M., and Hand, S.J. 2009. Palaeoecological analyses of Riversleigh's Oligo-Miocene sites: implications for Oligo-Miocene climate change in Australia. *Palaeogeography, Palaeoclimatology, Palaeoecology* 276: 24–37.

Voss, R.S. and Jansa, S.A. 2009. Phylogenetic relationships and classification of didelphid marsupials of New World metatherian mammals. *Bulletin of the American Museum of Natural History* 322: 1–177.

Wroe, S. 1996. *Muribacinus gadiyuli* (Thylacinidae; Marsupialia), a very plesiomorphic thylacinid from the Miocene of Riversleigh, northwestern Queensland, and the problem of paraphyly for the Dasyuridae (Marsupialia). *Journal of Paleontology* 70: 1032–1044.

Wroe, S. 1997a. *Mayigriphus orbus*, a new species of dasyuromorphian (Marsupialia) from the Miocene of Riversleigh, north-western Queensland. *Memoirs of the Queensland Museum* 41: 439–448.

Wroe, S. 1997b. A reexamination of proposed morphology-based synapomorphies for the families of Dasyuromorphia (Marsupialia). I. Dasyuridae. *Journal of Mammalian Evolution* 4: 19–52.

Wroe, S. 1998. A new 'bone-cracking' dasyurid (Marsupialia), from the Miocene of Riversleigh, north-western Queensland. *Alcheringa* 22: 277–284.

Wroe, S. 1999. The geologically oldest dasyurid (Marsupialia) from the Miocene of Riversleigh, north-western Queensland. *Palaeontology* 42: 501–527.

Wroe, S. 2001. A new genus and species of dasyuromorphian from the Miocene of Riversleigh, northern Australia. *Memoirs of the Association of Australasian Palaeontologists* 25: 53–59.

Wroe, S., 2003. Australian marsupial carnivores: recent advances in palaeontology. Pp. 102–123 in: Jones, M., Dickman, C. and Archer, M. (eds), *Predators with Pouches: the Biology of Marsupial Carnivores*. CSIRO Publishing: Collingwood.

Wroe, S., and Mackness, B.S. 1998. Revision of the Pliocene dasyurid, *Dasyurus dunmalli* (Dasyuridae: Marsupialia). *Memoirs of the Queensland Museum* 42: 605–612.

Woodhead, J., Hand, S.J., Archer, M., Graham, I., Sniderman, K., Arena, D.A., Black, K.H., Godthelp, H., Creaser, P., and Price, L. 2014. Developing a radiometrically dated chronologic sequence for Neogene biotic change in Australia, from the Riversleigh World Heritage Area of Queensland. *Gondwana Research*. doi:10.1016/j.gr.2014.10.004.

Memoirs of Museum Victoria 74: 151–171 (2016) Published 2016

ISSN 1447-2546 (Print) 1447-2554 (On-line)
http://museumvictoria.com.au/about/books-and-journals/journals/memoirs-of-museum-victoria/

Going underground: postcranial morphology of the early Miocene marsupial mole *Naraboryctes philcreaseri* and the evolution of fossoriality in notoryctemorphians

Robin M. D. Beck[1,*], Natalie M. Warburton[2], Michael Archer[3], Suzanne J. Hand[4], and Kenneth P. Aplin[5]

[1] School of Environment & Life Sciences, Peel Building, University of Salford, Salford M5 4WT, UK and School of Biological, Earth and Environmental Sciences, University of New South Wales, Sydney, NSW 2052, Australia (R.M.D.Beck@salford.ac.uk)
[2] School of Veterinary and Life Sciences, Murdoch University, 90 South Street, Murdoch, WA 6150, Australia (N.Warburton@murdoch.edu.au)
[3] School of Biological, Earth and Environmental Sciences, University of New South Wales, Sydney, NSW 2052, Australia (m.archer@unsw.edu.au)
[4] School of Biological, Earth and Environmental Sciences, University of New South Wales, Sydney, NSW 2052, Australia (s.hand@unsw.edu.au)
[5] National Museum of Natural History, Division of Mammals, Smithsonian Institution, Washington, DC 20013-7012, USA (aplink@si.edu)
* To whom correspondence should be addressed. E-mail: R.M.D.Beck@salford.ac.uk

Abstract

Beck, R.M.D., Warburton, N.M., Archer, M., Hand, S.J. and Aplin, K.P. 2016. Going underground: postcranial morphology of the early Miocene marsupial mole *Naraboryctes philcreaseri* and the evolution of fossoriality in notoryctemorphians. *Memoirs of Museum Victoria* 74: 151–171.

We present the first detailed descriptions of postcranial elements of the fossil marsupial mole *Naraboryctes philcreaseri* (Marsupialia: Notoryctemorphia), from early Miocene freshwater limestone deposits in the Riversleigh World Heritage Area, northwestern Queensland. Qualitative functional analysis of these elements suggest that *Na. philcreaseri* was very well-adapted for burrowing, albeit somewhat less so than the living marsupial moles *Notoryctes typhlops* and *N. caurinus*. Quadratic discriminant analysis of limb measurements suggests that *Na. philcreaseri* was subterranean, and its Index of Fossorial Ability is almost identical to that of *Notoryctes* species, being among the highest known for any mammal. These results suggest that notoryctemorphians evolved their specialised, "mole-like" subterranean lifestyle prior to the early Miocene. Given that forested environments predominated in Australia until the middle-late Miocene, this transition to subterranean behaviour may have occurred via burrowing in forest floors, in which case fossorial mammals that live in tropical rainforests today (such as the placental golden moles *Chrysospalax trevelyani* and *Huetia leucorhina*) may represent reasonable living analogues for early notoryctemorphians. However, alternative scenarios, such as a cave-dwelling or semi-aquatic ancestry, should be considered. Phylogenetic analysis using a Bayesian total evidence dating approach places *Naraboryctes* as sister to *Notoryctes* with strong support (Bayesian posterior probability = 0.91), and indicates that *Naraboryctes* and *Notoryctes* diverged 30.3 MYA (95% HPD: 17.7–46.3 MYA). The age and known morphology of *Na. philcreaseri* does not preclude its being ancestral to *Notoryctes*. Using estimates of divergence times and ratios of nonsynonymous to synonymous substitutions per site, we infer that the nuclear gene "Retinol-binding protein 3, interstitial" (*RBP3*), which plays a key role in vision, became inactive in the *Notoryctes* lineage ~5.4 MYA (95% HPD: 4.5–6.3 MYA). This is much younger than previous published estimates, and postdates considerably the age of *Na. philcreaseri*, implying that *RBP3* was active in this fossil taxon; hence, *Na. philcreaseri* may have retained a functional visual system. Our estimate for the inactivation of *RBP3* in the *Notoryctes* lineage coincides with palaeobotanical evidence for a major increase in the abundance of grasses in Australia, which may indicate the appearance of more open environments, and hence selection pressure on notoryctemorphians to spend less time on the surface, leading to relaxed selection on *RBP3*. Ultimately, however, a fuller understanding of the origin and evolution of notoryctemorphians – including when and why they became "mole-like" – will require improvements in the Palaeogene fossil record of mammals in Australia.

Keywords

marsupial moles; *Notoryctes*; *Naraboryctes*; Notoryctemorphia; fossorial; subterranean; postcranial; functional morphology; marsupial phylogeny; Riversleigh; Miocene; *RBP3*; *IRBP*

"Some people might say my life is in a rut,
But I'm quite happy with what I got"
Going Underground – The Jam

Introduction

The two living species of marsupial mole – *Notoryctes typhlops* (the Southern Marsupial Mole, or Itjaritjari) and *Notoryctes caurinus* (the Northern or Northwestern Marsupial Mole, or Kakarratul) – are remarkably specialised, subterranean mammals that live in the western deserts of continental Australia (Johnson and Walton, 1989; Benshemesh and Johnson, 2003; Benshemesh, 2008; Benshemesh and Aplin, 2008). The only extant representatives of the order Notoryctemorphia (Kirsch, 1977; Aplin and Archer, 1987), both species show extreme anatomical adaptations for burrowing, including a heavily fused and conical skull, loss of external ears and functional eyes, and a postcranial skeleton that is highly modified for parasagittal scratch-digging (Stirling, 1891; Carlsson, 1904; Sweet, 1906; Johnson and Walton, 1989; Warburton, 2006). One striking molecular feature of *Notoryctes* is also probably related to its subterranean lifestyle: the gene "Retinol-binding protein 3, interstitial" (*RBP3*, often referred to as "interphotoreceptor retinoid binding protein", or *IRBP*) of *N. typhlops* is non-functional, exhibiting both frameshift mutations and premature stop codons (Springer et al., 1997; Emerling and Springer, 2014). *RBP3* plays a key role in visual pigment regeneration (Pepperberg et al., 1993), and loss of function of this gene in *N. typhlops* is presumably related to its degenerate visual system: its eyes are tiny, lack lenses and are covered by skin, and the optic nerve is absent (Stirling, 1891; Sweet, 1906). The visual system of *N. caurinus* is similarly degenerate (Benshemesh and Aplin, 2008), but to date *RBP3* has not been sequenced for this species. *RBP3* has also been shown to be pseudogenic in some subterranean rodents (Kim et al., 2011: table 2; Emerling and Springer, 2014) and in several echolocating bat species (Shen et al., 2013); as in *Notoryctes*, vision is probably of limited importance in these species, and hence selection to maintain a functional copy of *RBP3* has presumably been relaxed (Kim et al., 2011; Shen et al., 2013; Emerling and Springer, 2014).

Both *Notoryctes* species spend the vast majority of their time below ground, surfacing only rarely (Johnson and Walton, 1989; Benshemesh and Johnson, 2003; Dennis, 2004; Benshemesh, 2008; Benshemesh and Aplin, 2008); because of this, many basic aspects of their ecology and life history are unknown. Fundamental questions regarding the evolutionary history of notoryctemorphians also remain unanswered. Resolution of their phylogenetic relationships has proven difficult due to their numerous morphological autapomorphies, lack of obvious close living relatives and, until recently, complete absence of a fossil record. Indeed, some studies have even questioned whether they are marsupials (Stirling, 1888; Cope, 1892; Turnbull, 1971). However, there is now overwhelming evidence that *Notoryctes* is indeed a marsupial (e.g. Horovitz and Sánchez-Villagra, 2003; Asher et al., 2004; Nilsson et al., 2004, 2010; Beck, 2008; Beck et al., 2008; Meredith et al., 2008, 2009b, 2011; Mitchell et al., 2014). Recent phylogenetic analyses, particularly those based on molecular data (e.g. Nilsson et al., 2004, 2010; Beck, 2008; Meredith et al., 2008, 2009b, 2011; Mitchell et al., 2014), typically place *Notoryctes* in a clade with the Australian marsupial orders Dasyuromorphia (predominantly carnivorous forms such as quolls, thylacines and the numbat) and Peramelemorphia (bandicoots and bilbies); Beck et al. (2014) named this clade Agreodontia. However, the precise branching relationship between Notoryctemorphia, Dasyuromorphia and Peramelemorphia is uncertain. The previous lack of fossil evidence has also meant that the underlying factors driving the evolution of the extreme fossorial adaptations of *Notoryctes*, and the timing of when they arose, remain enigmatic.

Crucial information regarding the evolutionary history of Notoryctemorphia is now being provided with the discovery of cranial and postcranial remains of the first known fossil member of the order, *Naraboryctes philcreaseri*, from early Miocene freshwater limestone deposits at Riversleigh (Gott, 1988; Warburton, 2003; Archer et al., 2011). *Na. philcreaseri* provides the first hard evidence showing how the zalambdodont molar dentition of *Notoryctes* evolved, namely via suppression of the paracone (Archer et al., 2011). In addition, postcranial elements tentatively referred to *Na. philcreaseri* show apparent fossorial specialisations, albeit not as extreme as in *Notoryctes* species (Warburton, 2003; Archer et al., 2011). The presence of these features in *Na. philcreaseri* is perhaps surprising because available evidence suggests that Riversleigh was a rainforest environment during the early Miocene (Travouillon et al., 2009; Archer et al., 2011; Bates et al., 2014). It had previously been suggested that notoryctemorphians acquired their fossorial adaptations in a desert milieu (Archer, 1984), but there is no evidence of deserts anywhere in Australia prior to the Pleistocene (McLaren and Wallace, 2010), nor extensive grasslands prior to the middle Pliocene (Martin and McMinn, 1994; Martin, 2006; Strömberg, 2011; Black et al., 2012). The discovery of *Na. philcreaseri* has led to an alternative hypothesis, namely that these adaptations evolved for burrowing through soft rainforest floors (Archer et al., 1994; Archer et al., 2011). In support of this, analogies have been drawn with the morphologically similar but unrelated placental chrysochlorids (golden moles) of sub-Saharan Africa (Archer et al., 1994), as some extant chrysochlorid species (e.g. *Chrysospalax trevelyani*, *Huetia leucorhina*) occur in wet forest environments (Bronner, 2013).

In this paper, we present the first detailed descriptions of the postcranial skeleton of *Naraboryctes philcreaseri*, including bones not discussed by Archer et al. (2011). We present a qualitative functional interpretation of its postcranial morphology, focusing on evidence for fossoriality, and test this within a quantitative framework using multivariate discriminant analysis (see Hopkins and Davis, 2009). We also calculate the widely-used Index of Fossorial Ability (Vizcaino et al., 1999; Vizcaino and Milne, 2002) for *Na. philcreaseri* and compare it to values for *Notoryctes typhlops* and for other burrowing mammals. We discuss the changes required to derive the postcranial morphology seen in *Notoryctes* species from that seen in *Na. philcreaseri*. We present the first phylogenetic

analyses to include *Naraboryctes*, using a dated Bayesian total evidence dating approach (Ronquist et al., 2012a), the first time this method has been applied to marsupials. Finally, we use the divergence dates from our phylogenetic analysis and estimates of non-synonymous to synonymous substitution ratios to estimate the timing of inactivation of the *RBP3* gene in the notoryctemorphian lineage (Chou et al., 2002; Zhang et al., 2008), and discuss its implications for our understanding of the ecology of *Na. philcreaseri*.

In 1971, Tom and Pat Rich undertook their first fieldwork in Australia, working with the American Museum of Natural History's Dick Tedford, and using "conventional" fossil collecting methods (Archer and Hand, 1984). In 1984, however, Tom, Pat and a team of brave volunteers turned to tunnelling as a way to obtain fossils from Dinosaur Cove, on the south coast of Victoria. This was apparently the first time that a tunnel had ever been dug solely to find fossils, and over the following ten years it proved a remarkable success, albeit one requiring immense efforts in terms of time and manpower. Tom has gone on to use a similar tunnelling approach in Late Cretaceous deposits in Alaska. We think, therefore, that a paper on the evolution of burrowing in marsupial moles is particularly appropriate for this volume celebrating Tom's long and productive career and his extraordinary contribution to Australian palaeontology.

Materials and methods

As with most other vertebrate specimens collected from fossil deposits in the Riversleigh World Heritage Area, the material of *Naraboryctes philcreaseri* described here was obtained by processing limestone blocks with 5–10% acetic acid, and subsequent microscope-assisted sorting of the concentrate. None of the postcranial elements were found in direct association with dental specimens of *Na. philcreaseri*; referral is based on compatible size and presence of apparent fossorial adaptations, particularly features that closely resemble the morphology seen in *Notoryctes*. It is possible that some or all of these elements in fact belong to a different taxon, but we consider this unlikely: no mammalian group present at Riversleigh besides Notoryctemorphia is known to have either living or fossil members that show extreme specialisations for digging. Nevertheless, as with all specimens not found in direct association, these referrals should be considered tentative. All known specimens of *Na. philcreaseri* are from Riversleigh Faunal Zone B sites, which have been interpreted to be early Miocene in age based on biostratigraphy (Archer et al., 1997; Archer et al., 2006; Travouillon et al., 2006), an age assignment that is now being validated by radiometric dating (Woodhead et al., 2014). A full list of *Na. philcreaseri* postcranial specimens is given in supplementary information; they are registered in the fossil vertebrate collection of the Queensland Museum (prefix QM F).

Description and functional interpretation of the postcranial morphology of *Na. philcreaseri* follows previous studies of fossorial and subterranean mammals, both living and fossil (e.g. Stirling, 1891; Thompson and Hillier, 1905; Chapman, 1919; Campbell, 1939; Orcutt, 1940; Reed, 1951; Lehmann, 1963; Puttick and Jarvis, 1977; Rose and Emry, 1983; Gasc et al., 1986; Lessa, 1990; Stein, 1993; Warburton, 2006), as well as more general studies of mammalian morphology (e.g. Coues, 1872; Barbour, 1963; Davis, 1964; Schaller, 1992; Evans, 1993). We consider mammals to be "fossorial" if they engage in regular burrowing activities below ground but nevertheless spend considerable periods of time above ground, and "subterranean" if they spend the clear majority of their time below ground (Nevo, 1999: character 2; Lessa et al., 2008); under this definition, both living *Notoryctes* species are subterranean. Measurements for *Na. philcreaseri* were taken from complete adult specimens, where available, while measurements for *N. caurinus* and *N. typhlops* were taken from Warburton (2003: Appendix 1) and an additional *N. typhlops* specimen (SAM M637).

To quantitatively test whether the known morphology of *Na. philcreaseri* supports its interpretation as a fossorial or subterranean mammal, we used a quadratic discriminant analysis based on the "limbs only" dataset of Hopkins and Davis (2009). This dataset comprises four measurements from the humerus, two from the ulna, and two from the femur, for 115 extant subterranean, fossorial and non-burrowing mammal species (including placentals, marsupials and monotremes; see Hopkins and Davis, 2009 for full details). Hopkins and Davis (2009) found this dataset to be 86.1% accurate at distinguishing burrowing (= subterranean + fossorial) and non-burrowing taxa, and 85.2% accurate for distinguishing subterranean, fossorial and non-burrowing taxa. Hopkins and Davis (2009) estimated measurements for *Notoryctes typhlops* from published images; we have replaced these with measurements taken directly from *N. typhlops* specimen SAM M637. We added a further three modern marsupial taxa to the Hopkins and Davis (2009) dataset, namely the non-burrowing dasyurid *Dasyurus viverrinus*, the non-burrowing peramelemorphians *Isoodon macrourus*, *I. obesulus* and *Perameles gunnii*, and the fossorial peramelemorphian *Macrotis lagotis*. *Na. philcreaseri* was then added, with measurements taken from the most complete specimens and with its fossorial ability treated as unknown. Measurements for these additional taxa are given in supplementary information. The quadratic discriminant analysis was implemented in JMP, assuming equal prior probabilities for the different locomotor modes, and a plot of the first two canonical axes was produced, following Hopkins and Davis (2009: fig. 3).

To further quantify the likely fossorial ability of *Na. philcreaseri*, we compared its Index of Fossorial Ability (IFA; sometimes referred to as Olecranon Length Index) – a commonly used metric that is strongly correlated with the degree of fossoriality in various groups of mammals (Vassallo, 1998; Vizcaino et al., 1999; Elissamburu and Vizcaíno, 2004; Lagaria and Youlatos, 2006; Warburton et al., 2013; Woodman and Gaffney, 2014) – with that of *Notoryctes* and other fossorial and subterranean mammals (table 1). We calculated IFA as (olecranon length/(total ulnar length-olecranon length))*100, following Vizcaino and Milne (2002). Olecranon length was measured to the distal margin of the trochlear notch, as in Hopkins and Davis (2009; see also comments by Woodman and Gaffney, 2014: table 1). For *Na. philcreaseri*

Table 1. Selected Recent and fossil mammals with an Index of Fossorial Ability (IFA) greater than 60. Identification of Recent taxa as subterranean, fossorial or non-burrowing follows Hopkins and Davis (2009). Fossil taxa are indicated by †, and their burrowing behaviour is treated as unknown. All measurements are taken from Hopkins and Davis (2009) except those for *Naraboryctes philcreaseri* (which were taken from QM F57706; see Figs. 4a, c, e) and *Notoryctes typhlops* (which were taken from SAM M637; see Figs. 4b, d, f). IFA is calculated as (olecranon length/(total ulnar length-olecranon length))*100, following Vizcaino and Milne (2002). IFA for *Na. philcreaseri* is likely a slight overestimate, as QM F57706 is missing the distal epiphysis (see Figs. 4a, c, e), and hence total ulnar length is slightly too short; the true value is probably the same as or slightly less than that for *N. typhlops*.

taxon	order	family	type	total ulnar length (mm)	Olecranon length (mm)	Index of fossorial ability (IFA)
†*Xenocranium pileorivale*	†Palaeanodonta	†Epoicotheriidae	unknown	38.46	22.08	134.7
Amblysomus hottentotus	Afrosoricida	Chrysochloridae	subterranean	17.56	8.96	104.2
Priodontes maximus	Cingulata	Dasypodidae	fossorial	131.96	67.07	103.4
Cabassous centralis	Cingulata	Dasypodidae	fossorial	58.15	27.88	92.1
†*Pentapassalus pearcei*	†Palaeanodonta	†Epoicotheriidae	unknown	55	26	89.7
†*Naraboryctes philcreaseri*	**Notoryctemorphia**	**Notoryctidae**	**unknown**	17.9	8.4	88.4
Notoryctes typhlops	**Notoryctemorphia**	**Notoryctidae**	**subterranean**	16.1	7.5	87.2
Scaptochirus moschatus	Eulipotyphla	Talpidae	subterranean	15.93	7.36	85.9
Scapanus orarius	Eulipotyphla	Talpidae	subterranean	16.95	7.8	85.2
Euphractus sexcinctus	Cingulata	Dasypodidae	fossorial	70.83	30.72	76.6
Spalax giganteus	Rodentia	Spalacidae	subterranean	49.81	21.44	75.6
Chaetophractus villosus	Cingulata	Dasypodidae	fossorial	60.44	25.84	74.7
Dasypus novemcinctus	Cingulata	Dasypodidae	fossorial	76.63	32.58	74.0
Nannospalax leucodon	Rodentia	Spalacidae	subterranean	33.3	14.04	72.9
Talpa europaea	Eulipotyphla	Talpidae	subterranean	18.27	7.57	70.7
Scalopus aquaticus	Eulipotyphla	Talpidae	subterranean	17.97	7.44	70.6
Eremitalpa granti	Afrosoricida	Chrysochloridae	subterranean	12.16	4.98	69.4
†*Mesoscalops montanensis*	?Eulipotyphla	†Proscalopidae	unknown	24.83	9.6	63.0
Manis pentadactyla	Pholidota	Manidae	non-burrowing	60.7	23.46	63.0
Parascalops breweri	Eulipotyphla	Talpidae	subterranean	15.66	6.04	62.8
†*Palaeanodon ignavus*	†Palaeanodonta	†Metacheiromyidae	unknown	71	27	61.4
Tolypeutes matacus	Cingulata	Dasypodidae	non-burrowing	42.71	16.1	60.5

and *N. typhlops*, we calculated IFA based on our own measurements, whereas values for other taxa were calculated from measurements for total ulnar length and olecranon length given in Hopkins and Davis (2009).

Our phylogenetic analysis is based on the total evidence matrix used by Beck et al. (2014), specifically the version that includes character scores from isolated tarsals tentatively referred to *Yalkaparidon*. This matrix comprises 258 morphological characters and 9012 bp from five nuclear genes, namely *APOB* (exon 26), *BRCA1* (exon 11), *RBP3* (exon 1), *RAG1*, and *VWF* (exon 28), and includes a range of fossil and extant metatherians and non-metatherian outgroups (see Beck et al., 2014, and supplementary information for full details). We subdivided character 192 of Beck et al. (2014), such that presence/absence of the transverse canal foramen and its position (if present) are now treated as separate characters (characters 192–193), and hence the morphological matrix used here comprises a total of 259 characters. We also deleted the indels and retroposons included by Beck et al. (2014) because we used a total evidence dating approach (see below) and it is not obvious how rare genomic changes should be treated in this framework. We added *Naraboryctes* to this matrix, with character scores based on the craniodental and postcranial material described by Archer et al. (2011) and here. As in Beck et al. (2014), an appropriate partitioning scheme for the nuclear sequence data was determined using PartitionFinder (Lanfear et al., 2012), with initial partitioning by gene and codon position, and assuming linked branch lengths. Only models implemented by MrBayes were tested, using the "greedy" heuristic search algorithm, with the Bayesian Information Criterion used for model selection. The morphological partition was assigned the Mk model (Lewis, 2001), assuming that only parsimony-informative characters were scored, and with a gamma distribution to model rate heterogeneity between characters. As in Beck et al. (2014), multistate morphological characters representing putative morphoclines were ordered.

We employed a Bayesian total evidence dating approach (Ronquist et al., 2012a; Beck and Lee, 2014), which simultaneously estimates phylogeny and divergence times for both extant and fossil taxa, as implemented in MrBayes 3.2.2 (Ronquist et al., 2012b). Each terminal taxon was assigned an age: Recent taxa were assigned a point estimate of 0 Ma, whilst each fossil taxon was assigned an age range as a hard-bounded uniform prior, based on current age estimates (see supplementary information for full justification). The age of the root was also constrained as an offset exponential prior, with a minimum of 176.15 Ma and a mean (expectation) of 201.3 Ma. The minimum is based on the minimum radiometric age of the Queso Rellado locality of the Cañadon Asfalto Formation (Cúneo et al., 2013), which contains the oldest known putative crown-group mammals, *Asfaltomylos* and *Henosferus*, which are usually recovered as stem-monotremes in published phylogenetic analyses (e.g. Rougier et al., 2007; Bi et al., 2014). The mean corresponds to the Triassic-Jurassic boundary, and is broadly congruent with recent molecular estimates for the age of Mammalia (Meredith et al., 2011; dos Reis et al., 2012; 2014). Analysis of eutherian mammals suggests that total evidence dating in which only the age of the root is constrained can result in implausibly ancient divergence dates for at least some nodes (Beck and Lee, 2014); we therefore specified 13 additional topological and temporal constraints on internal nodes, with ages specified as offset exponential priors, namely: Theria, Marsupialia, Didelphidae, Didelphinae, crown-group Australidelphia, Dasyuridae, Dasyurinae, Peramelidae, Diprotodontia, Phalangerida, Petauroidea, Macropodidae and Vombatiformes (see supplementary information for full details). To assist convergence of the Bayesian analyses, monophyly of Eutheria and Metatheria was also enforced *a priori*, but the ages of these nodes were not calibrated.

The independent gamma rates (IGR) model was used (Ronquist et al., 2012a), with a single clock model applied to the entire nuclear sequence partition and a separate clock model applied to the morphological partition. The MrBayes analysis comprised four runs of four chains, each run for 15 million generations and with the temperature of the heated chains increased to 0.2. A burn-in fraction of 25% (i.e. 3.75 million generations) was specified; examination of plots of log likelihood against number of generations revealed that stationarity and convergence between chains had been achieved prior to this. The post-burnin trees were then summarised using majority-rule consensus, with all compatible partitions retained. Bayesian posterior probabilities (BPPs) were used as measures of clade support. The MrBayes file used in our analysis and the post-burnin majority-rule consensus that resulted are included in supplementary information.

To calculate the time of inactivation of *RBP3* in the notoryctemorphian lineage we used the general approach of Chou et al. (2002; see also Zhang et al., 2008). We first pruned our *RBP3* exon 1 alignment and the final consensus tree from our dated total evidence analysis so that only extant marsupials were retained (i.e. all fossil taxa and the monotreme outgroups *Ornithorhynchus* and *Tachyglossus* were deleted). We then deleted all codon positions in the pruned alignment that contained insertions. The modified *RBP3* alignment and pruned tree were then used to calculate the ratio of non-synonymous substitutions per non-synonymous site to synonymous substitutions per synonymous site (ω, also referred to as d_N/d_S, or K_a/K_s). Using the codeml package of PAML 4.7 (Yang, 2007), we firstly calculated ω for all branches, and then calculated ω separately for: 1) the branch leading to *Notoryctes* (the "foreground" branch; ω_f), and 2) all other branches (the "background" branches; ω_b). We used a likelihood ratio test to compare the relative fit of the two models (i.e. single ω, versus ω_f for *Notoryctes* and ω_b for all other branches), with critical values taken from a χ^2 distribution with a single degree of freedom (see Jansa and Voss, 2011). Values for ω_f and ω_b were then entered into the equation of Zhang et al. (2008: supplementary materials), to calculate the time of gene inactivation (T_N): $T_N = T((\omega_f - \omega_b)/(1- \omega_b))$, where T is the estimated time of divergence of the *Notoryctes* lineage (which was taken from the results of our total evidence dating analysis). This method assumes that, after a gene becomes inactive, ω for that gene becomes 1 (i.e., that non-synonymous substitutions and synonymous substitutions occur with the same frequency).

Anatomical description

General. Most of the limb bones of *Na. philcreaseri* discovered to date are missing the epiphyses, indicating that the epiphyseal sutures were unfused. Those that do preserve the epiphyses retain open sutures. In part, this may reflect the general marsupial pattern of most epiphyseal sutures remaining unfused throughout adult life (Geiger et al., 2014). However, based on their small size and very porous metaphyseal surfaces, at least some of the *Na. philcreaseri* specimens appear to represent juveniles (e.g., QM F57696, a right femur; QM F57703, a partial left ulna). By contrast, limb epiphyseal sutures are consistently fused in the skeletal specimens of *Notoryctes typhlops* and *N. caurinus* that we have examined, but these all appear to be adults based on the presence of a fully erupted permanent dentition (juvenile specimens of *Notoryctes* are exceptionally rare in scientific collections). Consistent closure of the epiphyseal sutures in the limbs of *Notoryctes* adults (which contrasts with the condition observed in most other marsupial species; Geiger et al. 2014) may reflect the high mechanical loadings their limbs are subjected to during digging; however, we note that Geiger et al. (2014) examined both fossorial and non-fossorial mammals and found no clear relationship between locomotor mode and the sequence of epiphyseal closure (see also Meier et al., 2013).

Scapula. Three partial scapulae are referable to *Na. philcreaseri* (see supplementary information), of which the most complete (QM F57716, which lacks only the acromion) is illustrated here (fig. 1a). In *Notoryctes* (and also some other burrowing mammals, such as talpids and chrysochlorids; Edwards, 1937; Reed, 1951; Puttick and Jarvis, 1977: fig. 3; Gasc et al., 1986), the scapular spine is oriented roughly parallel to the anterior thoracic vertebral column; hence the so-called "dorsal" (or "vertebral") border of the scapula is actually positioned caudally (rather than dorsomedially, towards the vertebral column), the "cranial" border is positioned dorsomedially, and the "caudal" (or "axillary") border is positioned ventrolaterally (Warburton, 2006). Based on its morphology, it seems likely that the scapula was similarly oriented in *Na. philcreaseri.* Nevertheless, to avoid confusion and to maintain consistency with anatomical descriptions of other mammals, we will refer to "cranial", "dorsal" and "caudal" borders in the scapula of *Na. philcreaseri* and *Notoryctes* following the terminology of, *inter alia*, Schaller (1992) and Evans (1993).

In dorsal view, the scapula appears narrow and elongate compared to those of most other marsupials. The supraspinous fossa is subtriangular in shape, and much larger in surface area than the infraspinous fossa. The infraspinous fossa is elongate and uniform in breadth along its length; its length-to-width ratio is approximately 10:1. Although slightly damaged in all three specimens, the scapular spine is clearly well-developed along its entire length, and its glenoid third is markedly broadened, slightly overhanging the infraspinous fossa. The angle between the "cranial" and "dorsal" borders of the scapula is approximately 80°, but is smoothly rounded. The "dorsal" border is short, rounded, and thickened for muscle attachment (principally the m. rhomboideus).

The glenoid third of the "caudal" border is markedly raised, forming a prominent secondary scapular spine that is separated from the scapular spine by the intervening infraspinous fossa. Although slightly damaged in QM F57716, the "caudal" angle appears rounded, thickened and slightly extended "caudally" (parallel to the "dorsal" border), for attachment of the m. teres major. The subscapular fossa is smoothly concave. The glenoid is large relative to the size of the supra- and infraspinous fossae, and the glenoid cavity is elliptical and relatively long. A small raised area from the "cranial" side of the glenoid cavity marks the coracoid process. The acromion is not preserved in any of the three specimens.

The elongate scapula of *Na. philcreaseri* bears a strong resemblance to that of *Notoryctes* (fig. 1b) and is broadly similar in size: maximum length of QM F57716 is 15.7 mm, compared to 13–13.5 mm in *N. caurinus* and 14.3–18.4 mm in *N. typhlops.* However, the modifications of the muscular attachment sites are markedly less extreme in the fossil species. Most notably, the "cranial" and "caudal" angles of the scapula (for attachment of the m. subscapularis and m. teres major respectively) appear to be gently rounded in *Na. philcreaseri* (although the caudal angle is slightly damaged in QM F57716, and hence its exact shape when intact is unclear), whereas in *Notoryctes* they are elongated and modified into recurved, hook-shaped processes, particularly the "caudal" angle, giving the bone an overall fan shape. *Notoryctes* also has a prominent postscapular fossa "caudal" to the secondary scapular spine,

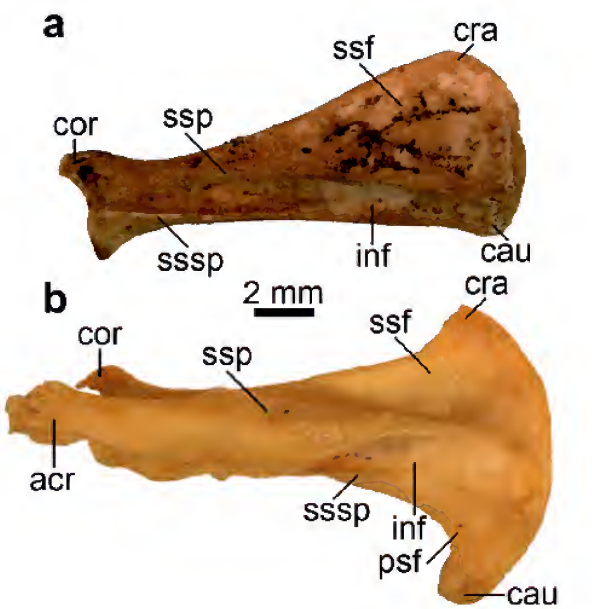

Figure 1. Comparison of scapulae of *Naraboryctes philcreaseri* and *Notoryctes typhlops* in lateral view: a, left scapula of *Naraboryctes philcreaseri* (QM F57716); b, right scapula (reversed) of *Notoryctes typhlops* (SAM M637). Abbreviations: acr, acromion process; cau, "caudal" angle; cor, coracoid process; cra, "cranial" angle; inf, infraspinous fossa; psf, postscapular fossa; ssf, supraspinous fossa; ssp, scapular spine; sssp, secondary scapular spine.

reflecting enlargement of the scapular (long) head of the m. triceps brachii. Enlargement of the triceps is common in fossorial mammals, particularly scratch diggers, and is also associated with elongation of the olecranon on the ulna (resulting in a larger IFA; Windle and Parsons, 1899; Taylor, 1978; Gasc et al., 1986; Stein, 1986; Lagaria and Youlatos, 2006; Warburton, 2006; Warburton et al., 2013). In *Na. philcreaseri*, the development of the secondary scapular spine reflects enlargement of the triceps compared to non-fossorial mammals. However, the absence of a postscapular fossa suggests that this muscle was probably not as well developed in *Na. philcreaseri* as it is in species of *Notoryctes*. The scapular spine is markedly broadened over two-thirds of its length in *Notoryctes*, towards the glenoid end, whereas only a third of the scapular spine is broadened in *Na. philcreaseri*. Furthermore, in *Notoryctes*, the scapular spine curves towards the secondary scapular spine, forming a tube-like structure that almost completely encloses the infraspinous fossa and infraspinatus muscle (this feature is better developed in *N. typhlops* than in *N. caurinus*; Warburton, 2006); no such tube is present in *Na. philcreaseri*.

Humerus. 31 humeri referable to *Na. philcreaseri* are known (see supplementary information). Their morphology is clearly indicative of fossoriality, and they are very similar in size and overall shape to those of *Notoryctes* species (see brief description by Archer et al., 2010: appendix 1). Most have lost their proximal and distal epiphyses. The specimen illustrated here, QM F57719, has the epiphyses in place, but the epiphyseal sutures remain unfused (figs. 2a, c).

The humeral head is large relative to the length of the bone, roughly hemispherical in shape, and protrudes posteromedially. The proximal tubercles are relatively low and broad; the greater tubercle extends slightly higher than the humeral head, while the lesser tubercle is slightly lower. The greater tubercle bears a short proximal crest, and is more than twice the breadth of the much smaller, ovoid lesser tubercle. The bicipital (intertubercular) groove is moderately broad and deep, and somewhat displaced medially due to the disproportionate sizes of the tubercles. The humeral neck is deeply constricted, particularly on its posterior aspect. The proximal half of the humeral shaft is relatively robust, and is marked by broad rugosities cranially and a broad sulcus caudally. The deltopectoral crest is massive and protrudes cranially and laterally from roughly the midpoint of the humeral shaft. This crest is thick and robust, with numerous rugosities, and its proximal end is distinctly concave in cranial view. Distal to this, a crest that appears continuous with the deltopectoral crest sweeps distally and medially, toward the medial epicondyle and over the supratrochlear foramen (which is proximal to the medial edge of the trochlea), giving the impression that the distal and proximal halves of the humerus are twisted relative to each other. Distally, the humerus broadens rapidly, primarily due to massive enlargement of the medial epicondyle; the maximum distal width of the humerus is slightly less than half its length. The medial epicondyle projects medially and is long and robust, with a bluntly rounded terminus. The trochlea and capitulum are smoothly contiguous, with only a slight medial constriction, and the combined articular surface is broad and convex. The coronoid

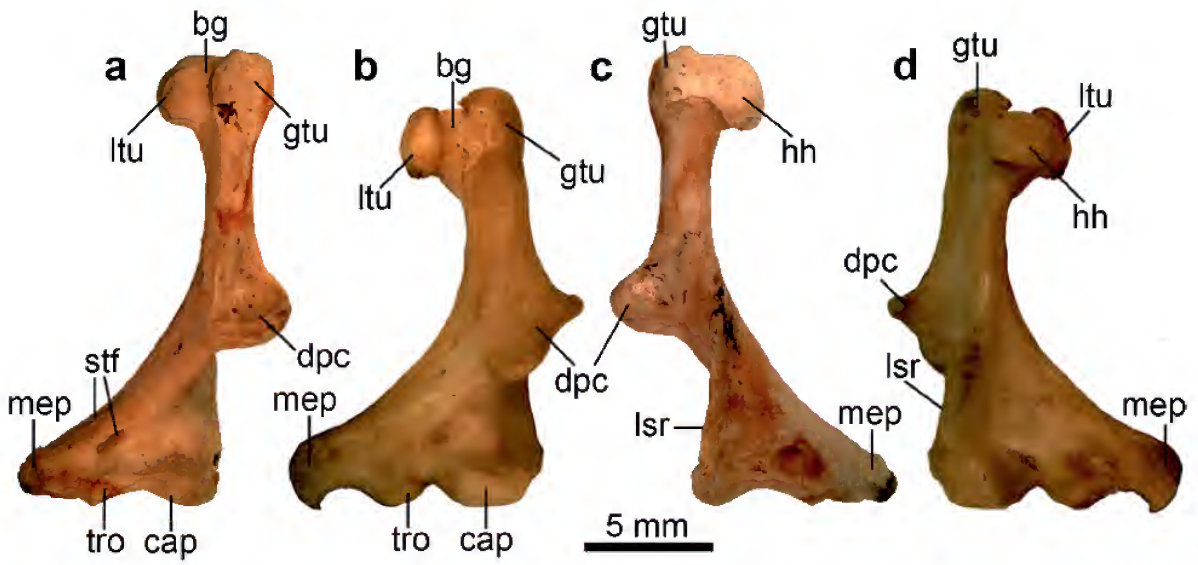

Figure 2. Comparison of humeri of *Naraboryctes philcreaseri* and *Notoryctes typhlops*: a, left humerus of *Naraboryctes philcreaseri* (QM F57719) in cranial view; b, right humerus (reversed) of *Notoryctes typhlops* (SAM M637) in cranial view; c, QM F57719 in caudal view; d, SAM M637 (reversed) in caudal view. Abbreviations: bg, bicipital groove; cap, capitulum; dpc, deltopectoral crest; gtu, greater tuberosity; hh, humeral head; lsr, lateral supracondylar ridge; ltu, lesser tuberosity; mep, medial epicondyle; stf, supratrochlear foramen; tro, trochlea.

fossa, proximal to the trochlea, is broad and shallow. The lateral epicondyle extends only slightly beyond the lateral border of the capitulum. The lateral supracondylar ridge is strongly developed, and extends proximally for more than one-third of the length of the humeral diaphysis, before merging with the mid-posterior surface of the shaft.

Although very robust compared to the humeri of non-fossorial mammals, the humerus of *Na. philcreaseri* is proportionately somewhat more elongate and gracile than that of *Notoryctes* (figs. 2b, d): maximum length and distal width of the most complete adult humeri of *Na. philcreaseri* (QM F23710, F57652 and F57719) are 15.1-17.2 mm and 7.9-8.3 mm respectively, whereas in *N. caurinus* they are 11.9-12.7 mm and 7.5-8.2 mm, and in *N. typhlops* they are 13.4-15.6 mm and 7.6-10.4 mm. As noted by Archer et al. (2011: appendix 1), the humeral shaft is oval in cross-section in *Na. philcreaseri*, rather than triangular as it is in *Notoryctes*, the proximal surface of the deltopectoral crest is concave rather than convex, and a supratrochlear foramen is present whereas this foramen is absent in *Notoryctes*. In addition, the bicipital groove is distinctly shallower than it is in *Notoryctes*, and the deltopectoral crest, medial epicondyle and lateral supracondylar ridge are all smaller and less strongly developed in the fossil species. A further key difference is that in *Notoryctes* the capitulum is relatively broader and more cylindrical, and there is a distinct separation of the capitulum and trochlea, whereas these form a single, continuous articular surface in *Na. philcreaseri*.

Radius. The 11 radii attributed here to *Na. philcreaseri* (see supplementary information) are very robust for their overall size. Both the proximal and distal ends of the bone are expanded, and are approximately equal width, although most are missing the proximal and distal epiphyses; QM F57679, however, is complete and is illustrated here (figs. 3a, c). The fovea is ovoid and smoothly concave, and demarcated by a well-marked border. Along the posterolateral aspect of the shaft is an obvious groove; this groove is also present in *Notoryctes*, where it houses a tendinous sheet (the interosseous membrane) that binds the shafts of the radius and ulna together (Warburton, 2006). The distal end of the radius (for the radiocarpal articulation) is very broad, and possesses a short styloid process. In its general size, shape and robustness, the radius of *Na. philcreaseri* is very similar to that of *Notoryctes* (figs. 3b, d), although this bone is slightly longer in the fossil species (10.7 mm in QM F57679; 10.3 mm in QM F57680) than in either *N. caurinus* (6.9-7.2 mm) or *N. typhlops* (7.4-9.3 mm).

Ulna. 30 ulnae referable to *Na. philcreaseri* are known (see supplementary information). Together with the humerus, the ulna of *Na. philcreaseri* arguably exhibits the most obvious evidence of fossorial adaptations, as briefly discussed by Archer et al. (2011: appendix 1). The ulnar shaft is robust and relatively deep in the cranial-caudal plane, but narrow mediodistally. The olecranon is long, robust and somewhat curved medially; measured from the distal margin of the trochlear notch (following Hopkins and Davis, 2009), it forms more than 40% of the total length of the ulna, although the exact percentage is uncertain as none of the ulnae of *Na. philcreaseri* are fully intact; most are missing either the proximal or distal epiphysis or both. The most complete specimen, QM F57706, is illustrated here (figs. 4a, c e) and was used to calculate IFA for *Na. philcreaseri* (table 1); however, QM F57706 lacks the distal epiphysis, and hence the calculated IFA is undoubtedly a slight overestimate (see below).

The trochlear (semilunar) notch is moderately deep, and its distal (coronoid) surface is very steep in comparison to the proximal (anconeal) surface. The trochlear notch is broad and lies in somewhat oblique alignment, from proximomedial to distolateral. The proximal anconeal process is long and extends laterally. A crest extends proximally from the medial margin of the proximal anconeal process, along the cranial aspect of the olecranon. A crest also extends distally along the cranial aspect of the ulnar shaft. The broad radial notch is on the lateral side of the anconeal process, slightly distal to the articular surface for the trochlea of the humerus. Medial and lateral coronoid processes surround the radial notch in a slightly oblique orientation. In medial view, a very prominent flexor sulcus extends from the proximal ulnar shaft onto the olecranon.

The ulna of *Na. philcreaseri* resembles that of *Notoryctes* (figs. 4b, d, f), and is similar in size; total preserved length of QM F57706 is 17.9 mm (when intact, this bone may have been 0.5-1.0 mm longer), whereas the length of this bone is 13.4-14.2 mm in *N. caurinus* and 15.4-18.7 mm in *N. typhlops*. However, the ulnar shaft is proportionately longer and mediolaterally narrower in *Na. philcreaseri*, and therefore appears more gracile. The morphology of the ulnar articular surfaces are very similar between the fossil and extant species, particularly in the distinct distal displacement of the radial articulation; however, the trochlear notch is not as broad and

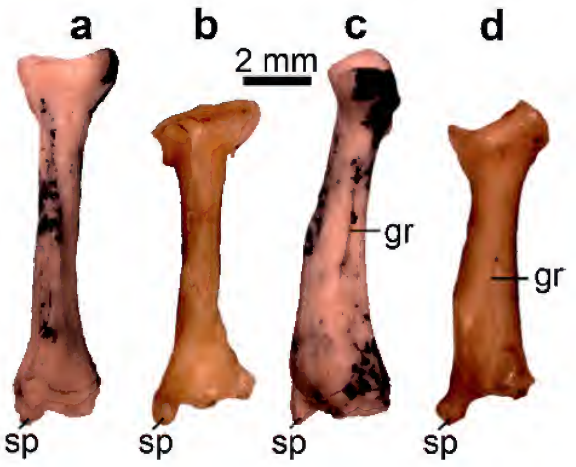

Figure 3. Comparison of radii of *Naraboryctes philcreaseri* and *Notoryctes typhlops*: a, left radius of *Naraboryctes philcreaseri* (QM F57679) in cranial view; b, right radius (reversed) of *Notoryctes typhlops* (SAM M637) in cranial view; c, QM F57679 in lateral view; d, SAM M637 (reversed) in lateral view. Abbreviations: gr, groove for interosseous membrane (tendinous sheet binding shafts of radius and ulna together); sp, styloid process.

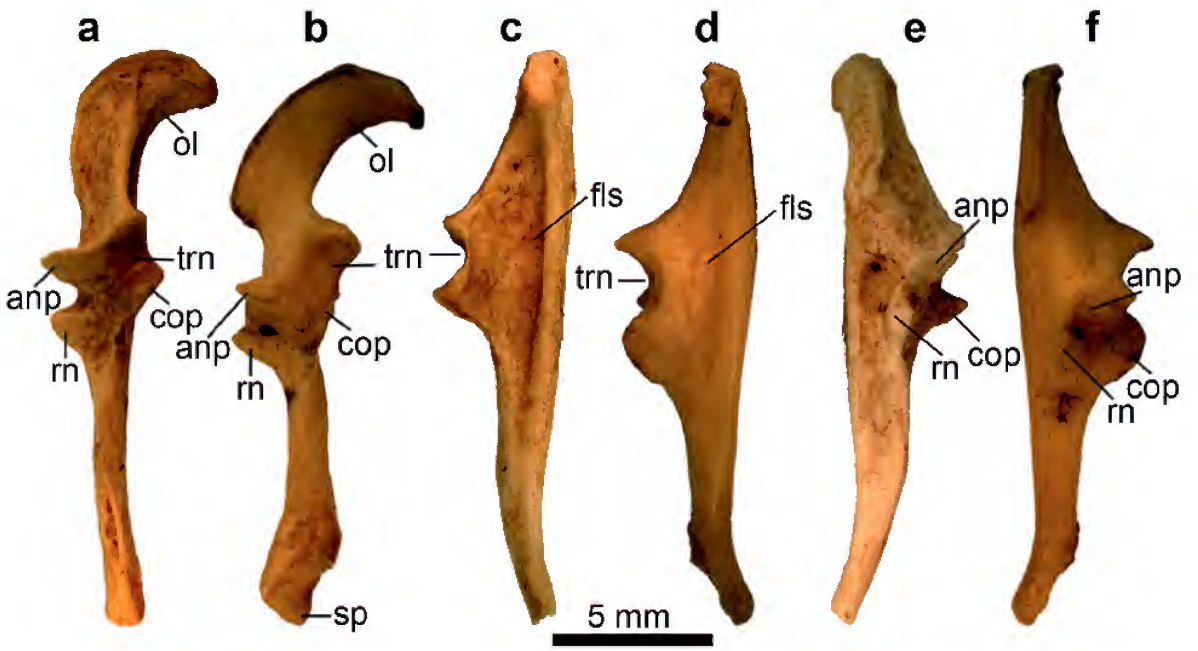

Figure 4. Comparison of ulnae of *Naraboryctes philcreaseri* and *Notoryctes typhlops*: a, right ulna of *Naraboryctes philcreaseri* (QM F57706) in cranial view; b, right ulna of *Notoryctes typhlops* (SAM M637) in cranial view; c, QM F57706 in medial view; d, SAM M637 in medial view; e, QMF 57706 in lateral view; f, SAM M637 in lateral view. Abbreviations: anp, anconeal process; cop, coronoid process; fls, flexor sulcus; ol, olecranon; rn, radial notch; sp, styloid process; trn, trochlear notch.

the radial notch not as deep in *Na. philcreaseri*. Interestingly, in QM F57706 at least, the flexor sulcus on the medial aspect of the ulna is deeper in *Na. philcreaseri* than in *Notoryctes*. The olecranon is also less curved medially in the fossil species; as a result, although the total length of the olecranon, measured following its curvature, is clearly proportionately greater in *Notoryctes*, the anteroposterior length of the olecranon, measured parallel to the ulnar shaft, is proportionately similar between the fossil and extant species.

Femur. The 17 femora referred here to *Na. philcreaseri* (see supplementary information) are highly distinctive (figs. 5a, c), but are broadly similar in size to femora of *Notoryctes* species; based on the three most complete *Na. philcreaseri* specimens (QM F57678, F57718, F57708), total length is 13.6-17.3 mm, compared to 12.4-14.1 mm in *N. caurinus* and 14.3-16.8 mm in *N. typhlops*. The femoral head is essentially spherical in shape. The greater trochanter is broad and laterally extended. In specimens in which the proximal femoral epiphyses are intact (e.g. QM F57678), the greater trochanter is very slightly lower than the femoral head. The lesser trochanter is broad and rounded in outline and does not extend proximally as far as the femoral head. In some specimens (e.g. QM F57708), the lesser trochanter is deeply excavated such that its cranial face forms a distinct 'pocket', whereas in others (e.g. QM F57678) a somewhat shallower, less well-defined depression is present. In caudal view, a small, shallow trochanteric fossa is visible in a quite lateral position, on the caudal face of the greater trochanter. The femoral shaft is robust for its length and oval in cross-section. The distal shaft flares towards the enlarged condylar region. The intercondylar groove is relatively broad. A large, anteroposteriorly-compressed process, the third trochanter, protrudes laterally from the mid-shaft. At the level of the third trochanter, the maximum transverse width of the femur is more than one-fifth of femoral length.

The femur of *Na. philcreaseri* is substantially modified from those of more generalised marsupials in its being particularly robust, the strong development (relative to absolute size) of the greater and lesser trochanters, and the presence of a very large third trochanter. In comparison to *Notoryctes* (figs. 5b, d), the femoral shaft of *Na. philcreaseri* is not as robust with respect to femoral length, nor is the greater trochanter as robust or broad. The lesser trochanter is located in a more proximocaudal position in *Notoryctes*, such that it is proximodistally level with the femoral head (Warburton, 2006: fig. 13). *Na philcreaseri* retains a small trochanteric fossa, whereas no such fossa is found in *Notoryctes*. A particularly striking difference between *Na. philcreaseri* and *Notoryctes* is that the latter lacks a distinct third trochanter. However, the greater trochanter of *Notoryctes* is very large and extends distally as a wing-like process along

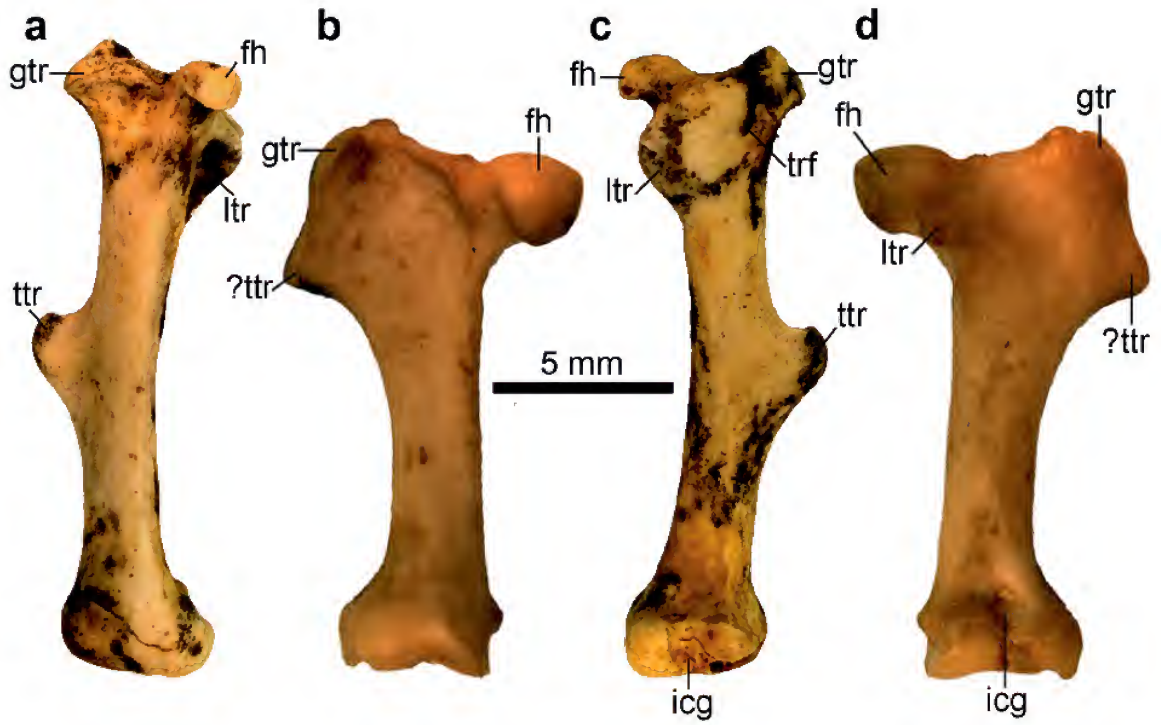

Figure 5. Comparison of femora of *Naraboryctes philcreaseri* and *Notoryctes typhlops*: a, right femur of *Naraboryctes philcreaseri* (QM F57678) in cranial view; b, right femur of *Notoryctes typhlops* (SAM M637) in cranial view; c, QM F57678 in caudal view; d, SAM M637 in caudal view. Abbreviations: fh, femoral head; gtr, greater trochanter; icg, intercondylar groove; ltr, lesser trochanter; trf, trochanteric fossa; ttr, third trochanter.

the lateral margin of the proximal quarter of the femur; we suspect that this process originated via ancestral fusion of the greater and third trochanters, with the distal end of this process homologous with the third trochanter of *Na. philcreaseri*, as we discuss in more detail below (see Discussion).

Tibia. The five tibiae described here are referred to *Na. philcreaseri* (see supplementary information) on the basis of their size and unusual morphology (figs. 6a, c), which somewhat resembles that observed in *Notoryctes* (figs. 6b, d). All known specimens are missing the proximal and distal epiphyses, with preserved lengths ranging from 10.2 to 12.7 mm. By comparison, intact tibial length is 10.1-10.5 mm in *N. caurinus* and 12.6-13.6 mm in *N. typhlops*. The most distinctive feature of the *Na. philcreaseri* tibiae is the massively developed tibial crest on the cranial aspect, which extends along the proximal two-thirds of the length of the tibia and more than doubles its craniocaudal depth. The development of the massive tibial crest is strongly reminiscent of the strong development of the same feature in *Notoryctes*. Unlike the flat, blade-like tibial crest of *Notoryctes*, however, the crest in *Na. philcreaseri* is curved in cross-section, such that it is slightly convex on its medial surface and slightly concave on its lateral surface. In addition, whereas the crest is most extensive cranially at its proximal end (adjacent to the articulation with the femur) in *Notoryctes*, in *Na. philcreaseri* it is most extensive more distally, reaching its maximum extent about two-thirds along its length from the proximal end of the tibia. The tibial crest of *Notoryctes* is mediolaterally broad and concave at its proximal end, for articulation with the distinctive enlarged patella. By contrast, the crest in *Na. philcreaseri* is mediolaterally narrow, and there is no sulcus that might have housed a patella. It is therefore unclear whether or not a patella was present in *Na. philcreaseri*. Absence of the proximal and distal epiphyses also means that the precise morphology of the femoral and tarsal articular surfaces is unknown; in particular, it is unclear whether or not the peculiar, rounded process present posterolaterally at the proximal end of the tibia in *Notoryctes* (which articulates with the lateral condyle of the femur and also with the fibula; Stirling, 1891: 179) was present in *Na. philcreaseri*. However, proximally, it appears that the medial condyle was probably slightly larger than the lateral condyle in *Na. philcreaseri*, as in *Notoryctes*. The distal shaft is also short and very robust, although slightly less so than in *Notoryctes*.

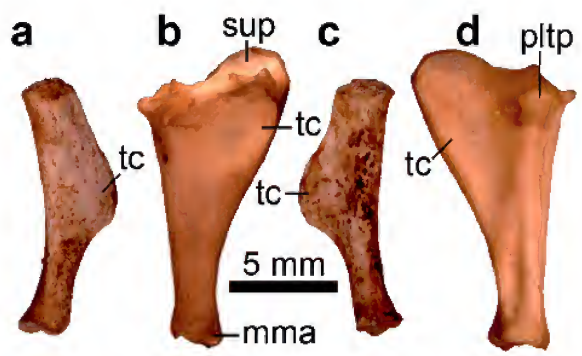

Figure 6. Comparison of tibiae of *Naraboryctes philcreaseri* and *Notoryctes typhlops*: a, left femur of *Naraboryctes philcreaseri* (QM F57686) in medial view; b, left femur of *Notoryctes typhlops* (SAM M637) in medial view; c, QM F57686 in lateral view; d, SAM M637 in lateral view. Abbreviations: mma, medial malleolus; pltp, posterolateral tibial process for articulation with lateral femoral condyle and fibula; sup, sulcus for patella; tc, tibial crest.

Functional interpretation of the postcranial skeleton of *Naraboryctes philcreaseri*

Forelimb. The scapula of *Na. philcreaseri* (fig. 1a) is elongate and narrow in comparison to those of more generalised mammals. In *Notoryctes* (fig. 1b) and many other fossorial and subterranean mammals, the scapula is similarly elongate and narrow (Reed, 1951; Gasc et al., 1986; Warburton, 2006; Salton and Sargis, 2008). In these forms, this morphology reflects the reduction of dorsally-placed muscles between the thoracic vertebral column and scapula (e.g. the m. rhomboideus), which allows posterior rotation of the scapula. It is also correlated with the more cranio-caudal alignment of the long axis of the scapula (Reed, 1951; Puttick and Jarvis, 1977; Gasc et al., 1986; Warburton, 2006), which results in enhanced mobility of the pectoral girdle along the cranial-caudal axis (as demonstrated in *Eremitalpa*; Gasc et al., 1986). As a result, the pectoral girdle is highly mobile, facilitating protraction and retraction of an extended forelimb, as is required for scratch-digging (Hildebrand, 1985; Nevo, 1999: 71).

The humerus (figs. 2a, c), radius (figs. 3a, c) and ulna (figs. 4a, c, e) of *Na. philcreaseri* are all very robust for their length, and the articular surfaces of these bones are relatively large in surface area. Short, robust limb bones are characteristic of semi-fossorial and fossorial mammals (Casinos et al., 1993; Farina and Vizcaino, 1997; Vizcaino et al., 1999; Campione and Evans, 2012), being better able to withstand the high muscular and reaction forces acting through the bones during digging (Hildebrand and Goslow, 2001; Elissamburu and Vizcaíno, 2004). The relatively large surface area of humeral head, capitulum and radial fovea of *Na. philcreaseri* would have acted to improve the stability and structure of the joint by spreading large mechanical forces over a greater area. Similarly enlarged articular surfaces are found in the forelimb of many other fossorially-adapted mammals, including chrysochlorids (Gasc et al., 1986) and anteaters (Taylor, 1978).

The enlarged and strengthened muscle attachment sites of the forelimb of *Na. philcreaseri*, notably the development of a secondary spine on the scapula (fig. 1a), the enlarged deltopectoral crest and medial epicondyle of the humerus (figs. 2a, c), and the proportionately robust and elongate olecranon of the ulna (fig. 4a), are also all characteristic of a fossorial or subterranean lifestyle (Reed, 1951; Lehmann, 1963; Taylor, 1978; Thorington et al., 1997; Warburton, 2006; Warburton et al., 2013). Collectively, they reflect enlargement of the m. triceps longus, mm. pectorales, m. flexor carpi radialis, and m. flexor carpi ulnaris and m. flexor digiti profundus, each of which contribute during the power stroke of digging and thus require increased power in order to act against the resistance of the substrate.

Besides muscle enlargement, power can also be increased by migration of muscle attachment sites to improve mechanical advantage: typically, fossorial mammals enhance mechanical advantage by increasing the length of the in-lever relative to the out-lever length (Lehmann, 1963; Nevo, 1979; Nevo, 1999; Hildebrand and Goslow, 2001). The distally placed deltopectoral crest of the humerus (figs. 2a, c) and greatly enlarged olecranon of the ulna (fig. 4a) of *Na. philcreaseri* would have acted to functionally increase the in-lever length of their respective muscles by moving the insertions further from the joint across which they act, while the relatively short limb bones would have reduced the length of the out-lever. In comparison to other fossorial mammals, the deltopectoral insertion is more distally placed in *Na. philcreaseri* than in digging armadillos (MacAlister, 1875a; Macalister, 1875b; Burne, 1901; Hildebrand and Goslow, 2001) and fossorial rodents (Lehmann, 1963), but less distally placed than the homologous structure in some chrysochlorids (Gasc et al., 1986). Similarly, the elongate medial epicondyle of *Na. philcreaseri* (figs. 2a, c) reflects improved mechanical advantage by providing a long lever arm of the forearm flexor musculature (as well an enlarged area for muscle attachment), for strong flexion of the wrist against the substrate during digging. This is convergent with other scratch diggers, particularly where the elbow is somewhat extended during limb retraction in the power-stroke of digging (Gasc et al., 1986; Warburton, 2006). It is also characteristic of fossorial mammals that utilise a partially abducted (half-sprawling) or sprawling posture of the carpus during digging (Gambaryan and Kielan-Jaworowska, 1997).

Turning now to the ulna, IFA for *Na. philcreaseri* is 88.4, which is slightly higher than that for *Notoryctes typhlops* (87.2; see table 1). However, the specimen used to calculate IFA in *Na. philcreaseri*, QM F57706, is missing the distal epiphysis (see fig. 4a, c, e) and so this value is undoubtedly a slight overestimate; the true value for *Na. philcreaseri* is probably the same as, or slightly less than, that for *N. typhlops*. It should also be noted that IFA is based on the anteroposterior length of the olecranon; it does not take into account the degree of medial curvature of the olecranon, which is greater in *Notoryctes* species (fig. 4b; Warburton, 2006: fig. 9) than in *Na. philcreaseri* (fig. 4a). The IFA values for *Na philcreaseri* and *N. typhlops* are some of the highest seen in mammals

(table 1); of the taxa measured by Hopkins and Davis (2009), only the chrysochlorid *Amblysomus hottentotus* (which is subterranean), the dasypodids *Priodontes maximus* and *Cabassous centralis* (which are both fossorial), and the fossil epoicotheriid palaeanodonts *Xenocranium pileorivale* and *Pentapassalus pearcei* exhibit higher values. Other subterranean mammals, such as talpids and spalacid rodents are characterised by lower IFA values (table 1).

Hind limb. The femur of *Na. philcreaseri* is robust, and the greater and lesser trochanters are very large for a bone belonging to a mammal of this size (figs. 5a, c). The lateral expansion of the proximal femur compared to more generalised marsupials seen in *Na. philcreaseri* is largely due to enlargement of the greater trochanter. Lateral extension of the proximal femur is even more extreme in *Notoryctes*, due to its very wide greater trochanter (figs. 5b, d). Although not as large as in *Notoryctes*, the transversely wide greater trochanter of *Na. philcreaseri* would have improved the mechanical advantage of the gluteal muscles for limb abduction by increasing the length of the in-lever; this suggests a strongly abducted posture of the hind limbs, most likely to brace the hind part of the body during digging, but potentially also during the propulsive phase of locomotion.

The prominent third trochanter protruding laterally from the midshaft of the femur of *Na. philcreaseri* is highly distinctive (figs. 5a, c). A much smaller, more proximally-positioned third trochanter occurs in caenolestids, vombatids and some stem-metatherians (Szalay and Sargis, 2001; Horovitz et al., 2008; Abello and Candela, 2010). However, no such distinct process is observed in *Notoryctes* (figs. 5b, d) or most other marsupials. Among placental mammals at least, the third trochanter (where present) is for attachment of the gluteal muscles. The gluteal musculature of *Notoryctes* is modified compared with that of other marsupials, due to the highly modified morphology of the pelvis and the expanded greater trochanter (Warburton, 2006). While there is no indication in the living species of an insertion by the gluteal musculature on the mid-lateral femur, the morphology of the femur of *Naraboryctes* may represent an adaptation for increasing the leverage of the gluteal muscles for limb abduction. If so, this may indicate that the hindlimbs were strongly abducted in *Na. philcreaseri* (at least during burrowing), which would be a plausible intermediate stage between the parasagittal stance of generalised terrestrial mammals and the highly specialised stance of *Notoryctes*, where the legs appear to project laterally from the body and no longer play a role in supporting the body off the substrate. In addition, among extant and fossil xenarthrans, a prominent third trochanter has been proposed as a mechanism to mitigate, by muscular action, bending forces acting through the femur (Milne and O'Higgins, 2012). The hypothesised shift to a strongly abducted hind limb position in *Na. philcreaseri*, potentially for bracing or active excavation of substrate, would tend to increase bending moments through the femur; if so, this may have favoured the evolution of enlarged gluteal musculature to mitigate these forces, with concomitant development of a large third trochanter. In *Notoryctes*, there is a well-developed crest extending from the greater trochanter along the proximal third of the length of the bone (figs. 5b, d). We suggest that this proximally-extended lateral crest in *Notoryctes* is the result of ancestral fusion of the third trochanter seen in *Na. philcreaseri* with the greater trochanter, and that the distal end of this crest in *Notoryctes* is homologous with the third trochanter of *Na. philcreaseri*.

Discriminant analysis

Compared to Hopkins and Davis' (2009) original "limbs only" dataset, our quadratic discriminant analysis based on a slightly expanded and modified dataset showed slightly better accuracy for discriminating burrowing from non-burrowing mammals (13.2% misidentified, versus 13.9% in Hopkins and Davis, 2009), but was somewhat less accurate at determining the degree of fossoriality, i.e. distinguishing between non-burrowing, fossorial and subterranean mammals (18.2% misidentified, versus 14.8% in Hopkins and Davis, 2009). In the "burrowing" versus "non-burrowing" analysis, *Na. philcreaseri* was identified as burrowing with very high probability (p = 0.99), and in the "non-burrowing" versus "fossorial" versus "subterranean" analysis it was identified as subterranean, again with very high probability (p =1.00). A plot of the first two canonical axes from the non-burrowing versus fossorial versus subterranean analysis indicates that the first axis encompasses 91.2% of the total variability, with subterranean taxa exhibiting the lowest values and non-burrowing taxa the highest values (fig. 7). *Na. philcreaseri* exhibits a very low value for the first canonical axis, even lower than for *N. typhlops*, and plots closest to the subterranean chrysochlorid *Eremitalpa granti* (fig. 7).

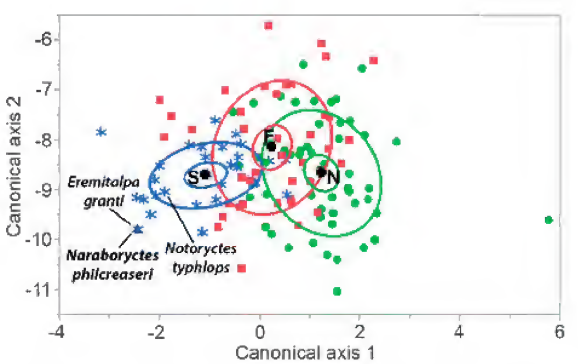

Figure 7. Plot of first two canonical axes from quadratic discriminant analysis of degree of fossoriality (non-burrowing versus fossorial versus subterranean) in mammals based on an expanded version of the "limbs only" dataset of Hopkins and Davis (2009). Non-burrowing species are represented by green circles, fossorial species by pink squares and subterranean species by blue asterisks. Inner ellipses represent 95% confidence intervals for the means for each class, whilst the outer ellipses represent the 50% prediction intervals. *Naraboryctes philcreaseri* is represented by a black triangle and was treated as unknown, but falls among subterranean species and is predicted to be subterranean with very high probability (p = 1.0). Abbreviations: F, fossorial; N, non-burrowing; S, subterranean.

Phylogeny and divergence times

The dated phylogeny that results from Bayesian analysis of our total matrix using the IGR clock model is given in Figure 8. The topology is broadly congruent with that found in analyses of a similar version of the matrix by Beck et al. (2014). As expected, *Na. philcreaseri* is recovered as sister-taxon to *Notoryctes*, with strong support (BPP=0.91). Notoryctemorphia (i.e. *Naraboryctes* + *Notoryctes*) is sister to Peramelemorphia (i.e. *Echymipera* + *Perameles*), with Dasyuromorphia (i.e. *Dasyuroides* + *Dasyurus* + *Phascogale*) outside this, but support values for these two nodes are very low (BPP <0.5). There is somewhat stronger support (BPP = 0.71) for the clade comprising Notoryctemorphia, Peramelemorphia, Dasyuromorphia and *Yalkaparidon*, which corresponds to Agreodontia *sensu* Beck et al. (2014).

In terms of divergence times, the base of Agreodontia is estimated to be 55.2 MYA (95% HPD = 48.0-63.9 MYA), with Dasyuromorphia diverging at 54.4 MYA (95% HPD = 46.8-63.9 MYA), and the Notoryctemorphia-Peramelemorphia split estimated at 52.2 MYA (95% HPD = 43.6-60.7 MYA). The point estimate for the split between *Notoryctes* and *Naraboryctes* is 30.3 MYA, which is considerably older than the age of *Naraboryctes* inferred here (19.4 Ma old; 95% HPD = 16.0-22.6 Ma old). However, the 95% HPD for this split is wide (17.7-46.3 MYA) and overlaps the inferred age of *Na. philcreaseri*. Furthermore, the 95% HPD for the effective branch length leading to *Naraboryctes* (i.e. the estimated change relative to that inferred for the last common ancestor of *Naraboryctes* and *Notoryctes*) is 0.0000-0.0733 substitutions/site (= changes/character) for the morphological partition (see supplementary information); this encompasses the possibility that *Na.philcreaseri* exhibits no morphological apomorphies relative to the *Naraboryctes-Notoryctes* common ancestor. Thus, when 95% HPDs are taken into account, the age and morphology of *Na. philcreaseri* are both compatible with its being ancestral to *Notoryctes* (M.S.Y. Lee, pers. comm.).

RBP3 inactivation

Specifying separate values of ω for the *RBP3* alignment for *Notoryctes* (the "foreground" branch, ω_f) and for all other branches (the "background" branches, ω_b) did not result in a significantly better fit than the null model of a single value of ω for all branches ($p >> 0.05$). However, entering the values for ω_f (0.244) and ω_b (0.15635) into the equation of Zhang et al. (2008), and assuming that *Notoryctes* diverged from (*Echymipera* + *Perameles*) at 52.2 MYA (see above) gives an estimate of 5.4 MYA for the timing of inactivation of *RBP3* in the *Notoryctes* lineage, with a range of 4.5–6.3 MYA if the

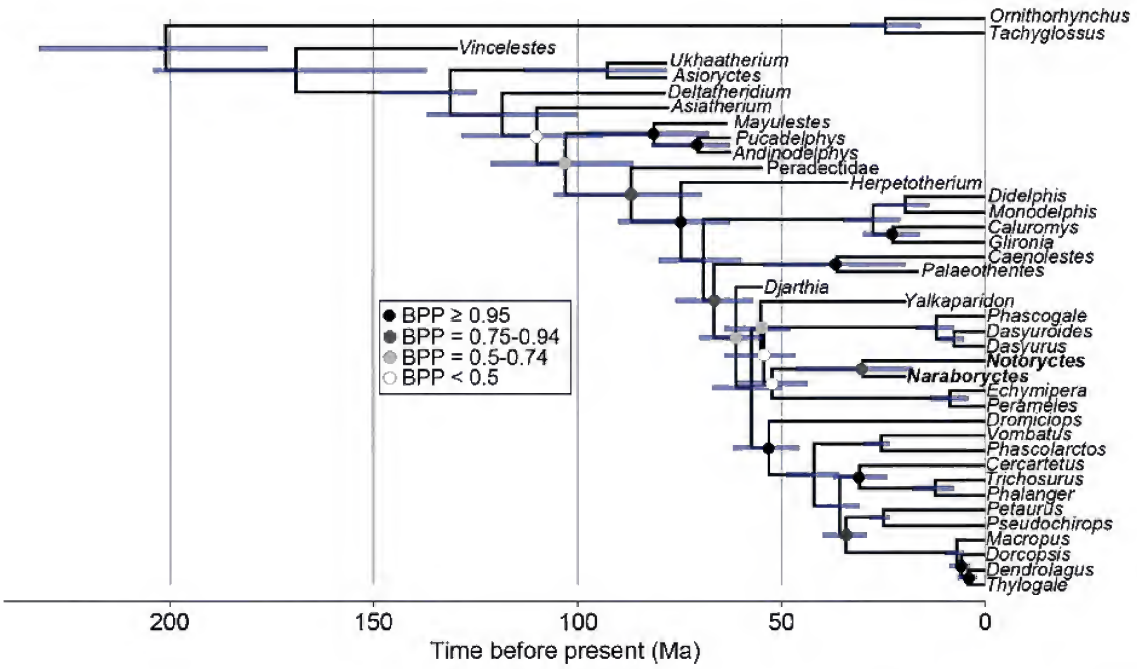

Figure 8. Dated total evidence phylogeny based on 259 morphological characters and 9012 bp of sequence data from five nuclear genes (*APOB*, *BRCA1*, *RBP3*, *RAG1*, and *VWF*) analysed using MrBayes 3.2.2 assuming the Independent Gamma Rates (IGR) clock model, with topological and temporal constraints applied to selected internal nodes (see supplementary information). *Notoryctes* and *Naraboryctes* are indicated in bold. Blue bars represent 95% highest posterior density intervals (HPDs) on the divergence times. Nodes without Bayesian posterior probability (BPP) were constrained *a priori*.

95% HPD for the time of divergence is taken into account (fig. 9; see above). This corresponds to the latest Miocene-earliest Pliocene, and considerably postdates the age of *Na. philcreaseri* (fig. 9), suggesting that *RBP3* was functional in this fossil taxon. Interestingly, it is similar to Mitchell et al.'s (2014) relaxed molecular clock estimate of 4.5 MYA for the divergence between the living species *Notoryctes typhlops* and *N. caurinus*.

Discussion

Qualitative functional analysis of the postcranial anatomy of *Na. philcreaseri* indicates that it was well-adapted for scratch-digging. Of particular significance are the narrow, elongate scapula with secondary scapular spine, very robust humerus with enormously enlarged deltopectoral crest and medial epicondyle, and greatly enlarged and medially-inflected olecranon of the ulna. All of these are characteristic of extant scratch-diggers, and of fossil mammals that have been interpreted to exhibit similar burrowing behaviour, such as the early Miocene meridiolestidan *Necrolestes* and the late Eocene epocoitheriid palaeanodonts *Epoicotherium* and *Xenocranium* (Turnbull and Reed, 1967; Rose and Emry, 1983). This interpretation is bolstered by the results of our quadratic discriminant analysis, in which *Na. philcreaseri* is predicted

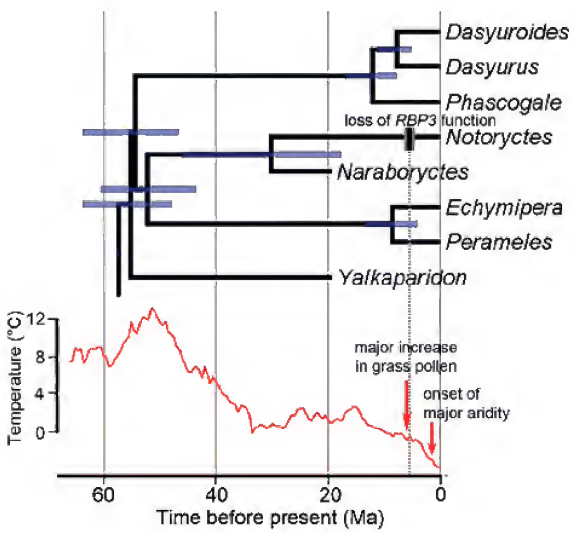

Figure 9. Part of the dated total evidence phylogeny shown in Figure 8, restricted to the clade Agreodontia (which includes Notoryctemorphia), with divergence dates compared to global temperatures and environmental change in Australia. The estimated time of inactivation of the *RBP3* gene in the *Notoryctes* lineage is indicated: the black bar represents the point estimate (5.4 MYA), whilst the grey bars represent 95% HPDs (4.5-6.3 MYA). The global temperature curve is modified from Zachos et al. (2001). The date for the major increase in grass pollen is taken from Martin and McMinn (1994: fig. 2) whilst the date for the onset of major aridity in Australia (~1.4-1.5 MYA) is taken from McLaren and Wallace (2010).

to be subterranean based on its limb proportions, and lies closest to the subterranean chrysochlorid *Eremitalpa granti* in our plot of the first two canonical axes. In addition, although the IFA value calculated for *Na. philcreaseri* (88.4) is undoubtedly a slight overestimate, it is almost identical to that for *N. typhlops* (87.2), and is greater than that for many fully subterranean mammals (table 1). In summary, all available morphological evidence supports the conclusion that *Na. philcreaseri* was a specialised, most probably subterranean, scratch-digger.

These results indicate that specialised fossorial, probably subterranean, behaviour originated in the notoryctemorphian lineage some time before the early Miocene. The Faunal Zone B deposits at Riversleigh from which all known specimens of *Na. philcreaseri* have been recovered appear to represent rainforest environments (Travouillon et al., 2009; Archer et al., 2011; Bates et al., 2014), and forests likely predominated throughout Australia until the middle-late Miocene (Martin, 2006). This may be an indication that the burrowing specialisations of fossil notoryctemorphians were well-suited to, and potentially evolved in, such closed forest environments. If so, the golden moles *Chrysospalax trevelyani* and *Huetia leucorhina* (which forage in or above leaf litter as well as digging burrows in the rainforests of sub-Saharan Africa; Bronner, 2013) and possibly other fossorially-adapted mammals that live in rainforest environments (e.g. the tenrec *Oryzorictes hova* of Madagascar, and the peramelemorphian *Microperoryctes murina* of New Guinea) may represent reasonable living analogues for early notoryctemorphians. However, rainforest soils are typically thin and do not appear favourable for the evolution of a truly subterranean lifestyle. Furthermore, Riversleigh appears to have been a karst environment during the early Miocene (Arena, 2004; Arena et al., 2014), and karst (including karst in rainforest) typically has exposed rocky surfaces only partially covered by thin soils (although deep, dirt-filled fissures may be present; D.A. Arena, pers. comm.). We therefore propose two further scenarios for the origin of specialised fossorial behaviour in notoryctemorphians.

It is interesting that all specimens of *Na. philcreaseri* collected to date are from sites at Riversleigh that are interpreted as representing cave deposits (Arena, 2004; Arena et al., 2014). An alternative hypothesis is therefore that notoryctemorphians acquired fossorial behaviours foraging for invertebrates within cave environments, burrowing through guano-rich cave floors. However, we note that no modern mammal or other terrestrial vertebrate of which we are aware occupies such a niche, nor is their compelling evidence for occupation of this niche by any other fossil vertebrate species. Furthermore, all Riversleigh sites representing the early Miocene Faunal Zone B appear to be cave deposits (D. A. Arena, pers. comm.). Thus, the presence of *Na. philcreaseri* fossils at these sites may simply be because notoryctemorphians only occurred in the Riversleigh area during the early Miocene, and are present in cave deposits because those are the only deposits preserved from this time period, not because they were cave-dwelling. Several other Riversleigh mammal species are known only from Riversleigh Faunal Zone B (and

hence are found only in cave deposits), including the thylacinids *Wabulacinus ridei* and *Ngamalacinus timmulvaneyi* (see Muirhead, 1997) and species of the miralinid possum *Durudawiri* (e.g. Crosby and Archer, 2000; Crosby, 2002), none of which are likely to have been cave-dwellers. However, remains of these species are admittedly much rarer than those of *Na. philcreaseri*. On the other hand, Rzebik-Kowalska (2013) reported very large numbers of individuals of the talpid "true moles" *Talpa europaea* and *T. minor* in early Pleistocene deposits at Zabia Cave in Poland, and suggested that the cave acted as a natural trap for moles due to their burrowing activities. This might explain the abundant remains of *Na. philcreaseri* in Faunal Zone B cave deposits, without needing to assume that it was a specialised cave dweller.

A third hypothesis is that early notoryctemorphians were semi-aquatic, and that their semi-aquatic adaptations subsequently became exapted for fossoriality. Several species of talpid moles are semi-aquatic, and some authors have proposed that modern talpids all descend from a semi-aquatic ancestor (Campbell, 1939; Whidden, 1999; but see Reed 1951; Hickman 1984). Similarly, the fossorial adaptations of the living platypus (which is semi-aquatic) and echidnas (which are terrestrial) may represent exaptations from a semi-aquatic monotreme ancestor (Phillips et al., 2009; Phillips et al., 2010; Mirceta et al., 2013; but see Camens 2010; Ashwell 2013; Musser 2013). However, there is only a single extant semi-aquatic marsupial, the yapok or water-opposum *Chironectes minimus* (see Marshall, 1975; Stein and Patton, 2008), and only one questionably semi-aquatic stem-metatherian, *Didelphodon vorax* (Szalay, 1994; Longrich, 2004; but see Fox and Naylor, 2006). This suggests that marsupials are, in general, poorly adapted to semi-aquatic or aquatic niches, probably due to their reproductive mode (Lillegraven, 1975; Phillips et al., 2009). We consider it unlikely, based on available evidence, that Na. *philcreaseri* was an exception to this general rule. However, this hypothesis can be tested: Mirceta et al. (2013) showed that mammals with some degree of aquatic ancestry show elevations in myoglobin net surface charge, which is correlated with maximal skeletal muscle concentration of myoglobin, which in turn is linked with maximal active dive time underwater. Mirceta et al.'s (2013) study suggests that scalopine talpids (members of other talpid subfamilies were not sampled) and modern monotremes derive from at least semi-aquatic ancestors, but that chrysochlorids apparently do not. Using this approach, sequencing of the myoglobin locus for one or both living *Notoryctes* species should reveal whether or not they have semi-aquatic ancestry. Histological analysis of humeral microanatomy, specifically bone compactness, may also indicate whether or not *Na. philcreaseri* was semi-aquatic (Canoville and Laurin, 2010). However, a recent study of bone compactness in the humeri of talpids found no significant difference between fossorial and semi-aquatic taxa (Meier et al., 2013).

The point estimates for the age of *Na. philcreaseri* (19.4 Ma) and the timing of the *Naraboryctes-Notoryctes* split (30.3 Ma) imply that *Na. philcreaseri* post-dates the divergence between the *Naraboryctes* and *Notoryctes* lineages. However, when 95% HPDs are taken into account, these estimates overlap. In addition, the 95% HPD for the effective branch length leading to *Naraboryctes* encompasses a zero length branch. Collectively, this means that the age and known morphology of *Na. philcreaseri* is compatible with its being ancestral to *Notoryctes*. Furthermore, the postcranial differences observed between *Na. philcreaseri* and the extant *Notoryctes* species (*N. typhlops* and *N. caurinus*) appear to represent further developments of morphological trends that are apparent when comparing *Na. philcreaseri* to more generalised marsupials. They can plausibly be interpreted as reflecting more extreme specialisation towards burrowing in *Notoryctes*.

Specifically, derivation of the postcranial morphology seen in the extant *Notoryctes* species, *N. typhlops* and *N. caurinus*, from a *Naraboryctes*-like ancestor would require the following major changes. In the scapula: lengthening of the "vertebral" border and modification of the coracoid and axillary angles into hook-like processes for attachment of the subscapularis and teres major muscles; lengthening of the secondary scapular spine towards the "caudal" angle; and enlargement of the scapular spine, which curves medially towards the secondary scapular spine to enclose the infraspinatus muscle within a nearly complete tube; development of a postscapular fossa, reflecting enlargement of the triceps muscle group. In the humerus: further enlargement of the deltopectoral crest; further expansion of the medial epicondyle, increasing the surface area of origin for the forearm flexor musculature; enlargement of the lateral supracondylar ridge, increasing the surface area of origin for the forearm extensors. In the ulna: further elongation of the olecranon and development of a more marked medial curvature; broadening of the trochlear notch; deepening of the radial notch. In the radius: increased concavity of the articular surfaces for the humerus and ulna at the proximal end; broadening of the distal end. In the femur: further enlargement of the greater trochanter and the head of the femur; loss of the third trochanter, probably by proximal migration and fusion with the greater trochanter; a slight proximocaudal shift in the position of the lesser trochanter, such that it is proximodistally level with and caudal to the femoral head; increased robusticity of the femoral shaft. In the tibia: increased robusticity of the tibial shaft and further enlargement of the tibial crest, particularly at its proximal end, with development of a proximal sulcus that houses an enlarged patella.

As discussed by Archer et al. (2011), the apomorphic dental morphology of extant *Notoryctes* species can also be plausibly derived from that seen in *Na. philcreaseri*, via loss of a premolar locus (P1 is tiny in *Na. philcreaseri*), complete suppression of the paracone on the upper molars (this cusp is greatly reduced and shifted labially in *Na. philcreaseri*), and loss of the talonid on the lower molars (the talonid is present but narrow in *Na. philcreaseri*). Thus, the known dental and postcranial morphology of *Na. philcreaseri* renders it a plausible model for a plesiomorphic ancestor of *Notoryctes*.

If our estimate for the timing of inactivation of *RBP3* in the *Notoryctes* lineage, 5.4 MYA (95% HPD = 4.5–6.3 MYA;

latest Miocene to earliest Pliocene), is correct, then *RBP3* was presumably functional in the early Miocene *Na. philcreaseri*. In turn, this might be an indication that *Na. philcreaseri* still retained some visual capabilities. If so, we might predict that orbit will be more obviously identifiable on the cranium of *Na. philcreaseri* than in *Notoryctes*, in which osteological evidence for the orbit is minimal (Stirling, 1891; Carlsson, 1904; Johnson and Walton, 1989); for example, the frontal process of the jugal (for attachment of the postorbital ligament) might be more strongly developed. However, testing of this hypothesis will require the discovery of additional, more complete cranial material of *Na. philcreaseri*. Archer et al. (2011) noted that the jaw and dentition of *Na. philcreaseri* seem adapted for somewhat harder food items than those of modern *Notoryctes* species which may be an indication that the fossil taxon foraged at least some of the time on the surface (particularly soft-bodied invertebrates such as insect larvae and worms being more common below ground). Based on this combined genetic and morphological evidence (and pending the discovery of more complete cranial remains that would reveal the degree of development of its orbit), we suggest that *Na. philcreaseri* probably spent a greater proportion of its time above ground than does *Notoryctes* today, which surfaces only rarely (Johnson and Walton, 1989; Benshemesh and Johnson, 2003; Dennis, 2004; Benshemesh, 2008; Benshemesh and Aplin, 2008).

The late Miocene saw the replacement of rainforest with more open woodland environments across much of Australia, in response to a general global drying and cooling trend (Martin, 2006; Black et al., 2012). This coincided with a period of extensive faunal turnover among Australian terrestrial vertebrates (Black et al., 2012), probably including major radiations of dasyurids (Krajewski et al., 2000) and macropodids (Prideaux and Warburton, 2010).This is followed by palaeobotanical evidence for a sudden increase in the abundance of grasses in the latest Miocene (~6 MYA), from 1–2% to ~35% of the total pollen count (Martin and McMinn, 1994: fig. 2). However, true grasslands did not become widespread in Australia until the middle Pliocene (Martin, 2006; Strömberg, 2011; Black et al., 2012). If our value for the timing of *RBP3* inactivation in *Notoryctes* of 5.4 MYA (95% HPD = 4.5-6.3 MYA) is correct, it is tempting to postulate that loss of *RBP3* function is causally linked to the development of more open environments – probably open sclerophyllous woodland with a grassy understory (Strömberg, 2011), rather than true grasslands – at this time. This reduction in vegetation cover would have led to strong selection pressure on the *Notoryctes* ancestor to spend minimal time on the surface (where it would be particularly vulnerable to predators), leading to relaxation of selection on *RBP3*.

Our estimate for the timing of *RBP3* inactivation in the *Notoryctes* lineage is markedly more recent than that of Springer et al. (1998), which was 18.5–24.7 MYA, and that of Emerling and Springer (2014), which was 12.23 MYA (range of 6.87–17.84 MYA). There are a number of potential explanations for this. Springer et al.'s (1998) estimate was based on the presence of three or four indels in the *RBP3* sequence of *N. typhlops*, and the assumption that indels occur in pseudogenes at a rate of 0.17/kb/Ma. This value is a weighted average calculated from four nuclear pseudogenes (none of them *RBP3*) for seven primates, five of which (*Homo*, *Pan*, *Gorilla*, *Pongo*,and *Hylobates*) were hominoids (Saitou and Ueda, 1994). Rates varied between 0.14 and 0.24/kb/Ma across the four genes examined by Saitou and Ueda (1994), but it is unclear how much additional rate variation would be observed if more genes were to be examined. Furthermore, molecular rates of evolution vary considerably within mammals (Bininda-Emonds, 2007; Welch et al., 2008), and rates are particularly slow in hominoids relative to most other mammals, including marsupials (Bininda-Emonds, 2007). Thus, the indel rate assumed by Springer et al. (1998) may be an underestimate, in which case their estimate for the timing of *RBP3* inactivation is too old.

The approach of Emerling and Springer (2014) is conceptually similar to that used here, namely using estimated values of ω and divergence times to infer the timing of gene inactivation (see Meredith et al., 2009a). However, their estimate for ω_b (0.1007–0.1385) was lower than that calculated here (0.15635), and their estimate for ω_f (0.2928–0.3355) was higher than ours (0.244). These discrepancies may be due to differences in taxon sampling: Emerling and Springer's (2014) *RBP3* sequence alignment included 13 placentals but only five marsupials, whereas our alignment comprises 23 marsupials. In addition, Emerling and Springer (2014) used empirical estimates for ω after inactivation of *RBP3* (0.9071–1.1489) based on bat sequence data, whereas our method assumes *a priori* that ω after gene inactivation is 1, and they assumed a somewhat older estimate for the divergence of *Notoryctes* from other extant marsupials (61.28 MYA; Meredith et al., 2011) versus that used here (52.2 MYA; 95% HPD: 43.6–60.7 MYA).

Conclusion

Our qualitative and quantitative analysis of the postcranial morphology of *Na. philcreaseri* indicate that it was most likely subterranean, albeit somewhat less specialised in this regard than the living species of *Notoryctes*; the fact that *RBP3* was probably functional in *Na. philcreaseri* might be an indication that vision was more important to the fossil taxon than to *Notoryctes*, which might be evidence that it spent more time on the surface than the two living marsupial mole species. Nevertheless, it appears that notoryctemorphians had already evolved specialised, probably fully subterranean, burrowing behaviour prior to the early Miocene. A single upper molar, (NTM P2815–6) from the late Oligocene Pwerte Marnte Marnte Local Fauna in the Northern Territory, probably represents a notoryctemorphian, albeit more plesiomorphic than *Na. philcreaseri* based on its larger paracone and metaconule (Murray and Megirian, 2006: 151; Beck et al., 2014). This is the only other fossil occurrence of Notoryctemorphia currently known. A fuller understanding of the evolution of notoryctemorphians, including when and why they evolved "mole-like" behaviour, will therefore require marked improvements in the Palaeogene fossil record of mammals in Australia.

Acknowledgements

We thank Laura Wilson and Rick Arena for discussion, Sharon Jansa for help with PAML, Hayley Bates for access to JMP, and Mike Lee for assistance and advice with our Bayesian phylogenetic analyses. Kenny Travouillon provided helpful information regarding the taxonomic composition of different Riversleigh sites. Financial support for this research has been provided by the National Science Foundation (via grant DEB-0743039, in collaboration with Robert Voss at the American Museum of Natural History) and the Australian Research Council (via Discovery Early Career Researcher Award DE120100957). Additional support for research at Riversleigh has come from the Australian Research Council (LP0989969, LP100200486, and DP130100197 grants to MA and SJH), the XSTRATA Community Partnership Program (North Queensland), the University of New South Wales, Phil Creaser and the CREATE Fund, the Queensland Parks and Wildlife Service, Environment Australia, the Queensland Museum, the Riversleigh Society Inc., Outback at Isa, Mount Isa City Council, and private supporters including K. and M. Pettit, E. Clark, M. Beavis, and M. Dickson. Many volunteers, staff and students of the University of New South Wales have also assisted in field work at Riversleigh. We thank Sandrine Ladevèze and the editor Erich Fitzgerald for their helpful and constructive comments that greatly improved the final draft.

References

Abello, M. A., and Candela, A. M. (2010). Postcranial skeleton of the Miocene marsupial *Palaeothentes* (Paucituberculata, Palaeothentidae): paleobiology and phylogeny. *Journal of Vertebrate Paleontology* 30: 1515–1527.

Aplin, K., and Archer, M. (1987). Recent advances in marsupial systematics with a new syncretic classification. In M. Archer (Ed.), *Possums and opossums: studies in evolution*. (pp. xv–lxxii). Sydney: Surrey Beatty and Sons and the Royal Zoological Society of New South Wales.

Archer, M. (1984). The Australian marsupial radiation. In M. Archer, and G. Clayton (Eds.), *Vertebrate zoogeography and evolution in Australasia* (pp. 633-808). Perth: Hesperian Press.

Archer, M., Arena, D. A., Bassarova, M., Beck, R. M. D., Black, K., Boles, W. E., et al. (2006). Current status of species-level representation in faunas from selected fossil localities in the Riversleigh World Heritage Area, northwestern Queensland. *Alcheringa* 31: 1-17.

Archer, M., Beck, R. M. D., Gott, M., Hand, S., Godthelp, H., and Black, K. (2011). Australia's first fossil marsupial mole (Notoryctemorphia) resolves controversies about their evolution and palaeoenvironmental origins. *Proceedings of the Royal Society B: Biological Sciences* 278: 1498-1506.

Archer, M., and Hand, S. (1984). Background to the search for Australia's oldest mammals. In M. Archer, and G. Clayton (Eds.), *Vertebrate zoogeography and evolution in Australasia. (Animals in space and time)* (pp. 517-565). Carlisle, Western Australia: Hesperian Press.

Archer, M., Hand, S. J., and Godthelp, H. (1994). *Riversleigh: the story of animals in ancient rainforests of inland Australia*. Sydney: Reed Books.

Archer, M., Hand, S. J., Godthelp, H., and Creaser, P. (1997). Correlation of the Cainozoic sediments of the Riversleigh World Heritage fossil property, Queensland, Australia. In J.-P. Aguilar, S. Legendre, and J. Michauz (Eds.), *Actes du Congrès BiochroM'97* (pp. 131-152). Montpellier: École Pratique des Hautes Études, Institut de Montpellier.

Arena, D. (2004). *The geological history and development of the terrain at the Riversleigh World Heritage Area during the middle Tertiary*. Ph.D. dissertation, University of New South Wales, School of Biological, Earth and Environmental Sciences, Sydney.

Arena, D. A., Black, K. H., Archer, M., Hand, S. J., Godthelp, H., and Creaser, P. (2014). Reconstructing a Miocene pitfall trap: recognition and interpretation of fossiliferous Cenozoic palaeokarst. *Sedimentary Geology* 304: 28-43.

Asher, R. J., Horovitz, I., and Sánchez-Villagra, M. R. (2004). First combined cladistic analysis of marsupial mammal interrelationships. *Molecular Phylogenetics and Evolution* 33: 240-250.

Ashwell, K. W. S. (2013). Reflections: monotreme neurobiology in context. In K. Ashwell (Ed.), *Neurobiology of monotremes: brain evolution in our distant mammalian cousins* (pp. 285-298). Collingwood, Australia: CSIRO Publishing.

Barbour, R. A. (1963). The musculature and limb plexuses of *Trichosurus vulpecula*. *Australian Journal of Zoology* 11: 488-610.

Bates, H., Travouillon, K. J., Cooke, B., Beck, R. M. D., Hand, S. J., and Archer, M. (2014). Three new Miocene species of musky rat-kangaroos (Hypsiprymnodontidae, Macropodoidea): description, phylogenetics, and paleoecology. *Journal of Vertebrate Paleontology* 34: 383-396.

Beck, R. M. D. (2008). A dated phylogeny of marsupials using a molecular supermatrix and multiple fossil constraints. *Journal of Mammalogy* 89: 175-189.

Beck, R. M. D., Godthelp, H., Weisbecker, V., Archer, M., and Hand, S. J. (2008). Australia's oldest marsupial fossils and their biogeographical implications. *PLoS ONE* 3: e1858.

Beck, R. M. D., and Lee, M. S. Y. (2014). Ancient dates or accelerated rates? Morphological clocks and the antiquity of placental mammals. *Proceedings of the Royal Society B: Biological Sciences* 281: 20141278.

Beck, R. M. D., Travouillon, K. J., Aplin, K. P., Godthelp, H., and Archer, M. (2014). The osteology and systematics of the enigmatic Australian Oligo-Miocene metatherian *Yalkaparidon* (Yalkaparidontidae; Yalkaparidontia; ?Australidelphia; Marsupialia). *Journal of Mammalian Evolution* 21: 127-172.

Benshemesh, J. (2008). Itjaritjari, *Notorytes typhlops*. In S. Van Dyck, and R. Strahan (Eds.), *The Mammals of Australia, 3rd edition* (pp. 412-413). Sydney: Reed New Holland.

Benshemesh, J., and Aplin, K. P. (2008). Kakarratul, *Notoryctes caurinus*. In S. Van Dyck, and R. Strahan (Eds.), *The Mammals of Australia, 3rd edition* (pp. 410-411). Sydney: Reed New Holland.

Benshemesh, J., and Johnson, K. (2003). Biology and conservation of marsupial moles (*Notoryctes*). In M. Jones, C. R. Dickman, and M. Archer (Eds.), *Predators with pouches: the biology of carnivorous marsupials* (pp. 464-474). Melbourne: CSIRO Publshing.

Bi, S., Wang, Y., Guan, J., Sheng, X., and Meng, J. (2014). Three new Jurassic euharamiyidan species reinforce early divergence of mammals. *Nature* 514: 579-584.

Bininda-Emonds, O. R. P. (2007). Fast genes and slow clades: comparative rates of molecular evolution in mammals. *Evolutionary Bioinformatics* 3: 59-85.

Black, K. H., Archer, M., Hand, S. J., and Godthelp, H. (2012). The rise of Australian marsupials: a synopsis of biostratigraphic, phylogenetic, palaeoecologic and palaeobiogeographic understanding. In J. A. Talent (Ed.), *Earth and Life: Global Biodiversity, Extinction Intervals and Biogeographic Perturbations Through Time* (pp. 983-1078). Dordrecht: Springer Verlag.

Bronner, G. N. (2013). Family Chrysochloridae: golden moles. In J. Kingdon, D. C. D. Happold, T. M. Butynski, M. Hoffmann, M. Happold, and J. Kalina (Eds.), *Mammals of Africa. Volume I: introductiory chapters and Afrotheria* (Vol. Volume 1, pp. 223-257). London: Bloomsbury Publishing.

Burne, R. H. (1901). A contribution to the myology and visceral anatomy of *Chlamydophorus truncatus*. *Proceedings of the Zoological Society, London.*: 104-121.

Camens, A. B. (2010). Were early Tertiary monotremes really all aquatic? Inferring paleobiology and phylogeny from a depauperate fossil record. *Proceedings of the National Academy of Sciences of the United States of America* 107: E12-E12.

Campbell, B. (1939). The shoulder anatomy of the moles. A study in phylogeny and adaptation. *American Journal of Anatomy* 64: 1-39.

Campione, N. E., and Evans, D. C. (2012). A universal scaling relationship between body mass and proximal limb bone dimensions in quadrupedal terrestrial tetrapods. *BMC Biology* 10: 60.

Canoville, A., and Laurin, M. (2010). Evolution of humeral microanatomy and lifestyle in amniotes, and some comments on palaeobiological inferences. *Biological Journal of the Linnean Society* 100: 384-406.

Carlsson, A. (1904). Zur Anatomie des Notoryctes typhlops. *Zoologische Jahrbücher. Abteilung für Anatomie und Ontogenie der Tiere* 20: 81-122.

Casinos, A., Quintana, C., and Viladiu, C. (1993). Allometry and adaptation in the long bones of a digging group of rodents (Ctenomyinae). *Zoological Journal of the Linnean Society* 107: 107-155.

Chapman, R. N. (1919). A study of the correlation of the pelvic structure and the habits of certain burrowing mammals. *American Journal of Anatomy* 25: 185-219.

Chou, H. H., Hayakawa, T., Diaz, S., Krings, M., Indriati, E., Leakey, M., et al. (2002). Inactivation of CMP-N-acetylneuraminic acid hydroxylase occurred prior to brain expansion during human evolution. *Proceedings of the National Academy of Sciences of the United States of America* 99: 11736-11741.

Cope, E. D. (1892). On the habits and affinities of the new Australian mammal, *Notoryctes typhlops*. *American Naturalist* 26: 121–128.

Coues, E. (1872). The osteology and myology of *Didelphys virginiana*. *Memoirs of the Boston Society of Natural History* 2: 41–154.

Crosby, K. (2002). A second species of the possum *Durudawiri* (Marsupialia: Miralinidae) from the early Miocene of Riversleigh, northwestern Queensland. *Alcheringa* 26: 333-340.

Crosby, K., and Archer, M. (2000). Durudawirines, a new group of phalangeroid marsupials from the Miocene of Riversleigh, northwestern Queensland. *Journal of Paleontology* 74: 327-335.

Cúneo, R., Ramezani, J., Scasso, R., Pol, D., Escapa, I., Zavattieri, A. M., et al. (2013). High-precision U–Pb geochronology and a new chronostratigraphy for the Cañadón Asfalto Basin, Chubut, central Patagonia: Implications for terrestrial faunal and floral evolution in Jurassic. *Gondwana Research* 24: 1267-1275.

Davis, D. D. (1964). The giant panda: a morphological study of evolutionary mechanisms. *Fieldiana: Zoology Memoirs* 3: 1-339.

Dennis, C. (2004). Zoology: a mole in hand. *Nature* 432: 142-143.

dos Reis, M., Donoghue, P. C. J., and Yang, Z. (2014). Neither phylogenomic nor palaeontological data support a Palaeogene origin of placental mammals. *Biology Letters* 10: 20131003.

dos Reis, M., Inoue, J., Hasegawa, M., Asher, R. J., Donoghue, P. C., and Yang, Z. (2012). Phylogenomic datasets provide both precision and accuracy in estimating the timescale of placental mammal phylogeny. *Proc Biol Sci* 279: 3491-3500.

Edwards, L. F. (1937). Morphology of the forelimb of the mole (*Scalops aquaticus*, L.) in relation to its fossorial habits. *The Ohio Journal of Science* 37: 20-41.

Elissamburu, A., and Vizcaíno, S. F. (2004). Limb proportions and adaptations in caviomorph rodents (Rodentia: Caviomorpha). *Journal of Zoology* 262: 145-159.

Emerling, C. A., and Springer, M. S. (2014). Eyes underground: Regression of visual protein networks in subterranean mammals. *Molecular Phylogenetics and Evolution* 78C: 260-270.

Evans, H. E. (1993). *Miller's anatomy of the dog*. Philadelphia: W.B. Saunders.

Farina, R. A., and Vizcaino, S. F. (1997). Allometry of the leg bones of living and extinct armadillos. *Mammalian Biology* 62: 65-70.

Fox, R. C., and Naylor, B. G. (2006). Stagodontid marsupials from the Late Cretaceous of Canada and their systematic and functional implications. *Acta Palaeontologica Polonica* 51: 13-36.

Gambaryan, P. P., and Kielan-Jaworowska, S. (1997). Sprawling *verses* parasagittal stance in multituberculate mammals. *Acta Palaeontologica Polonica* 42: 13-44.

Gasc, J. P., Jouffroy, F. K., Renous, S., and Von Blottnitz, F. (1986). Morphofunctional study of the digging system of the Namib Desert golden mole (*Eremitalpa granti nambiensis*): cinefluorographical and anatomical analysis. *Journal of Zoology, London* 208: 9-35.

Geiger, M., Forasiepi, A. M., Koyabu, D., and Sanchez-Villagra, M. R. (2014). Heterochrony and post-natal growth in mammals - an examination of growth plates in limbs. *Journal of Evolutionary Biology* 27: 98-115.

Gott, M. (1988). *A Tertiary marsupial mole (Marsupialia: Notoryctidae) from Riversleigh, northeastern Australia and its bearing on notoryctemorphian phylogenetic systematics*. Masters Thesis, School of Biological Science, University of New South Wales,

Hickman, G. C. (1984). Swimming ability of talpid moles, with particular reference to the semi-aquatic *Condylura cristata*. *Mammalia* 48: 505-513.

Hildebrand, M. (1985). Digging of quadrupeds. In M. Hildebrand, D. M. Bramble, K. F. Liem, and D. B. Wake (Eds.), *Functional vertebrate morphology* (pp. 89-109). Cambridge, Massachusetts: Belknap Press.

Hildebrand, M., and Goslow, G. E. J. (2001). *Analysis of vertebrate structure*. USA: John Wiley & Sons, Inc.

Hopkins, S. S. B., and Davis, E. B. (2009). Quantitative morphological proxies for fossoriality in small mammals. *Journal of Mammalogy* 90: 1449-1460.

Horovitz, I., Ladevèze, S., Argot, C., Macrini, T. E., Martin, T., Hooker, J. J., et al. (2008). The anatomy of *Herpetotherium* cf. *fugax* Cope, 1873, a metatherian from the Oligocene of North America. *Palaeontographica Abteilung A* 284: 109-141.

Horovitz, I., and Sánchez-Villagra, M. R. (2003). A morphological analysis of marsupial mammal higher-level phylogenetic relationships. *Cladistics* 19: 181-212.

Jansa, S. A., and Voss, R. S. (2011). Adaptive evolution of the venom-targeted vWF protein in opossums that eat pitvipers. *PLoS ONE* 6: e20997.

Johnson, K. A., and Walton, D. W. (1989). 23. Notoryctidae. In D. W. Walton, and B. J. Richardson (Eds.), *Fauna of Australia: Volume 1B Mammalia* (pp. 1-24). Canberra: AGPS.

Kim, E. B., Fang, X., Fushan, A. A., Huang, Z., Lobanov, A. V., Han, L., et al. (2011). Genome sequencing reveals insights into physiology and longevity of the naked mole rat. *Nature* 479: 223-227.

Kirsch, J. A. W. (1977). The comparative serology of Marsupialia, and a classification of marsupials. *Australian Journal of Zoology, Supplementary Series* 52: 1-152.

Krajewski, C., Wroe, S., and Westerman, M. (2000). Molecular evidence for the pattern and timing of cladogenesis in dasyurid marsupials. *Zoological Journal of the Linnean Society* 130: 375-404.

Lagaria, A., and Youlatos, D. (2006). Anatomical correlates to scratch digging in the forelimb of European ground squirrels (*Spermophilus citellus*). *Journal of Mammalogy* 87: 563-570.

Lanfear, R., Calcott, B., Ho, S. Y., and Guindon, S. (2012). Partitionfinder: combined selection of partitioning schemes and substitution models for phylogenetic analyses. *Molecular Biology and Evolution* 29: 1695-1701.

Lehmann, W. H. (1963). The forelimb architecture of some fossorial rodents. *Journal of Morphology* 113: 59-76.

Lessa, E. P. (1990). Morphological evolution of subterranean mammals: integrating structural, functional, and ecological perspectives. *Progress in Clinical and Biological Research* 335: 211-230.

Lessa, E. P., Vassallo, A. I., Verzi, D. H., and Mora, M. S. (2008). Evolution of morphological adaptations for digging in living and extinct ctenomyid and octodontid rodents. *Biological Journal of the Linnean Society* 95: 267-283.

Lewis, P. O. (2001). A likelihood approach to estimating phylogeny from discrete morphological character data. *Systematic Biology* 50: 913-925.

Lillegraven, J. A. (1975). Biological considerations of the marsupial-placental dichotomy. *Evolution* 29: 707-722.

Longrich, N. (2004). Aquatic specialization in mammals from the Late Cretaceous of North America. *Journal of Vertebrate Paleontology* 24: 84A.

MacAlister, A. (1875a). Report on the anatomy of the insectivorous edentates. *Transactions of the Royal Irish Academy* 24: 491-508.

Macalister, M. B. (1875b). A monograph of the anatomy of *Chlamydophorus Truncatus* (Harlan) with notes on the structure of other species of Edentata. *Transactions of the Royal Irish Academy* 25: 219-278.

Marshall, L. G. (1975). *Chironectes minimus*. *Mammalian Species* 109: 1-6.

Martin, H. A. (2006). Cenozoic climatic change and the development of the arid vegetation in Australia. *Journal of Arid Environments* 66: 533-563.

Martin, H. A., and McMinn, A. (1994). Late Cainozoic vegetation history of north-western Australia from the palynology of a deep sea core (ODP site 765). *Australian Journal of Botany* 42: 95-102.

McLaren, S., and Wallace, M. W. (2010). Plio-Pleistocene climate change and the onset of aridity in southeastern Australia. *Global and Planetary Change* 71: 55-72.

Meier, P. S., Bickelmann, C., Scheyer, T. M., Koyabu, D., and Sanchez-Villagra, M. R. (2013). Evolution of bone compactness in extant and extinct moles (Talpidae): exploring humeral microstructure in small fossorial mammals. *BMC Evolutionary Biology* 13: 55.

Meredith, R. W., Gatesy, J., Murphy, W. J., Ryder, O. A., and Springer, M. S. (2009a). Molecular decay of the tooth gene enamelin (*ENAM*) mirrors the loss of enamel in the fossil record of placental mammals. *PLoS Genetics* 5: e1000634.

Meredith, R. W., Janecka, J. E., Gatesy, J., Ryder, O. A., Fisher, C. A., Teeling, E. C., et al. (2011). Impacts of the Cretaceous Terrestrial Revolution and KPg extinction on mammal diversification. *Science* 334: 521-524.

Meredith, R. W., Krajewski, C., Westerman, M., and Springer, M. S. (2009b). Relationships and divergence times among the orders and families of Marsupialia. *Museum of Northern Arizona Bulletin* 65: 383-406.

Meredith, R. W., Westerman, M., Case, J. A., and Springer, M. S. (2008). A phylogeny and timescale for marsupial evolution based on sequences for five nuclear genes. *Journal of Mammalian Evolution* 15: 1-36.

Milne, N., and O'Higgins, P. (2012). Scaling of form and function in the xenarthran femur: a 100-fold increase in body mass is mitigated by repositioning of the third trochanter. *Proceedings of the Royal Society B: Biological Sciences* 279: 3449-3456.

Mirceta, S., Signore, A. V., Burns, J. M., Cossins, A. R., Campbell, K. L., and Berenbrink, M. (2013). Evolution of mammalian diving capacity traced by myoglobin net surface charge. *Science* 340: 1234192.

Mitchell, K. J., Pratt, R. C., Watson, L. N., Gibb, G. C., Llamas, B., Kasper, M., et al. (2014). Molecular phylogeny, biogeography, and habitat preference evolution of marsupials. *Molecular Biology and Evolution.*

Muirhead, J. (1997). Two new early Miocene thylacines from Riversleigh, northwestern Queensland. *Memoirs of the Queensland Museum* 41: 367-377.

Murray, P. F., and Megirian, D. (2006). The Pwerte Marnte Marnte Local Fauna: a new vertebrate assemblage of presumed Oligocene age from the Northern Territory of Australia. *Alcheringa* Special Issue 1: 211-228.

Musser, A. M. (2013). Classification and evolution of the monotremes. In K. Ashwell (Ed.), *Neurobiology of monotremes: brain evolution in our distant mammalian cousins* (pp. 1-16). Collingwood, Australia: CSIRO Publishing.

Nevo, E. (1979). Adaptive convergence and divergence of subterranean mammals. *Annual Review of Ecology and Systematics* 10: 269-308.

Nevo, E. (1999). *Mosaic evolution of subterranean mammals: regression, progression and global convergence.* Oxford: Oxford University Press.

Nilsson, M. A., Arnason, U., Spencer, P. B. S., and Janke, A. (2004). Marsupial relationships and a timeline for marsupial radiation in South Gondwana. *Gene* 340: 189–196.

Nilsson, M. A., Churakov, G., Sommer, M., Tran, N. V., Zemann, A., Brosius, J., et al. (2010). Tracking marsupial evolution using archaic genomic retroposon insertions. *PLoS Biology* 8: e1000436.

Orcutt, E. E. (1940). Studies on the muscles of the head, neck, and pectoral appendages of *Geomys bursarius*. *Journal of Mammalogy* 21: 37-52.

Pepperberg, D. R., Okajima, T. L., Wiggert, B., Ripps, H., Crouch, R. K., and Chader, G. J. (1993). Interphotoreceptor retinoid-binding protein (IRBP). Molecular biology and physiological role in the visual cycle of rhodopsin. *Molecular Neurobiology* 7: 61-85.

Phillips, M. J., Bennett, T. H., and Lee, M. S. Y. (2009). Molecules, morphology, and ecology indicate a recent, amphibious ancestry for echidnas. *Proceedings of the National Academy of Sciences of the United States of America* 106: 17089-17094.

Phillips, M. J., Bennett, T. H., and Lee, M. S. Y. (2010). Reply to Camens: How recently did modern monotremes diversify? *Proceedings of the National Academy of Sciences of the United States of America* 107: E13-E13.

Prideaux, G. J., and Warburton, N. M. (2010). An osteology-based appraisal of the phylogeny and evolution of kangaroos and wallabies (Macropodidae: Marsupialia). *Zoological Journal of the Linnean Society* 159: 954-987.

Puttick, G. M., and Jarvis, J. U. M. (1977). The functional anatomy of the neck and forelimbs of the Cape Golden Mole, *Chrysochloris asiatica* (Lipotyphla: Chrysochloridae). *Zoologica Africana* 12: 445-458.

Reed, C. A. (1951). Locomotion and appendicular anatomy in three soricoid insectivores. *American Midland Naturalist* 45: 513-665.

Ronquist, F., Klopfstein, S., Vilhelmsen, L., Schulmeister, S., Murray, D. L., and Rasnitsyn, A. P. (2012a). A total-evidence approach to dating with fossils, applied to the early radiation of the Hymenoptera. *Systematic Biology* 61: 973-999.

Ronquist, F., Teslenko, M., van der Mark, P., Ayres, D. L., Darling, A., Hohna, S., et al. (2012b). MrBayes 3.2: efficient Bayesian phylogenetic inference and model choice across a large model space. *Systematic Biology* 61: 539-542.

Rose, K. D., and Emry, R. J. (1983). Extraordinary fossorial adaptations in the Oligocene palaeanodonts *Epoicotherium* and *Xenocranium* (Mammalia). *Journal of Morphology* 175: 33-56.

Rougier, G. W., Martinelli, A. G., Forasiepi, A. M., and Novacek, M. J. (2007). New Jurassic mammals from Patagonia, Argentina: a reappraisal of australosphenidan morphology and interrelationships. *American Museum Novitates* 3566: 1-54.

Rzebik-Kowalska, B. (2013). *Sorex bifidus* n. sp. and the rich insectivore mammal fauna (Erinaceomorpha, Soricomorpha, Mammalia) from the Early Pleistocene of Żabia Cave in Poland. *Palaeontologia Electronica* 16: 12A.

Saitou, N., and Ueda, S. (1994). Evolutionary rates of insertion and deletion in noncoding nucleotide sequences of primates. *Molecular Biology and Evolution* 11: 504-512.

Salton, J. A., and Sargis, E. J. (2008). Evolutionary morphology of the Tenrecoidea (Mammalia) forelimb skeleton. In E. J. Sargis, and M. Dagosto (Eds.), *Mammalian Evolutionary Morphology: A Tribute to Frederick S. Szalay* (pp. 51-72). Dordrecht, The Netherlands: Springer.

Schaller, O. (Ed.). (1992). *Illustrated veterinary anatomical nomenclature*. Stuttgart: Enke.

Shen, B., Fang, T., Dai, M., Jones, G., and Zhang, S. (2013). Independent losses of visual perception genes *Gja10* and *Rbp3* in echolocating bats (Order: Chiroptera). *PLoS ONE* 8: e68867.

Springer, M. S., Burk, A., Kavanagh, J. R., Waddell, V. G., and Stanhope, M. J. (1997). The interphotoreceptor retinoid binding protein gene in therian mammals: implications for higher level relationships and evidence for loss of function in the marsupial mole. *Proceedings of the National Academy of Sciences of the United States of America* 94: 13754-13759.

Springer, M. S., Westerman, M., Kavanagh, J. R., Burk, A., Woodburne, M. O., Kao, D. J., et al. (1998). The origin of the Australasian marsupial fauna and the phylogenetic affinities of the enigmatic monito del monte and marsupial mole. *Proceedings of the Royal Society B Biological Sciences* 265: 2381-2386.

Stein, B. R. (1986). Comparative limb myology of four arvicolid rodent genera (Mammalia; Rodentia). *Journal of Morphology* 187: 321-342.

Stein, B. R. (1993). Comparative hindlimb morphology in geomyine and thomomyine pocket gophers. *Journal of Mammalogy* 74: 86-94.

Stein, B. R., and Patton, J. L. (2008). Genus *Chironectes* Illiger, 1811. In A. L. Gardner (Ed.), *Mammals of South America. Vol. 1. Marsupials, xenarthrans, shrews, and bats* (pp. 14-17). Chicago: Chicago University Press.

Stirling, E. C. (1888). Preliminary notes on a new Australian mammal. *Transactions of the Royal Society of South Australia* 11: 21-24.

Stirling, E. C. (1891). Description of a new genus and species of Marsupialia, *Notoryctes typhlops*. *Transactions of the Royal Society of South Australia* 14: 154-187.

Strömberg, C. A. E. (2011). Evolution of grasses and grassland ecosystems. *Annual Review of Earth and Planetary Sciences* 39: 517-544.

Sweet, G. (1906). Contribution to our knowledge of the anatomy of *Notoryctes typhlops*, Stirling. Part III - the eye. *Quarterly Journal of Microscopical Science* 50: 547-572.

Szalay, F. S. (1994). *Evolutionary history of the marsupials and an analysis of osteological characters*. Cambridge: Cambridge University Press.

Szalay, F. S., and Sargis, E. J. (2001). Model-based analysis of postcranial osteology of marsupials from the Palaeocene of Itaboraí (Brazil) and the phylogenetics and biogeography of Metatheria. *Geodiversitas* 23: 139-302.

Taylor, B. K. (1978). The anatomy of the forelimb of the anteater (*Tamandua*) and its functional implications. *Journal of Morphology* 157: 347-368.

Thompson, P., and Hillier, W. T. (1905). The myology of the hindlimb of the marsupial mole (*Notoryctes typhlops*). *Journal of Anatomy and Physiology* 34: 308-331.

Thorington, R. W. J., Darrow, K., and Betts, A. D. K. (1997). Comparative myology of the forelimb of squirrels (Sciuridae). *Journal of Morphology* 234: 155-182.

Travouillon, K. J., Archer, M., Hand, S. J., and Godthelp, H. (2006). Multivariate analyses of Cenozoic mammalian faunas from Riversleigh, northwestern Queensland. *Alcheringa* Special Issue 1: Proceedings of CAVEPS 2005: 323-349.

Travouillon, K. J., Legendre, S., Archer, M., and Hand, S. J. (2009). Palaeoecological analyses of Riversleigh's Oligo-Miocene sites: implications for Oligo-Miocene climate change in Australia. *Palaeogeography, Palaeoclimatology, Palaeoecology* 276: 24-37.

Turnbull, W. D. (1971). The Trinity therians: their bearing on evolution in marsupials and other therians. In A. A. Dahlberg (Ed.), *Dental morphology and evolution* (pp. 151-179). Chicago: University of Chicago Press.

Turnbull, W. D., and Reed, C. A. (1967). *Pseudochrysochloris*, a specialized burrowing mammal from the early Oligocene of Wyoming. *Journal of Paleontology* 41: 623-631.

Vassallo, A. I. (1998). Functional morphology, comparative behaviour, and adaptation in two sympatric subterranean rodents genus *Ctenomys* (Caviomorpha: Octodontidae). *Journal of Zoology* 244: 415-427.

Vizcaino, S. F., Farina, R. A., and Mazzetta, G. V. (1999). Ulnar dimensions and fossoriality in armadillos. *Acta Theriologica* 44: 309-320.

Vizcaino, S. F., and Milne, N. (2002). Structure and function in armadillo limbs (Mammalia : Xenarthra : Dasypodidae). *Journal of Zoology* 257: 117-127.

Warburton, N. M. (2003). *Functional morphology and evolution of marsupial moles (Marsupialia; Notoryctemorphia)*. Unpublished Ph.D. dissertation, University of Western Australia,

Warburton, N. M. (2006). Functional morphology of marsupial moles (Marsupialia, Notoryctidae). *Verhandlungen des Naturwissenschaftlichen Vereins in Hamburg* 42: 39-149.

Warburton, N. M., Gregoire, L., Jacques, S., and Flandrin, C. (2013). Adaptations for digging in the forelimb muscle anatomy of the southern brown bandicoot (*Isoodon obesulus*) and bilby (*Macrotis lagotis*). *Australian Journal of Zoology* 61: 402-419.

Welch, J. J., Bininda-Emonds, O. R., and Bromham, L. (2008). Correlates of substitution rate variation in mammalian protein-coding sequences. *BMC Evolutionary Biology* 8: 53.

Whidden, H. P. (1999). The evolution of locomotor specializations in moles. *American Zoologist* 39: 135A.

Windle, B. C. A., and Parsons, F. G. (1899). On the myology of the Edentata. *Proceedings of the Zoological Society, London* 67: 314-339.

Woodhead, J., Hand, S. J., Archer, M., Graham, I., Sniderman, K., Arena, D. A., et al. (2014). Developing a radiometrically-dated chronologic sequence for Neogene biotic change in Australia, from the Riversleigh World Heritage Area of Queensland. *Gondwana Research.*

Woodman, N., and Gaffney, S. A. (2014). Can they dig it? Functional morphology and semifossoriality among small-eared shrews, genus *Cryptotis* (Mammalia, Soricidae). *Journal of Morphology* 275: 745-759.

Yang, Z. (2007). PAML 4: phylogenetic analysis by maximum likelihood. *Molecular Biology and Evolution* 24: 1586-1591.

Zhang, Z. D., Cayting, P., Weinstock, G., and Gerstein, M. (2008). Analysis of nuclear receptor pseudogenes in vertebrates: how the silent tell their stories. *Molecular Biology and Evolution* 25: 131-143.

Memoirs of Museum Victoria 74: 173–187 (2016) Published 2016

ISSN 1447-2546 (Print) 1447-2554 (On-line)
http://museumvictoria.com.au/about/books-and-journals/journals/memoirs-of-museum-victoria/

New specimens of ektopodontids (Marsupialia: Ektopodontidae) from South Australia

Neville S. Pledge

South Australian Museum, Adelaide, South Australia 5000 (neville.pledge@samuseum.sa.gov.au)

Abstract

Pledge, N.S. 2016. New specimens of ektopodontids (Marsupialia: Ektopodontidae) from South Australia. *Memoirs of Museum Victoria* 74: 173–187.

Knowledge about the extinct phalangeroid family Ektopodontidae is increased by the discovery of new material from several localities. Previously unknown teeth of *Chunia illuminata* and *Ektopodon stirtoni* are described respectively from White Sands Basin and Mammalon Hill, Lake Palankarinna, Lake Eyre Basin, South Australia, with M^1 being recorded for the first time for any species of *Chunia*., and a full maxilla of *Ektopodon stirtoni* showing the positional relationship between P3 and M1 for the first time; this is even more extreme than the arrangement postulated previously. Another species *Ektopodon litolophus* has been described on the basis of an M^1 found at the Leaf Locality, Lake Ngapakaldi, Lake Eyre Basin. Material from Lake Tarkarooloo, referred to *Ektopodon stirtoni*, is redescribed as a new species *Ektopodon tommosi*. Comparisons of M^1 of *Chunia* and *Ektopodon* species now allow evolutionary trends, such as increasing number of cusps on the molar lophs, and simplification of the cusps, to be discerned.

Keywords

Marsupialia, Ektopodontidae, *Chunia*, *Ektopodon*, Ditjimanka, Ngama, Kutjamarpu, Etadunna Formation, Wipajiri Formation, Tertiary, Oligocene, Miocene, Lake Eyre Basin, Australia.

Introduction

Ektopodon is a genus of extinct possum-like marsupials established by Stirton et al. (1961) for isolated teeth found at the early Miocene Leaf Locality at Lake Ngapakaldi, northeastern South Australia. Further specimens from this locality were described and interpreted by Woodburne and Clemens (1986b), together with new, slightly older late Oligocene species in the plesiomorphic genus *Chunia* (*C. illuminata*, *C.* sp. cf. *C. illuminata* and *C. omega*) from sites in the Lake Eyre Basin (e.g. Tedford Locality, Lake Palankarinna) and the Frome Embayment (e.g. Tom O's Quarry, Lake Tarkarooloo). A second, later Oligocene species of *Ektopodon* (*E. stirtoni*) was described by Pledge (1986) from Mammalon Hill, Lake Palankarinna (fig. 1.), and specimens also from Lake Tarkarooloo were also referred to *E. stirtoni*.

Rich (1986) described *Darcius duggani* from Hamilton, western Victoria, a deposit radiometrically determined to be Pliocene in age (ca. 4.46 Ma), and *E. paucicristata* from Pliocene sediments near Portland, also in western Victoria (Rich et al., 2006). By 1986 the rich deposits of Riversleigh, northwestern Queensland, were beginning to yield many new species including an unidentifiable ektopodontid, and a second species of *Ektopodon* was found in the Kutjamarpu Local Fauna of South Australia (Pledge et al. 1999). New specimens from Lake Palankarinna referable to *Chunia illuminata* and *Ektopodon stirtoni* are described in this paper. The status of the Tarkarooloo specimens referred to *E. stirtoni* is re-evaluated and a new species erected.

Age

Although Stirton (Stirton et al., 1961) initially assessed the age of the Etadunna Formation and its faunas to be Oligocene, it became customary to interpret these central Australian deposits as middle Miocene in age (approximately 12–15 Ma; Woodburne et al., 1985), following preliminary analyses by W. K. Harris of pollen, wrongly identified as grasses, from the Etadunna Formation; this was amended to Restionacea (sedge) pollen by Martin (1990). Later work with foraminiferans (Lindsay 1987) suggested that at least some of these deposits may be as old as Late Oligocene. This assessment was based on the abundant presence of the foraminiferan *Buliminoides* sp. cf. *B. chattonensis*. The older age is also supported by Truswell et al. (1985) on the basis of pollens from the Geera Clay (which appears to be a lithological equivalent of basal Namba Formation, itself correlated with the Etadunna Formation), and by Norrish and Pickering (1983) who reported a Late Oligocene Rb-Sr date for authigenic illite from the Etadunna Formation.

Collection methods

Specimens from the Lake Eyre Basin were found by excavation of the fossiliferous horizons or by screen-washing the dried sediment through window screen with mesh of 6 x 6 wires per cm^2.

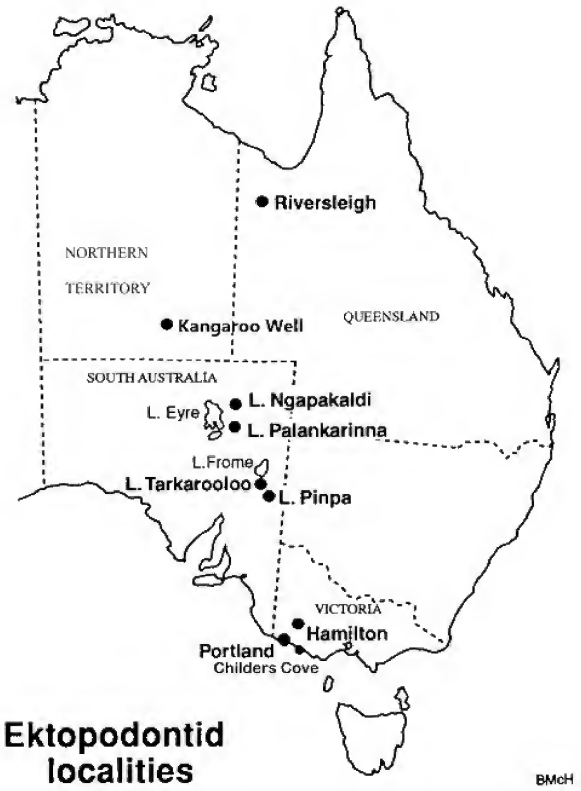

Figure 1. Locality map. Ektopodontid localities.

Terminology

Molar homology follows Luckett (1993). The terminology for the crown morphology of ektopodontid teeth used here is that of Woodburne & Clemens (1986a) with modifications to cusp homology as recommended by Tedford & Woodburne (1987).

Museum abbreviations

SAM, South Australian Museum; NMV, Museum Victoria; UCMP, University of California, Berkeley; UCMP V, University of California Museum of Paleontology locality number; UCR, University of California, Riverside; SAM PL, South Australian Museum Palaeontological locality.

Systematic Palaeontology

Marsupialia (Illiger, 1811) *sens.* Cuvier (1817)

Diprotodontia Owen, 1866

Phalangeroidea (Thomas, 1888) sens. Aplin & Archer (1987)

Ektopodontidae Stirton, Tedford & Woodburne, 1967

***Chunia* Woodburne & Clemens, 1986**

Chunia illuminata Woodburne & Clemens, 1986

(Figs. 3A–D)

Holotype. SAM P17997. In their original description of *Chunia illuminata*, Woodburne & Clemens (1986b) described the RM^2 holotype SAM P17997 (= RM^3 in their notation following Archer 1978), together with QM F10641 (maxilla fragment with partial LM^2), UCR 15228 (LM_2) and UCR 15227 (LM_2).

New Specimens. SAM P29081, left M^1 (figs. 3A–D) collected by J. McNamara 9 July 1987; also SAM P33944, left M^3, collected by J. Case and J. Clemitson, June 1992, from Tedford Locality.

Locality. White Sands Basin (SAM locality PL 7719), 200 m south of Tedford Locality (UCMP V5375, the Type Locality for the species).

Stratigraphy and Age. Stratigraphically, White Sands Basin is about one metre below the sandy clay layer in Tedford Locality that produced the holotype. This fauna from the Etadunna Formation is considered to be Late Oligocene in age (see above).

Revision of specific diagnosis. In addition to the features noted by Woodburne & Clemens (1986b), including the upper dental formula I^2, C^1, P^{1-3}, M^{1-4}, the M^1 of *Chunia illuminata* differs from that tooth in all other ektopodontids in being smaller, having fewer cusps on its lophs and in having a parastyloph that is less loph-like and more cusp-like than that structure in any known species of *Ektopodon*. The face is 'longer' and less obtuse than that of *Ektopodon stirtoni*.

Description. The M^1 of *Chunia illuminata* has the same basic outline as that tooth in other species of *Ektopodon* but differs in several ways noted below. The cusps on the 'protoloph' and 'metaloph' are all worn apically, so some detail has been obscured.

The parastyloph ("paraloph" of Pledge, 1986) is simpler than that structure in other species, being an oblique blade confluent with the buccal face of the tooth and having three cusps. The minute lingual cusp is offset posteriorly from the end of the loph and gives rise to a pair of postcristae that initially diverge, then converge slightly linguad. A weak precrista descends basally from the point of inflection of the loph. The central cusp is by far the largest of the three but, apart from the loph crest, gives rise only to a short postcrista at right angles to it. However, a strong postcrista arises from near the buccal end of the cusp and continues transversely to almost meet the converging postcristae from the lingual cusp. The buccal cusp is separated from the median cusp by a narrow crevice. There are two postcristae, a buccal one forming part of the "parastyloph" and a lingual one that curves transversely and extends half the width of the loph.

The protoloph has four distinct cusps and a complex structure at the buccal end that could represent either two or three smaller cusps. The lingual cusp, the protocone, is a trigonal pyramid with the precrista being stronger than either the postcrista or the lingual extension of the loph crest. Cusp 2 is the smallest with a short precrista cut off by converging precristae from the protocone and cusp 3. Its postcrista is the

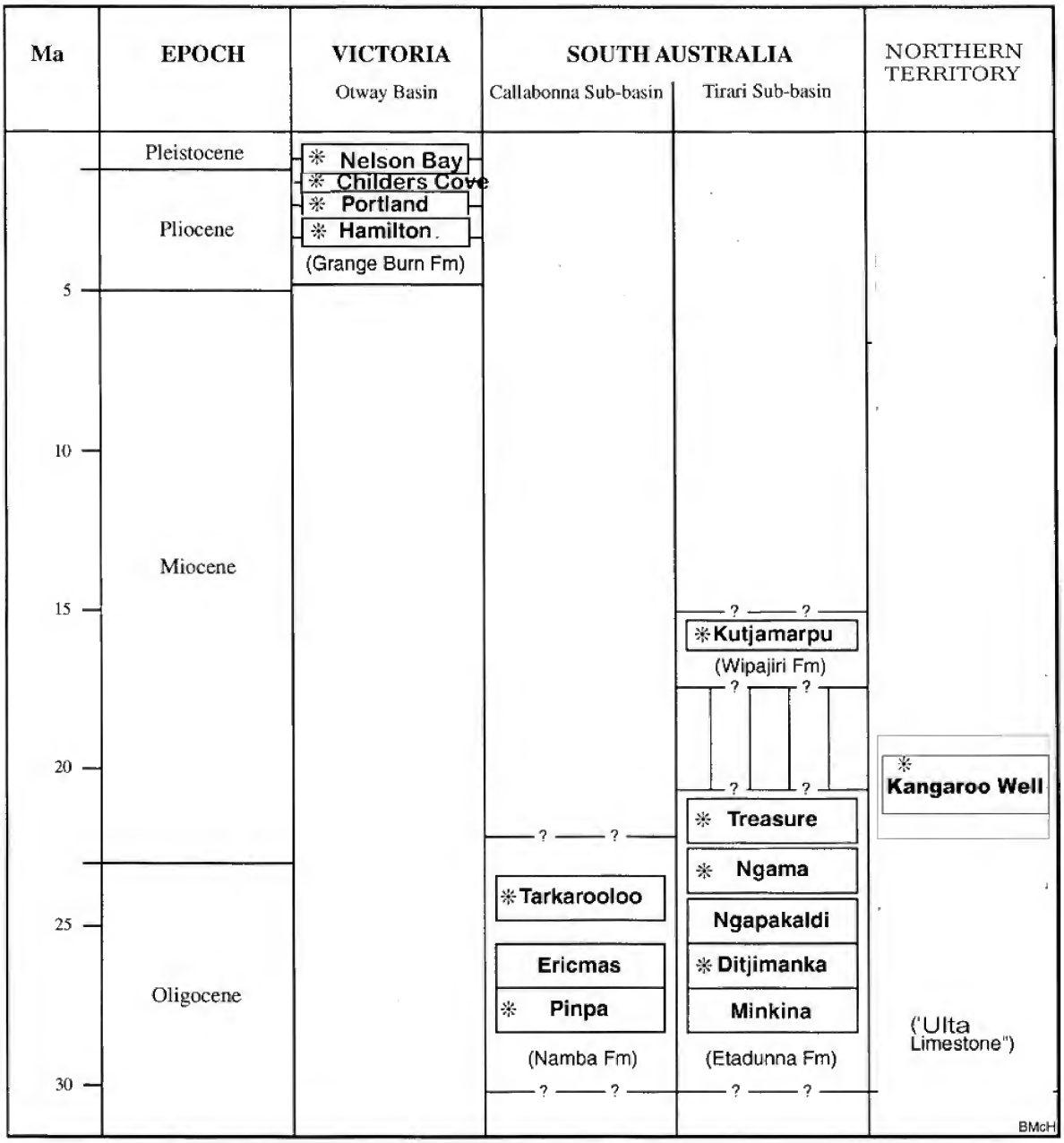

Figure 2. Stratigraphic distribution of named ektopodontid species.

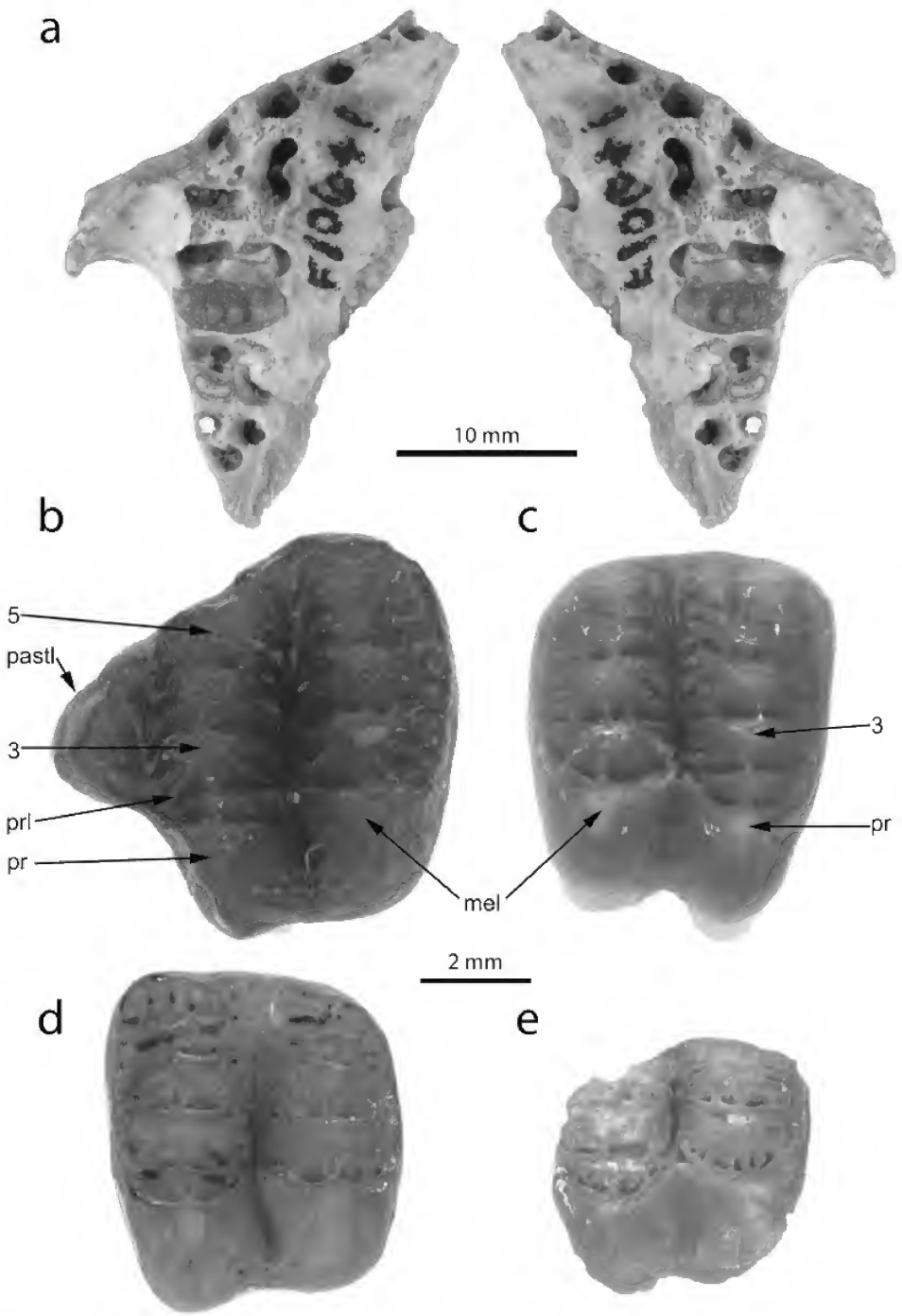

Figure 3. *Chunia* spp. teeth: **a-d**. *Chunia illuminata*, Woodburne and Clemens, 1986. **a**. right maxilla. QM F10641, mirror-imaged to show angle of face, Tedford Locality; **b**. M^1 SAM P29081, White Sands Basin; **c**. SAM P17997, (type) M^2 Tedford Locality; **d**. M^3 SAM P33944, Tedford Locality, Lake Palankarinna, Ditjimanka Local Fauna; **e**. *Chunia omega* Woodburne and Clemens, 1986, half of M3? (type) SAM P23065, Tom O's Quarry, Lake Tarkarooloo, Tarkarooloo Local Fauna. Abbreviations: mel, metaconule; pastl, parastyloph; pr, protocone; prl, protoloph; 3, cusp 3; 5, cusp 5.

simplest (after that of the protocone) and extends to the transverse valley; a weak lingual spur arises about halfway along its length and the distal (posterior) end curves lingually to parallel the transverse valley. Cusps 3 and 4 are basically similar, each being large and having a pair of subparallel precristae and postcristae that are angled slightly linguad. Cusp 3, however, also has a third slightly sinuous precrista, two weak ribs on the buccal face of the outermost precrista and a bifurcation of the buccal postcrista. Cusp 5 shows two strong postcristae reaching the transverse valley and a shorter, bifurcating buccal postcrista. Anteriorly, two sinuous precristae are linked by two or more near-apical struts and a basal strut. The lingual precrista bifurcates just below a strut linking it with the buccal precrista of cusp 4. All cusps (1–5) are linked apically by a fine transverse strut. Cusp 6 is displaced posteriorly and is a small trigonal structure with pre-, post- and transverse cristae.

The transverse valley is deep, trenchant, slightly curved and anteriorly convex. No structures cross it except at the lingual end where there is a notched cingulum. Buccal to this are three weak irregular postcristae at the base of the protocone and four irregular precristae on the metaconule, none of which cross the valley. The lingual cingulum curves and extends up the lingual face of the metaconule (i.e. the posterolingual cusp of diprotodontians previously called the hypocone; see Tedford & Woodburne, 1987).

The metaconule is stronger and more bulbous than the protocone. Besides the irregular basal precristae, there are two short postcristae that form a small pocket on the posterior face. The main precrista is aligned with the main postcrista and with the postcrista of cusp 2 of the protoloph. Cusp 2 of the metaloph is similar in size to cusp 3 of the protoloph. Besides the strut linking it to the metaconule, both of the pre- and postcristae bear several transverse ribs on the lingual face of the lingual cristae and the buccal cristae bifurcate basally. Cusp 3 is similar but with fewer and weaker ribs; only its buccal postcrista bifurcates. However, the apex of the cusp appears to be a triangle of short crests with its base aligned with the buccal cristae. Buccally from here, the structure is unclear. Cusp 4 appears to be a relatively simple structure with a single precrista and a postcrista bearing several weak lingual ribs. Near its apex, however, a short crest leaves posterobuccally to join one coming anterolingually from another, posteriorly offset cusp. A short postcrista arises at the junction of these crests but does not reach the posterior cingulum. This posterior cusp also bears four other radiating crests, two being aligned longitudinally and the others antero- and posterobuccally. Buccal to cusp 4 are three or four weak cusps defined by four simple precristae alternating with three short postcristae that do not meet the cristae from the posterior cusp. At the base of these precristae a low transverse crest parallels the transverse valley. A distinct postcingulum extends from the buccal-most postcrista to the metaconule. Pledge (1986) attempted to equate these buccal structures (in species of *Ektopodon*) with the cusp and crest patterns common in diprotodontians but it now appears, even in this relatively plesiomorphic species, that the homology of these cusps in ektopodontids is unclear.

M^3. The new specimen found by Case and Clemitson SAM P33944 is almost identical to, but the mirror image of, the holotype SAM P17977, and paratype SAM P22722 M^2s from the same locality. It differs in being slightly longer and narrower, with slightly more prominent equiradial development of crests and struts, and is thus accorded here a more posterior position. This tooth bears some resemblance to the incomplete type specimen of *Chunia omega* (fig. 3E) from the Tarkarooloo Local Fauna (Woodburne and Clemens 1986).

Ektopodon Stirton, Tedford & Woodburne, 1967.

Distribution. Kutjamarpu Local Fauna, Wipajiri Formation, Lake Ngapakaldi; Ngama Local Fauna, Etadunna Formation, Lake Palankarinna; Tarkarooloo Local Fauna, Namba Formation, Lake Tarkarooloo; Portland Bay Local Fauna, Whalers Bluff Formation, Portland.

Age. Late Oligocene to early-mid Miocene, Pliocene.

Diagnosis (revised). As for Woodburne and Clemens (1986b) but with the revision of the dental formula which is now understood to be: I?/1, C1/1, P3/3, M1-4/1-4. This revision involves recognition of the presence of only a single premolar.

Ektopodon serratus Stirton, Tedford & Woodburne, 1967.

Holotype. SAM P 13847. (Fig. 6B).

Ektopodon tommosi sp. nov.

Ektopodon sp. cf. *E. stirtoni* Pledge 1986, pls 3.1D, F, G; 3.2; 3.3D-E (fig. 4).

Holotype. SAM P19962 (RM^1).

Paratypes. NMV P48750-48751 (LM^1), SAM P19963 (RM^2), SAM P19950 (RM_1), NMV P48752 (LM^2), NMV P48753 (LM^3), NMV P48757 (LM^4), NMV P48764 (LM_2), NMV P48765 (RM_3), NMV P48766 (RM_4).

Referred specimens. NMV P48758 (right lower incisor), NMV P48769 (partial LP^3), SAM P19965 (RP_3).

Locality. Tom O's Quarry, western shore of Lake Tarkarooloo, Callabonna Basin. 31°8.5'S., 140°6.3'E.

Horizon. A sandy channel deposit within the Namba Formation (Callen & Tedford, 1976).

Age. Late Oligocene, Tarkarooloo Local Fauna. Biocorrelation suggests this is faunistically equivalent to the Ngapakaldi Local Fauna of the Lake Eyre Basin (Rich and Rich, 1987), which is a little older than the latest Oligocene Ngama L.F. of Lake Palankarinna, but younger than the Pinpa L.F. from Lake Pinpa.

Diagnosis. The molar teeth are generally 5–10% smaller than comparable elements of *E. stirtoni*, and the loph(id)s generally have one less cusp. The protostyloph on M^1 is shorter and less loph-like with two cusps, one less than in *E. stirtoni*. The P^3 is larger than that tooth in *E. stirtoni*. The mandible is slightly larger than in other species, with a longer diastema.

Etymology. The species name reflects the source of these specimens, Tom O's Quarry site, (discovered by Cpl. John Thompson – 'Tom O' to distinguish him from Tom Rich – of 3rd RAAME which provided logistic support for Rich's 1974 expedition; Rich and Archer, 1979), at Lake Tarkarooloo.

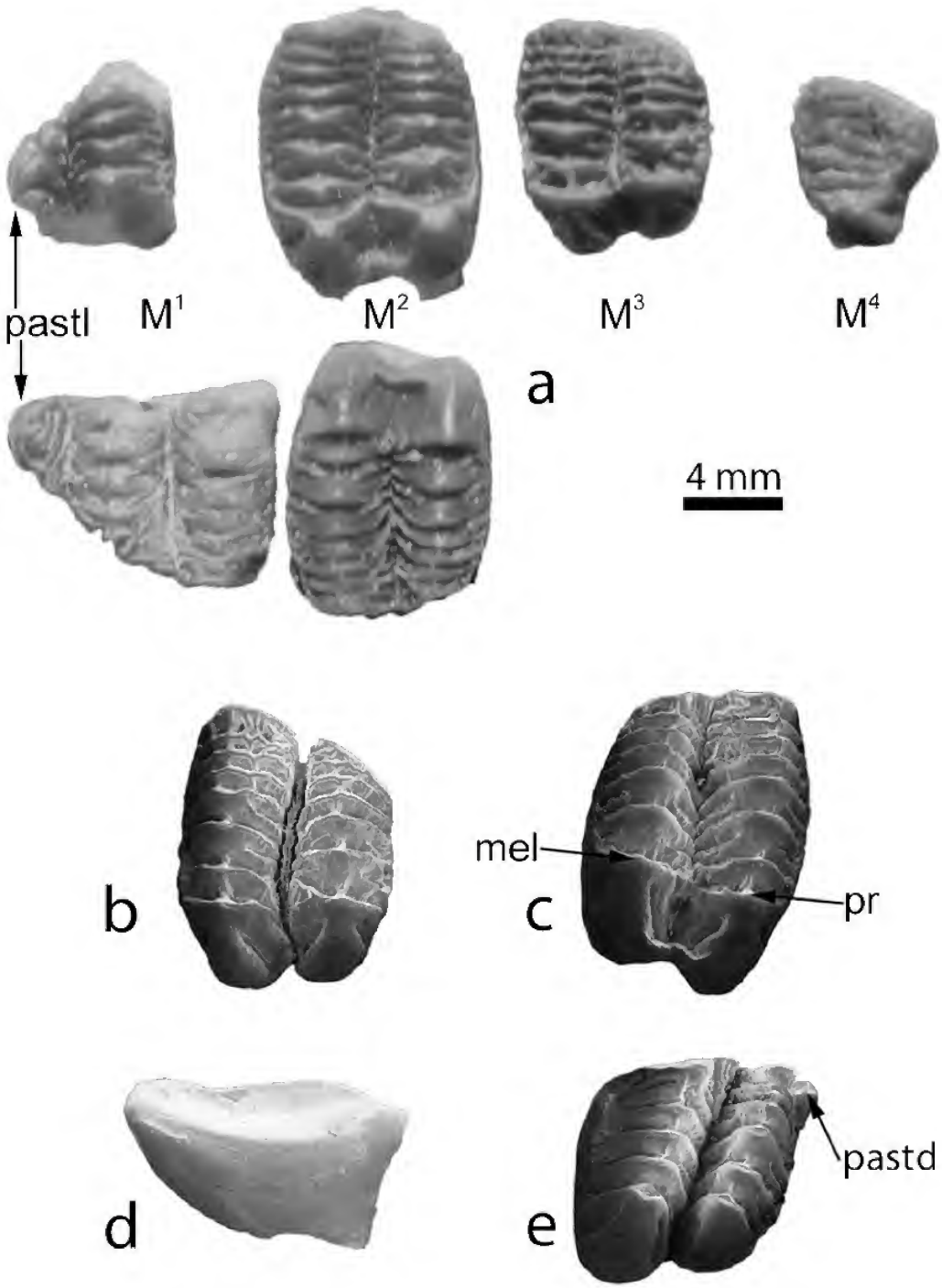

Figure 4. Dentition of *Ektopodon tommosi* nom. nov. **a**. composite upper dentition, anterior at left: LM^1 fragment (NMV P48750), partial RM^1 (SAM P19962), LM^2 (NMV P48752), RM^2 (SAM P19963), LM^3 (NMV P48753), LM^4 (NMV P48757); **b**. LM^3 (NMV P48753); **c**. RM^2 (SAM P19963); **d**. RI_1 (NMV P48758); **e**. RM_1 (SAM P19950. Tom O's Quarry, Lake Tarkarooloo; Tarkarooloo Local Fauna. Abbreviations: mel, metaconule; pastd, parastylid; pastl, parastyloph; pr, protocone.

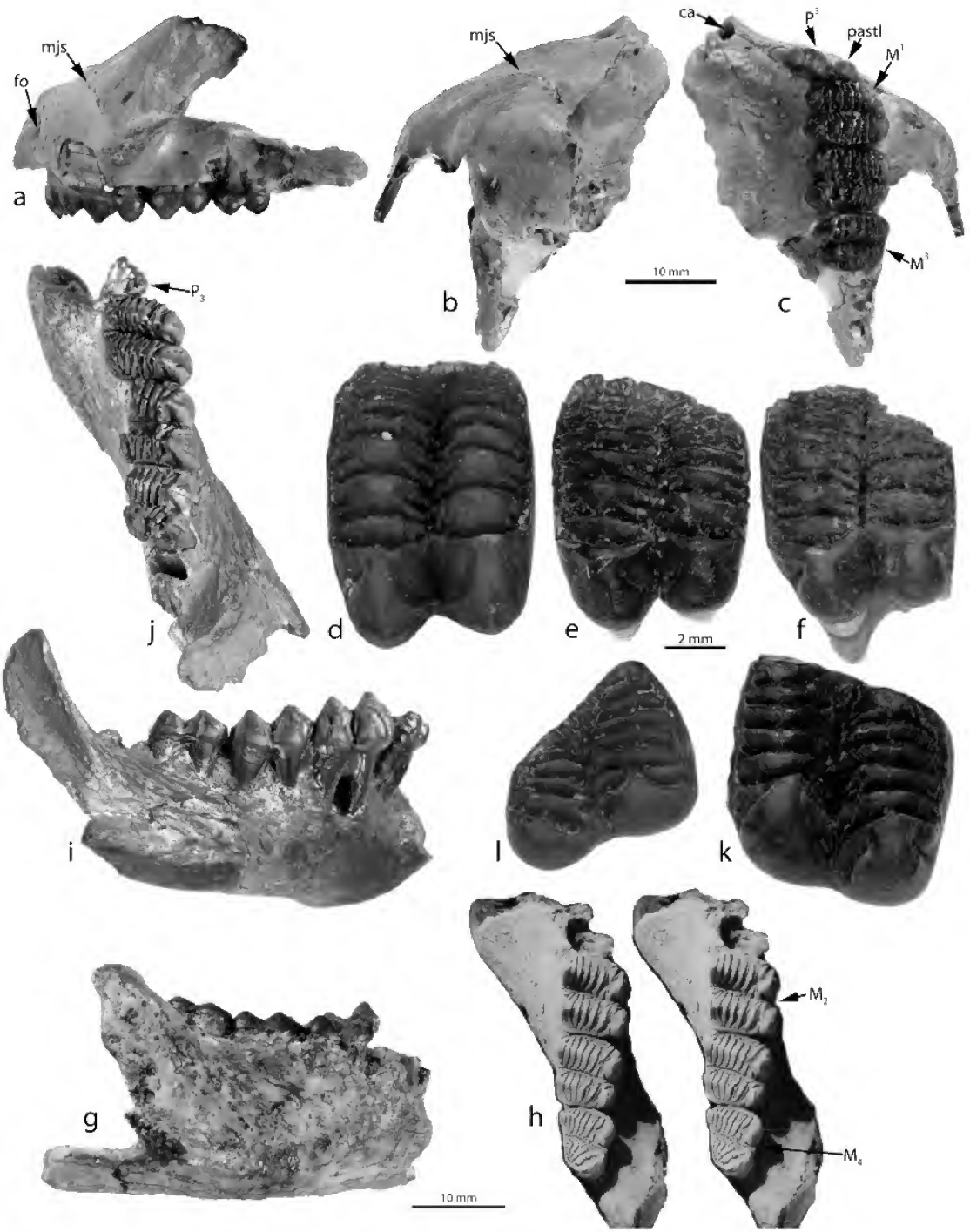

Figure 5. *Ektopodon stirtoni* Pledge, 1986, holotype dentary and new material. **a-c**. new maxilla (SAM P35309): **a**. lateral; **b**. dorsal; **c**. palatal; **d**. RM^2 (P23854); **e**. LM^3 (P30175); **f**. LM^3 (SAM P30156); **g**. right dentary (SAM P29577), lateral aspect; **h**. right dentary with M_{2-4} (SAM P29577) stereo pair; **i**, **j**. holotype right dentary with P_3, M_{1-3} (SAM P19509); **k**. LM_3 (P31638); **l**. RM4 (SAM P33451). Ngama Quarry, Mammalon Hill, Lake Palankarinna; Ngama Local Fauna.

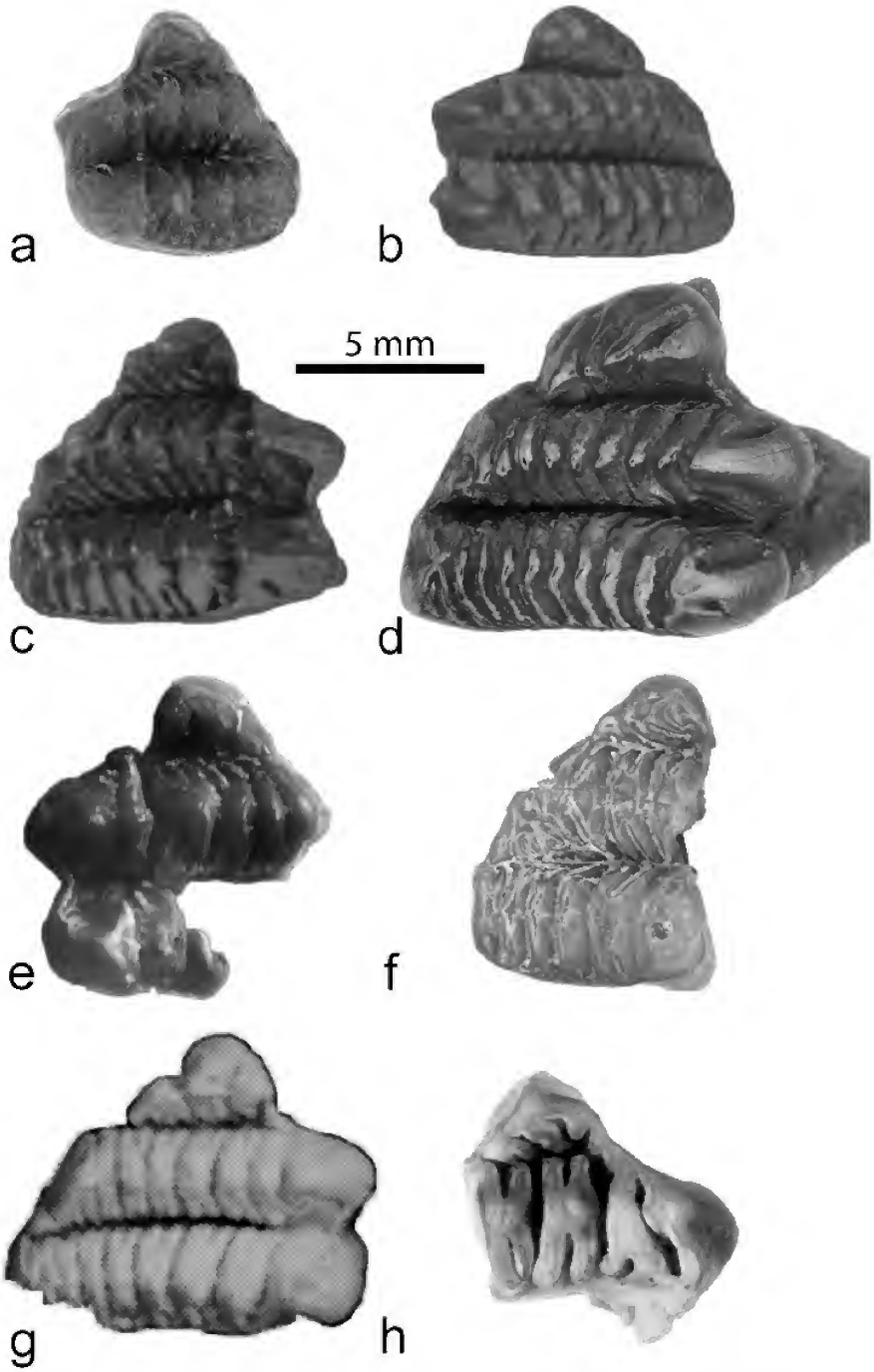

Figure 6. Ektopodontid spp.; comparison of first upper molars. **a**. *Chunia illuminata* SAM P29081 (left); **b**. *Ektopodon serratus* SAM P13847 (left); **c**. *Ektopodon stirtoni* SAM P22504 (right); **d**. *Ektopodon litolophus* SAM P30176 (right); **e**. *Ektopodon tommosi* NMV P48750-1 (left); **f**. *Ektopodon tommosi* SAM P19962 (right); **g**. *Ektopodon ulta* (from Megirian et al. 2004:719, fig. 15A); **h**. *Ektopodon paucicristatus* (from Rich et al. 2006:137, fig. 3D). Scale bar approximately 1 cm, for a-d; others about same scale. Abbreviations: ca, canine alveolus; fo, infraorbital foramen; mjs, maxillojugal suture; pastl, parastyloph.

Description. See Pledge (1986: 53–60) for a more-complete description. The following is abbreviated and has updated terminology.

P^3. There are still only two fragments known; the incomplete specimen (NMV48769) referred to this taxon by Pledge (1986) is correctly ascribed. It agrees morphologically with the P^3 of *E. stirtoni* (see below) as far as can be compared, but is noticeably larger (length >5.6, width 4.1 vs. length 5.5, width 3.4). The curving longitudinal crest extends from a conspicuous anterior cusp at the anterolingual corner of the tooth. At the midway point, a deep angular saddle divides the crest, separating the anterior cusp from two closely-linked larger posterior cusps. The latter are separated by a deep narrow crevice. The crest ends at the posterolingual corner of the tooth. Its lingual face has a weak basal cingulum with two small cusps.

M^1 (fig. 4A). Only three fragmentary teeth have been found, the holotype, SAM P19962 being one of them. The latter is quite worn and lacks the lingual margin, but compares well with P22504, the M1 of *E. stirtoni* from Mammalon Hill. However, it differs, apparently, in having one less cusp on each loph and a shorter protostyloph with only two well-developed cusps and the trace of an incipiently-developed third cusp.

M^2 (figs. 4A, C). This molar is broad, roughly trapezoidal, and the largest of the upper molars having only two lophs. The protoloph, with eight cusps, is slightly longer than the metaloph, which has seven, and the crests of the lophs slightly twisted rather than being in the same plane. The crests are also not as sharp as those structures on M^1, nor the transverse valley as deep. On the protoloph, the protocone bears a pair of deep grooves on its anterior and posterior sides, but the resulting ridges do not bifurcate. Similarly, the cristae of the second protoloph cusp do not bifurcate, but those of the 3rd, 4th, 5th and 6th cusps do (the last only on the posterior side). Similarly on the metaloph, the metaconule has a pair of deep grooves, and the 2nd, 3rd, 4th and 5th cristae bifurcate, the last only on the anterior side. The posterior groove of the protocone joins with the anterior one on the metaconule to form a deep buccal pocket. All cusps on a loph are joined by a fine, deep-set apical 'strut' along the axial plane of the loph. All cristae are cut off by the pre- and post-cingula.

M^3 (figs. 4A, B). This tooth is of similar length to M^2 but is noticeably narrower, and therefore trapezoidal in outline. The protoloph has eight cusps and extends beyond the metaloph at each end. The metaloph probably has seven cusps, but the count is uncertain because of the difficulty in distinguishing between primary cristae and bifurcations. Fine linking struts between cristae increase in number buccally to at least four at the paracone.

M^4 (fig. 4A). This tooth appears to be a stunted version of M^3. It is triangular, and bears only the protoloph which is of low relief and has seven or eight cusps (number uncertain because of the irregular bifurcation of the cristae). The missing metaloph is replaced by the third corner of the triangle: an inchoate network of low crests. The metaconule appears to have merged into the protocone, and that combination presents as a square extension of the protoloph.

Dentaries. Three dentaries are known, one retaining a fragment of the hypolophid of M_3; the others may be a pair. They are relatively massive, are slightly larger than those of *E. stirtoni.* Compared with the latter, they have a more convex ventral profile, and a longer diastema, but the alveolar cheek-tooth length is shorter. A minute alveolus (for a canine?) immediately follows that of the incisor on its dorso-lateral corner.

I_1 (fig. 4D). An isolated right incisor is referred to this position, based on size and its semicircular cross-section to fit the alveolus. It is short, high and somewhat spatulate, but it cannot be proven to relate to this species.

P_3. This tooth is represented by three specimens. It is smaller than the P_3 of *E. stirtoni*, and more subdued in its features, but otherwise similar. It is ovate in outline, and has on the lingual side a longitudinal cristid that bears four cuspids. An isolated anterior cuspid is followed by a central slightly larger one, then a third even larger one to which is appressed a smaller fourth cuspid. A posterobuccal cingulum forms a small pocket.

M_1 (Fig. 4E). SAM P19950 is the only complete specimen of this tooth known. It can be recognised by its distinctive 'parastylid'. The tooth is roughly rhomboid in outline and wider than long. The 'parastylid', at the anterolingual corner of the tooth, is more prominent than that structure in *E. stirtoni.* The lingual face of the tooth is relatively flat; the buccal ends of the lophids are quite swollen. Lophid crests are sharp and parallel to themselves, but not to the anterior and posterior faces of the tooth. The six protolophid cuspids are not as well-graded as in *E. stirtoni.* The two most buccal are very closely appressed, while the other four are well-spaced. The same pattern of distribution of cuspids characterizes the hypolophid. The precristids of cuspids 2–4 on the protolophid bifurcate. The same occurs for cuspids 1–3 on the hypolophid.

M_2. This tooth is relatively longer than M_1 and has a more open transverse valley. Each lophid has seven cuspids, the inner-most two being combined. On the protolophid, only the precristid of the protoconid divides, and its lingual branch divides again. On the hypolophid, the hypoconid and cuspid 2 divide on both sides. Although this occurs on cuspid 3, it does so only on the precristid. The precristid of the metaconid has a small notch, as it does in M_1, but it does not develop a 'parastylid' at the precingulum.

M_3. This tooth is not represented by a complete specimen. A fragment of hypolophid is preserved in the dentary NMV P48767, Although another M_3, NMV P48765, is more complete, it lacks the protoconid and hypoconid. Based on what is preserved, these specimens show a morphology similar to that of *E. stirtoni*, with low lophids and a wide transverse valley. On both lophids, the postcristids of cuspids 2 and 3 divide, and on the hypolophid, the precristids also. The lingual part of the crown develops into a network of fine cristids and struts, which differs in the extent of this network development from that in the M_3 of *E. stirtoni.*

M_4. Despite their superficially different appearances, two specimens, SAM P19966 and NMV P48766, have been identified as M_4s. The former is incomplete and slightly more worn than the other; both are from right dentaries. They are roughly triangular as a result of reduction of the entoconid, and are low-crowned with very low, broad lophids. There are six to seven cuspids on each lophid, the number uncertain because of similarities and irregularities of cristids and ribs. The transverse

valley is an irregular network of anastomosing cristids and ribs. These teeth are elongate (length:width ratio about 1.14). NMV P48766 fits the alveolus of jaw NMV P48767.

Ektopodon stirtoni Pledge, 1986.

(Fig. 5)

Pledge (1986) named this taxon on the basis of a right dentary with P_3 M_{1-3} (SAM P19509) and an isolated RM^1 (P22504). The new material described here adds considerably to knowledge about this species.

New specimens. SAM P23854, RM^2 with lingual root, collected by J. McNamara, 13 July, 1981; SAM P24541, LM_2 hypolophid, collected by N. Pledge, August, 1983; SAM P23989, RM_3 hypolophid with root, collected by N. Pledge on 5 September, 1982; SAM P23988, LM_4 crown, collected by N. Pledge, 5 September, 1982. All the above were noted (per measurements only) in Pledge (1986). The following have not previously been noted. SAM P29577, right dentary with M_{2-4}, collected by D. Williams, 3 July, 1988; SAM P30156, LM^3, collected by H. Aslin, 1 September, 1989; SAM P30175, LM^3, found by J. Thurmer, 1 November, 1989 (fig. 4); SAM P31637, left maxilla with M^2, found by J. McNamara, 27 July 1990; SAM P31638, a left M_2 found by B. McHenry, August 1990; SAM P33451, a right M_4 collected by G. Aldridge, October 1991; and SAM P35309, a left maxilla, with P^3M^{1-3} but missing the canine and M^4, collected by N. Haines, 8 August, 1995.

Locality. Mammalon Hill (SAM locality PL7611; the Type Locality for the species), northwestern shore of Lake Palankarinna, South Australia.

Age. The Ngama Local Fauna comes from the Mammalon Hill beds (zone D) of the Etadunna Formation. The age of this horizon is uncertain but considered to be Late Oligocene (Pledge, 1984; Woodburne, 1986; Woodburne et al., 1994).

Revision of specific diagnosis. In addition to the diagnostic features noted by Pledge (1986), these additional specimens of *Ektopodon stirtoni* demonstrate that this species differs from *E. serratus*, in greater size, greater length/width ratio of the molars and fewer cusp(id)s. It differs from *E. litolophus* (Pledge et al., 1999) in its smaller size, relatively narrower M^1, relatively less regular parastyloph with less uniformly sized cusps, fewer and less uniformly-sized cusps on main lophs with obvious ribs and struts, presence of posterior cingulum. The face is blunter than that of *Chunia illuminata* (compare figs. 3A and 5B, C).

The original description of *E. stirtoni* (Pledge 1986) dealt with the holotype dentary and an M^1 (ibid. plate 3.1B). In the dentary, only the P_3 and M_1 were complete. The present work includes descriptions of the other lower molars (M_{2-4}) as well as that of P^3, M^2 and M^3. These descriptions incorporate specimens previously noted only in the table of measurements (ibid. table 3.1).

Descriptions. Maxilla. Although the (mostly edentulous) maxilla of *Chunia illuminata* had been known for some time (Woodburne and Clemens, 1986b), it did not fully prepare us for the morphology shown by the new specimen of *Ektopodon*. SAM P35309 is virtually complete, lacking only the thin bone on the medial edge of the palate at the midline suture, the dorsal wing of the maxilla with the nasal contact, the small canine, and the last molar M^4 (figs. 5A-C).

However, part of the jugal which forms the lower border of the orbit and part of the zygomatic arch is also present. This enables us to form a picture of the face of *Ektopodon*. The orbits had an estimated diameter of up to 15 mm, and were directed forwards and upwards in a wide (est. 50 mm across cheekbones) flat face with a short, narrow muzzle. The lateral face of the maxilla is gently convex, almost flat, from canine to malar process of the zygomatic arch. There is no malar depression or fossa. The maxillo-jugal suture is gently sinuous from just behind the malar to the anterior 'corner' of the orbit, with the jugal tapering from less than 3 mm below the orbit and being a uniform 3 mm wide inside the edge of the orbit. The bottom edge of the eye socket is 5.5 mm above the molar occlusal surface. The infraorbital foramen is ovate and situated about 4 mm behind the canine and 3–4 mm above the diastemal crest; it emerges 12 mm posterior in the orbital floor.

The molar occlusal surface shows a slight torsion along its length. The combined length of the cheektooth row, P^3 to M^3 is 23.2 mm. The maximum bone length, from canine alveolus to posterior extremity of the palate, parallel to the molar tooth-row, is 37.3 mm. The width of the maxillary palate to the lingual margin of the molars is (2x) 12.7 mm. The maximum palate width measured to the buccal edge of the molars is 22.2 mm. M^4 is represented by three alveoli.

Canine. Not much can be said of this tooth based on its alveolus, apart from its existence and its gingival diameter: maximum 2 mm. The alveolar depth of 5 mm suggests it was neither a large nor particularly functional tooth. It is situated at the extreme corner of the maxilla, next to the premaxillar suture.

P^3 (fig. 5C). Previously, the ektopodontid P^3 was known only from two referred fragments from Lake Tarkarooloo (Pledge, 1986). These have here been reinterpreted (below) to represent *E. tommosi* n. sp.

The P^3 of SAM P35309 is somewhat recumbent, with its anterior root extending well into the diastema. However, it is almost transverse to the long axis of the molar-row, and its posterolingual corner is tucked neatly into the angle formed by the 'protostyloph' and the protoloph of the first molar. The tooth is fairly typical of the permanent premolars of many diprotodontans: somewhat rectangular with a longitudinal ridge just buccal of the centre-line bearing two major cusps, and a shorter, lower lingual cingular ridge with an anterior expansion that forms a prominent anterolingual corner and is the base for a strong transverse ridge ascending to the anterior cusp. Anterior to this ridge is a slightly weaker and shorter one, midway between the transverse ridge and the trenchant anterior extension of the longitudinal ridge. The longitudinal ridge is crossed by a deep valley that separates the anterior cusp from the slightly lower, double, posterior cusp; the crest from the hind part of this cusp curves around to connect with the posterior end of the lingual cingulum. There are two or three small transverse crenulations in the cingular valley. The longitudinal crest is slightly convex buccally, and is almost perfectly aligned with the anterior transverse crest (the 'parastyloph') of M^1.

M^1. This tooth in SAM P35309 is almost identical to the paratype SAM P22504 described by Pledge (1986).

M^2. In Pledge (1986), the M^2 of *Ektopodon tommosi* from Lake Tarkarooloo was depicted for purposes of illustrating morphology in Text Fig 3.5 (ibid.) as that of *E. stirtoni*, the tooth having not then been found at Mammalon Hill. This deficiency has now been rectified with discovery of specimen SAM P23854 – an RM^2 still partly *in alveolo* in a fragment of maxilla (it lacks only the buccal face of the tooth), SAM P31637 with a complete LM^2 in most of the maxilla, and SAM P35309, an almost complete maxillary dentition (figs. 5A–C).

This bilophodont tooth is wider than long. The protoloph is slightly wider transversely than the metaloph. The tooth's length is 6.8 mm; its maximum width is 9.5 mm.

The protoloph has eight distinct cusps and an indication of at least one more (as does the metaloph). This is more than in *E. tommosi* (from the slightly older Tarkarooloo LF). The apices of the protocone and metaconule are equal in height, but the lingual extremity of the base of the former is more acute and thus extends slightly farther in a lingual direction. There is a large, deep groove on the anterior face of the protocone and a slightly weaker posterolingual one that extends into the pocket formed by the short but strong lingual cingulum at the end of the transverse valley. Strong pre- and postprotocristae extend in a slightly buccal direction (in the same way that comparable crests extend from the metaconule) giving a hint of remnant selenodonty. The preprotocrista meets the lingual end of the anterior cingulum. The other pre-cristae do not join or only just contact the precingulum. Cusp 2 is smaller and simpler than either the protocone or cusps 3 or 4. It has a single undivided longitudinal crest and is linked to the protocone by an apical strut and a basal strut from the postcrista. Cusp 3 has a strong pre- and postcrista, with a somewhat weaker parallel set arising lower on the lingual face. It is linked to cusps 2 and 4 by a fine low apical strut. Cusp 4 is similar but the lingual pair of cristae is slightly stronger. Cusps 5 to 8 bear undivided pre- and postcristae which are linked by 2 or 3 subapical struts and several short basal ribs. The extent of the median valley indicates at least one more cusp and possibly two.

In occlusal view, only the metaconule on the metaloph is opposite its counterpart cusp (the protocone) on the protoloph. The metaconule is rounder than the protocone and the two grooves diverge antero- and posterolingually, the anterolingual groove running into the cingular pocket. The postmetaconulecrista runs into a very narrow postcingulum to which the other postcristae are weakly joined. Cusp 2 is large and well-spaced from both the metaconule and cusp 3. Its precrista bifurcates basally, with the new rib extending lingually towards the thickened basal ends of the premetaconulecrista and the postprotocrista. Short struts link it anterobasally and apically to the metaconulecrista and there is a short lingual rib from the postcrista. Cusp 3 is similar to that of the protoloph. Cusp 4 is finer with a bifurcating precrista and a short basal lingual rib from the postcrista. It is linked by an apical strut to cusps 3 and 5. Cusps 5 and 6 are similar with undivided cristae that bear a few short irregular ribs. Cusp 6 joins apically to cusps 5 and 7 with a fine strut. Cusp 7 is irregular, having a fine wavy crista bearing several short ribs or broken struts that link with the remnants of cusp 8.

Of the roots, only the double lingual one supporting the protocone and metaconule is preserved, although its tapered tip is missing. Anterior and posterior transverse roots are represented by their bases which support the buccal ends of the protoloph and metaloph respectively.

SAM P 23854 (fig. 5D) is similar in appearance and construction to the M^2 referred by Pledge (1986) to *E.* sp. cf. *E. stirtoni* (=*E. tommosi*) from the Tarkarooloo LF. It differs in two obvious respects: (1) the relatively and absolutely greater width of the Mammalon Hill M^2 resulting from (2) at least one extra cusp at the buccal end of each loph. In these features, it appears to be autapomorphic within the genus. In P 31637, by some aberrant occlusal wear or damage, cusps 2–4 on the protoloph and cusp 3 on the metaloph are exceedingly worn, far more so than the other cusps.

M^3. This tooth is represented by two specimens, SAM P 30156 (fig. 5F) and SAM P 30175 (fig. 5E), both slightly damaged by the loss of enamel on the buccal face. The former is the better preserved. M^3 has been described from *E. tommosi*, e.g. NMV P48753, at Lake Tarkarooloo, hence a direct comparison is possible with these two additional specimens.

The M^3 of *Ektopodon stirtoni* is slightly larger than that of *E. tommosi* and in occlusal outline is less tapered posteriorly since the metaloph is relatively longer and less acutely truncated. The detailed structure of cusp ribs and struts is also less complex. The tooth is 6.7 mm long.

The protoloph is 8.9 mm wide and has eight distinct cusps. It is similar in most respects to that of M^2, differing in that the posterolingual groove of the protocone does not flow into a pocket formed by a lingual cingulum, and in that there are more links joining the crests of cusps 7 and 8. By the same token, the protoloph differs from that of *E. tommosi*, in having fewer subapical links and struts between the crests of cusps 5 to 8. They are similar in lacking the lingual basin.

The metaloph is 7.6 mm wide with six distinct cusps and a buccal complex. The metaconule is situated somewhat more buccally than the protocone, but not level with cusp 2 of the protoloph. However, the crests of the metaconule do align with those of protoloph cusp 2. Similarly the cristae of metaloph cusps 2 and 3 align with those of protoloph cusps 3 and 4. The pre- and post-cristae of cusp 2 each have an accessory crista that is rather sinuous and arises from further down on the lingual face, parallel to the main crista. This is similar to cusp 3 of the protoloph. Cusp 3 is a smaller version of cusp 2; both have a basal bifurcation of the precrista. Cusp 4 is smaller still, with both pre- and post-cristae bifurcating. The cristae of cusp 5 do not bifurcate, but have several struts and/or ribs on the buccal face alongside the fine apical strut linking the cusp to cusp 6. The cristae of cusp 6 are rather zig-zag because of the several struts linking them to cusp 5 and to the missing buccal face. The putative apical strut linking to cusp 7 is displaced anteriorly and there is a short simple precrista from the apex. Parallel to this is an even shorter precrista (half the length of that of cusp 7), which would arise from the buccal edge of the tooth.

The metaloph thus differs from that of M^2 in ways consistent with the posterior narrowing of the tooth and the molar gradient. It differs from that of *E. tommosi* in its greater relative and absolute width, and lesser buccal angular truncation, with consequent better development of the postcristae of cusps 5 to 7.

The maxilla of *Chunia illuminata* (QM F10641) (fig. 3A) suggests from its alveoli that there is a steep molar gradient in that species. The dentary of *Ektopodon stirtoni* (SAM P19509) indicates that the gradient is less in this species. The new specimens of M^3 described in this paper confirm that it is also less than in *E. tommosi*, although the alveoli preserved in maxilla P31637 are too damaged to enable tooth gradients to be determined with confidence.

The maxilla SAM P31637 is damaged on all sides. The root of the zygoma is split and the maxilla is broken anteriorly through the alveolus of M^1. The alveolus of M^3 is damaged buccally and that of M^4 is broken across, while the medial edge of the fragment is irregular with no part of the median suture being preserved. While the endocranial surface of the palatal wing of the maxilla is smooth and relatively flat (slightly concave anteriorly), the oral (ventral) surface is noticeable convex anteroposteriorly, rather as it is in *Phascolarctos cinereus*. This characteristic is not evident in *Chunia illuminata* where the palate is relatively flat.

Lower dentition. Dentary, SAM P29577, (figs. 5G, H) is broken off just anterior to the position of M_1, which is missing. It preserves molars M_{2-4} in good but more-worn condition than the holotype. The horizontal ramus is torted, and the tooth-row lies at an angle of about 30° to this portion of the dentary.

M_2. In the holotype, this tooth is incomplete, having been reconstructed from numerous tiny fragments. Dentary SAM P29577 presents a complete but worn M_2, while SAM P24541 is a slightly worn hypolophid of an M_2 and SAM P31638 a perfect M_2 crown. The following description is based on the last, with additional comments on the others where appropriate.

The M_2 is somewhat rhomboidal in occlusal outline with protolophid and hypolophid having about the same transverse width. In P29577, both protoconid and hypoconid are extremely worn with the enamel breached and the dentine deeply excavated, but only a few of the adjacent cuspids have been breached. In contrast, P31638 is virtually unworn.

The protolophid in P31638 has seven cuspids (eight in P29577) with the protoconid being much larger than the others. Its crest is oblique (at about 80°) to the lingual face. The protoconid in P29577 is so deeply worn that it merges with the second cuspid and the two are difficult to distinguish. In P31638, as in the holotype SAM P19509, cuspid 2 is a single, simple plate closely appressed to the protoconid. On the protoconid, the anterobuccal groove is flanked buccally by a low crest and lingually by a parallel crest that seems (in P29577) to arise from the precristid of cuspid 2. The precristid curves buccally to merge with the remnant of the precingulid. Posteriorly the posterobuccal groove of the protoconid is flanked by a fine cristid arising from the postprotocristid. The postcristid of cuspid 2 has a short buccal rib. The enamel of cuspids 3–6 of P29577 is breached, leaving a thicker and higher ridge on the buccal side. Precristids of cuspids 3–5 are simple but divide slightly as they merge with the precingulid. Their postcristids expand slightly in the base of the transverse valley and each has a minor buccal rib. Cristids of cuspid 6 (and 7 in P29577) are simple. The innermost cuspid (7 of P31638 and 8 of P29577) has a bifid precristid with a basal cuspule (homologous with the larger structure in M_1 of the holotype) developed at the lingual corner of the precingulid.

The hypolophid parallels the protolophid. The hypoconid has deep anterobuccal and posterior grooves separating the bulbous buccal part from the rather sinusoidal cristid. The precristid curves buccally and the postcristid lingually to merge with the postcingulid. All six cuspids of P29577 have breached enamel. Precristid 2 has a weaker buccal rib and an expanded base; postcristid 2 is bifid at its base. On cuspid 3, the precristid is trifid with a weak buccal rib, a stronger lingual rib and the main crest expanded in the bottom of the transverse valley. The postcristid is bifid at its base. Cuspids 4 and 5 are similar, with simple undivided cristids. Cuspid 6 is complex with three parallel anterobuccal cristids which decrease rapidly in size lingually as they are truncated by a low, transverse cristid in the transverse valley. There are two parallel postcristids, the lingual one of which is shorter and cut off by the curving end of the postcingulid. The postcingulid is well developed.

The hypolophid (SAM P24541) has a transverse width (i.e. normal to the lingual face) of 6.4 mm. Characteristically for lower molars of *Ektopodon* spp., the lophids are oblique to the tooth row with an acute anterolingual corner. There are seven cuspids, the inner two being combined. The hypoconid is large, its apex just buccal of the mid-line of the tooth. It has a deep anterobuccal groove that swings out basally and an almost longitudinal posterobuccal groove. The cristid obliqua curves buccally and divides basally. The posthypocristid is longitudinal. Cuspid 2 is on the midline of the tooth. Its pre- and postcristids parallel those of the hypoconid and give rise to shorter, basal supplementary cristids on the buccal side. A notched apical strut links the cuspids. Cuspid 3 is more complex with the precristid bifurcating and the postcristid trifurcating. Cuspids 4 and 5 are similar, simple cuspids, linked apically by fine struts. Their cristids do not divide. Cuspids 6–7 are complicated in being almost inseparable but having two diverging pre- and postcristids. The lingual-most precristid is short and notched to produce a basal cusp that extends as a "cingulum" along the transverse valley to the precristid of cuspid 4. All but the penultimate postcristid merge into the postcingulum.

This tooth fragment is similar to that of *E. tommosi* (NMV P48764) but its ornamentation is less developed. It is smaller than both that specimen and the holotype of *E. stirtoni* but larger than M_3 of *E. stirtoni*.

M_3. This tooth is incomplete in the holotype and poorly known in *E. tommosi*. It is now represented, however, by a complete (but worn) tooth in dentary SAM P29577 and by hypolophid SAM P23989.

The M_3 resembles that of P29577 except for its lesser degree of wear. Only cuspids 1–3 of the protolophid and cuspids 1–5 of the hypolophid have been breached. There are eight protolophid cuspids and six or seven hypolophid cuspids. The anterolingual

cuspule is smaller than in M_2 but slightly larger than in M_4. The tooth is smaller than M_2 and less rhomboid in outline, with the hypolophid narrower than the protolophid.

Hypolophid SAM P23989 is rectilinear and orientated obliquely at about 75–80° to the longitudinal axis of the tooth. The width of the hypolophid is 5.6 mm. There are seven cuspids. The buccal-most cuspid, the hypoconid, is at about one quarter the distance from the buccal end. It has a broad, shallow anterobuccal groove and a shallower posterior groove. The cristid obliqua is longitudinal but swings buccally at the base as it joins a basal strut from the second precristid. The posthypocristid curves lingually and joins the well-developed postcingulum. Cuspid 2 has simple undivided pre- and postcristids; the precristid of cuspid 3 divides halfway; and cuspids 4 and 5 have simple undivided cristae. Cuspid 6 lacks a postcristid but has a short precristid, parallel to that of cuspid 5, that divides basally. Cuspid 7 is displaced anteriorly and gives rise to two slightly diverging postcristids, the lingual one of which merges with the postcingulum. Its precristid is short and apparently joins the last postcristid of the protolophid.

This specimen preserves the posterior root, a long, tapering transverse fang-like structure, 9.8 mm long on the lingual side.

M_4. Three teeth represent M_4. Apart from its high degree of wear, which has reduced the crest angle of the protolophid to 140° or more and almost flattened the hypolophid, SAM P29577 from the dentary (fig. 5H) is virtually identical to the unworn SAM P23988 and P33451 (fig. 5I). Our description of this tooth will be based on the second specimen.

Previously, M_4 was only known from *E. tommosi* from Lake Tarkarooloo. The new specimens should, therefore, be compared with NMV P48766 (Pledge, 1986, plate 3.2H), NMV P160517 and SAM P19966. SAM P23988 is less worn than the Tarkarooloo specimens and shows a similar occlusal outline although with more buccal constriction at the transverse valley. The lophids are low and broad, though possibly higher than in *E. tommosi*. The primary cuspids, the protoconid and hypoconid, stand markedly higher than their subordinate cuspids.

The protolophid is much wider than the hypolophid and its crest is orientated at about 60° to the lingual face. The anterior edge of the tooth is convex and has a widening precingulid extending from the anterolingual corner, curving backwards, almost to the inner preprotocristid. The protolophid has seven cuspids, as in *E. tommosi*. The protoconid is situated about one third the distance from buccal end of the lophid. It is relatively high and lacks the obvious buccal grooves present on the protoconids of more anterior teeth. Instead, it has a strong anterobuccal preprotocristid and a subordinate lower cristid parallel to it on the lingual side. A pair of subparallel postprotocristae extends posterolingually to the transverse valley, with the lingual one having two buccally directed ribs.

Cuspid 2 is plate-like. Its precristid almost meets the precingulum at a cuspule but instead swings buccally and parallels it (as a rib) almost reaching the lesser preprotocristid. The postcristid bifurcates basally. Cuspid 3 is also plate-like, its precristid being simple and undivided and its postcristid only thickening at the posterior end. Cuspid 4 is a weaker irregular plate, thick anteriorly, with several minor ribs. It is shorter than cuspid 3 and larger than cuspid 5, which is otherwise similar although posterobuccally curved. Most cuspids are linked by fine, deep-set, apical struts, but on cuspid 6 these are as strong as the pre- and postcristids. The precristid is short and rather bulbous while the postcristid is finer and longer and curves buccally to join distally at the transverse valley the postcristids from cuspids 4 and 5. Cuspid 7 is low and on the extreme edge of the tooth. It is linked to cuspid 6 by a strut stronger than its pre- and postcristids. The precristid is short and merges into the precingulum. The postcristid is little more than a lingual cingulum with several strong basal ribs that increase in size towards the transverse valley. No postcristids actually cross the transverse valley.

The hypolophid is short with only five distinct cusps – fewer than in *E. tommosi*. The hypoconid is rounder than the protoconid and has a small anterobuccal groove that joins a larger posterobuccal groove on the protoconid to form a shallow pocket. There is no buccal cingulid. The cristid obliqua curves almost in a semicircle to a small basal cusp in the transverse valley, where it joins the precristid from cuspid 2. The posthypocristid curves lingually to join the short postcingulid. Cuspid 2 is a simple cristid with no discernable apex. Posterolingually, it joins the postcingulid at a small cuspule. Cuspid 3 is also a simple cristid bifurcating at the anterior end and not reaching the postcingulid. Cuspid 4 is irregular and links with a transverse cristid in the transverse valley. It is posteriorly short. Cuspid 5 is very low; its cristid is irregular and buccally curved. It converges with but does not meet ribs from the lingual cingulum and posteriorly parallels the postcingulid.

Morphologically SAM P23988, P29577 and P33451 are similar to the M_4s of *E. tommosi* but the fine ornamentation of cristids, ribs and struts is simpler. The teeth are also marginally larger.

Remarks. Overall, these newly described teeth of *E. stirtoni* confirm the distinction of this taxon from *E. tommosi* from the Tarkarooloo LF and appear to represent a relatively derived species. This is in keeping with the perceived greater age of the Tarkarooloo LF (e.g. Woodburne et al., 1985).

Ektopodon litolophus Pledge et al. 1999.

Holotype. SAM P30176, an isolated right M^1 (fig. 6D).

Locality. Leaf Locality (UCMP V-6213), Wipajiri Formation, eastern edge of Lake Ngapakaldi, South Australia.

Local Fauna and Age. The Kutjamarpu Local Fauna is estimated to be approximately early Miocene (see above).

Remarks. This unique specimen is noticeably larger than its contemporary *E. serratus*, and has a simpler morphology, with a longer, more loph-like parastyloph, suggesting that it is the most autapomorphic member of the family.

Discussion

There are now at least five known species of *Ektopodon* (*E. serratus*, *E. stirtoni*, *E. litolophus*, *E. tommosi*, a Riversleigh taxon, and *E. paucicristata*); two or three species of *Chunia*

(*C. illuminata*, *C.* sp. cf. *C. illuminata*, *C. omega*); and the monotypic *Darcius duggani*. No ektopodontid species, except *E. paucicristata* and *D. duggani*, occurs in more than a single local fauna, and in all but two local faunas (Tarkarooloo and Kutjamarpu) there is only a single ektopodontid species. Further, most are not common in their respective local faunas and three (*E. litolophus*, *C. omega* and the Riversleigh taxon) are known only from a single tooth. In the faunas where more than one species occurs, the sympatric forms are distinct in terms of size and morphology, a situation that may indicate ecological partitioning of species into feeding guilds. Food preferences for these possums are unclear but possibilities include grains, nuts and insects/grubs (Pledge, 1982, 1986, 1991).

Species of *Ektopodon* range in age from late Oligocene to late Pliocene. The oldest (*E. tommosi*) occurs in the Tarkarooloo LF of late Oligocene age. *Ektopodon serratus* and *E. litolophus* in the Kutjamarpu LF are probably Early to Middle Miocene in age. *Ektopodon ulta* (Megirian et al., 2004; fig. 6G) from the Kangaroo Well LF of the Northern Territory may be slightly younger than *E. stirtoni*. The age of the Riversleigh ektopodontid has been interpreted by Archer et al. (1989) to be most probably Early Miocene. The youngest reported *Ektopodon* is *E. paucicristata* (Rich et al., 2006) from the Pliocene Whalers Bluff Formation (Dutton Way, Portland) and Childers Cove of southwestern Victoria. This species is a temporal anomaly, in so far as its authors regarded it to be relatively plesiomorphic. In its short protostyloph with few cusps, low number of deeply bifurcated cusps on the lophs, and equidimensional molars, it resembles species of *Chunia*. While the original authors considered the teeth of *E. paucicristata* to be upper molars, their outline suggests they may in fact be lower molars. Species of *Chunia* range in age from Late Oligocene (Ditjimanka LF) to latest Oligocene (Tarkarooloo LF) in age. *Darcius duggani* (Rich, 1986) is known from the Early Pliocene Hamilton LF, and from the apparently early Pleistocene Nelson Bay Formation (Rich et al., 2006), both in southwestern Victoria. Rich (1986) regards *D. duggani* to be structurally intermediate between the species of *Chunia* and *Ektopodon*.

The fragmentary *Ektopodon serratus*-like ektopodontid tooth from the Wayne's Wok LF (Pledge et al., 1999) confirms previous suggestions that Riversleigh's Faunal Zone B local faunas share taxa with the Kutjamarpu LF (Archer et al., 1989). A *Darcius*-like form, also from one of the numerous Riversleigh localities, is noted by Long et al. (2002: 142) but is yet to formally described.

Woodburne & Clemens (1986c) interpreted the phylogenetic relationships of ektopodontids known at the time. Now, *Ektopodon litolophus* (Pledge et al., 1999) is best regarded as a sister taxon of *E. serratus*, and both may have been derived from an *E. stirtoni*-like ancestor. This conclusion follows from the observation that *E. litolophus* and *E. serratus* share the evidently synapomorphic condition of transversely widened lophs which also contain a relatively larger number of cusps. Considering that both of the more derived species are apparently contemporaneous, neither is likely to be the other's ancestor.

Acknowledgements

I thank the owners and managers of Etadunna Station for permission for us and our predecessors (R. A. Stirton and his students/colleagues) to work on their land, and for their forbearance of our activities over the years. Thomas H. Rich allowed me to participate in his early expeditions to Lake Tarkarooloo, which resulted in some of the material described here. Numerous volunteers helped me in the field; notable amongst them have been J. McNamara and J. Thurmer. A. Tindall helped with some photography and digital processing, and H. Hamon got the figures into presentable order.

References

Aplin, K.P. and Archer, M. 1987. Recent advances in marsupial systematics with a new syncretic classification. Pp. xv-lxxii in: M. Archer (ed) *Possums and Opossums: Studies in Evolution*. Surrey Beatty & Sons Pty Ltd and the Royal Zoological Society of N.S.W., Sydney.

Archer, M., Godthelp, H., Hand S. and Megirian D. 1989. Fossil mammals of Riversleigh, Northwestern Queensland: Preliminary overview of biostratigraphy, correlation and environmental change. *Australian Zoologist* 25: 29-65.

Callen, R.A. and Tedford, R.H. 1976. New late Cainozoic rock units and depositional environments, Lake Frome area, South Australia. *Transactions of the Royal Society of South Australia* 100: 125-167.

Lindsay, J.M. 1987. Age and habitat of a monospecific foraminiferal fauna from near-type Etadunna Formation, Lake Palankarinna, Lake Eyre Basin. *South Australian Department of Mines Report* 87/93.

Long, J. M., Archer, Flannery, T. and Hand, S. 2002. *Prehistoric mammals of Australia and New Guinea. One hundred million years of evolution*. University of New South Wales Press, Sydney. 244 pp.

Luckett, W. P. 1993. An ontogenetic assessment of dental homologies in therian mammals. Pp. 182-204 in: Szalay F. S., Novacek M. J., and McKenna M. C. (eds), *Mammal Phylogeny: Mesozoic Differentiation, Multituberculates, Monotremes, Early Therians and Marsupials*. Springer-Verlag, New York.

Martin, H. A. 1990. The palynology of the Namba Formation in the Wooltana-1 bore, Callabonna Basin (Lake Frome), South Australia, and its relevance to Miocene grasslands in central Australia. *Alcheringa* 14: 247-255.

Megirian, D., Murray, P., Schwartz, L. and von der Borch, C. 2004 Late Oligocene Kangaroo Well Local Fauna from the Ulta Limestone (new name), and climate of the Miocene oscillation across central Australia. *Australian Journal of Earth Sciences* 15 (5):701-741.

Norrish, K. and Pickering, J.G. 1983. Clay minerals; pp. 281-308 *in Soils: an Australian viewpoint*. CSIRO/Academic, Melbourne.

Pledge, N.S. 1982. Enigmatic *Ektopodon*: a case history of palaeontological interpretation. Pp. 479-488 in: Rich, P.V., and Thompson, E.M. (eds), *The Fossil Vertebrate Record of Australasia*. Monash University Offset Printing Unit, Clayton, Victoria.

Pledge, N.S. 1984. A new Miocene vertebrate faunal assemblage from the Lake Eyre Basin: a preliminary report. *Australian Zoologist* 21: 345-355.

Pledge, N.S. 1986. A new species of *Ektopodon* (Marsupialia; Phalangeroidea) from the Miocene of South Australia. *University of California Publications in Geological Sciences* 131: 43-67.

Pledge, N.S. 1991. Reconstructing the natural history of extinct animals - *Ektopodon* as a case history. Ch. 9, pp. 247-266 in: Vickers-Rich, P., Monaghan, J.M., Baird, R.F. and Rich, T.H. (eds). *Vertebrate Palaeontology of Australasia*. Pioneer Design Studio. Monash University, Melbourne.

Pledge, N.S., Archer, M., Hand, S.J. and Godthelp, H. 1999. Additions to knowledge about ektopodontids (Marsupialia: Ektopodontidae): including a new species *Ektopodon litolophus*. *Records of the Western Australian Museum* Supplement No. 57: 255-264.

Rich, T.H.V., 1986. *Darcius duggani*, a new ektopodontid (Marsupialia; Phalangeroidea) from the early Pliocene Hamilton Local Fauna, Australia. *University of California Publication in Geological Sciences* 131: 68-74.

Rich, T.H.V. and Archer, M. 1979. *Namilamadeta snideri*, a new diprotodontan (Marsupialia, Vombatoidea) from the medial Miocene of South Australia. *Alcheringa* 3: 197-208.

Rich, T.H., Piper, K.J., Pickering, D. and Wright, S. 2006. Further Ektopodontidae (Phalangeroidea, Mammalia) from southwestern Victoria. *Alcheringa* 30: 133-140.

Rich, T.H.V. and Rich, P.V. 1987. New specimens of *Ngapakaldia* (Marsupialia: Diprotodontoidea) and taxonomic diversity in medial Miocene palorchestids. Pp. 467-476, in: Archer M. (ed.) *Possums and Opossums: Studies in Evolution*. Surrey Beatty & Sons Pty Ltd and the Royal Zoological Society of New South Wales, Sydney.

Stirton, R.A., Tedford, R.H. and Miller. A.H. 1961. Cenozoic stratigraphy and vertebrate palaeontology of the Tirari Desert, South Australia. *Records of the South Australian Museum* 14: 19-61.

Tedford, R.H. and Woodburne, M.O. 1987. The Ilariidae, a new family of vombatiform marsupials from Miocene strata of South Australia and an evaluation of the homology of molar cusps in the Diprotodontia. Pp. 401-418, in: Archer, M. (ed.) *Possums and Opossums: Studies in Evolution*. Surrey Beatty & Sons Pty Ltd and the Royal Zoological Society of New South Wales, Sydney.

Truswell, E.M., Sluiter, I.R. and Harris, W.K. 1985. Palynology of the Oligocene–Miocene sequence in the Oakvale-1 corehole, western Murray Basin, South Australia. *Bureau of Mineral Resources Journal of Australian Geology and Geophysics* 9: 267-95.

Woodburne, M.O. 1986. Biostratigraphy and biochronology. *University of California Publications in Geological Sciences* 131: 87-93.

Woodburne, M.O. and Clemens, W.A. (eds). 1986a. Revision of the Ektopodontidae (Mammalia; Marsupialia; Phalangeroidea) of the Australian Neogene. *University of California Publications in Geological Sciences* 131: 1-114.

Woodburne, M.O. and Clemens, W.A. 1986b. A new genus of Ektopodontidae and additional comments on *Ektopodon serratus*. *University of California Publications in Geological Sciences* 131: 10-42.

Woodburne, M.O. and Clemens, W.A. 1986c. Phyletic analysis and conclusions. *University of California Publications in Geological Sciences* 131: 94-102.

Woodburne, M.O., MacFadden, B.J., Case, J.A., Springer, M.S., Pledge, N.S., Power, J.D., Woodburne, J.M. and Springer, K.B. 1993. Land mammal biostratigraphy and magnetostratigraphy of the Etadunna Formation (Late Oligocene) of South Australia. *Journal of Vertebrate Paleontology* 13: 483-515.

Woodburne, M.O., Tedford, R.H., Archer, M., Turnbull, W.D., Plane, M.D. and Lundelius, E.L. 1985. Biochronology of the continental mammal record of Australia and New Guinea. *Special Publication South Australian Department of Mines and Energy* 5: 347-363.

Table 1. Measurements (in mm) of recently discovered ektopodontid molar teeth. Pstl = parastyloph width.

Specimen Number	tooth	length	Pstl	Anterior width	Posterior width
Ektopodon stirtoni					
SAM P35309	LP^3	5.5		3.4	
(left maxilla)	LM^1	8.8	3.2	8.5	9.1
"	LM^2	6.9		9.3	8.7
"	LM^3	6.3		8.2	6.5
SAM P31637	LM^2	6.8		9.3+	8.7
SAM P23854	RM^2	7.9		9.5+	9.2+
SAM P30156	LM^3	6.7		8.9	7.6
SAM P30175	LM^3	6.7		8.5+	-
SAM P31638	LM_2	7.7		7.0	6.7
SAM P29577	RM_2	8.1		7.8	7.5
(right dentary)	RM_3	8.0		6.9	6.1
"	RM_4	7.5		5.5	4.3
SAM P24541	LM_2	-		-	6.4
SAM P23989	RM_3	-		-	5.6
SAM P23988	LM_4	6.8		5.95	5.0
SAM P33451	RM_4	6.7		6.0	5.1
Ektopodon litolophus					
SAM P30176	RM^1	10.6	6.0	11.7	12.1
Chunia illuminata					
SAM P29081	LM^1	5.0	1.9	4.5	4.8

Table 2. Dimensions (in mm) of cheek teeth in maxilla, *Ektopodon stirtoni* SAM P35309. Molar row length, 26.0; preserved molar length, 21.7; preserved cheek row length, 23.5; half-palate width, 22.0; clear half palate, 13.2; angle of premolar crest to inner line of molar row, 65°. 'Stylewidth' = parastyloph width.

Tooth	Length	Stylewidth	Ant. Width	Post. Width	Ant. Cusps	Post. cusps
P^3	5.00	N/A	3.20	3.20	1.00	1.00
M^1	8.50	3.2	8.50	9.10	7.00	8.00
M^2	6.50	N/A	9.10	8.25	9.00	8.00
M^3	5.70	N/A	8.00	6.70	8.00	7.00
M^4	–	–	–	–	–	–